Regulation of potassium currents in the sino-atrial node

A thesis presented for the degree of Doctor of Philosophy
Trinity Term 2003

By

Paul A.D. Mattick

Hertford College, Oxford
University Department of Pharmacology, Oxford

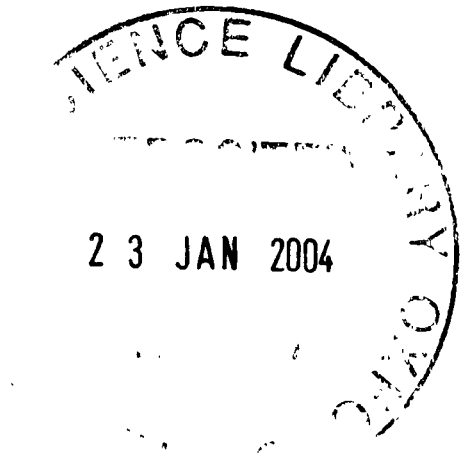

Regulation of potassium currents in the sino-atrial node

Paul AD Mattick
Hertford College, Oxford
Submitted for the degree of Doctor of Philosophy, Trinity 2003

Regulation of potassium channels by cytosolic calcium and other factors was studied in guinea-pig isolated sino-atrial node cells. Rapidly activating I_{Kr} and slowly activating I_{Ks} were identified on the basis of biophysical factors (range of activating depolarisations, time of activation, rectification) and selective blockers (E4031 to suppress I_{Kr}). The protein channels carrying I_{Kr} and I_{Ks} were localised to the sarcolemmal membrane using specific antibodies in immunohistochemical experiments. Loading cells with a calcium chelator (BAPTA) caused substantial reduction of I_{Kr} and I_{Ks}. Both currents were also reduced by the CAMK inhibitor KN-93. It therefore appeared that cytosolic calcium plays a role in regulating I_{Kr} and I_{Ks} and that this effect was mediated at least in part through CAMK. AC may also be calcium sensitive, and production of cAMP and PKA activity may therefore be calcium dependent. cAMP appeared to regulate pacemaking; basal AC turnover is though to be high, and elevated cAMP appear to augment I_{Kr} via PKA activity. Upon cAMP elevation (via AC stimulation or isoprenaline) I_{Ks} augmentation was greater than I_{Kr}. Agents that interfered with the function of the sarcoplasmic reticulum (ryanodine and cyclopiazonic acid) also reduced I_{Kr} and I_{Ks}, but to a lesser extent than BAPTA-loading or KN-93, and these observations indicate that calcium from the SR contributed partially to (was not the sole source) the calcium regulating I_{Kr} and I_{Ks}. The effects of the cytosolic BAPTA and of the other agents listed above were re-investigated after stimulation of beta-adrenoceptor pathways with isoprenaline, and it was concluded that increased calcium entry and rises in cytosolic calcium play a significant role in mediating the effects of beta-adrenoceptor stimulation on I_{Kr} and I_{Ks}. Inhibitors with differential specificity for protein kinase subtypes showed a range of inhibitory effects, reflecting complex interactions between the different protein kinases upon I_{Kr} and I_{Ks}.

Abstract word count: 299
Thesis word count: 64890

Full Papers

Rigg, L., P. A. Mattick, et al. (2003). "Modulation of the hyperpolarization-activated current (I_f) by calcium and calmodulin in the guinea-pig sino-atrial node." Cardiovasc Res 57(2): 497-504.

Papers submitted

Rakovic, S., L. Sanders, P.A. Mattick, M. Lowe & D.A. Terrar (2003)."Fundamental importance of Na^+-Ca^{2+} exchange for the pacemaking mechanism in guinea-pig sino-atrial node."

Rakovic, S., L. Sanders, P.A. Mattick, H. Ishida & D.A. Terrar (2003)."Investigation of the role of T-type calcium current, and its relationship to local and whole-cell calcium transients, in pacemaking of guinea-pig sino-atrial node cells."

Papers in preparation

Mattick, P.A. & D.A. Terrar. "Calcium regulation of I_{Kr} and I_{Ks} in guinea-pig sino-atrial node cells."

Mattick, P.A. & D.A. Terrar. "Investigation of augmentation of I_{Kr} and I_{Ks} by isoprenaline in guinea-pig sino-atrial node cells."

Abstracts

Mattick, P.A., B.M. Heath, L. Rigg & D.A. Terrar (2001)."Ca^{2+} regulation of delayed rectifier K^+ currents (I_K) in guinea-pig sino-atrial node (SAN) cells." Biophys. J. (Annual Meeting Abstracts) 2001: 638a

Mattick, P.A. & D.A. Terrar (2001)."Effects of β-adrenergic stimulation on spontaneous rate, I_K, I_f and I_{CaL} in isolated guinea-pig sino-atrial node (SAN) cells." IUPS (New Zealand): 271P

Mattick, P.A. & D.A. Terrar (2002)."Modulation of the delayed rectifier K^+ current (I_K) in guinea-pig sino-atrial node (SAN) cells by adenylate cyclase." Biophys. J. (Annual Meeting Abstracts): 607c

Mattick, P.A & D.A. Terrar (2002)."Ca^{2+} modulates I_K, possibly via calmodulin kinase and the SR partially mediates isoprenaline augmentation of I_K." J. Physiol: 544P

I would like to primarily thank my supervisor, Dr. Derek A. Terrar, for giving me the opportunity to undertake this work at Oxford and for the guidance and advice his has given me throughout my period of study.

The people of the department of pharmacology have been especially helpful, both in academic and social terms. My funding body was the British Heart Foundation, but the department of pharmacology also provided some financial support in the latter stages. I would like to thank Jayne Watson (Veterinary Services) and Derek Blake for their respective parts in raising antibodies, Sarah Busby for her help with the immunohistochemistry and Alexia Roberts for some of the preliminary experimental work. I am especially grateful to Steve Rakovic and Lauren Rigg, who taught me the techniques I have used in this thesis and the Terrar laboratory in general for their good company.

My friends have been a good source of support over the years, some I have known only briefly, but I hope to know them for a long time.

Over my time at Oxford I found I needed an outside interest apart from science, and I found an impressive distraction in the form of rowing for Hertford College 1st VIII and Oxford University Lightweight Rowing Club (Nephthys 2003).

Finally and probably most importantly, I would like to thank my parents for all their support, direction and for having faith in me when I didn't deserve it.

CHAPTER 1: Introduction **1**

The sino-atrial node 1

Ion channels and currents 4

Action potential shape in ventricular, atrial and sino-atrial node myocytes 6

Ionic current of the sino-atrial node 10

Role of ionic in DD and AP 32

Sarcoplasmic reticulum and other calcium sinks 35

Intracellular regulation pathways 39

Sino-atrial node heterogeneity 42

Autonomic regulation of the sino-atrial node 43

Summary 46

Aims of thesis 47

Figures 48

CHAPTER 2: Methods **51**

Figures 71

CHAPTER 3: Immunohistochemistry **77**

Results 83

Discussion 93

Figures 101

CHAPTER 4: Description of I_K and other ionic currents **120**

Results 124

Discussion 150

Figures 169

CHAPTER 5: Calcium and the SR **209**

Results 213

Discussion 221

Figures 226

CHAPTER 6: Adenylate cyclase **241**

Results 246

Discussion 255

Figures 262

CHAPTER 7: Kinase regulation of I_K **274**

Results 279

Discussion 288

Figures 293

CHAPTER 8: β-adrenergic stimulation **312**

Results 316

Discussion 331

Figures 343

CHAPTER 9: General discussion **367**

CHAPTER 1: Introduction

The heart's pumping of blood around the body is well known; this circulation facilitates delivery of oxygen and glucose to metabolically active cells (such as muscle cells) and removal of toxic by-products of the ATP generation processes.

The heart is a sophisticated pump and valve system; the two chambers in the right side of the heart drive deoxygenated blood (with a high concentration of carbon dioxide) to the lungs where oxygen is replenished and carbon dioxide removed. The blood then proceeds to the left-hand side of the heart, where another set of two chambers combine to forcefully propel blood out of the heart and to the rest of the body. The used of uni-directional valves between cardiac chambers and the ability of the large arteries to distend, creates affective blood circulation that is continuous (but pulses).

The rhythm of the heart is fundamental to the propulsion of blood around the body. The atria contract momentarily before the ventricular chambers of the heart (figure 1.1) and when this rhythmical process falters, the system can degenerate into fibrillation and circulation may fail. Sequential timing of cardiac activity is vital; to accomplish this the heart has a specialised conduction pathway, and at the origin of this arrangement is the sino-atrial node.

The sino-atrial node

The sino-atrial node is a very specialised area of the heart, situated on the upper surface of the right atria in-between the venae cavae (as illustrated in figure

1.1), bordered by the crista terminalis and the intra atrial septum. The sino-atrial node is only a few cells in depth, but spans all the way across the wall of the right atria.

The cells from the sino-atrial node are quite distinct morphologically from other cardiac cells, regarding both size and shape. Sino-atrial node cells range in length between 30 and 100 μm, being only 2 to 25 μm wide and deep; the smallest cells are thought to originate from the most central regions of the sino-atrial node (Honjo, Boyett et al. 1996). Atrial and ventricular myocytes tend to be much larger, being more than 75 μm long, by 50 μm in the other two dimensions. There is a morphological spectrum of cell shape from the sino-atrial node; ranging between spindle, elongated spindle and so-called spider cells. The naming of these cell types is based purely upon appearance (figure 1.2), spindle cells being bulbous around the nucleus, with two limbs extending from this region, elongated spindles being a larger version of this morphology and spider cells having numerous branching appendages extending from a central body. There are some reports that cells from the very centre of the node are slightly different to cells from the so-called peripheral sino-atrial node. These central cells are thought to be of the spider type morphology. These have very few (if any) striations, posses less sarcoplasmic reticulum and have smaller action potential amplitude (Wu, Schuessler et al. 2001). Few studies have been able to distinguish central and peripheral node cells, and many have not found such functional differences. It is apparent that cells of any morphology are capable of being the primary pacemaker. However, we should not consider just one cell as they interact to such an extent that the characteristic of a single cell (even if it were from the primary pacemaker) would not be the same as the *in vivo* pacemaker. For this reason, a mixed population of sino-atrial node cells should be studied. Each type of

sino-atrial node cell is quite different to any other cardiac myocyte, therefore it is relatively easy to morphologically discriminate between myocyte populations.

Ventricular myocytes have membrane invaginations named transverse-tubules regularly spaced along the sarcolemma, and have important roles in ventricular calcium handling; these are absent in the sino-atrial node and atria. Sino-atrial node cells are heterologous (Boyett et al, 2000), but all are considerably smaller (and thinner) than ventricular cells, still have a relatively high ratio of sarcolemmal membrane to cell volume.

Sino-atrial node cells contain fewer contractile fibres than other myocytes, therefore are not able to develop the same magnitude of contractile force as ventricular cells for example. Contractile units containing actin and myosin are precisely arranged in cardiac myocytes, with the Z-lines orientated to the transverse tubule system found in the ventricular myocytes. This organisation causes the appearances of striations in isolated ventricular and atrial cells, which are absent or faint in sino-atrial node cells (Rigg and Terrar 1996; figure 1.2).

By far the most interesting specialisation of sino-atrial node cells is their electrical properties. Ionic gradients are set up across all cell membranes and an action potential is a brief reversal in this gradient, which in muscle cells triggers contraction. To generate affective contraction of the heart, it is necessary for there to be a single stimulus for contraction and this is generated by the spontaneous development of the sino-atrial node action potential. Spontaneous action potential generation is absent from all healthy myocytes, except those from the action potential

conduction pathway. The sino-atrial node determines the beating rate, as the inherent rhythm of these cells is the quickest in the conduction pathway and the action potential is then propagated to the other regions, which are them-selves spontaneous, before they are able to initiate an action potential.

Ionic channels and currents

An electrochemical gradient is set up across virtually all lipid cell membranes, so that useful ions and molecules are concentrated inside the cell and those that are detrimental to function are excluded. This is accomplished by a system of molecular/ionic pumps (powered by ATP degradation) and form concentration gradients in excess of 1:1000, assuming the substrate is membrane insoluble. These gradients can then be used to mediate movement of other desirable molecules (such as glucose), signal a cellular action (calcium in contraction) and even produce the energy-storing molecule ATP. To utilise the ionic gradients set up in electrically excitable cells, flux pathways have been developed, the most simple of these is the ionic channel.

The ionic system that is present in cardiac myocytes requires the investigators of this system to use electrical recording (in association with other techniques) to gain a full understanding of the system. In order to study cellular electric activity a number of physics laws have to be applied to this biological system. The most important of these is the relationship between voltage, current and resistance (Ohm's law); voltage (or potential difference) is a measure of the separation of charge and is

equal to current (describing the movement of charge across a separation) multiplied by the resistance (hindrance encountered by the current).

Ion channels are sophisticated pores in the membrane, which can display selectivity for certain ionic species and are activated in various ways. The ion channels that are of most importance to this thesis are those that are sensitive to the voltage across the cell membrane. This characteristic has been accredited in sodium channels and some potassium channels, to a region in the fourth transmembrane domain; these contain positively charged residues at every third amino acid (Isacoff, Papazian et al. 1990). When the voltage sensor is activated it moves inside the channel (associated with a gating current), subtly changing the structure of the protein and causing the opening of the channel pore (Fedida, Chen et al. 1998). This pore is filled with water and facilitates the movement of large numbers of hydrophilic ions across the lipid membrane. The conduction of these ions can only occur down the electrochemical gradient.

The naming of channels has not been systematic, nomenclature having been derived from various properties of the channel (selectivity, pharmacology, activating agents and kinetics), and more recently molecular identification has also been utilised. Naming of ionic channels using both functional and molecular terminology can lead to confusion. Native currents are produced by heteromultimers of slightly different channel subunits (particularly in the case of potassium channels), often being associated with regulatory subunits; whereas channels have been primarily molecularly expressed in cultured cell lines as homomultimers, generally without

accessory units. The native and the expressed currents of the same ionic channel may therefore be quite dissimilar.

Ionic channels can pass both negatively (anions) and positively (cations) charged ions both in and out of the cell (depending upon their selectivity). Movement of cations into the cell (or anions out), tends to depolarise the membrane, whereas movement of cations out of the cell (or anions in) causes repolarisation. The complexity of voltage dependency and kinetics varies between ionic channels.

The physiological relevance of each type of ionic channel depends primarily upon the level of expression of the channel sub-units (known as the α-subunit) in that specific tissue type. However the co-expression of non-pore forming subunits should be also considered, as these can determine voltage dependency, conductance and kinetics of the current (England, Uebele et al. 1995). There is an expanding diversity of channels (especially potassium channels), due partially to the continued discovery of new channels, but also to the heteromerization of α-subunits (Isacoff, Jan et al. 1990; Po, Roberds et al. 1993) and the modification of channel activity by association with additional non-pore forming subunits.

Action potential shape in ventricular, atrial and sino-atrial node myocytes

The action of the heart was found by Galvani & Volta to be associated with an electrical activity more than 2 centuries ago, but only comparatively recent technological developments have facilitated the direct recording of cardiac cellular

electrical activity. Cardiac action potentials are substantially longer in duration than those of other excitable cells; this is due to the influx of calcium ions during the action potential plateau associated with an inward depolarising current; this calcium binds to troponin and initiates cross bridge cycling of the actin and myosin fibres in these myocytes. The shape of every action potential is a product of the functional channels that are expressed in that tissue and different channel expression in the heart creates the heterogeneous action potential waveform (figure 1.3).

The action potential of sino-atrial node cells does not include the period of stable negative membrane potential, commonly known as diastole in the rest of the heart. The form of the action potential is similarly in sino-atrial node cells from all species, however the precise parameters vary due to differential ion channel densities; action potential parameters in the same species are therefore similar, but interspecies comparison show some differences. Most initial studies of the sino-atrial node were undertaken upon rabbit tissue (Sanguinetti and Jurkiwicz, 1990), there are fewer more recent studies of guinea-pig tissue (Anumowo and Delmar et al 1992). The way in which the parameters are measured may also vary between studies.

	Present Study	Rigg 2000	Ono 1995	Lei 2002
N number	50	9	16	11
Species	Guinea-pig	Guinea-pig	Rabbit	Rabbit
Beating rate (bpm)	171 ± 10	132 ± 9	204 ± 7	166 ± 16
Most negative potential (mV)	–58 ± 2	–57 ± 2	–71 ± 1	–59 ± 1
Diastolic depolarisation rate (V/s)	2 ± 1	1.5 ± 0.4	0.1 ± 0	0.1 ± 0
Rate of Upstroke (V/s)	4 ± 1			10 ± 2
Overshoot (mV)	14 ± 1	16 ± 4	25 ± 2	37 ± 3
APD_{50} (ms)	62 ± 3	68 ± 5		120 ± 18
APD_{90} (ms)	101 ± 5	123 ± 9		151 ± 25

The action potential is generated in the sino-atrial node region and propagated to the surrounding atrial muscle. However, the atrial cells juxtaposed to the sino-atrial node play an important role in pacemaking. It has been mentioned that sino-atrial node cells display a relatively positive diastolic potential (around –60 mV) and that these cells propagate the cardiac action potential to the atria; to accomplish this the sino-atrial node is electrically coupled to atria, via macromolecular channels known as connexins (Davis, Kanter et al. 1994; Davis, Rodefeld et al. 1995). When the atria are removed from a sino-atrial node preparation, the origin of action potential generation is shifted, indicating that hyperpolarising atrial load affect the site of action potential generation in the sino-atrial node (Watanabe, Honjo et al. 1995; Honjo, Boyett et al. 1996). The atrial action potential is much more negative during diastole (figure 1.3b) and this is imposed upon peripheral sino-atrial cells due to the electrical connection. This hyperpolarisation slows diastolic depolarisation in the periphery of the sino-atrial node and result in the central cells being the primary pacemaker, as although they may not have the fastest inherent pacemaking rate, they are not subjected to the hyperpolarising atrial load. Atrial myocytes are found in the population isolated from the sino-atrial node region. The functional role and distribution of these cells is still under debate, but it is thought that these are absent from the very centre of the node (Honjo, Boyett et al. 1996).

As mentioned above the atrial action potential has a relatively more negative resting potential during diastole (around –80 mV) and upon propagation of the sino-atrial node action potential to this region, there is a very rapid depolarisation during which the membrane potential overshoots 0 mV. This depolarised state is maintained for a few hundred 100 ms before the membrane is once again repolarised to its resting

membrane potential. The atria are unable to propagate this electrical activity directly to the ventricular mass as a ring of non-conducting fibrous tissue separates the two chambers and the only possible route is the atrio-ventricular node, another part of the cardiac conduction pathway. The atrio-ventricular node is similar to the sino-atrial node in some ways, expressing similar ionic channels (Hancox and Levi 1994; Hancox and Howarth 1995) and having similar cell morphology (Howarth, Levi et al. 1996). The spontaneous action potential generation from this region is secondary only to the sino-atrial node itself. The atrio-ventricular node introduces a delay in the passage of the cardiac action potential to the ventricular tissue, thus facilitating complete transfer of the atrial blood volume to the ventricles (figure 1.1). After a 100 ms delay, the action potential is passed down the Purkinje fibres and the bundle of His, before diverging into the ventricular muscle mass.

The ventricles themselves are composed of a number of different cell types, but these do not need to be discussed. A classic description of the ventricular action potential is as figure 1.3a illustrates; a resting ventricular membrane potential of –90 mV is maintained until an action potential is propagated to the region, where-upon a very rapid depolarising upstroke is initiated, taking the membrane to positive potentials (40 mV). There is then an extended plateau period in which these positive potentials are preserved, and in some cell types a notch and dome can be seen during this period, before repolarisation occurs and the resting potential is re-established. The ventricular mass is electrically couple to a much greater degree than the sino-atrial node, via connection with adjacent myocytes through intercalated disks, creating an affective functional syncitium.

Ionic currents of the sino-atrial node

The sino-atrial node action potential has previously been described in form and the basics of ionic currents have been introduced. There are a large number of ion channels, with various ionic species in virtually every biological membrane and in this respect sino-atrial node cells are no exception. Sino-atrial node cells contain many voltage sensitive channels, which are sequentially activated during different phases and define action potential morphology. The majority of these channels are selective for cationic species, but the role of anions should still be considered, especially regarding non-selective currents. It is worth noting that due to the small size of this type of cell, in addition to the relatively small action potential amplitude, the high input resistance of between 0.5-1 GΩ, whereas ventricular myocytes vary between 40-300 MΩ. This creates a finely balanced diastolic depolarisation (0.5 V/second) of the sino-atrial node. Even currents of relatively small amplitude (~3 pA) play a substantial role in pacemaking (Accili and DiFrancesco 1996).

The ionic channels of primary concern to this thesis are located in the sarcolemmal membrane, that is the lipid membrane separating the internal cytosol from the extracellular space. Functional ionic channels are distributed along the surface membrane of the sino-atrial node cell, with other channels possibly being contained in vesicles in the cytoplasm prior to sarcolemmal insertion. There are also ionic channels on the membranes of intracellular organelles, one of which will be described later in this chapter.

The initial studies of the sino-atrial node were generally upon cells isolated from the rabbit heart (Noma, Yanagihara et al. 1977). Procedures were subsequently developed to isolate the corresponding cells from the guinea-pig heart (Anumonwo, Freeman et al. 1992), and recently mouse (Anumonwo, Tallini et al. 2001), pig (Ono, Shibata et al. 2000) and rat (Shinagawa, Satoh et al. 2000) sino-atrial cells have been isolated. These studies of different species indicate that the precise ionic mechanisms and regulation varies between the sino-atrial node cells of different species, but the general activation sequence of the ionic currents during the pacemaking cycle remains relatively consistent.

Most studies of sino-atrial node pacemaking have been undertaken upon isolated cells; but some studies have used multicellular preparations with reasonable success. The use of multicellular preparations gives a better insight into how the different regions of the sino-atrial node function, and how they interact with surrounding atrial cells.

The best order in which to describe the various ionic currents, and major electrogenic exchange mechanisms, in the pacemaking cycle is to discuss them in the sequence in which they are *activated*;

- Most negative potential — Hyperpolarisation activated current (I_f)
- Diastolic depolarisation — Sustained Inward current (I_{St})
  T-type Calcium current (I_{CaT})
  Sodium-Calcium exchange current (I_{NCX})

Sodium dependent background current (I_{bNa})

- Upstroke — L-type Calcium current (I_{CaL})

- Repolarisation — Delayed rectifier Potassium current (I_K)

composed of- Rapid component (I_{Kr})

Slow component (I_{Ks})

Hyperpolarisation activated current (I_f)

At negative (hyperpolarised) voltages this channel is activated and opening mediates the influx of various cationic species into the cell, therefore contributing an inward depolarising current.

I_f was initially described in rabbit sino-atrial node cells in the 1970's, and (after some initial confusion) in other regions of the cardiac conduction pathway; being quite different from previously described currents, it was initially named the "funny current" and hence gained the nomenclature I_f (Anumonwo, Delmar et al. 1994). This current displays slow activation kinetics (Tau 1300 ms), being activated in the voltage range –50 to –110 mV and exhibiting substantial amplitude at more negative voltages (DiFrancesco 1991; DiFrancesco and Tortora 1991). The main ions passed by this non-specific current are sodium and potassium monovalent cations (the channel that underlies I_f is most closely related to the potassium channel), but other cationic species do pass through the channel, as there is not an extensive selectivity filter. This is demonstrated by the reversal potential of I_f having been found to be –25 mV (Yanagihara and Irisawa 1980). I_f time-dependently activates upon membrane

hyperpolarisation, exhibiting exponential activation after an initial instantaneous current component. The exact identity of the instantaneous current is unknown, but has been reported previously to be I_{K1} (Shinagawa, Satoh et al. 2000), although there is thought to be no I_{K1} expression in the sino-atrial node (Vassalle 1995). This instantaneous current could possibly be related to tandem-pore potassium channels (Verkerk, Wilders et al. 2002). There is an analogous current to I_f found in the nervous system (known as I_h, derived from is activation upon hyperpolarisation) and in other tissue that possess rhythmical activity (cells of cajal). Caesium has previously been used to describe I_f (Denyer and Brown 1990), but the specificity of this divalent cation to I_f is not complete and can have affects upon potassium channels. Consequently the drug ZD-7288 was developed and has shown much greater specificity (BoSmith, Briggs et al. 1993).

The molecular entity underlying I_f has been recently cloned from the mouse heart (Shi, Wymore et al. 1999) and has been named the Hyperpolarisation Cyclic Nucleotide (HCN) gated family of ionic channels. To date there have been 4 HCN channels found and they are named HCN_{1-4} respectively, with each tissue expressing different levels of each sub-type. In addition, the same tissue expresses differential sub-units in other species; HCN_4 is expressed most in the sino-atrial node, with HCN_1 (and in some animals HCN_2) also being present in the rabbit (Altomare, Terragni et al. 2003) and probably in the guinea-pig heart (Robinson and Siegelbaum 2003). An accessory protein is often expressed in association with HCN channels, known as $mirP_1$, and HCN channel interaction with this protein alters the ionic characteristics of the channel (Shi, Wymore et al. 1999). The voltage sensing mechanism of I_f is very

similar to delayed rectifier potassium channels, but this current is an inward current and the gating mechanism really is rather funny.

HCN channels are closely related to the cyclic nucleotide gated family of channels and display a similar characteristic in binding cyclic Adenosine Mono Phosphate (cAMP). Upon the binding of cAMP to HCN channels the voltage dependent activation range is shifted to more depolarised potentials in excess of 10 mV (DiFrancesco and Tortora 1991). In the voltage range in which these channels operate, the influence of cAMP leads to an increased probability that the HCN channel will be open (DiFrancesco and Tortora 1991; Bois, Renaudon et al. 1997), elevating the physiologically relevance of I_f in the sino-atrial node action potential. Other cyclic nucleotides (such as cGMP) can also bind and modulate the voltage dependent activation of I_f (Yoo + 1998). Any action to alter the cytosolic concentration of cAMP, modulates the voltage dependent activation of I_f (Accili, Redaelli et al. 1997). Both β-adrenergic and muscarinic receptor activation, mediating the affects of the sympathetic and parasympathetic nerves, modulate cAMP levels by respectively activating and inhibiting the action of adenylate cyclase (AC), the enzyme which catalyses the production of cAMP (DiFrancesco 1987; Renaudon, Bois et al. 1997). The cAMP shift of voltage-dependency is independent of magnesium, ATP, GTP and PKA (DiFrancesco and Tortora 1991), re-affirming the direct interaction of cAMP with the HCN channel. Analogues of cAMP that inhibit PKA have been found to activate I_f in a manner similar to cAMP itself (Bois, Renaudon et al. 1997), indicating a PKA independent modulation which maybe mediated by structural interaction. Non-cyclic nucleotides failed to modulate I_f activation, whilst other cyclic nucleotides caused a positive shift in voltage dependent

activation, although to a smaller degree (Renaudon, Bescond et al. 1998). Sympathetic stimulation increases the role of I_f in pacemaking via elevating cAMP levels, whereas the converse occurs during parasympathetic tone. In addition to cAMP, intracellular calcium seems to alter I_f amplitude (Hagiwara and Irisawa 1989) and high calcium concentrations (100 nM) cause a depolarised shift in the activation threshold of I_f. The calcium sensitivity of I_f has been reported by various groups, although it is not clear whether this is a direct action this could be mediated by calcium regulation of AC (Luthi and McCormick 1998; Luthi and McCormick 1999; Luthi and McCormick 1999; Rigg, Mattick et al. 2003). Alternatively, it could be mediated by interaction with calcium-calmodulin, or by phosphorylation via calcium sensitive kinases, such as calmodulin kinase or protein kinase C (Tesmer and Sprang 1998).

There is a theory that earlier in evolution all cardiac myocytes were similar to sino-atrial node cells, all possessing I_f and capable of pacemaking (Brown, Kimura et al. 1984). As the size of the animal grew and a bipedal form was assumed, the heart needed to pump more forcefully and therefore ventricular myocytes specialised to accomplish more forceful contraction, supplying effective circulation. Embryonic ventricular myocytes still possess substantial amounts of I_f, which is extensively down regulated before birth (Yasui, Liu et al. 2001), but can present in pathological states such as hypertrophy and initiate abnormal automaticity.

Sustained Inward current (I_{st})

Upon blockade of various ion channels, a nicardipine sensitive inward current has been recorded in guinea-pig (Guo, Mitsuiye et al. 1997) and rabbit sino-atrial

node (Guo, Ono et al. 1995), as well as rabbit atrio-ventricular node (Guo and Noma 1997). Nicardipine primarily acts upon calcium currents; but I_{st} utilises sodium as the charge carrier (Mitsuiye, Guo et al. 1999) and is activated from voltages as negative as -70 mV, being maximal (~100 pA) at –40 mV (Guo, Mitsuiye et al. 1997). Voltages that are experienced during sino-atrial node diastolic depolarisation would activate this inward current. I_{st} has faster activation kinetics than I_f, but this inward current is of smaller amplitude. However I_{st} is found only in spontaneous cells and should be considered when fully describing pacemaking (Guo, Mitsuiye et al. 1997).

I_{st} was also found to be sensitive to cAMP concentration, with phosphorylation by cAMP sensitive protein kinase (PKA) which was thought to mediate this activity, in a similar way to some calcium currents (Mitsuiye, Shinagawa et al. 2000).

T-type Calcium current (I_{CaT})

I_{CaT} is a calcium selective inward current, which is activated at potentials positive to –70 mV and displays rapid voltage dependent inactivation. I_{CaT} has a bell-shaped voltage dependent activation curve, maximal around –50 mV (Hirano, Fozzard et al. 1989; Tytgat, Vereecke et al. 1990).

I_{CaT} was originally so named because compared to other calcium currents I_{CaT} was tiny and transient. The voltage range of activation of I_{CaT} and other calcium currents is nearly overlapping, with I_{CaT} being activated at slightly more negative potentials (Hirano, Fozzard et al. 1989). I_{CaT} is distributed throughout the heart (Zhou and Lipsius 1994), including in the sino-atrial node region. The voltage dependency

and the use of low nickel concentrations to specifically inhibit I_{CaT} have allowed characterised of this current (Tytgat, Vereecke et al. 1990; Martinez, Heredia et al. 1999). The inward I_{CaT} is activated in the voltage range of diastolic depolarisation, hence I_{CaT} would accelerate pacemaking. In addition to this, I_{CaT} may have a role in the activation of calcium release from intracellular stores (Huser, Blatter et al. 2000; Lipsius, Huser et al. 2001). I_{CaT} however does not mediate the sino-atrial node action potential upstroke (Doerr, Denger et al. 1989).

I_{CaT} is generally considered not to be affected by autonomic stimulation (Tytgat, Nilius et al. 1988), whereas other calcium currents demonstrate large increases upon sympathetic stimulation (Golard and Siegelbaum 1993; Zaza, Robinson et al. 1996).

Sodium-Calcium exchange current (I_{NCX})

This current is mediated by the action of an ion exchanger, rather than an ionic channel, but the high rate of electrogenic exchange of calcium for sodium (Chapman and Tunstall 1980), creates a substantial current. This current is inward whilst the cell is extruding calcium during some parts of the action potential.

I_{NCX} is the current that is generated as 1 divalent calcium cation is transferred across the sarcolemmal membrane in exchange for 3 monovalent sodium cations (Pitts 1979; Giles and Shimoni 1989). This results in a single net charge being passed across the membrane in the direction of sodium movement for every cycle of the exchanger (Bers, Philipson et al. 1980; Philipson, Bers et al. 1980). The exchanger is bi-directional, so I_{NCX} can be an inward or an outward current depending upon the

electrochemical gradients. The exchanger's primary role (in parallel with the sarcolemmal calcium pump) is thought to be the extrusion of calcium that has entered the cytosol via calcium channels during the action potential. Ironically this extrusion of calcium is associated with an inward current, which depolarises the sino-atrial node cell and contributes to activation of the subsequent action potential. This direction of exchange is electrogenically favoured during diastolic depolarisation, as this is a movement of a positive towards a relatively negative region; this is against the calcium concentration gradient but is powered by the large sodium concentration gradient (set up by the sodium-potassium pump). There is a perpetual sodium gradient into the cell, so calcium extrusion (and therefore an inward current) is likely to be occurring throughout the pacemaking cycle (Bers, Philipson et al. 1980). There is evidence that I_{NCX} is outward (mediating calcium influx) during the early stages of the ventricular action potential, when the polarisation of the membrane has been reversed and before significant intracellular calcium entry (Noble and Shimoni 1981; Boyett 1986). The action potential of the sino-atrial node does not overshoot 0 mV by as much as in ventricular myocytes, in addition the sino-atrial node upstroke is mediated by calcium entry and so it is unlikely that there will be any outward I_{NCX}. Blockade of this current caused significant slowing of pacemaking and removal of sodium from the extracellular solution caused cessation and has affects upon calcium handling (Huser, Blatter et al. 2000).

The different nature of the sodium-calcium exchanger to ion channels is demonstrated at the molecular level, as the exchanger current is mediated by a 12 membrane spanning system, possessing a large intracellular domain (Nicoll, Longoni et al. 1990; Frank, Mottino et al. 1992). The intracellular domain has a number of

regulatory possibilities, including calmodulin binding and phosphorylation sites (Nicoll, Longoni et al. 1990). There has been a study of ventricular mocytes in which the current thought to be I_{NCX} was increased by actions which stimulate sympathetic stimulation, via a cAMP/PKA mediated pathway (Perchenet, Hinde et al. 2000). This fits in with the molecular study that found phosphorylation sites on the intracellular regulatory domain of the sodium-calcium exchanger.

Sodium dependent background current (I_{bNa})

This is another non-specific inward current that has been recorded when all other currents have been blocked. I_{bNa} is a time-independent current, which is selective for mono-valent cations and has a reversal potential of about –20 mV. I_{bNa} can only be observed in the presence of sodium in the extracellular medium (Hagiwara, Irisawa et al. 1992). This current is insensitive to nickel and therefore cannot be related to I_{NCX}. The fast sodium current (see later) has been found to be absent from the cells of the central node (Honjo, Boyett et al. 1996).

Few groups have reported the presence of I_{bNa} and Noble, Denyer et al (1992) pointed out that any inward current developed by I_{bNa}, would reduce the activation of inward I_f. However I_{bNa} is enhanced by sympathetic stimulation and the role of this non-specific inward background current to accelerate diastolic depolarisation would therefore be increased (Hagiwara, Irisawa et al. 1992).

L-type Calcium current (I_{CaL})

The role of I_{CaL} has been well described in ventricular (Qu and Campbell 1998), but the action of I_{CaL} is different in the sino-atrial (Boyett, Kodama et al. 1995;

Honjo, Boyett et al. 1996). The absence of the fast sodium current (see additional currents of interest, page 27) in the sino-atrial node, requires I_{CaL} to mediate the action potential upstroke.

The inward I_{CaL} is rapidly activated (<10 ms) by depolarisations positive of –30 mV and is of large amplitude, but both depolarised voltages and calcium itself inactivate I_{CaL} (Yatani, Wilson et al. 1983; Mangoni, Couette et al. 2003). Recovery from inactivation at diastolic potentials means that there is a progressively increasing contribution of inward I_{CaL} to diastolic depolarisation. The L-type calcium channel facilitates the influx of calcium ions that triggers calcium release from intracellular stores. Calcium influx mediated by I_{CaL}, I_{CaT}, possibly I_{NCX} (if current is ever outward) and that calcium released from the intracellular stores (primarily the SR), all combine to increase the cytoplasmic concentration and initiate contraction.

An I_{CaL} mediated action potential upstroke has also been observed in crustacean striated muscle and various smooth muscle (Liu and Huizinga 1994), but in most tissue and species the sodium currents fulfil this role. The reversal potential for calcium is very positive (+120 mV), due to the large calcium concentration gradient that is set up across the sarcolemma. However the reversal potential for I_{CaL} is +80 mV, due to potassium outward leak through the relatively calcium selective (1 potassium: 1000 calcium) pore. The massive concentration of potassium in the cell results in a significant efflux of potassium through I_{CaL}, which shifts the I_{CaL} reversal potential towards that of potassium (-80 mV). Even so upon opening of the L-type calcium channels there's a rapid depolarisation, over-shooting 0 mV and if

inactivation did not block the channel then the membrane potential would approach the I_{CaL} reversal potential.

I_{CaL} channels seem to be preferentially located/clustered in the transverse tubules of ventricular myocytes (Tsien 1983; Gathercole, Colling et al. 2000; Takagishi, Yasui et al. 2000)Takagishi, Yasui et al (2000) calculated that there are between 10 and 50 L-type calcium channels in every μm^2 of sarcolemma (including transverse tubules). I_{CaL} is much larger in ventricular myocytes, although channel density maybe similar since sino-atrial node has much less membrane (Qu and Campbell 1998).

The α-subunit of the L-type calcium channel is composed of 4 homologous regions, containing 6 transmembrane domain in each; the 4 regions are thought to arrange themselves into a square, containing a central pore which facilitates the passage of calcium ions across the sarcolemma (Catterall 1988; Ahlijanian, Westenbroek et al. 1990). The selectivity of this channel is relatively high for calcium, passing calcium over 4000 times more readily than another divalent cation caesium (Tsien, Hess et al. 1987). The α-subunit has numerous regulatory sites (phosphorylation and calmodulin binding sites) and has an extracellular receptor site for the binding of dihydropyridine agents (e.g. nifedipine) that modulate I_{CaL}. There are also a number of other sub-units that interact with the α-subunit of the L-type calcium channel, altering both kinetics and regulation.

Autonomic regulation has been quite extensively investigated after Reuter and Wollert (1967) found I_{CaL} to be augmented by sympathetic tone. β-adrenoceptor

activation of stimulatory GTP-binding protein (G_s), activates AC which leads to cAMP production, which then prompts PKA phosphorylation of the L-type calcium channel (Osterrieder, Brum et al. 1982; Trautwein and Kameyama 1986; Habuchi, Yamamoto et al. 1996). At the channel level I_{CaL} is increased by PKA mediated phosphorylation that shifts the voltage-dependency to more negative potentials, thus increasing the window current, as the voltage dependent inactivation remains constant (Brum, Osterrieder et al. 1984). More recently, an additional faster, direct G_s augmentation of I_{CaL} has also been described (Yatani, Seidel et al. 1987); this type of direct channel interaction with GTP-binding proteins has been previously described. Parasympathetic activity, or any course of action to mimic it, reduces cAMP levels (via an inhibitory GTP-binding protein (G_i) down-regulation of AC). These actions directly antagonise the well described sympathetic pathway.

Delayed rectifier potassium current (I_K)

The delayed rectifier potassium current is the chief outward current, mediating repolarisation of the sino-atrial node action potential. I_K is activated upon depolarisation (positive to –40 mV), but displays slow activation kinetics and therefore I_K mediated repolarisation is not instantaneous. In addition, the deactivation kinetics of this channel are slow, causing a component of outward I_K still being present when the depolarised voltages (which activated this current) have ceased.

The delayed rectifier potassium current is a voltage and time dependent potassium current originally described in sheep cardiac Purkinje fibres (Noble and Tsien 1969; Noble and Tsien 1969); I_K displays a reversal potential of –65 mV, which indicates only mediocre selectivity for potassium ions (Sanguinetti and Jurkiewicz

1990; Chinn 1993). Two components of I_K have been separated on the basis of the activation kinetics: a rapidly activating current called I_{Kr} and slowly activating component called I_{Ks} (Sanguinetti and Jurkiewicz 1990; Chinn 1993; Heath and Terrar 1996; Lei and Brown 1996). These components can be separated pharmacologically, using class III anti-arrhythmic drugs such as E4031, which selectively inhibit I_{Kr} (Carmeliet 1993). Using class III anti-arrhythmic drugs to isolate the I_K components, I_{Kr} has been found to be maximally activated with depolarisation's as short as 40 ms. I_{Ks} however does not begin to activate until depolarisation durations in excess of 75 ms and continues to activate further as the duration is extended (Sanguinetti and Jurkiewicz 1990; Anumonwo, Freeman et al. 1992; Lei, Brown et al. 2000). The voltage dependencies of the two components of I_K are also different: I_{Kr} is activated by less a positive voltage than I_{Ks}, and this characteristic varies between species to a relatively small degree.

Species	I_K $V_{1/2}$	I_{Kr} $V_{1/2}$	I_{Ks} $V_{1/2}$	Reference
Guinea-pig	8 mV	-23 mV	15 mV	Present Study
Guinea-pig	32 mV			Anumonwo et al 1992
Guinea-pig		-26 mV	17 mV	Matsuura et al 2002
Pig	21 mV			Ono et al 2000
Rabbit		-23 mV		Ono & Ito 1995
Rabbit		-25 mV		Shibasaki et al 1987

I_{Kr} actually shows rectification at positive potentials, being characterised by an inverse current voltage relationship at voltages positive to 0 mV (Sanguinetti and Jurkiewicz 1990), but it rapidly recovers from inactivation. The difference in time and voltage dependent activation (and inactivation) of I_{Kr} and I_{Ks}, cause them to have slightly different roles in repolarisation: I_{Kr} maybe involved in initial repolarising phase and I_{Ks} subsequently activates to affect full repolarisation. Inhibition

experiments using guinea-pig cardiac myocytes have found the two components to be of similar magnitude during the action potential (Sanguinetti and Jurkiewicz 1990).

It has been mentioned that I_K has delayed deactivation kinetics. Both components of this current exhibit this characteristic, which results in a component of both I_{Kr} and I_{Ks} (activated by depolarisation) remaining for a period after the membrane has been repolarised. The remaining outward component, known as a tail current, decays with time (Chinn 1993). The rate of I_K tail current decay is bi-exponential, being described by the time constants 188 and 2510 ms (Heath and Terrar 1996); the decay of I_{Ks} primarily contributes to the fast time-constant at –40 mV, whereas I_{Kr} has both fast and slow kinetics.

There are a number of structural similarities in the channels that pass I_{Kr} and I_{Ks}. The α-subunits of I_{Kr} and I_{Ks} are similar to one of the four homologous domains that form the L-type calcium channel and it is thought that the association of 4 such channel subunits can form functional tetramers. The homology with the L-type calcium channel (and the fast sodium channels) continues: hydrophobicity analysis has indicated 6 predicted transmembrane-spanning regions, with both N and C termini located intracellularly and the presence of the voltage-sensor in the fourth transmembrane domain.

The channels of two current components are from different potassium channel sub-families; I_{Kr} is formed by the protein known as ERG_1 (Curran, Splawski et al. 1995) in the ether-a-go-go channel sub-family (Sanguinetti, Jiang et al. 1995), often referred to as HERG (Human ERG) and I_{Ks} which is the product of $KvLQT_1$ (Wang,

Curran et al. 1996). Early studies of kinetics were undertaken upon whole I_K, without separating I_{Kr} and I_{Ks} (Shibasaki 1987; Ito and Ono 1995; Ono and Ito 1995), therefore are not relevant when discussing these molecularly channels, unless rabbit I_K is presumed to not contain I_{Ks}. Mutations in the genes that encode both ERG_1 and $KvLQT_1$ can cause cardiac arrhythmia's, known as LQT syndrome (where $KvLQT_1$ acquired its name), indicating a functional role of I_{Kr} and I_{Ks} in rhythm generation. $KvLQT_1$ requires the small accessory protein minK, to become a functional channel recognisable as I_{Ks} (Barhanin, Lesage et al. 1996; Sanguinetti, Curran et al. 1996). However, co-localisation of ERG_1 with minK has also been described (McDonald, Yu et al. 1997), but a study by Abbot et al (1999) identified ERG_1 to actually interact with minK related protein ($mirP_1$) rather than minK itself. $KvLQT_1$ in association with minK is the molecular correlate of I_{Ks}, whereas I_{Kr} is produced by the integration of ERG_1 with $mirP_1$. I_{Kr} and I_{Ks} are important targets for anti-arrhythmic drugs, as class 3 anti-arrhythmic drug reduction of I_{Kr} is thought to help prevent certain types of arrhythmia, but excessive I_{Kr} block is actually pro-arrhythmic, in a similar manner to LQT syndrome (Sanguinetti, Jiang et al. 1995).

Upon sympathetic stimulation via β-adrenoceptors, the beating rate of heart is elevated. This is mediated via activation of the AC production of cAMP (Iijima and Taira 1989) by G_s and subsequent cAMP-sensitive kinase phosphorylation of various intracellular protein targets (Kiehn, Wible et al. 1995). In regard to I_K, β-adrenergic stimulation causes a shift in the voltage dependency to more negative potentials (by -10 mV), in addition to increasing the amplitude (Lei, Brown et al. 2000; Lei, Cooper et al. 2002). The augmentation of I_K activated upon depolarisation is paralleled by a corresponding increase in magnitude of the tail current. There have also been some

reports that the rate of tail current deactivation is also quickened, via a PKA mediated pathway (Lei, Brown et al. 2000) although others disagreed with this (Giles, Nakajima et al. 1989). In addition to the well described β-adrenergic stimulation pathway above, another has been found, which connects the β-adrenoceptors more directly (and rapidly) to I_K via a GTP-binding protein pathway independent of kinase activity (Freeman, Kwok et al. 1992). It does this in a similar manner to the dual regulation pathways of I_{CaL}. It is also possible that other molecules released at the sympathetic nerve termini such as ATP, may have additional I_K regulatory roles (Matsuura, Tsuruhara et al. 1996; Matsuura and Ehara 1997)

When the rapid component of I_K has been isolated by either pharmacological or voltage protocols, it has generally been reported not to be sensitive to β-adrenergic stimulation (Sanguinetti and Jurkiewicz 1990; Cui and Zhao 1995; Heath and Terrar 1996; Lei and Brown 1996), and in this it differs from recordings of I_K that are augmented by all actions that mimic β-adrenergic stimulation. However, when less intrusive measurements of I_{Kr} are undertaken, either using perforated patch or sharp electrode techniques, an enhancement of I_{Kr} by both adrenaline (Brown and Difrancesco 1980) and isoprenaline has been described (Heath and Terrar 1996). Brown and Difrancesco (1980) were actually attempting to activate I_K that is not separated, but the voltage protocol they used (10 mV step to –35 mV for 200 ms) would fail to activate any significant I_{Ks}, so the current is presumably only I_{Kr}. In fact Heath and Terrar 2000 described a calcium dependent reduction in the rectification of I_{Kr} at positive potentials during sympathetic stimulation, which effectively enlarged I_{Kr} during a depolarisation event such as an action potential.

Cardiac I_{Ks} is regulated by the sympathetic nervous system. β-adrenoceptor enhancement of I_{Ks} has been demonstrated; this is similar to other channels such as I_{CaL} and is similarly thought to be mediated through activation of cAMP-dependent protein kinase and phosphorylation of the channel protein (Lo and Numann 1998). The relative contribution of the I_K components to repolarisation during β-adrenergic stimulation is thought to change, with I_{Ks} having a much larger importance (Sanguinetti, Jurkiewicz et al. 1991); however this could be a facet of many studies finding no I_{Kr} enhancement. Regulation of I_{Ks} by calcium has also been described in the absence of β-adrenergic stimulation. Elevations of intracellular calcium increase I_{Ks} amplitude, without altering the voltage dependency (Walsh and Kass 1991), by increasing the open probability of these channels (Tohse, Kameyama et al. 1990). There are a number of regulators, including protein kinase C (PKC) and calmodulin, which are sensitive to calcium concentration; also additional regulatory pathways of I_{Ks} have been described in various cardiac cells (Tohse, Kameyama et al. 1987; Nitta, Furukawa et al. 1994). PKC has been found to regulate only I_{Ks}, without having any affects upon the more rapid component I_{Kr} (Mamas and Terrar 2001) or I_{CaL} (Walsh and Kass 1988); PKC is also thought to mediate the α-adrenoceptor enhancement of I_K (Walsh and Kass 1988; Tohse, Nakaya et al. 1992).

Additional currents of interest;

- Inward rectifier potassium current (I_{K1})

- Fast sodium current (I_{Na})

- Transient outward current (I_{TO})
- Ultra-rapid delayed rectifier potassium current (I_{Kur})
- Acetylcholine activated potassium current (I_{KAch})
- ATP sensitive potassium current (I_{KATP})
- Sodium-potassium pump current (I_{NaK})

I_{K1} in the heart maintains the resting membrane potential in atrial and ventricular myocytes, but is not usually found in myocytes of the conduction pathway. The outward I_{K1} is activated upon hyperpolarisation, which exhibits inward rectification that allows negligible current at potentials positive to about -40 mV. The large outward current at negative potentials allows cells to maintain a stable resting membrane potential (Ishii, Yamagishi et al. 1994). The absence of this current in sino-atrial node cells results in the variable resting potential, which is associated with pacemaking. Functional I_{K1} has however been reported in rat sino-atrial node (Shinagawa, Satoh et al. 2000). A recent study by Zaritsky, Redell et al 2001 of I_{K1} knockout ventricular myocytes, found that in the absence of this inward rectifier, ventricular myocytes actually exhibited spontaneous activity. The most negative potential reached during rest in cells of the sino-atrial node is not as negative as in other myocytes. The absence of this large current means that the smaller currents are

of more importance, as any additional current flowing during the finely balanced diastolic depolarisation will have an affect on the rate of depolarisation.

I_{Na} mediates the rapid action potential upstroke in cardiac myocytes. This current has been described in various tissues by its sensitivity to blockade by tetrodotoxin. However the pacemaking rate of sino-atrial node cells of most species, with the possible exception being mouse (Mangoni, Couette et al. 2003), are not affected by tetrodotoxin (Okada 1976; Honjo, Boyett et al. 1996). There maybe some I_{Na} in sino-atrial node cells isolated from regions that are not central, as the peripheral/transitional cells have been found to contain I_{Na} (Honjo, Boyett et al. 1996). Some groups define central sino-atrial node cells, as those beating rates are not effected by tetrodoxin. In addition, atrial cells can be found in some regions of the sino-atrial node and these cell types contain I_{Na}, but are however not spontaneous. This large inward current is voltage dependently activated upon depolarisation, then it undergoes quick inactivation, creating a brief inward current that reverses the membrane potential. The fast sodium channels recovery from inactivation is much more rapid than I_{CaL}, which slowly recover during diastolic depolarisation, and this allows the fast sodium channel to mediate the action potential of much more rapidly firing cells (e.g. neurones). This sodium channel has a similar structure to calcium channels, being composed of 4 homologous regions, each having 6 transmembrane domains (Emerick and Agnew 1989). The I_{Na} mediated depolarisation activates various other currents in ventricular myocytes, including the calcium currents that initiate contraction and potassium currents that subsequently facilitate repolarisation. In sino-atrial node cells, I_{Na} is either absent or voltage-dependently inactivated and so I_{CaL} mediates the action potential upstroke.

I_{TO} has been described in ventricular (and atrial tissue), as being responsible for the brief repolarisation that is sometimes observed prior to the plateau phase of the ventricular action potential. I_{TO} is transient due to its rapid activation (maximal in 10 ms) and ensuing voltage dependent inactivation (Campbell, Rasmusson et al. 1993; Boyett, Honjo et al. 1998; Honjo, Lei et al. 1999). Guo, Mitsuiya et al (1997) characterised their guinea-pig sino-atrial node cells partly by a lack of I_{TO} however others have describe I_{TO} in rabbit (Irisawa 1987; Boyett, Honjo et al. 1998) and more importantly in human sino-atrial node cells (Guo, Mitsuiya et al. 1997). Species dependent differences of ion channel expression seem prevalent and so in this investigation of guinea-pig sino-atrial node cells, I_{TO} shall be considered to be absent and this is recognised as a limitation in comparison to human sino-atrial node cells.

I_{Kur} is another component of the delayed rectifier potassium current, which has been described in some species, primarily in atrial myocytes (Guo and Noma 1997). I_{Kur} is an outward current with half-maximal activation occurring by depolarisation as brief as 15 ms (Fedida, Chen et al. 1998). This takes place within in a similar timescale to I_{TO}, although I_{Kur} does not display such a large degree of inactivation (Snyders, Tamkun et al. 1993; Schmalhofer, Bao et al. 2002). I_{Kur} in canine atrial cells is increased upon sympathetic stimulation (Snyders, Tamkun et al. 1993). This current has not been found in the sino-atrial node region of the heart in the guinea-pig and therefore is irrelevant in subsequent discussions.

Acetylcholine is released from the termini of parasympathetic nerves and stimulation of this pathway, slowing the beating rate of the heart (Boyett, Kodama et

al. 1995; Renaudon, Bois et al. 1997). At high acetylcholine concentrations, in excess of 50 nM an outward potassium current is time-independently activated and this tends to slow (or stop) diastolic depolarisation (Boyett, Kodama et al. 1995). The binding of Acetylcholine to muscarinic (M_2) receptors activates a membrane-delimited G-protein (G_K), which binds to I_{KACh} channels and stimulates opening (DiFrancesco 1987; Renaudon, Bois et al. 1997). This channel has been described in sino-atrial node cells and maybe some basal I_{KACh} due to turnover of G_K in the absence of parasympathetic stimulation.

I_{KATP} is passed by a similar class of channel to I_{KAch}, a ligand gated inwardly rectifying potassium channel. Molecularly I_{KATP} (and I_{K1} and I_{KAch}) are ancestral predecessors of I_K, with each subunit having 2 transmembrane domains, forming functional tetramers; these monomers are analogous to the S5 and S6 regions of I_K and contain the pore domain (see review by Wickenden 2002). This outward current was originally discovered in cardiac muscle and is physiologically inhibited by ATP. Although when ATP levels fall (or ATP degradation by-products concentrate) the inhibition of I_{KATP} ceases (Ogbaghebriel and Shrier 1995); this acts as a link between the metabolic state of the myocytes and their electrical activity. The activity of this current is thought to be cardioprotective (Findlay 1994) by shortening the action potential duration in conditions of metabolic stress (such as ischaemia and hypoxia), but there are also some reports that I_{KATP} is linked to re-entrant arrhthymias (Parratt and Kane 1994).

The sodium/potassium-ATPase is a ubiquitous plasma membrane pump, coupling the hydrolysis of one molecule of ATP with the electrogenic transfer of

three sodium ions for two potassium ions; it is associated with a current flowing in the direction of sodium movement known as I_{NaK}. I_{NaK} is generally an outward current, as this pump primary function is to extrude sodium. Although this current would be relatively small,(Noble and Tsien 1969; Vassalle 1987) found I_{NaK} to be able to alter the membrane potential of sino-atrial node and therefore the rate action potential generation.

Role of ionic currents in DD and AP

The most important aspect to comprehend when considering the ionic mechanism of pacemaking in the sino-atrial node is that there is not just one current that defines the rate of action potential generation, it is a complex interaction of ionic currents forming a precisely balanced unstable system. The absence of the comparatively massive I_{K1} and I_{Na} cause the sino-atrial node to lack current redundancy; any small ionic movement will have an affect upon the generation of action potentials, as there are no large currents to obscure them. The generation of action potentials in the sino-atrial node is also relatively slow and gradual, so fast time-dependent activation becomes less pivotal and inactivation more critical (Zaza, Micheletti et al. 1997). One view is outlined below and can be regarded as a working hypothesis, based upon the model of Brown, Kimura et al (1984).

When the membrane potential is at its most negative, repolarisation will have ceased and diastolic depolarisation will not yet have commenced. This is effectively an instance of membrane potential stability. There are various inward and outward

ionic currents activated, but they are in equilibrium and so no voltage change is affected. The major outward currents at this point would be predominately I_{Ks} and then I_{Kr}; these would be voltage dependently closing, but this process is quite delayed and so a component of both outward I_{Ks} and I_{Kr} would be present at this point in time. The inward I_f would be voltage dependently activating due to the negative potential, in association with the I_{NCX} which is generated by the final stages of electrogenic calcium extrusion. The presence of I_{St}, I_{bNa} and I_{CaT} also contribute to the inward currents, but the sum of all these inward currents, is only equal to the deactivating I_K component at this point.

As the various inward currents mentioned above become more fully time-dependently activated and only slightly exceed the remaining component of I_K that is time-dependently reducing, diastolic depolarisation begins to develop. I_{Ks} deactivates more quickly than I_{Kr}, but I_{Kr} is of smaller amplitude, with total remaining outward I_K taking over 250 ms to halve in amplitude. It is worth noting at this point that the higher the beating rate, the more deactivating I_K will still be present when the subsequent action potential is initiated; this affect is cumulative and results in an large component of deactivating I_K always being present. I_K will be opposed by the time-dependent activation of I_f, although the voltage-dependent activation will successively become less. I_{St} activation is more rapid than I_f and increases as the voltage approaches –40 mV. I_{bNa} continues to contribute a small inward current, whereas I_{CaT} develops into a substantial contributor to pacemaking; the calcium influx associated with I_{CaT} is opposed by the sodium-calcium exchanger, which itself contributes a sizeable depolarising current.

This trend continues as diastolic depolarisation takes the membrane potential to more positive voltages. As the diastolic depolarisation reaches its last third, I_K has nearly decayed fully, most of the inward currents are maximally activate, the I_{CaT} mediated influx of calcium is initiating a progressively large I_{NCX} and so depolarisation is accelerated. I_f is the exception as it has progressively contributed less, due to its voltage dependency. In addition, I_{CaL} gradually begins to activate; this is the largest current in the sino-atrial node cell and again accelerates depolarisation of the membrane potential past –40 mV.

At around –40 mV I_{CaL} becomes fully activated and there is a smooth transition to a rapid phase of depolarisation, as divalent calcium ions flow down the large electrochemical gradient. During this period I_{CaT} is inactivated, I_f ceases, whilst I_{NCX} and I_{St} are reduced. In addition the calcium influx (primarily via I_{CaL}) has activated calcium release from the intracellular calcium stores and caused the increase in cellular calcium that is required to initiate contraction. The inside of the myocyte becomes relatively depolarised, and I_{CaL} begins to inactivate (calcium and voltage dependently), ending the rapid depolarisation associated with the upstroke of the sino-atrial node action potential. This depolarisation has activated I_{Kr} and, after a brief period of maintained positive membrane potential, I_{Ks}.

The membrane potential is only briefly depolarised, and as I_{CaL} declines, the outward I_{Kr} slowly develops, creating another very brief time point of balance between outward and inward currents, before I_{Ks} develops and the I_K components initiate repolarisation. Intracellular calcium is being rapidly lowered by sequestration back into the intracellular calcium stores, extrusion across the membrane on a calcium

pump and via the sodium-calcium exchanger, which generates an inward current that actually prolongs the action potential slightly. As I_K activates over 10's of ms and causes a delay in repolarisation, but there are no substantial inward currents flowing during this period, in contrast with the ventricle where I_{CaL} would be now activating; therefore repolarisation is almost directly related to the development of I_K. As this occurs, outward current accumulates with the I_K that was still deactivating from the previous action potential and mediates repolarisation. The rate of repolarisation is relatively constant as there is not a large I_{K1} present and therefore the final stage repolarisation just becomes progressively slower as the most negative potential is re-established.

Sarcoplasmic reticulum and other calcium sinks

The sarcoplasmic reticulum (SR) is the major intracellular store of calcium. It is present in all cardiac myocytes, as calcium release from these stores is fundamental to the contraction process. These stores are membrane bound networks, independent of the nucleus and the surface sarcolemmal membrane (Rigg, Heath et al. 2000), and they contain a high concentration of calcium that is actively pumped into these structures. Large amounts of calcium can also be rapidly released from the SR, by means of the ryanodine receptor, which is actually a calcium channel that is expressed on the SR. Ryanodine receptors are named due to their affinity for ryanodine, a plant alkaloid. Although they have a similar function to sarcolemmal calcium channels, they are much larger, being both molecularly and structurally complex (Coronado, Morrissette et al. 1994). Calcium release is initiated by binding of multiple calcium

ions to the cytoplasmic side of the ryanodine receptor, known as Calcium-induced Calcium release (CIRC), however direct voltage dependent SR calcium release has also been described in some species and tissues (see review by (Bers and Perez-Reyes 1999). Ryanodine receptors are located at the ends of the SR and calcium release causes very high local calcium concentration (probably in excess of 1 μM), which is then either sequestered back into the SR or extruded across the sarcolemma. Other regions of the SR contain calcium pumps and buffers, to accumulate and store the high concentration of calcium. The Sarcoplasmic/Endoplamic Reticulum Calcium ATPase (SERCA) is activated by high cytosolic calcium, which utilises the breakdown of ATP to move calcium against its concentration gradient into the SR (Misquitta, Sing et al. 1999). Phospholamban is an inhibitory molecule that associates with the SERCA SR calcium pump; although, phosphorylation of phospholamban (by sympathetic activity) removes the inhibition of SERCA (Pan, Hannon et al. 1999).

A healthy myocyte will be in calcium equilibrium regarding the release and sequestration into the SR each cycle. This is a fine balance between calcium channel mediated calcium entry, SR calcium release, SR calcium sequestration, calcium sarcolemmal pump and the sodium-calcium exchanger (reviewed by (Wier 1990). The amount of calcium being released and returning to the SR will be constant, therefore the amount crossing the sarcolemma must also be constant, otherwise this system would either lead to calcium depletion or overloading, and both of these situations have severe pathophysiology. Calcium handling is altered upon autonomic stimulation (Choate, Edwards et al. 1993; Choate, Klemm et al. 1993).

The release of calcium from the SR has been thought to be an all or nothing event, either all the ryanodine receptors are open or none of them. However there are some studies that dispute this theory (Stern, Pizarro et al. 1997). A number of studies have found local release of calcium by a limited number of ryanodine receptors in close proximity; this activity has been called a calcium spark (Song, Stern et al. 1997; Smith, Keizer et al. 1998). Huser, Blatter et al (2000) undertook some elegant studies in latent pacemaker cells and proposed that calcium influx via I_{CaT} activated calcium sparks. Both I_{CaT} and spark activity would increase sub-sarcolemmal calcium concentration and therefore activate I_{NCX}. The I_{NCX} inward current would accelerate depolarisation, and activate I_{CaL} mediated calcium influx, which activates all SR ryanodine receptors (although only a fraction of SR calcium is released) and these calcium sources would combine to increase the global concentration (Huser, Blatter et al. 2000). This possible mechanism requires more investigation in pacemaking cells.

In the sino-atrial node, the SR network is not as extensive as in other types of cardiac myocyte, but these cells are much smaller in volume they are also not primarily a force-developing population and hence probably do not require massive calcium storage capacity. The absence of transverse-tubules in the sino-atrial node is of importance when considering SR function, due to the fact that in other myocytes the ryanodine receptors are juxtaposed to these structures, possibly physically linked to channels/receptors on the sarcolemmal membrane of the transverse-tubule. The absence of transverse-tubules does not alter the SR localisation of ryanodine receptors to the myofibril regions (the Z-line) that would in other tissues, be the location of the transverse-tubules (Rigg, Heath et al. 2000). Clearly, the SR and ryanodine receptors have an important role in excitation-contraction coupling, but the primary role of

sino-atrial node cells is an electrical one; in order to fully describe the pacemaking of the heart, the activity of the SR in pacemaking should be considered.

Inhibition of SR function has been found to reduce the beating rate of the heart in various species, presumably by modulating pacemaking (Rigg and Terrar 1996; Hata, Sakamoto et al. 1998; Ju and Allen 2000). Various ionic currents have been found to be reduced when SR function is inhibited, more prominently affecting inward currents associated with diastolic depolarisation, such as I_f, I_{St} and possibly I_{CaL}. Although no direct reduction of I_{CaL} was observed upon SR function inhibition, the rate of action potential upstroke was reduced which is known to be mediated by I_{CaL} (Rigg and Terrar 1996), although outward I_K was reduced (Hata, Sakamoto et al. 1998). A reduction in I_{NCX} would also be expected. SR activity, presumably mediated by calcium release, modulates a number of different ionic currents involved in pacemaking. SR inhibition tends to decelerate the beating rate, and this indicates that SR function accelerates pacemaking.

The major calcium handling pathways have been described: very briefly, calcium entry via I_{CaL} and I_{CaT} activate calcium release from the SR, combining to raise intracellular calcium concentration and to initiate contraction, with the subsequent sequestration of calcium into the SR or extrusion across the sarcolemma (Vinogradova, Bogdanov et al. 2002). There are also some other minor calcium stores and sinks that need to be briefly mentioned. The mitochondria are thought to only play a minor role in beat-to-beat calcium handling, except in pathophysiological situations such as ischaemia, in which they are able to buffer a large amount of calcium as an insoluble phosphate in mitochondrial matrix (Budd and Nicholls 1996).

Calcium can also be buffered by negatively charged binding sites on the internal sarcolemmal surface, which are formed by inositol-based phospolipids.

Intracellular regulation pathways

The interaction between ionic channels is a dynamic relationship; the role of each current in pacemaking changes to mediate the autonomic nervous system requirement for an alteration in sino-atrial node beating rate. To achieve this ionic channels are sensitive to the intracellular concentration of certain important molecules; interaction with these molecules, or an indirect action of these molecules upon the channel, alters the characteristics of the current. In many cases a regulatory signal needs to be amplified so that a small change in the concentration of one molecule will result in a large affect. For example, the activation of an enzyme by a single molecule causes many molecules of product to be formed, each of which can have a signalling affect.

The activity of certain classes of G-protein result in the stimulation of the membrane bound adenylate cyclase (AC) enzyme; this catalyses the conversion of ATP to cAMP. Results from various groups (Petit-Jacques, Bois et al. 1993; Habuchi, Nishio et al. 1996; Zaza, Robinson et al. 1996; Heath and Terrar 2000) indicate cAMP to be at high concentrations in the sino-atrial node. The cAMP molecule has very important direct affects upon I_f (DiFrancesco 1999) and possibly I_{Kr} (Cui, Kagan et al. 2001), both of which have vital role in pacemaking. In addition, the presence of raised cAMP levels activates PKA, resulting in the phosphorylation of

various targets, including phosphorylation of I_{CaL} causing augmentation (Tanaka, Clark et al. 1996). There maybe an intrinsic turnover of the AC enzyme in the sino-atrial node in the absence of stimulation (personal communication, Terrar & Mamas; (Petit-Jacques, Bois et al. 1993; Habuchi, Nishio et al. 1996; Zaza, Robinson et al. 1996), as parasympathetic stimulation decreased basal I_{CaL}; for such an affect there must be some cAMP being produced by AC. Phospodiesterase's (PDE) are important enzymes that degrade the cyclic nucleotide product of AC. Both AC and PDE are highly active in all cardiac tissue (Arch and Newsholme 1976), so this system will have a high throughput and small modifications to this system would have substantial affects upon cellular cAMP levels. PDE inhibitors increase the cytosolic cAMP levels and therefore have similar affects to AC activators such as forskolin.

Calcium has a pivotal role in every myocyte, as the presence of calcium activates the myofibrils, initiates cross-bridge cycling and therefore contraction. Calcium also has a regulatory role. Calcium concentration in the sino-atrial node is thought to be higher than in other cardiac myocytes (Huser, Blatter et al. 2000), with basal concentrations being reported to be as high as 200 nM, reaching a peak of 800 nM during contraction (Verheijck 2000). Calcium itself binds to I_{CaL} causing inactivation (Xiao, Cheng et al. 1994), and to I_K (Tohse, Kameyama et al. 1987), I_f (Hagiwara and Irisawa 1989), ryanodine receptors (Lipp and Niggli 1994) and probably a variety of other channels. Importantly, calcium has also been found in neurones to regulate the turnover of AC and hence cAMP production (Luthi and McCormack 1999); this would be especially important in the sino-atrial node cell, which have such high cytosolic calcium levels.

Calcium can also bind to calmodulin, which is a ubiquitous regulatory molecule that is activated upon association with calcium. Calcium binding to calmodulin causes the complex to translocate to the membranes where the construct binds and modulates the function of various channels, including I_{CaL} (Wu, Schuessler et al. 2001), I_K (Nitta, Furukawa et al. 1994) and the SR calcium pump SERCA (Narayanan and Xu 1997).

To complicate the regulation further there is a kinase that is sensitive to the calcium-calmodulin complex. When calcium (which has regulatory actions) concentration is increased, it binds and activates calmodulin that can subsequently interact with various ion channels, and in addition calcium-calmodulin itself activates a kinase. In the heart, this calcium-calmodulin dependent kinase is generally of the second subtype discovered and therefore abbreviated to $CaMK_{II}$. $CaMK_{II}$ has been found to be vital in pacemaking and to regulate I_{CaL} (Vinogradova, Zhou et al. 2000), I_{Na} (Deschenes, Neyroud et al. 2002), I_{CaL} (Wu, Dzhura et al. 2001) and I_{NCX} (Isosaki, Minami et al. 1994).

A parallel pathway to the above regulation mechanisms, is that of PKC; it is activated by various compounds (phosphatidylserine and diacylglycerol), but the PKC_β isoform expressed in the heart is most importantly activated by calcium (Way, Chou et al. 2000). To achieve contraction, calcium levels are elevated, and there will be a corresponding increase in PKC phosphorylation. The timescale of PKC activation by calcium should be considered, as cellular calcium concentration varies according to autonomic stimulation, both in rate and calcium handling. The calcium dependent regulation, direct and indirect is complicated to investigate. For example,

PKC increases I_K in the presence of >100 nM calcium; although in the presence of full PKC inhibition, raising calcium still increased I_K, therefore indicating a direct calcium augmentation of I_K, in addition to a PKC mediated component (Tohse, Kameyama et al. 1987). PKC has also been found to regulate most sino-atrial node ionic currents, including I_{CaL} (Satoh 1994).

Sino-atrial node heterogeneity

There is some evidence of variability within the cells of the sino-atrial node, with cells from only the very centre of the area being true pacemaking cells and the peripheral population being progressively more transitional in morphology and function, as they are located nearer the surrounding atria.

According to this theory, the true pacemaking cells are very small (approximately 10 μm by 60 μm) containing very few (if any) visible striations. Some reports claim that the small spindle shaped cells are the primary pacemakers (Honjo, Boyett et al. 1996), whilst others find that it is the spider type morphology (Wu, Schuessler et al. 2001). However it is thought that the primary pacemaking cells have a smaller amplitude action potential, less SR and a lower density of most of the ionic currents involved in pacemaking, including I_{Kr}, I_{Ks}, I_f, I_{NCX}, I_{CaL} (reviewed by Boyett, Honjo et al 2000). Kodama, Nikmaram et al (1997) found that rabbit peripheral sino-atrial node cells expressed the fast sodium channel, which mediates the action potential upstroke in most other tissues, but the central cells did not. Mouse sino-atrial node cells have been found to express I_{Na} (Zhang, Holden et al.

2000) and there is some preliminary data that infers I_{Na} mutation effects normal rhythm development in humans (Benson, Wang et al. 2003). Most surprisingly these central node cells have also been found to have a slower intrinsic pacemaking rate, although transitional cells will be exposed to the hyperpolarizing load of the atria and will electronically shield the central primary pacemaker cells (Watanabe, Honjo et al. 1995). When all of these factors are taken into account the small central cells are still thought to be the primary pacemaker of the sino-atrial node.

Only some groups have found this sino-atrial node cell heterogeneity, but it should be considered that a pathophysiological atrial cell which is calcium overloaded may well display apparently spontaneous activity, as the SR spontaneously releases calcium from a store which is unbalanced. In a healthy sino-atrial node cell the action potential should always precede the major release of calcium from the SR. In a calcium-overloaded sino-atrial node cell, similar to an atrial myocyte, the spontaneous release of calcium from the SR would result in a large inward I_{NCX}, which could activate an action potential (Janiak and Lewartowski 1996). The separation of sino-atrial node cells from other myocytes is therefore paramount, and further separation of sino-atrial node cells into central and peripheral populations (if they exist) should be considered.

Autonomic regulation of the sino-atrial node

Although the heart is myogenic, it is modulated on a beat-by-beat interval by the autonomic nervous system. The resting heart rate is predominantly defined by the

amount of parasympathetic tone (via the vagal nerve), but during exercise the heart rate is raised by sympathetic nervous activity. The resting human heart rate is approximately 100 beats per minute (bpm) lower than it would be without parasympathetic stimulation and an athlete undertaking extreme exercise their resting beating rate can be quadrupled, mediated by strong sympathetic stimulation.

These modulations of heart rate are affected via cholinergic and adrenergic pathways, using acetylcholine and noradrenaline respectively as the neurotransmitter at the post-ganglionic neurone. Additionally ATP is released from sympathetic nerve termini, and the relevance of these should also be considered when studying autonomic regulation.

Sympathetic nerve stimulation is further sub-divided by the adrenergic receptor affinity for various catecholamines, creating α and β subtypes. β-adrenergic receptors are expressed to a much higher degree in the heart than the α subtype, and β_1-adrenoceptor (there are 3 classes) is by far the most prevalent in the sino-atrial node. β-adrenoceptors are coupled via a G-protein to AC, with adrenoceptor activation causing an elevation in cellular cAMP levels. In turn, cAMP modifies various ion channels either directly or indirectly; cAMP shifts $V_{1/2}$ of I_f to more depolarised potentials and it also activates PKA that can increase I_{CaL} (Sato, Ferguson et al. 1998), I_K (Lei, Brown et al. 2000) and possibly I_{NCX} (Perchenet, Hinde et al. 2000). There are other intracellular pathways that link β-adrenoceptor activation to various ion channels and other cellular proteins. For example, a direct G-protein modulation of I_K has been reported, in addition to the slower I_K modulation pathway that utilises cAMP and PKA (Xiong, Sperelakis et al. 1994; Xiong, Sperelakis et al.

1994). There maybe some expression of α-adrenoceptor (Tohse, Nakaya et al. 1992; Takei, Ikegaki et al. 1999) and β_2-adrenoceptor in the heart however only at very low levels (Walsh, Begenisich et al. 1989). No β_3-adrenoceptors have been found. β_1-adrenoceptor are the most important adrenergic receptors when considering cardiac sympathetic stimulation.

Sympathetic stimulation accelerates the beating rate of the heart. It does this by activating β-adrenoceptors, mediated by various pathways and modulating ionic currents involved in pacemaking. In general, stimulation increases the inward currents during diastolic depolarisation (e.g. I_f, I_{CaT}, I_{NCX}), but I_{CaL} and I_K are also increased. A functional SR has been found to be required in the β_1-adrenergic response by various groups (Hata, Sakamoto et al. 1998; Ju and Allen 1999). The SR does seem to play a vital role in sympathetic stimulation, as the beating rate seems to be directly related to the calcium load of the SR (Ju and Allen 1999). Such adrenergic stimulation causes phosphorylation of phospholamban and this leads to removal of inhibitory affect upon the SR calcium uptake pump SERCA, thus increasing SR calcium load (Pan, Hannon et al. 1999).

Regarding the parasympathetic modulation of the sino-atrial node, cholinergic neurones release acetylcholine at the post-ganglionic nerve terminal and acts on muscarinic receptors. So far 5 muscarinic sub-types have been pharmacologically described (reviewed by Dhein, van Koppen et al 2001). Muscarinic receptors are named according to their high affinity for a poisonous alkaloid found in some mushrooms, but they also readily bind the neurotansmitter acetylcholine. The most common cardiac sub-type is the M_2 muscarinic receptor. Cholinergic muscarinic

receptors are linked to multiple intracellular pathways, via G-proteins, including diacylglycerol/IP_3 production, and AC inhibition that is a well described M_2 pathway. M_2 activation resulting in AC inhibition explains the low concentration acetylcholine induced reduction in I_{CaL} and negative shift in I_f voltage dependency. Higher acetylcholine concentrations activate I_{KACh}, which dramatically slows the sino-atrial node beating rate.

Summary

Various inward currents, including I_f, I_{NCX} and I_{CaT} are activated during diastolic depolarisation and gradually overcome the diminishing outward I_{Ks} initially and subsequent I_{Kr} current, slowly causing the membrane potential to depolarise. When the voltage has reached the I_{CaL} threshold, this relatively large and fast current, mediates the upstroke of the sino-atrial node action potential, activating the I_K components that mediate repolarisation.

I_K is especially sensitive to intracellular regulation by pathways involving calcium, cAMP *and* protein kinase activity; however every other current in pacemaking can be altered by at least one of these pathways. Calcium handling appears to be important in defining the beating rate of these cells, especially the role of the SR.

Sympathetic stimulation of the sino-atrial node causes an alteration in the regulation pathways, increasing cytosolic cAMP and elevating SR calcium load. These affects, as well as their down stream affect upon protein kinases sensitive to

cAMP and calcium, result in an alteration in the amplitude of the ionic currents which facilitate diastolic depolarisation. Inward currents are augmented to a greater extent than outward currents, and hence diastolic depolarisation occurs more rapidly, which causes the heart rate to be raised.

The sino-atrial node region of the heart is small, but defines the rhythm of the heart and facilitates affective circulation of the body; the study of this region is therefore physiologically very important and modulators of function of this region have pharmacological applications.

Aims of thesis

- Determine the characteristics of I_{Kr} and I_{Ks} in of guinea pig sino-atrial node cells, using techniques that minimally disrupt cytosolic milieu.

- To evaluate the relative contribution of I_{Kr} and I_{Ks} in pacemaking of the guinea-pig sino-atrial node.

- To investigate the possible regulation of I_{Kr} and I_{Ks} by cytoplasmic calcium, both crossing the sarcolemma and released from the SR.

- To investigate the role of the SR in pacemaking.

- To study β-adrenergic stimulation, and describe the alterations of the roles of I_{Kr} and I_{Ks}.

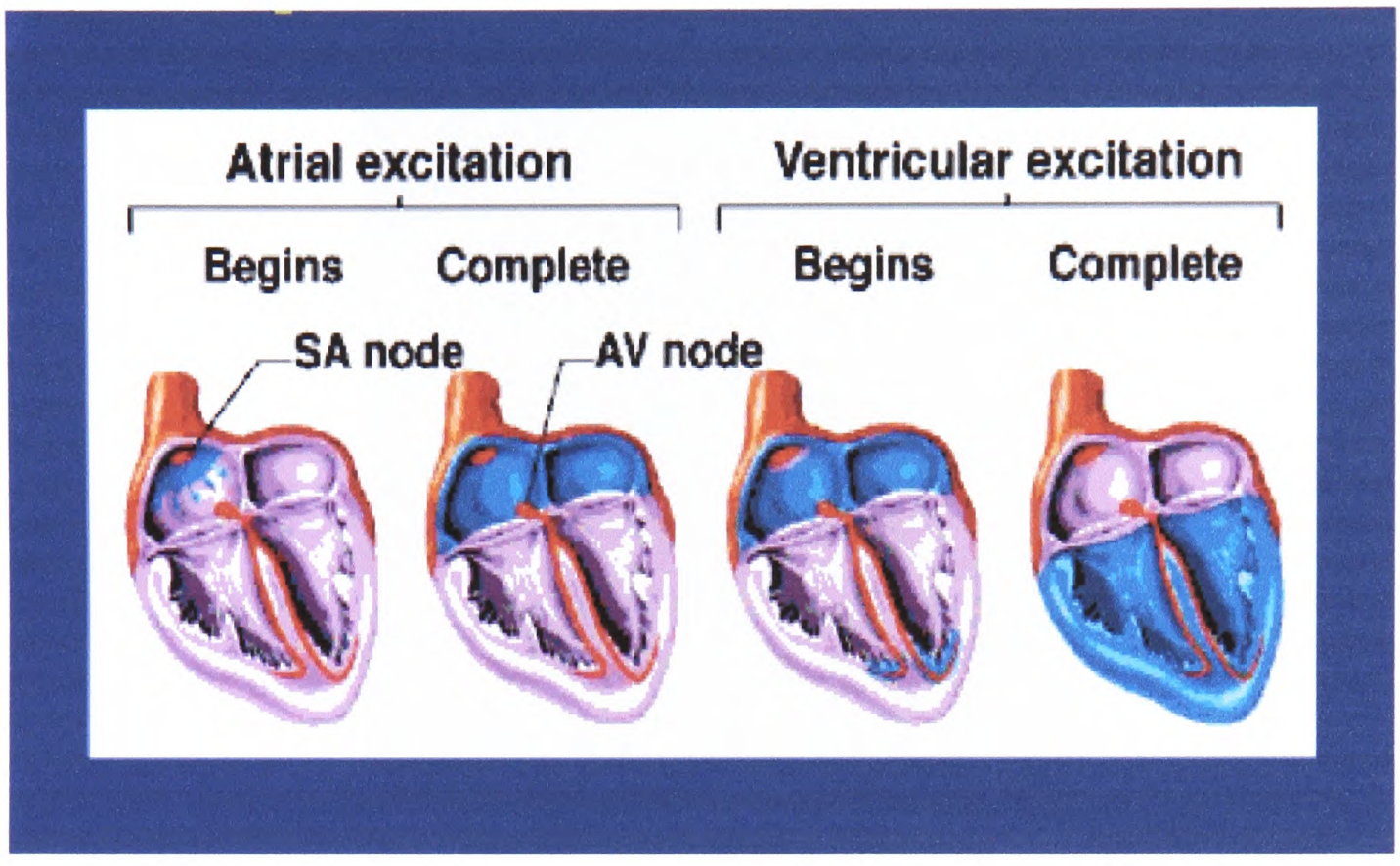

Figure 1.1 Page 48

Diagram of the conduction pathway involved in the transduction of the action potential to the rest of the heart (from Harvey's Biology notes). The sino-atrial node initiates the action potential; it is then propagated to the rest of the atria and then to the atrioventricular node, where a delay in conduction is introduced, before the action potential is propagated to the ventricles. This facilitates effective rhythmical pumping.

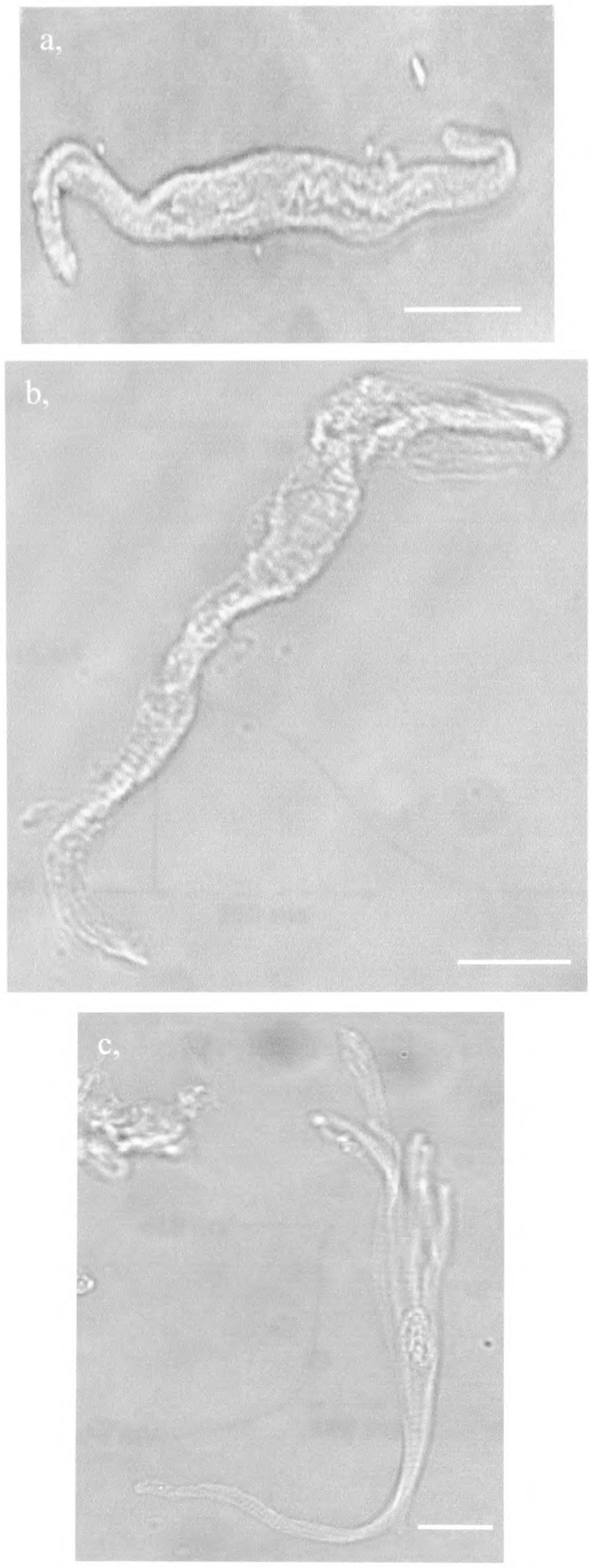

Figure 1.2

The three different sino-atrial node cell morphologies; spindle (a), elongated spindle (b) and spider (c). These sino-atrial node cells were isolated according to procedures described in the Methods section of this thesis. Bar measure 10 μm.

a,

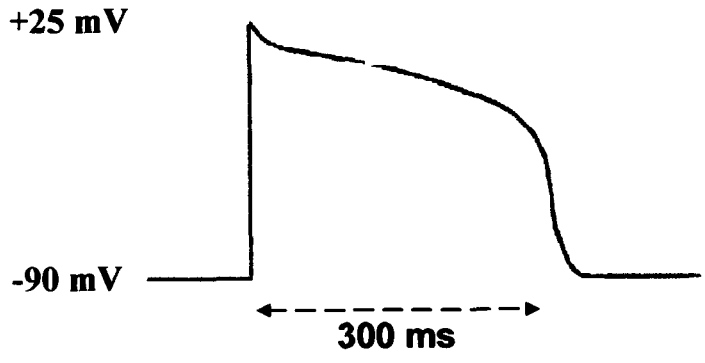

b,

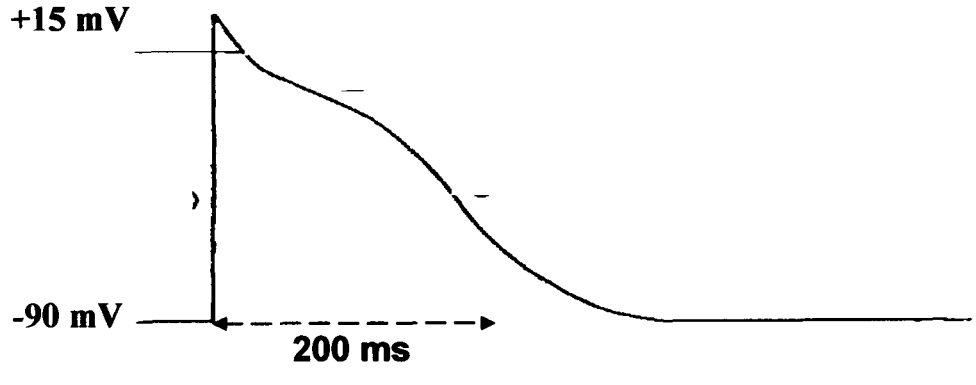

c,

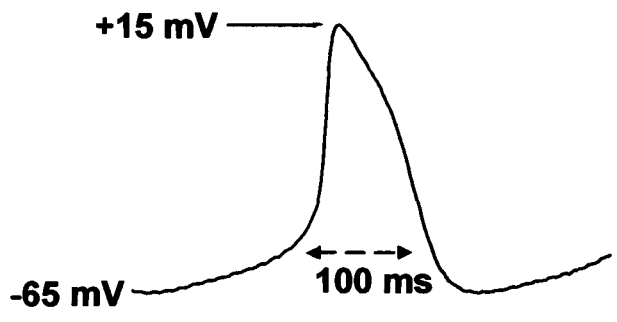

Figure 1.3 Page 50

Different action potential shapes of cardiac action potentials, from ventricular (a; Gintant, G. A. 1995; canine), atrial (b; Ogbaghebriel, A. and A. Shrier 1995; guinea-pig) and sino-atrial node cells (c; this study; guinea-pig). Note the different in time-scale and voltage amplitude, as well as the shapes.

CHAPTER 2: Methods

Male guinea-pigs (400-500 g body weight) were sacrificed in accordance with the Home Office Guidance On The Operation Of The Animals (Scientific Procedures) Act 1986 (H.M.S.O.): Schedule 1 killing by cervical dislocation subsequent to stunning.

Isolated atrial preparations

The protocol for the isolated atrial preparation is derived from Rigg and Terrar (1996). The heart was quickly excised, transferred into a chamber, continuously superfused with oxygenated, physiological saline solution (solution B; Methods, page 55) at room temperature. Any remaining ventricular tissue was cut away carefully, so that only the beating atria remained. Silk suture (Pearsalls Ltd, 5/0) loops were placed in the tips of each atria. The atrial preparation was then transferred to a water jacket pre-heated (37 ± 0.5 °C), oxygenated organ bath containing 50 ml solution B. The atria were vertically mounted, with the left atria attached to a stainless steel hook and the right atria being attached by the silk thread to a force transducer (HDE F30), amplified and the atrial preparation shortening illustrated on an oscilloscope (Gould, DRO). Beating rate was determined from the interval between contractions (using a trigger circuit to detect beats) and the signals displayed in real time. In addition to contraction measurements, electrical activity was recorded using a surface electrode, which was positioned in proximity to the inter-atrial septum. Hence atrial preparation contraction, electrical activity in proximity to the sino-atrial node and beating rate were simultaneously measured. Atrial preparations were allowed to stabilise for 60 minutes (or however long the beating rate took to become constant) before any experimental data were collected.

Isolated sino-atrial node cells

Sino-atrial node cells were isolated using a protocol derived from previously described techniques (Brown and Difrancesco 1980; Anumonwo, Freeman et al. 1992; Rigg, Heath et al. 2000). The heart was rapidly excised, placed in zero calcium solution (Methods, page 55) with 100 units of heparin, weighed and then cannulated at the aorta to allow retrograde perfusion by the Langendorff technique. The heart was initially perfused for 3 minutes with zero calcium solution. After 3 minutes the solution was substituted for one of similar composition, lacking EGTA but containing collagenase (Powell, Sturridge et al. 1981). The precise type/batch of collagenase used had a considerable effect upon the sino-atrial node cells isolated. Most batches did yield calcium tolerant, spontaneously active cells. The use of between 15 and 40 mg of the type 2 collagenase (332 units/mg activity) in 50 ml solution A (plus 10 µl of 0.1 M $CaCl_2$) facilitated the isolation of the best sino-atrial node cells. Collagenase was obtained from Worthington Biochemical Corporation, New Jersey, USA. The heart was perfused with collagenase containing solution for 12 minutes x the weight of the heart. Three 20 µl aliquots of 0.1 M $CaCl_2$ were added to the top reservoir at equally spaced intervals. Any heart larger than 3 g was superfused for a maximum of 36 minutes, with calcium aliquots being administered at 9, 18 and 27 minutes.

When this procedure was complete, the ventricular tissue was careful removed with a razor blade (figure 2.1a) and the atria were further dissected in solution A to isolate the sino-atrial node region. The sino-atrial node was identified as being located between anatomical markers defined in figure 2.1b. The exact size/location of the sino-atrial node varies considerably between preparations. The isolated sino-atrial node was cut into small strips (2 x 5 mm) perpendicular to the crista terminalis, to

avoid cutting against the cellular alignment, and transferred to a high potassium solution (KB, (Denyer and Brown 1990)). The solution containing the strips of sino-atrial node was then gently triturated with a fire polished Pasteur pipette with a tip diameter of approximately 2 mm. The cell suspension was kept at 4 °C for at least one hour before they were studied. Sino-atrial node cells were settled on a glass cover slip for 5 minutes (Menzel-Glaser, Germany) that formed the base of a small perspex chamber and were studied on an inverted microscope (Leica, DMIRB, Germany). After the sino-atrial node cells had been plating for an appropriate length of time, warmed, oxygenated solution B was superfused through the chamber.

Trituration separates single sino-atrial node cells; this procedure occurs in KB that helps the cells recover from enzymatic and physical assault during isolation. The yield and integrity of the sino-atrial node cells varied throughout this prolonged study. In some cases the variance appeared to be related to the type of collagenase used, however water quality and various other factors seem to drastically affect sino-atrial node cell isolation. In the KB storage solution there was normally a high yield of apparently healthy cells (70 % atrial, 30 % nodal), with some rounded and dead cells. Subsequent exposure to solution containing calcium reduced the number of viable sino-atrial node cells by approximately 50 %. Sino-atrial node cells were identified by spontaneous activity (contraction), in association with sino-atrial node cell morphology; cells that exhibited only one of these two characteristics were not used in this study. Sino-atrial node cells tend to be substantially smaller than other myocytes (Honjo, Boyett et al. 1996); a capacitance measurement (related to the surface area of the sarcolemma) was taken from each cell investigated and most figures in this thesis contain an average capacitance value (measured in pF) of the

cells studied. Previously Honjo, Boyett et al (1996) found an average capacitance of population of sino-atrial node cells to be 38 pF in rabbit sino-atrial node, which is comparably to the average capacitance of these guinea-pig sino-atrial node (38 pF).

Isolated ventricular myocytes

Ventricular myocytes were used in some experiments to allow comparison between cardiac cell types. Isolation of cardiac myocytes began in the 1970's with Gould and Powell (1972), using retrograde perfusion to non-round cells; this was further developed by Powell, Terrar et al (1980) to isolate electrically functional ventricular myocytes. The isolation procedure of ventricular and sino-atrial node myocytes is run concurrently. After the ventricular tissue is removed from the atria (see above, page 52), the ventricular tissue and 10 ml of collagenase containing solution was incubated in an agitator for 5 minutes. This suspension was then passed through a 250 μm mesh (R. Cadisch & Sons, London, UK) and split into 2 tubes of pre-warmed and gassed Dulbecco's MEM with 25 mM HEPES. A further 9 ml of collagenase solution was then added and the agitation/filtration procedure repeated 3 times, creating 8 (4 pairs) test tubes. Ventricular cells were allowed to settle for 15 minutes and the supernatent discarded; the pellets were resuspended in MEM/HEPES, then the pairs of test tubes combined and were allowed to sediment again. Again the supernatent was removed and myocyte pellets were resuspended in an appropriate volume of MEM/HEPES.

All chemicals used in both sino-atrial node and ventricular myocyte isolation procedures are required to be at least analaR grade or equivalent. All solutions were made using Purite de-ionised water that had been passed through a Purite Select

polishing unit (Purite Ltd, Thame, UK). The quality of the water and chemicals use appears to be of paramount importance in the isolation of sino-atrial node cells, probably due to their small number and extensive interactions.

Substance (mM)	*A*	*B*	*Zero calcium*	*KB*	*Patch*
NaCl	137	118.5	137		
KCl	5	4.2	5	70	150
$NaHCO_3$	12	14.5	12		
NaH_2PO_4	0.4	1.18	0.4		
$MgCl_2.6H_2O$	1		1		5
$MgSO_4.7H_2O$		1.18		5	
KH_2PO_4					
Glucose	5	11.1	5		
K_2ATP				5	1
K Glutamate				5	
Na Pyruvate	1		1		
Taurine				20	
Trisphosphocreatine				5	
Succinic acid					
HEPES				5	3
EGTA			0.1	0.04	
$CaCl_2$		2.5			
NaOH	1		1		
Gassed with 95%O_2/5%CO_2	Yes	Yes	Yes		
pH	7.4	7.4	7.4	7.2	7.2
pH with				KOH	KOH
Amphotericin B					240u/ml

Abbreviations: *A,* solution A, for making collagenase-containing solution and dissecting collagenase -treated sino-atrial node. *B,* solution B or physiological saline solution, used as the superfusing solution for all experiments. *Zero calcium* used initially in the isolation procedure to perfuse the cannulated heart. *KB,* high potassium

solution for dissociating and storing single sino-atrial node cells, kept at 4°C. *Patch*, patch electrode solution used for all perforated patch clamp experiments.

Superfusion

Myocytes were bathed in the chamber by a near physiological solution (solution B; Methods, page 55), the composition that is shown below. Solution B superfusion of the cells was gravity fed, maintaining a flow rate of ~7 ml/minute and the outflow was facilitated by a peristaltic pump (Hyflo, Medcalf Bros Ltd. England). Temperature was maintained at 36 ± 1 °C throughout the chamber, using a thermostatic heater located in proximity to the inflow port to administer drugs or change ionic environment, switching of solutions was required. Experimental recordings were taken from cells being perfused by solution B and then the same recordings were taken again after exposure to a drug diluted in solution B. To facilitate this switching of perfusing solutions, two mechanisms were used; bath exchange and rapid switch. Bath exchange has a delay of approximately 20 seconds, before the beginning of exchange of bathing solution, as a tap selector is located close to the solution reservoir and is manipulated to select an alternate reservoir containing drug solution. The solution heating procedure occurs close to the chamber and assuming equal flow rate (dependent upon reservoir height), the temperature of the superfusing solution, should be constant. The bath exchange method was generally used throughout the study, although a more rapid switch mechanism was used in some experiments. In certain experiments, solution switches were carried out using a local perfusion system (Warner Instrument Corporation) to allow rapid (< 0.5 second) application of alternate perfusing solution (containing drugs or solution of altered ionic composition). A triple-barrelled square glass capillary tube was positioned

close (< 100 μm) and slightly upstream of the experimental cell, such that the cell was bathed in solution (36 °C) flowing from only one barrel of the capillary tube. The central barrel of the triple-barrelled capillary tube was not used, so the local perfusions with different solutions are separated. Lateral movement of the glass capillary tube (driven by a stepper motor) achieved a rapid solution switch, such that the cell was then bathed with solution emerging from a different barrel of the triple-barrelled capillary tube. The flow of solution through the rapid switch system was driven by means of a syringe pump, which delivered a constant flow rate (100 μl/minute) through each barrel.

Electrophysiology

Sino-atrial node cells were studied using single electrode voltage-clamp and current-clamp, using Axopatch 200 amplifier (Axon Instruments, USA). The basic principle of the voltage clamp technique is the control of the membrane potential, facilitating the study changes in the flow of ions across the same membrane. Current (the flow of ions across a membrane) can be measured at a defined voltage, due the use of fast negative feedback amplifier, to introduce current into the cell that is proportional to the difference between the desired voltage and the actual voltage. Small amounts of current are continually applied until the membrane voltage equals the desired voltage. Membrane voltage is sensed and current passed back into the cell by the same electrode in single-electrode voltage clamp. Sino-atrial node cells were studied using the continuous voltage clamp technique, in which membrane potential is detected at the same time as current is passed. Continuous voltage clamp has a some draw backs due to the concurrent voltage detection and current passing, the most problematic of these are the capacitors and resistors in the biological system resulting

in disparity between command and membrane voltage (figure 2.2). The same factors reduced the temporal resolution of the voltage step, creating a more gradual membrane voltage alteration. Both voltage and temporal errors were partially ameliorated by compensation for electrode capacitance, series resistance and whole cell parameters, using prediction and correction functions of Axoclamp 200 (both > 40 %) to further increase precision of the voltage step. For example, 40 % compensation of a cell with 20 MΩ access resistance (ideal for amphotericin perforated patch) with a 200 pA current (typical I_K current after depolarisation to +40 mV), would develop a voltage error of 2.4 mV. Higher access resistance and larger currents would exacerbate this imprecision.

Current clamp is similar to the inverse of voltage clamp, in that one alters the current and measures the voltage. In all of the experiments in this study, no current was passed in current clamp and therefore voltage fluctuation was intrinsic to the cell.

The system requires two Ag/AgCl electrodes. At the Ag/AgCl electrode exchange of electrons for Cl^- ions and is fully reversible, so both inward and outward currents can be recorded. One electrode is situated in the centre of the microelectrode, consisting of a thin length of Ag wire, which is connected to the headstage recording circuitry. The Ag wire is regularly chlorided via electrolysis in 0.1 M HCl. The other electrode is a bath Ag/AgCl pellet reference electrode. The two electrodes are exposed to different Cl- environments, and cause a voltage offset, has been compensated for.

Borosilicate glass (1.0 mm E.D.) microelectrodes were created using a two-step, Narishige (Tokyo, Japan) vertical electrode puller. The resistance of these electrodes was between 3 to 5 MΩ when filled with internal patch solution.

Perforated patch clamp

(Kyrozis and Reichling 1995) used perforated patch clamp techniques to precisely measure neuronal activity, and it can be applied to measure both voltage and current from isolated sino-atrial node cells. This study has used amphotericin B (although various antibiotics such as nystatin have a similar pore-forming ability), that creates 0.8 nm diameter perforations in the cellular membrane that it is exposed to. The microscopic size of these punctures means that large molecules, and even divalent ions (such as calcium), are unable to diffuse through them. The perforations however allow the measurement of the electronic environment inside the cell being investigated, without disrupting the distribution of large molecules and divalent ions. The gradual "run-down" of certain ion channels measured in ruptured patch clamp, such as I_{CaL} (Kurachi, Asano et al. 1989), was thought to be related to the dialysis of the cellular cytosol with the solution inside the patch pipette. Not only do elements leak out of the cell and into the patch pipette solution, but also any buffers in the patch pipette solution can leak into the cytosol and alter physiological function. Perforated patch has the advantage of higher shunt resistance (better than internal microelectrodes), without the significant alteration of cytoplasmic constituents that would occur using the conventional patch method. Amphotericin was freshly prepared each day; a stock of 2 mg amphotericin in 100 µl DMSO was prepared and 12.5 µl were added to 1 ml of patch solution. The final amphotericin concentration was 240 µg/ml. Once seal formation had occurred between the microelectrode and

the cellular membrane, adequate perforation took between 5 and 15 minutes. Perforated patch clamp measurements were recorded only when the access resistance was stable; if control measurements were recorded at a different access resistance to the drug-treated measurements, these data were disregarded.

Current and voltage measurement

The pClamp 6 software was used to measure both current and voltages. The current signal was filtered at 1.25 kHz with a low pass single pole RC filter in Clampex (digitisation/sampling rate 0.4 ms), whereas voltages were not filtered except in off-line analysis. Currents were analysed in Clampfit and expressed as a percentage of the maximum control current. The currents were normalised in such a manner to reduce the variability between cells and to allow comparison.

Action potentials were analysed using software design in this laboratory (Dr Rakovic); maxima and minima were fitted to each action potential in 2 second sections, various parameters were measured and an average of at least 6 action potentials were taken.

Curve fitting

Curves were fitted to the activation/deactivation of various currents in this study; activation and deactivation of I_K, voltage dependent activation of I_K and its components, time-dependent activation of I_K and I_{Kr}, activation and voltage dependent activation of I_f. The most common fit to these relationships was the sigmoidal curve (voltage dependent activation of I_K and I_f), which was fitted with the Boltzmann equation.

$$y = 1 / \{1+\exp[(V_{1/2}-V_{max})/\text{Slope factor}]\}$$

Exponential curves were used to fit the activation/deactivation of I_K, using 1st and 2nd order exponentials respectively. Deactivation was measured over 8 seconds at various voltages. Box Lucas curves were also fitted to the time-dependent activation of the E4031 sensitive curve.

1st order exponential decay function

$$y = V_{min} + Amp_1 . e^{-(x - x_o) / Tau_1}$$

2nd order exponential decay function

$$y = V_{min} + Amp_1 . e^{-(x - x_o) / Tau_1} + Amp_2 . e^{-(x - x_o) / Tau_2}$$

Box Lucas curve function

$$y = V_{min} + a . (1- e^{-bx})$$

Tau_1 and/or Tau_2 define the rate of decay in this function, Tau_1 is the rapid time-constants and Tau_2 can be a secondary, slower phase of decay. In the BoxLucas function the value of 'b', which quantifies the activation constant, whereas 'a' is the value associated with the maximal value.

I_K decay has been measured in this study and these data were used to create a model. This model is recognised to be very basic, with some of the assumptions being incorrect and therefore the power of this model is limited. This model does however demonstrate the decay of I_K (and cellular calcium levels would be similar) is effected by rate. An increased beating rate means there is less time for I_K tail current to decay before subsequent I_K activation. This model of I_K decay has the following assumptions;

1. The full amount of I_K is available for activation in each action potential (no inactivation or deactivation)
2. I_K activated in the 2nd action potential is additive to I_K decaying from activating in 1st action potential.
3. I_K decay kinetics are not effected by the variation of voltage in subsequent action potentials.
4. I_K characteristics are not altered by a change in beating rate

Conductance values were calculated from measured currents, taking into account the driving force for the movement of the ions across the membrane.

Conductance = current / (step voltage - reversal potential)

Conductance is measured in Siemens (S), current in Amperes (A) and voltage/potentials in Voltage (V).

Drugs

Summary of information regarding drugs used in thesis. Storage refers to storage of the final stock solution. DMSO refers to dimethyl sulphoxide.

Compound	**Supplier**	**Solubility [stock]**	**Storage**
BAPTA-AM	Molecular Probes	DMSO 1 mM	-20 °
CPA	Sigma	DMSO 10 mM	-20 °
Isoprenaline	Sigma	Water 1 mM	fresh
Ryanodine	Calbiochem	Water 2 mM	4 °
E4031	Calbiochem	Water 50 mM	-20 °
Linopirdine	Sigma	DMSO 10 mM	4 °
DmBAPTA-AM	Molecular probes	DMSO 10 mM	4 °
Nifedipine	Sigma	DMSO 5 mM	4 °
Forskolin	Sigma	Water 10 mM	4 °
MDL-12,330A	Calbiochem	Water 10 mM	4 °
SQ 22536	Calbiochem	DMSO 25 mM	4 °
8 Bromo cAMP	Sigma	Water 25 mM	4 °
Dibutryl cAMP	Sigma	Water 25 mM	4 °
Sp-cAMP-AM	Calbiochem	Water 10 mM	-20 °
Staurosporine	Sigma	Methanol 3 mM	4 °
K252a	Calbiochem	DMSO 1 mM	-20 °
KT5720	Calbiochem	DMSO 10 mM	-20 °
Bisindolylmaleimide	Sigma	DMSO 2 mM	4 °
Ro-31-8220	Roche	DMSO 10 mM	-20 °
KN-92	Calbiochem	DMSO 1 mM	4 °
KN-93	Calbiochem	DMSO 1 mM	4 °
Calmidazolium	Calbiochem	DMSO 25 mM	4 °
W7	Sigma	Methanol 10 mM	-20 °
Acetylcholine	Sigma	DMSO 5 mM	-20 °
ZD-7288	Tocris	Water 10 mM	4 °
Thiopentone	Sigma	Ethanol N/A	20 °

General immunohistochemistry protocol

Sino-atrial node cells were isolated using the technique described above and were plated onto glass coverslips (22 mm x 22 mm, Menzel-Glaser, Germany) and left to settle for at least 15 minutes. Some immunohistochemical studies of ventricular cells were also undertaken, primarily for comparison. In order to improve cell adhesion the coverslips were passed several times through a Bunsen flame and allowed to cool before the cells were plated. To fix the cells, the coverslips were transferred into 4 % paraformaldehyde (PFA) in phosphate buffered saline solution (PBS) for 15 minutes, and then were moved into clean PBS 3 times, after a 15 minute initial PBS wash. All antibodies used in this study have epitopes on the interior of the cell; therefore membrane integrity has to be disrupted to facilitate entry of the antibody to locate the specific peptide targeted. In most cases permeabilisation was undertaken by placing each coverslip into a 1 % Triton-X 100 detergent solution for 30 minutes. An alternate freeze-thaw permeabilisation procedure was used in some experiments. This involved dipping a plastic beaker containing approximately 250 mls of iso-pentane into liquid nitrogen for 15 minutes, whilst covering the microscope slide (with cells adhered to) with cryoprotectant (25 g sucrose, 10 ml glycerol, 25 ml 0.2 M PBS, pH 7.4, made up to 100 mls with distilled water). The cyroprotectant was then drained off slide and the iso-pentant was removed from the liquid nitrogen. The slide was dipped into the iso-pentane for 10 seconds and then transferred to liquid nitrogen until the solution stops 'boiling'. The slide was then rapidly submerged in a Coplin jar containing PBS. When the slide had returned to room temperature and any frozen cryoprotectant was dissolved, the slide was washed thoroughly in PBS. This procedure required the use of thicker microscope slides (1 mm thick, Blue Star, England) to avoid cracking of the glass induced by the low temperature. Cells were

thoroughly washed in PBS before incubation in various dilutions (titres) of primary antibody. The duration of primary antibody incubation varied between antibodies, being either between 1 hour at room temperature, or overnight at 4 °C. The coverslips were washed 3 times in PBS for 15 minutes each and then incubated in secondary antibody. The secondary fluorescent-labelled antibody was raised in a different animal to the primary, and therefore recognises it as foreign and binds to it (figure 2.3); for example, most of the primary antibodies used were raised in rabbit, and were used in association with goat anti-rabbit IgG conjugated to fluorescein isothiocyanate (ITC). Multiple fluorescent secondary antibodies become localised to the target of the primary antibody. Secondary antibodies have been used at 1:40 and 1:100, as suggested by suppliers (Sigma Aldrich, Molecular probes). The secondary antibody was incubated for 1 hour at room temperature, in the dark to protect the fluorescence from bleaching. Coverslips were again thoroughly washed in PBS and mounted onto microscope slides with a small amount of Vectashield® mounting medium (Vector laboratories), which delays photobleaching using an anti-fade substance. Coverslips were sealed onto slides using clear nail varnish and viewed within 2 days. Controls slides were created with each immunohistochemical run; in these the same protocol was undertaken, but either the primary, or the secondary, antibody was omitted.

Antibodies and probes used in this study

Antibody/Probe	**Target**	**Description**	**Supplier**	**Catalogue #**
Anti-Kir2.1	I_{K1}	Rabbit polyclonal	Alomone	APC-026
Anti-HERG	I_{Kr}	Rabbit polyclonal	Alomone	APC-016
Anti-$KCNQ_1$	I_{Ks}	Goat polyclonal	Santa-Cruz biotechnology	Sc-10646

Anti-phospholamban	Phospholamban	Mouse monoclonal	Upstate technology	05-205
Anti-$P2X_2$	$P2X_2$ receptor	Rabbit polyclonal	Alomone	APR-003
Phalloidin	Actin	*Amanita Phalloides*	Molecular probes	P-3457
ER tracker	SR	Dapoxyl dye	Molecular probes	E-12353

The above commercial primary antibodies/probes were used in this study of the sino-atrial node. Subsequent immunolocalisation of antibodies was undertaken using fluorescently tagged secondary antibodies. The fluorescent tags used were Fluorescein isothiocyanate (ITC, Sigma), Texas Red ITC (Vector laboratories) and Alexa fluor (Molecular Probes). These fluorescent labels were conjugated to antibodies raised in various species, against foreign molecules (including other antibodies) from the species in which the primary antibody was raised (figure 2.3). For example, the anti-Kir2.1 was raised in rabbit, so a suitable fluorescent secondary antibody would be raised in goat (goat anti-rabbit) by injection of rabbit cells.

Fluorescent probes

Phalloidin and an ER tracker were used to describe actin and SR distribution in ventricular and sino-atrial node cells. Phalloidin was incubated with the cardiac myocytes (in KB/MEM) for 60 minutes at a 1:20 dilution. The ER tracker was incubated with the cardiac myocytes (in KB/MEM) for 30 or 60 minutes at concentrations between 100 nM and 1 μM. The myocytes were then plated as described for electrophysiology (Methods, page 57). These probes themselves emit fluorescence when excited appropriately, which was at 374 nM for the ER tracker (emission 430-640 nM) and so required an UV lamp.

Raising an antibody against $KvLQT_1$

When the initial immunohistochemical studies were undertaken, there was no antibody against I_{Ks} available. Therefore an antibody was raised against a peptide (a short amino-acid sequence) in the $KvLQT_1$ sequence, the channel protein which mediates I_{Ks}. The amino-acid sequence of $KvLQT_1$ has been defined in the Norway rat (Schreiber et al, unpublished) and house mouse (Barhanin, Lesage et al. 1996), being 669 and 604 amino-acids in length respectively (figure 2.4a). In addition an UK HGMP centre search revealed a number of groups had defined Homo sapiens $KvLQT_1$ (Sanguinetti, Curran et al. 1996; Wang, Curran et al. 1996). In Homo sapiens this gene for the voltage gated potassium channel $KvLQT_1$ maps to 11p15.5 (HGMP). The peptide sequence of the Norway rat was used to identify possible antigenic site in the sequence, which were not in inaccessible locations in the transmembrane regions. There were various peptide sequences that could have been targeted, but 15 amino-acids at the carboxyl terminus of the peptide were chosen (figure 2.4);

654 669

...YEQLTVPQTGPDEGS - COOH

There was full amino-acid homology within this region in rat and mouse, with only a 2 amino-acid variation with the Homo sapiens sequence. The carboxy terminus is known to be in the cytosol (figure 2.4a), so this would provide a better target than an amino-acid sequence that is antigenic, but maybe enclosed in a transmembrane domain.

Peptide synthesis and conjugation and antibody production

The 15mer peptide (1620.7 molecular weight) was synthesised commercially by Sigma Genosys (Cambridge), HPLC purified to 80 % and 20 mg was conjugated

to BSA. Mass spectral analysis and HPLC were undertaken by Sigma Genosys for the peptide, and the BSA conjugated peptide, to verify the purity of the peptide.

The use of rabbit in the production of antibodies is highly regulated due to animal welfare concerns, the Terrar Laboratory/Department of Pharmacology do not have the appropriate home office project/site license for this procedure to be undertaken. Therefore Oxford University Veterinary Services (Jane Watson) were contacted and agreed to immunise animals and harvest blood. Two rabbits were immunised with the peptide, to produce the antibody following standard protocol (figure 2.5):

Day 0- Pre-bleed rabbits, taking between 5-10 mls. Shave animals back.

Day 1- 0.5 ml of antigen is mixed with 0.5 ml Complete Freunds Adjuvant.

Day 14- An emulsion is made of Freunds Incomplete adjuvant as day one and injected sub-cutaneously at fresh sites as day 1.

Day 21- Collect blood sample for assay to determine antibody level. Repeat as required.

(*Harvest*- Animals were anaesthetised and exsanguinated by cardiac puncture)

This protocol was repeated 3 times, before an appropriate antibody titre was attained, as identified by the use of ELISA. The blood of both rabbits was then harvested and frozen. The sample was subsequently thawed and centrifuged at 2000 rpm for 30 and left in 10 ml vials overnight, to separate off the serum from the erythrocytes (and other cellular matter) which should pellet in the bottom of the container. Unfortunately, the serum should have been separated from the blood cells before the sample was frozen. Upon thawing, there was a large degree of haemolysis.

The procedure was continued and the serum, (probably with some cellular components) was separated.

Antibody purification

To try to ameliorate the haemolysis, the sample was further separated using an ammonium phosphate cut. A precipitate was developed by introduction 0.4 and 1.6 M ammonium sulphate, after pH adjustment (with glycine sulphate) and centrifugation at 11,600 rpm for 30 minutes at both cuts, but this pellet was discarded and the supernatant was retained. A final 2.4 M ammonium sulphate cut was carried out and the pellet was resuspended in 7 ml of 0.2 M sodium thiosulfate and 1 mM sodium acetate (pH 4.5). The suspension was then dialysed with 3 mM disodium thiosulfate.

A column was then prepared using AminoLink® Plus Coupling Gel (Pierce biotechnology, Rockford, USA) to immobilize the protein antibody. The peptide antigen was covalently linked to the column using cyanoborohydride, non-specific binding sites blocked and a top porous disk was place on the gel bed (Pierce biotechnology, Procedure for Immobilising a Protein, sections C, H and E). The binding of the peptide to the column was measured in a non-quantitative manner, using the Bicinchronic acid protocol, by the relative absorbance at 562 nm: the binding efficiency was 53 %.

The rabbit serum containing antibodies against the peptide was run through the affinity column incubated for 1 hour/0.5 ml and then drained. When all the serum had been incubated in the gel, the gel was washed and then treated with an elution buffer, neutralised and protein content was monitored by absorbance at 280 nm.

Confocal microscopy

For imaging, a Leica TCS NT confocal scanning head was coupled to a DMIRB microscope with a 63x magnification, water immersion objective lens (1.2 NA, Leica). Illumination was provided by a 488 nm Ar laser, and a 515 nm long pass filter was used in the collection of emitted fluorescence (figure 2.6). Emissions were detected at 515 nm (Fluorescein ITC), 568 nm (Texas Red ITC) and 594 nm (Alexa fluor). The ER tracker was excited with an ultraviolet lamp at 374 nm, the peak emission spectra was dependent upon environment but ranged between 430-640 nm (visualised with a DAPI or UV longpass filter).

Analysis of confocal images

Confocal laser-scanning microscopy was used to visualise the distribution of various cellular structures, and quantification of intensity and distribution was carried out to draw conclusions from these results. Two analysis packages were utilised (Leica TCS NT and Scion Image), both of which describe the presence of non-black pixels in a user-defined area. In this manner the distribution of fluorescence across a region including areas of interest can be quantified.

Statistical Analysis

Results are presented as means ± standard error of the mean, and statistical comparisons were primarily made using the paired Students's *t* test, but in some stated cases the unpaired Students's *t* test was used. All data was described by parametric (normal) distribution. Statistical significance was assumed for P values less than 0.05. In some figures the standard error bars are smaller than the data symbols.

a,

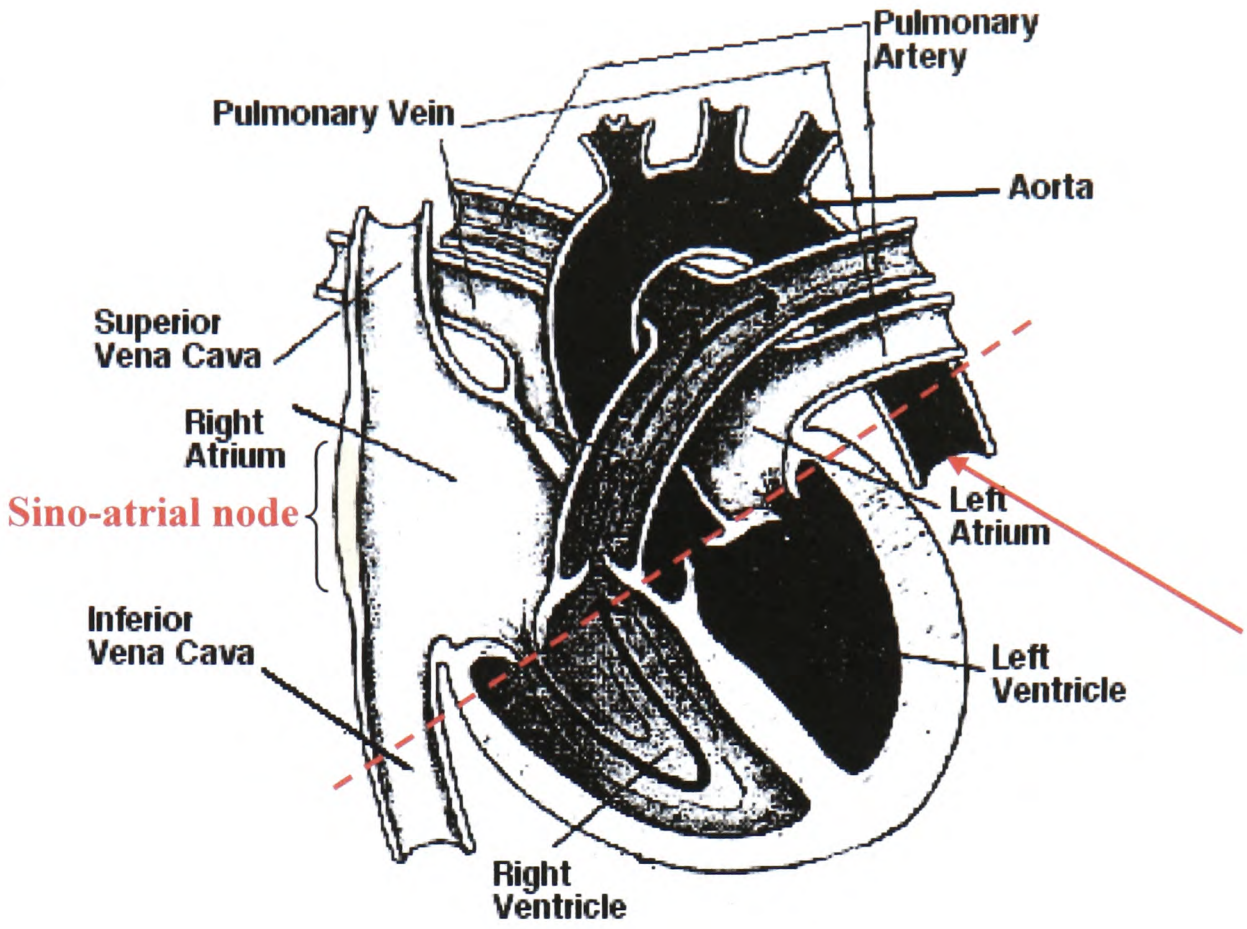

b,

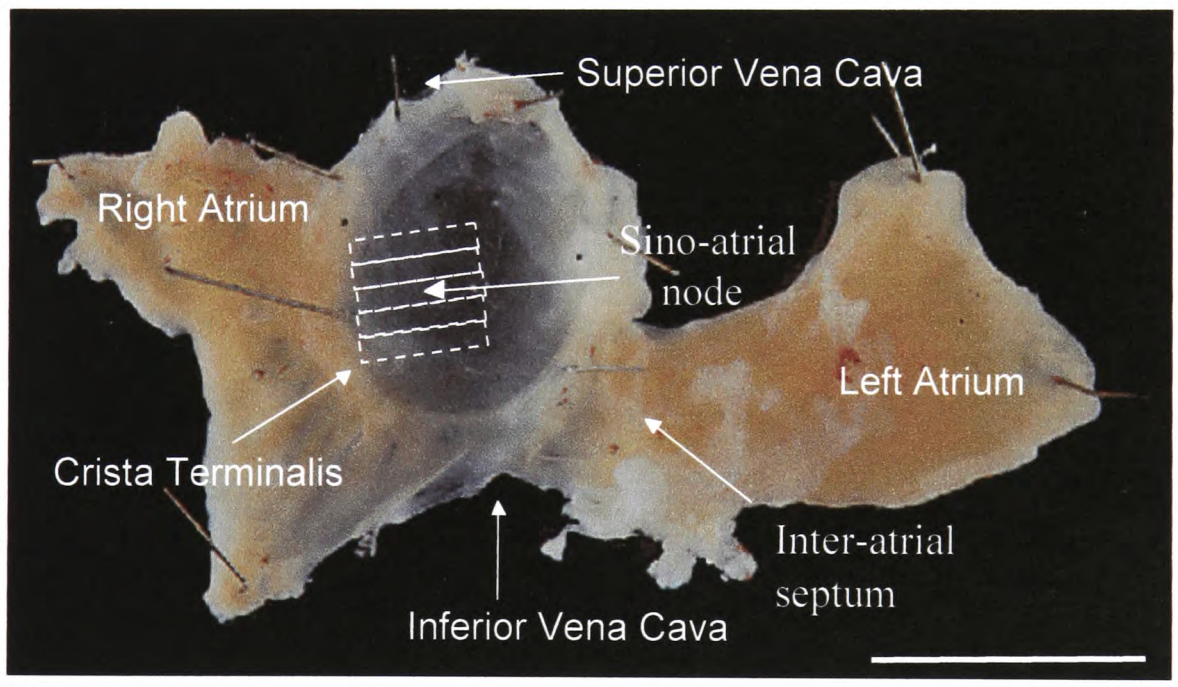

Figure 2.1 Page 71

Schematic of the heart (a, from Harveys's Biological Notes). Retrograde Llangendorf perfusion is accomplished by cannulating the aorta (in the manner indicated by the arrow) and after enzymatic digestion, the heart is bisected along the dotted line (a). Note the location of the superior and inferior venae cavae in the right atrium. The nodal is located on the upper surface in-between the venae cavae. The photograph (kindly provided by Dr L Rigg; b) shows the atria and sino-atrial node region after separation from the ventricular tissue. Morphological structures can be seen, with the sino-atrial node region being clearly visible as a more translucent area. Bar (bottom right hand side) measures approximately 10 mm. Dotted lines represent region dissected.

a,

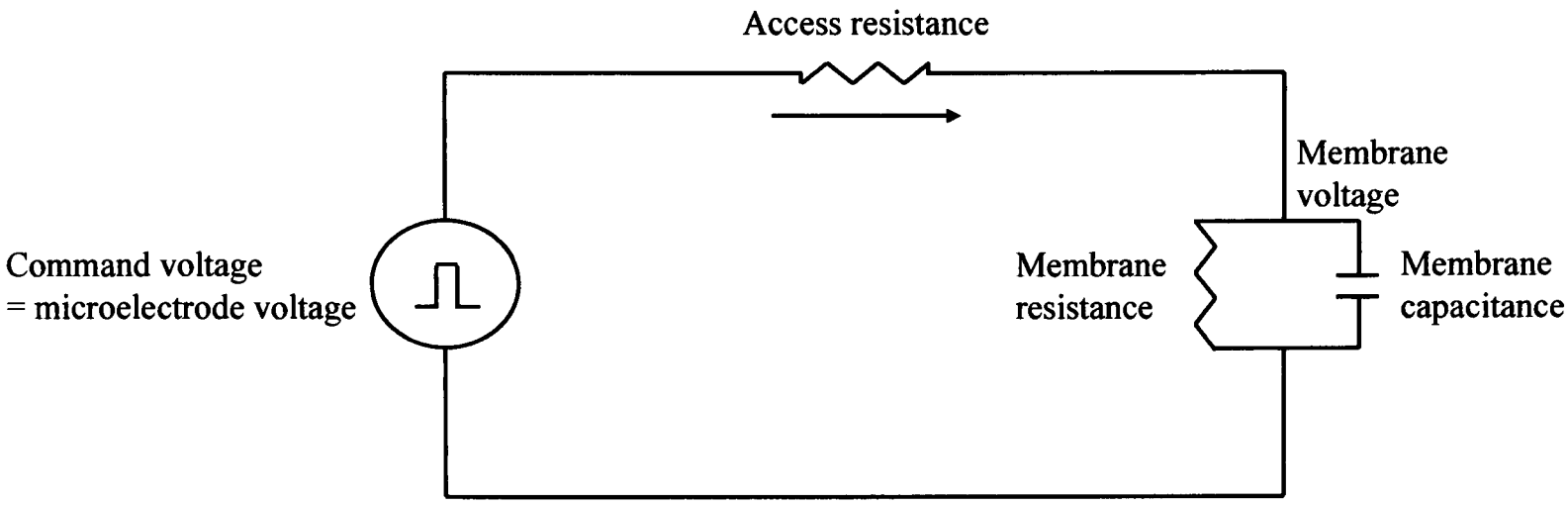

b,

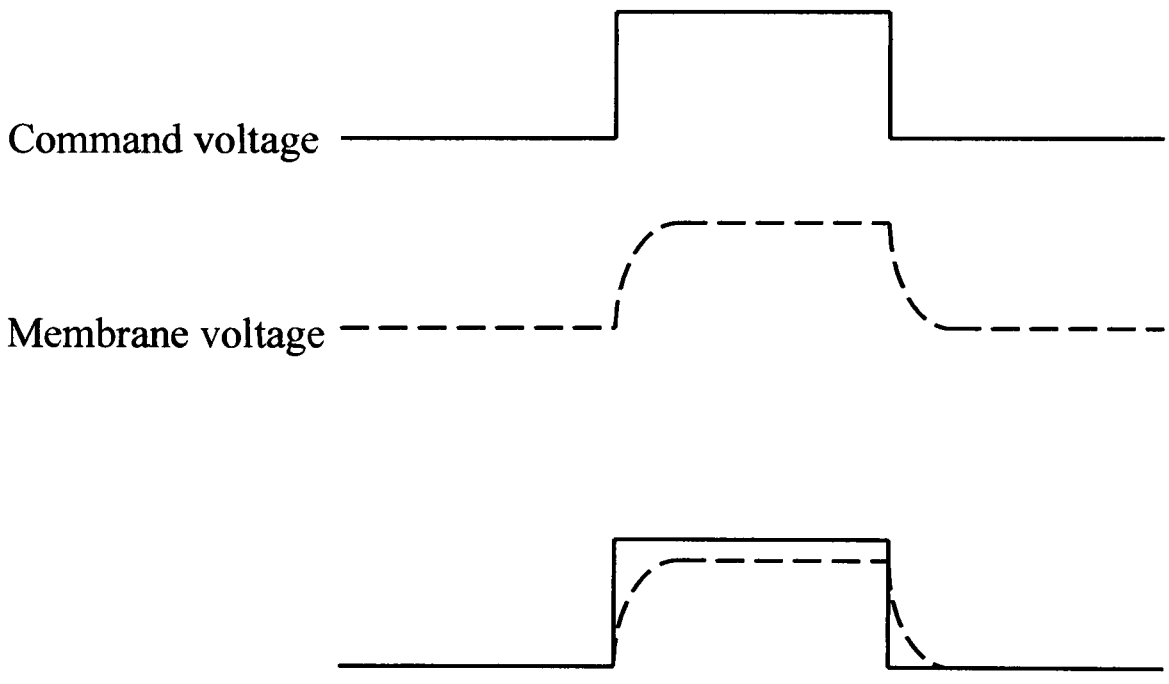

Figure 2.2 Page 72

Block diagram of the voltage clamp circuitry (a). The command and microelectrode voltage are maintained as close to equal as possible with a rapid feedback amplifier, but the cell membrane voltage is effected by the access and membrane resistance and the membrane capacitance. A cell is represented by a resistor and a capacitor in parallel. If command voltage is a square wave, both the amplitude and temporal definition will be compromised due to the capacitors and resistors in the system (b). This will result in stepping to a slightly less extreme voltage and the step occurring in a exponential manner, rather than square wave (lower panel); these errors can be partially compensated for using Axopatch 200.

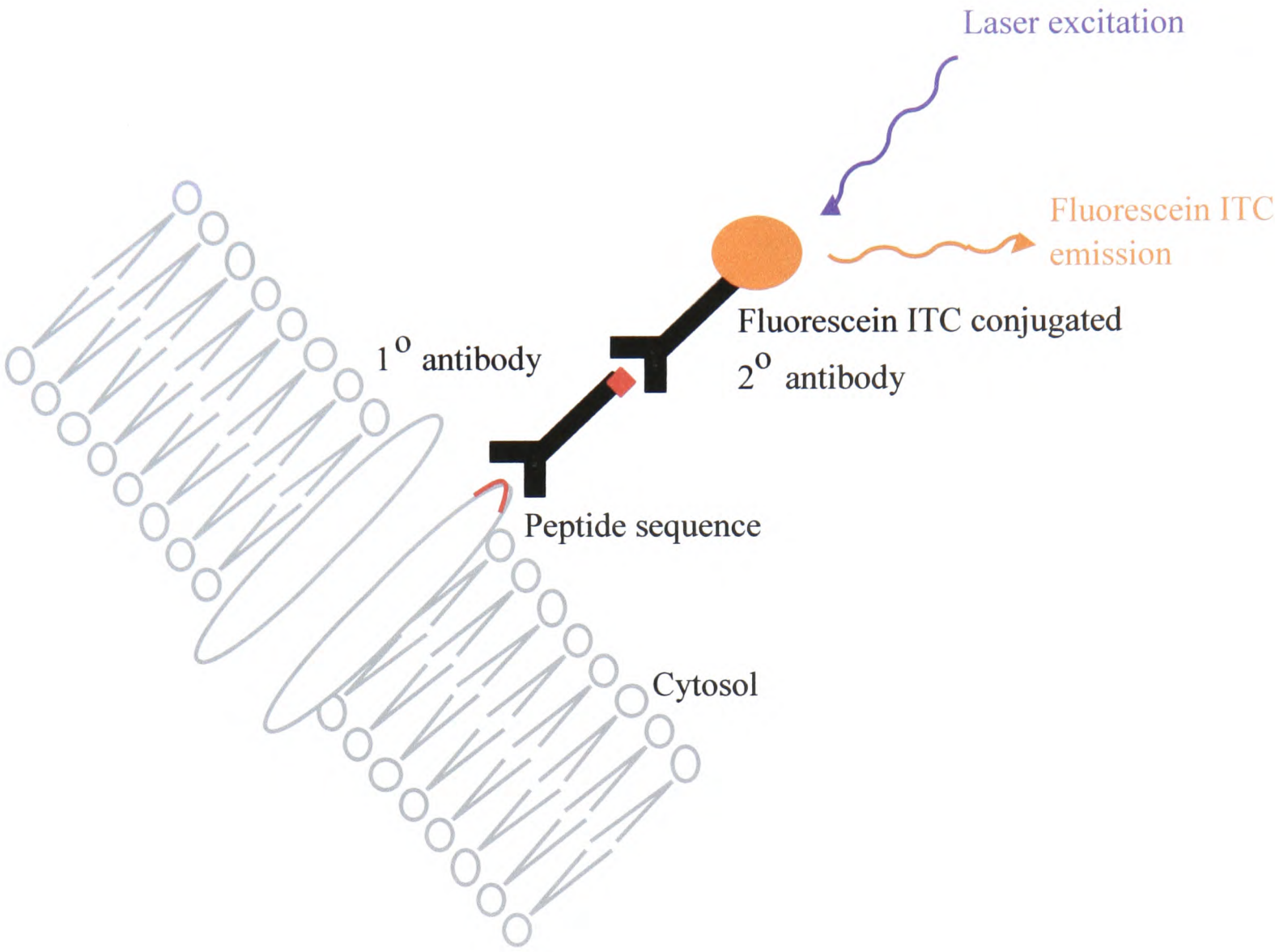

Figure 2.3 Page 73

Scheme of immunohistochemistry theory. The peptide sequence in the channel (located on the cytosolis of the sarcolemma) was recognised by the primary antibody, which is in turn recognised by secondary antibody which is conjugated to FITC, which emits fluorescence upon laser excitation. 1° and 2° are abbreviations of primary and secondary [antibodies].

a,

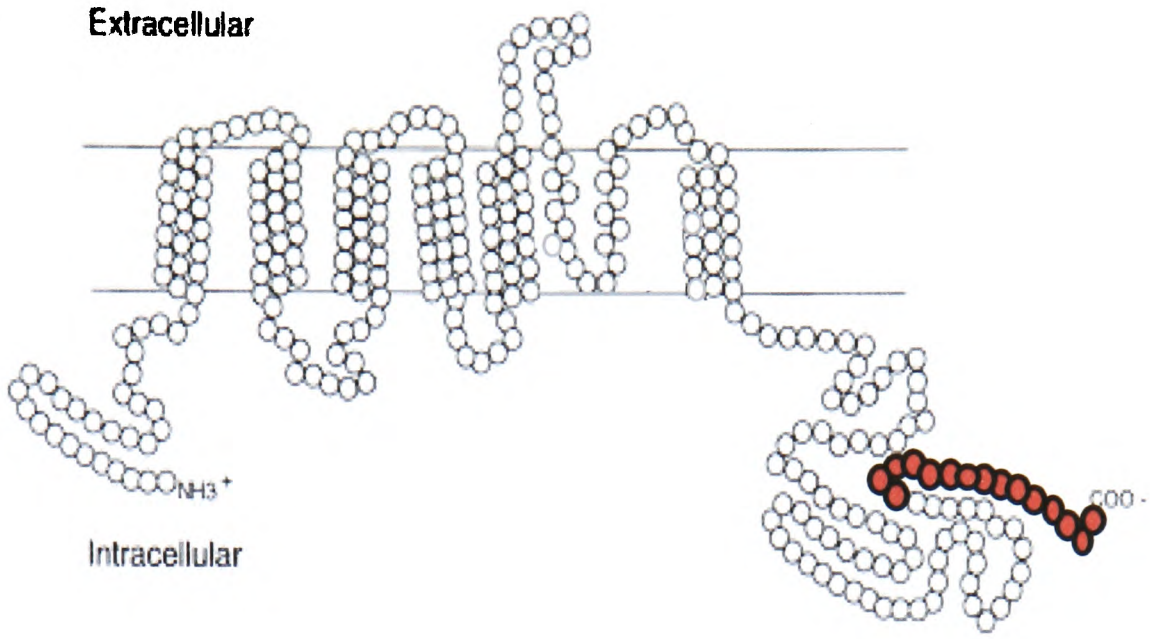

b,

ORIGIN

1 mstpvspapa padlgprprv sldprvsiys arrpllarth iqgrvynfle rptgwkcfvy
61 hftvflivlv clifsvlsti eqyaalatgt lfwmeivlvv ffgteyvvrl wsagcrskyv
121 giwgrlrfar kpisiidliv vvasmvvlcv gskgqvfats airgirflqi lrmlhvdrqg
181 gtwrllgsvv fihrqelitt lyigflglif ssyfvylaek davnesgrie fgsyadalww
241 gvvtvttigy gdkvpqtwvg ktiascfsvf aisffalpag ilgsgfalkv qqkqrqkhfn
301 rqipaaasli qtawrcyaae npdsatwkiy vrkparshtl lspspkpkks vmvkkkkfkl
361 dkdngmspge kmfnvphity dppedrrpdh fsidgydssv rksptllels tphflrtnsf
421 aedldleget lltpithvsq lrdhhratik virrmqyfva kkkfqqarkp ydvrdvieqy
481 sqghlnlmvr ikelqrrldq sigkpslfip isekskdrgs ntigarlnrv edkvtqldqr
541 lviitdmlhq llsmqqggpt cnsrsqvvas neggsinpel flpsnslpty eqltvpqtgp
601 degs

A-Ala	C-Cys	D-Asp	E-Glu	F-Phe
G-Gly	H-His	I-Ile	K-Lys	L-Leu

Figure 2.4

$KvLQT_1$ mouse peptide sequence and amino-acids chosen for targeting of antibody. Predicted protein structure and location (a) and amino-acid sequence (b) of the mouse $KvLQT_1$ potassium channel. The cytosolic location (a) of the 15 amino-acid region which is to be investigated is highlighted in red, as have the precise amino-acids in the peptide (b). The full amino-acid sequence is shown (604 amino-acids) and inset describes amino-acid code (b). Illustration modified from Lei et al 1997.

RAISING ANTIBODIES IN ANIMALS

Antibodies can be made in the laboratory by injecting an animal al (usually a mouse, rabbit, sheep, or goat) with antigen A.

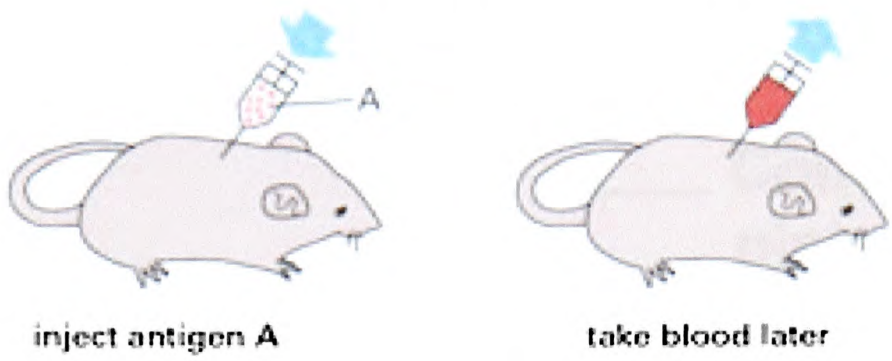

Repeated injections of the same antigen at intervals of several weeks ks stimulates specific B cells to secrete large amounts of anti-A antibodies into the bloodstream.

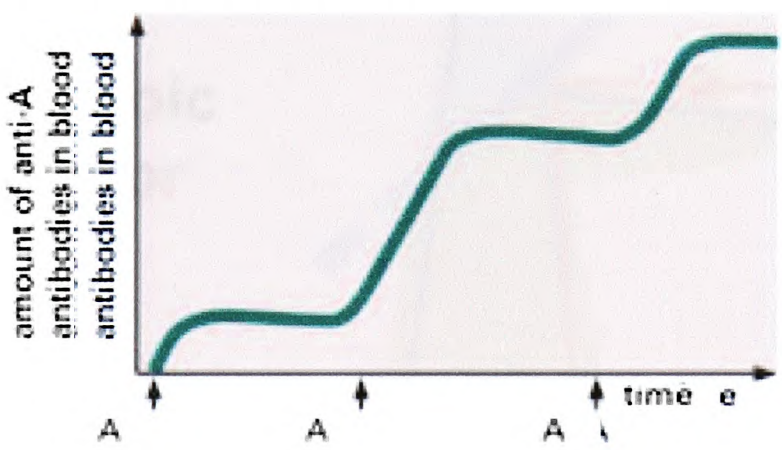

Figure 2.5

Schematic protocol for raising antibodies in animals. Rabbits were used in this study, however the protocol was similar and the injection of antigen A ($KvLQT_1$ peptide) occurred as illustrated. The rabbits in this study were immunised 3 times, causing the antibody titre to increase after each injection, as illustrated in the bottom panel. Illustration modified from Essential cell Biology, 1998.

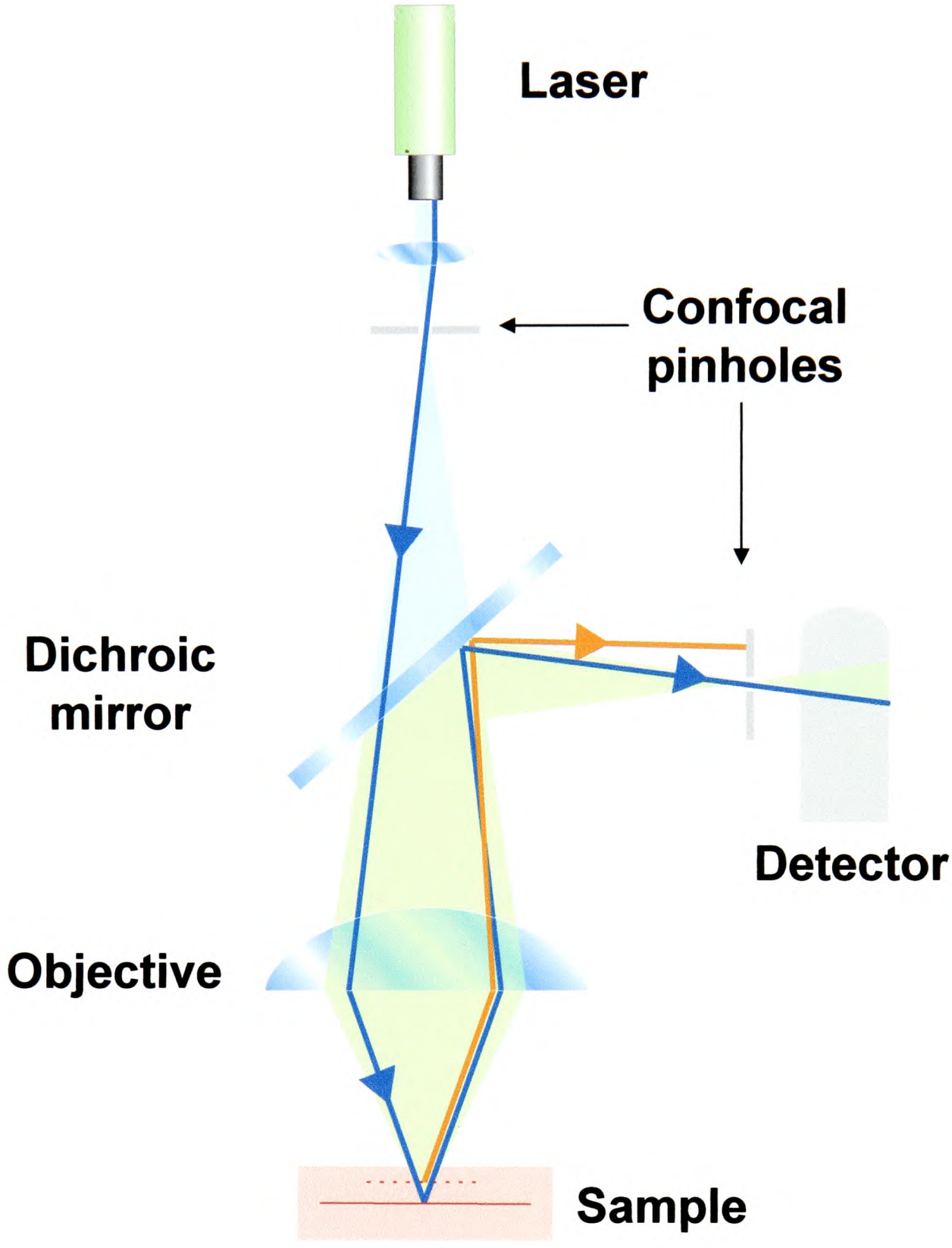

Figure 2.6 Page 76

Principle of the laser scanning confocal microscope. Excitation light is precisely focussed upon a point of the sample. Fluorescence from this region and no other (defined by pinhole) is sampled by the detector. The point of focus in the sample can be changed and successive layers through the sample can be assembled. The term confocal is due to the length of the light-path between 1st pinhole to sample and sample to 2nd pinhole are exactly the same. Illustration modified from that developed by Dr SJ Trout.

CHAPTER 3: Immunohistochemistry

The sarcolemma in ventricular cells is complex, as it has regularly spaced transverse tubule invaginations. These greatly increase the membrane surface area and results in the centre of the large ventricular cell being relatively close to extracellular fluid. In most cell-types an even distribution of ion channels across the exterior membrane is correctly presumed, however not only do ventricular cells have more complex sarcolemmal morphology, the transverse tubules also have a higher ion channel density (Gathercole, Colling et al. 2000; Takagishi, Yasui et al. 2000). The transverse tubule network is associated with the cellular distribution of the contractile apparatus, with these membrane invaginations coinciding with Z-lines in ventricular cells.

The sino-atrial node and cells from this region have been studied with both light and electron microscopy (Boyett, Honjo et al. 2000; Wu, Schuessler et al. 2001). Variable cell morphology has been found in this region and the amount of connective tissue in the sino-atrial node increases with age. Isolation of these cells was first achieved in rabbit (Brown and Difrancesco 1980), using various enzymatic and physical processes, however isolation of sino-atrial node cells from the guinea pig was even more problematic as the region is 1 mm^3, rather than 5 mm^3 in the rabbit. Eventually guinea pig sino-atrial node cells were isolated (Anumonwo, Freeman et al. 1992) and were a similar range of shapes to those found in the rabbit; spindle, elongated spindle and spider. These cell types are quite different to other cardiac myocytes, being smaller, less striated, but most importantly spontaneously beating when healthy. The smallest of these sino-atrial node cells (generally spindle shaped) maybe predominately located in the central node region (Boyett, Honjo et al. 2000), exhibit lower current density and therefore smaller action potential amplitude (Boyett,

Kodama et al. 1995; Rigg, Heath et al. 2000; Wu, Schuessler et al. 2001). Larger cells posses more I_f and I_{Na} (Honjo, Boyett et al. 1996) and tend to originate from the peripheral regions, in close proximity to atrial cells (Kodama, Nikmaram et al. 1997). However other studies have found the spider cells to have a higher intrinsic beating rate, whichever cell type (if any) has faster beating rate would *in situ* determine the rate of development of spontaneous action potentials and hence the heart rate (Wu, Schuessler et al. 2001).

To develop contraction of any muscle cell, actin and myosin must interdigitate in the way described previously (Bers 1993). In cardiac myocytes the filaments are structured around a rigid backbone of actin that is regularly distributed every 1.8 to 2 μm along the long axis of the cell; actin localisation has been used to define the distribution of antibody labelling. This actin scaffolding forms the Z-line and can be seen under a microscope as the dark striations (especially in ventricular cells). The Z-line is at the two ends of the contractile unit known as a sarcomere. From these anchor points actin filaments converge without actually meeting and are intersperse with myosin filaments. The two actin fibres are not quite long enough to reach each other (approximately 0.7 μm in length) and the region in-between (where there is only myosin) is called the M-line (Bers 1993). Titin is another microfilament type that is present in the cardiac sarcomere (Granzier and Labeit 2002), which run parallel to actin and myosin, but this protein with elastic properties provide the passive stiffness of myocytes. In ventricular myocytes there are transverse tubular sarcolemmal invaginations at the Z-lines, which propagate electrical activity deep into the central regions of the ventricular myocyte and therefore facilitate rapid movement of ions

(most importantly calcium). The same contractile apparatus is present in atrial and sino-atrial node cells, but transverse-tubules are absent (Huser, Blatter et al. 2000; Rigg, Heath et al. 2000), possibly due to lack of requirement because of their small cell size.

The role of calcium is still vital in the sino-atrial node, although the primary role of these cells is action potential generation, rather than force development. Calcium appears to regulate numerous currents and be involved in nearly all intracellular pathways. Release from the SR contributes the majority of calcium into the cytosol during excitation of ventricular myocytes (Bers 1993), with sarcolemmal calcium currents acting as a trigger for such release, and so the distribution of the SR in sino-atrial node cells is of paramount importance. The role of the SR is fundamental in pacemaking (Rigg and Terrar 1996; Hata, Sakamoto et al. 1998; Huser, Blatter et al. 2000; Rigg, Heath et al. 2000), and may mediate the adrenergic enhancement of beating rate (Ju and Allen 1999). Part of these sympathetic actions maybe mediated through pathways which are non-noradrenalin activated, but are initiated by co-transmitters such as peptides and ATP (Matsuura, Tsuruhara et al. 1996; Matsuura and Ehara 1997). Some of these sympathetic actions are a result of binding to sino-atrial node receptor for these compounds, such as the purinergic receptors for ATP (Matsuura, Tsuruhara et al. 1996). The SR is thought to be less extensive in the sino-atrial node, the SR surrounds myofibrils in ventricular myocytes (Bers 1993), presumably to provide the SR calcium release which is required for sarcomere contraction. SERCA calcium ATPases are located throughout the SR, mediating the re-uptake of calcium after an action potential. SERCA is basally inhibited by phospholamban (PLB), until this regulatory element is phosphorylated

(Pan, Hannon et al. 1999). Calcium is then stored in the SR until the calcium release channels (ryanodine receptors) are activated; these tend to be distributed near the Z-line (Rigg, Heath et al. 2000), so the local I_{CaL} mediated change ion calcium concentration can be detected and initiates an increase in cytosolic calcium.

Cells from the sino-atrial node do not have the transverse-tubule network seen in ventricular myocytes, having only an exterior plasma membrane, without the invaginations that form transfer tubules. Therefore all sarcolemmal ionic channels are present on the surface membrane. In ventricular cells there have been reports of channel clusters in the transverse tubules (Gathercole, Colling et al. 2000; Takagishi, Yasui et al. 2000); for example channels that pass I_{CaL} are in close proximity to both the SR, creating a more efficient excitation-contraction. The SR calcium release ion channel (ryanodine receptor) is located in the SR near the Z-line in both ventricular and sino-atrial node cells (Bers 1993; Rigg, Heath et al. 2000).

There are at least two components to the delayed rectifier potassium current, I_{Kr} and I_{Ks} (Sanguinetti and Jurkiewicz 1990). These currents are mediated via channel proteins named ERG and $KvLQT_1$ respectively and each associate with β-sub-units to form functional ion channels (Curran, Splawski et al. 1995; Barhanin, Lesage et al. 1996; Sanguinetti, Curran et al. 1996). To this point I_{Kr} has been more fully investigated, due to the class III anti-arrhythmic activity of I_{Kr} selective inhibitors, and hence there are commercially available monoclonal antibodies against I_{Kr}. Fewer studies have focused upon I_{Ks}, and when an extensive search to find an antibody against this channel was undertaken, none was found. Therefore an attempt to develop the antibody against the $KvLQT_1$ channel was undertaken in this study. Ion

channels are complex formations of amino-acid chains inserted into the lipid membrane. The amino-acid sequence of the $KvLQT_1$ subunits was elucidated by Barhanin, Lesage et al (1996) and is illustrated in figure 2.4. The long protein chains fold back upon themselves and create self-interactions, forming a secondary structure in addition to the amino-acid sequence. This results in each protein crossing the membrane 6 times, as assessed by hydrophobicity plots (Barhanin, Lesage et al. 1996; Sanguinetti, Curran et al. 1996) and having both termini located in the cytosol. In the case of the delayed rectifier potassium, 4 protein sub-units are required to combine to form a tetrameric functional channel (Barhanin, Lesage et al. 1996; Sanguinetti, Curran et al. 1996). The tetramer requires the additional presence of minK sub-unit to form a fully functional channel (Barhanin, Lesage et al. 1996; Sanguinetti, Curran et al. 1996). Ion channel protein subunits are constructed in the rough endoplasmic reticulum, as they are formed of long amino-acid chains. From the rough endoplasmic reticulum these amino-acid chains are transferred into vesicles, from which they can either be immediately transferred to the membrane, or they can be stored for later insertion. Non-functional ion channels can therefore be found concentrated in vesicles in the cytosol.

Antibodies can be raised against the proteins that form ion channels and can therefore be used to localise these proteins to different cell types and to different regions of individual cells. Fluorescent markers can be used to illustrate the distribution of the antibody localised to the channel protein, either by directly linkage to the primary antibody, or by the use of a secondary fluorescent-labelled antibody that detects the present of primary antibody. This technique requires the primary and secondary [antibodies] to have been raised in different species (goat and rabbit for

example). This dual antibody system provides an amplified signal of the fluorescent labelling at each channel.

To develop a primary antibody, a short amino-acid sequence from an accessible region of the channel protein should be identified, synthesised and conjugated to a large plasma protein such as bovine serum albumin. When the peptide (A in figure 2.5) is introduced to a non-bovine system, an immune response is initiated that results in the production of selective antibodies (anti-A antibodies), and memory cells, to the short amino-acid sequence. If the conjugated peptide is re-introduced a month or so later, memory cells will be activated and a much larger and more rapid development of antibodies will be initiated (figure 2.5). Once an appropriate amount of antibody is present in the animal's blood stream, they were humanly harvested and the antibody was subsequently purified.

This chapter aims to localise some of the ion channels, which mediate currents that are important to pacemaking in the sino-atrial node. Antibodies to nearly all of the currents (etc.) mentioned in the thesis have been attempted (including I_f, I_{CaL}, connexins and $P2X_1$), but effective labelling of channels in the sino-atrial node appears to be precarious. The results presented represent the more successful labelling procedures, however these give good indication of the tissue and cellular location of various ion channels. This chapter contains data from when an antibody was develop to describe the distribution of I_{Ks}; this antibody would be used to localise I_{Ks} in ventricular and sino-atrial node cells.

Results

Sino-atrial node cell morphologies

Mosaics of transmission photomicrographs (figure 3.1 and 3.2), illustrate the different types of sino-atrial node cell dissected from the guinea-pig sino-atrial node. There is a diverse morphological population, ranging from the elongated spindle (as described by (Brown and Difrancesco 1980), to complex forms having multiple appendages known as spider cells (Wu, Schuessler et al. 2001). Figure 3.1 demonstrates two examples of spindle cells (a and b), which are relatively squat, with a central nuclear mass and two tails, which form to make the classic spindle shaped sino-atrial node cell. Cells c and d in figure 3.1 are examples of spider shaped cells; both of these cells have multiple projections from only one end of the soma. However any cell with more than 2 'tails' can be described as a spider cell. The last two examples (figure 3.2) are elongated spindle sino-atrial node cells; these are similar to the first category, except they have extended tails that reach up to around 75 μm. All these types of sino-atrial node cells had a diameter of approximately 10 μm or less, but cell length varied between 35 and 100 μm according to morphological type. The bar in each photomicrograph is 10 μm. All healthy sino-atrial node cells had clear defined sarcolemmal membranes. Some had faint striations and most healthy sino-atrial node cells showed regular spontaneous activity. All sino-atrial node cells in this chapter were defined by morphology only, as they are fixed before microscopic investigation.

The cardiac myocyte sarcomere described using phalloidin labelling of actin.

The smallest contractile unit of any muscle is the sarcomere. This is the formation of myosin, around the rigid backbone of actin (the Z-line); the interaction of these two structures mediates the physical shortening of the myocyte. Titin provides an elastic structure when muscle is relaxed, running parallel to the other myofilaments.

Figure 3.3 illustrates a guinea-pig ventricular myocyte that had been exposed to phalloidin at 4 different confocal planes. The organisation of actin into cellular bundles is shown, as is the actin rich Z-line across the cell is spaced regularly along the long axis of the ventricular myocyte. The same actin organisation at the Z-line is shown by the fluorescently labelled phalloidin (figure 3.4), an extract from the deadly mushroom *Amanita phalloides* (Wieland 1986), which directly binds to the actin filaments of the sarcomere. The resolution of the phalloidin fluorescence is very good and can localise sub-sarcomere organisation. The region beside the white line on the confocal image has been investigated due to good definition of labelling in this vicinity. From the confocal images (figure 3.3 and 3.4) it is apparent that there is a repetitive type of labelling, consisting of a central thin bright region of fluorescence, in the centre of a less bright but much broader area, which is flanked with an area of little fluorescence. The intensity of the labelling of this region has been quantified and figure 3.4 demonstrates the profile of the phalloidin (and therefore actin) distribution. The thin line of highly concentrated actin, was surrounded by a broad band of lower intensity (although in some cases this merged into a gradual reduction), which was a bordered by region either side where there appeared to be no actin. The distance between peak to peak of this repetitive structure was found to be approximately 1.8 to 1.9 μm. This structure can be closely related to a cardiac

sarcomere, in which the Z-line (formed of actin) hold the shape of the myocyte and have been found every 1.85 μm; this ties in with the interval found between the high intensity lines. The fluorescence peaks were surrounded by regions of less intensity and these are most probably describing the filaments which interdigitate with myosin in the sarcomere. These peaks also co-inside with the dark lines of the ventricular transmission image, which are located at the Z-line of these cardiac myocytes. These regions will be of lower intensity as these structures are not continuous and are distinct from each other on the z-plane (going back into the page) of the myocyte. At some points of the profile, around 2 and 6 μm on XY-position axis (figure 3.4b), there are distinct steps between levels of fluorescence, which probably means this region of the sarcomere is in good alignment in the z-axis. There is in addition a region in which there appears to be very little phalloidin fluorescence, therefore presumably no actin present; this is again in agreement with a region called the M-line, at which myosin is present in-between the actin filaments. Similar images were developed in many ventricular myocytes in which the sarcomere structure was self-evident, but experiments using atrial and sino-atrial cells, developed similar but far less obvious actin alignment. In brief the phalloidin labelling of actin in this ventricular myocyte, illustrates the very good resolution of this system, which allows precise definition of sub-sarcomere structures.

Sarcoplasmic reticulum distribution

The cellular location of the endoplasmic reticulum, known as the sarcoplasmic reticulum (SR) in muscle cells, was investigated using a tracker that was excited using UV (374 nM). Much of this work was undertaken upon ventricular myocytes, as the Z-line of these cells were easy to define (they appear dark on a transmission image),

however some sino-atrial node cells were investigated. Ventricular myocytes were incubated in the ER-tracker for 30 minutes at 100 nM – 1 μM. Upon viewing with the confocal microscope, striations were apparent in the transmission image. The tracker was then excited with a UV lamp and similar striations were found, although these tended to be negative staining, i.e. a lack of ER tracker at the Z-lines. The transmission and fluorescence images were then overlaid, and the presence of ER in the regions in-between the Z-lines was confirmed (figure 3.5). There appeared to be an inter-nuclear ER network in most of the ventricular cells investigated, but sino-atrial node cells are generally mono-nucleated. Similar Z-line negative ER labelling were found in the atrial myocytes, although there appeared to be less, if any organisation of the ER in sino-atrial node cells.

PLB distribution

The regulatory compound phospholamban (PLB) inhibits the activity of the SERCA calcium ATPase on the SR, but upon PLB phosphorylation this inhibition of calcium sequestration is reduced. The cellular distribution of PLB was investigated in ventricular and sino-atrial node cells, using a monoclonal antibody and a FITC conjugated secondary antibody. In ventricular cells PLB was found to label the two shorter ends of the rectangular ventricular myocytes (figure 3.6), the region around the nucleus and a distinct band in the region of the Z-line. There also appears to be some generalised sub-sarcolemmal labelling by PLB, just inside of the ventricular cell. The first region at the end of the myocytes are know to interact closely with the next ventricular myocytes in the muscle fibre, actually being physically linked by large inter-cellular pores known as gap junctions, composed of connexins. These structures facilitate effective electrical coupling of ventricular myocytes through this

region of intercalated disks. A high PLB concentration has been found in the intercalated disks (Jorgensen and Jones 1987). The same studies have found PLB to be localised to the peri-nuclear region, which there is also evidence for here, although this labelling looks to be confined to the nuclear envelope, rather than a diffuse region around the nucleus. Most importantly for this study PLB also appears to be localised to the Z-line of ventricular myocytes, as figure 3.6 (right panel) illustrates the dark lines on the transmission image correspond to the fluorescence of the PLB labelling. The invagination of the transverse tubule from the sarcolemma can be observed in figure 3.6 (middle panel), especially in the PLB binding photomicrograph overlaid onto the transmission image. These findings indicate PLB is localised to relatively broad regions around the Z-line and to after the sub-sarcolemmal region, in addition to the peri-nuclear and intercalated disk regions of ventricular myocytes. PLB distribution in sino-atrial node cells is similar to that in the ventricle in some ways, but quite different in others (compare figure 3.6 and 3.7). Both peri-nuclear and labelling close to the sarcolemma are present in sino-atrial node cells, but there is no evidence for PLB distributed at the extreme end of the cell (sino-atrial node cells do not posses intercalated disks) or any regular banding-like distribution through the cytosol. Figure 3.7 indicate that there is some cytosolic PLB, although there appears to be no pattern, except for more PLB distributed near the nucleus. The lack of PLB distribution at the Z-lines, may well be related to the lack of transverse tubule invaginations at this point in myocytes of the sino-atrial node.

Phalloidin and PLB localise PLB to Z-line in ventricular cells

The location of actin (via phalloidin labelling) has been accurately described in ventricular myocytes (see above) and the precise location of the Z-line is illustrated

by the distinct fluorescence peak. The phalloidin labelling of the actin Z-line can be used to describe the location of other intracellular compounds, such as PLB. Photomicrogrhaphs after co-incubation of phalloidin and an antibody against PLB (figure 3.6), indicate that PLB (in red) is distributed in the region around the Z-line, although there seem to be no specific localisation at the Z-line. Peri-nuclear PLB distribution can again be identified. There also appears to be some longitudinal PLB distribution bands and if the area indicated by the white line is again studied, it becomes apparent that the longitudinal PLB bands coincide with regions in which phalloidin (and therefore actin) are absent. This probably indicates actin filaments (identified by phalloidin) being surrounded by the SR on which PLB is located. In the sino-atrial node, there was no PLB labelling coinciding with phalloidin labelling.

The sino-atrial node lacks I_{K1}.

I_{K1} is an important current in cardiac myocytes, providing a current that generates a resting potential in ventricular myocytes that is quite negative (-85 mV), being close to potassium reversal potential. Figure 3.8 illustrates the punctate distribution of I_{K1} in ventricular myocytes, as assessed by the labelling of antibodies raised against Kv2.1 (the I_{K1} channel protein subunit), possibly describing clustering of I_{K1} channels. Note the relative lack of I_{K1} distributed on the surface membrane. The fluorescent spots (approximately 500 nm across) are however localised to the dark bands of the transmission image (see overlay figure 3.8b), as illustrated in the region on the arrow, which correspond with the Z-line and therefore the sarcolemmal invaginations. The punctate spots of anti-I_{K1} labelling are distributed approximately every 2 μm. The presumed clusters of I_{K1} channel appeared to be located in the transverse tubule system, which is continuous with the extracellular fluid and

therefore acts as if the channels were located on the exterior sarcolemma. There is some additional generalised labelling of the nucleus in the ventricular myocytes. The sino-atrial node cell in figure 3.8c does not have these localised regions of high fluorescence, but does exhibit the low-level nucleus labelling and a small amount of cytosolic fluorescence. These sino-atrial node cells have no transverse tubule system and appear to not express I_{K1} on the sarcolemma. This is consistent with the absence of I_{K1} in the sino-atrial node, which has been found to be one of the reasons why diastolic depolarisation exist and hence can generate spontaneous action potential generation (Boyett, Honjo et al. 2000; Terrar and Rigg 2000).

The location of ERG (I_{Kr}) in cardiac myocytes.

When the protein α sub-unit ERG associates with $MiRP_1$, a current thought to be the correlate of the native I_{Kr} is developed (McDonald, Yu et al. 1997). To investigate the distribution of I_{Kr} in the sino-atrial node (and ventricle) antibodies to human ERG were utilised. Initial studies reveal surprising results, identifying nuclear and Z-line labelling of ERG in both ventricular and sino-atrial node cells (figure 3.9). There are no sarcolemma invaginations in sino-atrial node cells, so localisation of ERG to the Z-line, throughout the cell (figure 3.9c, inset), appears confusing. These experiments were undertaken with triton X-100 to permeabilise the cell, this facilitates antibodies access to the cell and intracellular epitopes. It transpires that the concentration of Triton X-100 (1 %) that was initially used, may have been stripping the myocytes of their sarcolemma. A different method of sarcolemmal permeabilisation was subsequently used, which involved a rapid freeze-thaw protocol (Methods, page 63), that disrupts the sarcolemmal membrane producing large holes, but leaves it intact. This modified protocol was used in association with the same

commercial antibody against human ERG (alomone), with an alexa fluor conjugated secondary antibody (Molecular probes). The new methodology facilitated more a believable description of ERG in sino-atrial node cells, as shown in figure 3.10 and 3.11. ERG was distributed at the sarcolemma of these cells, as the fluorescence profiles demonstrate; there is some cytosolic fluorescence, however the labelling at each end of the cell is approximately double that in the centre. In addition the cellular membrane of sino-atrial node cells in transmission images were found to coincide with the peak ERG fluorescence. These experiments indicate that ERG is distributed on the sarcolemma of sino-atrial node cells and therefore imply the presence of I_{Kr} in this cell type.

Distribution of KvLQT$_1$ in ventricular and sino-atrial node cells

$KvLQT_1$ is known to associate with minK protein to form a functional channel, which has characteristics very similar to I_{Ks} (Barhanin, Lesage et al. 1996; Sanguinetti, Curran et al. 1996; Suessbrich and Busch 1999; Seebohm, Lerche et al. 2001). Protocols similar to the one described above were used with a commercial antibody against $KvLQT_1$ (Santa-cruz biotechnology, cal), with the freeze-thaw and alexa fluor conjugated secondary antibody.

Antibody raised in-house

A population of sino-atrial node cells was investigated for the presence of specific fluorescence associated with the labelling of $KvLQT_1$. Two separate immunohistochemical procedures on different days were undertaken, using a range of antibody titres (1:50 to 1:500) and two different fluorescent probes (FITC and Alexa Fluor) were used, after freeze-thaw permeabilisation of the sino-atrial node cells

(Methods, page 63). Approximately 25 sino-atrial node cells were visualised after being treated with the antibody raised in this study, however, in no cell was there found any significant fluorescence indicative of the presence of $KvLQT_1$. Three sino-atrial node cells, one of each morphology, have been illustrated (figure 3.12). Some fluorescence can be observed in each cell (right panel), however the labelling is very faint and does not appear to be associated with any specific cellular structure; this labelling is likely to be non-specific. The labelling in figure 3.12b may be associated with the nuclear envelope, but there is no obvious reason for this to be a location of $KvLQT_1$. Similar numbers of ventricular myocytes, to sino-atrial node cells, were treated with the $KvLQT_1$ antibody that was raised in this study. Immunohistochemistry was undertaken on two separate occasions, with a range of antibody titres, two fluorescent indicators, with freeze-thaw permeabilisation. At least 10 ventricular myocytes were recorded after treatment with the primary antibody and goat anti-rabbit alexo flour conjugated secondary antibody. When the ventricular myocytes were visualised with a confocal microscope, no/very little fluorescence was observed upon laser excitation (figure 3.13) and only the small amount of fluorescence that can be seen in figure 3.13b, appears to be associated with the nucleus. $KvLQT_1$ would not be hypothesised to be located primarily in the nucleus, but this region is known to non-specifically bind a range of antibodies.

Commercial antibody

The distribution of $KvLQT_1$ with this antibody was initially investigated in ventricular myocytes and figure 3.14 illustrates that although there was some diffuse cytosolic fluorescence, the sarcolemmal membrane had visibly more labelling than other regions using this commercial antibody. This was further defined by

quantification of pixelation in the box indicated by the dotted line and from this a slightly increased labelling could be seen at the edges of the ventricular myocytes, indicating sarcolemmal localisation of $KvLQT_1$ and presumably functional I_{Ks}. Note the lack of t-tubule fluorescence when $KvLQT_1$ is localised in the ventricle (figure 3.14), indicating differential distribution of these ionic channels to I_{K1} that were mostly found to be local in discrete clusters in the transverse tubules. Figures 3.14b and 3.15 are sino-atrial node cells in which $KvLQT_1$ has been investigated. The fluorescence was found to generally localised to the edges of these sino-atrial node cells (figure 3.16), although there was some cytosolic labelling, again indicating the presence of $KvLQT_1$ in the sino-atrial node and implying localisation to the sarcolemma (see fluorescence profile), which seems probably for an ion channel. There appears to be relatively more fluorescence in sino-atrial node cells compared to that of ventricular myocytes, possibly indicating a higher expression of I_{Ks} in the sino-atrial node cell. No striations can be seen in sino-atrial node cells labelled with $KvLQT_1$.

Purinergic receptor distribution in the sino-atrial node

In addition to noradrenaline being released at the sympathetic nerve terminals, certain peptide neurotransmitter and ATP can be found in the vesicles (Matsuura, Tsuruhara et al. 1996; Matsuura and Ehara 1997), and are released into the cleft. Purinergic receptors that detect the presence of ATP maybe present in the sino-atrial node. To investigate the distribution of purinergic receptors, a commercial monoclonal antibody was used (Alomone), in association, with the freeze-thaw techniques and an alexa fluor conjugated secondary antibody. Such investigation into receptor ($P2X_2$) distribution in sino-atrial node cells identified good sarcolemmal

labelling (at two confocal planes in figure 3.17), with a small amount of generalised cytosolic fluorescence and in some cases a slight nuclear stain. The low level of cytosolic fluorescence facilitated good definition of the sarcolemmal labelling (approximately 4 times the magnitude of cytosolic fluorescence), as identified in the fluorescence profiles across the cytosol, sarcolemma and surrounding regions in these sino-atrial node cells (figure 3.18). There were no striations as seen previously (PLB) and no punctate spots of fluorescence when this purinergic receptor was investigated. Other purinergic receptors were investigated, however labelling was not as strong in $P2X_1$ and P2Y receptor subtypes (data not shown).

Discussion

The cells that originate from the sino-atrial node region have a diverse range of shapes (Boyett, Honjo et al. 2000; Wu, Schuessler et al. 2001), and are similar to those described previously; spindle, elongated spindle and spider. Each sino-atrial node cell has a single nucleus, which is relatively large compared with the cell size and so leads to a bulbous region of the cell containing the nucleus. Elongated spindle sino-atrial node cells maybe big enough for the large nucleus to not define the shape of the cell. From the nuclear region of the sino-atrial node cell appendages diverge, if this occurs at opposing poles then the cell appears to be spindle shaped (or elongated spindle), but if more than 2 limbs are present from the central soma-like region, then these cells are known are spider sino-atrial node cells. There are a large variety of spider shaped cells, ranging from a relatively simple spindle like arrangement with one of the tails splitting, to star like cells in which projections go off at all angles.

Cells originating from the sino-atrial node can therefore be easily identified by morphology, but in addition, healthy cells exhibit spontaneous action potential generation and hence intrinsically beat even when isolated. There have been some reports that different shaped sino-atrial node cells originate from different regions, Honjo, Boyett et al (1996) found that spindle cells were derived from the central region. Wu, Schuessler et al (2001) theorised that spider cells were the primary pacemakers due to their more frequent intrinsic spontaneous beating rate. No determination of central node cell type was attempted in this study, as from other data indicates that the entire node is a mixed population of sino-atrial node cell types. Some groups have not found the existence of peripheral and central sino-atrial node cell types and most do not differentiate between cell types when studying sino-atrial node cells (Yanagihara and Irisawa 1980; DiFrancesco and Mangoni 1994; Lei and Brown 1996; Rigg, Heath et al. 2000). In addition to the true sino-atrial node cells, atrial cells appear to also be present throughout this region. Distribution of atrial cells in the sino-atrial node has been contentious, with some groups finding progressively less atrial cells in the central node (Honjo, Boyett et al. 1996), whilst others report strands of atrial cells delving towards the centre of this region (Wagner, Namiki et al. 1999). The amount of connective tissue (including collagen) increases as the sino-atrial node ages and this is a serious consideration for cell isolation procedures, as enzymatic digestion/physical trituration are not as effective in the presence of connective tissue and therefore young mature animals are used.

The sino-atrial node functions as a single unit *in situ* and so only the spontaneous action potential generation of the primary pacemaker is relevant. However upon isolation the characteristics of sino-atrial node cells will be altered, as

there will be an absence of cell-to-cell electrical interaction, including an absence of atrial hyperpolarizing load and action potential conduction. The isolated sino-atrial node cell is however a useful system to study, to understand the processes and regulation underlying sino-atrial node action potential generation, which can subsequently be applied to multicellular and entire node preparations.

The sarcomere structure of every cardiac myocytes is very similar. The contractile unit has been described previously (Bers 1993); in brief actin and myosin interdigitate and cross-bridge cycling facilitates shortening of the sarcomere and this is translated into a propulsive force. The use of the actin specific labelling properties of phalloidin has allowed this study to effectively describe the sarcomere structure in ventricular cells and these findings can be translated to any cardiac myocytes, including the sino-atrial node. The distribution of actin in the sarcomere identifies the Z-lines and M-line of each sarcomere, which represent the two edges and the centre of a sarcomere respectively.

Previous studies of sino-atrial node cells have found the SR to fill up to 1/3 of the total cell volume (Bouman and Jongsma 1986), with a lesser myofilament density than in ventricular myocytes. In ventricular myocytes this study found an inter-nuclear SR network, possibly with the rough endoplasmic reticulum. There was an additional SR network interspersed between the Z-line/transverse tubule regions, this pattern probably exist due to the lack of physical space in the myocytes. In the absence of transverse-tubule network the organisation of the SR appears similar in the sino-atrial node and other tissue (Sommer and Johnson 1968; Jewett, Leonard et al. 1973), seemingly aligning itself with the sarcomere Z-lines. This organisation

produces regular distribution of ryanodine receptors (Rigg, Heath et al. 2000) and other SR associated components. The high acuity description of the sarcomere can be used to compare against the location of other intracellular components, such as PLB an inhibitory protein found in association with the SR calcium SERCA pump (Pan, Hannon et al. 1999). PLB has been found to roughly coincide with actin labelling, indicating z-line distribution of PLB in ventricular myocytes. This finding is initially confusing, as PLB regulates the pump that sequesters calcium back into the SR, and therefore would be primarily located in the regions between Z-lines, where most of the calcium re-uptake occurs. In fact there is a lower SR PLB density at the Z-line (Jorgensen and Jones 1987), however previous studies have found the same finding and have concluded that PLB localisation to the Z-line is due to a greater surface area of folded SR network (Jorgensen and Jones 1987; Hori, Takamoto et al. 1989). A phosporylated form of PLB can also be found in the intercalated disks of ventricular myocytes (Calaghan, White et al. 1998; Calaghan, White et al. 1998). In some sino-atrial node cells cytosolic PLB labelling has been identified, although it appears to be diffuse and unorganised. PLB also appears to be distributed in-between myofilaments in ventricular myocytes, in the peri-nuclear region and at the sarcolemma of both sino-atrial node (Hori, Takamoto et al. 1989).

Channel proteins can also be localised, the majority tend to be distributed upon the sarcolemmal membrane, however there are ion channels/transporters/exchange mechanisms on intracellular membranes; calcium release channels (ryanodine receptors) are located upon the SR membrane in proximity to the Z-line of sino-atrial node (Rigg, Heath et al. 2000). The two delayed rectifier potassium currents have been found to play a vital role in sino-atrial node

function (see Description of I_K and other ionic current, page 122;(Sanguinetti, Jurkiewicz et al. 1991; Sanguinetti, Jiang et al. 1995; Lei and Brown 1996; Anumonwo, Tallini et al. 2001; Lei, Cooper et al. 2002) and so the location of the channel proteins that mediate I_{Kr} and I_{Ks} (ERG and $KvLQT_1$) are of interest.

ERG has been localised to the sarcolemma of smooth muscle cells and other tissue (Wymore, Gintant et al. 1997), has been identified in cardiac myocytes including sino-atrial node cells (Heath and Terrar 1996; Brahmajothi, Morales et al. 1997). Two attempts at localising ERG, the channel protein underlying I_{Kr}, were made and provided interesting results, but the labelling from the latter set were more insightful. ERG was initially probed with antibodies against human ERG (Alomone), after Triton X-100 permeabilisation of the myocyte sarcolemma. Labelling indicated ERG to be present throughout the cytosol at the Z-line in both ventricular and sino-atrial node cells, with no sarcolemmal labelling described at all. It was possible that I_{Kr} maybe localised to the transverse tubule system in ventricular myocytes, as some channels have been reported to do this (I_{K1}), however sino-atrial node cells have no transverse-tubules and therefore the channel protein appears to be distributed in the cytosol. A high concentration of antibody had to be used and the Z-line has been found to non-specifically bind many antibodies. The lack of sarcolemmal labelling was surprising and so the alternative less destructive mechanism for permeabilisation, freeze-thaw, was used to describe distribution of ERG. In this case ERG and therefore I_{Kr} was localised to the sarcolemmal membrane in sino-atrial node cells, with some degree of cytosolic fluorescence. ERG channel protein localisation to the sarcolemma has been described in other cell types (Curran, Splawski et al. 1995; Wymore, Gintant et al. 1997) and would be functionally relevant to pace-making.

The $KvLQT_1$ antibody that was raised in rabbits, harvested and then purified in-house. When utilised, there was no significant fluorescence detected in the cells studied. The apparent lack of immunohistochemical labelling of $KvLQT_1$ in ventricular and sino-atrial node cells, could indicate two possibilities; either there is no $KvLQT_1$ in these cells types, or the antibody which was raised in this study was not effective. There are a large number of electrophysiological and molecular studies, but not immunohistochemical, that have found I_{Ks} (or the gene product) to have an important role in both ventricular and sino-atrial node cells. The interaction of minK and $KvLQT_1$ has been described (Barhanin, Lesage et al. 1996; Sanguinetti, Curran et al. 1996). The review by Suessbirch and Busch (1999) described how the data from various groups strongly indicated that the association of minK and $KvLQT_1$ underlie the native current known as I_{Ks} (Curran, Splawski et al. 1995). This indicates that the antibody isolation and purification was unsuccessful. The first thing that needs to be recognised is that this was a one off project, this group has never before isolated antibodies and as much help/advice was received, could not change the fundamental lack of experience. This lack of knowledge and bad communication resulted in the final harvested blood samples being immediately frozen. Upon thawing there was a large degree of haemolysis. In retrospect the separation of the serum, should have been undertaken prior to freezing. The haemolysis experienced may contribute to the ineffectiveness of the antibody isolation.

Santa Cruz Biotechnology Incorporated (California, USA) developed similar antibodies (sc-10646, sc-10645 and sc-20816) to those attempted by this study. The Santa Cruz antibodies (sc-10646 and sc-10645) were raised (in goat) against a short

internal peptide epitope on the $KvLQT_1$ channel, mapping at/near (respectively) the C-terminal of this channel protein, in a similar region to that which the in-house antibody was raised upon. Using the commercial antibody, $KvLQT_1$ was immuno-localised to the sarcolemmal membrane in both ventricular and sino-atrial node myocytes, with some scattered low-level cytosolic labelling. This is in agreement with Roche, Westenbroek et al (2002) that found members of the channel family to be localised at cellular membranes. There appeared to be no $KvLQT_1$ in the transverse-tubule system of the ventricular cells, which is a differential finding to that regarding ion channel proteins passing I_{K1} (see above) and I_{CaL} (Takagishi, Yasui et al. 2000) which concentrate in this system.

Channel protein complexes (minK/$KvLQT_1$, $MiRP_1$/ERG) are regulated by various intracellular pathways (Bian, Cui et al. 2001; Cui, Kagan et al. 2001), including pathways activated by extracellular ATP (Matsuura, Tsuruhara et al. 1996). ATP interacts with purinergic receptors on the surface membrane, of which $P2X_2$ was identified to be localised to the sino-atrial node cell sarcolemma. The binding of ATP to $P2X_2$ receptors on the sino-atrial node would initiate a cascade of intracellular events that modifies various cellular functions. Purinergic receptor activation also alters the PKC regulation of ion channels that contribute to spontaneous action potential generation in the sino-atrial node; including that of I_{Ks} as identified by $KvLQT_1$/IsK inhibition in cells of the central nervous system (Marcus, Sunose et al. 1997). In the sino-atrial node ATP has been found to change the contribution of I_{CaL} (Qu and Campbell 1998) and I_{KATP} (Findlay 1994; Parratt and Kane 1994) to diastolic depolarisation, but only the former is mediated via purinergic receptors.

As described previously, cells from the sino-atrial node have various morphologies; spindle, elongated spindle and spider. Confocal microscopy was used to describe the distribution of various ionic channels and other cellular components in both ventricular and sino-atrial node cells. A probe was used to show the position of the SR in ventricular myocytes, demonstrating Z-line negative labelling. Phalloidin was used to elegantly describe the distribution of actin in each sarcomere, having peak fluorescence precisely at the Z-line. PLB was found in locations such as the sarcolemmal and at the Z-lines (using co-incubation with phalloidin) in ventricular myocytes, but the Z-line labelling was absent in cells from the sino-atrial node. Another ion channel I_{K1} was found to be distributed on the sarcolemma and in punctate spots in ventricular myocytes, but appeared absent in sino-atrial node cells. After initial methodological problems, ERG and $KvLQT_1$ were distributed at the sarcolemma of ventricular and sino-atrial node cells. Purinergic receptors were also found distributed across the sarcolemma of sino-atrial node cells.

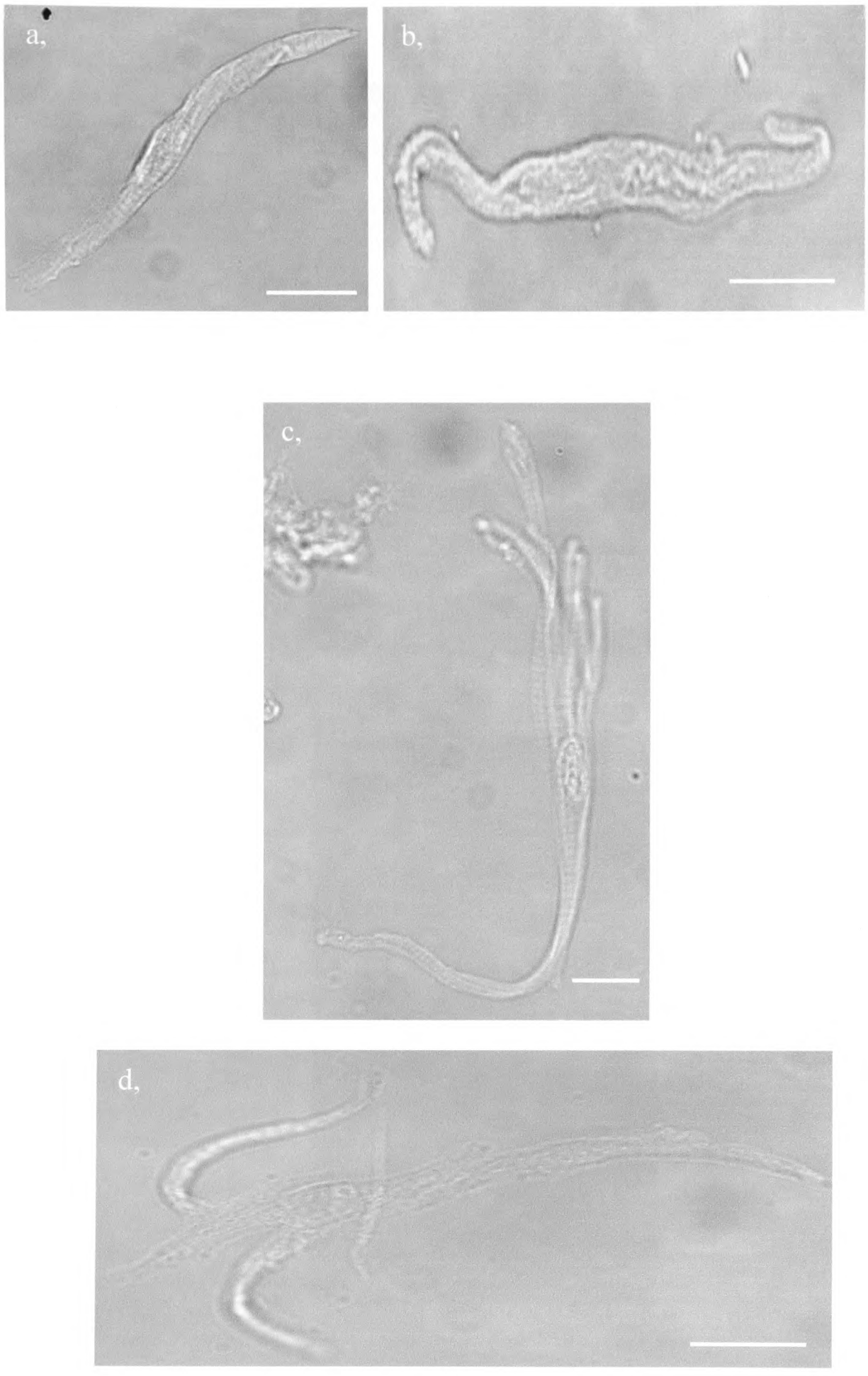

Figure 3.1

Spindle (a and b) and spider (c and d) shaped sino-atrial node cells. Images are transmission from a confocal microscope. Distinct morphologies are illustrated with spindle cells having two protrusions from a central bulbous region and spider cells being larger and having numerous appendages at either one or both poles of the cell. Bar measures 10 μm.

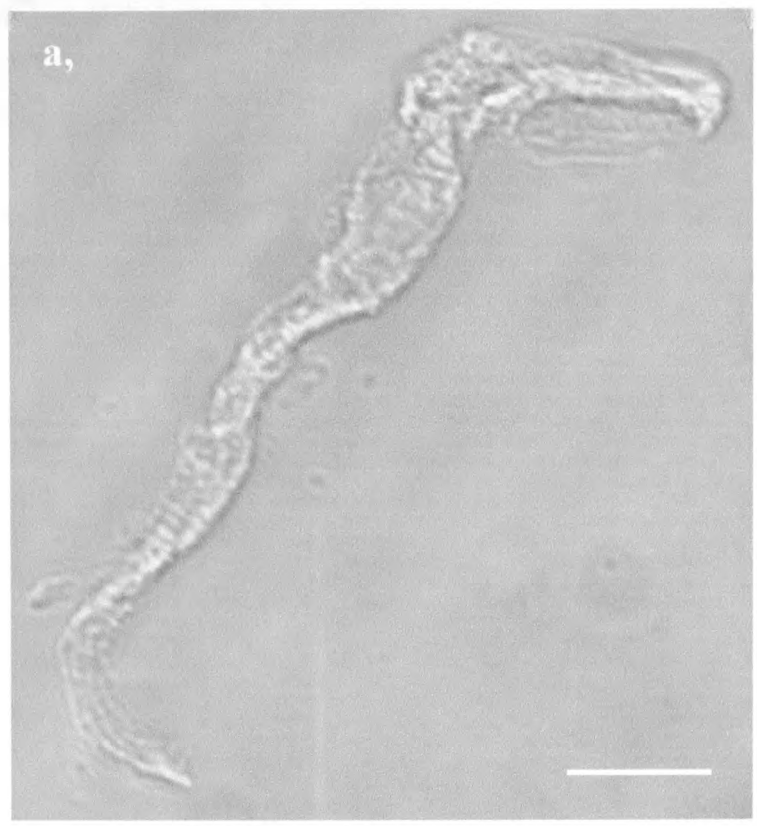

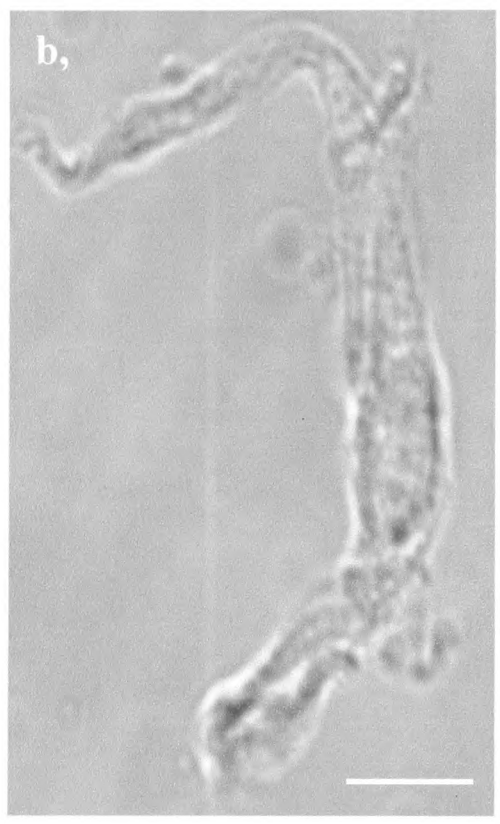

Figure 3.2 Page 102

Two examples (a and b) of elongated spindle sino-atrial node cell morphology. Images are transmission from a confocal microscope. These cell are considerably larger than spindle cell (see figure 3.1a and 3.1b), but similarly have two limbs protruding in opposite directions from a central region containing the nucleus. Bar measures 10 μm.

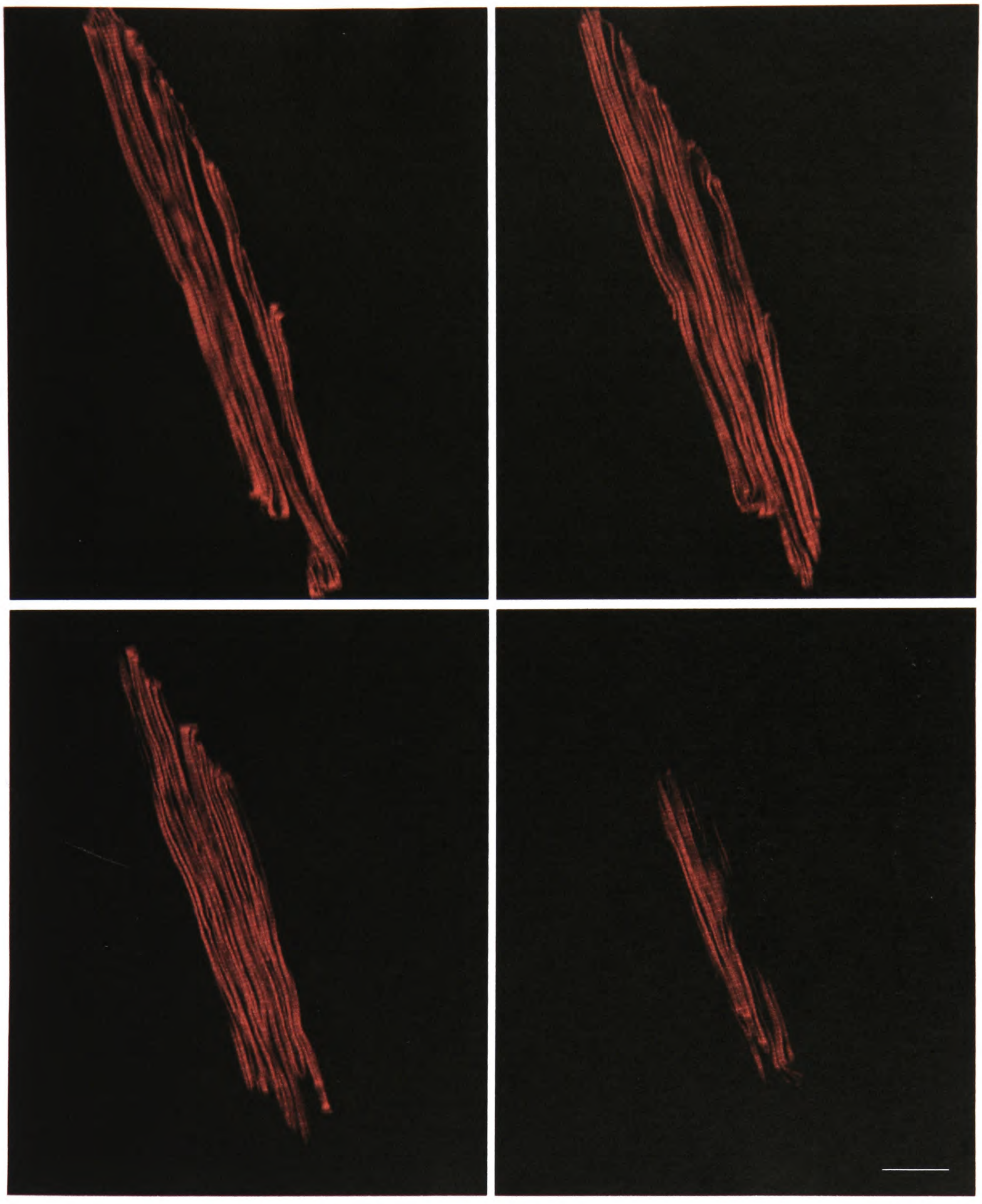

Figure 3.3 Page 103

Phalloidin fluorescence is located in actin filaments in ventricular myocyte in 4 different confocal planes. The texas red ITC conjugated fungal product phalloidin has a high affinity for actin and describes its distribution in myocytes. Phalloidin 1:20 dilution (Molecular probes). Phalloidin fluorescence in define in distinct bundles running the long axis of the ventricular myocyte and has regular fluorescence peaks approximately every 2 μm. Bar measures 10 μm.

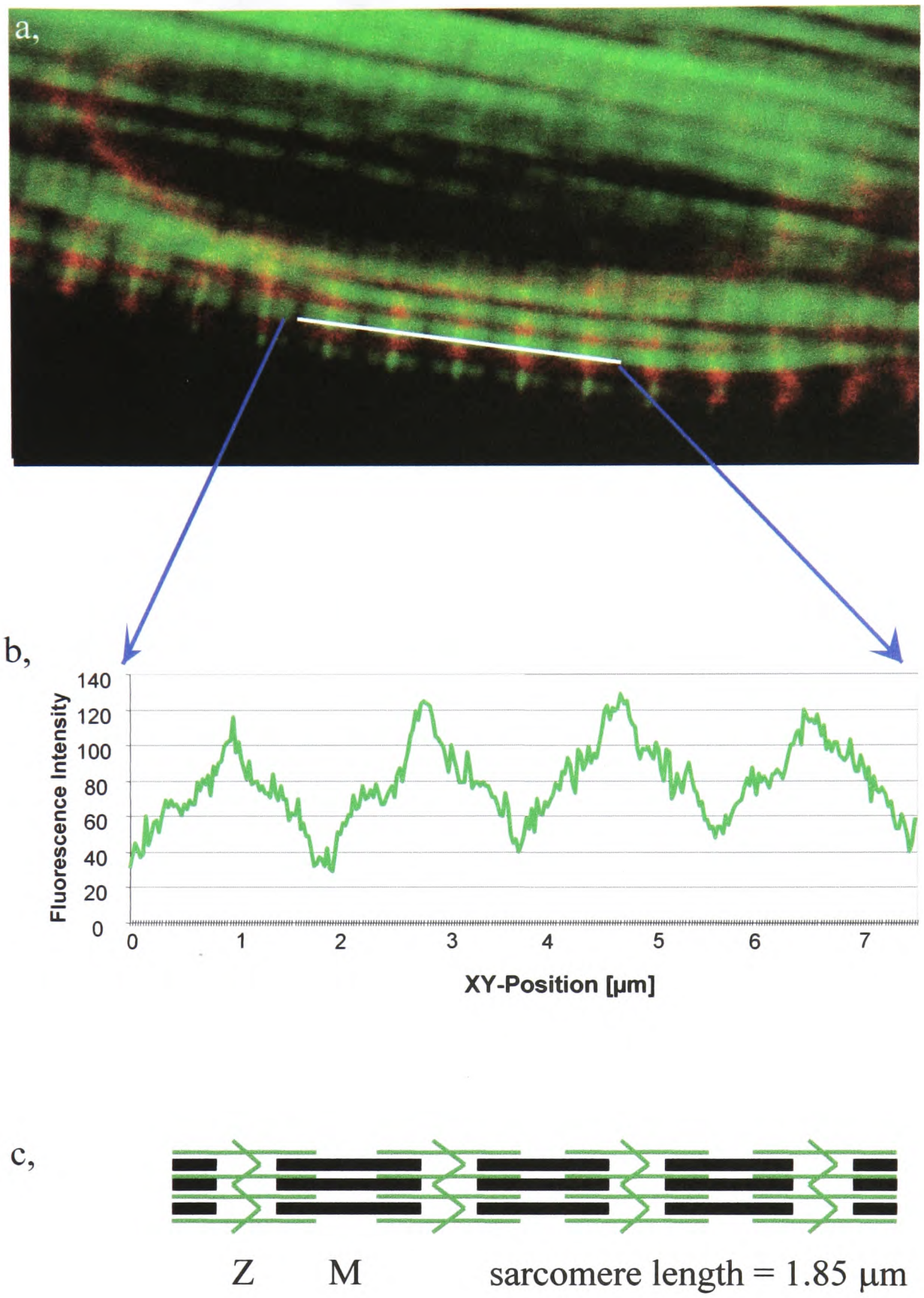

Figure 3.4 Page 104

Phalloidin fluorescence in figure 3.3 appears green describing the location of actin filaments (red staining describes PLB distribution) in ventricular myocyte (a), fluorescence intensity plot (b) and sarcomere organisation (c). Phalloidin fluorescence demonstrates a regular peak (~120) every 1.85 µm (b), with a subsequent intermediate level (between 60 and 100) and a trough at 40 fluorescence units. The phalliodin fluorescence in figure 4.3b appears to be similar to the actin (green) distribution in the sarcomere (c), being most concentrated at the Z line and least at the M line.

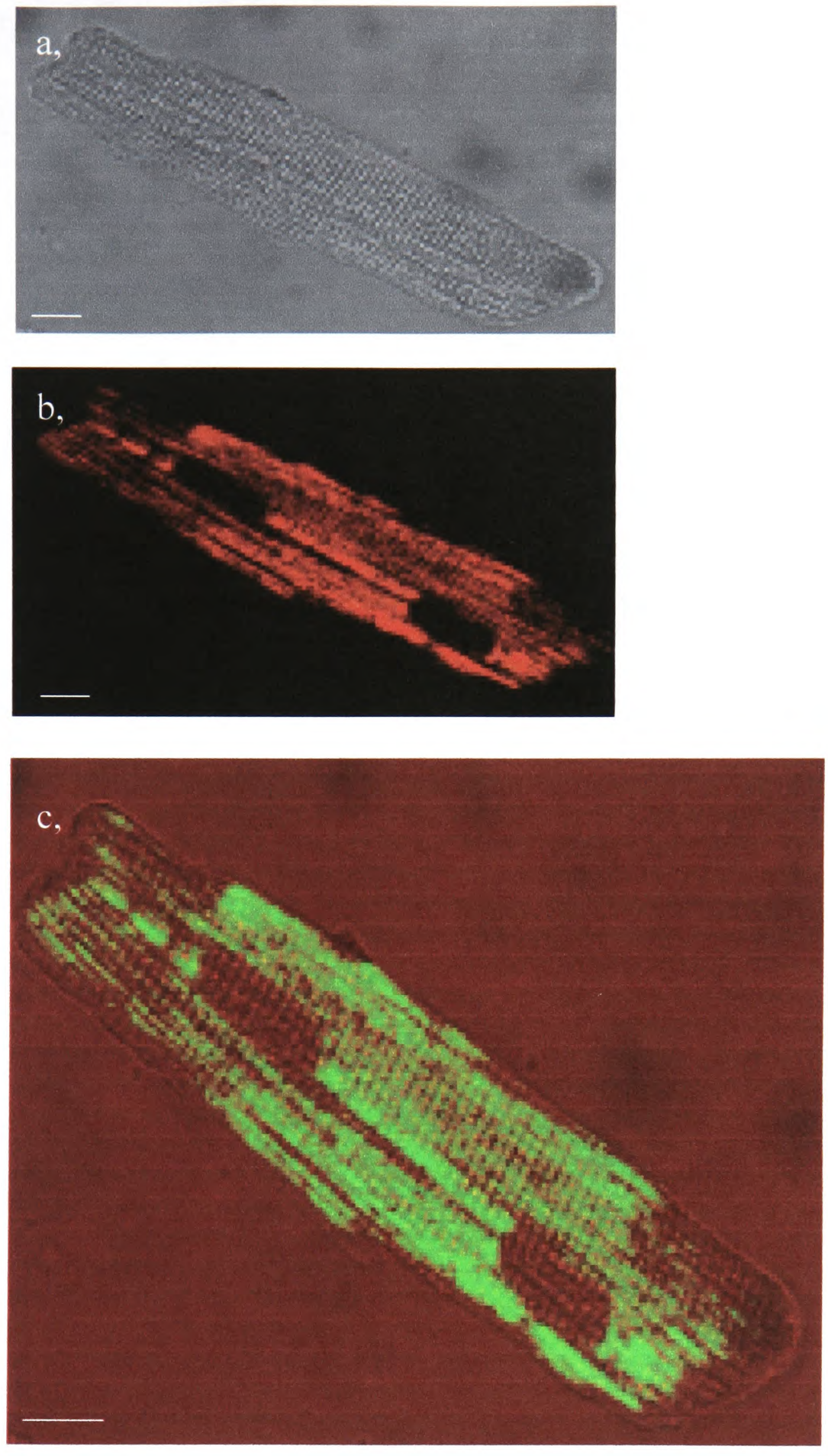

Figure 3.5 Page 105

Labelling of an ER-tracker (Molecular Probes) in ventricular mocytes. Transmission (a) and fluorescence images are shown (b), and the composite overlay image (c) indicates the Z line region of the ventricular myocyte is not labelled. The ER-tracker was used at concentrations between 100 nM to 1 μM and incubated with a similar volume of ventricular myocytes and incubated for 30 minutes. Excitation was accomplished using a ultra-violet (374 nm) lamp. Bar measures 10 μm. Also note the inter-nuclear ER network and the negative staining of the nuclei.

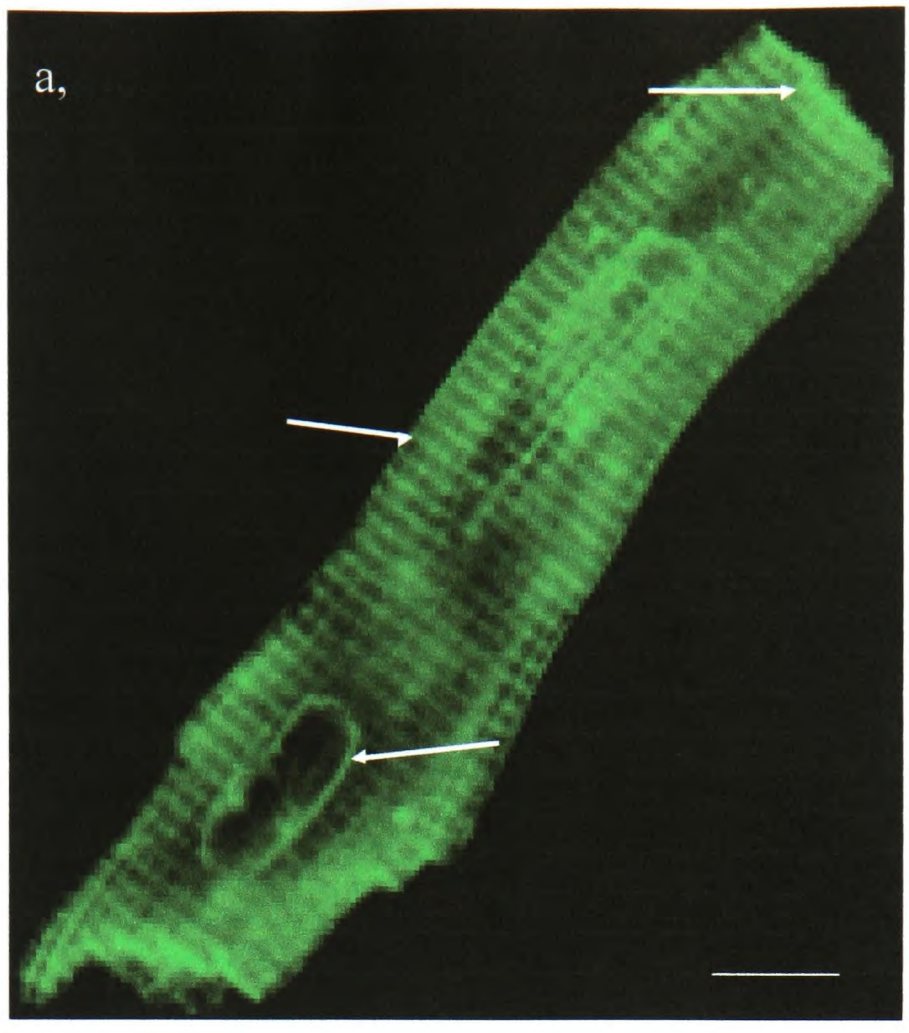

b,

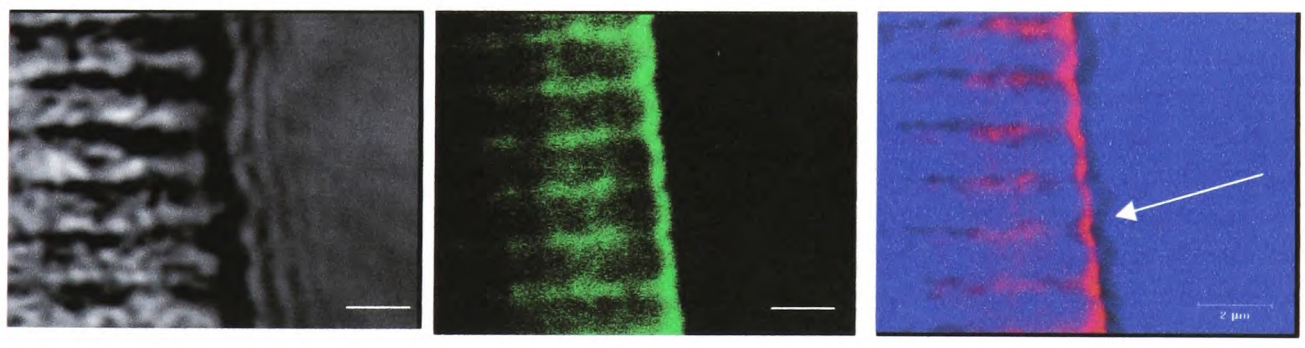

Figure 3.6

Fluorescence images of ventricular myocytes labelled against PLB (a), monoclonal antibody at 1:100 dilution (Upstate Biotechnology). Note the labelling within the cell either organised in bands at the Z-line (b) or around the nucleus (arrows), with additional labelling of the cell membrane and intercalated disks. Further evidence for PLB localisation to the Z-line is found in the overlay image (right panel), in which slight indentation can be observed at the Z line (arrow). Bar measures 10 and 2 μm in a and b respectively.

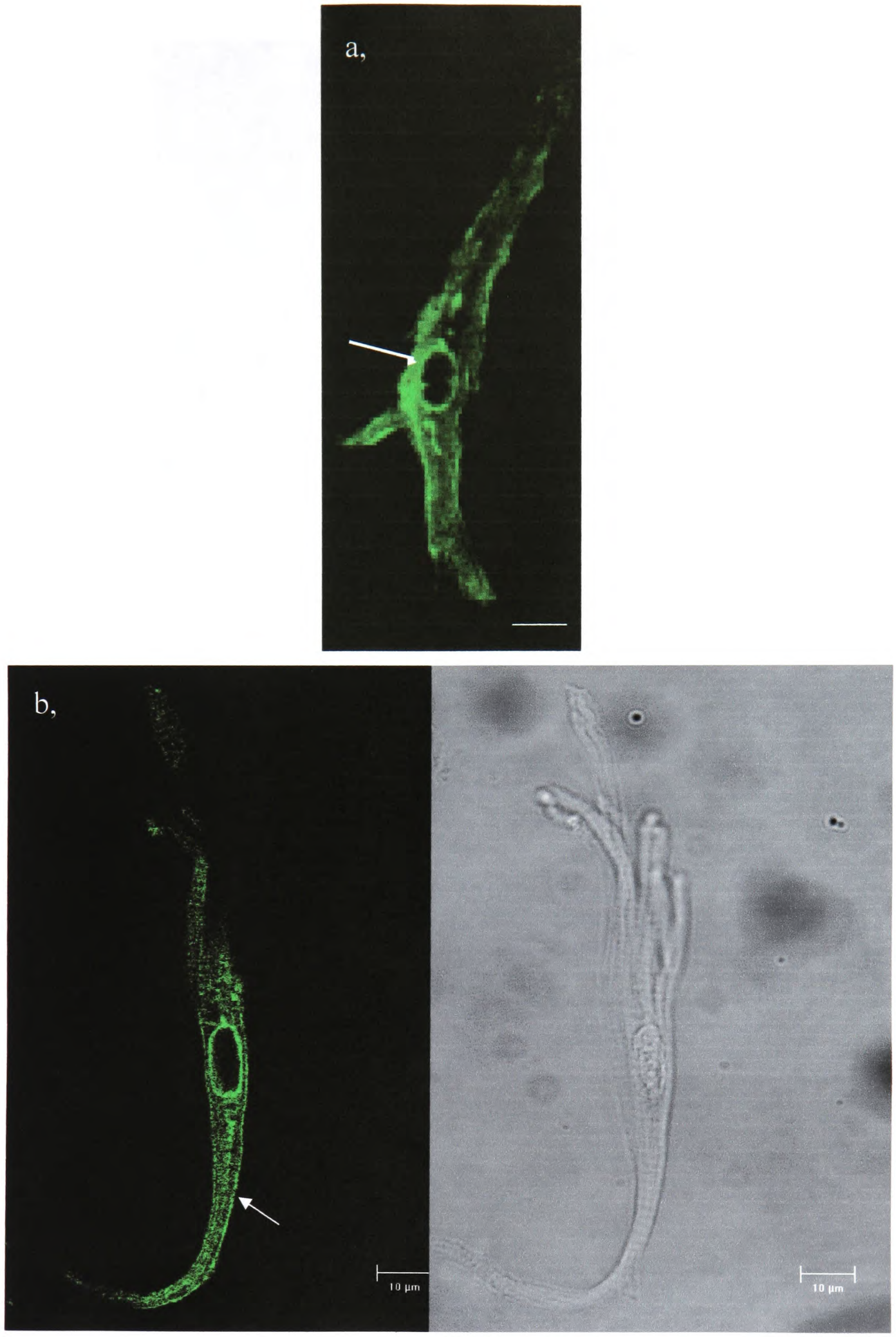

Figure 3.7

Fluorescence images of sino-atrial node cells labelled against PLB. Monoclonal antibody (Alomone, 1:100 dilution) was incubated with sino-atrial node cells for 1 hour. Note the presence of perinuclear and sarcolemmal labelling (see arrows), but the absence of axial banding, but possibly some organised cytosolic labelling. Both of these cells have numerous limbs, and these can be seen in the transmission image (right panel) of figure 3.6b. These limbs are often in different confocal planes and often do not appear in fluorescence images. Bar measures 10 µm.

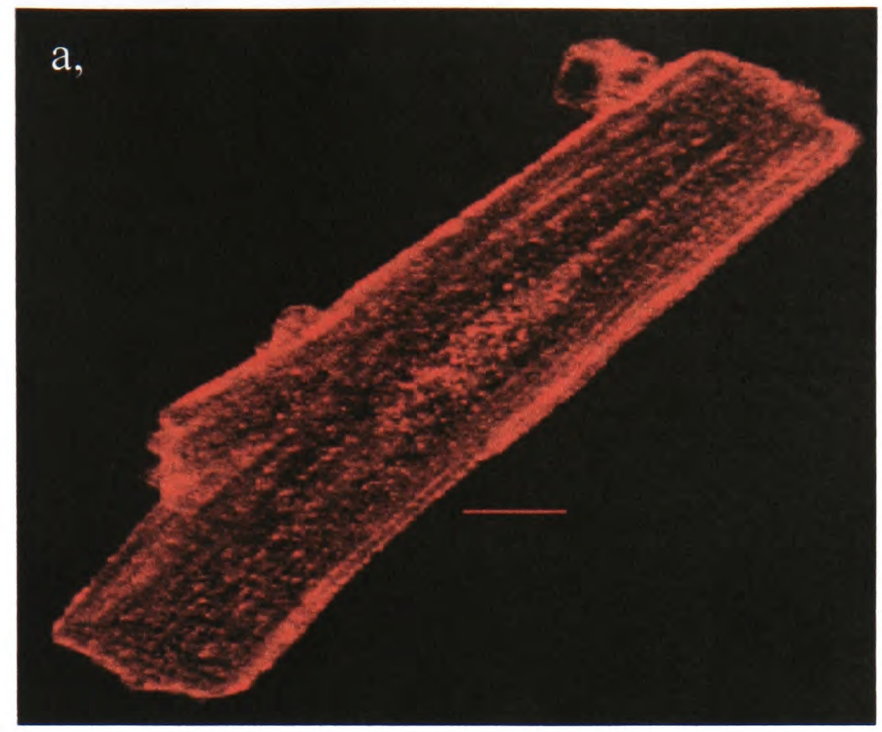

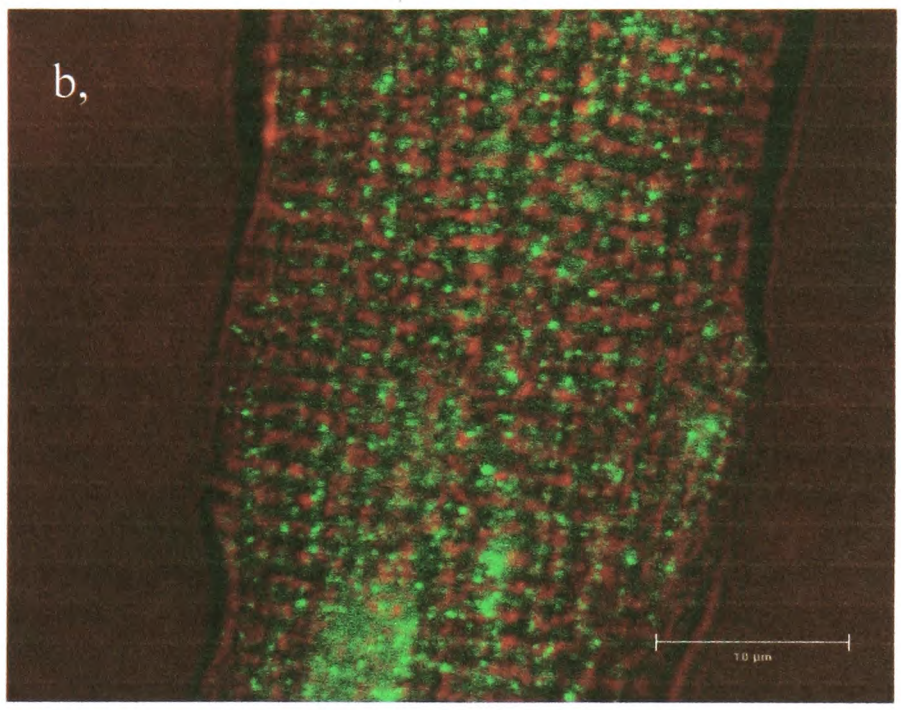

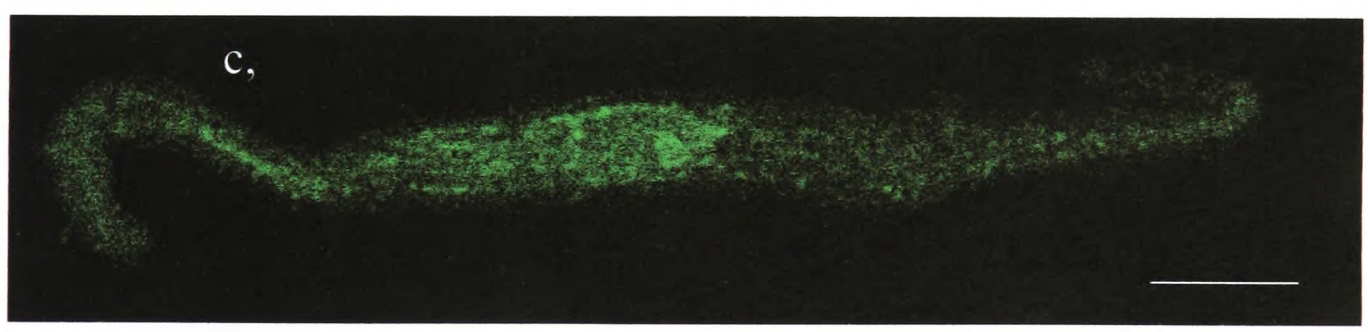

Figure 3.8 Page 108

I_{K1} labelling of a ventricular myocyte (a), overlay image comprising of fluorescence and transmission images (b; transmission appears red) and a fluorescence image of a sino-atrial node myocyte (c). The primary antibody (Alomone) was used at 1:100 dilution and incubated over a period of 1 hour. Note the sarcolemmal I_{K1} labelling (a) and the punctate spots of diameter less than 500 nm in the ventricular myocyte distributed throughout the interior, co-incidental with dark regions of the transmission image (b). There are no fluorescent spots in sino-atrial node cells (b), only diffuse cytoplasmic fluorescence. Bar measures 10 μm.

a,

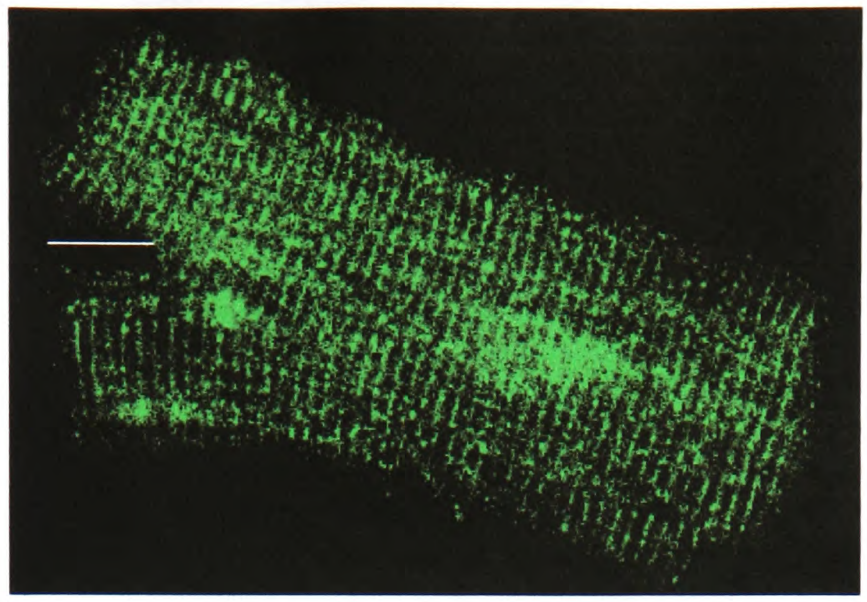

b,

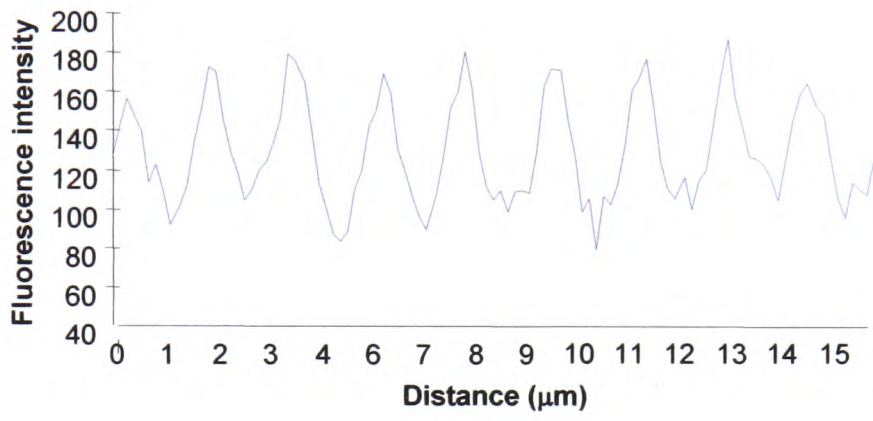

c,

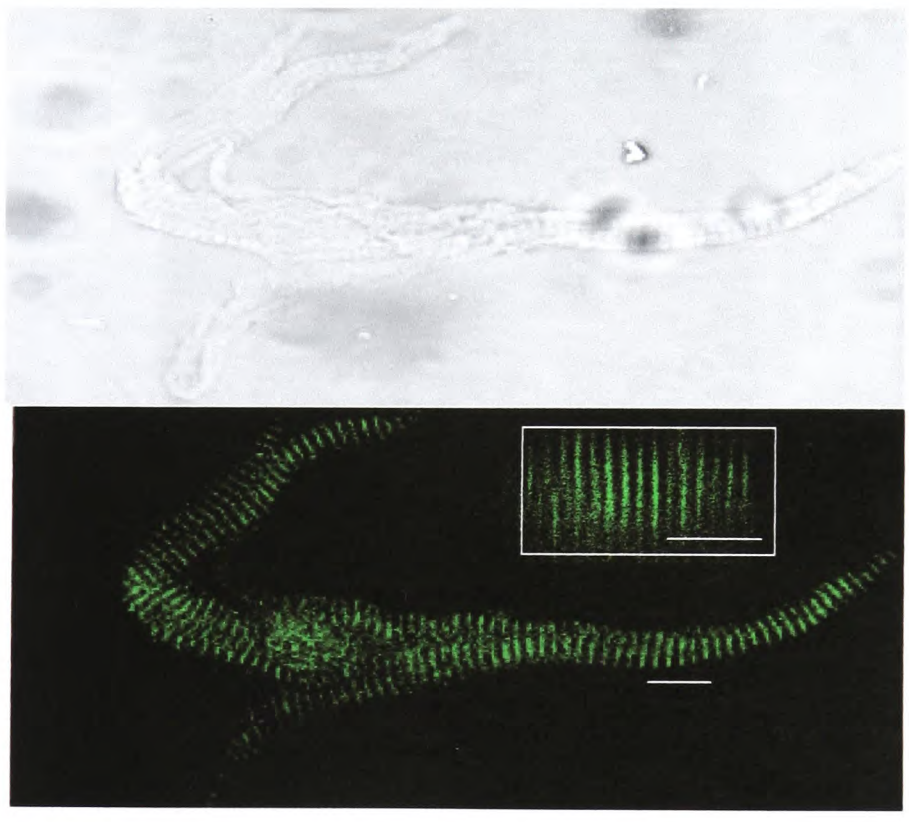

Figure 3.9

Fluorescence images of ERG (I_{Kr}) in ventricular (a) and sino-atrial node (c) myocytes, using triton permeabilisation. Monoclonal antibody (Alomone) 1:100 dilution. Bar measures 10 μm. Fluorescent labelling in ventricular cells was regularly distributed every 1.75-1.85 μm (b), when a fluorescent profile of the region adjacent to the bar (blue) in figure 3.8a was measured. Similar striations can be seen in the sino-atrial node cell (c, bottom panel), which lacks the transverse tubule network present in ventricular myocytes, but labels throughout the cytosol as indicated by the XZ confocal micrograph (inset), possibly indicating non-specific binding (see text).

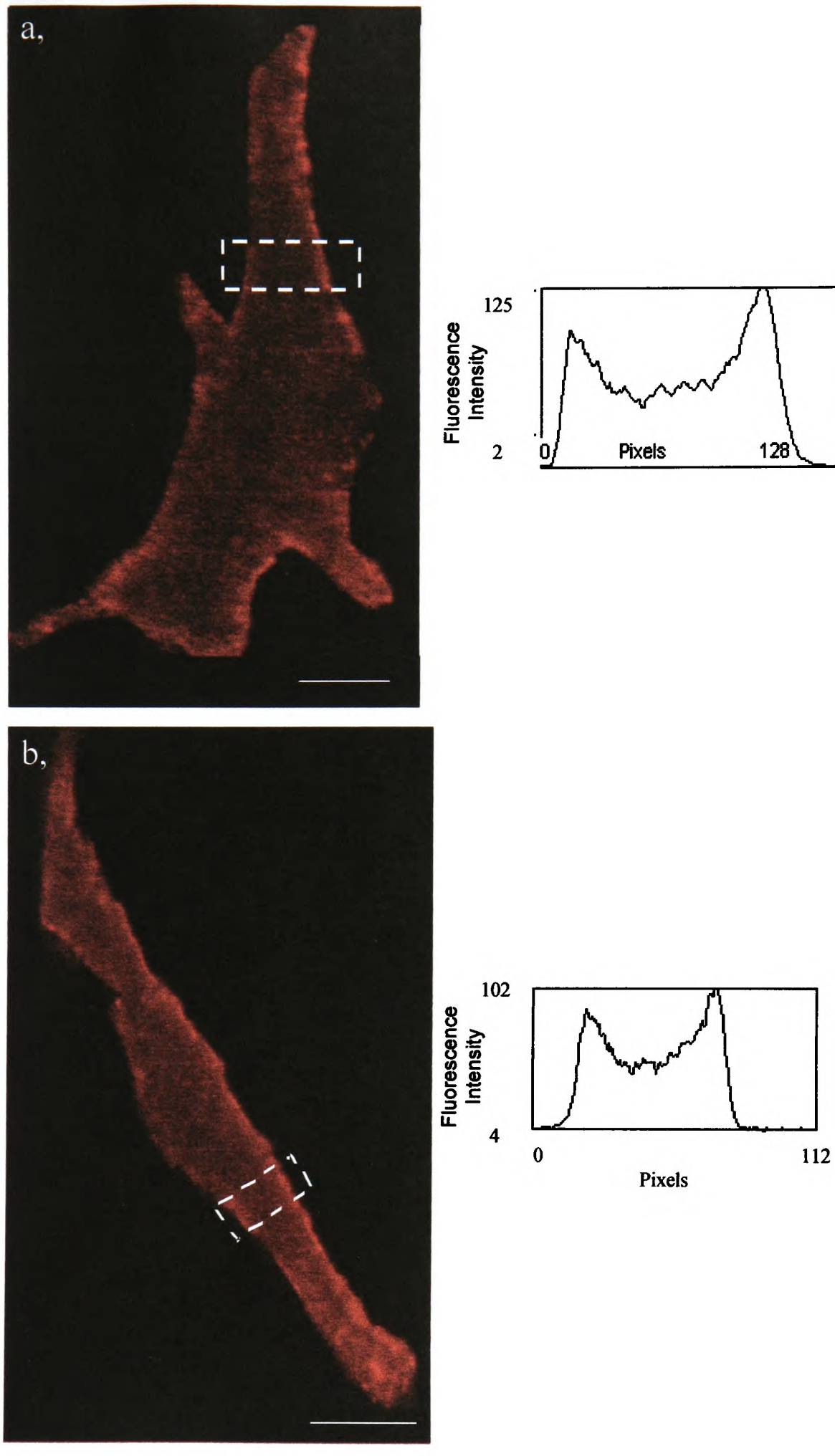

Figure 3.10

Fluorescence images of sino-atrial node cells labelled against human ERG (a and b). Monoclonal antibody 1:100 dilution (Alomone), using a protocol including freeze-thaw and alexa fluor conjugated secondary antibody. Bar measures 10 μm. Fluorescence is profiled in the region of the box indicated in both a and b, with peaks at the sarcolemma (see right panel).

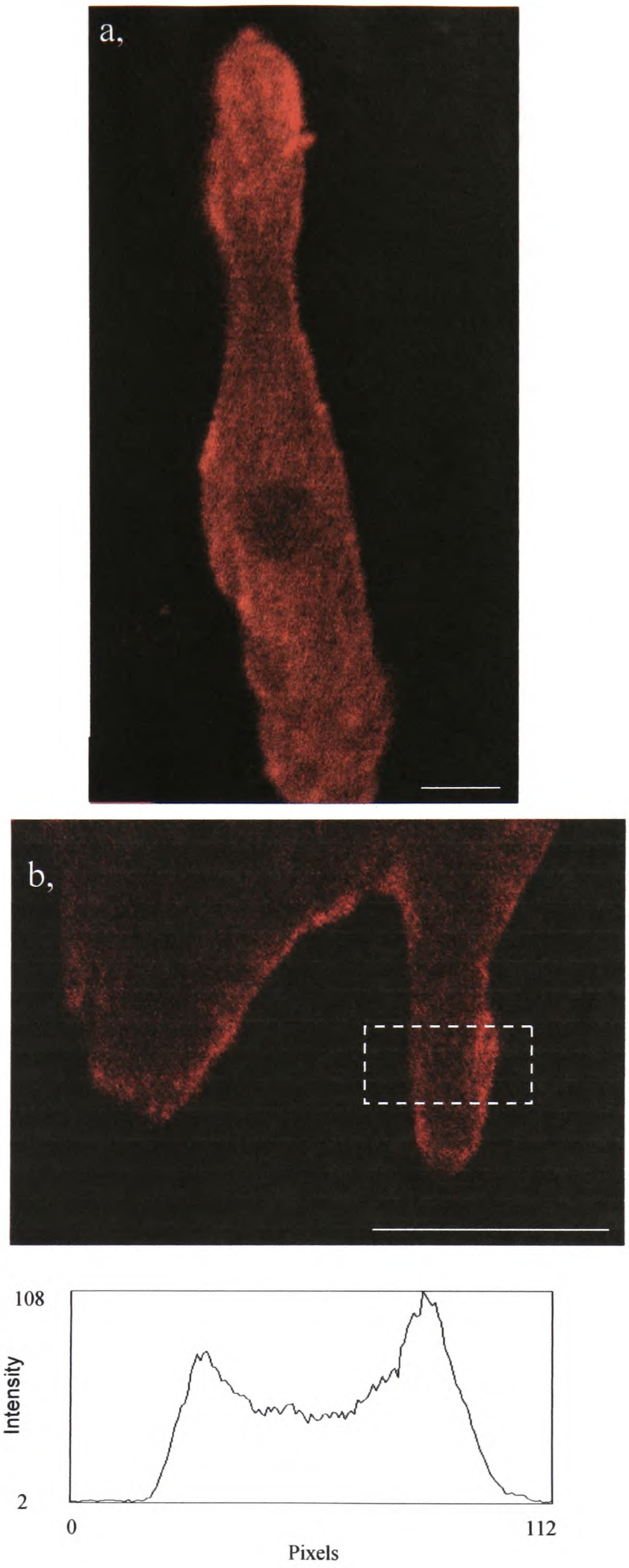

Figure 3.11 Page 111

Fluorescence images of atrial (a) and sino-atrial node cell (b) labelled against human ERG. Monoclonal antibody 1:100 dilution (Alomone), using a protocol including freeze-thaw permeabilisation and alexa fluor conjugated secondary antibody. Bar measures 10 μm, note that figure 3.10b is at a higher magnification. Fluorescence is profiled in the region of the box indicated and peaks are found at the sarcolemma (lower panel).

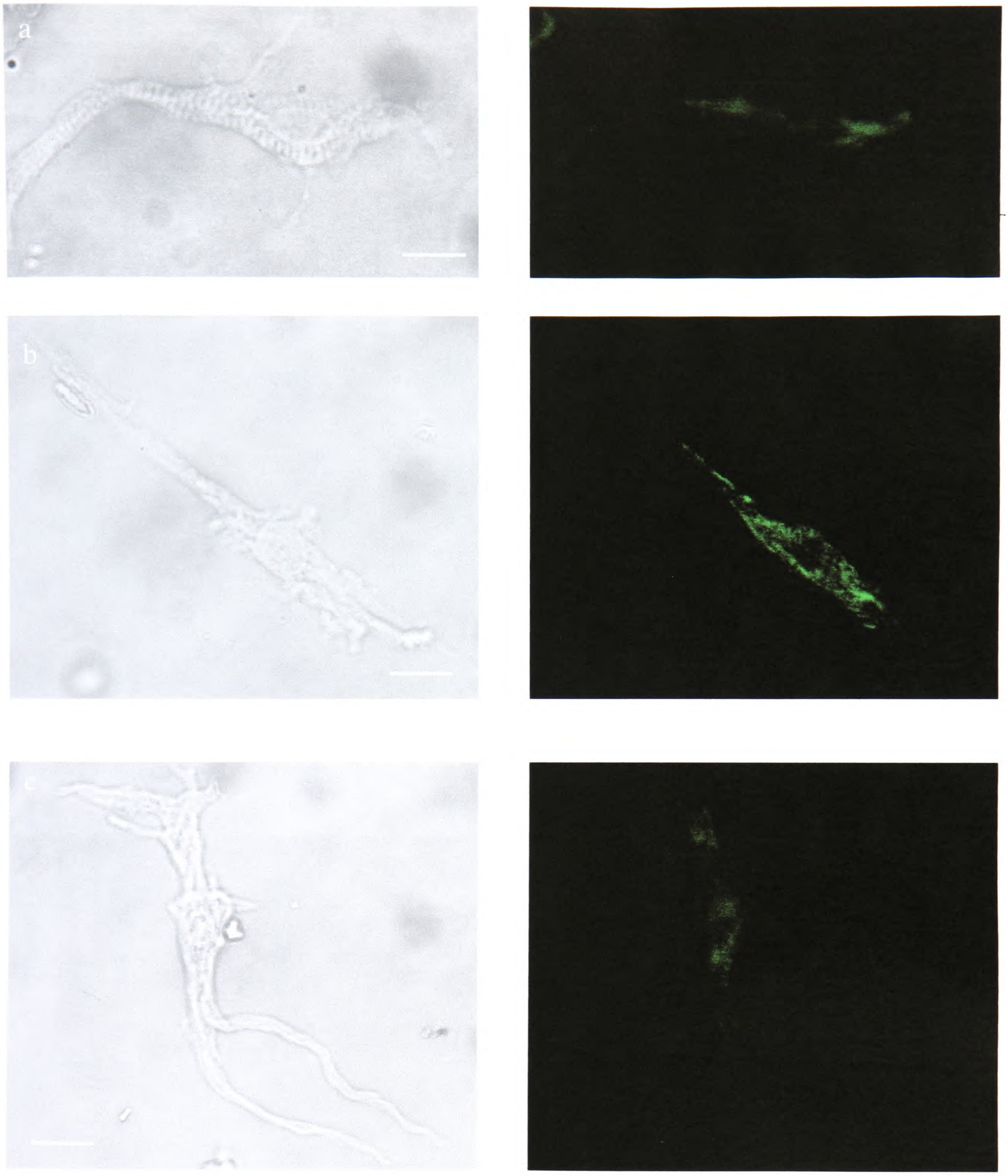

Figure 3.12

$KvLQT_1$ antibody labelling of sino-atrial node cells. The distinct sino-atrial node morphology can be seen in the left hand panel of each figure (a, b and c). These representative of a large population and appear to exhibit minimal fluoresence. A range of antibody dilutions were used, with freeze-thaw permeabilisation and Alexa fluor conjugated secondary antibody. Bar measures 10 μm.

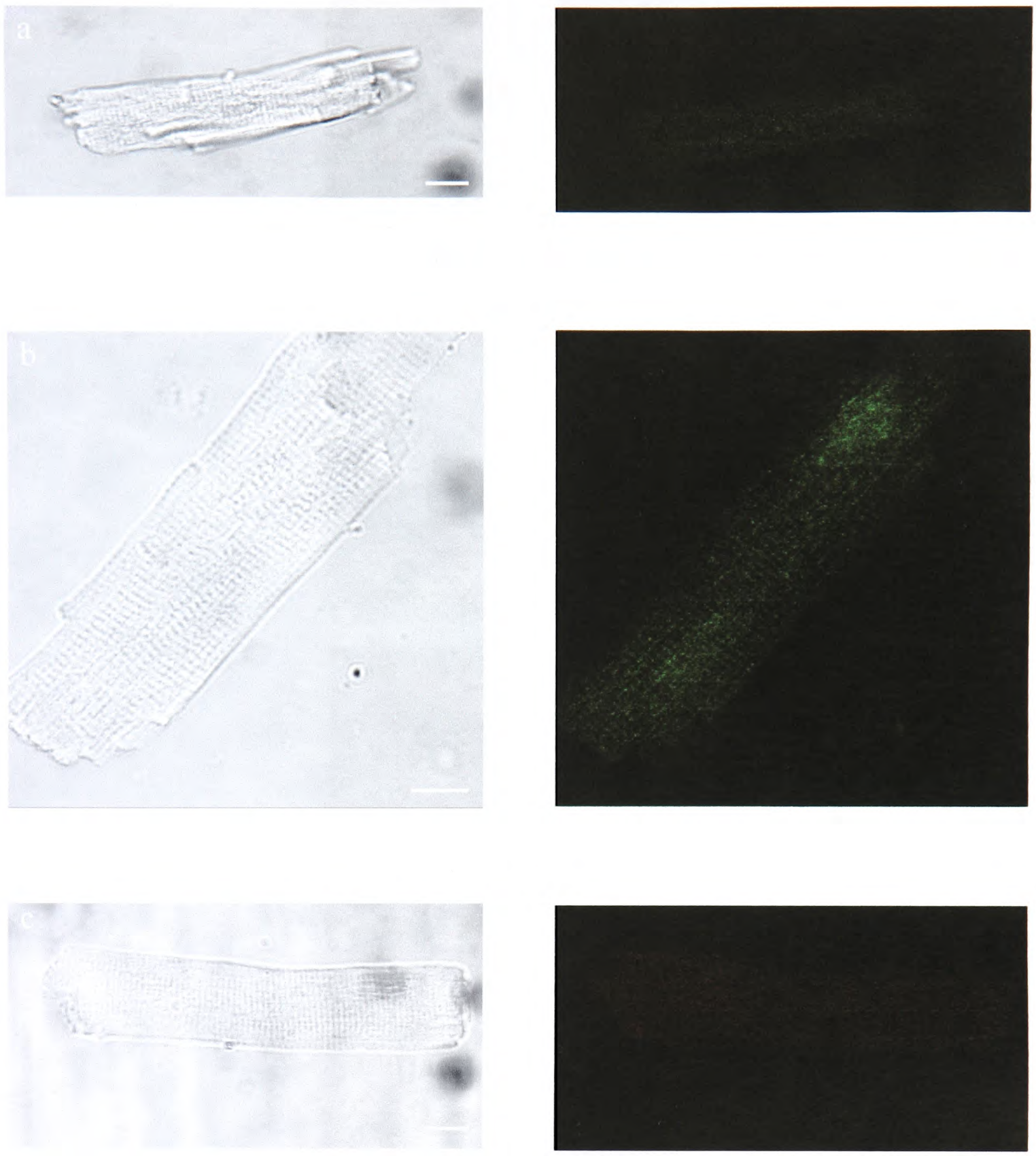

Figure 3.13

$KvLQT_1$ antibody labelling of ventricular myocytes. Three different ventricular myocytes (a, b and c) representing a larger population of myocytes, which appear to not fluoresence after immunohistochemcial investigation. Dilution of antibody in population ranged from 1:50 to 1:500. Freeze-thaw permeabilisation and Alexa fluor conjugated secondary antibody were used in association with this antibody. Bar measures 10 μm.

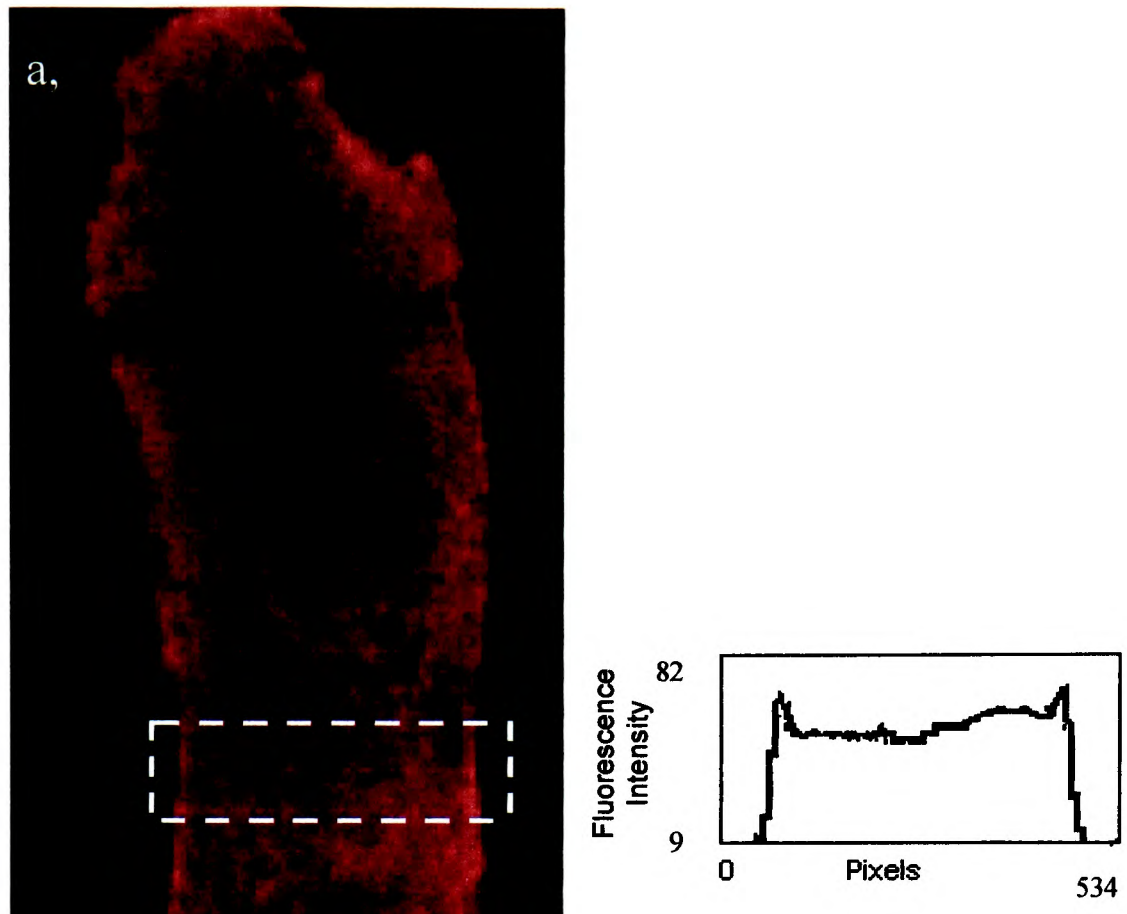

Figure 3.14

Fluorescence images of ventricular (a) and sino-atrial node cell (b) labelled against $KvLQT_1$. Polyclonal antibody against $KvLQT_1$ dilution 1:100 (Santa Cruz) was utilised, with a freeze-thaw permeabilisation procedure and alexa fluor conjugated secondary antibody. Bar measures 10 μm. Fluorescence is profiled in the region of the box indicated in both a and b, with both ventricular and sino-atrial node cells demonstrating fluorescence intensity peaks at the sarcolemma (see right panels). Note the lack of striations, as seen with other antibodies (figure 3.8), in either cell type.

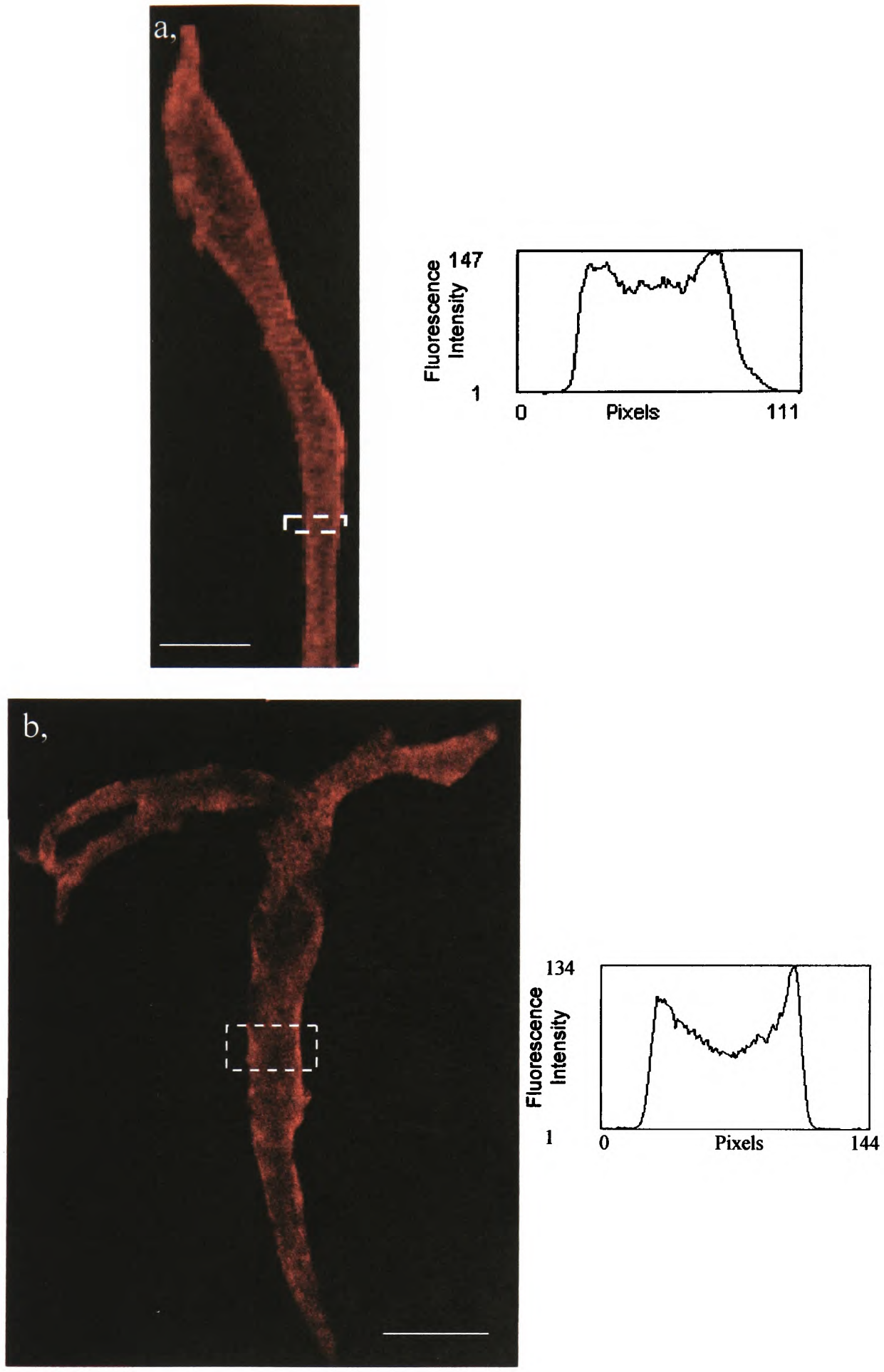

Figure 3.15 Page 115

Fluorescence images of sino-atrial node cells labelled against $KvLQT_1$. Polyclonal antibody against $KvLQT_1$ 1:100 dilution (Santa Cruz) were utilised, with freeze-thaw permeabilisation procedure and alexa fluor conjugated secondary antibody. Bar measures 10 μm. Fluorescence is profiled in the region of the box indicated in both a and b, with both sino-atrial node cells demonstrating fluorescence intensity peaks (if only slight in the case of figure 3.13a) at the sarcolemma (see right panels).

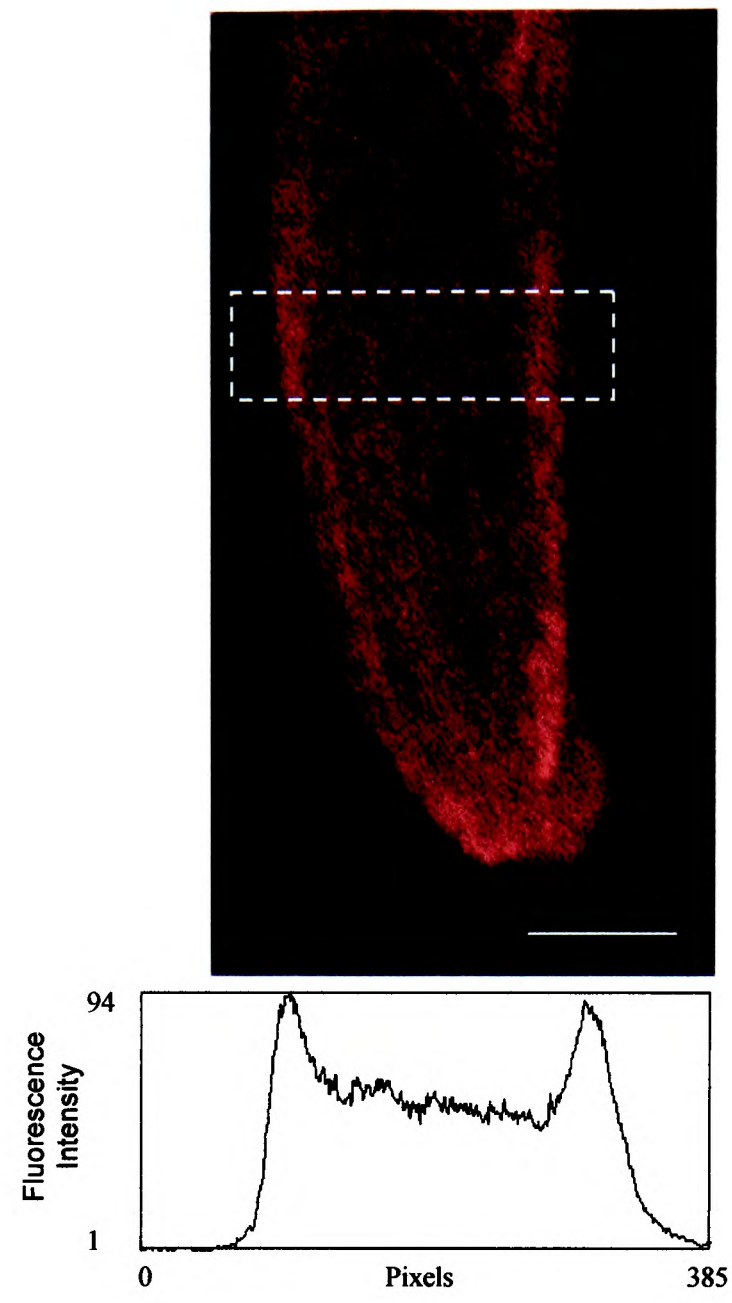

Figure 3.16 Page 116

Fluorescent labelling against $KvLQT_1$ focusing on a limb of a sino-atrial node cell. Polyclonal antibody against $KvLQT_1$ 1:100 dilution (Santa Cruz) was utilised, with a freeze-thaw permeabilisation procedure and alexa fluor conjugated secondary antibody. Bar measures 10 μm. Fluorescence is profiled in the region of the box below and sarcolemmal fluorescent peaks can be seen.

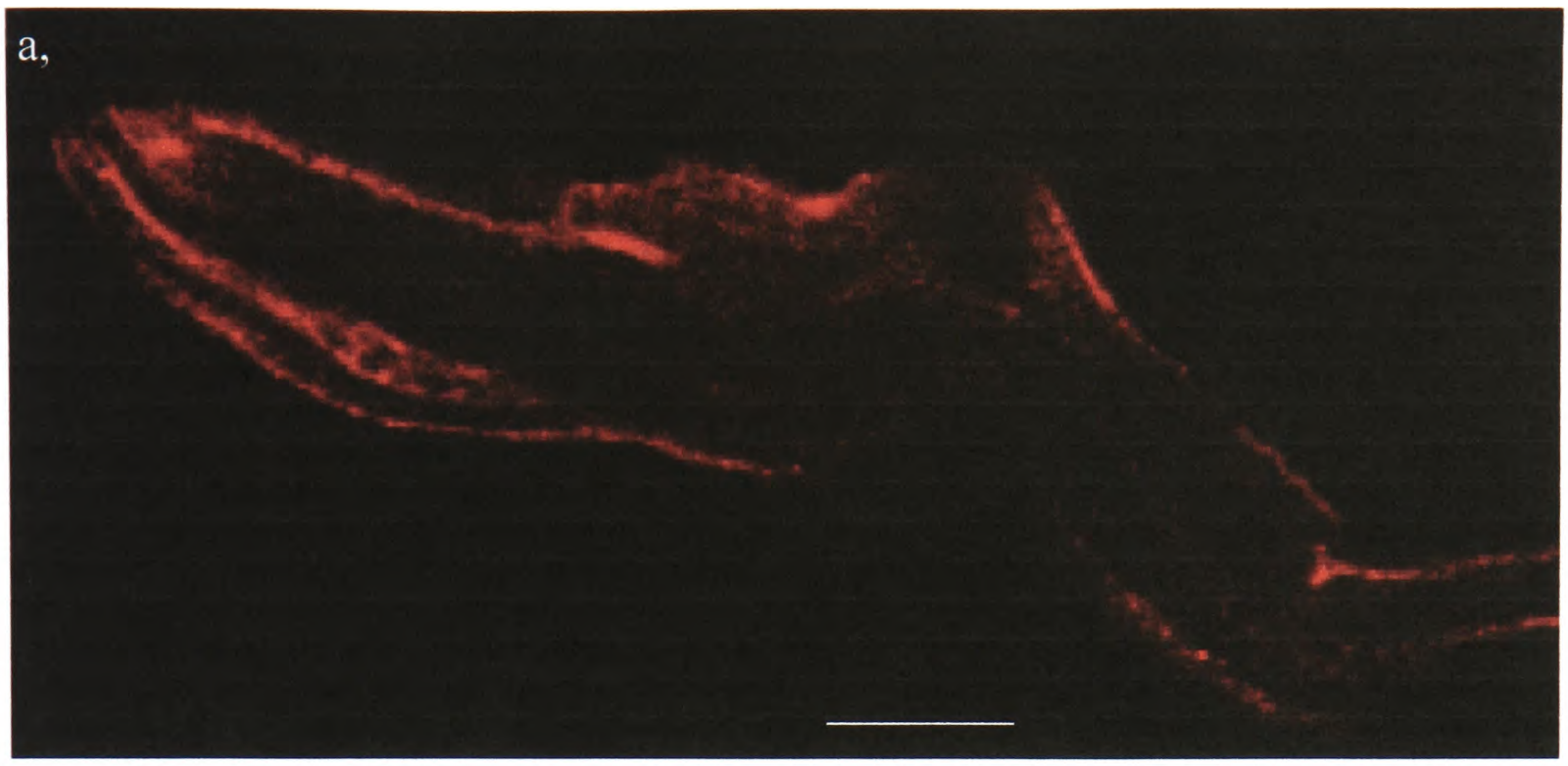

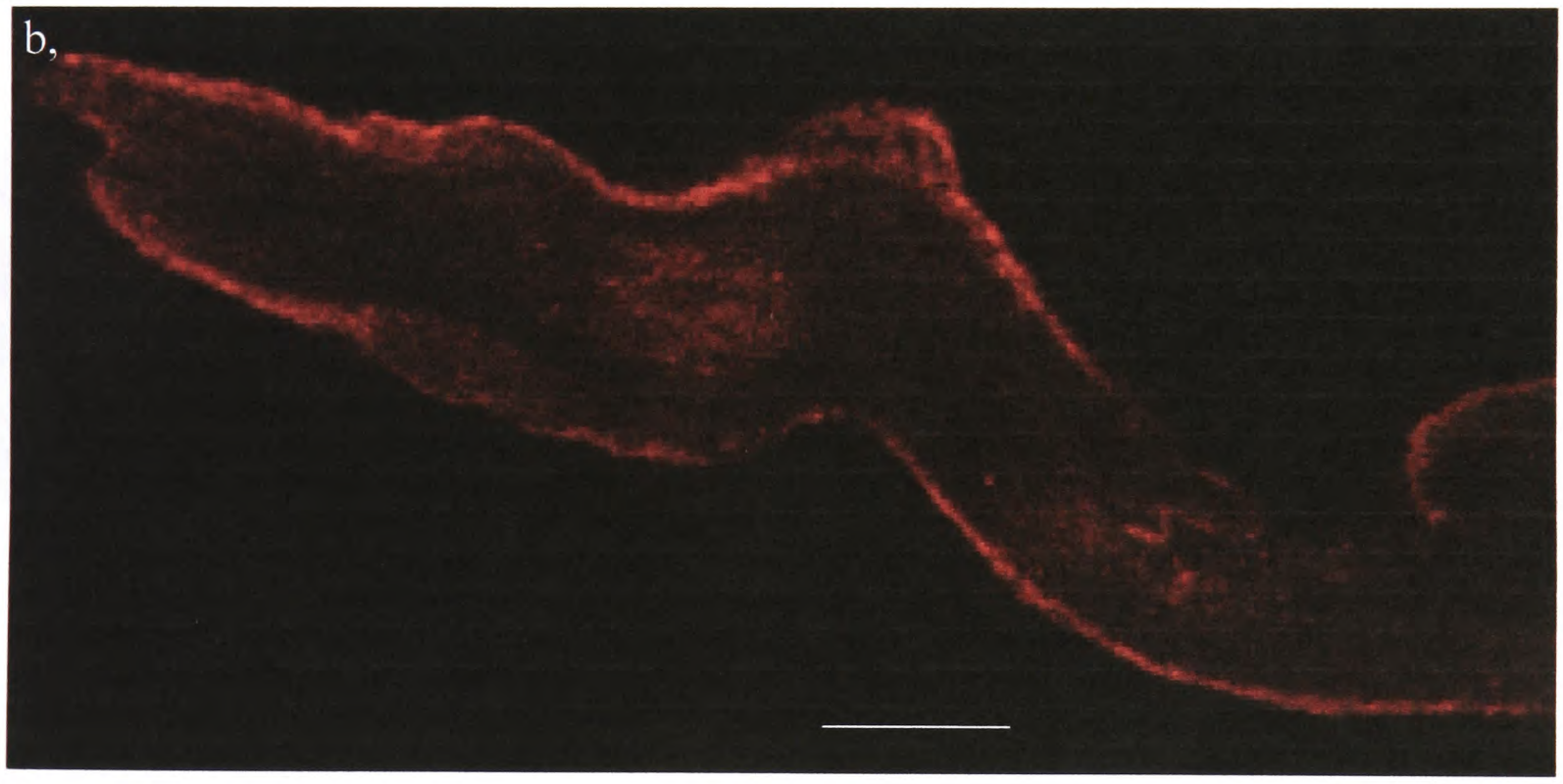

Figure 3.17

Fluorescent labelling of two confocal planes of the same sino-atrial node cell, labelled against $P2X_2$ purinergic receptors. Figure 4.15a is on a plane across the top of the sino-atrial node cell and figure 3.15b is in a more central region of the cell, identified by nuclear fluorescence. Polyclonal antibody (Alomone) dilution 1:100 against $P2X_2$ was utilised, with a freeze-thaw permeabilisation procedure and alexa fluor conjugated secondary antibody. Bar measures 10 μm. Fluorescence can be seen to enclose the cell, indicative of sarcolemmal labelling.

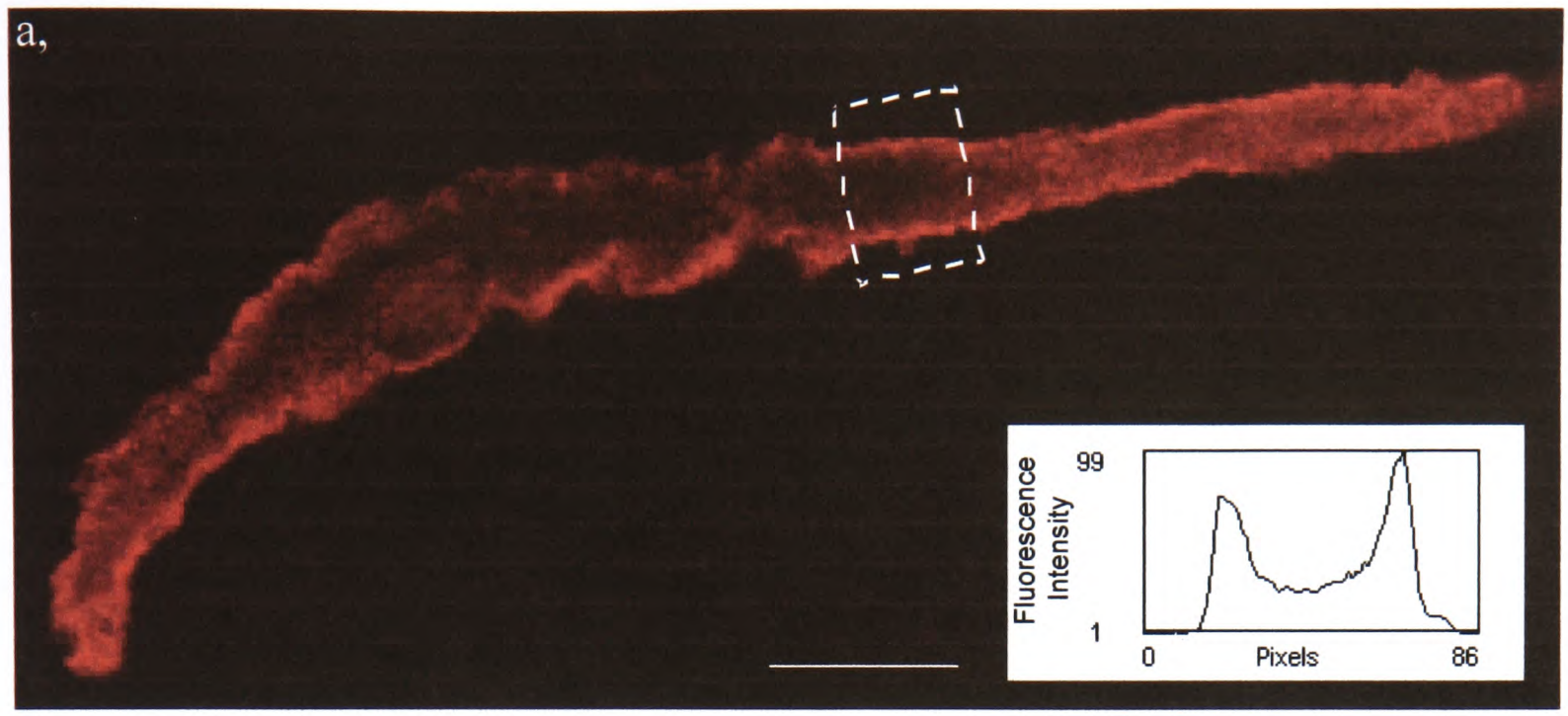

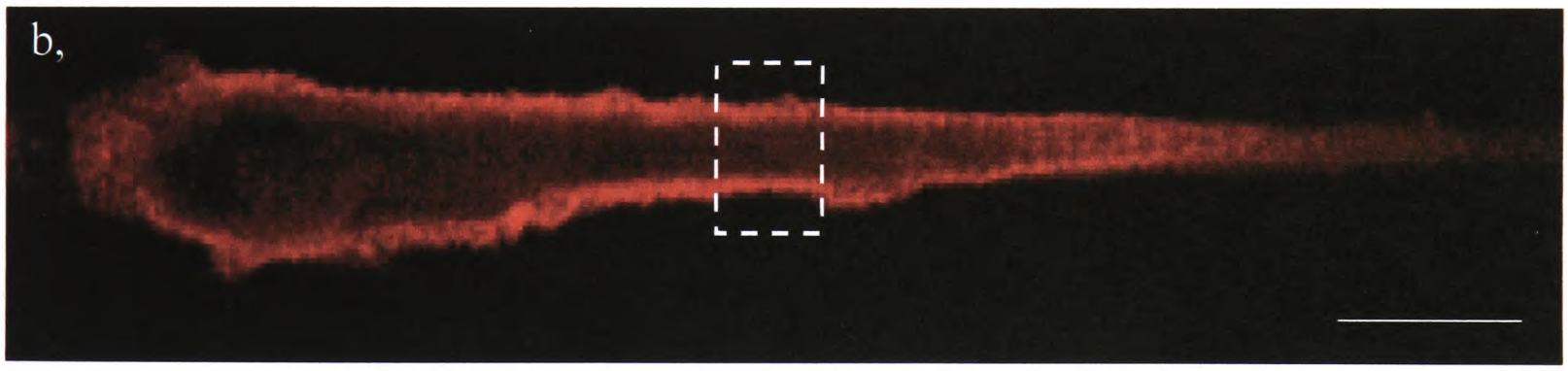

Figure 3.18 Page 118

Fluorescent labelling of two sino-atrial node cells (a and b), labelled against $P2X_2$ purinergic receptors. Polyclonal antibody against $P2X_2$ dilution 1:100 (Alomone) was utilised, with a freeze-thaw permeabilisation procedure and alexa fluor conjugated secondary antibody. Bar measures 10 μm. Fluorescence can be seen to enclose the cell, indicative of sarcolemmal labelling. Fluorescence is profiled in the region of the box and strong peaks at the edges of the sino-atrial node cell, indicate sarcolemmal localisation of $P2X_2$ receptors.

Antibody/probe	Target	Cell type	Localisation
Phalloidin	Actin	Ventricle	Z-line, absent at M-line
ER tracker	ER/SR	Ventricle	Absent at Z-line
Anti-PLB	Phospholamban	Ventricle Sino-atrial node	Z-line, sarcolemma, peri-nuclear and intercalated disks. Sarcolemma, peri-nuclear
Anti-I_{K1}	I_{K1}	Ventricle Sino-atrial node	Sarcolemmal and punctate spots None
Anti-ERG	ERG (I_{Kr})	Ventricle Sino-atrial node	Sarcolemmal Sarcolemmal
Anti-$KvLQT_1$ (made in-house)	$KvLQT_1$ (I_{Ks})	Ventricle Sino-atrial node	Non-specific Non-specific
Anti- $KvLQT_1$	$KvLQT_1$ (I_{Ks})	Ventricle Sino-atrial node	Sarcolemmal Sarcolemmal
Anti-$P2X_2$	$P2X_2$	Sino-atrial node	Sarcolemmal

Figure 3.19

Summary table of findings in this chapter. Cells were either isolated from the sino-atrial node region or from the ventricles.

CHAPTER 4: Description of I_K and other ionic currents

There have been many studies that have investigated cardiac I_K; the majority of have focused upon ventricular myocytes. However, there have been a number of groups that have studied the sino-atrial node and the role of I_K in this process (Anumonwo, Freeman et al. 1992); early studies used rabbit sino-atrial node cells (Giles and Shimoni 1989). Other species, such as guinea-pig (Anumonwo, Freeman et al. 1992), mouse (Mangoni and Nargeot 2001) and cat (Huser, Blatter et al. 2000), have only been studied in the last 10 years. The general mechanism of pacemaking appears similar in all species, although ion channel density (therefore action potential morphology) and precise regulation mechanisms are species dependent.

In the early 1990's (Sanguinetti and Jurkiewicz 1990) found guinea-pig ventricular I_K was a composite of more than one current (Noble and Tsien 1969), with different voltage and time dependent activation and distinct pharmacology; these components are known as I_{Kr} and I_{Ks}. Various groups continue to study whole I_K, without separating I_{Kr} and I_{Ks}. Descriptions of I_{Kr} using subtraction analysis has been pharmacologically accomplished using various class III anti-arrhythmic agents, such as E4031. But there is not a readily available and effective blocker of I_{Ks} and so it has not been as fully described. Some groups have used the chromanol derivative 293B (Bosch, Gaspo et al. 1998; Lei, Cooper et al. 2002), however a recent study by (Ding, Toyoda et al. 2002) has identified I_{Ks} blockade to be greater when the depolarisation is prolonged.

I_K was not investigated in guinea-pig sino-atrial cells until 1992 (Anumonwo, Freeman et al. 1992; Freeman, Kwok et al. 1992), when it was found to be substantially different to I_K described in guinea-pig ventricular myocytes (Heath and

Terrar 1996) and rabbit sino-atrial node I_K (Lei and Brown 1996). The relative expression of I_{Kr} and I_{Ks} varies both between tissue and species; I_{Kr} was found by Anumonwo, Freeman et al (1992) not to be a major component of the guinea-pig sino-atrial node I_K, as there was an absence of rectification at positive potentials (Sanguinetti and Jurkiewicz 1990; Clay, Ogbaghebriel et al. 1995; Heath and Terrar 1996; Howarth, Levi et al. 1996; Lei and Brown 1996). In addition, the same study found guinea-pig sino-atrial node I_K activated at more depolarised voltages (sigmoid with $V_{1/2}$ 32 ± 3 mV, reversal potential –65 ± 4 mV) than guinea pig ventricular and rabbit sino-atrial node cells, which both have a $V_{1/2}$ of approximately –25 mV (Matsuura, Ehara et al. 1987). Both activation and deactivation of guinea-pig sino-atrial node I_K are slow (approximately 0.5 and 2 sec respectively) and deactivation can be fitted with a biexponential curve with a bell-shaped voltage dependency around 0 mV. Matsuura, Ehara et al (2002) recently used the I_{Kr} specific blocker E4031 to describe I_{Kr} by subtraction analysis, identifying a $V_{1/2}$ of –26 mV and rectification at voltages positive to –50 mV; the I_K resistant E4031 (presumably I_{Ks}) was found to have a $V_{1/2}$ of 17 mV and display only slight rectification.

Sino-atrial node inward currents

I_f was originally defined in rabbit sino-atrial node cells (Brown, DiFrancesco et al. 1979), as a non-specific current that was increased upon hyperpolarisation. There has subsequently been much debate regarding the precise role of I_f in the sino-atrial node, as the very negative voltages which some groups find are required to substantially activate I_f, may not be relevant during pacemaking (Zhang and Vassalle 2001). However the group of Difrancesco and various others, have championed the role of I_f in pacemaking, after finding the $V_{1/2}$ of I_f to be –67 mV in rabbit sino-atrial

node cells and the value to be substantially shifted by cAMP (DiFrancesco and Tortora 1991). Cytosolic calcium has also been found to regulate, probably indirectly, I_f amplitude (Zaza, Maccaferri et al. 1991; Rigg, Heath et al. 2000). Blockade of I_f using ZD-7288 is not accompanied by inhibition of potassium current, which have previously been found with such agents as caesium (DiFrancesco and Ojeda 1980) and alinidine (BoSmith, Briggs et al. 1993).

The currents associated with calcium movement (I_{NCX}, I_{CaT} and I_{CaL}) have complex actions upon sino-atrial node cell. As calcium plays such a pivotal role in this cell type, diastolic calcium levels have been found to be directly related to beating rate (Ju and Allen 1999). Calcium extrusion via I_{NCX} is associated with depolarising current and may play an important role at various stages of the pacemaking cycle (Ju and Allen 1998; Lipsius, Huser et al. 2001; Vinogradova, Bogdanov et al. 2002). Calcium is being extruded in the diastolic period of the action potential and therefore I_{NCX} would provide a depolarising current at this stage. I_{NCX} can be inhibited by various agents, however one of the best ways to study I_{NCX} blockade is by a rapid reduction in extracellular sodium (Huser, Blatter et al. 2000). Such sodium removal techniques have been used to inhibit I_{NCX} have been found to rapidly and dramatically increase intracellular calcium concentration; this infers substantial I_{NCX}, as each calcium ion efflux would be associated with a stochastic depolarisation.

The role of I_{CaT} in pacemaking has been disputed and like other currents, the description of I_{CaT} has been hampered due to a lack of an appropriately specific blocker (Protas and Robinson 2000). Low concentrations of nickel (below 50 μM)

have been used by various groups and maybe the most appropriate I_{CaT} inhibitor (Satoh 1995; Huser, Blatter et al. 2000); in sino-atrial node cells of other species, nickel has been found to slightly reduce the rate of late diastolic depolarisation (Satoh 1995; Huser, Blatter et al. 2000). I_{CaT} has been found to activate at voltages as negative as –70 mV, being maximal between –50 and –30 mV, has been found to be of approximately 10 pA/pF in rat atrial myocytes (Leuranguer, Monteil et al. 2000).

I_{CaL} mediates the action potential upstroke of sino-atrial node cells, as functional fast sodium channels are absent, or voltage dependently inactivated, in most species. Voltages positive to –40 mV activate I_{CaL} and the take-off potential is a good indication of where the majority of sino-atrial node I_{CaL} becomes activated, whilst maximal I_{CaL} is achieved at 0 mV when the amplitude is approximately 12 pA/pF (Vinogradova, Zhou et al. 2000). This current has a number of good specific blockers, of which nifedipine is generally used. I_{CaL} mediated influx of calcium is thought to initiate the SR release of calcium, and the subsequent rise in cytosolic calcium results from the combined calcium entry and release. The blockade of I_{CaL} causes sino-atrial node quiescence by both abolishing action potentials and preventing actions of raised cytosolic calcium.

Various inward currents are activated during the sino-atrial node pacemaking cycle. During diastolic depolarisation I_f, I_{NCX} and I_{CaT} (plus others) slowly drive the membrane potential to depolarised voltages, activating the large I_{CaL} that mediates the sino-atrial node action potential upstroke. The rapid I_{CaL} mediated depolarisation activates I_K, both I_{Kr} and I_{Ks} components, which cause repolarisation. The decay of I_K

contributes to diastolic depolarisation by revealing the previously mention inward currents.

This chapter aims to describe ionic currents involved in the pacemaking of the guinea-pig sino-atrial node, focussing upon I_{Kr} and I_{Ks}, so that regulation and the β-adrenergic augmentation of these currents can subsequently be investigated.

Results

The delayed rectifier potassium current (I_K)

To investigate the effect of inhibiting the repolarising I_K upon the beating of the heart, a combination of E4031 (an I_{Kr} specific blocker) and thiopentone (which is a relatively selective inhibitor of I_{Ks}) were added to an organ bath containing isolated atrial preparations. Thiopentone has no effect upon I_{Kr} (Heath and Terrar 1996), but which causes an additional small reduction of calcium current at the concentration used. Atrial muscle contraction was recorded by a force transducer attached to one tip of the atria by a suture. The rate of beating of the atrial preparation was continuously monitored during the addition of the I_K inhibiting combination (5 μM E4031 and 200 μM thiopentone). The beating rate, measured in beats per minute (bpm) fell from 108 ± 4 (in the presence of E4031) to 39 ± 5 bpm ($n=7$, $P<0.05$) upon addition of the I_K blocking concoction (figure 4.1c), over a period of around 15 minutes (or when beating rate was stable), a reduction of 73 ± 5 % of control ($n=7$, $P<0.05$). In fact, 3 of the 7 atrial preparations developed oscillatory electrical (figure 4.1a) and contractile (figure 4.1b) activity in the presence of E4031 and thiopentone.

These effects are consistent with the importance of both components of I_K for pacemaking, though the small effects of thiopentone on calcium current complicate interpretation.

Electrophysiological description of I_K

I_K is an outward current that is activated upon depolarisation, having slow deactivation kinetics that result in a I_K tail current remaining after depolarisation has ceased (figure 4.2a/b); the magnitude of the tail current can be effectively used describe I_K amplitude (figure 4.2c). The membrane potential of a sino-atrial node cell can be controlled using voltage clamp techniques and by holding this cell at –40 mV and by introducing a step depolarisation of varying voltage (constant duration), the voltage dependent activation of I_K can be investigated (figure 4.2b). Activation of I_K was found to increase with the magnitude of depolarisation, and the relationship between I_K and membrane potential was sigmoidal (figure 4.3). This sigmoidal voltage relationship is the sum of the voltage dependencies of I_{Kr} and I_{Ks} and has been described previously (Sanguinetti and Jurkiewicz 1990; Anumonwo, Freeman et al. 1992; Heath and Terrar 1996). In experiments in which the maximum depolarisation was +40 mV (1000 ms in duration), curve fitting indicated a voltage of half-maximal activation ($V_{1/2}$) to be 6 ± 3 mV and the slope factor of this curve to be 14 ± 4 mV (figure 4.3a, n=14). The maximal I_K current was activated upon depolarisation to +40 mV and was 267 ± 55 pA. In a similar set of experiments encompassing more depolarised potentials (up to + 80 mV), $V_{1/2}$ was found to be 8 ± 3 mV, with a slope factor of 22 ± 2 mV (figure 4.3b, n=6).

The activation of outward current during a depolarising episode was also investigated. The current during the pulse may be composed of other currents in addition to I_K, but comparisons with I_K measured from tail currents can be made. Exponential curves (Methods, page 62) were fitted to the activating outward current, after the initial, 'instantaneous' inward current (including I_{CaL} and capacitance transient), at each voltage in 9 cells (figure 4.4a). Data indicated that the amplitude of the exponential increased rapidly (figure 4.4b), which was linear at voltages more depolarised than –10 and the time-constants of outward current activation composed a near bell-shaped curve around 0 mV (figure 4.4c, 532 ± 87 ms). The relationship of exponential amplitude to voltage, is similar to the current-voltage relationship described by the I_K tail currents, although guinea-pig sino-atrial node I_K is know to activate at relatively negative potentials and display rectification at positive (Nerbonne 2000).

I_K tail current deactivation can also be quantified using a bi-exponential function (Methods, page 62). To study the voltage dependence of tail current decay, the potential to which the cell was repolarised (from +40 mV) was varied over the range -60 to –10 mV (figure 4.5a). Bi-exponential fitting to I_K tail currents revealed two time constants to be longest at –20 mV (n=6); 298 ± 48 and 1731 ± 277 ms, referred to as Tau_1 and Tau_2 respectively. Both time-constants were abbreviated at more negative potentials (figure 4.5b). Tau_2 appeared to be relatively prolonged at –60 mV, which may perhaps be the consequence of I_f activation. Amp_2 increased as the voltage became more depolarised and was maximal at –20 mV (figure 4.5c, 131 ± 29 pA), whereas the amplitude of the other component (Amp_1) was relatively constant

around 130 pA, except at –60 and –10 mV where amplitude decreased slightly.

In addition to studying voltage dependent activation of I_K, the effect of extending the duration of depolarisation was also investigated (with a constant depolarisation). In all of these experiments the membrane was depolarised to +40 mV, as a large outward tail current was activated at this potential and could easily be measured. Depolarisations as brief as 10 ms and as long as 700 ms (figure 4.2a) were used to activate I_K (figure 4.6a). At the holding potential of –40 mV, de-activation of calcium currents and capacity transients were rapid, in comparison with the slowly de-activating potassium current. I_{NCX} can complicate the measurement of outward tail currents upon very brief depolarisations. The general trend is that when the duration of depolarisations was extended, I_K was increased. The time-dependent activation of I_K showed two phases (n=28) reflecting activation of I_{Kr} and I_{Ks} (Anumonwo, Freeman et al. 1992). The x-axis, labelled pulse duration, contains a section (0 to 105 ms) with an expanded scale to illustrate activation of the rapid I_K component (figure 4.6c).

An initial rapid phase of I_K activation was observed during the first 30/40 ms, with a subsequent slower secondary phase of activation at durations in excess of approximately 100 ms that continues to increase as duration was extended. A 700 ms depolarisation activated I_K tail currents which were 209 ± 40 pA (n=11), however currents are expressed as a % of the maximum current recorded from that cell (generally 700 ms), e.g. a 40 ms depolarisation activated tail currents of 17 ± 2 % of control max current (figure 4.6b, 31 ± 6 pA). Tail current amplitude is related to outward current during the depolarisation, when plotting tail current amplitude

against step current amplitude (figure 4.7c), a linear relationship was described (y=0.34x – 2.2, r=0.95, n=10, 96 points).

To further investigate the possible contribution of multiple components to I_K, an envelope of tails test was used (figure 4.8). This describes the tail current amplitude, relative to the outward current activated during the depolarisation, against the duration of depolarisation; if I_K is composed of just one component, then the ratio of tail to pulse current, would remain constant irrelevant of depolarisation duration. After brief depolarisations the tail current amplitude was on average slightly larger than the current activated during the depolarisation; therefore the ratio was >1 (1.16 ± 0.31 at 10 ms, n=10). As the duration of depolarisation was prolonged the tail current amplitude became progressively smaller relative to the pulse current, after a 50 ms depolarisation the tail/step current ratio was 0.55 ± 0.08. This ratio value subsequently became constant between 0.42 and 0.44 as the depolarisation duration was extended beyond 70 ms (figure 4.8b). The inconsistent ratio indicates there was more than one current contributing to the depolarisation activated outward current.

The reversal potential of I_K was investigated by depolarisation to +40 mV, followed by repolarisation to voltages ranging between –100 and –20 mV (figure 4.9). To investigate the I_K reversal potential the direction and amplitude of the instantaneous tail current were plotted against repolarisation voltage. This indicates the voltage at which current does not flow through the channel underlying I_K, which was activated in the preceding depolarisation and this gives information about the ionic species and selectivity of the channel. A linear relationship (r=0.996) between –100 and –20 mV was found (figure 4.9c), which were associated with inward and

outward tail currents respectively, the voltage at which there was no current (the reversal potential) was found to be –70 ± 2 mV (n=7).

From multiple electrophysiological recordings of I_K, an average of amplitude and deactivation kinetics has been developed. By simulating the effects of an action potential activating I_K, with a tail current (359 pA) that subsequently bi-exponentially decays (time-constants 175 and 839 ms) upon repolarisation to the voltage clamp holding potential of –40 mV (n=62), a plot of I_K against time after the action potential can be created. In this model it takes 230 ms for the I_K tail current to decay by ½, 590 ms for ¾ and 1113 ms to reduce to a $^1/_8$ of its original amplitude (5.10a). A sino-atrial node action potential generally repolarises to approximately –60 mV (Rigg, Heath et al. 2000), therefore I_K tail current amplitudes and decay kinetics have been recorded upon repolarisation to various voltages including –60 mV; time-constants at –60 mV are 185 and 1493 ms (amplitudes 108 and 30 pA respectively). By fitting these into the bi-exponential function an I_K tail current decay plot can be developed for repolarisation to –60 mV (figure 4.10b). The guinea-pig sino-atrial node spontaneously gives rise to an action potential every 300 to 500 ms (120-200 bpm). Therefore a significant amount of the I_K tail current (between ½ and ¼) will fail to decay before the activation of the subsequent action potential. As action potentials are initiated the amount of residual decaying I_K tail current, will increase until the system becomes stable. The effects of subsequent depolarisations activating I_K have been modelled at different beating rates, as the faster the beating rate, the greater the amount of residual I_K. I_K was simulated for a the period of 10 action potentials, with I_K deactivation kinetics for –60 mV (as measured above); the effect of beating rate upon I_K accumulation was briefly investigated. When a 120 bpm rate (action potential

every 500 ms) was applied, the least I_K (diastolic measurement) after 9 action potentials was 82 pA (arrow in figure 4.10b). Whereas the simulated beating rate of 180 bpm (300 ms interval) produced a minimum I_K after 9 action potentials to be 100 pA (figure 4.10c). The higher simulated beating rate caused an apparent increase in diastolic I_K. The amplitude of I_K activated during the simulated action potential was the same each action potential, but after the first action potential there was a residual I_K component which increased with each subsequent action potential, until an equilibrium was reach. This representation is very basic, contains a number of assumptions, but it does however indicate the possible amounts of I_K flowing during all stages of the sino-atrial node action potential.

The rapid component of the delayed rectifier potassium current (I_{Kr})

When atrial preparations were exposed to increasing concentrations of the I_{Kr} specific inhibitor E4031, the rate of beating of the preparations was concentration-dependently reduced (figure 4.11b). At low nM E4031 concentrations there was only a small effect upon the spontaneous beating rate of the atrial preparations, but as the E4031 concentrations were increased to above 50 nM the rate of beating was significantly reduced. This concentration dependent trend continued until the low μM range, where the E4031 dependent reduction in rate appears to be maximal, causing a 25 ± 2 % decrease from control beating rates (figure 4.11a, n=5). The E4031 concentration dependent reduction in beating rate was therefore a sigmoidal relationship and the concentration required to attain half-maximal blockade was found to be 64 ± 26 nM (figure 4.11c, n=5).

When isolated sino-atrial node cells were exposed to 5 μM E4031, the spontaneous development of action potentials (measured using current clamp) slowed or failed (figure 4.12c). E4031 was introduced to 9 sino-atrial node cells with action potential values; overshoot 9 ± 5 mV, most diastolic potential -59 ± 3 mV, action potential amplitude 68 ± 8 mV, beating rate 116 ± 8 bpm, APD_{50} 83 ± 7 ms and APD_{90} 140 ± 3 ms. From these data the nodal nature of the cells tested can be implied. 8 of 9 of these isolated sino-atrial node cells became quiescent after exposure to E4031, however the period before the failing of beating varied between approximately 30 seconds (3 of 8), within 3 minutes (4 of 8) and 4 minutes 30 seconds (1 of 8). Only 1 of 9 sino-atrial node cells continued to beat for a prolonged period after being exposed to 5 μM E4031, however the beating rate of this cell was halved within a minute (165 to 84 bpm). On average E4031 caused a reduction in beating rate of isolated sino-atrial node cells, from 116 ± 8 to 98 ± 6 bpm ($P<0.05$, $n=9$) after 1 minute exposure to E4031 (or just prior to cessation in 3 of 9 cells), which was 86 ± 5 % of control beating rate ($P<0.05$, $n=9$). In addition the rate of repolarisation of the sino-atrial node action potential is prolonged by E4031, with a transitory increase in the APD_{50} during E4031 wash-in and a stable prolongation of the APD_{90} from 140 ± 3 to 152 ± 2 ms ($n=9$, $P<0.05$).

Further evidence for the presence of I_{Kr} and I_{Ks} was obtained by the using E4031, when the sino-atrial node cells were voltage clamped, to eliminate the rapid component of I_K. The current after a 40 ms pulse was reduced from 16 ± 2 % (30 ± 4 pA) of max control current to 2 ± 1 % (4 ± 1 pA; $n=9$, $P<0.05$). By using a repetitive washin protocol containing two depolarisations, one of 40 ms duration and the other 700 ms long (both to +40 mV), the presence of I_{Kr} and I_{Ks} can be investigated. In

control conditions the brief depolarisation activated a prolonged outward tail current upon repolarisation (figure 4.13a) of similar amplitude to the outward current during the depolarisation. A prolonged depolarisation activated a very large current and upon repolarisation a tail current (of much smaller amplitude to the pulse current) remained. The currents measured were expressed on a time-scale (x-axis) that was expanded between 0 and 500 ms to aid illustration of the rapid currents. Upon addition of 5 μM E4031, although the pulse currents appeared similar to control, the outward tail current activated by the brief depolarisation was abolished (figure 4.13a). There was also a small reduction in the pulse and the tail current amplitude associated with the prolonged depolarisation. The effects of E4031 upon the currents of the sino-atrial node cell are representative of the whole population studied.

When a plot of tail current amplitude against pulse current (at any depolarisation duration) was developed in the presence of E4031, it is noticeable that tail current are relatively small until the pulse current is approaching 250 pA (see arrow, figure 4.13b) and so linearly fitting this relationship will be imprecise. However, an imperfect linear relationship can be identified with the equation $y = 0.24 x - 51.42$ ($r=0.86$, 96 samples), this can be compared to control plot which was linearly fitted with the curve $y = 0.34 x - 2.2$ ($r=0.95$, 96 points); this indicates that the tail current amplitude is smaller relative to the pulse current in the presence of E4301 (probably underestimated due to imperfect fitting).

To investigate the contribution of I_{Kr} and I_{Ks}, an envelope of tails test was again used. When this test was used previously, the ratio of tail to pulse current was variable; being large (>1) initially and subsequently reducing to between 0.4 and 0.45,

after depolarisations greater than 70 ms. The envelope of tails test was again applied to currents developed upon depolarisation of variable duration, in the presence of the I_{Kr} selective inhibitor E4031 (5 μM). These data were compared to the previous data and the relationships are obviously different (figure 4.14). After brief depolarisations in the presence of E4031 the tail/pulse current ratio was not greater than 0.4 and the ratio remained between 0.09 and 0.28 at longer duration depolarisation. The tail/pulse current ratio in the presence of E4031 was significantly reduced with depolarisations of 10 to 90 ms ($P<0.05$, except 70 ms), when compared to the control ratio (control n=10, E4301 n=6). At durations in excess of 80 ms there was no significant difference in the tail/pulse current ratio in the presence or absence of E4031.

I_K tail current deactivation kinetics were studied in the presence of 5 μM E4031 (control data were taken in the same cells), after a 1 second depolarisation to +40 mV (figure 4.15). The results of fitting bi-exponential curves to the decaying outward current are shown in figure 4.15b, time-constants of 145 ± 18 and 621 ± 96 ms in control conditions were described and upon E4031 addition to the same cells the values were altered to 185 ± 18 and 880 ± 114 ms ($P<0.05$, n=12). Amp_1 and Amp_2 were 156 ± 46 and 86 ± 19 pA in control, whilst after 5 minute exposure to E4031 they were 161 ± 47 ($P>0.05$ and 49 ± 9 ($P<0.05$, n=12).

5 μM E4031 has been identified as an I_{Kr} specific inhibitor, hence subtraction of the E4031 resistant current from the current in control conditions, provides an accurate description of the E4031 sensitive current; this enables precise measurement of voltage and time-dependency of I_{Kr}. To explain further, the control I_K current

recorded is composed of I_{Kr}, I_{Ks} and some other currents, the current resistant to E4031 will be mainly I_{Ks} (possible plus I_{NCX}, I_{CaT}). The subtraction of the E4031 resistant current (I_{Ks} and other) from control (I_{Kr}, I_{Ks} and other) provides a selective record of I_{Kr}.

E4031 sensitive currents were recorded at a range of depolarised voltages, 1000 ms step at -30 to +40 mV (figure 4.16a). The I_{Kr} tail current amplitude increased as the voltage step became more depolarised (up to +10 mV), although at positive potentials (> +10 mV) the I_{Kr} tail current did not enlarge, but became smaller in amplitude (figure 4.16b). At negative voltages the E4031 sensitive current is activated to a greater degree than I_K (figure 4.17a); the E4031 sensitive has a more negative activation threshold than that of I_K. The slope relationship between voltage (-30 to –10 mV) and E4031 sensitive current is steep, indicating rapid voltage–dependent activation (figure 4.18a). The voltage which evoked greatest E4031 sensitive current varied between cells, ranging from –20 to +40 mV, but on average (of 22 cells) the maximum E4031 sensitive current was recorded at +10 ± 4 mV (58 ± 15 pA, n=22). However, this variation results in the E4031 sensitive current at +10 mV being defined as 80 ± 4 % (figure 4.17a). At voltages between 0 and +20 mV (and possibly –10 mV) the voltage dependency of the E4031 sensitive current is insubstantial, as the current is not increased as the depolarisation is extended. The E4031 sensitive current induced by depolarisations greater than +20 mV, have a negative voltage dependency; depolarisation causes a reduction in the E4031 sensitive current (figure 4.17b). This reduction in current at depolarised voltages is a ¼ of the maximum current (figure 4.17a). At depolarised voltages of less than +20 mV, the E4031 sensitive current was relatively larger than I_K. However, at voltages greater

than +20 mV the E4031 sensitive current was diminished, whilst the voltage dependent activation of I_K is progressing. At positive potentials (greater than 0 mV) the relative contribution of the E4031 sensitive current (I_{Kr}) to I_K would reduce therefore I_{Ks} must be increasing very rapidly. The voltage-dependent activation of the E4031 sensitive current was quantified by fitting a sigmoidal curve between -30 and +20 mV (figure 4.18b, +30 and +40 mV were excluded to aid curve fitting) and it was found that the E4031 sensitive $V_{1/2}$ was -23 ± 11 mV (slope factor 8 ± 6 mV).

The E4031 sensitive current activates rapidly (see later) and becomes maximal close to the beginning of the depolarisation, generally the attained outward current is maintained until the end of the depolarisation, whence upon a tail current is initiated. At some voltages (generally positive to 0 mV) the E4031 sensitive current recorded during the depolarisation, can be seen to progressively shrink (figure 4.16b, 10 and 20 mV, figure 4.18c). The I_K tail current is not normally greater than the current developed in the previous depolarising pulse (figure 4.17b, gradient <1), however at positive voltages the tail current amplitude of the E4031 sensitive component can be in excess of the current flowing at the end of the depolarising pulse; this may partially be the result of the progressive reduction in E4031 sensitive current during the depolarisation.

The time-dependent activation of the E4031 sensitive component can also be investigated. By recording I_K with various duration depolarisations (+40 mV, 10 to 700 ms), then exposing the sino-atrial node cell to E4031 and taking similar secondary data of the E4031 resistant current, subtraction analyse facilitates quantification of the time-dependent activation of the E4031 sensitive component

(figure 4.19). In this manner, the time-dependent activation of I_K and the E4031 sensitive current can be quantified for each sino-atrial node cell studied (figure 4.20a); in this plot I_K can be seen to have two phases of activation, whereas the E4031 sensitive current appears to have just one, similar to the first phase of I_K time-dependent activation (not significantly different <100 ms). The E4031 sensitive component activates rapidly, when the time-dependent activation is fitted with a curve (Methods, page 62), the time-constant of activation was found to be 8.2 ms attaining a maximal E4031 sensitive current of 66 ± 2 pA (figure 4.20b, n=6). When the E4031 sensitive current is compared to the time-dependent activation of I_K, similarities can be observed between the activation of both of these currents with brief depolarisations, as they tend to superimpose at depolarisation durations more brief than 70 ms. As the depolarisation duration is extended I_K diverges from the E4031 sensitive component, which remain constant as the depolarisation is extended up to 700 ms (figure 4.20b). As described previously, the I_K continues to develop as the depolarisation is extended and becomes significantly different than the E4031 sensitive current at durations greater than 100 ms ($P<0.05$, n=6). Maximally activated E4031 sensitive current (I_{Kr}) is approximately 26 % of the amplitude of I_K activated with 700 ms depolarisation in the absence of E4031 (including I_{Kr} and I_{Ks}). Assuming maximal activation of I_{Kr}, this implies 74 % of the I_K is I_{Ks} (not maximally activated); I_{Ks} can be deduced from these data to be 2.8 times the size of I_{Kr}.

The slow component of the delayed rectifier potassium current (I_{Ks})

Atrial preparations were treated with increasing concentrations of thiopentone, a rapidly acting barbiturate which is used for induction of anaesthesia, that has been reported to specifically inhibit I_{Ks} (Heath and Terrar, 1996) however the selectivity

has been questioned by some groups (Mamas & Terrar, unpublished data). Thiopentone concentration dependently reduced the atrial preparation's beating rate, to approximately 25 % of control beating rate at the highest concentration of 300 μM (figure 4.21a). At lower concentrations of thiopentone the reduction in beating rate was more modest; 10 and 100 μM lowered the atrial bpm by 4 ± 3 (n=6, P>0.05) and 37 ± 5 % respectively (n=6, P<0.05). The concentration-response curve assumed sigmoidal form and the thiopentone concentration that produced half-maximal inhibition of beating rate was found to be 151 μM (figure 4.21c). The time frame of the effect of thiopentone (300 μM) can be seen in figure 4.21a (scanned oscilloscope trace), in which thiopentone was introduced to the solution bathing the atria at the position of the arrow, when the beating rate of the preparation was stable at 135 bpm. Upon addition of thiopentone the beating rate immediately began to decline and within 5 minutes was below 100 bpm. As the beating rate dropped the rate counting device, which was activated by action potentials recorded from a surface electrode (figure 4.21b) began to default to zero intermittently (see *) and subsequently failed as the rate dropped below 50 bpm. The recording of the surface electrode has been identified in these cases to contain monophasic action potentials deflections of alternating polarity and of variable amplitude, whilst in control the deflections were repetitively downward (figure 4.21b).

In addition to thiopentone, linopridine has been claimed to be selective inhibitor of a current molecularly similar to I_{Ks}, having an IC_{50} of 2 ± 1 μM in hippocampal neurones (Schnee and Brown 1998). Linopirdine (10 μM) was tested upon 3 sino-atrial node cells which had the following action potential parameters; overshoot 13 ± 1 mV, most diastolic potential -58 ± 3 mV, action potential amplitude

71 ± 3 mV, beating rate 194 ± 3 bpm, APD_{50} 58 ± 0 ms and APD_{90} 95 ± 1 ms. Upon addition of 10 μM linopridine into the physiological saline solution bathing isolated sino-atrial node cells, the rate of spontaneous development of action potentials reduced over the first minute, from 194 ± 10 to 123 ± 10 bpm (64 ± 6 % of control, $P<0.05$) and subsequently failed or developed non-action potential waveform oscillations (figure 4.22, n=3).

I_{Ks} has been investigated by studying the I_K resistant to the I_{Kr} selective inhibitor E4031. Tail currents have been used to describe this current, which only delayed rectifier currents contribute towards, so in the absence of I_{Kr}, there should be very little contamination by other ionic currents. The voltage dependent activation of the current resistant to E4031 has been studied and it has been found that as the membrane is more greatly depolarised, the E4031 resistant currents becomes larger (figure 4.23b). Voltages of less than 0 mV fail to activate a significant tail current (n=10, $P>0.05$), but at 0 mV and above there is steep voltage-dependent activation of the E4031 resistant tail current (figure 4.23b); this relationship has been fitted with a sigmoidal curve, from this the $V_{1/2}$ of the E4031 resistant current was found to be 20 ± 2 mV (slope factor 12 ± 2 mV) and the maximal current was found to be 352 ± 54 pA. When the E4031 resistant data is compared to that of I_K, $V_{1/2}$ of 6 ± 3 mV and the slope factor of this curve to be 14 ± 4 mV (n=14). The $V_{1/2}$ of the E4031 resistant current was found to be 14 mV more depolarised ($P<0.05$).

When investigating the time-dependent activation of the E4031 resistant current, there was found to be an absence of activation with brief depolarisations (figure 4.24). Depolarisations of less than 60 ms failed to activate any significant tail

current in the presence of E4031, unlike control recordings taken from the same sino-atrial node cells (figure 4.24b). Significant tail currents (>5 %) were activated with depolarisation of 70 ms and longer and developed to be of similar amplitude to that recorded in control (figure 4.24a), as depolarisation was further extended (maximal at 100 ± 13 pA, n=15). The E4031 resistant current continues to be time-dependently activated with the longest duration depolarisation activating the largest current. In some sino-atrial node cells the tail current amplitude appear to be inward after a brief depolarisations of 10 ms (figure 4.24c, n=15, $P<0.05$).

The effect of linopirdine upon the voltage and time-dependent activation of I_K was investigated. The voltage dependent activation of I_K was initially studied and linopirdine (10 μM) was found to reduce the amplitude of the tail current measure at all voltages in excess of –20 mV (figure 4.25a, n=4, $P<0.05$) and formed a voltage-dependent curve that appear to be a scaled version of the control data (figure 4.25b). The $V_{1/2}$ and slope factor for control and linopirdine are not significantly different; 2 ± 4 versus 7 ± 5 mV and 19 ± 4 versus 16 ± 3 mV respectively. This indicates there is no change in voltage dependency, just a slight reduction in amplitude. The amplitude of the brief inward current activated upon depolarisation (figure 4.25a, inset), presumably I_{CaL}, was not affected by linopirdine at any voltage (n=4, $P>0.05$). There was no effect upon I_K decay time-constants (figure 4.25c), however both Amp_1 and Amp_2 were reduced (n=4, $P<0.05$). Linopridine can be observed to reduce the tail current amplitude of I_K activated by both short and long (40 and 700 ms) depolarisations (figure 4.26a). In 4 sino-atrial node cells linopirdine was found to reduce I_K at all depolarisation duration's longer than 70 ms and the maximal I_K

activated by 700 ms depolarisation was reduced from 473 ± 65 pA to 315 ± 82 pA (67 ± 12 % of control, n=4, P<0.05).

The selectivity of linopridine was also investigated using the envelope of tails test. The ratio of tail/pulse current was recorded as various depolarisation pulse durations and with very short depolarisations (10 ms) the ratio was >1 (1.01 ± 0.30 at 10 ms, n=4). As the duration of depolarisation was prolonged the tail current amplitude became progressively smaller relative to the pulse current, therefore the ratio gradually diminished, not becoming stable (between 0.30 and 0.39) until depolarisation were of at least 80 ms (figure 4.27). This waveform is similar to that of the control data were not significantly different at any depolarisation duration (P>0.05, n=10 in control and 4 in linopirdine) and indicates the continued presence of both I_{Kr} and I_{Ks} in the presence of linopirdine.

The hyperpolarisation activated inward current (I_f)

I_f is an inward current which is activated by very negative membrane potentials, this current is very large at these extreme potentials, but does this current contribute to physiological pacemaking? ZD-7288 (3 μM), a specific I_f inhibitor (BoSmith, Briggs et al. 1993) was perfused onto isolated sino-atrial node cells with the following action potential characteristics; overshoot 15 ± 3 mV, most diastolic potential -59 ± 3 mV, action potential amplitude 74 ± 6 mV, beating rate 187 ± 10 bpm, APD_{50} 72 ± 4 ms and APD_{90} 122 ± 8 ms. Action potential recordings were taken throughout application of ZD-7288 and indicate that ZD-7288 reduced the spontaneous beating rate of these cells to 86 ± 3 % of control; from 187 ± 10 to 160 ± 6 bpm (figure 4.28a, n=6, P<0.05). The reduction in rate upon exposure of

spontaneously beating sino-atrial node cells gradually occurred over a period of 5-10 minutes and beating rate subsequently settled.

I_f was activated using voltage clamp, with prolonged hyperpolarising voltage steps. Varying the amplitude of the hyperpolarisation (figure 4.28b) allowed description of the I_f voltage dependency, in regard to both the amplitude and the kinetics of activation. As the voltage step becomes more hyperpolarised the amplitude of the inward I_f increases, although the current activated voltage steps to –50 and –70 mV have been found to be comparatively meagre (figure 4.29c). Even so, upon hyperpolarisation to –80 mV I_f activates slowly (time-constant of 1284 ± 102 ms), but developed over the prolonged hyperpolarisation to produce an inward current of over 1000 pA. At more negative voltages the activation of I_f becomes progressively more rapid and the amplitude more massive; I_f activation at –130 mV has a time-constant of 198 ± 17 ms and was in excess of 5 nA (5000 pA, figure 4.29). I_f amplitudes have been expressed as a current in figure 4.29.

The reversal potential of I_f was required in order to construct conductance-voltage curves. To accomplish this, a two-phase voltage protocol was utilised in which I_f was activated with a hyperpolarizing step to –120 mV (1000 ms) and then a variable voltage (-100 to +40 mV, in 20 mV graduations) was imposed upon the sino-atrial node cell before returning the holding potential (-40 mV). The currents developed from such a protocol are illustrated in figure 4.30a; secondary steps to –100 and +40 mV have been excluded to aid clarity. I_f can be seen to be activated by the initial hyperpolarizing step and upon repolarisation by the secondary voltage step, an instantaneous tail current can be observed and this indicates the direction of flow

of ions through I_f at various voltages. This should not be confused with the current that subsequently develops at these various voltages of the second phase or the tail current upon return to the holding potential, which are far more obvious. The direction and magnitude of these instantaneous tail currents upon I_f repolarisation have been plotted against the voltage of the secondary voltage step; this reveals a linear relationship, which demonstrates an I_f reversal potential of -19 ± 1 mV. The I_f reversal potential was calculated by averaging the voltage at which no current was flowing in each sino-atrial cell (n=6), however figure 4.30b is an average of all the data points at each voltage fitted with a linear curve. This explains the slight discrepancy between the quoted reversal potential (-19 mV) for I_f and the voltage of no net current flowing (figure 4.30b, approximately –22 mV). Using the reversal potential for I_f (19 mV), a conductance value can be calculated using Methods (page 62). This value was normalised to –130 mV and shown in figure 4.30c; conductance values demonstrate the maximal activation of I_f better than currents, as conductance measurements contain a reference to the electronic driving potential (step voltage minus reversal potential). The use of conductance values is especially insightful at these very negative membrane potentials. When considering the voltage-dependent activation of I_f, a conductance-voltage curve has been constructed and takes the form of sigmoidal relationship (between –50 and –130 mV), with hyperpolarisations of –70 to –110 mV activating large amounts of I_f (figure 4.30c). –50 and –60 mV appear to be below the activation threshold of I_f and –120 and –130 mV above the maximal activation of I_f conductance, although more negative steps activate greater current due to an increased driving force.

The $V_{1/2}$ of I_f has been found in this study to be –90 ± 1 mV (n=6), however the value appears variable according to conditions, slope factor 13 ± 1 mV (figure 4.30b). In regard to the amplitude associated with the time-constants of I_f activation, it can again be seen that –50 and –60 mV activate little current and therefore the time-constants maybe rouge, but at voltages above –70 mV amplitudes are progressively larger (figure 4.29c); the amplitude of time-constant activated by -130 mV was approximately 1400 pA.

When assessing the I_f inhibitor ZD-7288 a brief (250 ms) hyperpolarizing (-80 mV) voltage step was repeated every 15 seconds during a period when control data had been taken and ZD-7288 (3 μM) was being introduced into the superfusing solution (figure 4.31a). ZD-7288 caused a near-full block of I_f over a period of 5 minutes, identified by the reduction in the hyperpolarisation activated time-dependent inward current being reduced from approximately 1250 to 300 pA. In this same cell the voltage dependent activation of I_f was found to be characterised by a $V_{1/2}$ of –81 ± 7 mV (slope factor 16 ± 3 mV), whilst ZD-7288 was found to reduce the amplitude of the maximally activated current and shift voltage dependent activation 23 mV more negative ($V_{1/2}$ –105 ± 4 mV, slope factor 8 ± 1 mV). This data is only one cell however and this therefore only preliminary data and will not be further discussed.

Caesium is another compound which has been reported to be a selective inhibitor of I_f (Herring, Rigg et al. 2001) and so an evaluation of caesium upon I_f undertaken. Caesium (2 mM) fully inhibited I_f at all hyperpolarized voltages (figure 4.32a, n=8, $P<0.05$), more negative than –60 mV (at which little I_f is activated); therefore caesium was found to effectively block I_f. The selectivity of caesium was

subsequently investigated, utilising voltage protocols to activate I_{Kr}, I_{Ks} and I_{CaL}. The time-dependent activation of I_K has previously been described (Sanguinetti and Jurkiewicz 1990; Heath and Terrar 1996; Lei and Brown 1996), containing two phase of time-dependent activation roughly related to I_{Kr} and I_{Ks}, and caesium was found to reduce I_K activated with any depolarisation in excess of 30 ms (figure 4.32b, n=7, $P<0.05$). More studies would have to be carried out to determine which I_K component is being modified by caesium. Similarly when I_{CaL} was investigated, caesium was found to cause a reduction in I_{CaL} (figure 4.32c), activated with depolarisation of greater voltage than –20 mV (n=6, $P<0.05$). In summary caesium was found to block I_f, however it was also found to reduce I_K and I_{CaL}, therefore can not be described as a selective inhibitor.

A large inward current has been identified upon repolarisation of the membrane to the holding potential, after hyperpolarisation intended to activate I_f (figure 4.33a). I_{Na} is thought to be absence in sino-atrial node cells, however it might be possible that I_{Na} is present, but is voltage dependently inactivated by the relatively depolarised voltage action potentials in the sino-atrial node region. Therefore, prolonged hyperpolarisation would enable I_{Na} to recover from voltage dependent inactivation, and upon repolarisation (effectively a depolarising voltage step) I_{Na} might be activated. This inward current was measured from the maximally activated I_f to the tip of the inward current upon repolarisation (see arrow and bar, figure 4.33a). The voltage (of the hyperpolarising step) dependent appearance of the inward current upon repolarisation was plotted and a strong relationship was identified (figure 4.33b); this inward current appear fully activated after hyperpolarisation to –90 mV and beyond, having a $V_{1/2}$ of -72 ± 2 mV and a slope factor of 5 ± 1 mV

(n=6). The magnitude of this fast inward current, presumably I_{Na}, did not correlate with the size (measured as membrane capacitance in pF) of the sino-atrial node cell (n=7).

The sodium-calcium exchange current (I_{NCX})

The activity of the sodium-calcium exchanger is dependent upon voltage, intracellular calcium and extracellular sodium, but essentially the large inward sodium gradient is utilised to expel calcium from the cell; this activity is associated with an inward current due to the stoichiometry. I_{NCX} has been studied by rapidly locally superfusing the experimental sino-atrial node with a saline solution that lacks sodium (Huser, Blatter et al. 2000). This reduction in extracellular sodium concentration (from 140 to 15 mM) inhibits the sodium-calcium exchange process, and hence the expulsion of calcium from the cytosol and the inward current that is associated with such an exchange. Other non-I_{NCX} mediated effects will occur in a reduced sodium solution, however the time-course of these actions is likely to be magnitudes longer. Action potential form was studied in control recordings and of the 6 cells studied these were the quantification values; overshoot 13 ± 3 mV, most diastolic potential -60 ± 3 mV, action potential amplitude 73 ± 6 mV, beating rate 141 ± 15 bpm, APD_{50} 86 ± 10 ms and APD_{90} 135 ± 13 ms. When the saline solution superfusing a sino-atrial node cell, was rapidly switched for one that contained only 15 % of the initial solutions sodium concentration, spontaneous activity immediately (within 1 action potential) failed (figure 4.35a, n=6, 16 switches). Action potential generation ceased close to the maximum diastolic potential and very gradually depolarised, but then either became stable (and noisy), alternatively fired single or

brief bursts of action potentials (3 of 16 cells). Quiescence was maintained for the period of exposure to low sodium solution, but in some cells after prolonged exposure, voltage oscillations developed (n=4, 14 ± 7 mV). If the sino-atrial node cells were exposed to low sodium solution for more than 30 to 60 seconds, the cell displayed terminal voltage oscillations. The cells that did not undergo terminal voltage oscillations, gradually re-established normal spontaneous activity upon reperfusion with solution B. The initial action potentials upon switching out of the low sodium solution were of reduced amplitude both the most negative potential and/or the overshoot were diminished in comparison to previous action potentials. This reduction in amplitude only recovered over the next 5-10 action potentials, as the most diastolic potentials and overshoot were re-established, with the overshoot returning formerly. Even so, the action potential amplitude was smaller 30 seconds after treatment with low sodium was reduced from 73 ± 6 to 70 ± 5 mV (n=6, $P<0.05$). At the same point, the APD_{90} was quickened to 85 ± 1 % of control duration (n=5, $P<0.05$). Beating rate was initially quickened upon reperfusion of solution B, from 141 ± 15 bpm, to 172 ± 12 bpm (13 switches, n=5, $P<0.05$).

Similar experiments with low sodium were undertaken when the cell was voltage clamped, with depolarising and hyperpolarizing steps to activate I_K and I_f respectively. Repetitive brief depolarising voltage (1 every second of 40 ms to +40 mV) activated an outward current (presumably I_{Kr}) and upon repolarisation a brief inward current was observed before the appearance of the I_K tail current (figure 4.35c); upon rapidly exchange of solutions to one containing low sodium, the activation of the outward current appear to be accelerated and the magnitude of the inward current upon repolarisation was reduced (figure 4.35c, approximately 1250 to

750 pA). The presence of I_{NCX} upon repolarisation may result in the under-estimation of I_{Kr} activated with brief depolarisations, as the inward I_{NCX} may hide the outward tail current of I_{Kr}. Studies of the effect of low sodium upon I_K activated by more prolonged depolarisation were not carried out. I_f alternatively was activated with repetitive hyperpolarizing voltage steps to –110 mV (250 ms), activating the inward I_f. The perfusion of the low sodium solution reduced the I_f amplitude from –466 ± 123 to –339 ± 97 pA (n=7, $P<0.05$), which is a reduction to 73 ± 2 % of control.

The exposure of these cells to low sodium rapidly reduced the amplitude I_f (and possibly increased I_K). This could indicate that the rapid cessation in action potential generation could be due to the inhibition of I_f during diastolic depolarisation. To investigate this sino-atrial node cells were treated with 3 μM ZD-7288, before exposure to low sodium. In experiments in which I_f was inhibited, the rapid perfusion of these cells with a solution containing low sodium still caused a rapid block of action potential generation, and other action potential characteristics as described above (n=4).

The L-type calcium current (I_{CaL})

In sino-atrial node cells I_{CaL} mediates the action potential upstroke that is unusual for muscle cells, but is due to the absence of functional fast sodium channels. I_{CaL} activation also contributes to the end-stages of diastolic depolarisation and produces a smooth action potential upstroke initiation.

I_{CaL} is an inward current that is rapidly activated upon moderate depolarisation, but is inactivated by voltage and calcium, and causes only a brief

inward current at the start of depolarisation (arrow in figure 4.36a). I_{CaL} is progressively activated by depolarisation from –30 to 0 mV, attaining a maximal inward current of –331 ± 102 pA (n=6), however the amplitude of I_{CaL} was extremely variable between sino-atrial node cells. At voltages above 0 mV, I_{CaL} becomes successively smaller in an almost linear manner (figure 4.36b, n=6). The dihydropyridine nifedipine has been well used as a I_{CaL} inhibitor and 5 μM fully inhibited the I_{CaL} current activated upon depolarisation at all voltages (figure 4.36b, n=6, $P<0.05$), leaving an only an outward current, which appeared to be linearly related to voltage and is therefore probably a leak current. To more selectively define I_{CaL} the nifedipine sensitive current was calculated. The nifedipine sensitive current is shown to rapidly increase in amplitude up to –10 mV, be slightly larger at 0 mV and the amplitude slowly reduces at more positive voltages (figure 4.36c). The nifedipine sensitive current (with the leak current subtracted, figure 4.36c) shows a less bell-shaped voltage dependency, compared to depolarisation activated instantaneous current (figure 4.36b). If this gradual voltage-dependent reduction is extrapolated, a point at which the nifedipine sensitive current changes from being an inward, to an outward current (nifedipine sensitive current reversal potential) can be estimated (figure 4.37); this rough estimation of the reversal potential of the nifedipine sensitive current in sino-atrial node cells, revealed a voltage of approximately +85 mV.

The voltage dependent effect upon the time to peak instantaneous inward current upon depolarisation, presumed to be I_{CaL} was also investigated (figure 4.38). Depolarised voltages were found to more quickly activate max inward current (figure 4.35b), irrelevant of max amplitude; the most rapid current activation was at +40 mV of 5 ± 2 ms, whereas the slowest (14 ± 3 ms) was at –30 mV ($P<0.05$, n=5).

To investigate whether nifedipine was as selective for I_{CaL} as reported, the effect of this agent upon I_K was investigated. Nifedipine was added to solutions bathing sino-atrial cells in which the time and voltage dependent activation of I_K had previously been defined; nifedipine (5 μM) caused a significant reduction of I_K activated at all voltages (figure 4.39a; n=12, $P<0.05$) and with depolarisation longer than 20 ms (figure5.39b; n=11, $P<0.05$). When the deactivation kinetics of the I_K tail current was studied in the presence of nifedipine, no alteration of the time-constant or the associated amplitude was identified (n=12, $P>0.05$). Whether these effects upon I_K were non-specific action of nifedipine, or secondary effects to a reduction in cellular calcium will be considered in the discussion.

The T-type calcium current (I_{CaT})

The role of I_{CaT} was briefly investigated using low concentrations of nickel (25-100 μM) to inhibit this current (Doerr, Denger et al. 1989; Hancox and Howarth 1995; Satoh 1995). Nickel has been used to block a number of currents at higher concentrations, such as I_{NCX} and I_{CaL}, but at these low concentrations, the effect of nickel should be selective.

Upon exposure of an atrial preparation to nickel, the rate of beating was slightly reduced (figure 4.40a); a concentration dependent effect within the range tested was described, significant at 25 (n=16, $P<0.05$), 50 (n=16, $P<0.05$) and 100 μM nickel (n=8, $P<0.05$), with 50 μM lowering the rate by approximately 10 % (n=16,

P<0.05). In addition, the effect of nickel (all concentrations) took a reasonable time to develop and did not become stable until 10-30 minutes after additions.

Similar experiments were undertaken with isolated sino-atrial node cells. Nickel (25 μM) caused a slight reduction in the rate of spontaneous action potential generation, that took approximately 5 minutes to develop and was a rate reduction of 19 ± 2 %; as defined by nickel increasing the cycle length between action potentials from 378 ± 24 to 489 ± 57 ms (figure 4.40b, n=7, P<0.05). This effect was fully reversible upon re-perfusion with control solutions (344 ± 2 ms; n=3, not significantly different versus control). The other action potential parameters in the presence of nickel were similar to control, which were; overshoot 15 ± 2 mV, most diastolic potential -57 ± 3 mV, action potential amplitude 72 ± 5 mV, APD_{50} 80 ± 6 ms and APD_{90} 130 ± 9 ms (n=7).

Discussion

Experimental data from atrial preparations indicate that both I_{Kr} and I_{Ks} have a role in the development of spontaneous electrical activity in the guinea pig sino-atrial node, as inhibition of either of these ionic currents reduces the beating rate of the atria. The selectivity of agents used to reduce these currents is vital in attempting to assess their contribution; the drug of choice for inhibition of I_{Kr} is E4031 (Ono, Shibata et al. 2000; Zhang and Vassalle 2001). E4031 caused a concentration dependent reduction of the atrial beating rate (IC_{50} 64 nM), producing a maximal effect of approximately 25 % inhibition. Good selectivity is indicated by the nM IC_{50}

found in this study and has been previously reported; IC_{50} 397 nM (Sanguinetti and Jurkiewicz 1990). Thiopentone has been described as an inhibitor of I_{Ks} (Heath and Terrar 2000) and concentration-dependently inhibited the atrial beating rate, having a IC_{50} of 151 μM and maximally reducing the beating rate by 75 %. Presuming selectivity of thiopentone for I_{Ks}, it appears that I_{Ks} has a larger role than I_{Kr} in the development of spontaneous beating of the atria; maximal I_{Kr} inhibition reduce rate by 25 %, whilst maximal I_{Ks} inhibition reduced the beating rate by 75 %. Guinea-pig I_K has previously been described to be composed of greater I_{Ks}, than found in rabbit in which I_{Kr} is the dominant contributor (Lei, Cooper et al. 2002). Sanguinetti and Jurkiewicz (1990) found maximally activated I_{Ks} to be 11.4 times the amplitude of maximally activated I_{Kr} in guinea-pig ventricular myocytes. This study of guinea pig sino-atrial node cells, I_{Ks} (non-maximal) was found to be 2.8 times the size of maximally activated I_{Kr}. These values appears to alter substantially between individual cells and brings variability into the evaluation of the components of the delayed rectifier potassium current. The differential expression of I_{Ks} and I_{Kr} in various species may, in part, account for the relatively slower heart rate of larger animal, such as pigs in which I_{Ks} is the principal I_K component, rather than some smaller animal where I_{Kr} tends to be the functionally dominant (Ono, Shibata et al. 2000).

Upon addition of a concoction of E43031 and thiopentone, atrial preparations developed oscillatory contractions of small amplitude and beating rates became irregular; this could be indicative of an action potential repolarisation failure, as the major repolarising currents of the guinea-pig sino-atrial node have been severely compromised.

Similar experiments were undertaken with sino-atrial node cells that had been enzymatically isolated and studied using patch clamp techniques. The exposure of these isolated sino-atrial node cells to 5 μM E4031 caused 8 out of 9 to stop beating and all reduced in rate (Verheijck, van Ginneken et al. 1995). There is a marked difference between the effects of E4031 upon atrial preparations and isolated sino-atrial node cells; the former causes only a 25 % in rate, whilst spontaneity in E4031 treat sino-atrial node cells tended to fail. This dichotomy has been reported previously (Boyett, Honjo et al. 2000) and is thought to be due to the intact sino-atrial node having alternative pacemaking mechanisms, such as the subsidiary pacemaking cells (Huser, Blatter et al. 2000), but upon isolation these back-up systems are lost and so blockade of the primary pacemaking mechanism can result in quiescence. The reportedly I_{Ks} selective inhibitor linopirdine (Schnee and Brown 1998) was investigated in isolated sino-atrial node cells and it was found to cause a reduction in beating rate, which degenerated into non-action potential oscillations or quiescence. The selectivity of this agent as an I_{Ks} inhibitor was scrutinised in this study and is discussed below. Both inhibition of I_{Kr} and I_{Ks} in isolated sino-atrial node cells caused a larger reduction in beating rate, generally leading to a failure of action potential generation, than that observed in an intact atria; isolated cells seem to be more sensitive to pharmacological intervention, possibly due to the lack of multiple heterogeneous pacemaking mechanisms.

I_K has been studied using patch clamp to define the voltage activation of I_K, and its components. Upon depolarisation an outward current is slowly activated (time-constants 300-550 ms), the amplitude of which is relatively small at voltages

below 0 mV, but the increase in current accelerates at positive potentials. When this depolarisation ends, a component of I_K remains and the tail current slowly decays in a bi-exponential manner; time-constants of 225 (70 pA) and 1100 ms (130 pA) upon repolarisation to –40 mV. When studying I_K in guinea pig sino-atrial node, the tail current is smaller than the pulse current associated I_K activation. The I_K tail current present upon repolarisation has been used to quantify I_K, as this component is exclusively dependent upon activation of delayed rectifier potassium currents and so more precise measurement of I_K can be taken. Tail current amplitude after depolarisation indicates that I_K is voltage dependently activated, with the greatest activation occurring between –10 and +20 mV; this produced a sigmoidal voltage-dependent activation curve, which has been quantified as having a $V_{1/2}$ of 6 mV and a slope factor of 14 mV (Sanguinetti and Jurkiewicz 1990; Ono, Shibata et al. 2000). The reversal potential of I_K was measured as -70 mV in this study, which is similar to previously reported values of –65 (Sanguinetti and Jurkiewicz 1990) and –75 mV (Ono, Shibata et al. 2000) and indicates an ionic current which is not entirely selective for potassium (reversal potential for potassium is –94 mV in 4 mM external potassium).

E4031 has been used to describe the voltage dependent activation of I_{Kr} (E4031 sensitive current) and the E4031 resistant tail current (presumably I_{Ks}). The current sensitive to E4031 displayed quite different voltage dependent activation than I_K, as I_{Kr} strongly activating at negative voltages, $V_{1/2}$ was –23 and slope factor 8 mV; the I_{Kr} $V_{1/2}$ and slope factor have previously been reported to be –22 and 8 mV in guinea-pig ventricular cells (Sanguinetti and Jurkiewicz 1990), -14 and 8 mV in human atrial myocytes (Wang, Curran et al. 1996) and –26 and 15 mV in guinea-pig

sino-atrial node cells (Matsuura, Ehara et al. 2002). The voltage dependent activation of I_{Kr} seems to be relatively well preserved between species and cell type. The I_{Kr} activation begins to plateau at activation voltages between –10 to +20 mV and the E4031 sensitive current activated with more depolarised voltages exhibits rectification. This rectification of I_{Kr} has previously been describe in various tissue and species (Sanguinetti and Jurkiewicz 1990; Heath and Terrar 1996; Wang, Curran et al. 1996) and is thought to be due to a C-type inactivation process in which the C-terminal amino acids interact with the pore and reduce channel conductance (Heath and Terrar 2000). The E4031 resistant component of the I_K tail current has also been quantified according to voltage dependent activation, this component was not activated until voltage steps more depolarised than –10 mV, but activation was rapid with positive depolarisations. The E4031 resistant current was found to exhibit a $V_{1/2}$ of 15 mV and have a slope factor of 13 mV, which are similar to previously published I_{Ks} data; +7 and 11 mV (Salata, Jurkiewicz et al. 1996), +20 and 13 mV (Wang, Curran et al. 1996), 17 mV (Matsuura, Ehara et al. 2002). There have been some reports that I_{Ks} displays a small amount of rectification at positive potentials (Nerbonne 2000), but this study did not find any regions of negative voltage-dependency, however the rate of voltage-dependent activation of the E4031 resistant current was decreasing at very positive potentials. The deactivation of the E4031 resistant current was measured and in comparison to the control (E4031 absent) I_{Kr} measurement, Amp_2 was approximately halved, and shifted slightly, whereas Tau_1 was delayed. I_{Kr} has been reported to contribute to both time-constants of I_K decay, whereas I_{Ks} is primarily be related to the rapid phase of deactivation. The effect of E4031 delaying the Tau_1 and reducing Amp_2 is in agreement with this hypothesis. When I_K is measured, what is actually being measured is the sum of the I_{Kr} and I_{Ks}

voltage dependent activation, with I_{Kr} activating at negative potentials and passing less current at positive depolarisation, while I_{Ks} does not activate until relatively depolarised potentials, but then continues to activate as the depolarisation is extended. When those activation characteristics are summated, sigmoidal voltage dependence is observed.

The time-dependent activation of I_K has also been investigated, by extending the duration of a depolarisation (to +40 mV) from 10 up to 700 ms and measuring the tail current amplitude. I_K has two phases of time-dependent activation, a rapid phase (0-80 ms) and a delayed phase (>90 ms) and these components have previously been described to be mediated by I_{Kr} and I_{Ks} respectively (Anumonwo, Freeman et al. 1992). The I_K tail current was found to be activated by brief depolarisations, with the fast phase being maximally (or close to) with depolarisations of 40/50 ms, at approximately 20-30 % of maximum recorded I_K. Another phase of time-dependent I_K activation occurs with depolarisations in excess of 80/90 ms, which is superimposed upon the first phase of activation. This component strongly activates with depolarisation up to 500 ms, but continues to increase at even more prolonged depolarisation durations.

These components have been studied according to the contribution of I_{Kr} and I_{Ks} to this description of the time-dependent activation of whole I_K. E4031 sensitive currents have identified the initial phase of time-dependent activation to be associated with the action of I_{Kr}, with this current activating rapidly (time-constant of 8 ms) being maximally activated by 30-50 ms depolarisations. This maximal activation is maintained all the way to 700 ms, the maximum duration of depolarisation utilised.

This has been assessed using the tail current amplitude, however if the pulse current is considered I_{Kr} has been found to exhibit time-dependent rectification; I_{Kr} is activated, but then dwindles as the depolarisation is maintained, however this rectification did not appear to reduce the tail current amplitude in some cases the amplitude of the tail current was as a result of time-dependent rectification, larger than the outward current during the end-stages of depolarisation.

E4031 sensitive tail currents appear to be much better defined than I_K tail currents measured after brief depolarisations (figure 4.19), possibly indicated an inward current which is activated by brief depolarisations and removes a bite of the instantaneous tail current, which is absent when I_{Kr} is quantified using subtraction analysis of E4031 sensitive currents. In addition outward pulse currents (presumed to be I_{Kr}) have been occasionally recorded in the absence of tail currents, which could imply that an inward tail current component was masking the presence of an I_K tail current totally. There are a number of possible candidates for this role, however I_{NCX} seems to be most probable, due to the depolarisation activation, direction of current etc.

The primary phase of time-dependent I_K activation becomes maximal rapidly (within 40-50 ms) and becomes constant. A secondary phase of I_K activation occurs (>70 ms), which is superimposed upon the initial I_K activation, but then continues to activate as depolarisation is extended. The initial phase is similar to the current sensitive to the I_{Kr} selective inhibitor E4031, whilst the secondary phase that is superimposed, has similar activation characteristics to the E4031 resistant current, the tail current of which is presumably I_{Ks} mediated. I_K activation by 40 ms

depolarisation activates only I_{Kr}, whilst longer depolarisations activate both I_{Kr} and I_{Ks}. Prolonged depolarisations activate maximal I_{Kr}, however I_{Ks} would be progressively increased as the depolarisations are extended. Sanguinetti and Jurkiewicz (1990) found I_{Ks} was over 10 times the amplitude of maximally activated I_{Kr}, therefore the I_K tail current associated with a 700 ms depolarisation would primarily be I_{Ks} mediated, with I_{Kr} only contributing <10 % of the current. I_{Ks} is not fully activated by 700 ms depolarisations (as the amplitude is still increasing), however the I_{Kr} current at 40 ms was found to be 17 % of the I_K activated with a 700 ms depolarisation; therefore only 17 % of the effects of agents upon the I_K tail current activated by a 700 ms depolarisation are mediated via an I_{Kr} effect and 83 % by I_{Ks}. The subsequent use of 40 and 700 ms depolarisations to describe effects upon I_{Kr} and I_{Ks} have been used, however the contribution (although comparatively minor) of I_{Kr} to the I_K tail current activated by 700 ms depolarisation will not be dismissed.

Linopirdine is reportedly specific blocking agent of a current which molecularly very similar to I_{Ks} (Schnee and Brown 1998), and has been found to have similar selectivity for I_{Ks}. Linopirdine (DUP 996) is a proposed cognitive enhancing agent, although this effect is disputed (Nordholm, Moore et al. 1995), as it increases acetylcholine, dopamine and serotonin release from various regions of the brain (Nordholm, Moore et al. 1995). Linopirdine inhibits various channels of the KCNQ family, of which I_{Ks} is molecularly composed of the primary member (Seebohm, Lerche et al. 2001). Linopirdine was used to attempt subtraction analysis that allows more specific description of an ionic current. Initially 5 μM linopridine was added to solutions superfusing a spontaneous sino-atrial node cell, of which the action potentials were being recorded and linopirdine was found to reduce the beating rate of

these isolated cells to 64 ± 6 % (n=3, P<0.05). This was similar to the effects of thiopentone upon atrial preparations (~75 % reduction) and other I_{Ks} inhibitors upon the rate of spontaneous action potential generation in the sino-atrial node (Lei, Cooper et al. 2002). Linopirdine was found to reduce the amplitude of the I_K, however it reduced tail current amplitude after both brief and prolonged depolarisation (n=4, P<0.05), but without altering I_{CaL}.

The envelope of tails test was used to further define the contribution of I_{Kr} and I_{Ks} to the time-dependent activation of I_K, in addition the specificity of E4031 and linopirdine was investigate in this manner. By dividing the outward current activated during the pulse, by the tail current amplitude, a ratio is developed. If the tail current is directly related to the pulse current, this indicates that just one time-dependent current is contributing to the ratio, and the value of this ratio should be constant whatever the duration of the depolarisation. When there are more than one current contributing, the value will alter as the depolarisation duration is extended according to different time dependent activation kinetics. This test was performed upon I_K under control conditions and the ratio was found to not be constant, as has been reported previously (Sanguinetti and Jurkiewicz 1990; Heath and Terrar 1996; Ono, Shibata et al. 2000), implying multiple components contributing to I_K. The ratio developed by the envelope of tails test did become constant with depolarisation in excess of 70 ms, indicating that subsequent I_K enlargement was mediated by one current (I_{Ks}). These findings are agree with the current-voltage relationships, time-dependent activation and E4031 sensitive currents of this study and the various other reports (Sanguinetti and Jurkiewicz 1990; Heath and Terrar 1996; Ono, Shibata et al. 2000). When the test was again performed upon E4031 treated sino-atrial node cells,

the ratio was less variable and could be described as being constant (ranging from 0.16 to 0.29 between 30 and 700 ms); this indicates only one current component in the presence of E4031. When similarly tested linopirdine did not alter the envelope of tails ratio from control at any depolarisation duration and indicates that there has not been any specific inhibition of either components; therefore the relative contribution of I_{Kr} and I_{Ks} to the time-dependent activation of I_K are not altered. Linopirdine was found to reduce I_K tail current amplitude, activated with both 40 and 700 ms depolarisations and both these data imply that linopirdine does not selectivity inhibit I_{Ks}, as it inhibits I_{Kr} to a similar degree.

I_K is activated upon depolarisation during action potentials, the membrane is subsequently repolarised by this current, but a component of the outward I_K remains and partially decays over the subsequent 200-400 ms before the next spontaneous action potential is generated. There is however a component of the I_K tail current which hasn't decayed when the subsequent action potential is initiated, this component will become additive to the I_K activated in the next action potential. The I_K decaying after the second action potential would therefore be greater than that of the first action potential, as a fraction of the first action potential will remain. I_K would accumulate as the number of action potentials increase, until a point at which the amount of I_K decaying between action potentials was equal to the amount remaining from previous action potentials. The equilibrium is dependent upon the rate of action potential generation, at higher rates the basal I_K current would be greater (less time to decay), and I_K deactivation kinetics. I_K decay has been recorded upon repolarisation to –40 and –60 mV, these bi-exponential decay kinetics have been used to model I_K. The repolarisation to –60 mV is more physiological, however more

deactivation data has been collected at –40 mV (time-constants of 175 and 839 ms, n=62). The amplitude of these time-constants and the amplitude of the maximal I_K activated upon depolarisation were used to calculate the absolute current flowing at each point of the modelled action potential. When the decay constants for –40 mV were used the basal I_K, once equilibrated over the first 10 action potentials (simulated to be beating 120 times per minute, was found to be 216 pA. Using decay constants for –60 mV diminished this value to 82 pA (at 120 bpm), however the rate of spontaneous action potential generation is generally higher than 120 bpm and when the –60 mV deactivation kinetics were modelled with a beating rate of 180 bpm, this value was increased to 100 pA. These computational simulations of I_K during the sino-atrial node action potential make some assumptions (Methods, page 62), which maybe flawed in terms of quantification, however these models indicate that there will be an outward I_K current at all points during pacemaking.

The hyperpolarisation activated current I_f, has previously been rarely described in guinea pig sino-atrial node cells (BoSmith, Briggs et al. 1993), as most studies of I_f being performed in rabbit sino-atrial node cells (DiFrancesco and Boyett groups etc). Between voltages of –50 to –70 mV <100 pA I_f is time-dependently activated, however this is still a comparatively large current, and I_f exhibits activation constants between 500 and 1000 ms. More substantial amounts of I_f are activated by more negative voltages, the activation constants are very long (1300 ms at–80 mV) but the current developed is quite substantial (300 pA). As voltage steps become more hyperpolarized the amplitude of the current increases and the time-constants reduce, until at –130 mV the activation constant was 300 ms and the amplitude 1400 pA.

The voltage of half activation ($V_{1/2}$) seems to vary between the cells isolated from the sino-atrial node, with some cells possessing an I_f $V_{1/2}$ as positive as –71 mV and others being as negative as –118 mV; the average $V_{1/2}$ obtained for guinea pig sino-atrial node cells was –90 mV (n=6), approximately half way between these voltages. This value is comparable to -85 mV the $V_{1/2}$ that of BoSmith, Briggs et al (1993) in guinea-pig sino-atrial node, as well as –87 mV described in Mangoni and Nargeot (2001) and –89 mV in pig (Shiabata 1999). However, the group of DiFrancesco has found the $V_{1/2}$ of rabbit I_f to be around –66 mV (DiFrancesco and Mangoni 1994; Accili and DiFrancesco 1996; Accili, Redaelli et al. 1997; DiFrancesco 1999). The variability of the $V_{1/2}$ in this study and between other studies in various species, maybe related to the intrinsic turnover rates of AC in sino-trial node cells; higher AC turnover produce more cAMP which shifts I_f activation to more depolarised potentials. The region of which the sino-atrial node cells originated and the isolation procedure may effect AC turnover in the absence of stimulation. In addition some studies have use phosphodiesterase inhibitors, to block the degradation of cAMP, which would elevate cAMP beyond normal levels.

The I_f reversal potential can be measured by activating I_f, then repolarising the membrane to various potential and plotting the instantaneous tail current against the voltage of repolarisation; the reversal potential is where this relationship dissects the abiscus. The reversal potential of I_f was found to be –20 mV, which is similar to previous values reported; -25 mV (Yanagihara and Irisawa 1980). This indicates I_f to not be very selective, as this value is not close to the reversal potential of any major

cations and previous studies have found I_f to be mediated by the non-selective flux of cations, primarily potassium and sodium (DiFrancesco 1987).

Millimolar concentrations of caesium have been used to effectively eliminate I_f (Herring, Rigg et al. 2001) and such additions were found to reduce beating rate by 29 % in rabbit sino-atrial node (Denyer and Brown 1990; Herring, Rigg et al. 2001). Caesium (2 mM) was found to totally inhibit I_f activated upon hyperpolarisation. However caesium was also found to inhibit both I_{Kr} and I_{Ks} (by approximately 20 %) and I_{CaL} (50 %); caesium was therefore found not to be selective for I_f. The reported effect on beating rate could underestimate the role of I_f in pacemaking, as reducing repolarising I_K would accelerate depolarisation and compensate for I_f inhibition. The effect of caesium upon I_{CaL} would probably in itself cause such a reduction in beating rate. The alternative I_f inhibitor ZD-7288 (BoSmith, Briggs et al. 1993) was also utilised and ZD-7288 (3 μM) was found to reduce the beating rate of isolated sino-atrial node cells by 14 %, from 187 ± 10 to 160 ± 6 bpm (n=6, $P<0.05$). Preliminary voltage clamp studies (n=1) indicated that ZD-7288 (3 μM) reduced maximally activated I_f, shifted the voltage dependent activation to more depolarised potentials, similar to that reported by BoSmith, Briggs et al (1993).

I_f is a very large current, which activates more quickly (but still relatively slowly) at very negative potentials, however the contribution of I_f to pacemaking maybe slight, as the most negative potential of these sino-atrial node cells is –58 ± 2 mV (n=50) and only slight I_f is activated at these potentials.

The fast sodium current is not thought to play a major role in the pacemaking of the sino-atrial node, however some groups have found this current to be present when studying I_f. The membrane (and holding) potential of sino-atrial node cells is quite depolarised and at these voltage the fast sodium current could be inactivated. When I_f is investigated with prolonged hyperpolarizing steps in guinea pig sino–atrial node, the fast sodium current may recover from voltage dependent inactivation and subsequently be observed upon repolarisation (effectively a depolarising step).

The I_{NCX} will probably be an inward current throughout the sino-atrial node action potential, outward I_{NCX} requires very positive voltages and low intracellular calcium which do not happen in the guinea-pig sino-atrial node. The sino-atrial node action potential upstroke is mediated by calcium and so cellular calcium concentration is linked to membrane potential. The overshoot of sino-atrial node action potential was found to be 14 ± 1 mV (n=50) and reverse (outward) I_{NCX} necessitates much more positive voltages. I_{NCX} is dependent upon voltage, and concentrations of both intracellular calcium and extracellular sodium; the inward I_{NCX} associated with a SR calcium dump can be blocked by using a sodium free superfusate (Huser, Blatter et al. 2000).

Rapid substitution to low sodium superfusate caused an instantaneous cessation of spontaneous action potential generation. The membrane voltage tended to then depolarise, occasionally to a threshold potential where upon a single (or sometimes a brief train) action potential was initiated. If the cell was exposed to low sodium solution for more than 30-60 seconds, voltage oscillations sometimes developed that where associated with cell demise. Upon low sodium solution

replacement with normal saline solution, action potentials were re-initiated in the next few seconds; the first action potential was of low amplitude and the overshoot and most diastolic potential gradually developed to control values over 2-10 seconds. This data in itself does not define the role for I_{NCX} in pacemaking, as a reduction in extracellular sodium may effect I_{bNa} and I_{Na} (if present). An alternative technique to block I_{NCX} has been used within this group; 10 μM KB-R7943 (Kanebo Co Ltd, Osaka, Japan) also caused guinea-pig sino-atrial node cells to slow/stop beating, however this effect was less marked and took a longer duration to develop (unpublished data). These data taken together indicate I_{NCX} to have a substantial role in the development of pacemaker activity.

I_f is mediated by the movement of potassium and sodium ions across the membrane, so the effect of low sodium upon I_f was investigated. Switching to low sodium containing solutions during voltage clamp, identified I_f to be partially blocked. However full I_f blockade does not cause the sino-atrial node cells to stop beating, and when similar low sodium switching experiments were undertaken in the presence of ZD-7288 (3 μM), the same quiescence and voltage characteristics where identified. Low sodium may have an additional effect upon I_K, as I_{Kr} activated with brief depolarisations (40 ms) were found to be larger in the presence of low sodium, however this was just preliminary data; this could however be explained by inward I_{NCX} being inhibited by low sodium perfusion and revealing more I_{Kr}, which was previously masked. This would concur with data that found E4031 sensitive currents to be larger than I_{Kr}, possibly indicating a fraction of I_{Kr} was hidden by some unknown inward current. The exchanger could be constantly active during

pacemaking, being associated with a constant inward I_{NCX}, which would increase after SR calcium release during the early stages of diastolic depolarisation.

The role of I_{CaL} in sino-atrial node pacemaking is fundamental; I_{CaL} mediates the action potential upstroke and initiates the calcium accumulation associated with excitation-contraction coupling. I_{CaL} activates rapidly upon depolarisation (maximal current within 8 ms at 0 mV), contributing to the immediate inward current upon depolarisation, which rapidly inactivates (voltage and calcium dependently) but is superseded by outward I_K. I_{CaL} recovers from inactivation during diastolic depolarisation and is gradually activated, until the beginning of the action potential upstroke where upon the whole I_{CaL} population is activated.

I_{CaL} is voltage dependently activated, becoming more inward as depolarisation is extended from –30 to 0 mV at which voltage I_{CaL} was found to be maximal. Progressive depolarisation above 0 mV reduces the current activated, even though the reversal potential for calcium is +120 mV and so indicates voltage-dependent deactivation or inactivation of the I_{CaL} channel. The reduction in current at positive potentials is gradual and the trend can be extended to intersect the absical axis to indicating an approximate I_{CaL} reversal potential of +85 mV. This is 35 mV less depolarised than the calcium reversal potential, but this has been reported previously and although I_{CaL} is calcium selective (1:1000 over potassium) is a result of small potassium ion leakage through I_{CaL}, due to the very high potassium concentrations in the cell; this shifts the reversal potential of I_{CaL} slightly towards that of potassium reversal potential (-90 mV).

Nifedipine is a selective I_{CaL} inhibitor (Hagiwara, Irisawa et al. 1988; Kodama, Nikmaram et al. 1997). Exposure of spontaneous sino-atrial node cells to nifedipine was not studied, as even partial blockade of I_{CaL} would probably stop these cells that rely so heavily on I_{CaL}, to generate spontaneous action potentials. 5 μM nifedipine totally inhibited the inward current activated upon depolarisation at all voltages; subtraction analysis facilitated better description of the voltage-dependence of I_{CaL} but led to no further insights, except illustrating a more rapid activation at negative voltages and a more gradual decline in I_{CaL} at positive potentials. Further investigation into the effect of nifedipine upon other ionic currents revealed a slight inhibition of I_K; this effect is not likely to be a direct inhibitory effect of nifedipine upon I_K, as dihydropyridines are thought to bind specifically with calcium channels and there has been no previous evidence for such an effect upon I_K. It is more likely that the nifedipine reduction in I_K is due to some secondary mechanism, such as inhibition of the I_{CaL} mediated calcium influx blocking calcium regulation of I_K.

The other major calcium channel expressed in cardiac myocytes is the T-type calcium channel; this current is activated at more negative potentials than I_{CaL}, ranging from –70 to –30 mV. I_{CaT} has been found to have a role in diastolic depolarisation (Doerr, Denger et al. 1989), and if this current is not specifically looked for, it could easily be mistaken for an aspect of I_{CaL} due to similar voltage-dependent activation. The slightly more negative voltage activation range will however mean I_{CaT} would contribute more to diastolic depolarisation and not to the action potential upstroke. It has been reported that I_{CaT} initiated local calcium release from the SR and therefore may have a role in excitation-contraction coupling (Huser, Blatter et al. 2000). Low concentrations (50 μM and less) of nickel are thought to

block I_{CaT} and have been found to reduce the beating rate of atrial preparations and isolated sino-atrial node cells alike, both to a similar magnitude of between 10 and 20 %. Assuming selectivity of nickel for I_{CaT}, the observed reduction in spontaneous beating in atrial preparations and isolated sino-atrial node cells would indicate I_{CaT} does indeed have a role in pacemaking, which is comparable to that of I_f (ZD-7288 caused a 19 % reduction). No voltage clamp studies were undertaken to investigate I_{CaT}, as this requires a very negative holding potential, which activate I_f and disrupts the integrity of the patch recording.

Summary

Both I_{Kr} and I_{Ks} are present in the guinea-pig sino-atrial node and contribute to the generation of spontaneous action potentials. Voltage dependent activation of I_{Kr} is rapid at negative potentials, but exhibits rectification at more depolarised potentials as described by the E4031 sensitive currents. I_{Ks} does not activate until more depolarised potentials, but progressively activates as depolarisation is extended; I_{Ks} can be satisfactorily described by the I_K current resistant to E4031. The components of I_K can also be described according to their time-dependent activation, with I_{Kr} activating rapidly and becoming maximal, whereas I_{Ks} only begins to activate after >70 ms, but continues to activate as the depolarisation is extended. I_K tail current activated with 40 and 700 ms are used to differentiate effects upon I_{Kr} and I_{Ks} (although the I_{Kr} contribution is considered) in later chapters.

Other ionic currents of the sino-atrial node were also investigated. I_f, the large inward current activated upon hyperpolarisation, was found to activate more rapidly at very negative potentials at which the I_f current is massive and to exhibit a reversal potential of –19 mV. In addition, caesium was found to be a non-selective inhibitor of I_f. I_{NCX} was found to have a substantial function in pacemaking, as inhibition with low sodium resulted in immediate cessation of beating, causing terminal voltage oscillation if the low sodium substitution was prolonged. The role of the calcium currents, I_{CaL} and I_{CaT}, were also briefly investigated and nickel inhibition of I_{CaT} indicated that this current maybe contributing to pacemaking to a greater extent than previously believed.

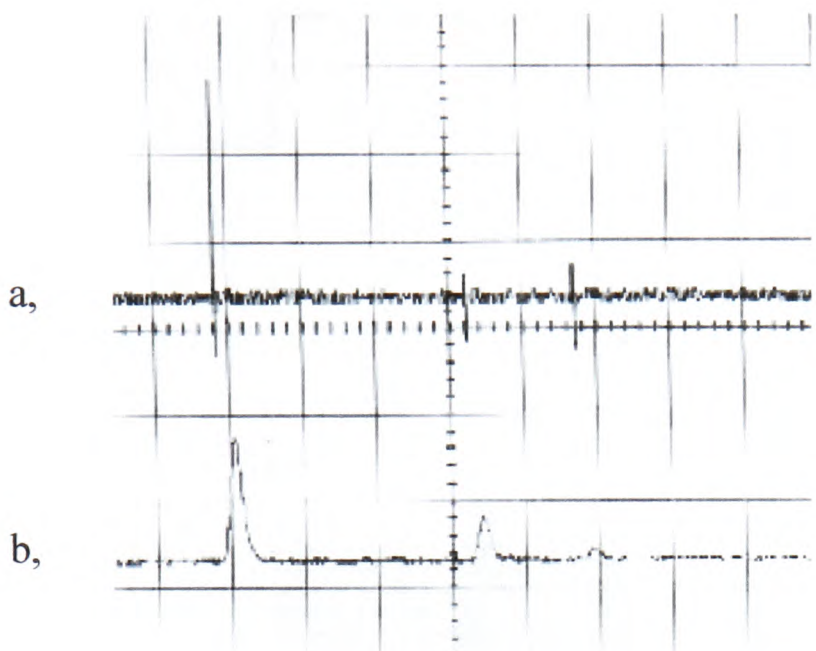

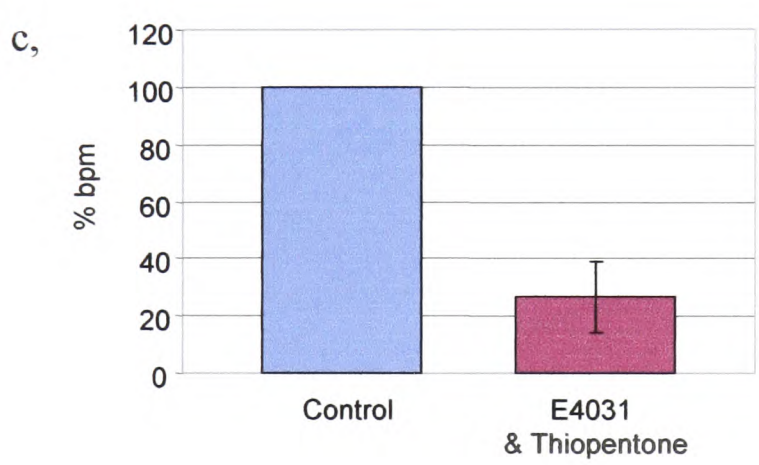

Figure 4.1

Blockade of I_K in guinea-pig atrial preparations reduced beating rate and induced arrhythmic activity. E4031 and thiopentone treatment (5 μM and 200 μM) appeared to make the electrical activity of atria more variable (a), as measured by a surface electrode, reducing the forced developed (b) and reduced the beating rate (c) by over 75 % (n=7, $P<0.05$). Beating in 4 of 7 atrial preparations failed and the other 3 developed variable electrical activity not conducive to effective contraction.

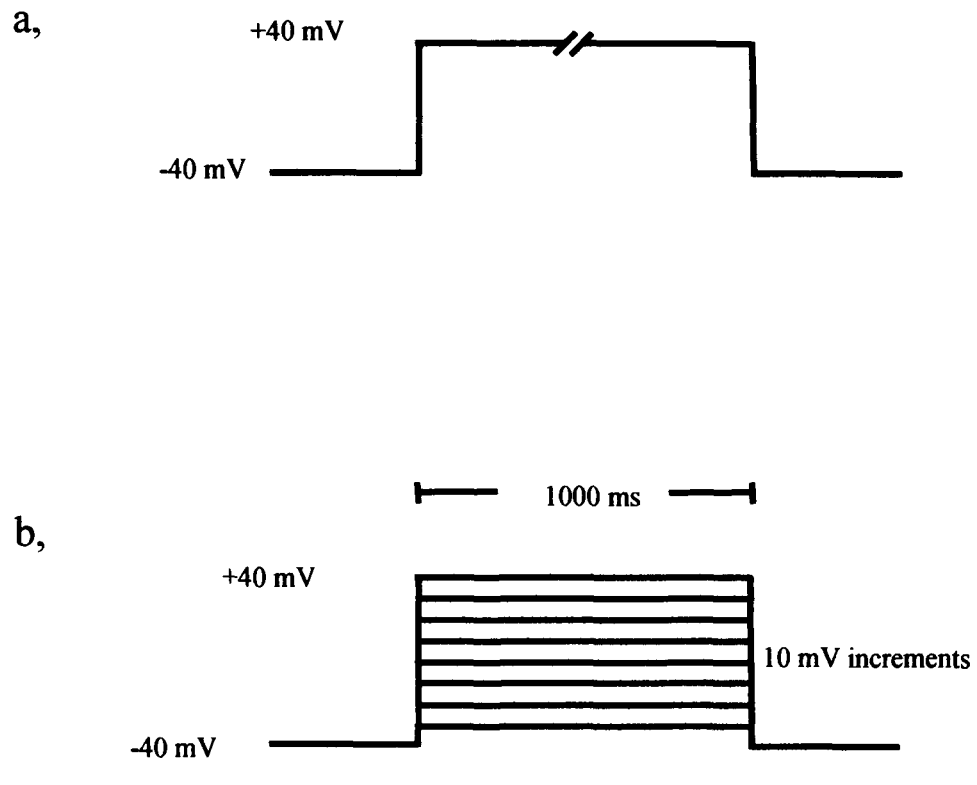

Figure 4.2

Voltage step protocol used to activate I_K (a and b), outward current activated by a 1000 ms depolarisation to +40 mV (c). Voltage steps are of duration range between 10 and 700 ms (a), with increments of 10 ms up to 100 ms, and subsequently with increments of 100 ms (to 700 ms). Voltage steps range between –30 and +40 mV, activating current with a 1000 ms depolarisation (b). Holding potential is always –40 mV. Both tail and step currents were measured (c), although tail currents are regarded as a more reliable measure of I_K (see text).

a,

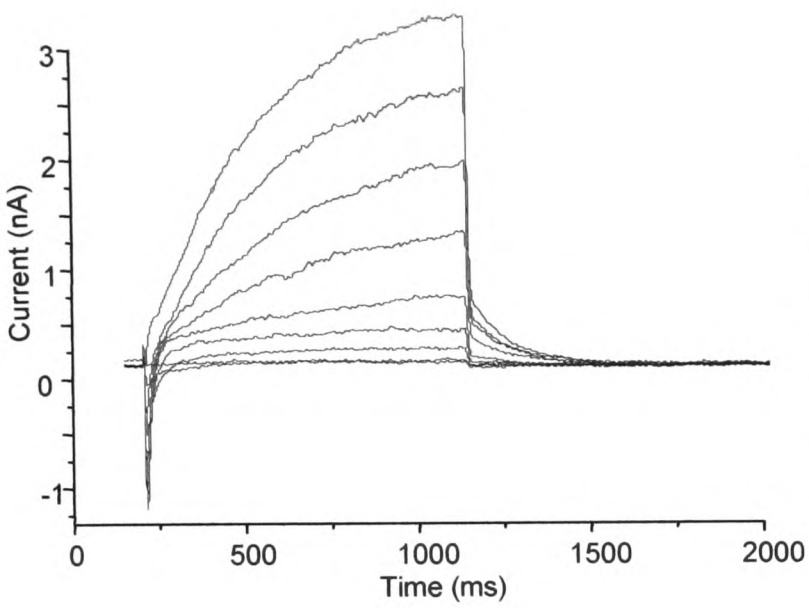

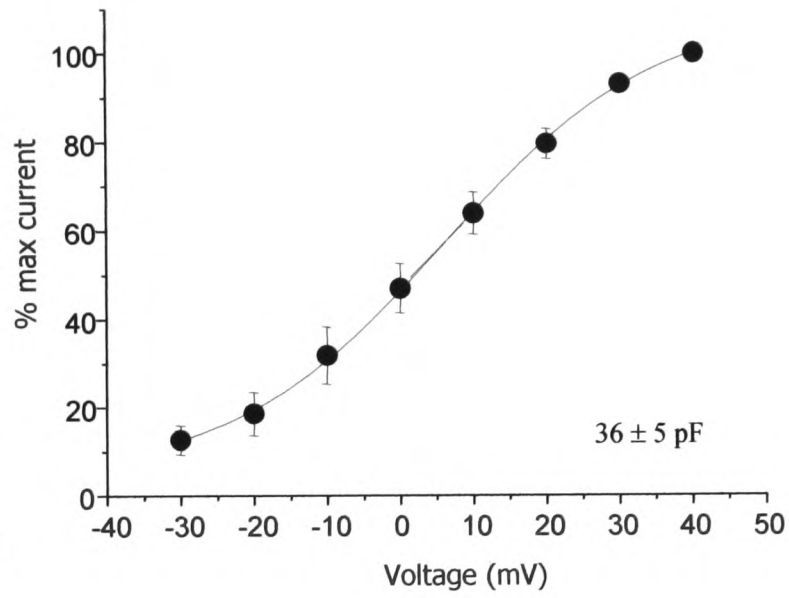

b,

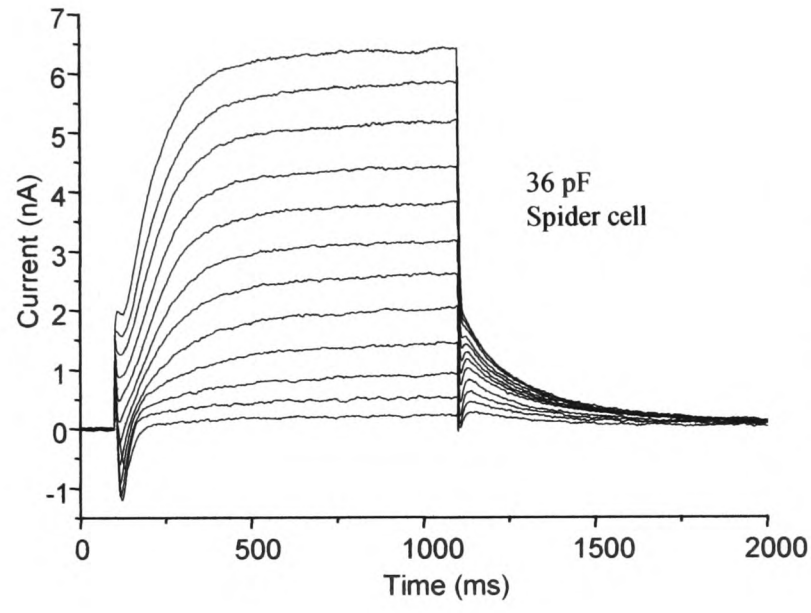

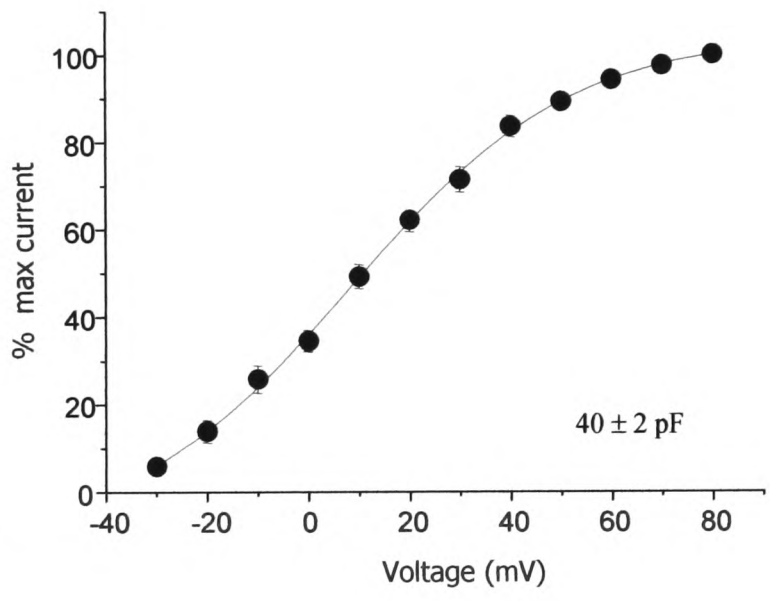

Figure 4.3

Currents activated by depolarisation to various voltages up to +40 mV (a) and +80 mV (b) displayed in left panel, and the I_K voltage dependence quantified from the tail current amplitude upon repolarisation in the right hand side panel. The $V_{1/2}$ and slope of activation were 6 ± 3 and 14 ± 4 mV (a) and 8 ± 3 and 22 ± 2 mV (b) in 14 and 6 cells respectively.

a,

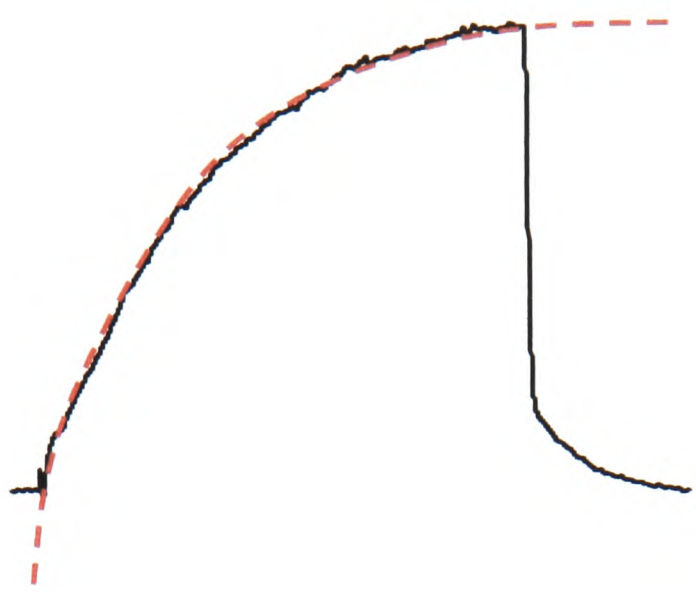

b,

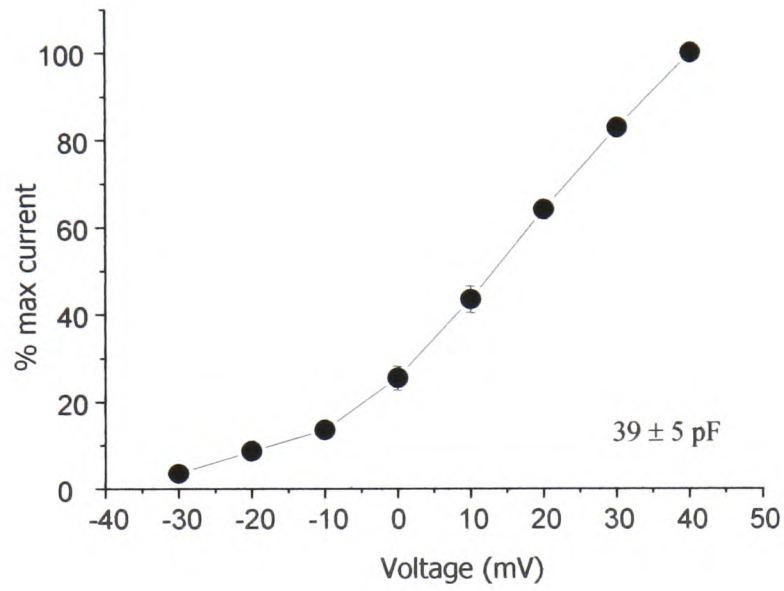

c,

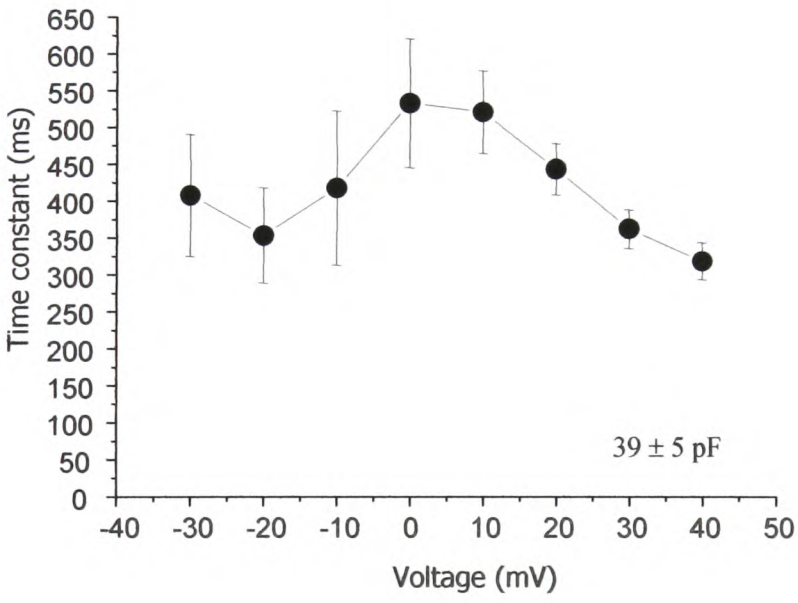

Figure 4.4 Page 172

Voltage dependent activation of outward current. The outward step current was fitted with a single exponential curve (a); both the amplitude (b) and the time-constant of activation (c) were recorded (n=9).

a,

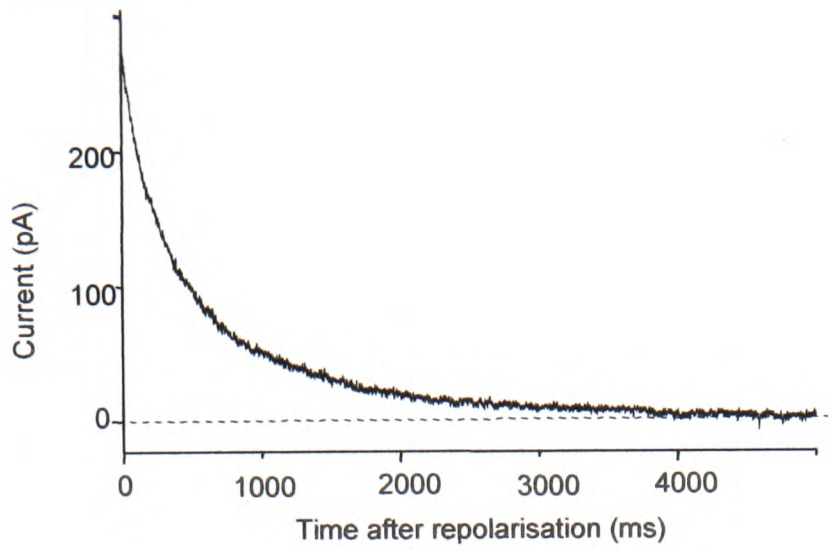

b,

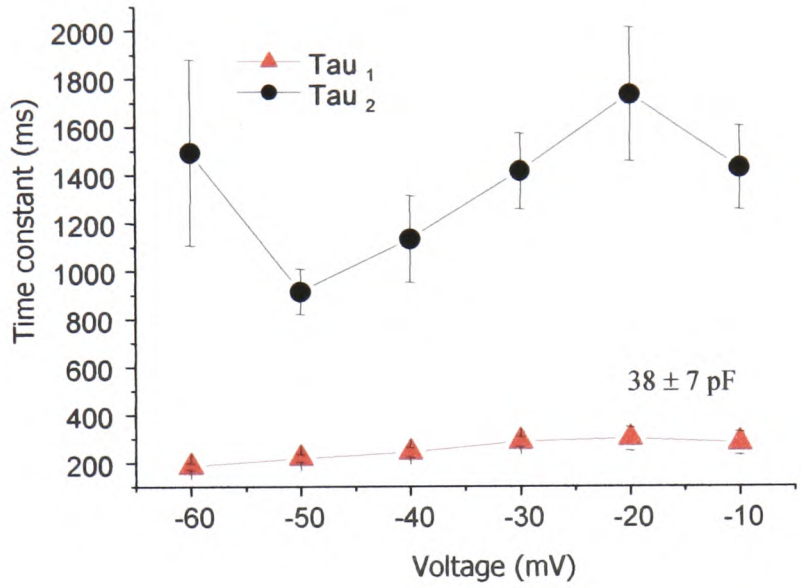

c,

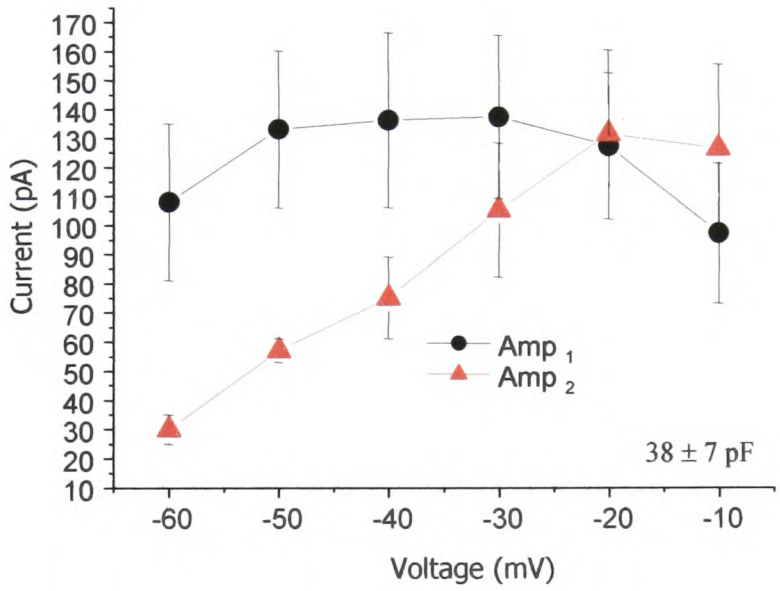

Figure 4.5 Page 173

Voltage dependent deactivation of the I_K tail current. The decay of the I_K tail current was fitted with a bi-exponential curve (a) and the voltage dependency of the time-constants (b) and of each components amplitude (c) were measured (n=6).

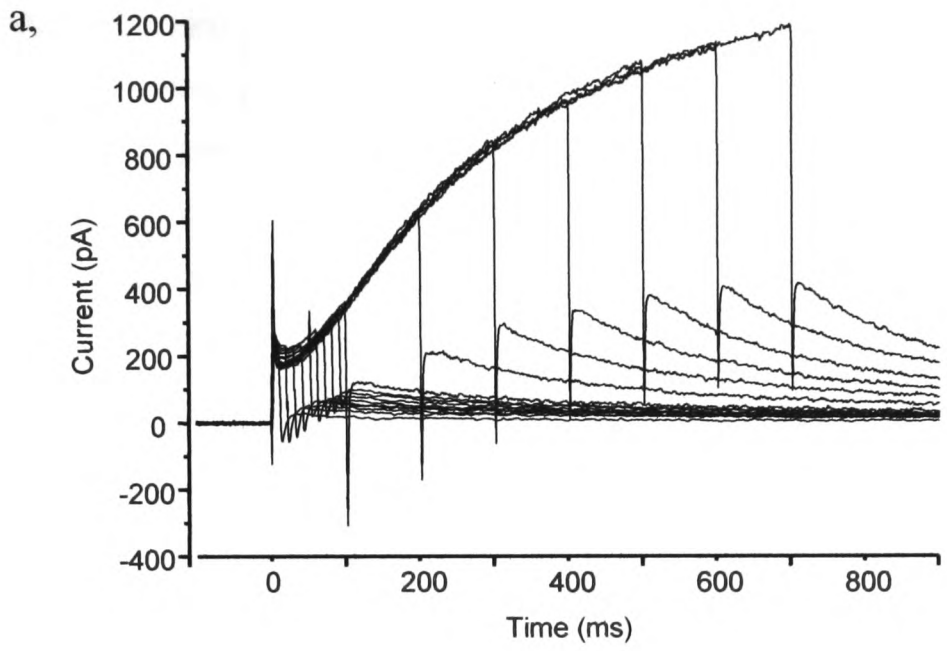

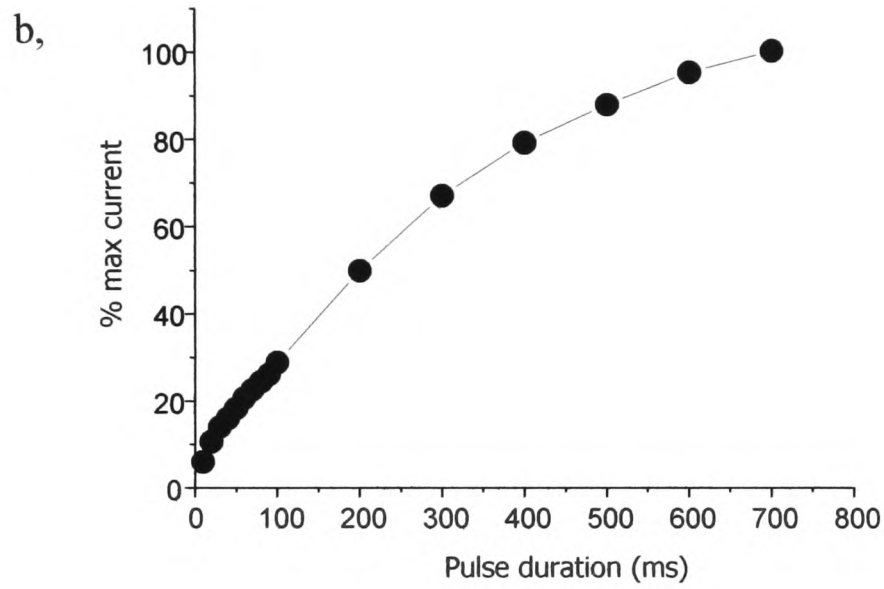

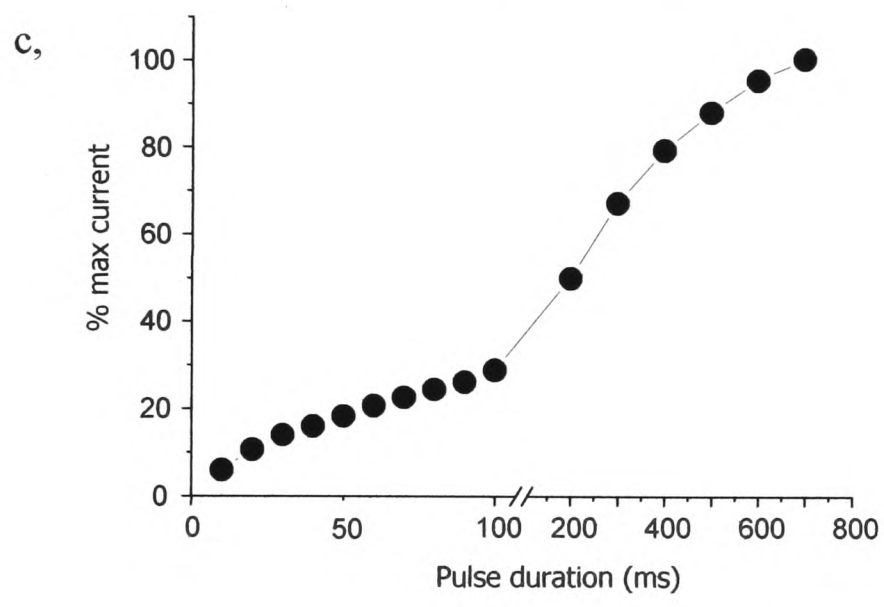

Figure 4.6 Page 174

Current traces showing pulse current and I_K tail current, activated by depolarisations of durations between 10 and 700 ms (a). Both step and tail current are progressively activated with depolarisation (a and b; n=28). Two phases of I_K time-dependent activation can be seen (b), and the use of an expanded time scale for the first 100 ms (c), makes this much easier to discern. Error bars maybe hidden within symbol (n=28). All measurements have been normalised to maximal current.

a,

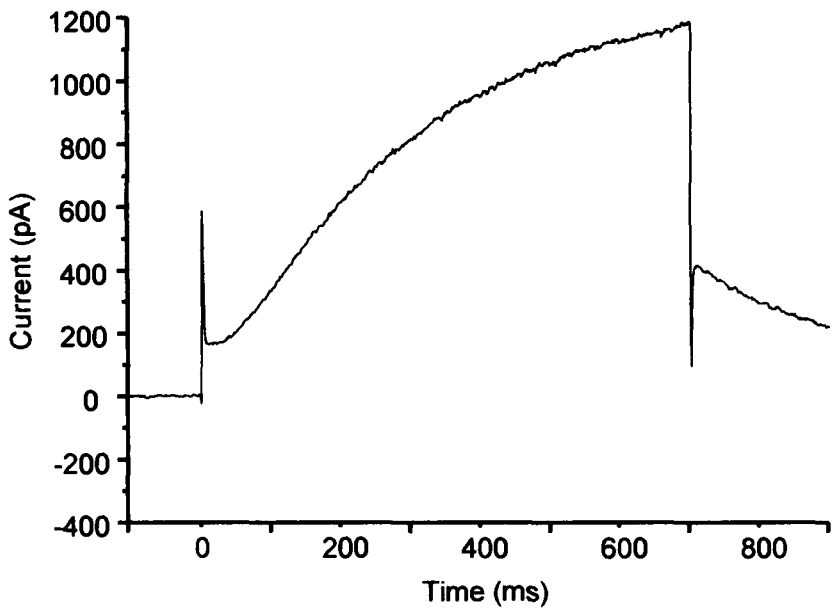

b,

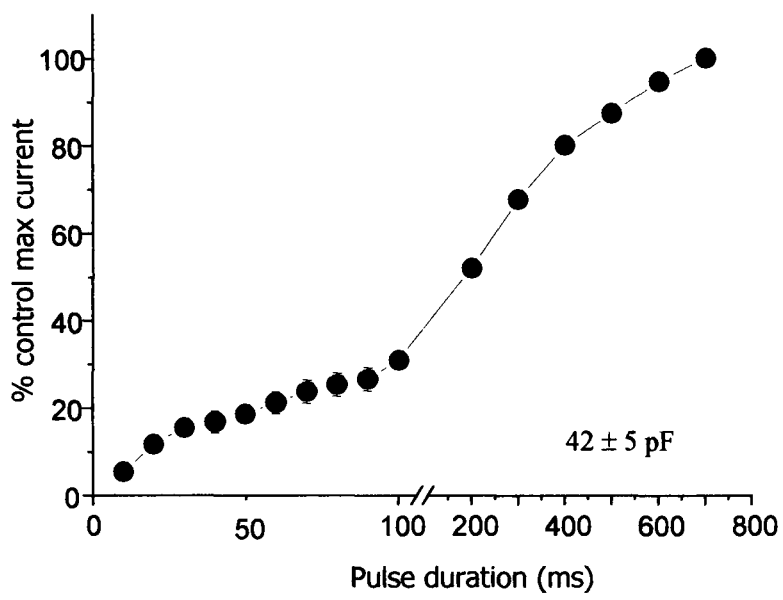

c,

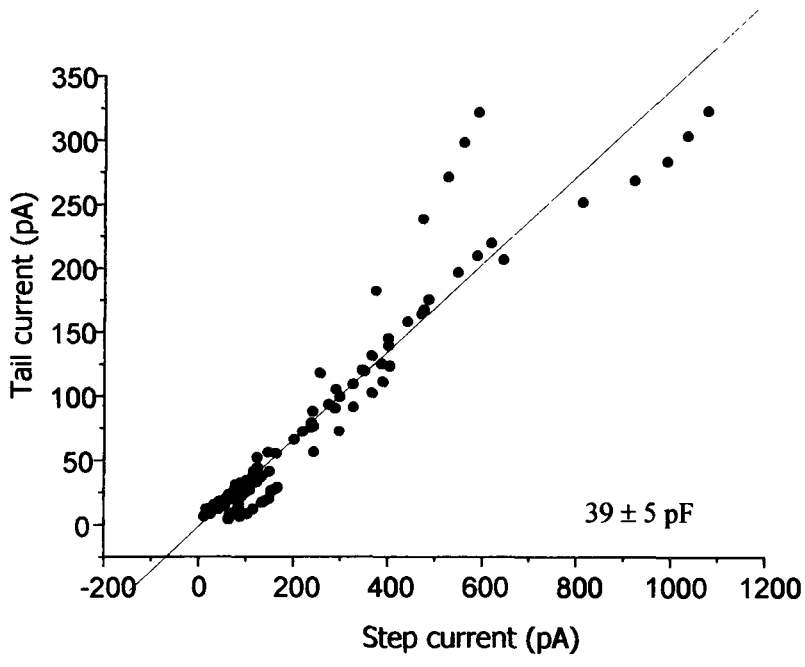

Figure 4.7 Page 175

Step and tail current activated upon depolarisation (a). Both step and tail currents were progressively activated by extended depolarisations (b); this relationship appeared to be linear (c), fitting the curve y=0.34x-2.2. These data were taken from 10 cells, each measured at 16 different depolarisation durations.

a,

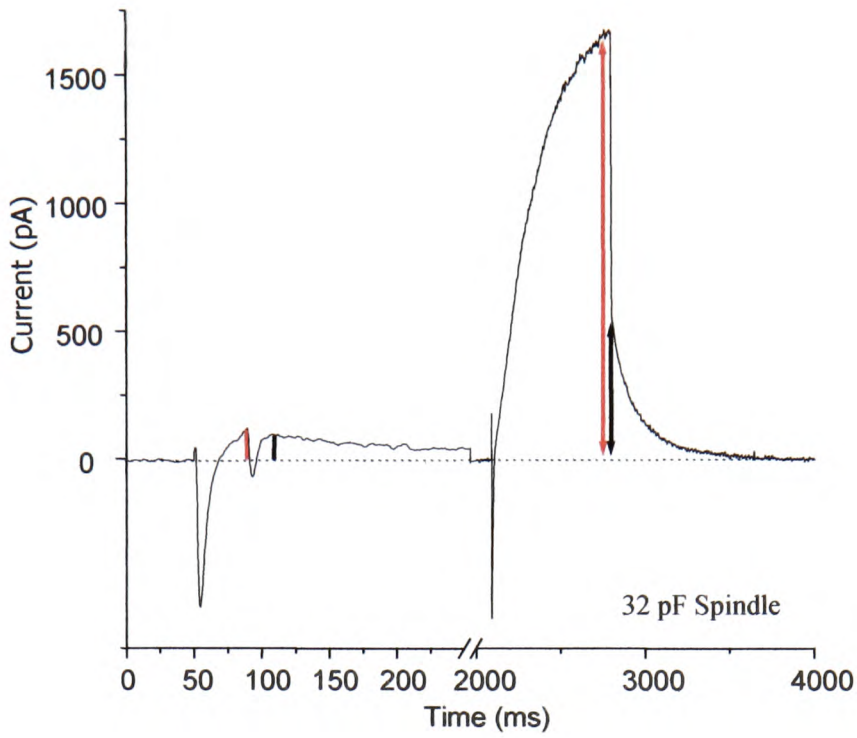

b,

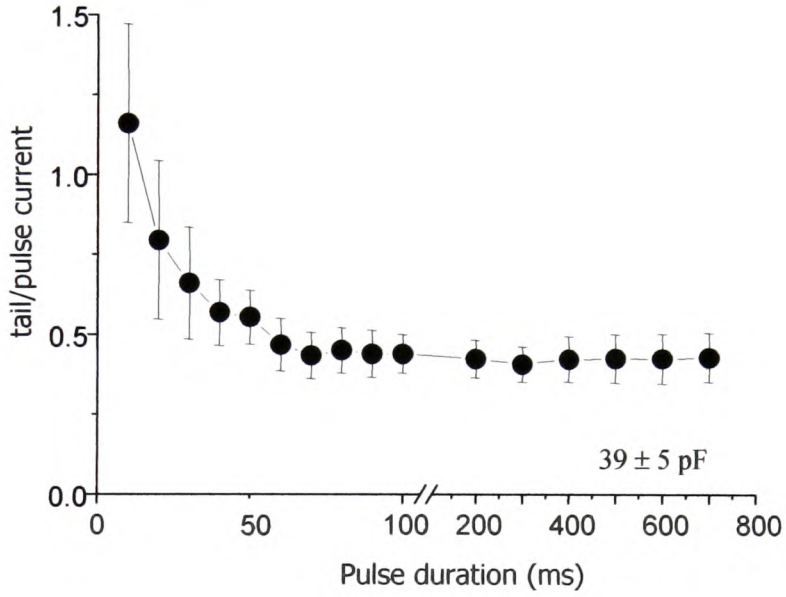

Figure 4.8 Page 176

Measurement of step and tail current at different duration depolarisations and application of the envelope of tails test. Figure 5.8a illustrates that the tail current amplitude (black arrows) is of comparable size to the step current (red arrow) at brief (40 ms), but not prolonged (700 ms) depolarisation. An envelope of tails test was undertaken (b) by taking a ratio of tail current:step current and plotting this against depolarisation duration (n=10).

a,

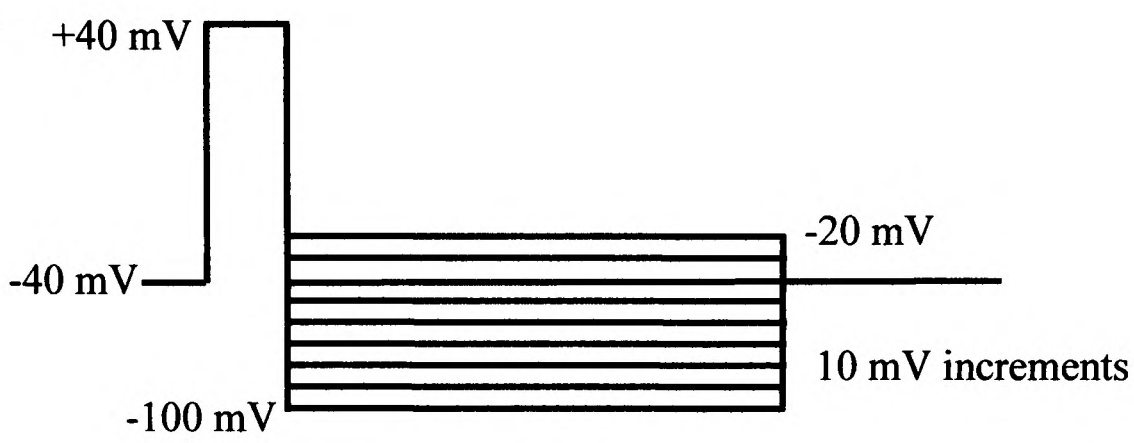

b,

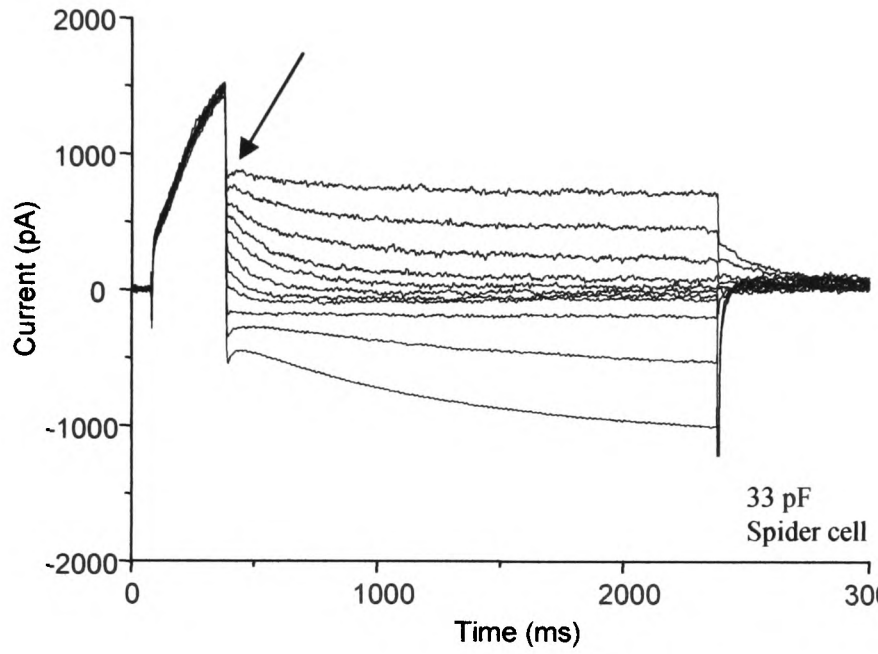

c,

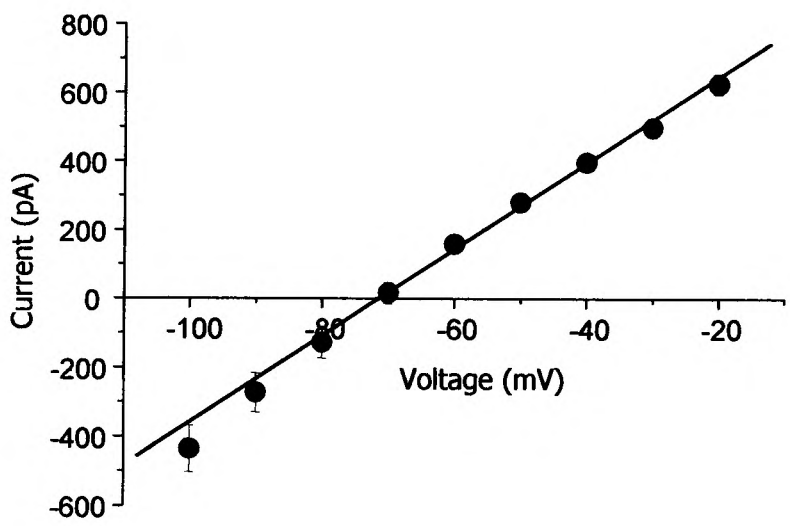

Figure 4.9

The reversal potential of I_K was found to be –70 ± 2 mV (n=7). Figure 5.9a illustrates the voltage protocol used to describe the instantaneous direction of current flow (arrow in figure 5.96) at various voltages, which had been previously activated by depolarisation. The instantaneous current was plotted against voltage and a linear relationship was found in figure 5.9c to reverse directions at –70 ± 2 mV (n=7).

a,

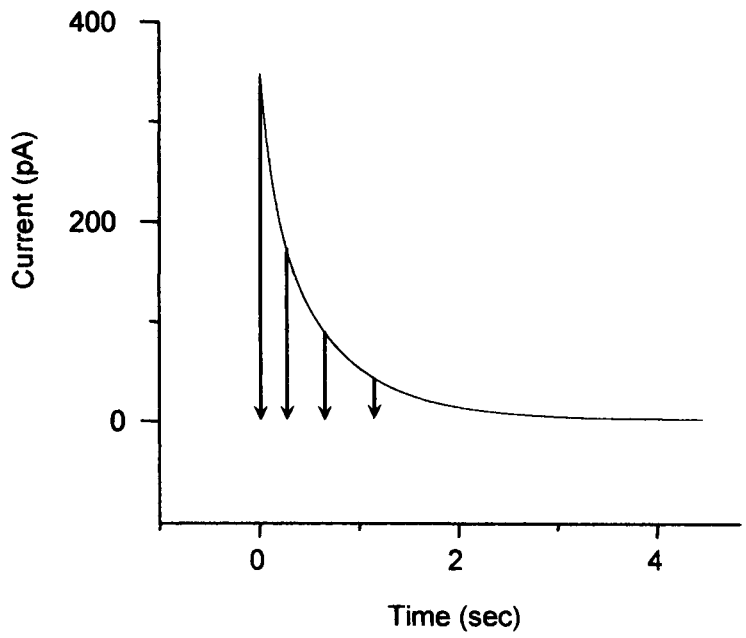

b,

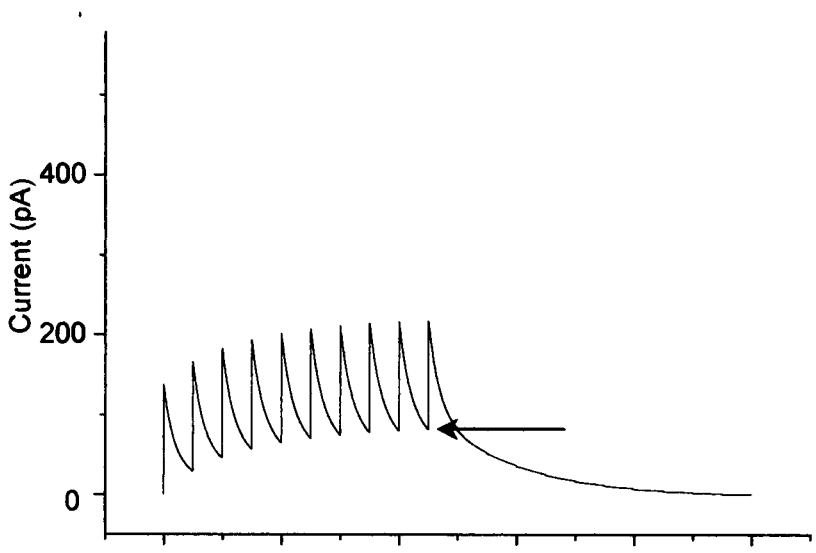

Repolarisation to -60 mV
Time-constants 185 and 1493 ms
Amplitudes 108 and 30 pA
120 bpm
Residual I_K = 82 pA

c,

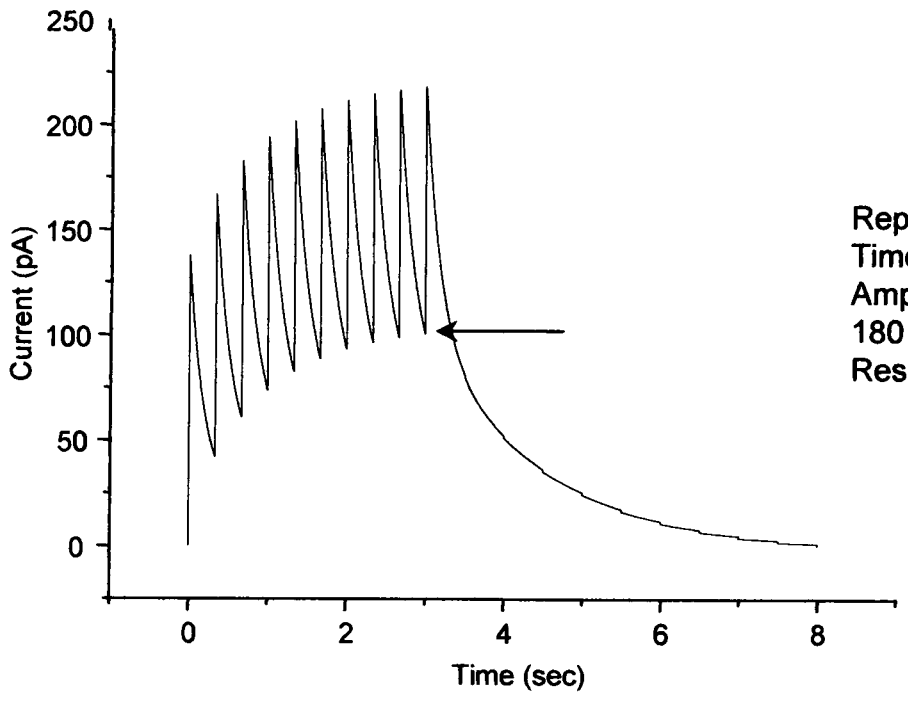

Repolarisation to -60 mV
Time-constants 185 and 1493 ms
Amplitudes 108 and 30 pA
180 bpm
Residual I_K = 100 pA

Figure 4.10

The time course of de-activation of an indivual current is shown in panel a. Modelling of I_K deactivation to –40 (a) and –60 mV in a system which simulates beating rates of 120 (b) and 180 bpm (c). Horizontal arrows in b, and c, show residual current at end of a sequence of depolarising pulses that simulate beating. The time-constants and amplitude of I_K tail current decay were incorporated into a system which illustrates the amount of residual I_K at 120 bpm. When the simulated beating rate was increased, a residual 100 pA current was identified (c).

a,

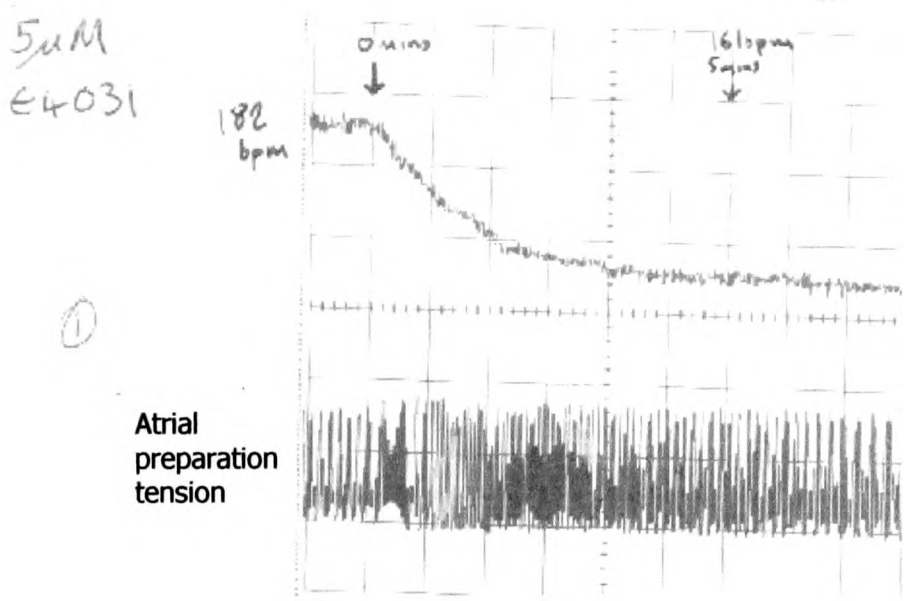

b,

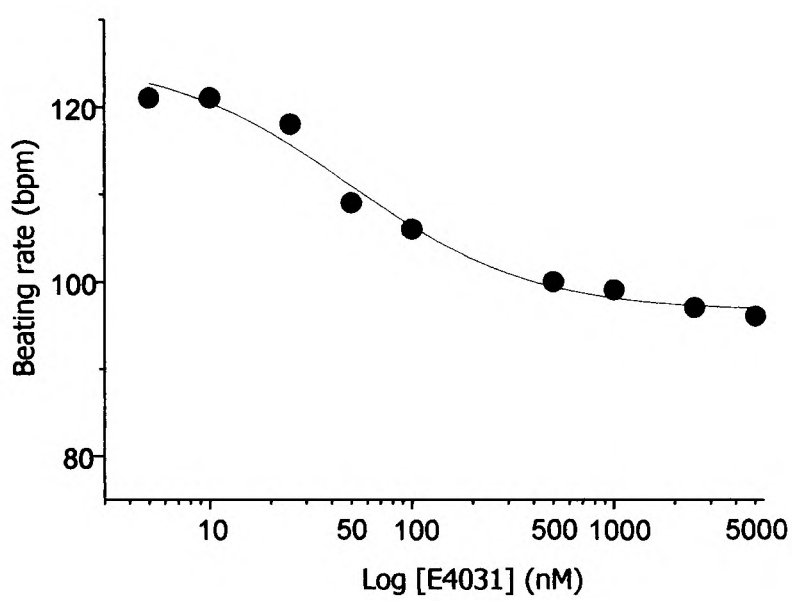

c,

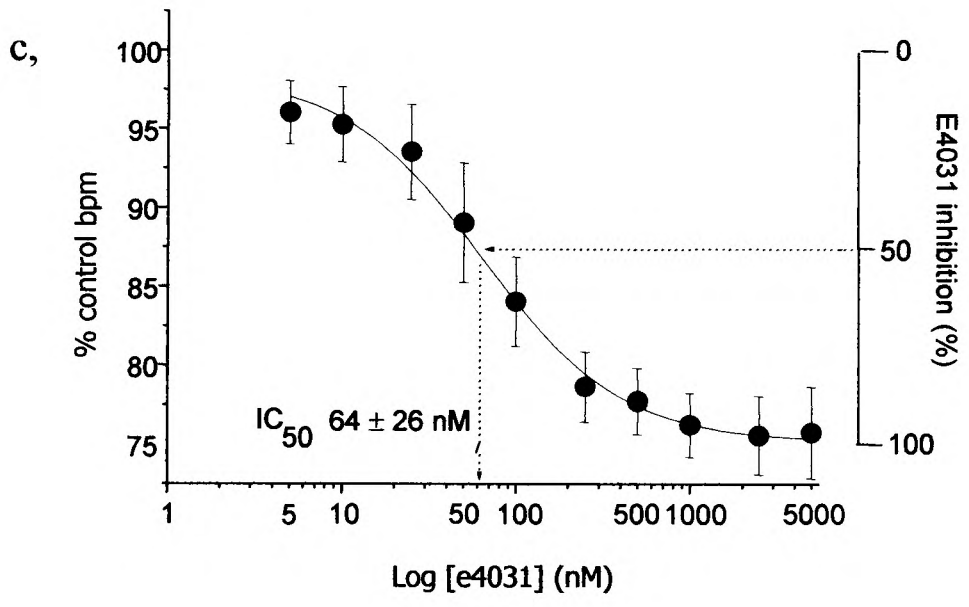

Figure 4.11 Page 179

Effects of the I_{Kr} specific inhibitor E4031 upon beating rate of isolated atrial preparations. Figure 5.11a is oscilloscope print-out of the beating rate (upper trace) and tension developed (lower trace) upon addition of 5 μM E4031, whilst figure 5.11b illustrates the concentration dependent effects of E4031 upon beating rate on the same preparation. The IC_{50} of E4031 was found to be 64 ± 26 nM (n=5), with the maximal E4031 effect reducing beating rate by approximately 25 % (c).

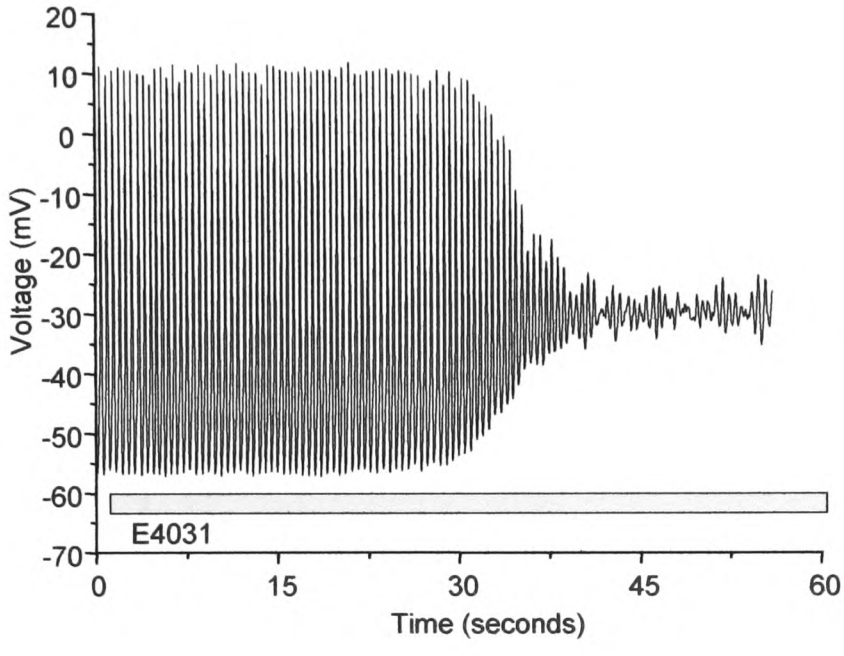

Figure 4.12 Page 180

E4031 causes spontaneously beating sino-atrial node cells to stop beating. An action potential recording from a spontaneously beating sino-atrial node cell, illustrates that 5 μM E4031 reduced the action potential amplitude, and usually (8 of 9 cells) stopped beating.

a,

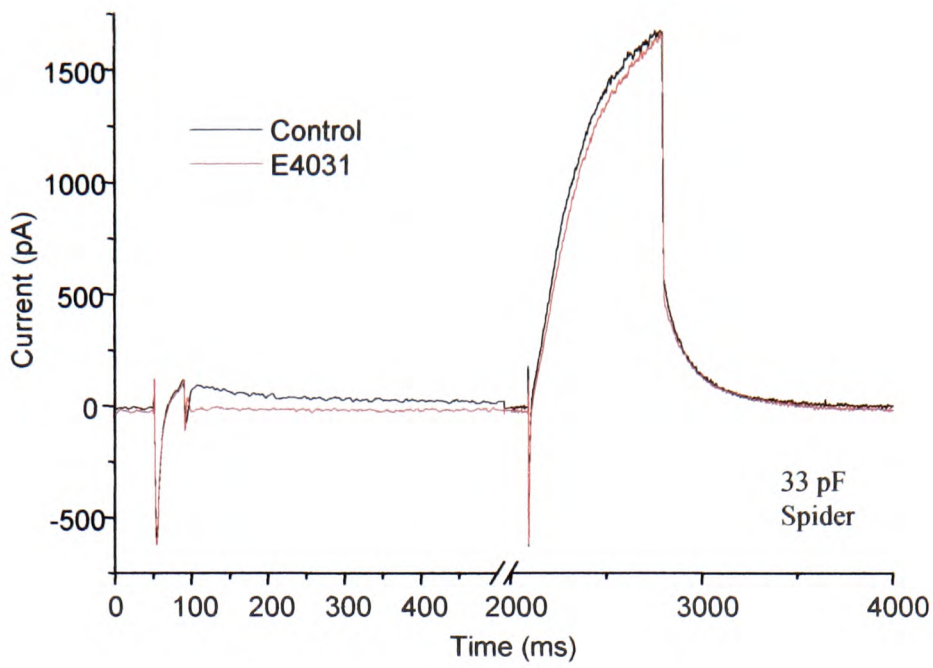

b,

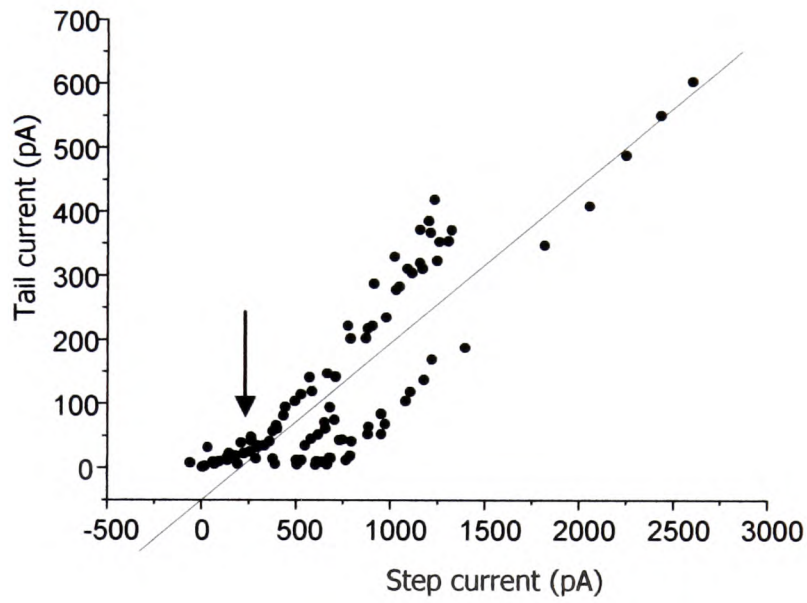

Figure 4.13 Page 181

Step and tail current activated upon 40 and 700 ms depolarisation (a) in the absence and presence of 5 μM E4031. Step currents were progressively activated by extended depolarisations, but tail current amplitude did not appear to increase until step current was approximately 250 pA (arrow in b). These data were taken from 10 cells, each measured at 16 different depolarisation durations.

a,

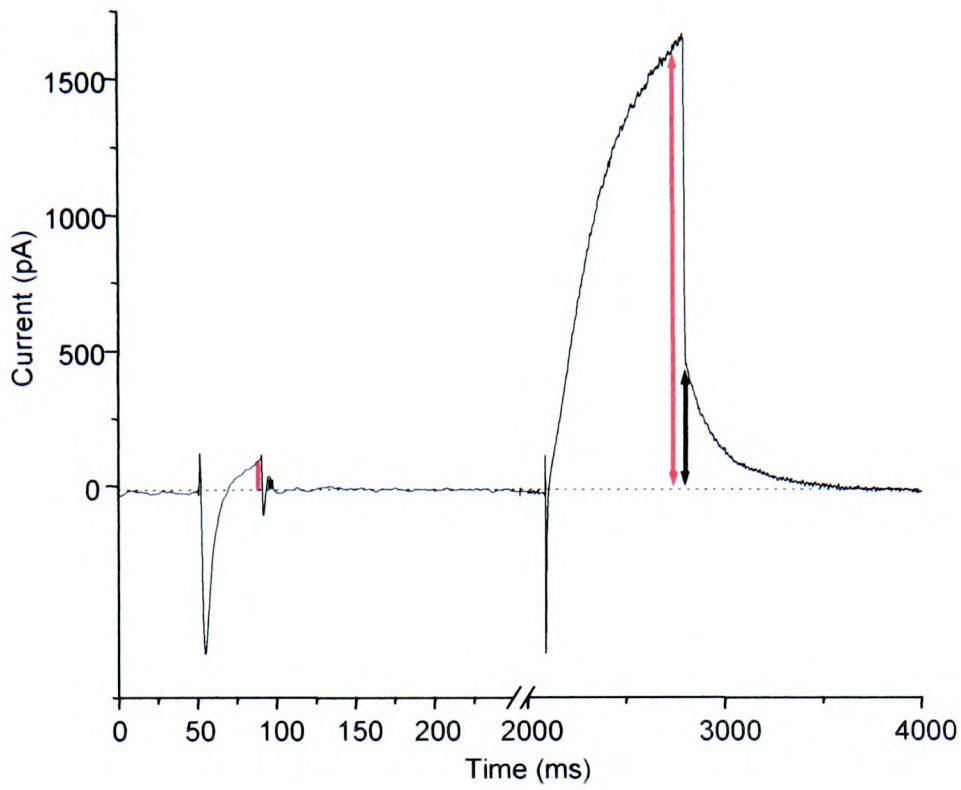

b,

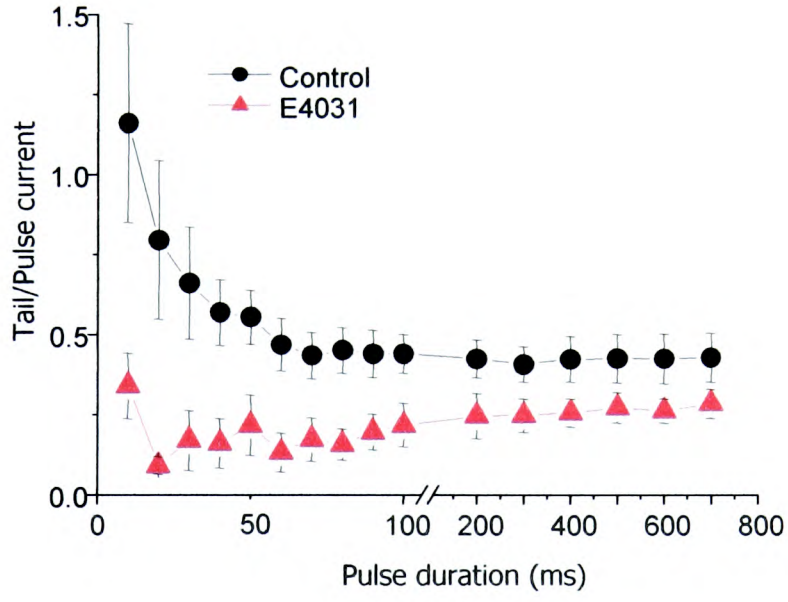

Figure 4.14 Page 182

Step and tail currents were measured at different duration depolarisations in the absence and presence of 5 μM E4031 and the envelope of tails test applied to these data. Figure 5.14a illustrates that in the presence of E4031 the tail current amplitude is smaller than the step current at both brief (40 ms) and prolonged (700 ms) depolarisation. An envelope of tails test was applied and compared to control (b); the ratio was reduced in the presence of 5 μM E4031 at durations briefer than 90 ms ($P<0.05$, excluding 70 ms), being relatively constant irrespective of depolarisation duration.

a,

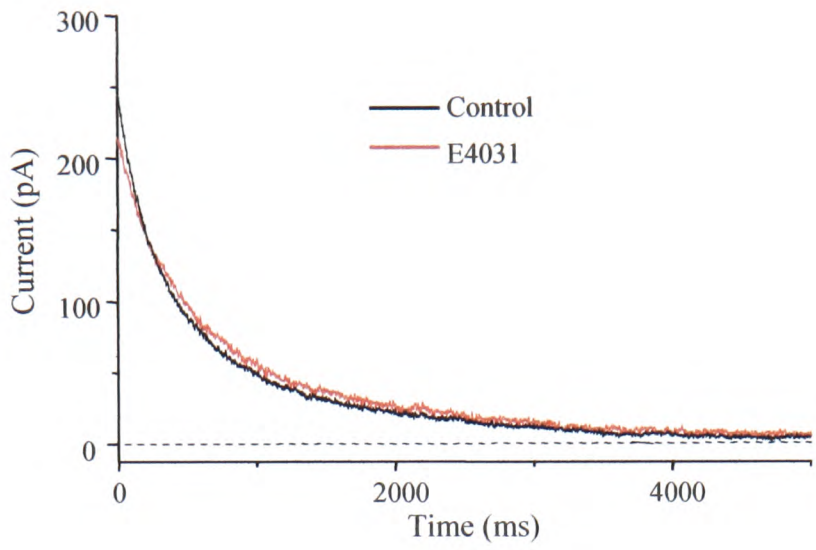

b,

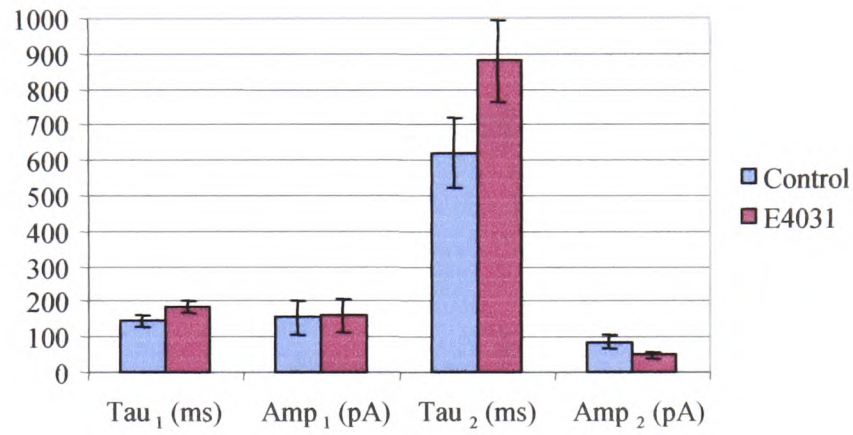

Figure 4.15 Page 183

I_K tail current deactivation in the presence of 5 μM E4031. Reduction in amplitude of the I_K tail current in the presence of E4031 (figure 5.15a), which has been quantified in 12 cells and found to be consistent with a reduction in the amplitude associated with the longer time constant (b). E4031 was also found to prolong both time-constants of I_K decay in the presence of E4031 (b).

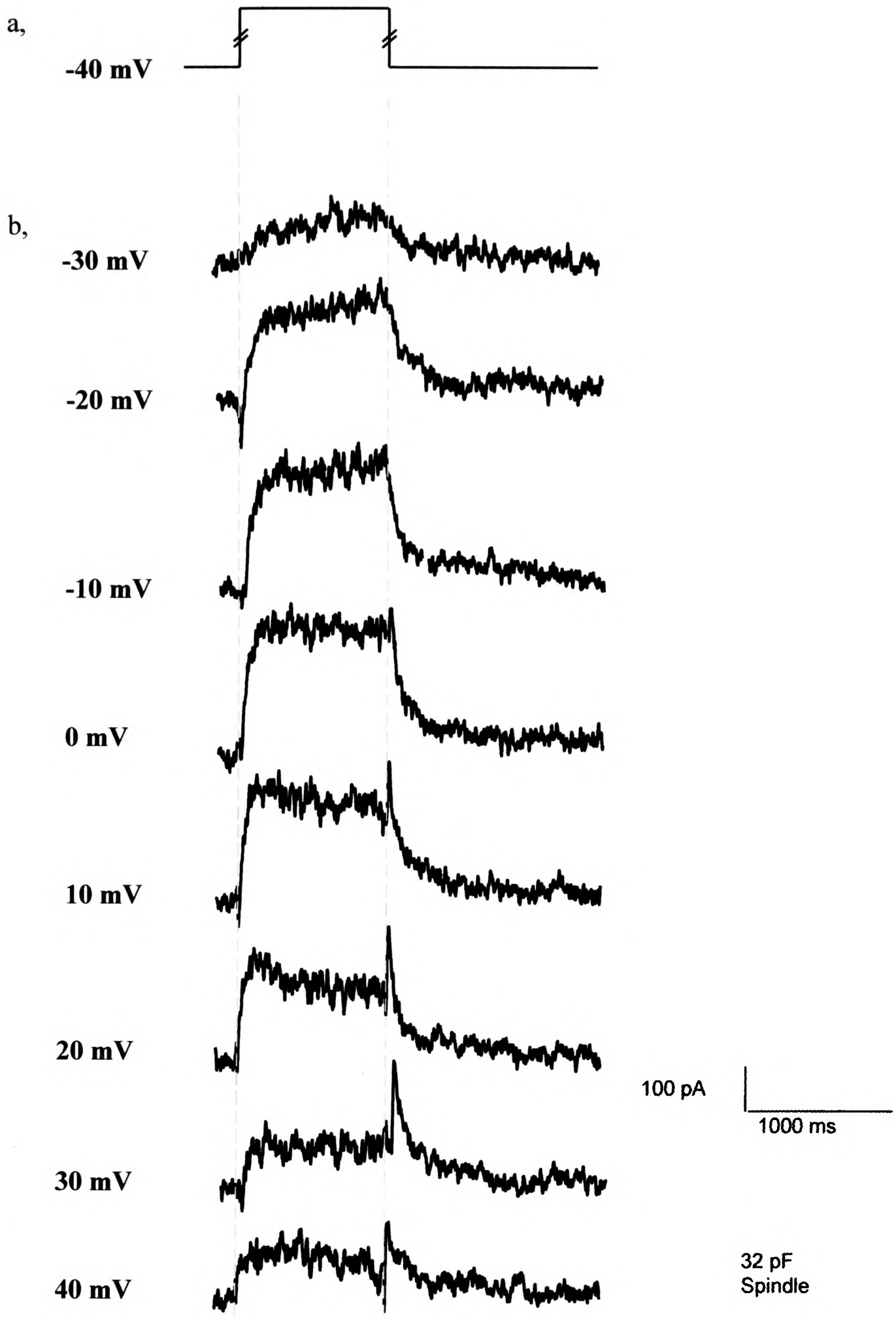

Figure 4.16 Page 184

Voltage dependent rectification of the E4031 sensitive current. The protocol described above (a) was used and subtraction analysis was undertaken to define the voltage dependent activation of the E4031 sensitive current (b). Both the step and the tail current sensitive to E4031 (5 μM) were maximal around 0 mV, whilst more depolarised voltages reduced both step and tail current amplitude (b). Note the reduction of the E4031 sensitive current *during* the step at 10 and 20 mV.

a,

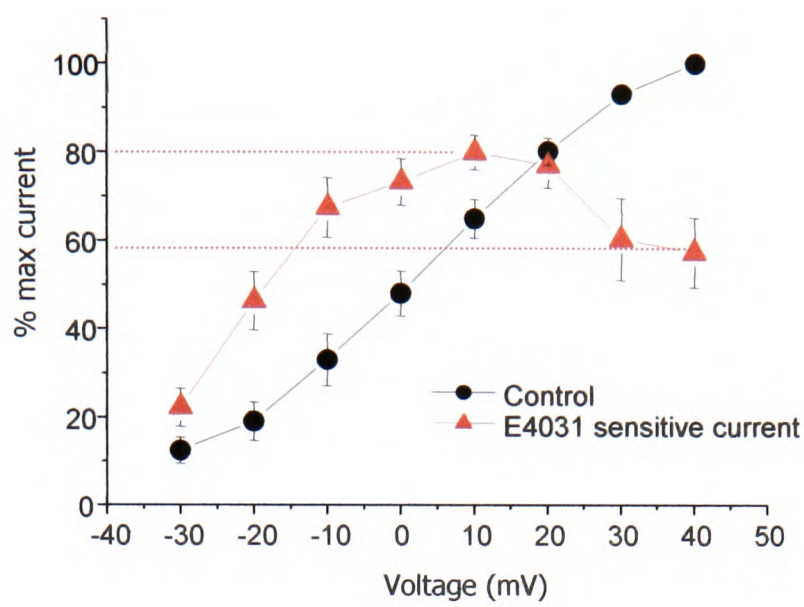

b,

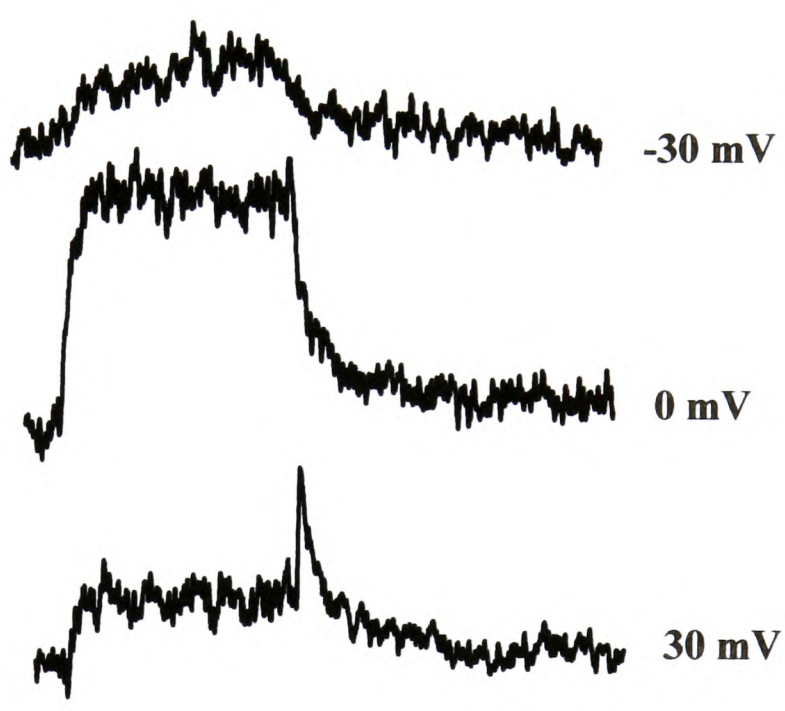

Figure 4.17

Voltage dependent rectification of E4031 sensitive current. E4031-sensitive tail current are compared with control tail currents in the absence of E4031 in panel a. Panel b shows individual traces of E4031 sensitive current at different potentials illustrating that rectification results in a smaller pulse and tail current at +30 mV than at 0 mV. At voltages greater than +10 mV there is a reduction in the E4031 sensitive tail current ($P<0.05$ at +30 and 40 mV). The E4031 sensitive current is reduced by approximately 25 % of max at +40 mV.

a,

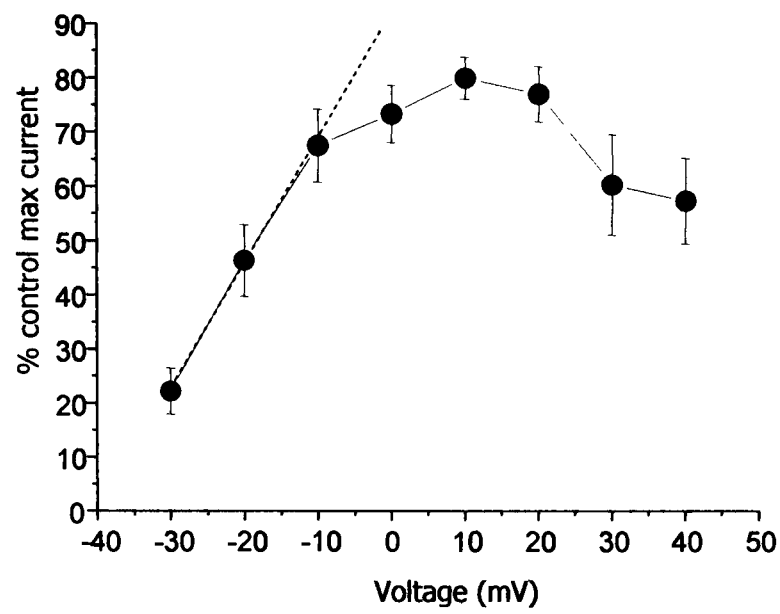

b,

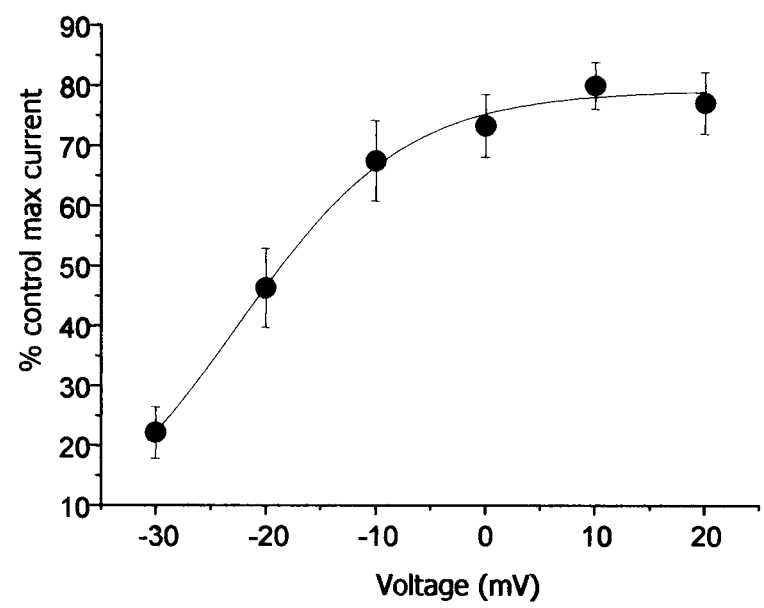

c,

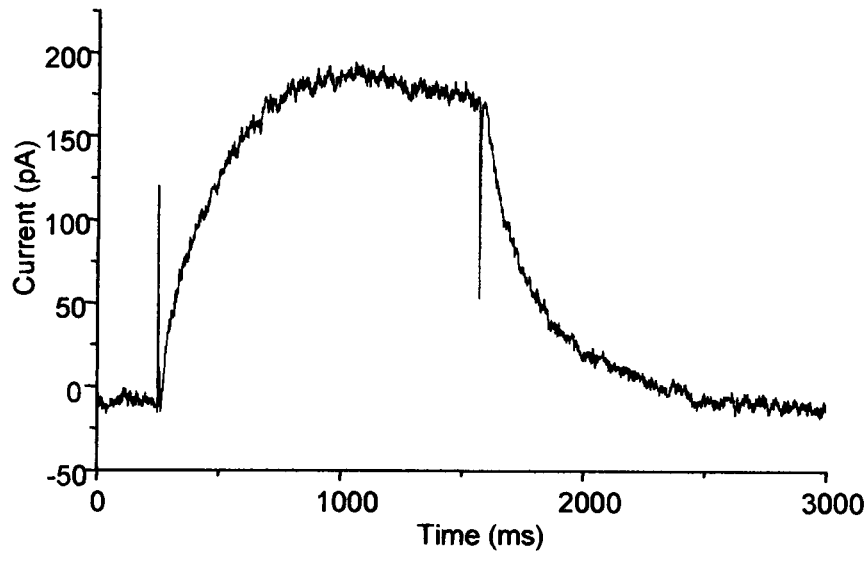

Figure 4.18 Page 186

Steep voltage dependent activation of the E4031 sensitive current. Depolarisation to –30 and –20 mV caused activation of bigger E4031 sensitive currents. When rectified current (+30 and +40 mV) were excluded, a sigmoidal voltage dependent activation curve was fitted and resulted in a $V_{1/2}$ and slope values of –23 ± 11 and 7 ± 6 mV (n=18). The E4031 sensitive step current was found to be progressively reduced in some recordings at more depolarised voltages (c and figure 5.16b, +10 and +20 mV).

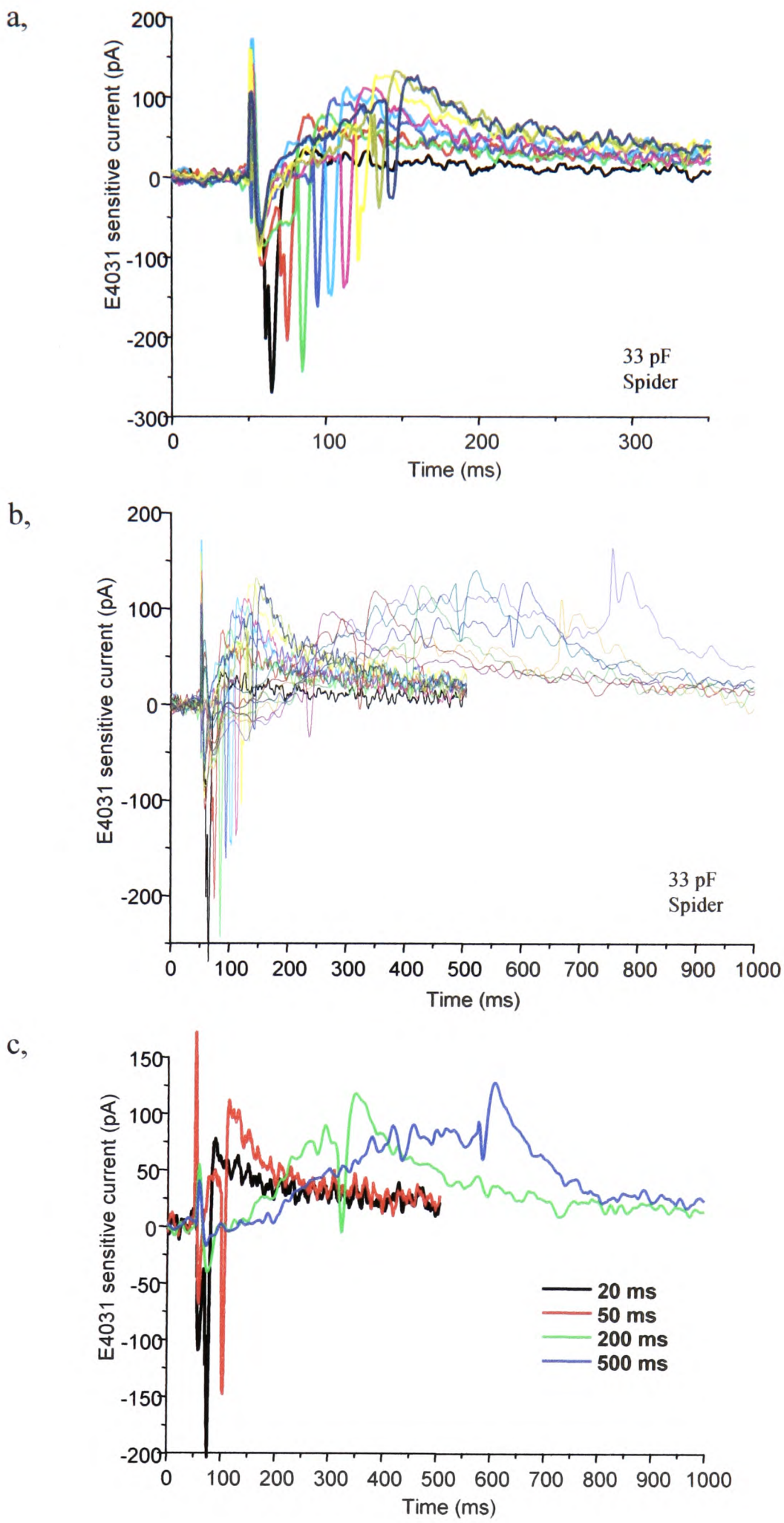

Figure 4.19

Time-dependent activation of the E4031 sensitive current. Progressively longer duration depolarisation activated bigger E4031 (5 μM) sensitive currents, but these were near-maximally activated between 50 and 70 ms (a). More extended depolarisations do not activate any additional E4031 sensitive current (b) and therefore these amplitudes were similar when activated with depolarisations of 50, 200 and 500 ms, approximately 125 pA in this sino-atrial node cell (c).

a,

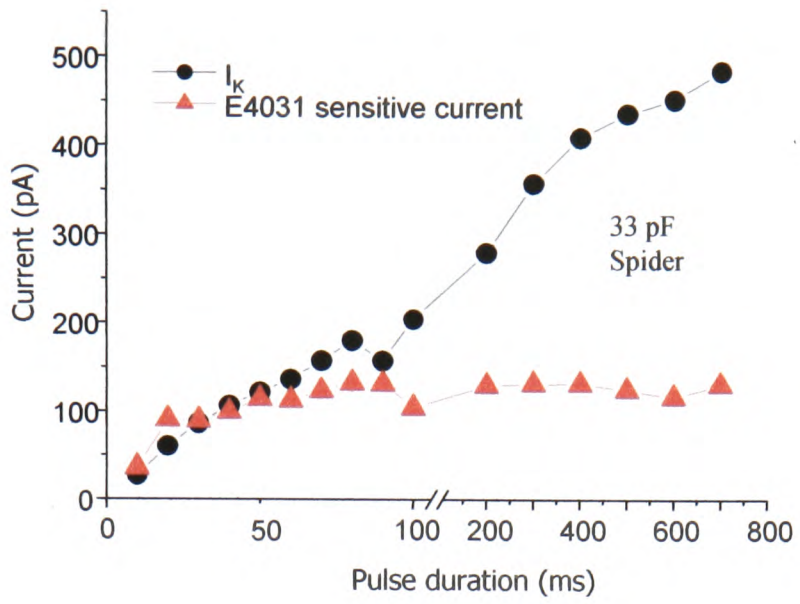

b,

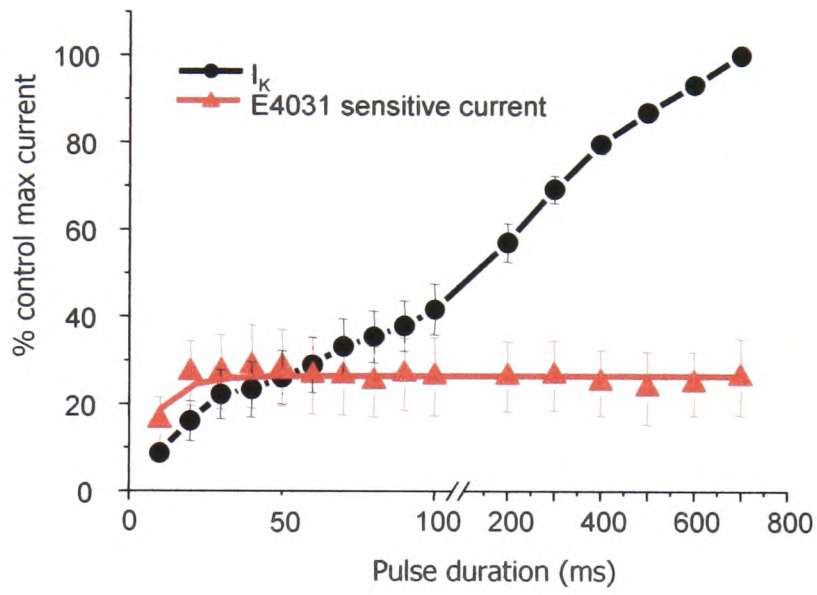

Figure 4.20 Page 188

Time-dependent activation of I_K and E4031 (5 μM) sensitive current. These data are taken from the same sino-atrial node cell (a). I_K amplitude progressively increased as depolarisation duration was extended, whereas E4031 sensitive current was maximally activated with a 40 ms depolarisations. I_K activated with depolarisation longer than 90 ms was larger than the E4031 sensitive current ($n=6$, $P<0.05$). E4031 sensitive current was fitted with a BoxLucas curve; max 26 %, time-constant 8 ms (rate constant of 0.12 ms).

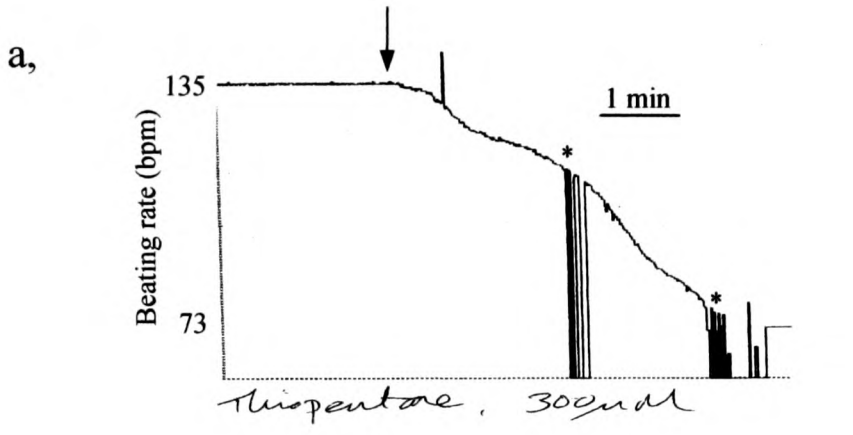

Figure 4.21 Page 189

Effect of thiopentone upon isolated atria preparations. The beating rate of atrial preparations was reduced immediately upon the addition (at the arrow) of 300 μM thiopentone (a). Thiopentone also caused the surface electrode recordings to become variable in regard to amplitude and direction of deflection (b); this maybe associated with ineffective rate measurement (*). Increasing concentrations of thiopentone were administered to atrial preparations (n=6) and the maximal thiopentone reduction of beating rate was evaluated (sigmoidal curve) to be approximately 100 % of beating rate (c); IC_{50} of thiopentone was estimated to be 151 μM.

a,

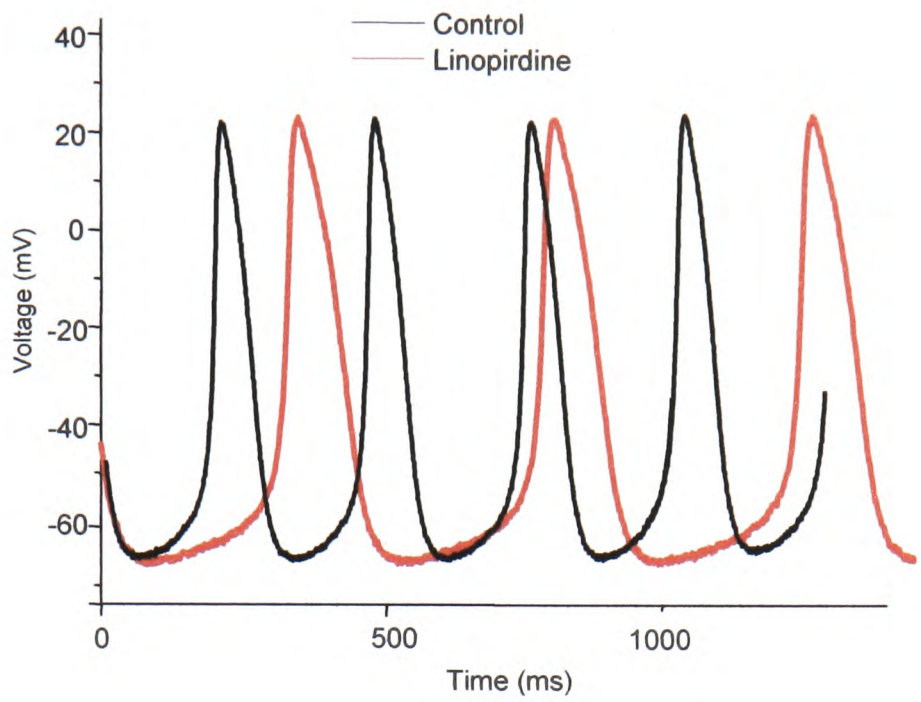

b,

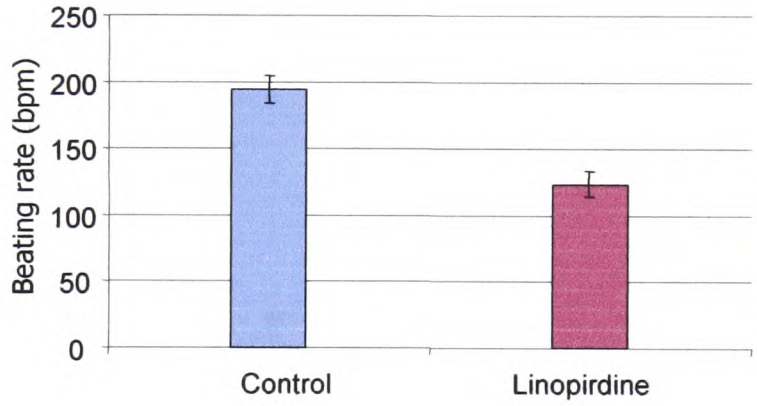

Figure 4.22 Page 190

linopirdine reduced spontaneous action potential generation of sino-atrial node cells. Linopirdine (1 μM) reduced the beating rate of sino-atrial node cells in the first minute of exposure, without alteration of other action potential parameters (a), to approximately 66 % of original rate (n=3, $P<0.05$). Note the tendency of the action potentials to be longer in duration after treatment with linopirdine. Prolonged exposure to linopirdine stopped spontaneous activity of sino-atrial node cells (n=3).

a,

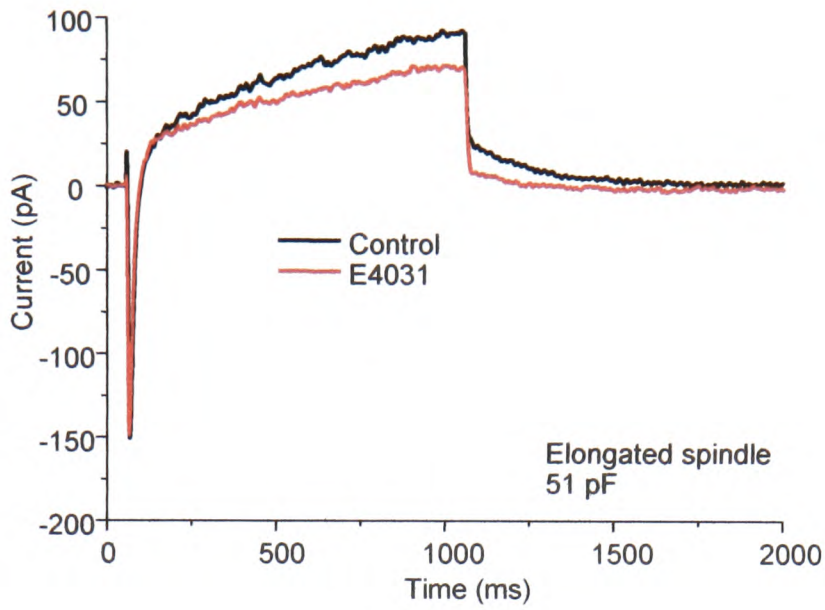

b,

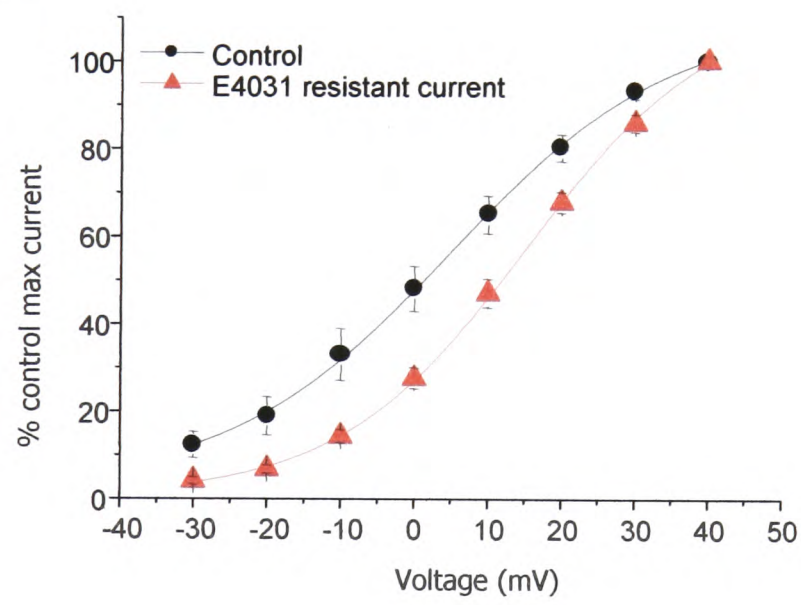

Figure 4.23 Page 191

Voltage-dependent activation of I_K resistant to E4031. I_K was activated with a depolarising step in control conditions, 0 mV in the above trace (a), and after perfusion with 5 μM E4031. The current remaining in the presence of E4031 is described as the E4031 resistant current. Note the lack of change of the initial inward current in the presence of E4031 (a). In figure 5.23b sigmoid curves were fitted to voltage-dependent I_K (n=14) and E4031 resistant current (n=10); $V_{1/2}$ 6 ± 3 versus 15 ± 2 mV ($P<0.05$) and slope 14 ± 4 versus 12 ± 2 mV respectively.

a,

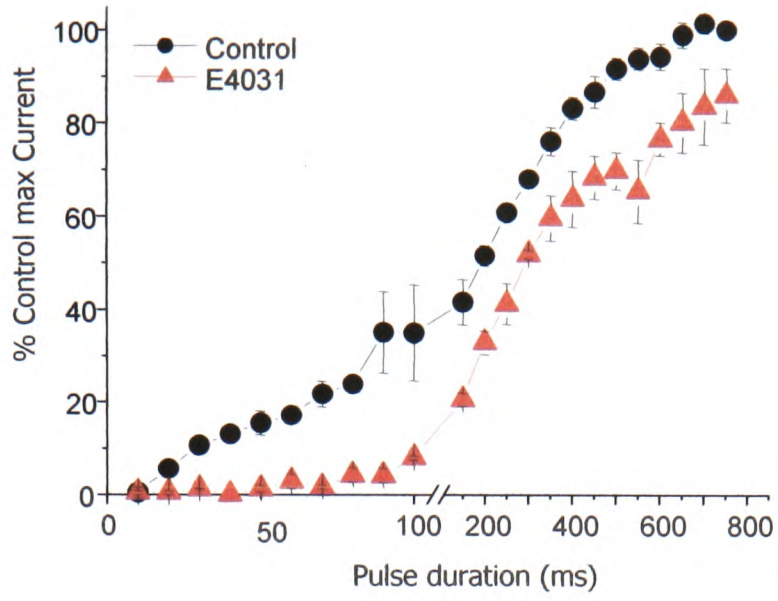

b,

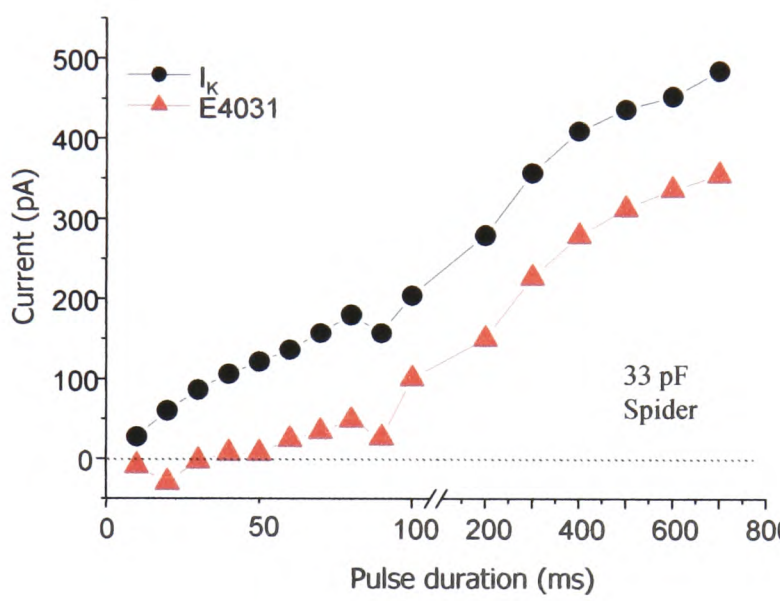

c,

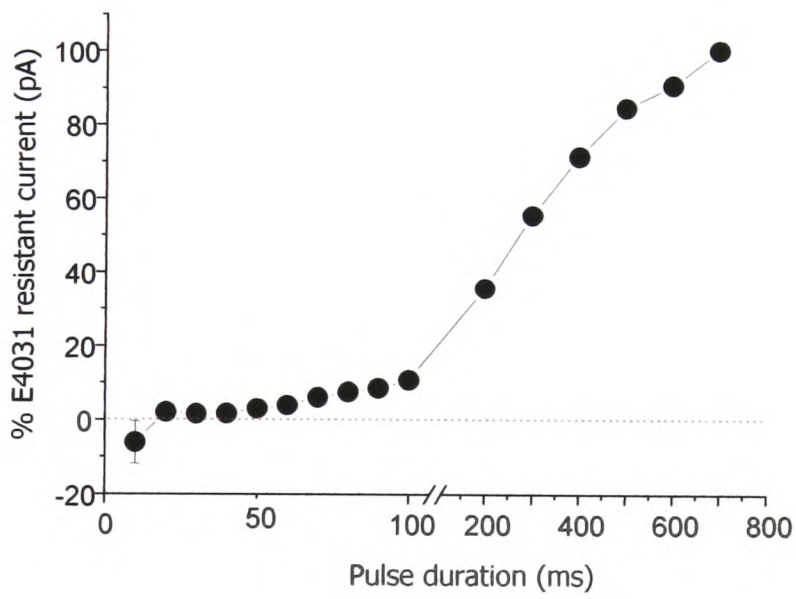

Figure 4.24 Page 192

Time-dependent activation of I_K resistant to E4031. I_K is activated with brief depolarisations (a), but little E4031 resistant current is activated with depolarisations shorter than 70 ms (a) and the E4031 resistant current was slightly less than I_K at longer depolarisation durations (n=10). The E4031 sensitive current amplitude (approximately 100 pA), was similar to the amplitude which the maximal current was reduced by (b). E4031 resistant tail current (c) was inward at very brief depolarisation durations (n=15, $P<0.05$), with no outward current until 70 ms and greater.

a,

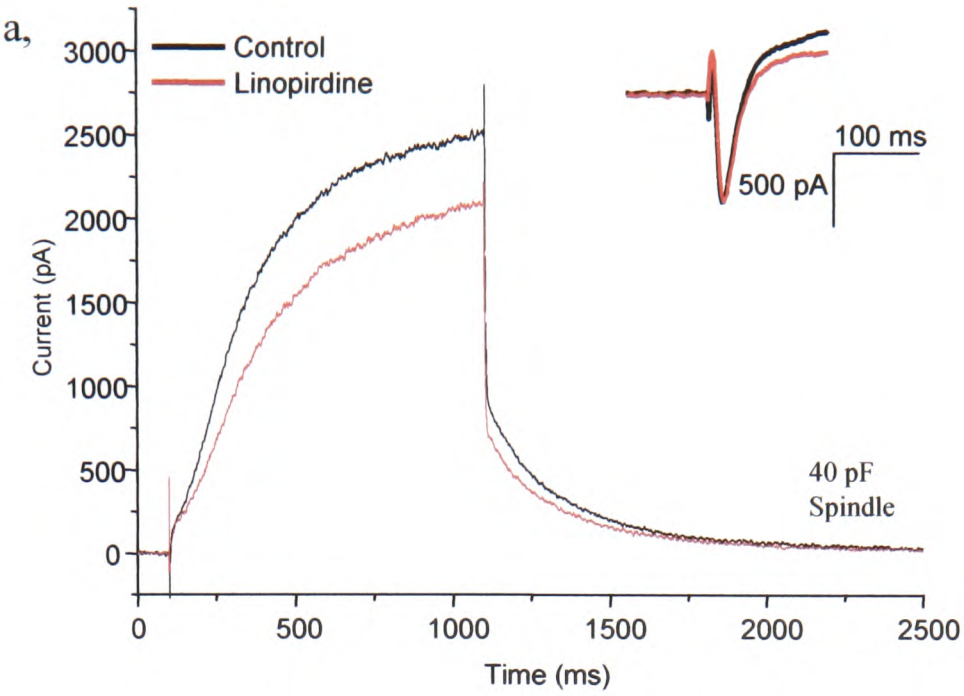

b,

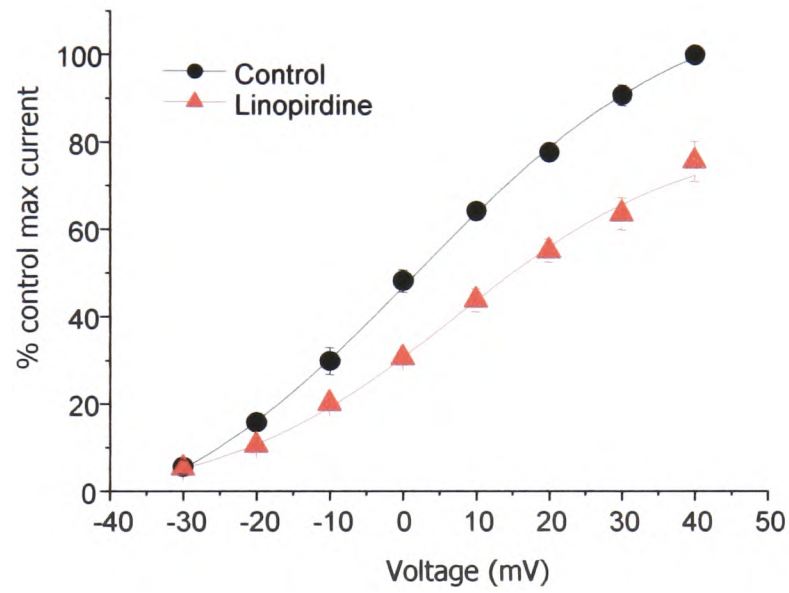

c,

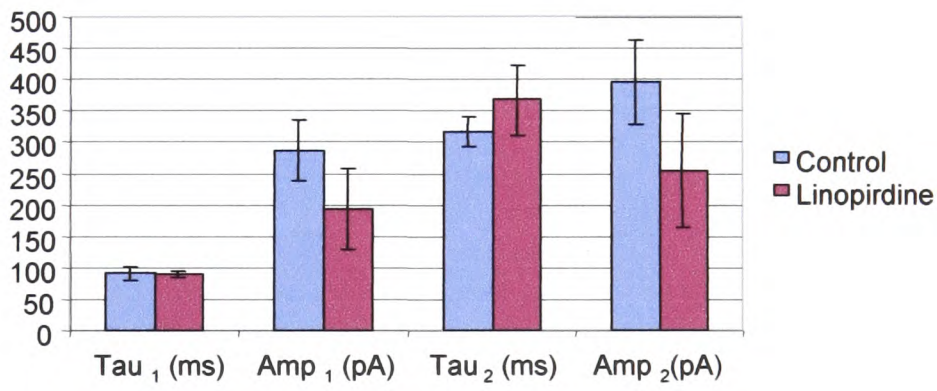

Figure 4.25 Page 193

Effect of linopirdine (1 μM) upon voltage dependent activation of I_K. 1 μM linopirdine reduced the amplitude of the step and tail current (a) upon depolarisation (to +40 mV), without having an effect upon the initial inward current which was maximally activated at 0 mV (inset). I_K was voltage dependently activated in the absence ($V_{1/2}$ 2 ± 2 mV and slope 19 ± 3 mV) and presence ($V_{1/2}$ 7 ± 3 and slope 16 ± 2 mV) of linopirdine (b), however linopirdine reduced I_K activated at voltages greater than –20 mV (n=4, $P<0.05$); to approximately 80 % of max control. The decay of the I_K tail current was quantified with a bi-exponential curve, and in the presence of linopirdine, neither time-constant were altered, but both Amp_1 and Amp_2 were reduced (c, n=4, $P<0.05$).

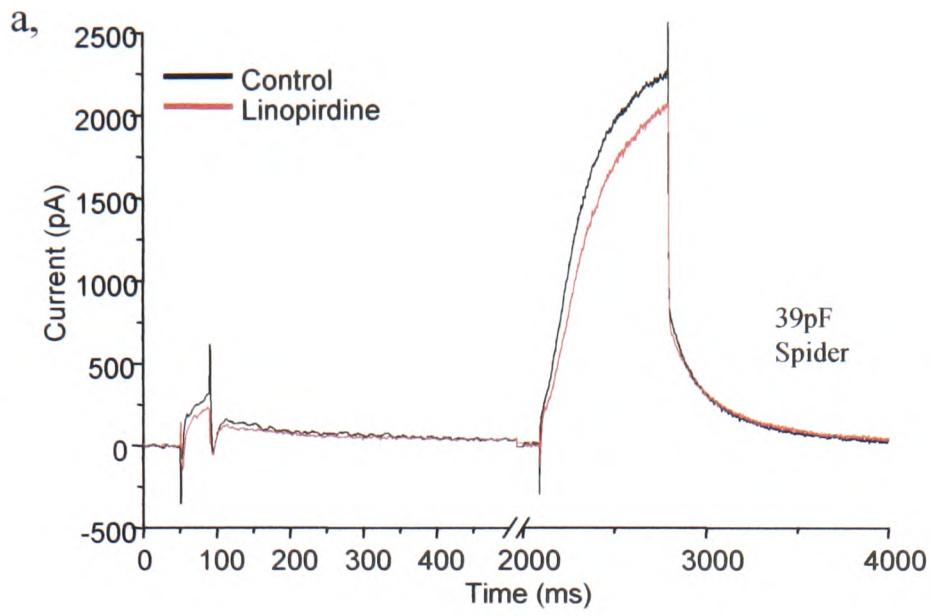

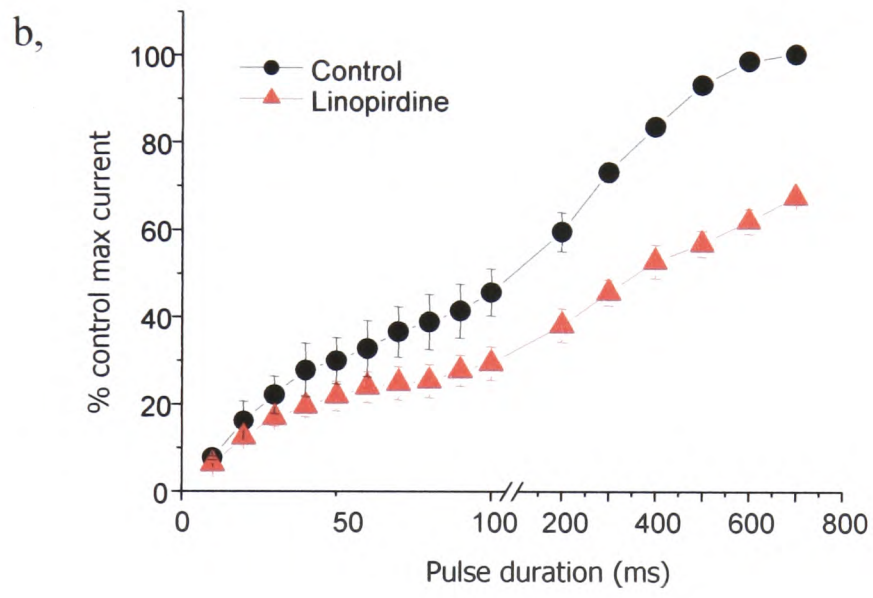

Figure 4.26

Time-dependent activation of I_K amplitude was reduced by linopiridine. Linopiridine (1 μM) reduced both I_K (step and tail current amplitude) activated with brief and prolonged depolarisations (a). I_K activated with depolarisations of between 10 and 700 ms activated both components of I_K (b). Linopiridine reduce I_K activated with depolarisations greater than 70 ms (n=4, $P<0.05$) and was approximately 70 % of control max (b).

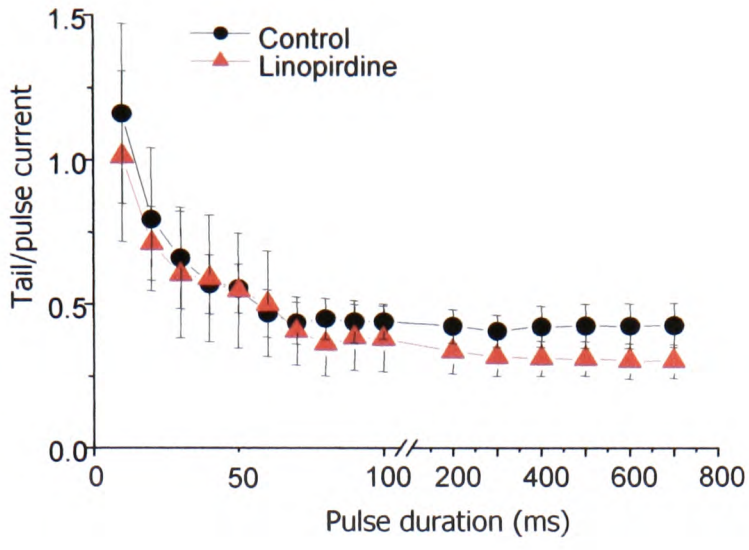

Figure 4.27 Page 195

Envelop of tails test in the presence of linopirdine. An envelope of tails test was applied and compared to control. The tail:pulse ratio was similar to control in the presence of 1 μM linopiridine at all duration depolarisation (n=4, P>0.05), only becoming constant with depolarisation durations in excess of 80 ms.

a,

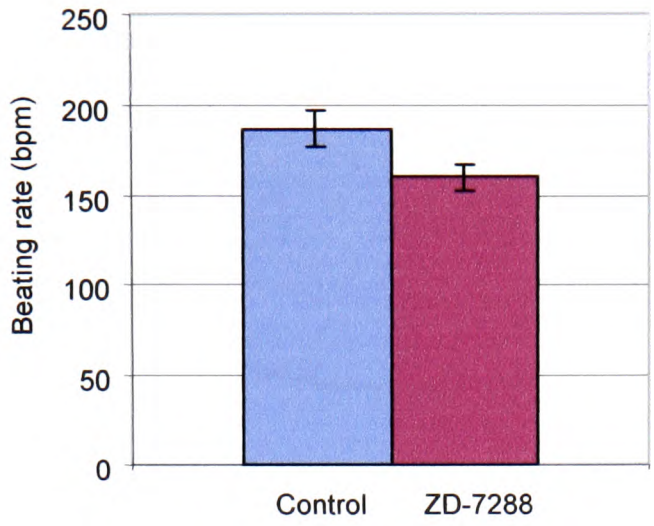

b,

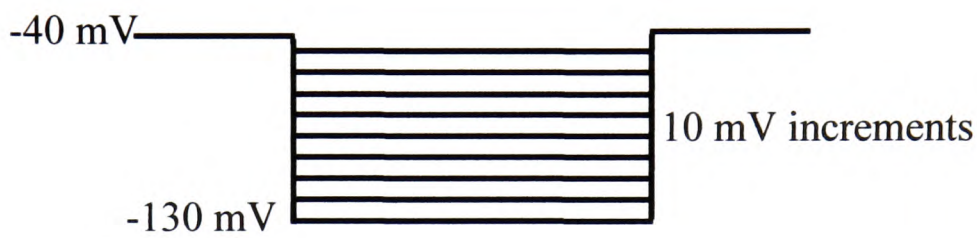

c,

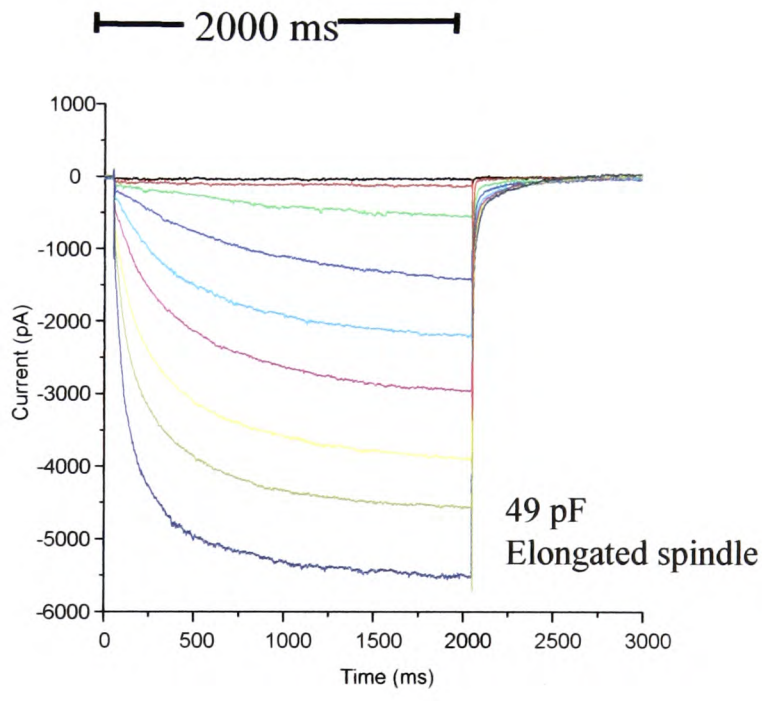

Figure 4.28 Page 196

Effect of ZD-7288 (3 μM) upon sino-atrial node cell beating rate and I_f. ZD-7288 reduced the spontaneous generation of action potentials from 187 ± 10 to 160 ± 7 bpm (a), a reduction to 86 ± 3 % of control (n=6, P<0.05). Voltage-dependent activation of I_f protocol (b). The large I_f was activated upon hyperpolarisation, with more negative voltages cause greater inward I_f currents (c).

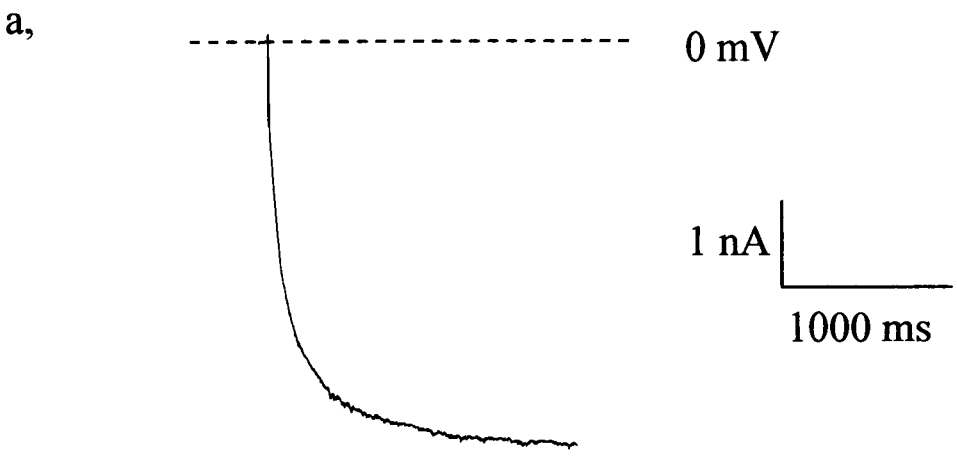

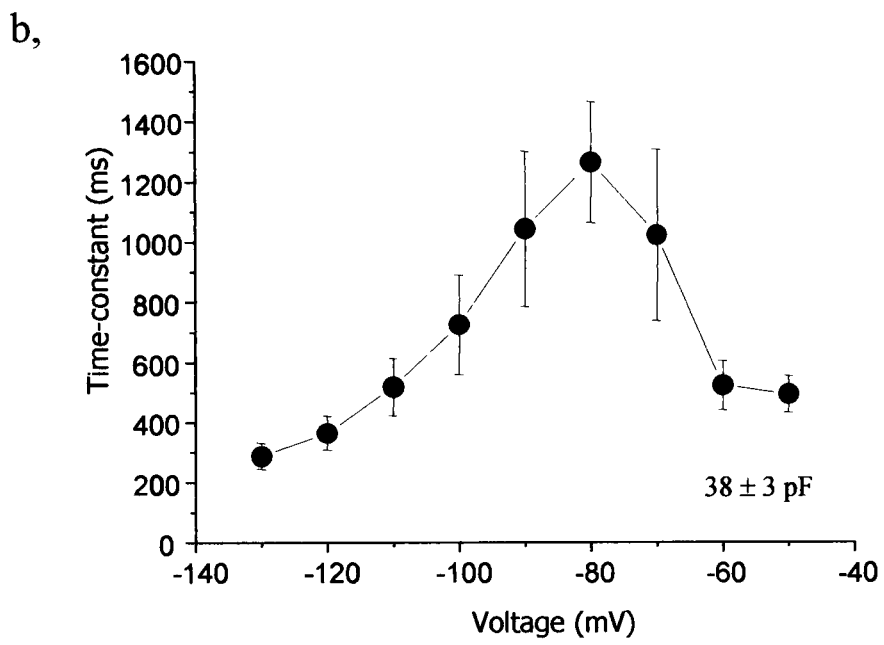

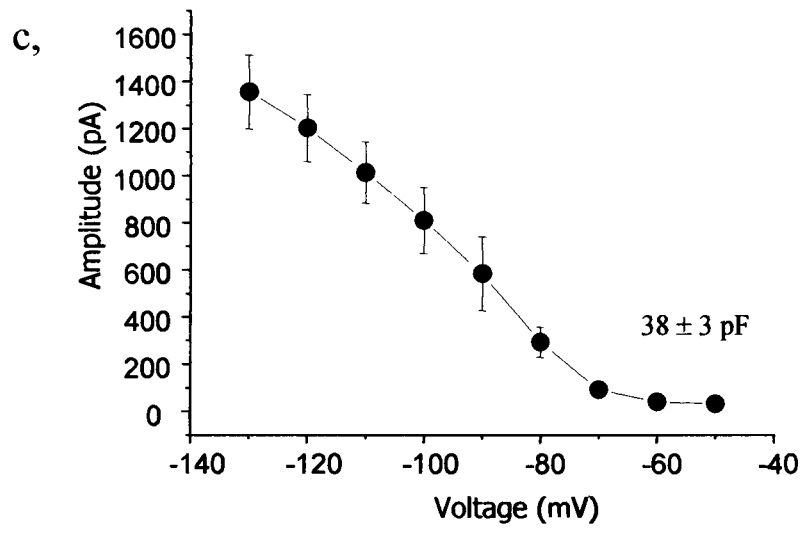

Figure 4.29 Page 197

Kinetics of I_f voltage-dependent activation. Large inward I_f currents are activated upon hyperpolarisation, with more negative voltages activating the greatest currents; steps to –130 mV activate many nA of inward current (a). The process of activation is slow (~1300 ms at –80 mV, n=5), but quickens to ~300 ms at very negative voltages (b); activation is also comparably rapid at –50 and –60 mV, but I_f amplitude is minimal (c). I_f amplitude is directly related to membrane voltage at potentials more negative than –70 mV (c).

a,

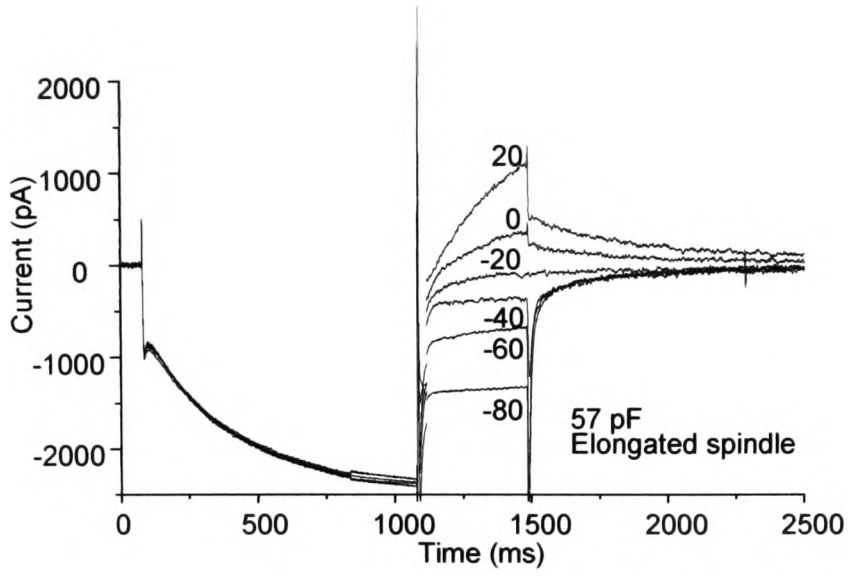

b,

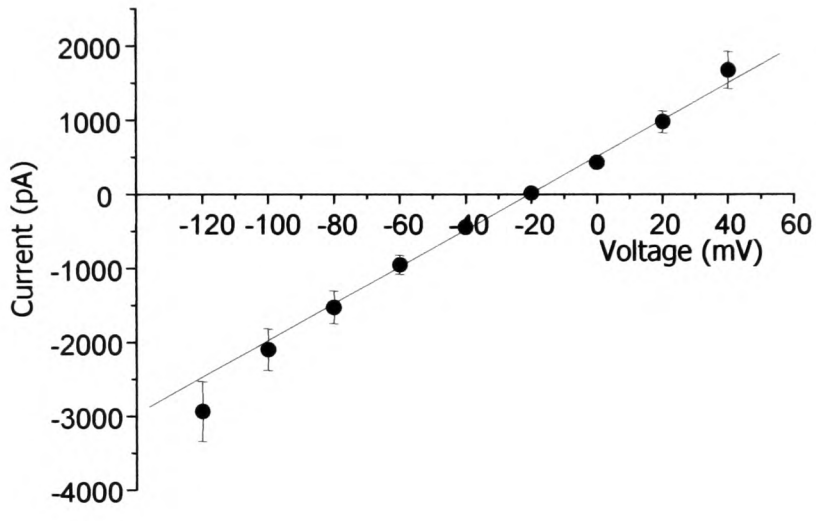

c,

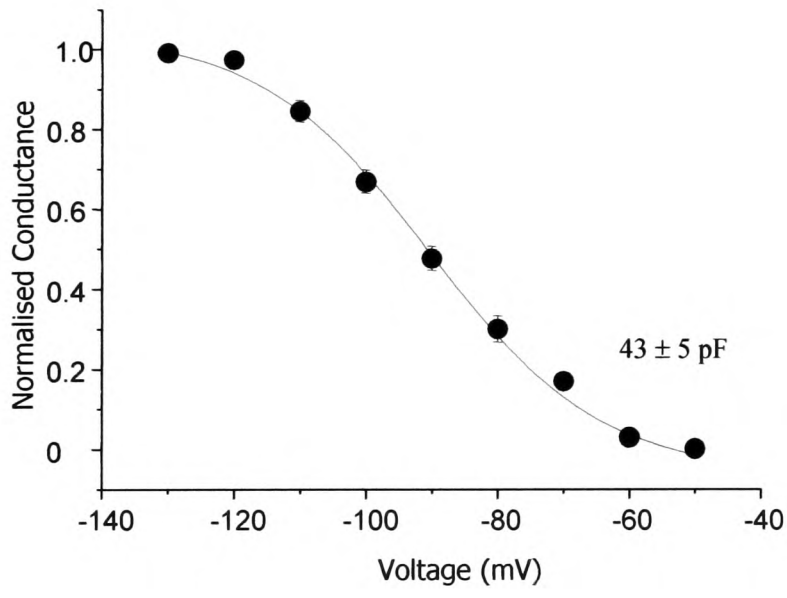

Figure 4.30 Page 198

Reversal potential of I_f and the conductance-voltage relationship. A voltage protocol similar to that in figure 5.9a was used with hyperpolarising step to –110 rather than a depolarising step to +40 mV. I_f is activated, the membrane is repolarised to various voltages (a) and the instantaneous tail current measured. Instantaneous tail currents were directly related to repolarisation voltage (b) and the linear relationship identified an I_f reversal potential of –19 ± 1 mV (n=6). The reversal potential was then used to conductance values, which take into account the electrochemical driving force; Conductance=current/(voltage-reversal potential). Conductance was normalised and plotted against voltage; $V_{1/2}$ –90 ± 1 mV slope 13 ± 1 mV (n=6).

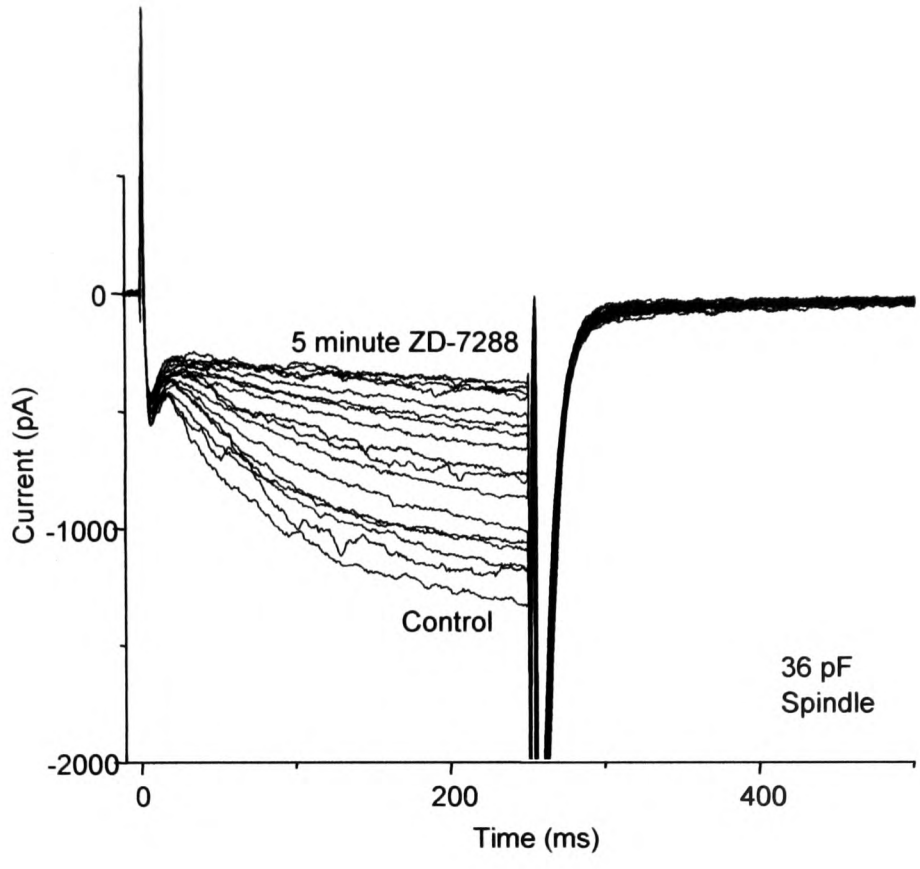

Figure 4.31 Page 199

In voltage clamp, repetitive steps to –80 mV activate I_f (every 15 seconds). Upon addition of ZD-7288 (3 μM) I_f amplitude was time-dependently reduced.

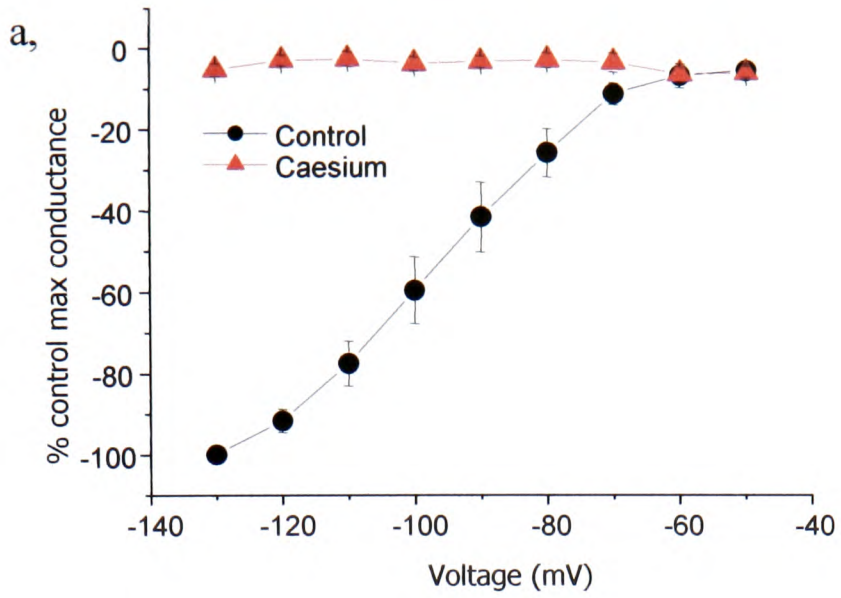

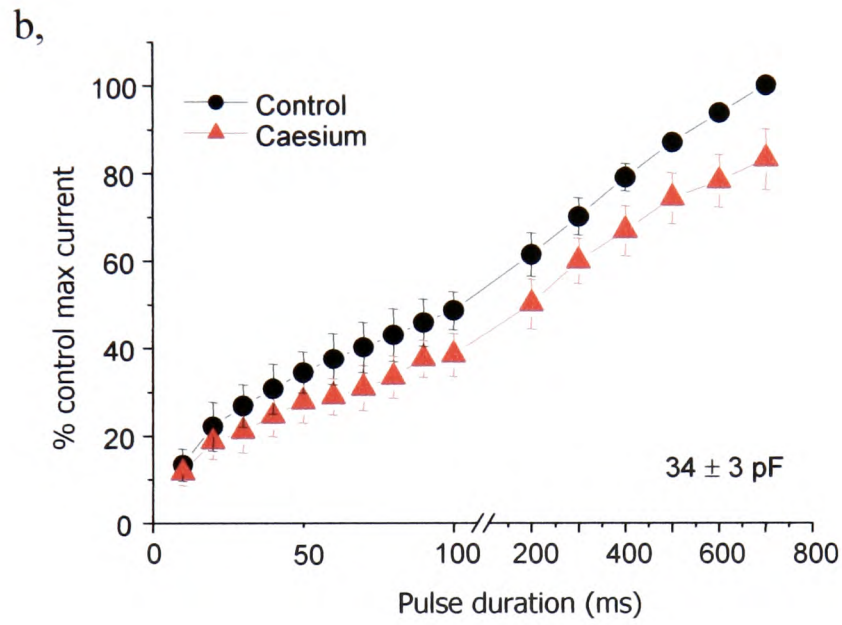

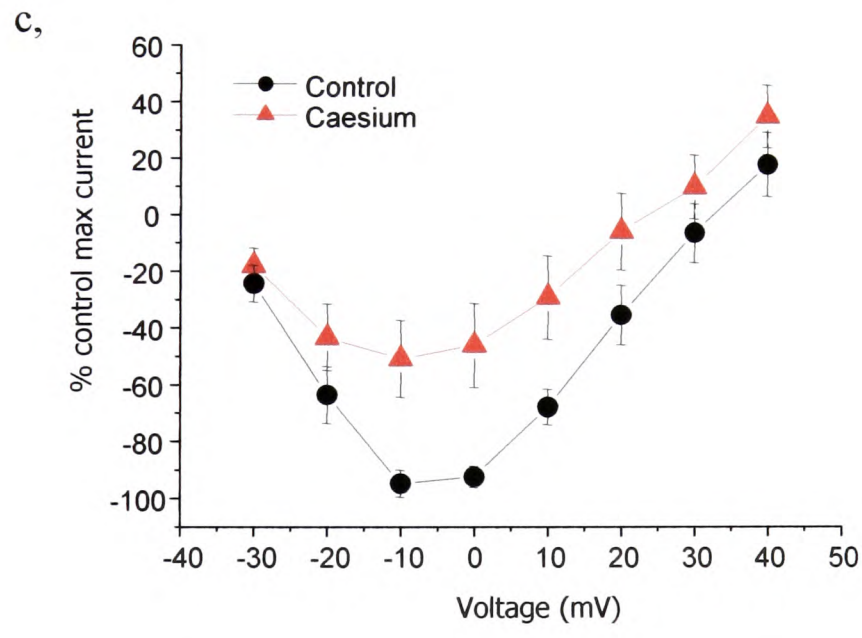

Figure 4.32 Page 200

Effect of 2 mM caesium upon I_f, I_K and I_{CaL}. Caesium was found to abolish voltage dependent activation of I_f (a), at potentials more negative than –60 mV (n=8, $P<0.05$). Caesium (2 mM) was also found to reduce I_K (b), upon depolarisations longer than 30 ms (n=7, $P<0.05$), and I_{CaL} (c) at voltages more positive than –20 mV (n=6, $P<0.05$).

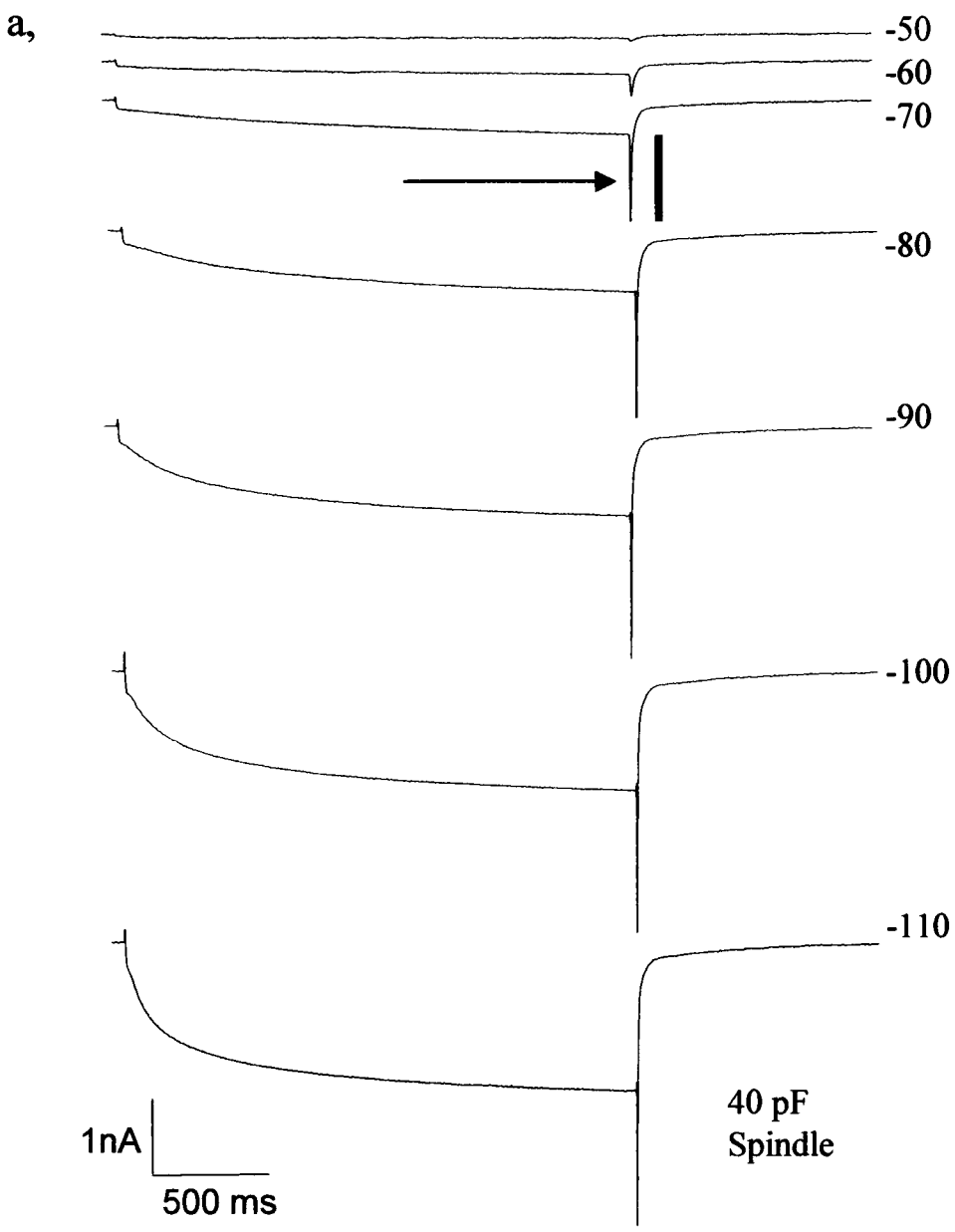

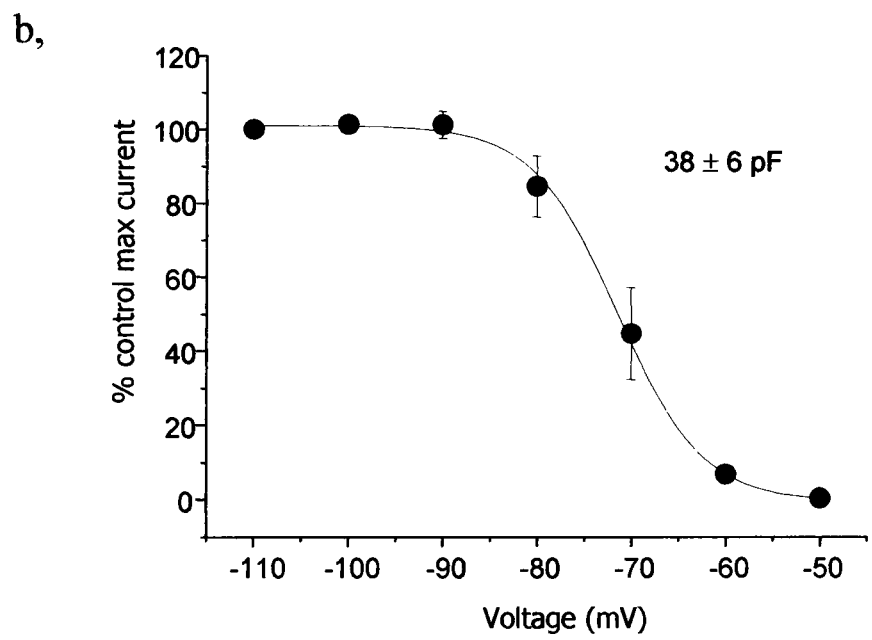

Figure 4.33 Page 201

Voltage steps to activate I_f reveals a rapid inward current thought to be I_{Na}. I_f was activated by hyperpolarising steps (-50 to –110 mV) and upon repolarisation (effectively a depolarisation) a large inward current was activated (see arrow in figure 5.33a). The amplitude of this inward current, measured from the maximal I_f current to the peak inward current (bar mark at –70) initially increased as the hyperpolarisation became more negative (b), but then became stable at voltages greater than –90 mV; n=6, $V_{1/2}$ –71 ± 2 mV, slope 4 ± 2 mV.

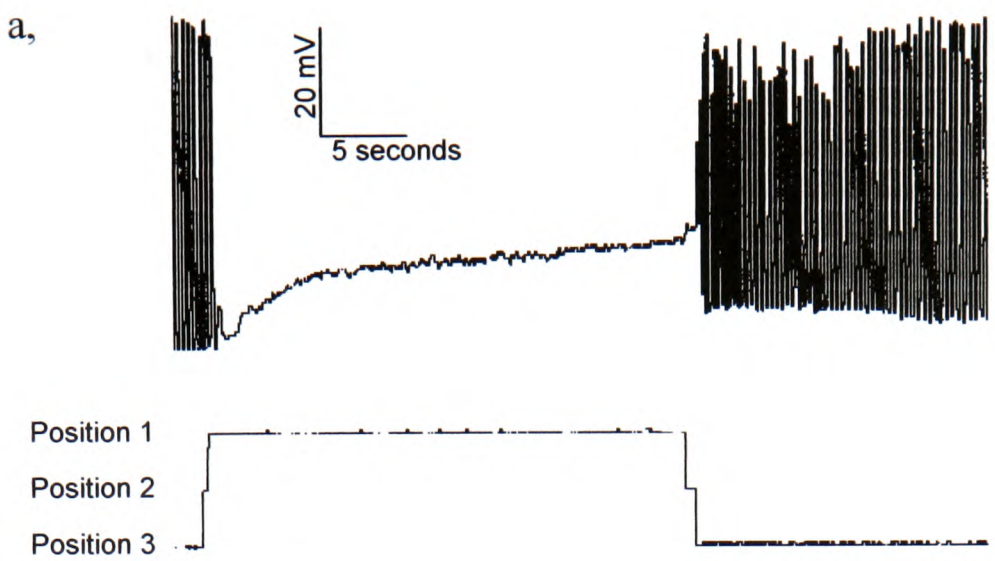

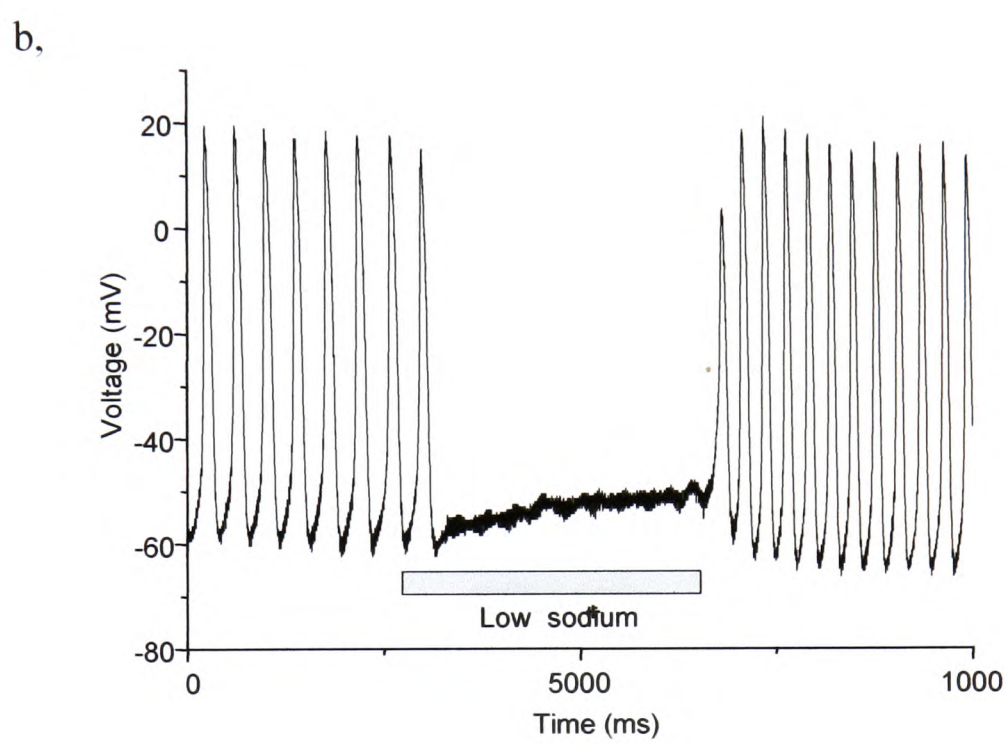

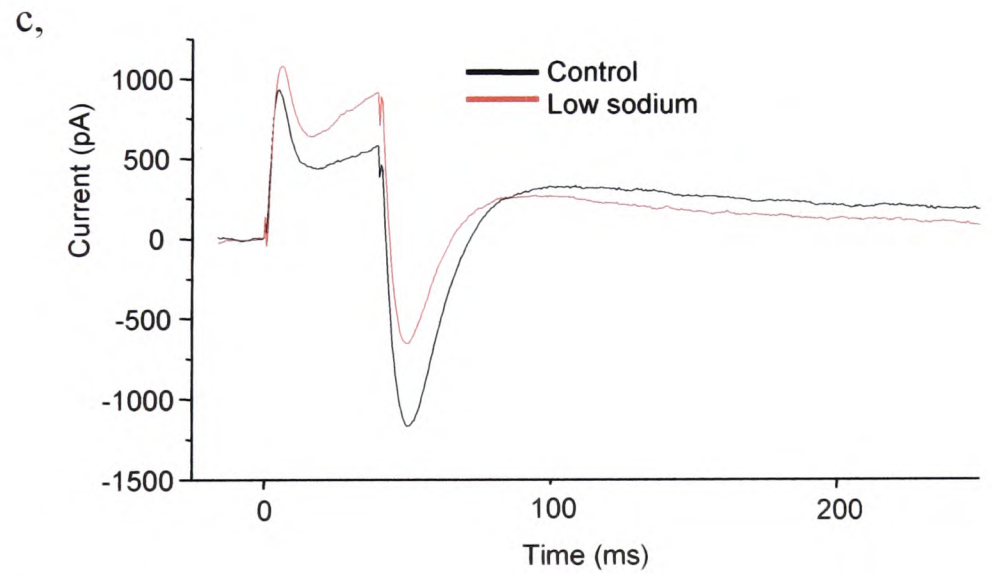

Figure 4.34 Page 202

Rapid switching of perfusing solution to one that was low in sodium caused immediate cessation of spontaneous action potential generation (n=6, 16 separate switches). Sodium concentration was lowered to 15 mM and replaced with lithium (a; position 1 was low sodium, position 3 was control) and was define by the bar (b). Note the gradual depolarisation when quiescent and the gradual development of action potential amplitude after quiescence. Low sodium also caused sino-atrial node cell quiescence in the presence of 3 μM ZD-7288 (n=4). Rapid switching of solutions to low sodium increased the current observed upon brief depolarisation (c, n=3)

a,

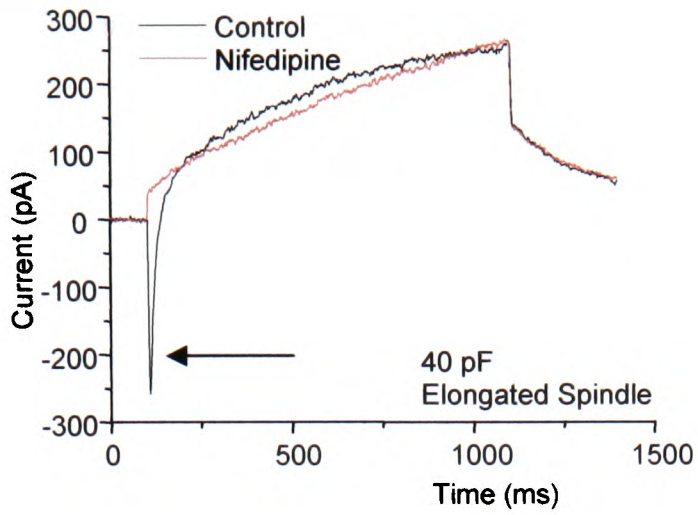

b,

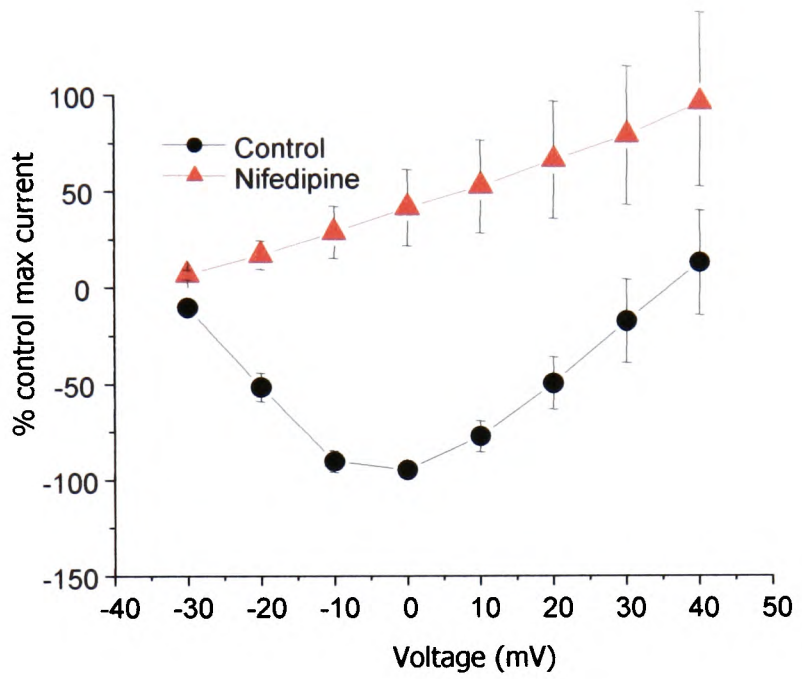

c,

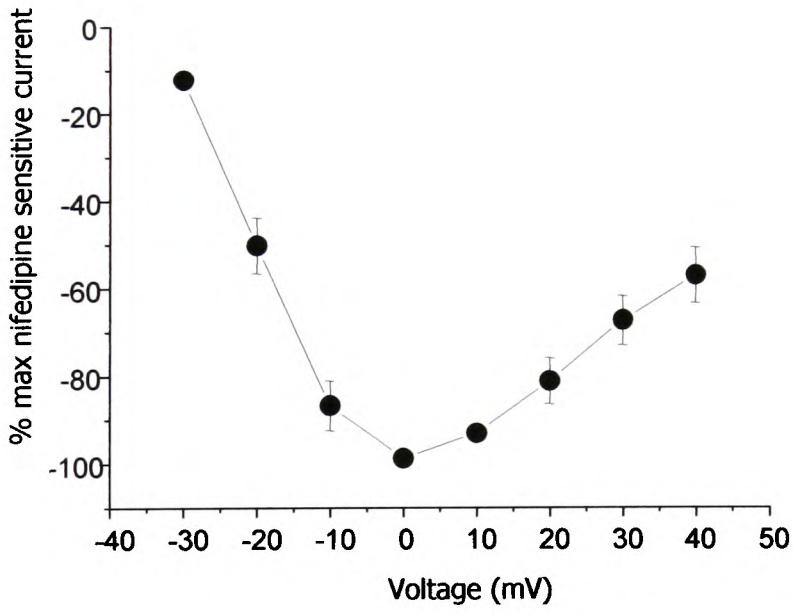

Figure 4.35 Page 203

Voltage dependent inhibition of I_{CaL} by nifedipine. The voltage dependent activation of the inward I_{CaL}, mediated the initial brief inward current upon depolarisation (indicated by the arrow in figure 5.36a), is inhibited with 5 μM nifedipine (a and b) at voltages between –30 and +40 mV (n=6, $P<0.05$). In the presence of nifedipine, no inward current was observed (a) and the remaining outward current was directly related to voltage (b). The nifedipine sensitive current was calculated (c) and has a steep voltage-dependently activation, attaining maximal current at 0 mV (n=6).

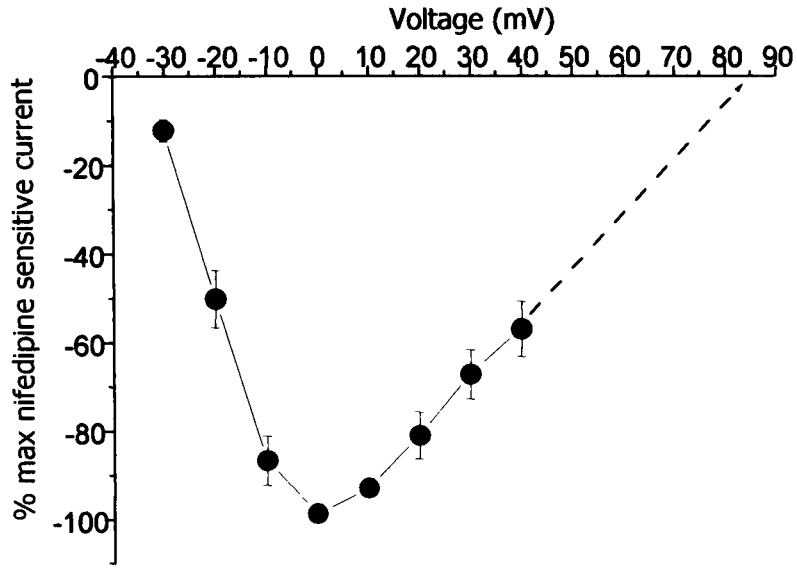

Figure 4.36 Page 204

Extrapolation of the voltage dependence of the nifedipine (5 μM) sensitive current, was used to estimate the reversal potential of I_{CaL}. The reversal potential of calcium is 120 mV, but the I_{CaL} reversed at potentials estimated to be around +85 mV (n=6).

a,

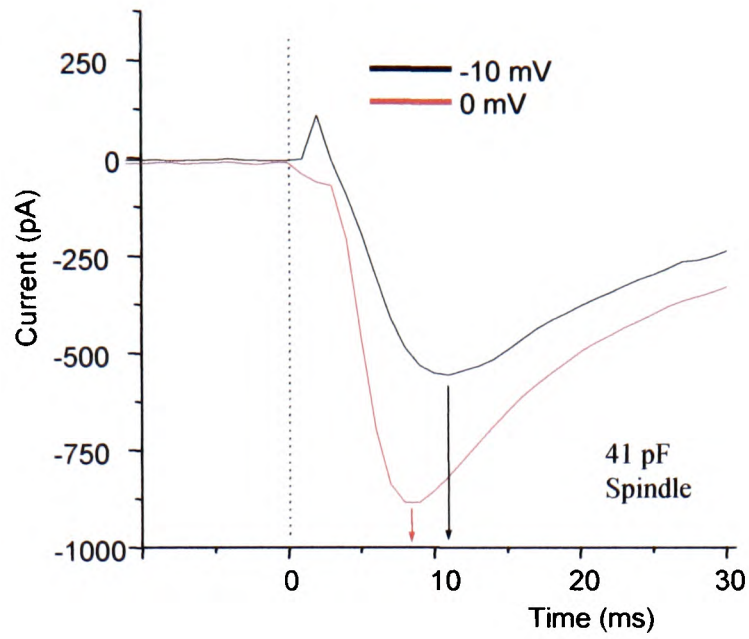

b,

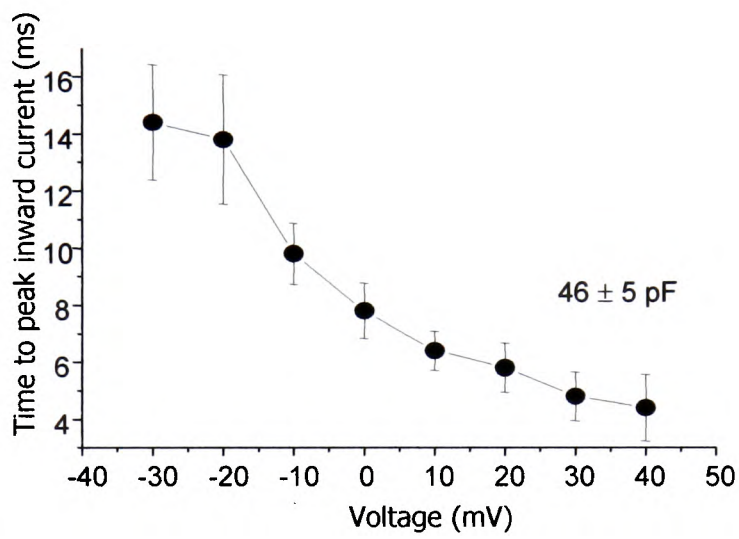

Figure 4.37 Page 205

Voltage dependent rapidity of I_{CaL} activation. Stronger depolarisations were found to activate peak I_{CaL} more quickly than steps to less positive potentials (a). Time to peak I_{CaL} was reduced as the depolarisation became more positive (b), from 14 ± 2 to 5 ± 2 ms when depolarisation was to –30 and +40 mV respectively (n=5, $P<0.05$).

a,

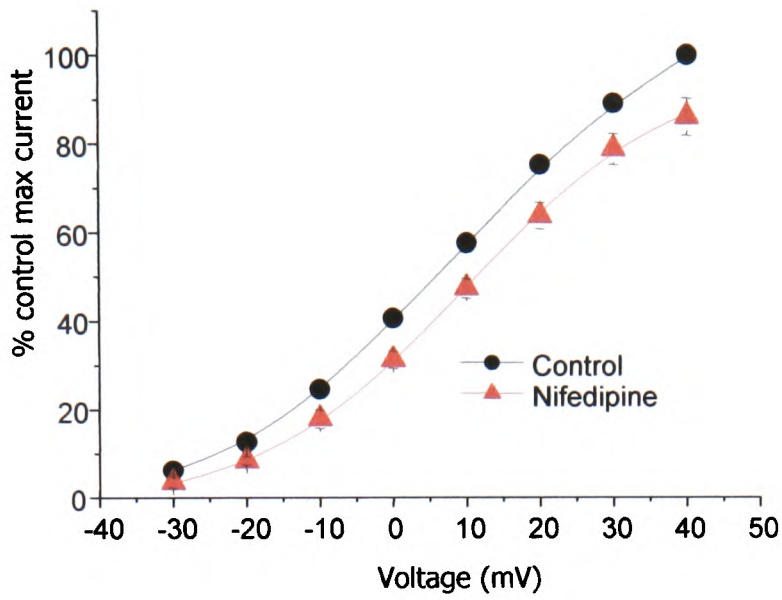

b,

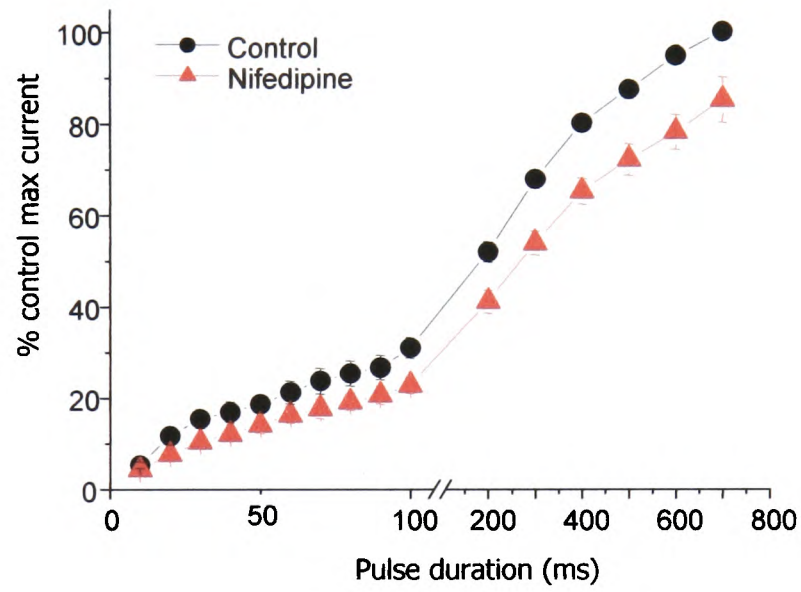

Figure 4.38 Page 206

Nifedipine reduced the voltage and time-dependent activation of I_K. Nifedipine (5 μM) reduced the amplitude of the I_K tail current activated in the voltage range –30 to +40 mV (n=12, $P<0.05$), causing I_K at +40 mV to reduce to 85 % of control (a). Neither the $V_{1/2}$ or the slope were altered in the presence of nifedipine; control 9 ± 1 and 16 ± 2 mV, nifedipine 10 ± 3 and 14 ± 2 mV (n=12). Nifedipine also diminished I_K activated with depolarisations longer than 20 ms (n=11, $P<0.05$), also reduce max nifedipine treated I_K to approximately 85 % of control max current (b).

a,

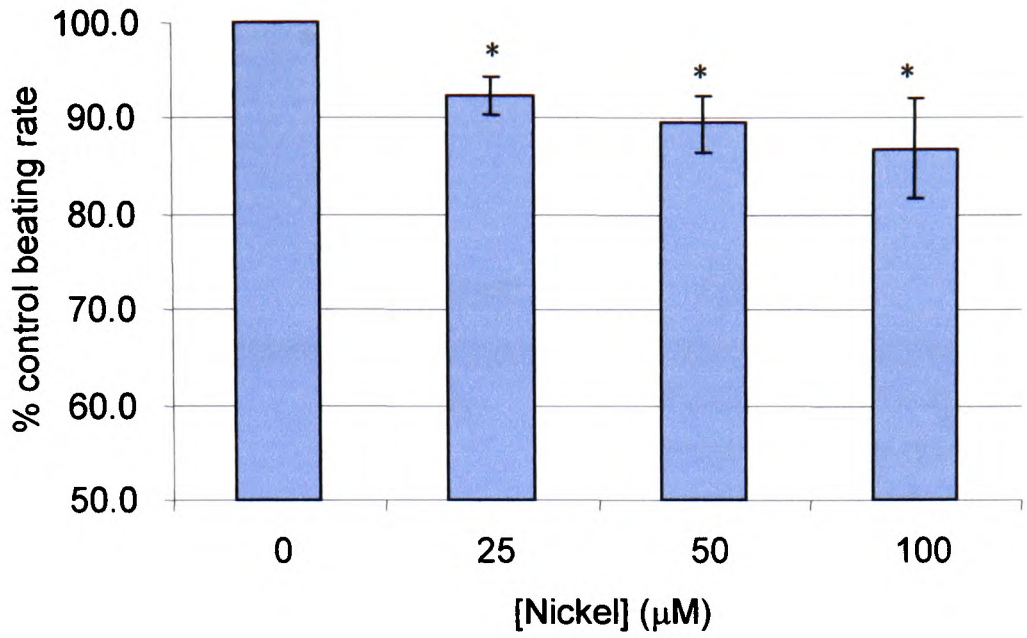

b,

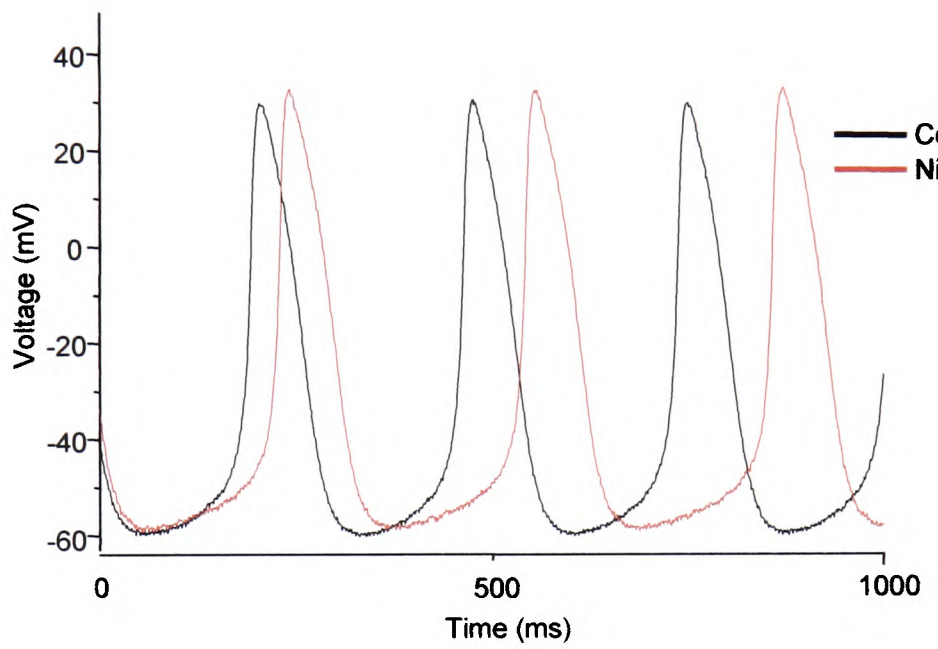

Figure 4.39 Page 207

Effects of nickel upon atrial preparation and sino-atrial node cell beating rates. Nickel concentration-dependently (25-100 μM) reduced the beating rate of atrial preparations (n=16, 16 and 8, $P<0.05$), causing a maximum inhibition of 13 % at 100 μM. Nickel (25 μM) similarly inhibited the spontaneous development of isolated sino-atrial node cell action potentials (b).

Agent	Target	Current	Affect
E4031	ERG	I_{Kr}	Reduction of beating rate (~25 %) tended to stop isolated cells. E4031 sensitive current describes I_{Kr}, including rectification
ZD-7288	HCN	I_f	Reduced isolated sino-atrial node cell beating rate by ~20 %.
Low sodium	Na-Ca exchanger	I_{NCX} (etc.)	Immediately stopped beating
Nifedipine	α-subunit of L-type Ca channel	I_{CaL}	Abolish I_{CaL} and slightly reduce I_K.
Nickel	α-subunit of T-type Ca channel	I_{CaT} (etc)	Reduce beating rate of preparations and isolated sino-atrial node cells

Figure 4.40 Page 208
Summary table of findings in this chapter. Isoprenaline was used at 100 nM, E4031 at 5 μM, BAPTA-AM at 10 μM, nifedipine at 5 μM, ryanodine at 2 μM and MDL at 10 μM.

CHAPTER 5: Calcium and the SR

'Excitation contraction coupling' links electrical activity to mechanical movement in the heart. Membrane depolarisation activates calcium channels, through which calcium flows and initiates further calcium release from the SR; these calcium contributions combine, raising cellular concentrations to bind with troponin, initiating cross bridge cycling of actin and myosin and hence cell shortening. Calcium induced calcium release is the central dogma of excitation contraction coupling, although the precise mechanisms of calcium entry and spatio-temporal characteristics of SR calcium release seems to be under perpetual review. In cells from the sino-atrial node and atrial tissue, neither of which have transverse tubules, both I_{CaT} and I_{CaL} (Hirano, Fozzard et al. 1989; Perez-Reyes, Yuan et al. 1994; Zhou and Lipsius 1994) are involved in mediating the trans-sarcolemmal entry of calcium. In the sino-atrial node I_{CaT} is activated by the negative voltages during diastolic depolarisation, the small amount of calcium entering may cause spark release of SR calcium (Huser, Blatter et al. 2000). Local increases in calcium activate I_{NCX}, which accelerates depolarisation. This would cause voltage dependent activation of I_{CaT} and then I_{CaL}, thus concentrating calcium and triggering whole SR ryanodine receptor activation and calcium dumping.

Cytosolic calcium is actively managed in sino-atrial node cells at a low concentration, but calcium concentrations appear to be unusually high in the sino-atrial node, with reports of 200 nM at rest and >800 nM during contraction (Huser, Blatter et al. 2000; Verheijck 2000). Calcium concentration needs to be well controlled as it acts as a messenger in many cellular pathways/activities, ranging all the way in a cells life cycle from fertilisation to apoptosis. The effects of calcium upon the sino-atrial node currents maybe via a direct calcium interaction or mediated

by calcium sensitive regulators. These would include protein kinases (Way, Chou et al. 2000), calmodulin interaction with cellular proteins (Vinogradova, Zhou et al. 2000) and the calcium stimulation of cAMP production by AC (Luthi and McCormick 1999; Luthi and McCormick 1999).

Every cardiac myocyte must be in calcium equilibrium each cycle, as overload and depletion are pathological (Choate, Edwards et al. 1993). Calcium channel mediated entry and SR calcium release are equal to SR calcium sequestration, plus extrusion on the sarcolemmal pump and the sodium-calcium exchanger. β-adrenoceptor activation increased SR calcium in frog sinus venosa (Ju and Allen 1999; Ju and Allen 2000) and the associated positive inotropy is SR dependent (Shah, Than et al. 1994; Hata, Sakamoto et al. 1998).

The rate of beating of sino-atrial node cells is determined by the sequential activation of sarcolemmal ionic currents (Irisawa 1987), although there is a substantial modification of these ionic currents (hence heart rate) upon modification of calcium handling (Ju and Allen 1999) and especially SR function (Satoh 1994; Hata, Sakamoto et al. 1998; Rigg, Heath et al. 2000; Lipsius, Huser et al. 2001). The SR regulation of beating rate is mediated by an effect upon these ionic currents of the sino-atrial node (Hata, Sakamoto et al. 1998; Ju and Allen 1999; Rigg, Heath et al. 2000), possibly by calcium sensitive kinase pathways such as PKC and CaMK (Ju and Allen 1999; Rigg, Heath et al. 2000; Wu, Dzhura et al. 2001; Vinogradova, Bogdanov et al. 2002).

The regulations of the ionic currents investigated in this chapter are described below. I_{Ks} is regulated by the cAMP/PKA pathway, which is activated upon β-adrenoceptor activation, and the AC production of cAMP maybe sensitive to cellular calcium concentrations, as this enzyme is regulated in this way (Luthi and McCormick 1999). Activation of the cAMP/PKA pathway causes channel phosphorylation, which both shifts the voltage dependency and increases the amplitude of I_{Ks}. In addition, direct elevation of intracellular calcium increases I_{Ks} amplitude by increased the open probability of these channels (Tohse, Kameyama et al. 1990; Walsh, Arena et al. 1991; Luthi and McCormick 1999). I_{Ks} is regulated by a number of other calcium sensitive pathways, including PKC and calmodulin (Tohse, Kameyama et al. 1987; Nitta, Furukawa et al. 1994). I_{Kr} in ventricular cells has been recently described to be augmented by β-adrenoceptor stimulation (Heath and Terrar 2000), and this may (similarly to I_{Ks}) be sensitive to cellular calcium via AC modulation; the increase in I_{Kr} is partially mediated by a reduction in rectification, however this alteration in rectification is calcium dependent.

I_{NCX} would be directly inhibited by a reduction in calcium, as calcium is the substrate of this exchanger and would therefore be very sensitive (Gao, Mathias et al. 1992). I_{NCX} amplitude is increased by sympathetic stimulation, via the calcium sensitive cAMP/PKA pathway (Perchenet, Hinde et al. 2000) and by increase calcium concentration itself. A reduction in cellular calcium would therefore decrease the contribution of this inward current to diastolic depolarisation.

I_{CaL} is also increased upon β-adrenoceptor activation by a pathway involving cAMP (Osterrieder, Brum et al. 1982; Trautwein and Kameyama 1986; Giles and

Shimoni 1989; Tanaka, Clark et al. 1996; Qu and Campbell 1998), whereas I_{CaT} is not (Tytgat, Nilius et al. 1988; Tytgat, Vereecke et al. 1990), and so I_{CaL} would be sensitive to calcium regulation of cAMP production, assuming a high AC turnover in the sino-atrial node. The local calcium ion concentration in the vicinity of intracellular C-terminal of the L-type calcium channel is also important, as calcium causes inactivation of I_{CaL}. The inactivation of I_{CaL} maybe altered by buffering, but during I_{CaL} mediated influx the local concentrations will be very high and the buffer will probably not be quick enough to mop up all the ions before they cause inactivation of I_{CaL}.

The $V_{1/2}$ of I_f is shifted to more physiological voltages by cAMP, and therefore may be sensitive to calcium concentrations via the regulatory effect of calcium upon AC (Hagiwara and Irisawa 1989; DiFrancesco and Tortora 1991). High calcium concentrations (100 nM) cause a shift in the $V_{1/2}$ to depolarised levels (Hagiwara and Irisawa 1989). I_f is sensitive to calcium, although it is not clear whether this is a direct action (although DiFrancesco disagree's with this), mediated by interaction with calcium-calmodulin (Liu and Huizinga 1994; Rigg, Mattick et al. 2003) or by phosphorylation via calcium sensitive kinases such as calmodulin kinase or protein kinase C.

Increasing calcium raises beating rate, and it therefore appears that the net inward current is preferentially increased under these conditions, to facilitate the observe quickening of diastolic depolarisation (Ju and Allen 1999; Vinogradova, Bogdanov et al. 2002). Conversely when spontaneous sino-atrial node activity is

stopped, calcium levels fall, as there is more time for the sequestration/expulsion mechanism to operate (Rakovic 2000).

It is the aim of this chapter to investigate the role of intracellular calcium (both cytosolic and SR released) in regulating I_{Kr}, I_{Ks} and the development of spontaneous activity by cells of the sino-atrial node.

Results

Atria have been isolated from the guinea pig heart, mounted in an organ bath and attached to a force transducer, to allow measurement of contractions and hence the beating rate of the preparation (Methods, page 51). The calcium concentration of the solution bathing the preparation was altered, using cumulative additions of calcium chloride to the bath of known volume. In this manner the calcium concentration of the bathing solution was increased from 1 mM, to 1.8 and then 2.5 mM calcium. Increasing the calcium caused a concentration dependent enhancement of the atrial preparation beating rate (figure 5.1); 106 ± 1 % at 1.8 mM and 110 ± 1 % at 2.5 mM calcium in the bathing solution ($n=5$, $P<0.01$). Similar results were found when atrial preparations were previously treated with E4031 (control rate in 1 mM calcium was 151 bpm), which reduced the rate to 74 ± 3 % ($n=5$, $P<0.05$), and subsequent calcium additions increased the beating rates to 79 ± 4 % at 1.8 mM and 80 ± 4 % at 2.5 mM ($n=5$, $P<0.05$).

Isolated sino-atrial node cells were continuously superfused with a saline solution, and an additional local perfusion of the cell, which facilitated a rapid switching of solution to one that contained 10 μM BAPTA-AM. Control recordings of action potentials were taken and displayed these characteristics; overshoot 12 ± 3 mV, most diastolic potential -61 ± 2 mV, action potential amplitude 73 ± 1 mV, beating rate 94 ± 16 bpm, APD_{50} 70 ± 4 ms and APD_{90} 116 ± 8 ms (n=3). BAPTA-AM caused the spontaneous action potential generation of the sino-atrial node cell to fail after 2-3 seconds of perfusion (figure 5.2), after a reduction of action potential amplitude. Upon quiescence the membrane potential remained constant at –25 ± 4 mV. Similar voltage characteristics upon perfusion with BAPTA-AM were found in 3 cells, although 1 cell did not completely stop beating and occasionally (every few seconds) fired an action potential. When the solution was rapidly switch back to the control, beating did not immediately restart: there was a gradual hyperpolarisation in all cells, which initiated small amplitude oscillations after approximately 10 seconds and subsequently developed over the next 80 seconds into action potentials which were similar to control (figure 5.2, inset).

Isolated sino-atrial node cells were exposed to BAPTA-AM 10 μM when the membrane potential was defined using voltage clamp. Repetitive depolarisations during a relatively slow solution change identified a progressive and substantial reduction (more than 50 %) in the amplitude of the outward current activated during depolarisation and the I_K tail current associated with repolarisation (figure 5.3a). After 5 minutes washin, I_K tail currents activated with both brief and prolonged depolarisation were found to be inhibited (figure 5.3b); 40 ms tail current was reduced from 33 ± 6 to 22 ± 5 % (n=6, $P<0.05$) and from 100 ± 0 to 44 ± 5 % (n=6, $P<0.01$).

Average currents at 40 and 700 ms were 176 ± 17 and 591 ± 73 pA respectively (n=6) and the effect of BAPTA-AM was significant at all depolarisations durations in excess of (and including) 40 ms.

The depolarisation voltage was also varied (1000 ms duration), as described in chapter 5; BAPTA-AM (10 μM) significantly reduced the amplitude of I_K at all voltages greater than –30 mV and I_K activated by a +40 mV depolarisation was reduced to 50 ± 3 % of control (figure 5.3c, n=6, $P<0.01$). There was, however, little or no effect in the voltage range over which I_K was activated since the $V_{1/2}$ of control (4 ± 3 mV, slope factor 18 ± 4 mV) was not altered in the presence of BAPTA-AM (1 ± 3 mV, slope factor 16 ± 5 mV). In addition the deactivation time constants of the I_K tail current were not altered in the presence of BAPTA-AM, while the amplitudes of both components were reduced (figure 5.4a, n=6, $P<0.05$).

I_{CaL} activated by depolarisation was also measured at voltages between –30 and +40 mV, and no effects of 10 μM BAPTA-AM were observed upon the bell-shaped voltage dependent activation of I_{CaL} (figure 5.4c, n=5, $P>0.05$); I_{CaL} was maximal at 0 mV, being on average –1014 ± 199 pA (n=5).

Hyperpolarisations between –50 and –110 mV were used to measure I_f in the absence and presence of 10 μM BAPTA-AM, to assess the effect of calcium chelation upon I_f voltage dependent activation and amplitude. I_f, measured as the inward time-dependent conductance was activated upon hyperpolarisation and recorded at a range of voltages, with maximal conductance at –110 mV. I_f was expressed as a normalised conductance, with reference to the maximal activated I_f (at –110 mV in all cells).

Sigmoidal conductance-voltage curves were fitted (figure 5.5) and the $V_{1/2}$ was found to be –86 ± 2 mV (slope factor 7 ± 1 mV). Upon exposure to 10 μM BAPTA-AM the maximal conductance did not appear to be reduced. Although in retrospect more negative hyperpolarisations would have made this easier to assess. The voltage dependent activation of I_f was shifted to more hyperpolarised potentials by approximately 10 mV; $V_{1/2}$ –96 ± 4 mV, slope factor 7 ± 1 mV ($P<0.05$, n=6).

Both the voltage and time-dependent activation of I_K have in addition been studied in the presence of 5 μM E4031. There was little current activated with depolarisation briefer than 100 ms, but an E4031 resistant current was recorded at longer duration depolarisation. This E4031 resistant current was time-dependently activated and was maximal at 700 ms, being an average of 238 ± 60 pA (n=3). Upon addition of 10 μM BAPTA-AM to the E4031 containing solution, the amplitude of the E4031 resistant current activated with depolarisation greater than 100 ms, were reduced to 50 ± 3 % (n=3) of control values of the E4031 resistant current at 700 ms. Concerning voltage dependent activation of the E4031 resistant current, control recordings were found to activate strongly with depolarisation greater than –10 mV (figure 5.7b), exhibiting a $V_{1/2}$ of 7 ± 1 mV (n=3) and a maximal E4031 resistant current at +40 mV of 218 ± 58 pA (n=3). BAPTA-AM caused a significant reduction of E4031 resistant current at all voltages (except –30 and –10 mV) and was reduced to 54 ± 6 % (n=3) at +40 mV. In addition the BAPTA treated E4031 resistant current displayed a $V_{1/2}$ that was shifted to 13 ± 9 mV (n=3).

The more potent analogue of BAPTA-AM, dimethylBAPTA-AM (dmBATPA-AM) was also used to evaluate I_K inhibition by calcium buffering.

dmBAPTA-AM was also used at 10 μM, but was superfused for 10 minutes (instead of 5 minutes); this ensured dmBAPTA (the de-esterified form) had attained maximal concentration in the cytosol and therefore calcium was buffered more fully. Figure 5.7 shows the effect of 10 minutes exposure of dmBAPTA-AM upon the outward current activated upon depolarisation; the I_K tail current (and the outward current during the depolarisation) were time-dependently reduced, but the effects appeared to be maximal after 10 minutes dmBAPTA. Upon exchange of perfusing solutions to one that did not contain dmBAPTA-AM, there was no reversal of the reduction of I_K. The effect of dmBAPTA-AM upon the voltage and time-dependent activation of I_K were investigated. The effect of dmBAPTA-AM were similar (no-significant difference detected using unpaired t-test) in both regards to the effects of BAPTA-AM; dmBAPTA-AM reduced time-dependent activation of I_K with depolarisations at 40 ms and 700 ms (figure 5.7b), to 53 ± 2 % of control at 700 ms (591 ± 163 pA, n=3, $P<0.05$) and also reduce I_K activated with voltages greater than –10 mV (n=3, $P<0.05$), without altering the $V_{1/2}$ or activation slope (figure 5.7c).

2 μM ryanodine was used to inhibit the release of calcium from the SR. I_K was activated using various duration depolarisations (10-700 ms) and two-phases of time-dependent activation were observed, which can be roughly assigned to I_{Kr} and I_{Ks} (figure 5.8). When 2 μM ryanodine was introduced, the I_K tail current activated with extended depolarisations (>100 ms) were reduced (to 82 ± 7 % at 700 ms), but I_K activated with brief depolarisations (≤100 ms) were not affected (n=9, $P>0.05$).

The effect of 2 μM ryanodine upon the voltage-dependent activation of I_K was also investigated and was found to be diminished at all voltages (n=9, $P<0.05$),

causing a reduction of I_K activated by a +40 mV depolarisation to 77 ± 9 % (figure 5.8b), without shifting the $V_{1/2}$ (14 ± 9 and 14 ± 4 mV respectively). The deactivation of the I_K tail current was also measured but the time-constants were not changed by ryanodine, 189 ± 12 ms and 810 ± 73 ms in the absence and 142 ± 10 ms and 833 ± 99 ms in the presence of ryanodine (n=8, P>0.05). Although the amplitude of the second component was reduced from 39 ± 10 to 17 ± 6 pA (n=8, P<0.05). A two-pulse protocol has been used to separate I_{Kr} from I_{Ks} (Carmeliet 1993), in which I_K is activated with a depolarisation to +40 mV, and the current de-activating at an initial repolarisation is to –10 mV is thought to reflect predominantly I_{Ks} deactivation (figure 5.9a). While current deactivating during a subsequent repolarisation to –40 mV is thought to reflect I_{Kr}. In this manner I_{Kr} and I_{Ks} can be separated and this protocol identified the tail current upon initial repolarisation to be reduced by ryanodine to 80 ± 6 % of control (n=8, P<0.05), whereas the tail current associated with the second repolarisation was not altered (figure 5.9b). The amplitude of I_{CaL} was also quantified in the voltage range –30 to +40 mV, to be of –243 ± 58 pA at +10 mV and the addition of 2 μM ryanodine did not cause any alteration in the voltage-dependent activation of I_{CaL} (figure 5.10, n=6, P>0.05).

The beating rates of atrial preparations were measured when treated with E4031 and then ryanodine. The control beating rate was 168 ± 11 bpm (n=5), this was reduced to 122 ± 9 bpm (73 ± 4 %, n=5, P<0.05) in the presence of E4031 and then was further reduced to 95 ± 8 bpm (57 ± 4 %, n=5, P<0.05) when E4031 and ryanodine were in the organ bath (figure 5.11a). To investigate a possible effect of ryanodine upon I_{Ks}, the sensitivity of the E4031 resistant current to ryanodine was studied. The E4031 resistant current was activated with depolarisation longer than 70

ms, and increased rapidly in amplitude with depolarisations between 200 and 400 ms, with longer durations still increasing the current (figure 5.11b). Ryanodine (2 μM) reduced the amplitude of the E4031 resistant current activated with depolarisations of 200 ms and longer (n=7, $P<0.05$); there was no significant current at 40 ms in the absence or presence of ryanodine, but the E4031 resistant current activated with a 700 ms depolarisation was reduced to 71 ± 7 % by ryanodine. The voltage dependent activation of the E4031 resistant current was found to activate with depolarisation to potentials more positive than 0 mV, having a $V_{1/2}$ of 23 ± 5 mV and an activation slope of 14 ± 3 mV (figure 5.11c). Ryanodine (2 μM) reduced the E4031 resistant current activated with depolarisation between 20-40 mV (n=6, $P<0.05$), having a $V_{1/2}$ to of 31 ± 20 mV and an activation slope of 17 ± 8 mV (n=6, $P>0.05$).

Cyclopiazonic acid (CPA) is another inhibitor of SR function. In contrast to ryanodine, CPA inhibits the conformational conversions associated with the SERCA ATPase sequestering of calcium (released during an action potential) back into the SR (Bers 1993); this therefore reduces the SR calcium available for release upon stimulation. The characteristics of spontaneous action potentials from isolated sino-atrial node cells have been measured as: overshoot 5 ± 1 mV, most negative potential -59 ± 0 mV, action potential amplitude 66 ± 1 mV, beating rate 156 ± 18 bpm, APD_{50} 68 ± 10 ms and APD_{90} 118 ± 18 ms (n=2). Locally superfused solution B was rapidly exchanged for one containing 5 μM CPA and the spontaneous activity was found to continue (figure 5.12a), although the interval between action potential development was increased by 141 ± 1 % (n=2, $P<0.05$). The beating rate also slowed from 164 ± 14 bpm to 120 ± 15 bpm (72 ± 3 %, n=3, $P<0.05$) upon addition of CPA (figure 5.12b). The effect of CPA on both time and voltage-dependent activation of I_K were

studied. The typical two-phases of time-dependent activation of I_K were found, with a 40 ms depolarisation activating 36 ± 4 % (199 ± 43 pA, n=6) of maximum current (700 ms, 591 ± 124 pA, n=6). CPA (5 μM) caused a reduction of I_K tail current amplitude activated with depolarisations of 40 ms and longer (figure 5.13a); in the presence of CPA I_K activated with a 40 ms depolarisation was 28 ± 5 % (143 ± 34 pA, n=6, $P<0.05$) and 80 ± 6 % (459 ± 105 pA, n=6, $P<0.05$) after a 700 ms depolarisation (figure 5.13b). I_K activated in the voltage range between –30 and +40 mV was quantified, identifying voltage-dependent activation of I_K with a $V_{1/2}$ of –5.8 ± 8 mV and a maximal current of 686 ± 160 pA (n=6). When 5 μM CPA was included in the superfusing solution there was a reduction in the amplitude of I_K activated with depolarisations to –10 mV and greater, reducing the current at 700 ms to 88 ± 4 % (figure 5.14a, 587 ± 133 pA, n=6, $P<0.05$). A sigmoidal curve could not be satisfactorily fitted to the CPA voltage-dependent activation and so no $V_{1/2}$ was described. I_{CaL} activated over the same range of potentials was measured, found to be maximal (-1318 ± 131 pA, n=3) at 0 mV and demonstrating a roughly bell-shaped curve over the voltages tested (figure 5.14b). In the presence of 5 μM CPA, I_{CaL} appear to be reduced between –20 and +10 mV (n=3, $P<0.05$).

As reported previously in this thesis (figure 5.38, page 207), the I_{CaL} blocker nifedipine (5 μM) was found to cause a slight reduction of I_K at depolarisation durations longer than 20 ms and similar inhibition of the voltage dependent activation of I_K. The effects of nickel (25-100 μM), a I_{CaT} inhibitor have also been reported (figure 5.39, page 208), describing a reduction in beating rate of atrial preparation and isolated sino-atrial node cells alike.

Discussion

Increasing the calcium concentration of the solution bathing an atrial preparation resulted in a concentration dependent elevation of beating rate, by approximately 10 % in the presence of 2.5 compared to 1 mM. An elevation of extracellular calcium would be expected to increase cytosolic calcium and increase the SR calcium load. Ju and Allen (1998) found beating rate of an amphibian pacemaker to increase when SR calcium load was increased and identified this mechanism as one that occurs upon adrenergic stimulation. Cardiac glycosides block the sodium-potassium pump, causing a high intracellular sodium, which favours influx of calcium on the sodium-calcium exchanger and limits extrusion on the same pathway; this causes cellular SR calcium load which increases rate of beating (Fischmeister, Brocas-Randolph et al. 1986). Conversely, Li et al (1997) used ryanodine to inhibit SR calcium release and found that this had a negative chronotrpic effect, again identifying the beating rate to be dependent upon SR function.

I_{Ks} has been reported to be more calcium sensitive than I_{Kr} (Nitta, Furukawa et al. 1994), so differential calcium modulation (including SR released) between species could be related to the relative expression of I_{Kr} and I_{Ks}. The effect of increasing calcium upon rate was not altered when the preparation was pre-treated with E4031, so the calcium sensitive increase in rate was not only mediated through I_{Kr} modification.

Rapid application of 10 μM BAPTA, via the AM membrane permeant delivery system, stopped spontaneous activity of isolated sino-atrial node cells. Cessation occurred within 2-5 action potentials and began with a gradual reduction in action potential amplitude, followed by a stable (but noisy) membrane potential of – 26 ± 4 mV in the presence of BAPTA. These effects of BAPTA upon spontaneous activity indicate that basal (as BAPTA will not be 'quick' enough to effectively buffer the SR calcium dump) cytosolic calcium critically regulates ionic currents that contribute to pacemaking. When buffering was removed the membrane potential gradually hyperpolarised, possibly indicating calcium buffering was inhibiting some outward current (I_{Ks}), until oscillations occurred and variable amplitude action potentials were initiated. The action potentials recovered slowly, only gradual developing the action potential amplitude described before BAPTA exposure. Both components of I_K were substantially reduced by buffering of cytosolic calcium with BAPTA, I_{Kr} by 30 % and I_{Ks} by approximately 50 %. There was no obvious reduction in I_f amplitude, however there was a 10 mV shift in the activation, to more negative potentials during BAPTA mediated calcium buffering, which would cause the I_f contribution to sino-atrial node pacemaking to be reduced (Hagiwara and Irisawa 1989). From these data, the most probable cause of action potential failure would be the I_K reduction, which would limit repolarisation therefore not activating the already diminished I_f. Upon removal of calcium buffering an outward current is activated, again the most likely candidate would be I_K; one interpretation would be that as I_K inhibition decreases, the membrane would become hyperpolarised and activate the de-inhibited I_f.

Another inhibitor of SR calcium release CPA, decreased the beating rate of isolated sino-atrial node cells by ~25 %. In concurrence with these findings, the beating rates of atrial preparations were reduced by E4031, but a further decreased was described after the addition of ryanodine; indicating a non-I_{Kr} mediated SR dependent reduction in beating rate. Hata, Noda et al (1996) and Rigg, Heath et al (2000) described the role of SR in pacemaking of the guinea-pig sino-atrial node, identifying a reduction of beating rate of various preparations upon inhibition of SR function, and other have reported a SR modulation of pacemaking currents (Ju and Allen 1998; Huser, Blatter et al. 2000; Lipsius, Huser et al. 2001).

SR calcium release inhibition with ryanodine resulted in a slight reduction in the amplitude of I_K, by reducing I_{Ks} by ~25 %, without having much effect upon I_{Kr}. CPA mediated reduction in SR calcium release was found to reduce I_{Ks} by approximately 20 %, but with CPA (unlike ryanodine) a similar reduction of I_{Kr}. The calcium sensitivity of I_K has been previously reported (Tohse, Kameyama et al. 1987), with the specific calcium released from the SR also having been reported by (Hata, Noda et al. 1996). It is worth noting that the SR calcium release does not modulate I_K to the same extent that BAPTA inhibition of cytosolic calcium, possibly indicating I_K calcium regulation to be related to the basal calcium levels, rather than the calcium dumped from the SR upon stimulation. Sino-atrial node cells do not have transverse-tubules, resulting in the junctional SR not being closely apposed to ion channels, so SR released calcium may not have a large a modulator role as in ventricular myocytes.

Inhibition of the T-type calcium current did cause a slight (15 %) reduction in beating rate of atrial preparations and isolated node cells alike, demonstrating at least a slight role of I_{CaT} in pacemaking (Hagiwara, Irisawa et al. 1988; Huser, Blatter et al. 2000). I_{CaT} activity could initiate spark-like calcium events during diastolic depolarisation (Huser, Blatter et al. 2000), which would activate the inward I_{NCX}. A reduction in I_{CaL} has been previously demonstrated to reduce the rate of the action potential upstroke (Rigg and Terrar 1996). Neither cytosolic calcium buffering or ryanodine reduced I_{CaL}, indicating sarcolemmal calcium currents to be relatively independent of cytosolic calcium, however at some non-maximal potentials CPA did reduce I_{CaL}. I_{CaL} is calcium dependently inactivated, however this is much more likely to occur upon I_{CaL} mediated calcium flux, which would result in very high local calcium concentrations, rather than cytosolic changes. The I_{CaL} blocker nifedipine reduced the amplitude of I_K, however this is likely to be due to the effect of blocking I_{CaL} upon intracellular calcium concentration; I_{CaL} inhibition would directly, and indirectly by not activating the SR calcium release, reduce the cytosolic calcium concentration and therefore I_K calcium regulation. Nifedipine has previously been found to reduce I_K (Sanjuinetti and Jurkiwicz 1990), and in this study the calcium sensitivity of I_K was concluded to be the reason for this reduction in amplitude. The macroscopic effect of calcium buffering and SR inhibition is to reduce/stop spontaneous action potential generation, this infers that SR function promotes sino-atrial node pacemaking.

A reduction of cytosolic calcium has previously been found to reduce I_f (Hagiwara and Irisawa 1989), there maybe a direct interaction of calcium with the I_f channel. Although it is more likely that calcium could up-regulate AC (Luthi and

McCormick 1999), thus increasing cAMP and hence I_f (Zaza et al 1991), or HCN could interact with calcium-calmodulin (Rigg, Mattick et al. 2003). Another mechanism of calcium modulation of I_f, could be calcium sensitive kinase activity. Whereas calcium has been identified to directly interact with I_{Ks} (Tohse, Kameyama et al. 1987; Tohse, Kameyama et al. 1990; Walsh, Arena et al. 1991), also being regulated by calmodulin and PKC (Tohse, Kameyama et al. 1987; Nitta, Furukawa et al. 1994). The removal of rectification of I_{Kr} has been found to be a calcium-dependent process (Heath and Terrar 2000). There may be an intrinsic turnover of AC in the sino-atrial node, which mimics partial sympathetic stimulation and I_{Kr} rectification would therefore be partially calcium-dependently removed.

Lowering of calcium levels reduces the rate of beating on isolated cells, and the intact sino-atrial node. Reducing cellular calcium diminishes the amplitude of both components of I_K, without altering decay or I_{CaL} amplitude. Calcium released from the SR is related to beating rate, augments I_{Ks} and possibly I_{Kr}, without having an effect upon I_{CaL}. These findings indicate calcium to have an important role in spontaneous activity of the guinea-pig sino-atrial node. Calcium regulates both I_{Kr} and I_{Ks}, partially mediated by calcium released from the SR.

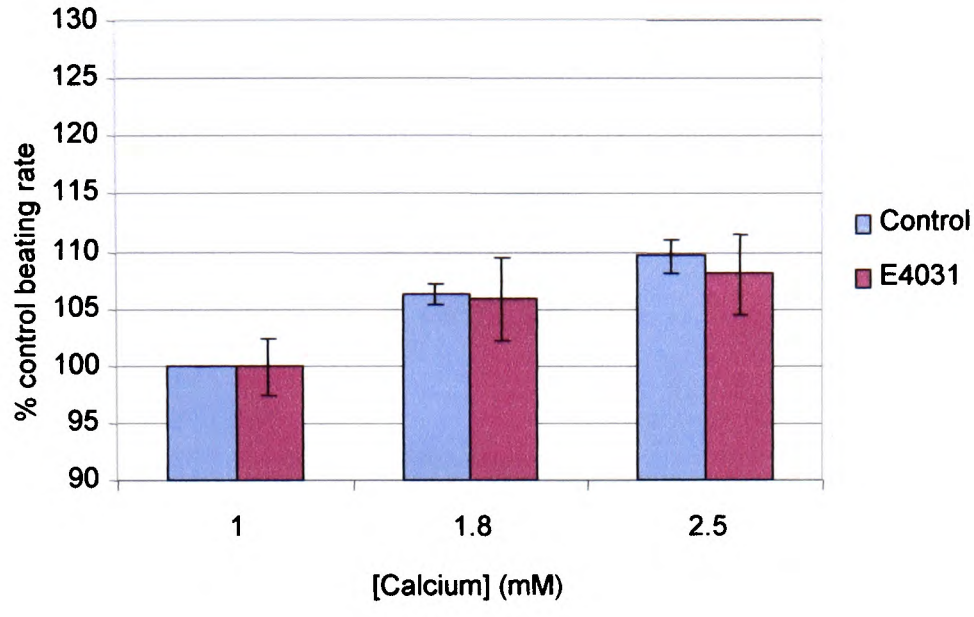

Figure 5.1 Page 226

Increasing the calcium concentration of the bathing solution around the atrial preparation, elevated the beating rate. Calcium concentration was increased from 1 to 1.8 mM and subsequently to 2.5 mM; this was associated with a quickening of atrial preparation being rate, to 106 ± 1 and then to 109 ± 1 % of control beating rate (n=5, $P<0.005$). In the presence of 5 μM E4031, which reduced beating rate to 74 ± 3 % (n=5, $P<0.001$), elevating calcium to 1.8 and 2.5 mM similarly increased relative beating rate (n=5, $P<0.05$).

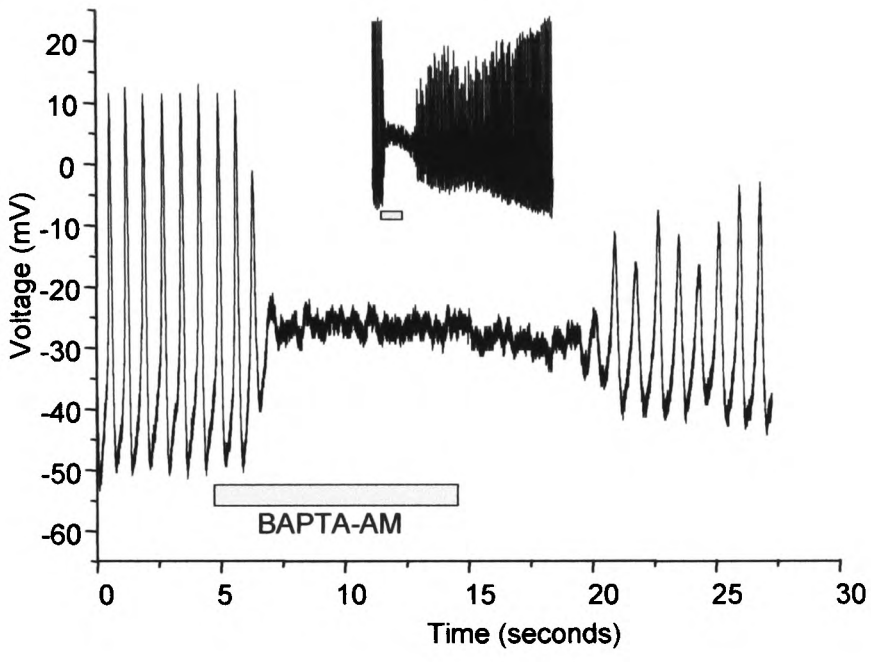

Figure 5.2 Page 227

Rapid switching of isolated sino-atrial node perfusing solution to one which contained BAPTA-AM (10 μM) caused immediate cessation of action potential generation. This trace is representative of the population tested (n=3) and illustrates the effect of transient exposure to BAPTA-AM. Reperfusion of control solutions did not immediately reverse this effect, the action potentials slowly regained amplitude over the subsequent few minutes (see inset of compressed time).

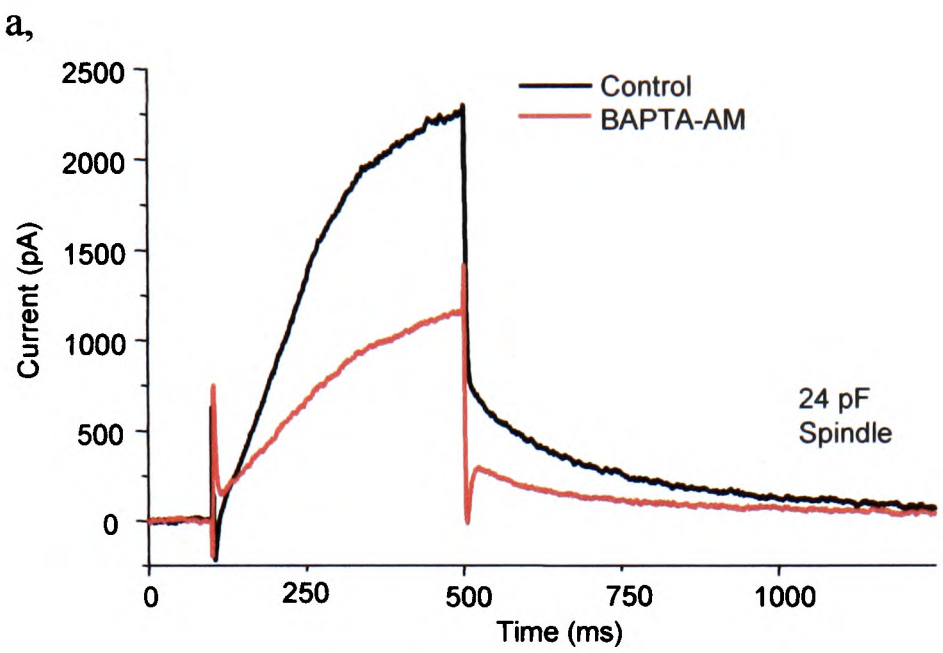

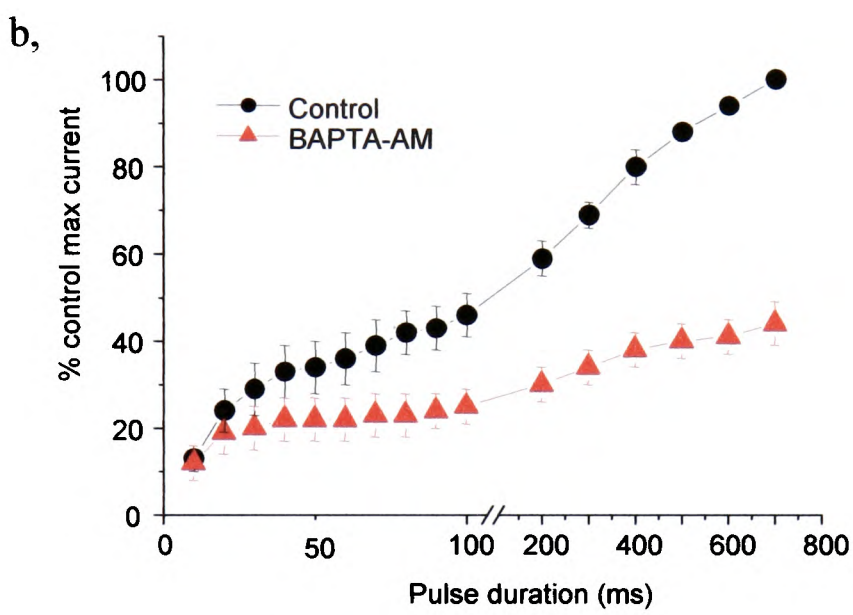

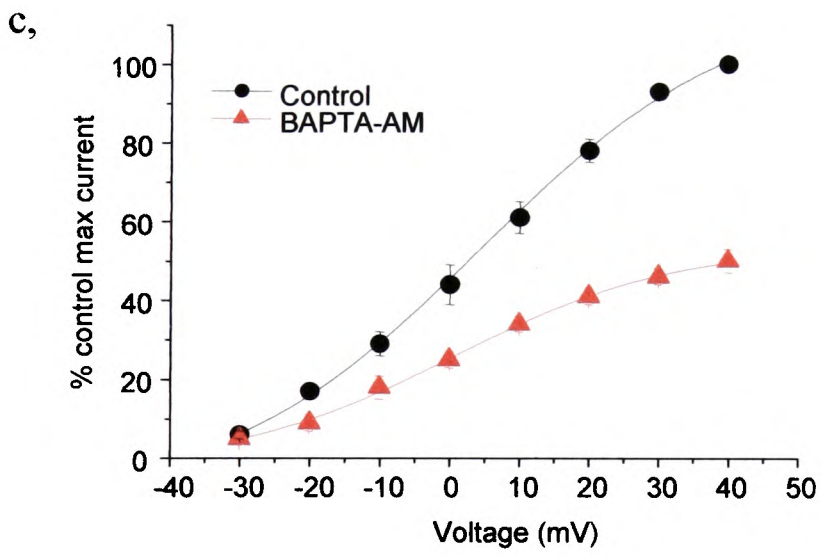

Figure 5.3 Page 228

Prolonged BAPTA-AM (10 μM) exposure (5 minutes) reduced the amplitude of the outward current activated upon depolarisation (to +40 mV) and the I_K tail current (a). I_K was examined after being activated by various duration depolarisations (b) and it was found that BAPTA-AM reduced I_K activated with depolarisations longer than 40 ms ($n=6$, $P<0.05$). Depolarisation between -30 to +40 mV were also investigated (c) and BAPTA-AM reduced I_K at -20 mV and greater ($n=6$, $P<0.05$), but neither the $V_{1/2}$ or the slope activation of I_K were altered (c).

a,

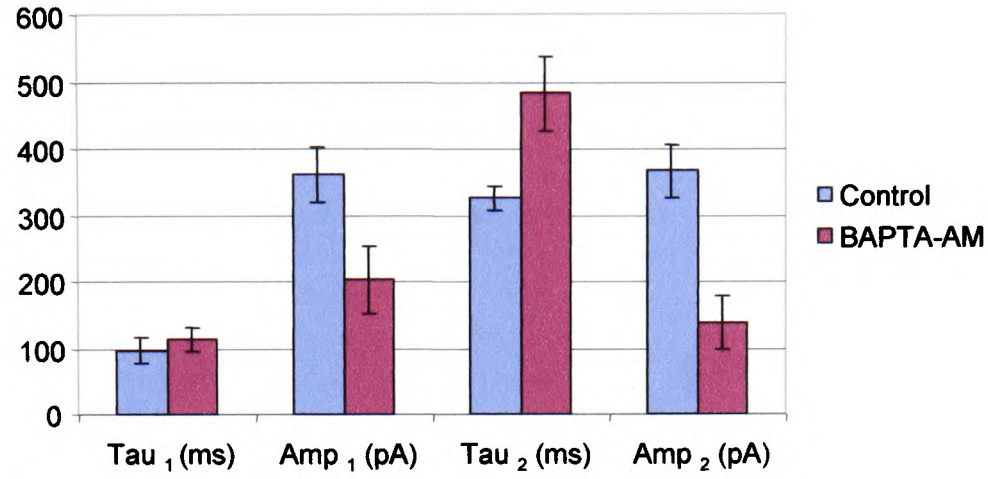

b,

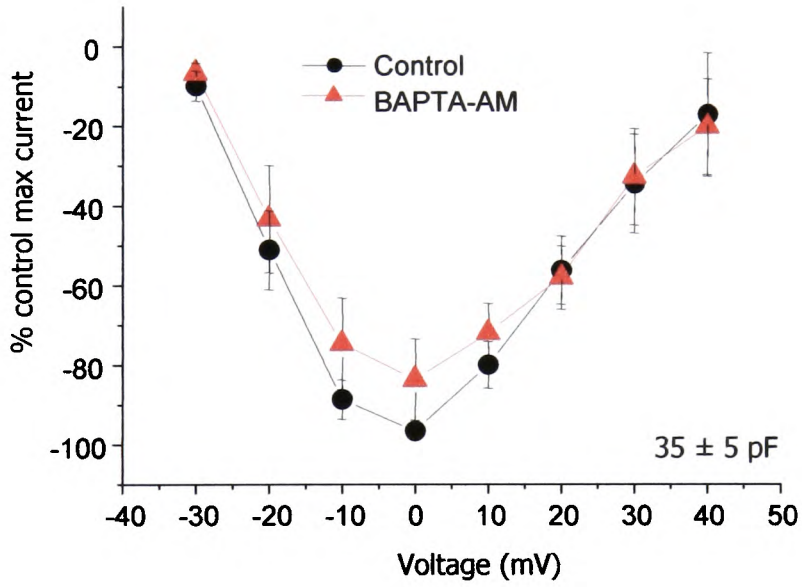

Figure 5.4 Page 229

BAPTA-AM (10 μM) did not alter the time-constants of I_K tail current decay (a), but both Amp_1 and Amp_2 were reduced (n=6, $P<0.05$). I_{CaL} was also investigated at voltages between -30 and +40 mV, but BAPTA-AM (10 μM) did not alter the amplitude (b), or the voltage which activated maximal I_{CaL} (n=5).

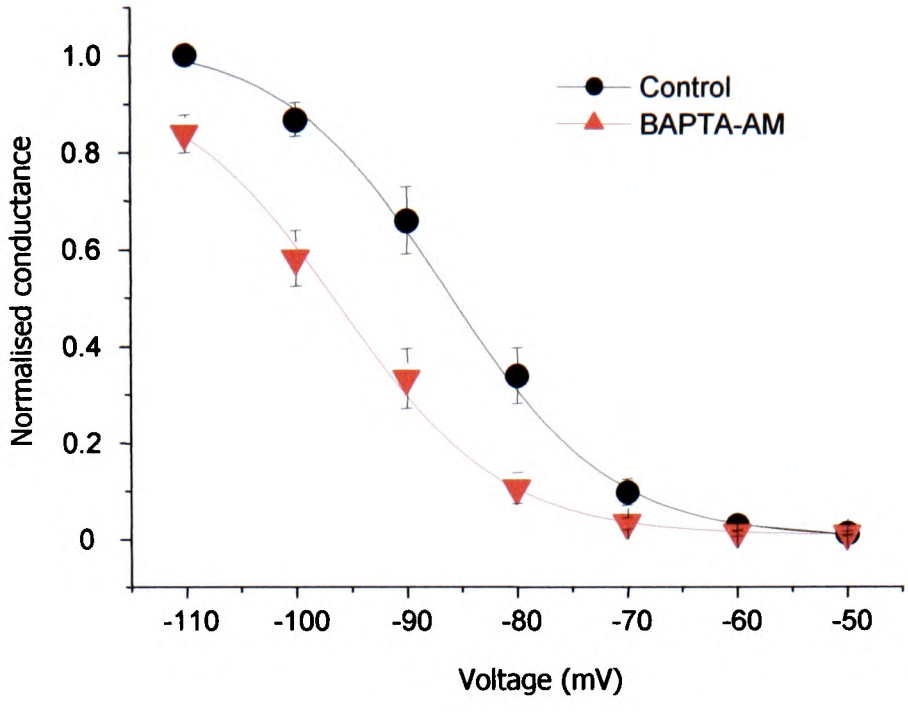

Figure 5.5 Page 230

BAPTA-AM (10 μM) shifted the voltage dependent activation of I_f to more negative potentials. The 5 minute exposure of isolated sino-atrial node cells to BAPTA-AM caused a shift in the $V_{1/2}$ from -86 ± 2 to -96 ± 2 mV (n=6, $P<0.05$), without changing the slope activation.

a,

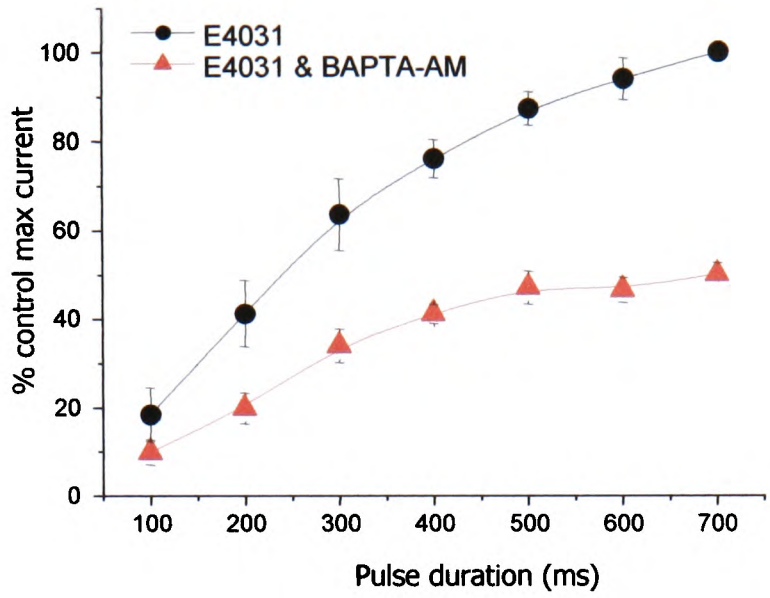

b,

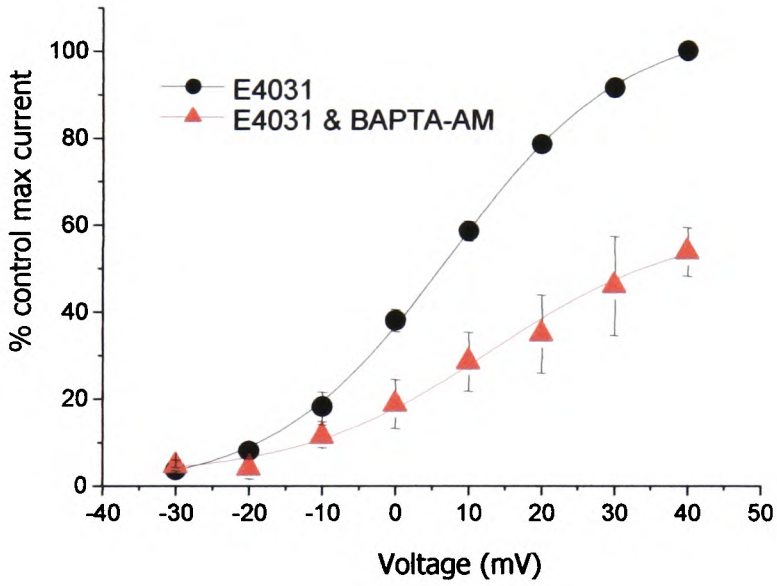

Figure 5.6 Page 231

In the presence of E4031 (5 μM), BAPTA-AM (10 μM) reduced the amplitude of I_K activated with depolarisations longer than 200 ms (a, n=3, $P<0.05$). In similar conditions I_K was activated with depolarisations to various voltages (b), BAPTA-AM reduced I_K activated with depolarisations to 0 mV and greater, as well as to -20 mV (n=3, $P<0.05$).

a,

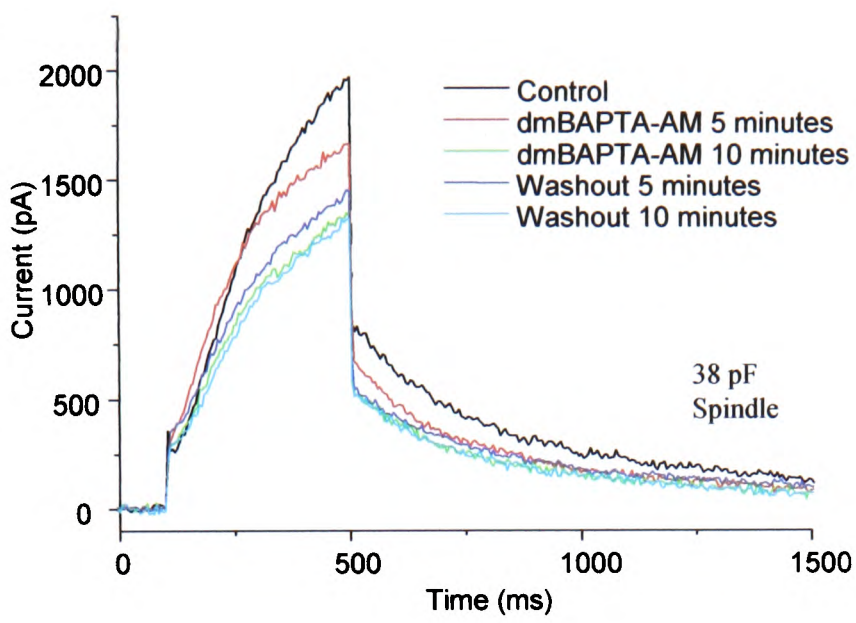

b,

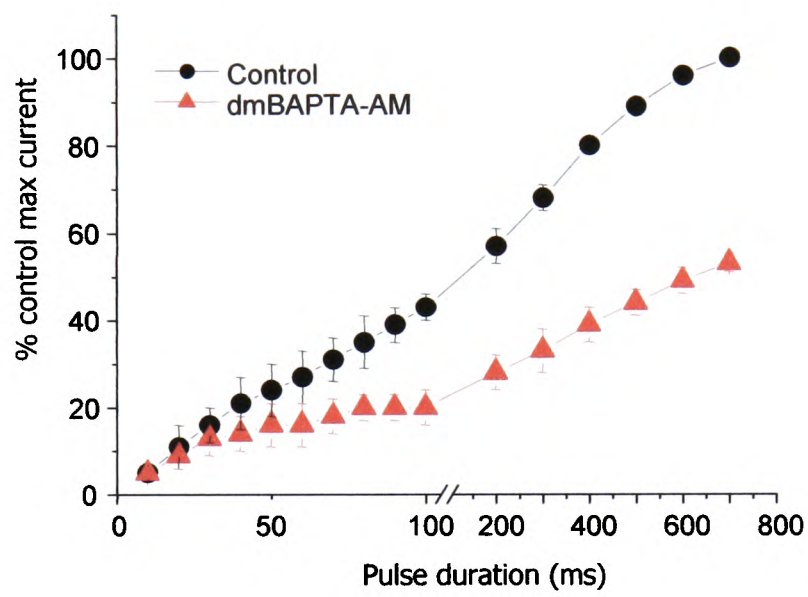

c,

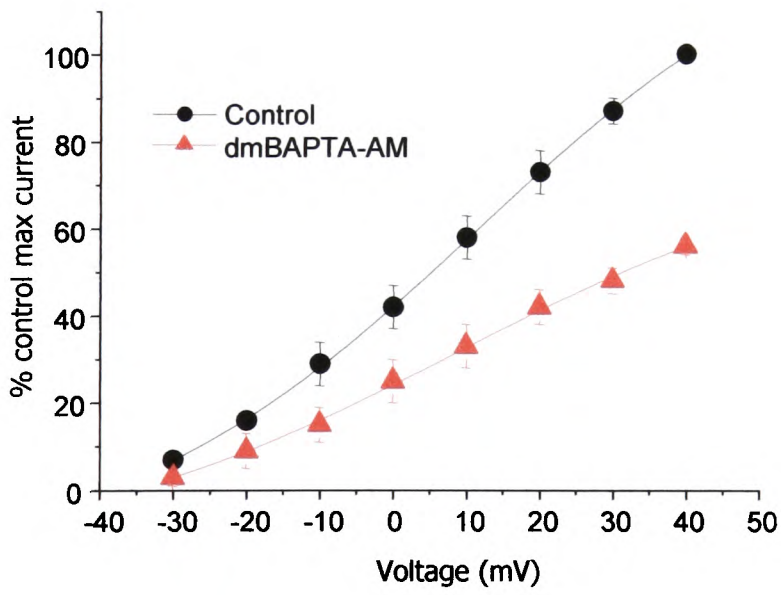

Figure 5.7 Page 232

The more potent BAPTA analogue dimethyl BAPTA (10 μM) was used, with the AM ester to facilitate cell membrane permeation (dmBAPTA-AM), and found to reduce I_K (a). The I_K tail current was progressively inhibited by dmBAPTA-AM (a). I_K was reduced by depolarisation of 40 ms and longer (n=3, $P<0.05$) upon exposure to dmBAPTA-AM for 10 minutes (b). I_K activated with voltages of -10 mV and greater was inhibited by dmBAPTA-AM (n=3, $P<0.05$), without effecting $V_{1/2}$ and activation slope (c).

a,

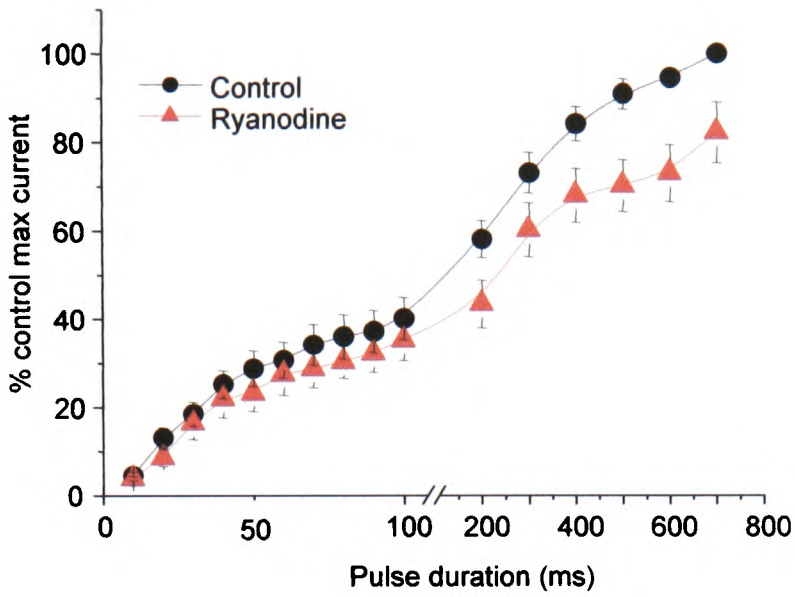

b,

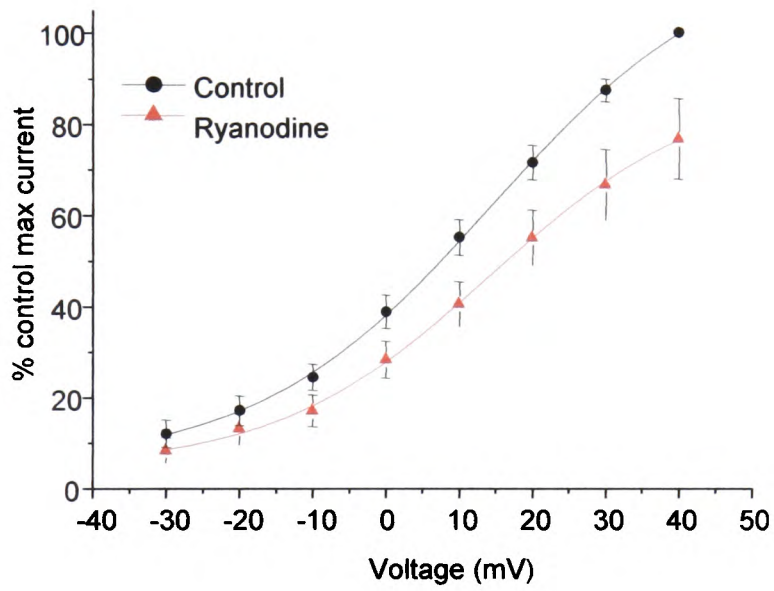

Figure 5.8 Page 233

The effect of SR calcium release channel blocker ryanodine (2 μM) upon I_K was investigated and found to reduce I_K amplitude activated with depolarisation longer than 200 ms (a, n=9, $P<0.05$). Although neither the $V_{1/2}$ or activation slope of I_K were altered (b), the amplitude of I_K was reduced by ryanodine (n=9, $P<0.05$).

a,

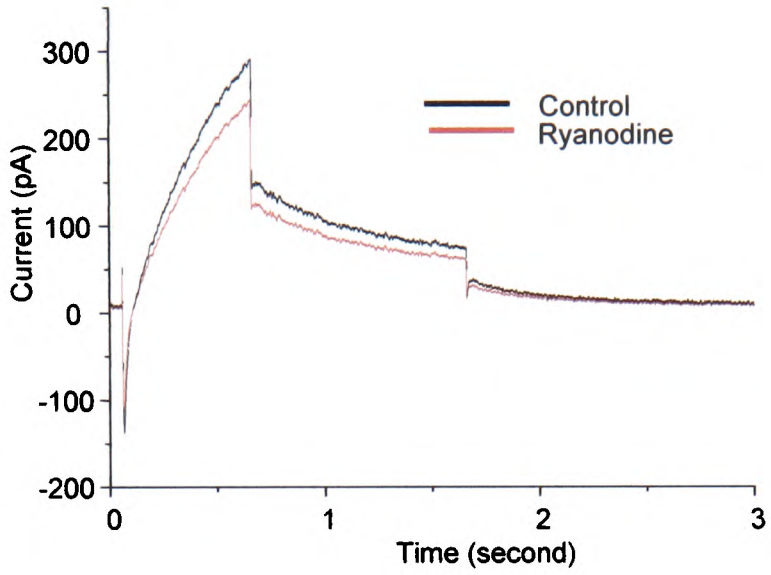

b,

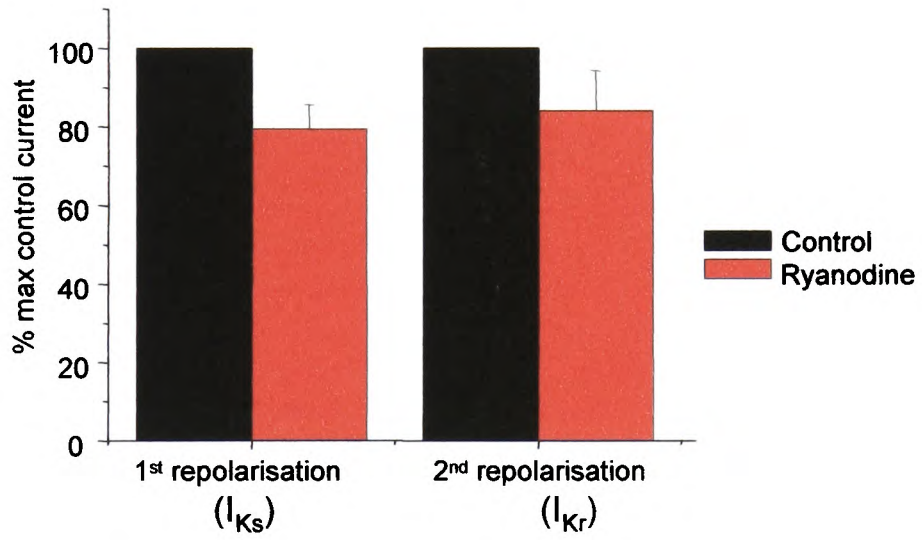

Figure 5.9 Page 234

I_K was found to be reduced by 2 μM ryanodine (a). Using the Carmeleit protocol, which contains two repolarisation steps, the I_K components can be separated (b). I_K was activated by the Carmeleit protocol and indicated that ryanodine reduced I_{Ks} ($n=8$, $P<0.05$), but not I_{Kr}.

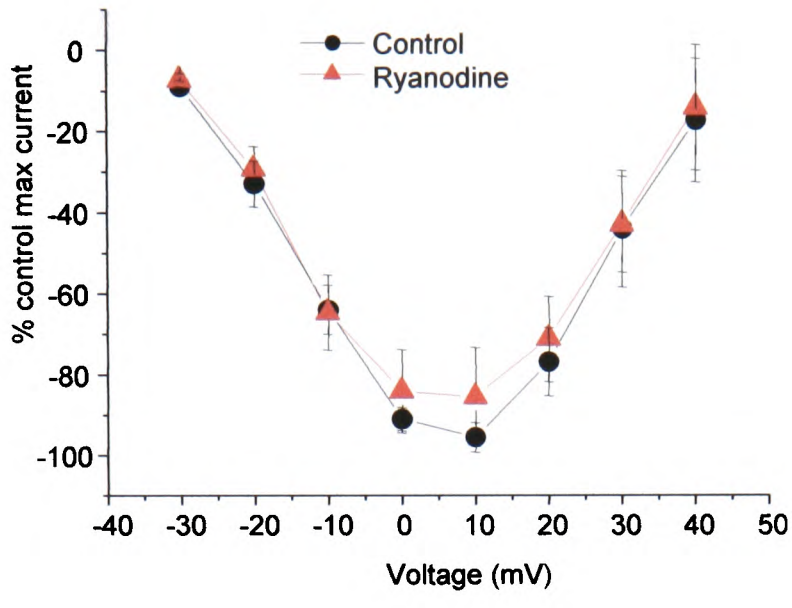

Figure 5.10 Page 235

Ryanodine did not effect I_{CaL}, activated between -30 and +40 mV and also did not alter the voltage which activated maximal I_{CaL} (n=6), which in this case was +10 mV.

a,

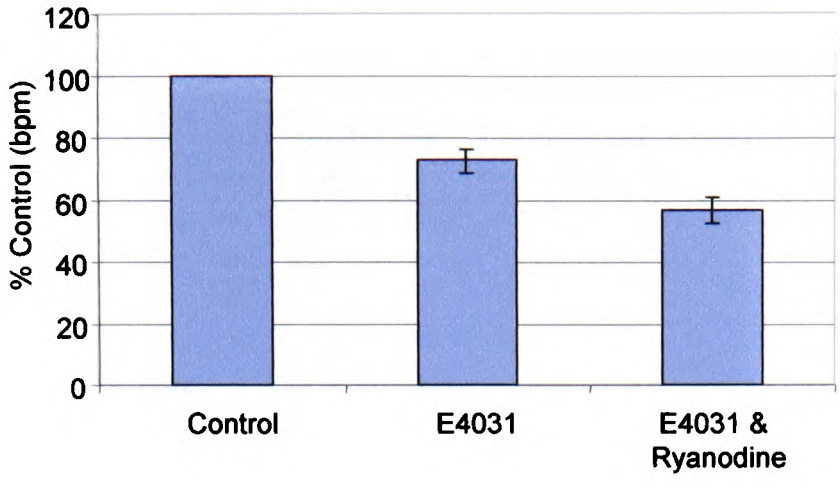

b,

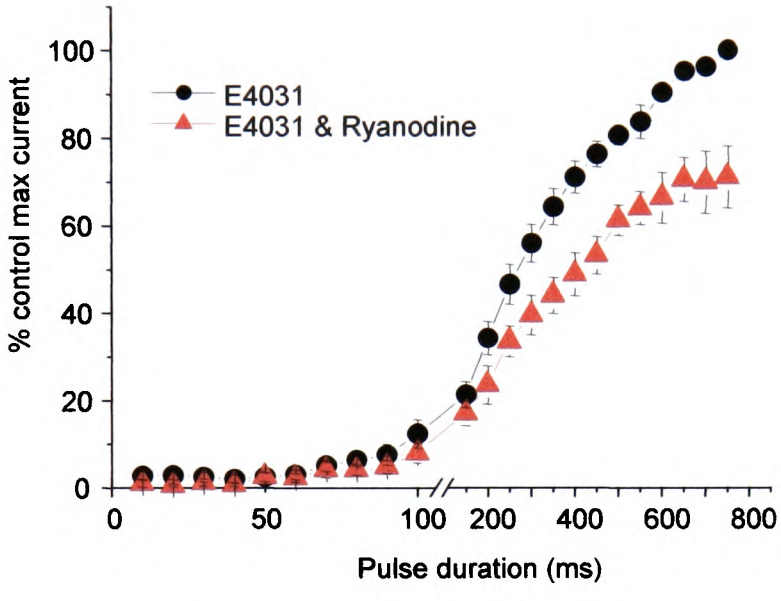

c,

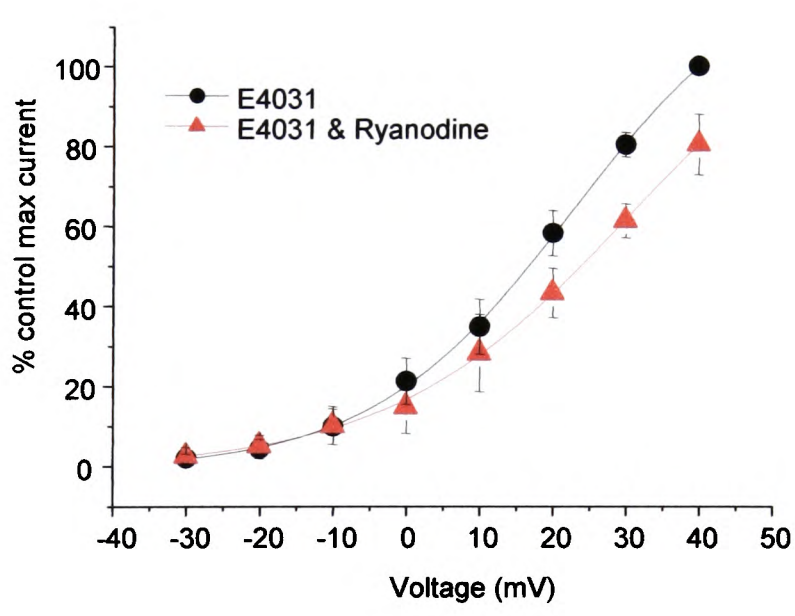

Figure 5.11 Page 236

Atrial preparations were treated with 5 μM E4031 (a), which caused a reduction from 168 ± 11 to 122 ± 9 bpm (n=5, $P<0.05$), and further addition of 2 μM ryanodine reduced beating rate to 95 ± 8 bpm (n=5, $P<0.05$). I_K was reduced by ryanodine in voltage clamped sino-atrial node cells in the presence of E4031 (b), with depolarisations in excess of 200 ms (n=7, $P<0.05$). The voltage dependent activation of I_K was reduced by ryanodine in the presence of E4031, at voltages greater than 20 mV (n=6, $P<0.05$), without changing the $V_{1/2}$ or slope activation (c).

a,

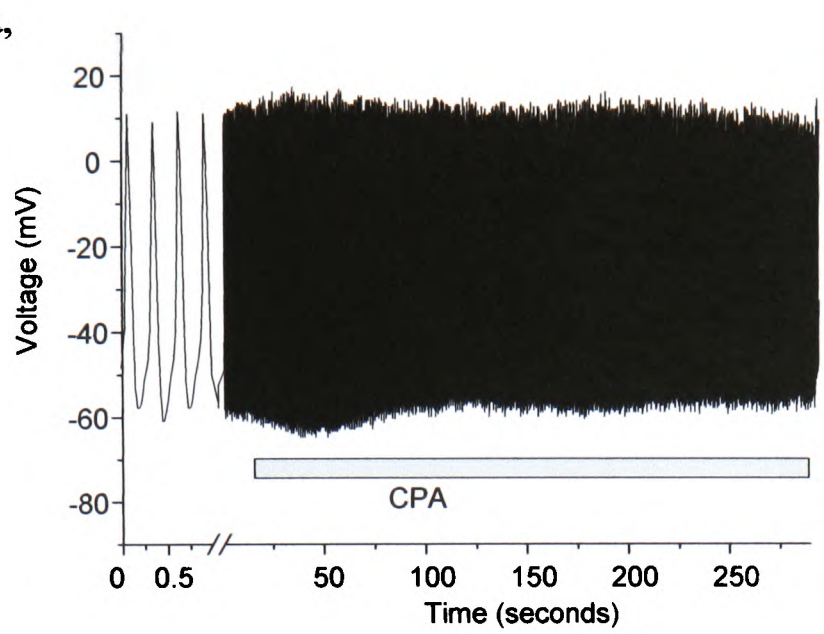

b,

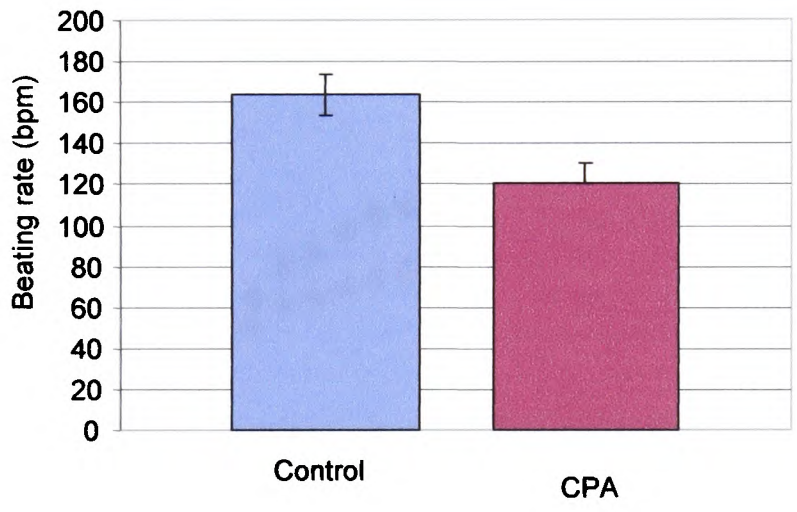

Figure 5.12 Page 237

5 μM cyclopiazonic acid (CPA) did not cause spontaneous sino-atrial node cells to become quiescent (a), but the beating rate was found to be reduced to 72 ± 3 % of control (b), after 5 minutes CPA exposure (n=3, $P<0.05$).

a,

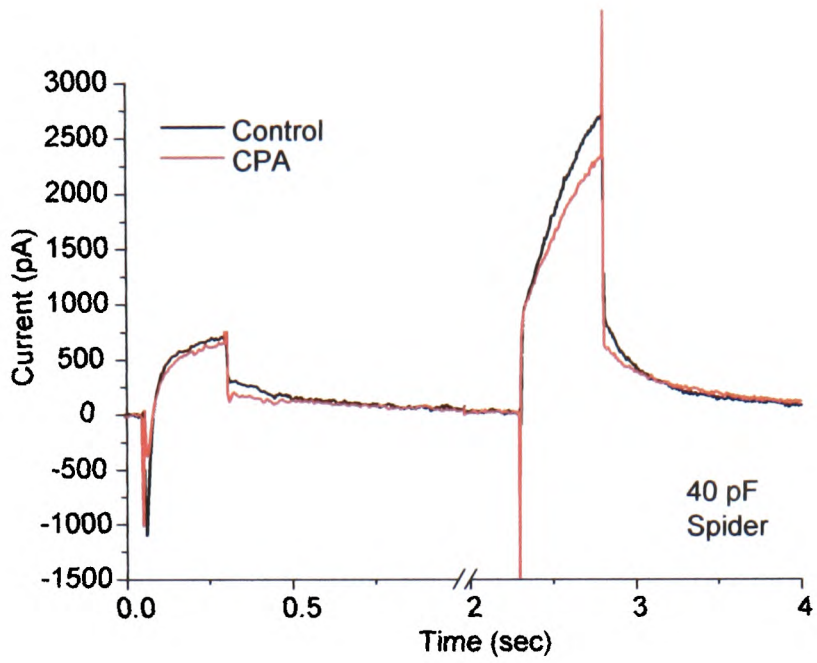

b,

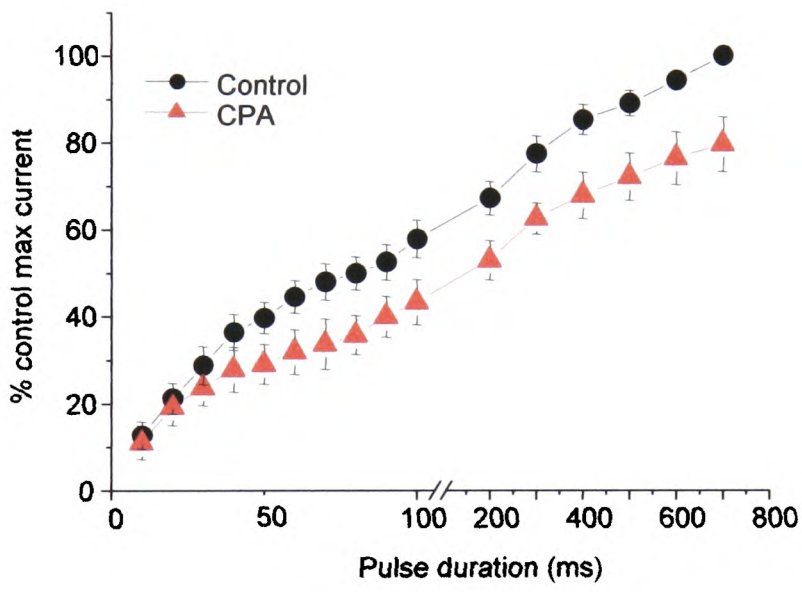

Figure 5.13 Page 238

5 μM CPA reduced I_K activated with both brief and prolonged depolarisations (a), being quantified to reduce I_K activated with depolarisation of 40 ms and longer (b, n=6, $P<0.05$).

a,

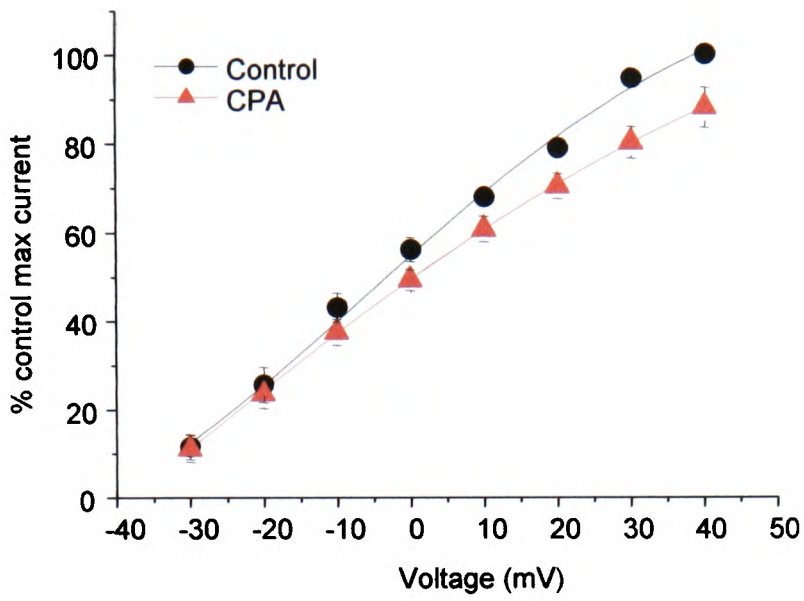

b,

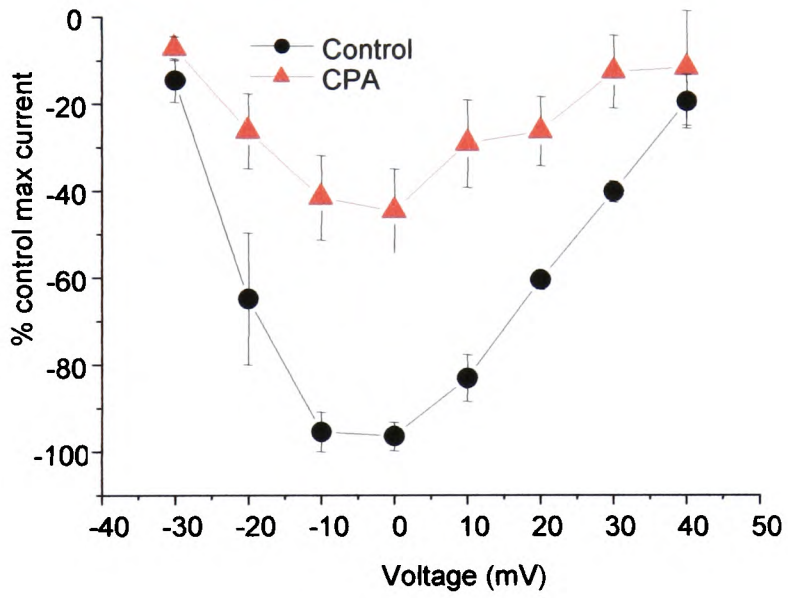

Figure 5.14 Page 239

I_K was activated with depolarisations in the voltage range -30 to +40 mV, activating I_K (a) and I_{CaL} (b). CPA (5 μM) was found to reduce I_K activated with depolarisations in excess of -10 mV (a, n=6, P<0.05) and I_{CaL} at -20 and -10 mV (b, n=3, P<0.05).

Agent	Target	Current	Affect
BAPTA	Cytosolic calcium	Various	Reduced I_{Kr}, I_{Ks} and shifted I_f
Ryanodine	SR calcium release	Various	Reduced I_{Ks}
CPA	SR calcium sequestering	Various	Reduced beating rate and I_K

Figure 5.15 Page 240
Summary table of findings in this chapter. Isoprenaline was used at 100 nM, E4031 at 5 μM, BAPTA-AM at 10 μM, nifedipine at 5 μM, ryanodine at 2 μM and MDL at 10 μM.

CHAPTER 6: Adenylate cyclase

The adenylate cyclase (AC) enzyme catalyses the production of cAMP from ATP. The most abundant isoforms of AC in the heart are AC V and AC VI (Cooper, Mons et al. 1995; Defer, Best-Belpomme et al. 2000), but most are expressed to some degree, with variation between ventricle and sino-atrial node being probable (Rigg, Mattick et al. 2003) and unquantified. AC participates in various intracellular pathways, but its role in autonomic stimulation is critical. During β-adrenergic stimulation of cardiac myocytes, a stimulatory guanine nucleotide binding protein subunit (G_s) is produced and this interacts with AC and increases turnover rate; this increases intracellular cAMP concentrations and partially mediates the β-adrenergic effects (Wang and Dhalla 2000). The activation of AC, does not mediate the full range of β-adrenergic effects (Bramich, Edwards et al. 1990; Choate, Edwards et al. 1993), as neuronal sympathetic stimulation (of guinea-pig sino-atrial node) differs in various characteristics to that of AC activation (Choate, Edwards et al. 1993). The non-AC effect may be mediated by co-transmitters which are released from the neurons in addition to noradrenaline, such as ATP (Bramich, Edwards et al. 1990). Acetylcholine stimulation of muscarinic receptors instigates the production of an inhibitory guanine nucleotide binding protein subunit (G_i), which also binds with AC, but G_i attenuates the production of cAMP. Both G-protein subunits and acetylcholine can directly interact with some ionic channels (Boyett, Kodama et al. 1995; Renaudon, Bois et al. 1997; Dhein, van Koppen et al. 2001), independent of AC, and hence alter the spontaneous generation of action potentials. Modulation of AC by the autonomic nervous system controls cAMP production, and consequently modulates ionic currents and pacemaking.

High AC activity

There is evidence that AC is actually partially stimulated in the sino-atrial node in the absence of β-adrenergic agonism (personal communication, Terrar & Mamas 2003). Acetylcholine regulates I_{CaL} in the ventricle and sino-atrial node by inhibiting the activation of PKA (Trautwein and Kameyama 1986; Giles, Nakajima et al. 1989; Tanaka, Clark et al. 1996); G_i interacts with AC, reduces cAMP production and hence lowers activation of PKA. In the absence of previous β-adrenergic pre-treatment, acetylcholine has no effect upon I_{CaL} amplitude in ventricular myocytes (Fischmeister, Brocas-Randolph et al. 1986; Fischmeister and Hartzell 1986), indicating that under basal conditions there is no AC turnover. Interestingly in both atrio-ventricular node (Habuchi, Nishio et al. 1996) and sino-atrial node cells (Petit-Jacques, Bois et al. 1993; Zaza, Robinson et al. 1996), acetylcholine decreased I_{CaL} in the absence of pre-treatment. For acetylcholine to have an effect there must be some cAMP being produced by AC and this supports the suggestion that there is baseline AC activity in node cells.

The voltage dependent rectification of sino-atrial node I_{Kr} has been described previously in this study (Description of I_K and other ionic currents, page 122), having a negative relation to voltage at potentials positive to +20 mV. I_{Kr} in ventricular myocytes (Heath and Terrar 2000) and ERG expressed in various cell-lines (Gintant, Datyner et al. 1985; Spector, Curran et al. 1996), demonstrates markedly more pronounced rectification from more negative potentials. Such rectification is removed upon β-adrenergic activation by a calcium dependent mechanism in which calcium entry as a consequence of AC stimulation leads to activation of other kinases including PKC (Heath and Terrar 2000), presumably involving AC stimulation. The

relatively weak rectification of I_{Kr} in the un-stimulated sino-atrial node could be taken to indicate raised levels of cAMP, due to basal turnover of AC

There is further evidence to indicate that there is no AC turnover in ventricular myocytes from the mechanisms of nitric oxide regulation of heart. Activation of the nitric oxide pathway causes the production of cGMP, which inhibits subtypes of PDE found in the ventricles (Cooper, Mons et al. 1995). Production of cGMP, would reduce cAMP degradation, but does not reduce I_{CaL}. But in the presence of isoprenaline (when AC is stimulated), I_{CaL} in ventricular myocyte was reduced by cGMP production (Fischmeister and Hartzell 1990; Hove-Madsen, Mery et al. 1996). These findings indicated that there is no basal turnover of AC in the ventricle, in the absence of stimulation.

Phospodiesterase's (PDE) are enzymes that promote the degradation of cyclic nucleotides. These include cAMP that is a product of AC, but other cyclic nucleotides (cGMP being the most relevant) are also substrates. There are four PDE subtypes, and specific subtypes are sensitive to calmodulin or cGMP, with 2 subtypes being cAMP specific (Komas, Le Bec et al. 1991). The neuronal production of nitric oxide (Herring, Rigg et al. 2001) causes activation of sino-atrial node guanylate cyclase (as does acetylcholine release) and the production of cGMP. Different PDE subtypes are stimulated or inhibited by cGMP (Komas, Le Bec et al. 1991; Herring, Rigg et al. 2001) and therefore alter cAMP levels according to the specific expression of AC sub-types in that tissue. Both AC and PDE's are found to have high activity in all cardiac tissue (Arch and Newsholme 1976), indicating that this system will have a high throughput and any modification of synthesis or degradation would have

substantial effects upon cellular cAMP levels. Upon β-adrenergic stimulation AC activity is altered, however there appears to be no modification of the PDE cAMP degradation; if PDE and AC were both altered by autonomic stimulation, there maybe no net effect upon cAMP. The level of PDE activity will partially define cellular cAMP and therefore cAMP-dependent kinase activity. Any action to inhibit PDE will increase cAMP, assuming constant AC activity. Milrinone can be used as a therapeutic agent during heart failure, due to its inhibitory action upon cardiac PDE's that cause increased cAMP levels (Ahn, Eardley et al. 1986) and therefore a positive inotropy. Many studies of autonomic regulation utilize PDE inhibitors to more easily describe the effects upon cAMP, with degradation reduced, however this creates a non-physiological environment, in which complexity such as possible cAMP oscillations (Cooper, Mons et al. 1995) maybe overlooked.

AC calcium sensitivity

There are 8 AC isoforms isolated so far, with at least half of the AC isoforms regulated (some indirectly via calmodulin) by calcium (Piascik, Babich et al. 1983; Piascik, Babich et al. 1986). AC calcium sensitivity has been described in smooth muscle (Piascik, Babich et al. 1986), the parotid gland and the thalamus (Piascik, Babich et al. 1983; Luthi and McCormick 1998; Luthi and McCormick 1999), in these cell calcium primarily increased cAMP production. In addition PKC can regulation AC via phosphorylation, with some PKC exhibiting calcium sensitivity (see review by (Defer, Best-Belpomme et al. 2000). The tissue dependent AC subtype expression has been investigated and the calcium inhibited isoforms V and VI, appear to be primarily expressed in homogenised heart (Cooper, Mons et al. 1995), however only a very small minority of these cells would have been sino-atrial

node cells. Considering differential morphology, expression of ionic channels and calcium handling apparatus in the sino-atrial node versus the rest of the heart, expression of other (calcium activated) AC subtypes maybe a possibility (Rigg, Mattick et al. 2003).

Intracellular messenger pathways of various cell types exhibit cross-talk, an interaction between two separate pathways; such as the dual-regulation of PDE's by PKA and calcium (Sharma, Flores et al. 1994). Classically AC is the starting point of the cAMP/PKA pathway, and calcium is a mediator in the PLC/PKC pathway and defines contraction.

One of the major inward ionic currents involved in pacemaking is directly regulated by cAMP, leading to a substantial shift in the voltage dependent activation of I_f (DiFrancesco and Tortora 1991; Accili, Redaelli et al. 1997). This activity is independent of any cAMP mediated kinase activity (Bois, Renaudon et al. 1997). In addition, there are some data indicating a direct interaction of cAMP with HERG, the protein mediating I_{Kr} (Cui, Kagan et al. 2001). PKA is activated by cAMP and PKA phosphorylation also regulates a large number of channels including I_{CaL}, which shows a negative shift in voltage-dependent activation and quadrupled amplitude (Brum, Osterrieder et al. 1984; Tanaka, Clark et al. 1996), I_{Kr} and I_{Ks} (Lo and Numann 1998). AC activation (subsequent to β-adrenoceptor stimulation) may cause an alteration in the contribution of the I_K components, as Sanguinetti, Jurkiewicz et al (1991) found I_{Ks} to be doubled, without effecting I_{Kr}, although Heath and Terrar (1996) and this study identified AC activation to increase I_{Kr} and I_{Ks}.

The ionic currents of the sino-atrial node are regulated by various mechanisms, but cAMP and cAMP-dependent phosphorylation are amongst the most influential. The cellular level of cAMP is the net product of AC production and PDE hydrolysis, unlike ventricular myocytes, sino-atrial cells are thought to have elevated basal cAMP levels. The aim of this chapter is to describe the role of cAMP produced by AC activity in the sino-atrial node.

Results

AC activation

Forskolin is a diterpene derivative of the India plant *Coleus forskolin*. Forskolin has been found to directly bind to the intracellular loops of AC (Seamon and Daly 1981; Seamon, Padgett et al. 1981) and promote a conformational change associated with an increased turnover rate of this enzyme; hence the cellular concentration of the AC product (cAMP) is increased. Spontaneously active sino-atrial node cells were investigated (n=5), with the following action potential parameters; overshoot 11 ± 3 mV, most diastolic potential -53 ± 9 mV, action potential amplitude 64 ± 10 mV, beating rate 165 ± 10 bpm, APD_{50} 66 ± 5 ms and APD_{90} 117 ± 7 ms (n=5). Forskolin (10 μM) increased the beating rate of these sino-atrial node cells by 165 ± 5 % to 273 ± 11 bpm ($P<0.001$) after 5 minutes. In addition to this increase in beating rate in the presence of forskolin, an abbreviation in the APD_{90} to 65 ± 5 % of control was observed; APD_{90} reduced from 117 ± 7 to 75 ± 6 ms (n=5, $P<0.05$). There was also an increase in the action potential overshoot upon exposure of these sino-atrial node cells to forskolin; the overshoot was increased from 11 ± 3 to 16 ± 0 mV (n=5, $P<0.01$).

I_K has been shown to activate time-dependently, with I_{Kr} activating initially and I_{Ks} subsequently as the depolarisation duration is prolonged. I_K activated with a 40 ms depolarisation was 20 ± 5 % of the control max current of 112 ± 20 pA recorded after 700 ms depolarisation (n=6). Forskolin (10 μM) increased the amplitude of I_K activated with any duration depolarisation (except the very brief 10 ms depolarisation), increasing the secondary phase of I_K time-dependent activation to a greater degree than that activated with briefer depolarisations (figure 6.1a); forskolin increased I_K activated with a 40 ms depolarisation to 28 ± 6 % (a 140 % increase compared to control) and 191 ± 20 % (220 ± 49 pA) with a 700 ms depolarisation (n=6, $P<0.05$). The voltage-dependent activation was studied, using tail current amplitude upon repolarisation to quantify I_K activation. A sigmoidal voltage-dependent activation of I_K was observed, demonstrating a $V_{1/2}$ of 14 ± 5 mV, an activation slope of 20 ± 7 mV and a maximal current (at +40 mV depolarisation) of 133 ± 27 pA (n=6). Upon exposure of these sino-atrial node cells to forskolin (10 μM), the amplitude of I_K was increased (figure 6.1b), by 203 ± 26 % to 283 ± 54 pA (n=6, $P<0.05$). In addition, the voltage-dependent activation of I_K was altered in the forskolin treated sino-atrial node cells which showed a $V_{1/2}$ of 4 ± 7 mV and an activation slope of 16 ± 8 mV, the former of which is significantly different to control data (n=6, $P<0.05$). The decay of the I_K tail current activated by depolarisation to +40 mV was investigated at potentials ranging from –10 to –60 mV (figure 6.2). The fast time-constant of deactivation (Tau_1) generally became more rapid as the repolarisation voltage became more negative. Forskolin did not alter these characteristics. Amp_1 was found to be maximal around –40 mV, whilst Amp_2 progressively reduced with more negative repolarisation. Forskolin appeared to approximately double the amplitudes of both components at all repolarisation

voltages. When significant differences are scrutinized, rather than trends, the time-constants indicated that only a few (3 of 12) were altered by forskolin (Tau_1 at –30 mV, Tau_2 at –10 and –30 mV). However the amplitude associated with these deactivation constants were increased in amplitude (figure 6.2, n=6, $P<0.05$) by forskolin (10 μM), especially upon more negative repolarisation.

The amplitude of the L-type calcium current was also found to be greatly augmented by forskolin (10 μM), with the current at 0 mV showing an increase from –143 ± 57 to –409 ± 90 pA (figure 6.3, n=5, $P<0.05$). The effects of forskolin on the amplitude of I_{CaL} were significant over the voltage range from –20 to +30 mV (n=5, $P<0.05$). The voltage at which maximal I_{CaL} was activated each cell varied in control; 1 at –10 mV, 3 at 0 mV and 1 at +10 mV. In the presence of forskolin (10 μM), a similar variation between the voltages that activated max I_{CaL} were found, but these were at more negative potentials; 1 at –20 mV, 3 at –10 mV and the remaining cell at 0 mV. Forskolin directly activates AC and consequently increase the production of cAMP, to which I_f is sensitive. Therefore, the effects of forskolin upon the voltage dependent activation of I_f were investigated. The voltage dependent activation of I_f was found to have a $V_{1/2}$ of –96 ± 3 mV and a slope factor of 10 ± 3 mV (n=5). Upon exposure to forskolin (10 μM) the former (but not the latter) were altered to –90 ± 1.3 mV (n=5, $P<0.05$) and 11 ± 1.9 mV respectively. The observations therefore show a 6 mV shift in the voltage dependent activation of I_f, by (10 μM) forskolin.

AC inhibition

10 μM MDL-12,330A (henceforth known as MDL) has been used to inhibit the activity of AC, however the converse action of forskolin (Ferretti, Sonetti et al.

1996). Rapidly switching of solutions to one in which MDL has been added caused spontaneous beating sino-atrial node cells to slow their beating rates (figure 6.4a). The sino-atrial node cells investigated (n=4) had the following action potential parameters; overshoot 18 ± 6 mV, most diastolic potential -61 ± 4 mV, action potential amplitude 80 ± 10 mV, beating rate 167 ± 12 bpm, APD_{50} 58 ± 5 ms and APD_{90} 96 ± 9 ms (n=4). The action potential amplitude of these cells then tended to reduce in the presence of 10 μM MDL (all 5), and in 4 of 5 cells low voltage (<30 mV in amplitude) rapid oscillations developed, with an increased rate of beating (n=5, $P<0.05$) as the amplitude diminished. These voltage oscillations lack the rapid upstroke and repolarisation observed in normal sino-atrial node action potentials (figure 6.4b). In a further 3 cells, the sino-atrial node cells became quiescent at –20 ± 22 mV.

An alternative AC inhibitor was also studied; SQ 22536 is thought to work similarly to MDL, possibly by physically blocking the active site of AC. An IC_{50} of 200 μM (Babenko and Vassort 1997) was found for SQ 22536 inhibition of parathyroid hormone activation of AC; this study used SQ 22536 at 250 μM. Spontaneously beating isolated sino-atrial node cells were investigated (n=2), with the following action potential parameters in control; overshoot 10 ± 1 mV, most diastolic potential -61 ± 2 mV, action potential amplitude 72 ± 1 mV, beating rate 153 ± 12 bpm, APD_{50} 51 ± 3 ms and APD_{90} 94 ± 6 ms (n=4). Exposure of spontaneously beating sino-atrial node cells to 250 μM SQ gradually reduced both amplitude and frequency of action potential generation (figure 6.4c, n=2). After 60 seconds the rate of action potential generation had reduced from 162 ± 23 to 146 ± 23 bpm (n=2, $P<0.05$), this trend continued over the next few minutes until the cell either stopped

beating (1 of 2) or developed low voltage oscillations (see trace), which occasionally activated action potentials.

Under voltage clamp conditions the effects of the AC inhibitor MDL (10 μM) upon the I_K components were studied. MDL reduced the amplitude of the I_K tail current at all depolarisation durations in excess of 10 ms (n=7, P<0.05); at 40 ms the I_K current was reduced from 113 ± 21 to 22 ± 7 pA (figure 6.5a, n=7, P<0.05). The current activated with a 700 ms depolarisation was reduced from 458 ± 97 to 359 ± 80 pA (76 ± 5 % of control, n=7, P<0.05). MDL nearly totally blocked I_K activated with rapid depolarisation (20 out of 25 % at 40 ms), a similar I_K inhibition continued as depolarisation was prolonged, with MDL reducing a 700 ms depolarisation by 24 %. The voltage–dependent activation of I_K was then investigated and under control conditions the current-voltage relationship was found to have a $V_{1/2}$ of 6 ± 3 mV and an activation slope of 22 ± 6 mV (n=7). The current activated by a +40 mV depolarisation was 537 ± 82 pA (n=7). After MDL, the amplitude of the I_K tail current was reduced at all voltages with the current at +40 mV reduced to 75 ± 4 % of the control value of 400 ± 78 pA (n=7, P<0.05). There appear to be no alterations in the voltage dependent activation (figure 6.5b) since the $V_{1/2}$ of I_K voltage dependent activation was found to be 8 ± 5 mV and the slope was 17 ± 6 mV (n=7, P>0.05) in the presence of MDL.

The deactivation of the I_K tail current has been investigated in the presence of MDL and an effect upon the brief time-constant and amplitude of the current associated with the longer time-constant have been identified (figure 6.6). The I_K deactivation in 7 cells were fitted with a bi-exponential curve with of Tau_1 of 117 ±

23 ms (Amp_1, 188 ± 54 pA) and Tau_2 of 493 ± 90 ms (Amp_2, 370 ± 54 pA). Upon exposure to 10 μM MDL the quick time-constant was prolonged to 280 ± 24 ms (n=7, $P<0.05$) and the amplitude of the second time-constant was reduced to 291 ± 51 pA (n=7, $P<0.05$).

The L-type calcium current was also studied and was found to be greatly reduced by 10 μM MDL at all voltages between –30 and +40 mV (n=5, $P<0.05$). There were a range of voltages (-20 to 0 mV) which activated maximal inward current in these sino-atrial node cells in control, but upon addition of MDL, very little in the way of inward current was found (figure 6.7a). I_{CaL} activated upon depolarisation to 0 mV was reduced from –570 ± 128 to –100 ± 101 pA in the presence of MDL (n=5, $P<0.05$). I_{CaL} in the presence of MDL was not (on average) more than 10 % of the current amplitude identified in control conditions. At voltages positive to 0 mV the current was actually found to be outward, indicating an absence of I_{CaL}.

MDL is thought to have the converse action upon AC to forskolin, inhibition rather than activation. MDL should therefore reduce the cytosolic cAMP levels, assuming there is some basal AC turnover (producing cAMP) at rest in the sino-atrial node. I_f is cAMP sensitive (DiFrancesco and Mangoni 1994; Renaudon, Bescond et al. 1998), and so the effects of MDL upon the amplitude and voltage dependent activation of I_f were investigated. 10 μM MDL caused a time-dependent shift in the $V_{1/2}$ of I_f voltage-dependent activation of I_f to more hyperpolarised potentials (figure 6.7b); in control the $V_{1/2}$ and slope factor were -97 ± 2 and 14 ± 1 mV, after 5 minutes exposure to 10 μM MDL these values were –106 ± 2 (n=6, $P<0.05$) and 11 ± 0 mV and with a further 5 minute exposure to MDL these values were -111 ± 1 (n=6,

P<0.05) and 10 ± 1 mV. The initial activation of I_f occurs at around –60 mV in untreated sino-atrial node cells, while in cells treated with MDL for 10 minutes this initial voltage-dependent activation does not occur until approximately –80 mV (figure 6.7c). Using the reversal potential of –19 mV (Description of I_K and other ionic currents, page 122), an I_f conductance-voltage relationship can be described. The conductance-voltage curve has a very similar form to current-voltage, however at very negative potentials the conductance can been seen not to increase as much as the current. The conductance-voltage curve illustrates that control and 10 minutes MDL treated conductance are similar at very negative potentials and so the maximal conductance is not altered (n=6, P>0.05). MDL (10 μM) shifts the voltage dependent activation of I_f to more hyperpolarised potentials, without having an effect upon the maximal current/conductance.

cAMP analogues

An alternative technique to simulate the modulation of AC is to introduce an exogenous source of the product of this enzyme, ie cAMP. Cell permeant analogues of cAMP can be used, including an AM ester of cAMP (similar to BAPTA-AM), that cannot be degraded by cellular phosphodiesterases. These cell permeable cAMP analogues are available commercially and include dibutyryl cAMP (db-cAMP) and 8bromo cAMP (8br-cAMP). The more potent cAMP analogue SP-cAMP (AM ester) was also used in some experiments. These agents will be differentiated, however the data are grouped when describing effects upon spontaneous action potentials and I_f. 3 spontaneously active sino-atrial node cells were studied, which had the following action potentials values; overshoot 10 ± 3 mV, most diastolic potential -62 ± 2 mV, action potential amplitude 74 ± 3 mV, beating rate 224 ± 7 bpm, APD_{50} 57 ± 14 ms

and APD_{90} 95 ± 24 ms (n=3). Upon exposure of these cells to the AM ester of the cAMP analogue (one cell with 500 μM 8br-cAMP and 2 using 100 μM SP-cAMP) no alteration of action potentials was identified (n=3).

Both 500 μM 8br-cAMP and 1 mM db-cAMP were found to increase IK activated with both brief (40 ms) and prolonged (700 ms) depolarization (figure 6.8); 13 ± 1 % and 25 ± 3 % of max I_K were activated by 40 ms depolarisation and this was increased to 15 ± 1 % and 30 ± 4 % in the presence of 8br-cAMP (n=6, $P<0.05$) and db-cAMP (n=4, $P<0.05$). 8br-cAMP did not increase the amplitude of I_K activated after a 50 ms depolarisation (n=6). After prolonged depolarisation (700 ms) the current was increased by 139 ± 9 % (351 ± 89 pA to 481 ± 116 pA) and 138 ± 9 % (656 ± 131 pA to 915 ± 202 pA) in the presence of 8br-cAMP (n=6, $P<0.05$) and db-cAMP (n=4, $P<0.05$). Additions of db-cAMP increased the tail current amplitude after depolarisation as brief as 20 ms (n=4, $P<0.05$), whereas 8br-cAMP had a similar effect with depolarisation greater than 40 ms (n=6, $P<0.05$). The effect of these cAMP analogues upon maximal I_K, were not significantly different; 8br-cAMP increased max current by 139 ± 9 %, db-cAMP (n=6) increased the value by 138 ± 9 % (n=4, $P>0.05$, unpaired t-test). The modification of the voltage dependent activation of I_K by cell permeant cAMP analogues was also studied, in this manner both 8br and db cAMP (at 500 μM and 1 mM) were found to increase I_K. The increase of I_K by cAMP analogues was progressive over the voltage range (-30 to +40 mV), however a significant increase was observed at voltages more positive than –20 mV by 8br-cAMP (n=5, $P<0.05$) and +10 mV by db-cAMP (figure 6.9, n=3, $P<0.05$). The level of 8br-cAMP and db-cAMP augmentation upon maximal current (observed upon depolarisation to +40 mV) was 133 ± 10 % (401 ± 135 pA to 505 ± 149 pA) and

152 ± 2 % (793 ± 93 pA to 1209 ± 153 pA); these effects of cAMP analogues are not statistically different (unpaired t-test). The voltage dependent activation of I_K, and the modification of this by cAMP analogues, has also been studied. 500 μM 8br-cAMP was found to shift the $V_{1/2}$ from 2 ± 2 to 7 ± 2 mV (n=5, $P<0.05$). Unlike the finding with 8br-cAMP, the AM ester of db-cAMP caused no shift in the $V_{1/2}$ of voltage dependent activation of I_K; $V_{1/2}$ values were 8 ± 2 and 9 ± 4 mV (n=3, $P>0.05$). The deactivation of the I_K tail current was studied after the addition of 8br-cAMP and no alteration in the time-constants or associated amplitudes from control were described (figure 6.9c, n=4, $P>0.05$); control Tau_1 was 249 ± 24 ms (Amp_1, 188 ± 78 pA) and Tau_2 was 1566 ± 272 ms (Amp_2, 73 ± 32 pA).

When regarding the voltage dependent activation of I_{CaL}, a maximal current was described at 0 mV, with voltage dependency having a roughly bell shaped form around these values (figure 6.10); currents at 0 mV were –148 ± 94 (n=3) and -1907 ± 67 pA (n=4). Upon addition of 500 μM 8br-cAMP there was no alteration in the voltage dependent activation of I_{CaL} in the voltage range tested (n=3, $P>0.05$) and the maximal current at 0 mV was –119 ± 70 (n=3). The effect of 1 mM db-cAMP upon I_{CaL} were however slightly different (figure 6.10b), as db-cAMP caused an increase in I_{CaL} in the voltage range –20 to +10 mV (n=4, $P<0.05$). This augmentation included the maximal current activated at 0 mV which was increased to –2262 ± 125 pA, 117 ± 6 % on control (n=4, $P<0.05$). The cAMP analogue db-cAMP, but not 8br-cAMP, caused a partial increase in I_{CaL} amplitude.

The effects of cAMP analogues upon I_f were also investigated, as this channel is directly modulated by intracellular cAMP (Renaudon, Bescond et al. 1998). The

data from the AM esters of cAMP analogues were grouped in this data set and include 500 μM 8br-cAMP (2 cells), 1 mM db-cAMP (2 cells) and 100 μM SP-cAMP (1 cell). These cAMP analogues had similar effects upon I_f, each causing a slight depolarised shift in the $V_{1/2}$, without having an effect upon the activation slope (figure 6.11); on average the $V_{1/2}$ was shifted from –97 ± 2 to –92 ± 2 mV (n=5, $P<0.05$). The slope values were 13 ± 1 and 12 ± 2 mV before and after the introduction of cAMP analogues (n=5, $P>0.05$).

Discussion

During autonomic regulation of the heart, AC is activated or inhibited according to the sympathetic or parasympathetic nature of stimulation. This effect is mediated by G-protein subunit (G_s and G_i) interaction with AC. Modulation of AC activity is the major mechanism of autonomic control of heart rate (Habuchi, Yamamoto et al. 1996; Babenko and Vassort 1997; Wang and Dhalla 2000), although there are direct G-protein to channel pathways (I_K and I_{CaL}) and acetylcholine acts directly upon I_{KAch} (Renaudon, Bois et al. 1997). Such modulation of AC function by the autonomic nervous system indicates that cAMP has powerful effects upon the ionic currents that determine pacemaking.

AC and PDE

Regarding cellular cAMP levels, the actions of PDE's must be considered in addition to AC activity. PDE's breakdown the product of AC activity, so these rates of generation and degradation define cAMP concentration. AC is modified by

autonomic stimuli, however PDE activity is also modified by autonomic stimulation (Herring, Rigg et al. 2001). A balance is struck between production of cAMP by AC and degradation by PDE's, whilst this balance is stable, cAMP levels will be constant. Upon autonomic intervention, AC activity is altered, so the cAMP concentration alters until a new balanced is developed.

There are various ways to increase cAMP concentration, such as direct activation of AC (forskolin), inhibition of PDE's (i.e. with IBMX) and introduction of non-hydrolysable cAMP analogues (8br-cAMP). Increasing cAMP mimics the major mechanism of β-adrenoceptor modification of ionic currents, and therefore the beating rate of the sino-atrial node cells (Calaghan, White et al. 1998). Actions to lower cAMP, do in part simulate parasympathetic stimulation, however other cellular pathways are additionally used. Forskolin elevates cellular cAMP and through this mechanism affects various ionic currents in a similar manner to β-adrenergic agonists; this modulation by forskolin increased the beating rate of cells isolated from the sino-atrial node (165 %). Forskolin also had other β-adrenergic agonists-like effects, as treatment abbreviated the action potential and increased the action potential overshoot; these changes in action potential characteristics have been described in the presence of isoprenaline (see chapter 7.23). When the ionic currents that underlie the action potential were investigated, forskolin was found to increase I_K without effecting deactivation kinetics, with a more substantial augmentation of I_{Ks} as described by (Heath and Terrar 1996). Enlargement of I_{Ks} by forskolin has previously been described (Heath and Terrar 1996). I_{Kr}, activated with brief depolarisations, was increased to approximately 140 % of control amplitude. Voltage dependent activation of the ERG current ($V_{1/2}$) has been found to be shifted 14 mV by forskolin (Kiehn,

Karle et al. 1998) when using perforated patch. (Heath and Terrar 2000) again using perforated patch/sharp electrodes described forskolin increased I_{Kr}. Most previous reports have found forskolin (or sympathetic) activation of I_{Kr} (Sanguinetti, Jurkiewicz et al. 1991; Heath and Terrar 1996; Cheng, Kamiya et al. 1999), and this new finding appears to be related to development of voltage clamp methodology. Kiehn, Karle et al (1998), Heath and Terrar (2000) and this study all used perforated patch recordings (Heath additionally used sharp electrodes), rather than ruptured patch, to investigate I_{Kr} modulation by AC activation. Perforated patch (amphotericin in this study) reduces the interference with the cytosol. I_{Kr} appears to be very sensitive to dialysis of intracellular components and forskolin mediated augmentation has previously been lost using the more rudimentary ruptured patch configuration.

Forskolin was also found to cause a 10 mV shift in the $V_{1/2}$ of I_K, which is similar to the 14 mV shift that (Kiehn, Karle et al. 1998) described upon forskolin treatment of human ERG expressed in Xenopus oocytes. The voltage dependent activation of I_f was shifted by forskolin, by 6 mV in the depolarised direction; cAMP directly interacts with I_f and has been previously found to cause such a shift (DiFrancesco and Mangoni 1994; Renaudon, Bescond et al. 1998). There was no augmentation of maximal I_f conductance, only the voltage dependent activation was effected. This effect of cAMP mediating shifts in I_f $V_{1/2}$ have been identified in isolated rabbit sino-atrial node cells, HCN expressed in cell lines, with both macroscopic and single channel recordings (Anumonwo, Delmar et al. 1994; DiFrancesco and Mangoni 1994; Accili, Redaelli et al. 1997; DiFrancesco 1999; Altomare, Terragni et al. 2003). Forskolin was also found to greatly increase I_{CaL} amplitude, activating three times the max I_{CaL} at 0 mV. This effect of β-adrenergic

activation causing a large increase in I_{CaL} has been reported in all cardiac myocytes and may be a mechanism of positive inotropism. Larger trigger calcium activates a greater SR release of calcium, rather than a direct effect of the I_{CaL} augmentation, as trigger calcium is relatively small. The effect of greater I_{CaL} and more SR released calcium would result in higher cytosolic calcium. Calcium is involved in numerous intracellular pathways and can activate various regulation pathways including calmodulin and protein kinase C. The net effect of forskolin treatment is an increase in inward currents during diastolic depolarisation, as the rate of spontaneous action potential generation was elevated. Therefore the increase of I_K must be exceeded by the augmentation of the inward currents, such as I_f and I_{CaL}.

An alternative mechanism to increase cellular cAMP is to artificially introduce this second messenger into the sino-atrial node cell. This can be accomplished using a cell membrane permeant cAMP analogue that is not subject to degradation from PDE's, thus cellular cAMP levels can be manipulated. A number of different types of cAMP analogue have been used, including 8br-cAMP, db-cAMP and SP-cAMP. Elevation of cAMP using these analogues increased various action potential parameters and ionic currents, however the effect of these analogues was not as large as that of forskolin or β-adrenoceptor activation. In fact no increase in beating rate was identified after the addition of cAMP analogues to a small number of sino-atrial node cells. This could be due to limited membrane permeability of the cAMP analogue, or the active expulsion of these analogues from the cytosol. However the ionic currents involved in pacemaking are modulated; I_{Kr} and I_{Ks} were found to be increased, as was inward I_{CaL} and I_f $V_{1/2}$ was shifted by 5 mV. Both inward and outward currents were augmented by these cAMP analogues, without a significant

effect upon beating rate measured in 3 cells, indicating a similar increase in both inward and outward currents. Most autonomic regulation studies use PDE inhibition to allow easier description of cAMP modulation, however PDE inhibition may hide some complexity of cAMP levels (Cooper, Mons et al. 1995) and so this study has not. This may be the reason that introduction of cAMP analogues did not have the expected large effect as previously observed (DiFrancesco 1991).

In summary, activation of AC and hence the production of cAMP increases the beating rate of sino-atrial node cells (Wang and Dhalla 2000). The increase in spontaneous activity is the result of an increase in the net inward current during diastolic depolarisation, however both depolarising (I_{CaL} and I_f) and repolarising currents (I_K) are augmented.

AC inhibiting agents such as MDL and SQ 22536 diminish the turnover of this enzyme and hence reduce the production of cAMP, as there is constant PDE activity. If PDE activity is inhibited, cAMP levels rise (Ahn, Eardley et al. 1986). The action of MDL and SQ 22536 are therefore opposed to forskolin, reducing the spontaneous rate of sino-atrial node action potential generation and in some cells causing quiescence. The action potential amplitude was also reduced by MDL and SQ 22536; these actions are directly opposed to the effect of forskolin (see above).

I_K was described using various duration depolarisations and MDL was found to reduce I_K activated with both brief and prolonged depolarisation. I_{Kr} is activated with both brief and prolonged depolarisation, whereas I_{Ks} is only activated with the longer depolarisations. MDL greatly reduced I_{Kr}, whilst the I_K activated with

prolonged depolarisation was inhibited to a level similar to the I_{Kr} reduction. There maybe no additional inhibition of I_{Ks}, indicating a possible specific action of MDL upon I_{Kr}. I_{Ks} was not isolated using E4031, but these effects of MDL primarily upon I_K activated with brief depolarisations implies no/little effect upon I_{Ks}. MDL was also found to prolong the fast time-constant of I_K deactivation. Such a large effect of MDL upon I_{Kr} could indicate a direct effect of this agent upon the channel, causing a physical block of this channel, rather than an AC mediated effect. However MDL has a large effect upon I_{CaL}, causing a substantial reduction in the amplitude of this inward current, without changing voltage-dependent activation. The reduction of cellular cAMP levels by MDL was found to cause a hyperpolarised shift in the voltage dependent activation of I_f. This effect upon I_f was time-dependent, with the I_f $V_{1/2}$ being shifted by 9 mV after 5 minutes in MDL and an additional 5 mV after 10 minutes. The MDL mediated reduction of cAMP causes a large shift in the voltage dependent activation of I_f, without altering the slope of activation or maximal conductance. This effect is in agreement with DiFrancesco's identification of I_f activation to be determined by intracellular cAMP levels (DiFrancesco and Mangoni 1994). From the various effects upon ionic currents, MDL was identified as an AC inhibitor; hence cAMP reduction can be shown to severely reduce I_{Kr}, indicating a strong cAMP sensitive mechanism of regulation.

This is the first time that AC inhibition has been found to modulate the amplitude of the delayed rectifier potassium current. Another interesting finding is that MDL reduced the amplitude of I_{CaL} and I_{Kr} in the absence of stimulation. This could indicate that basal turnover of AC, hence cAMP levels before any stimulation, is adequate to up-regulate these ionic currents. AC inhibition could remove any

continuous augmentation (by basal AC turnover) of these currents. Whereas I_{Ks} is not greatly affected by MDL, implying I_{Ks} is not increased by the resting cAMP levels, possibly due to a lower cAMP sensitivity.

Upon AC activation, I_{Kr} is modestly increased, so the resting cAMP augmentation is not maximal and stimulation further increased I_{Kr} amplitude. Similarly I_f voltage dependent activation is shifted to more depolarised potentials by forskolin, however the shift is relatively small and could indicate basal cAMP levels to be near maximally effecting I_f activation. I_{CaL} however is subject to a large degree of amplification by forskolin and inhibition by MDL, indicating a massive range of regulation by cAMP (presumably PKA mediated). The scope of I_{CaL} magnification by forskolin was over 10 times the MDL inhibited (lowest cAMP levels) I_{CaL} amplitude. I_{Ks} was not affected by AC inhibition, possibly indicating a lack of basal cAMP effect upon this current, however forskolin caused a large (relative to I_{Kr}) increase in I_{Ks}. The rate of sino-atrial node cell beating was affected by both AC inhibition and activation; causing reduction/stopping and acceleration of beating rate respectively. Therefore AC may have been found to exhibit some continuous tone, producing cAMP that modulate various ionic currents involved in pacemaking, in both resting situations and upon stimulation. The relative augmentation of these ionic currents by cAMP causes an increase in the rate of diastolic depolarisation.

The basal levels of cAMP in the sino-atrial node are thought to be elevated, and it appears that basal cAMP up-regulates I_{Kr} almost maximally, whereas I_{Ks} does not appear to be augmented. Upon AC inhibition I_{Kr} was diminished, with no effect upon I_{Ks}, whereas AC activation primarily augments I_{Ks}.

a,

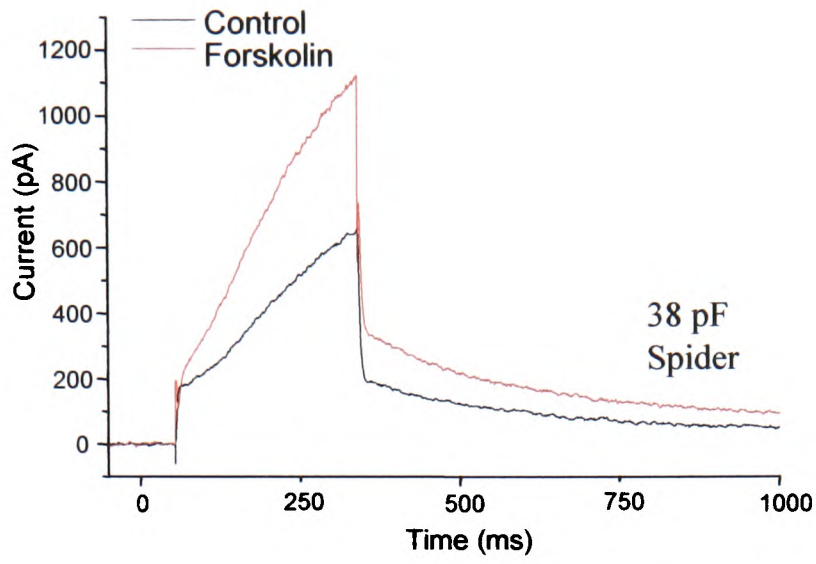

b,

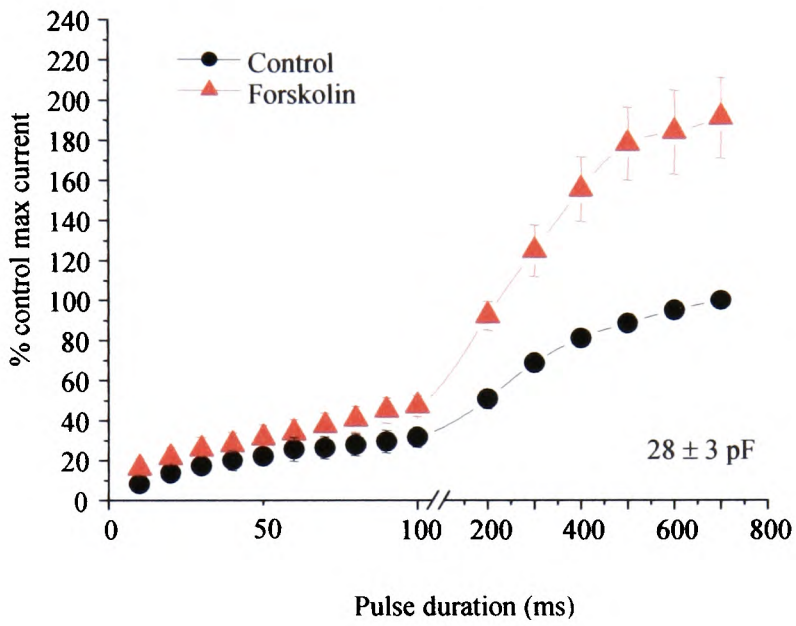

c,

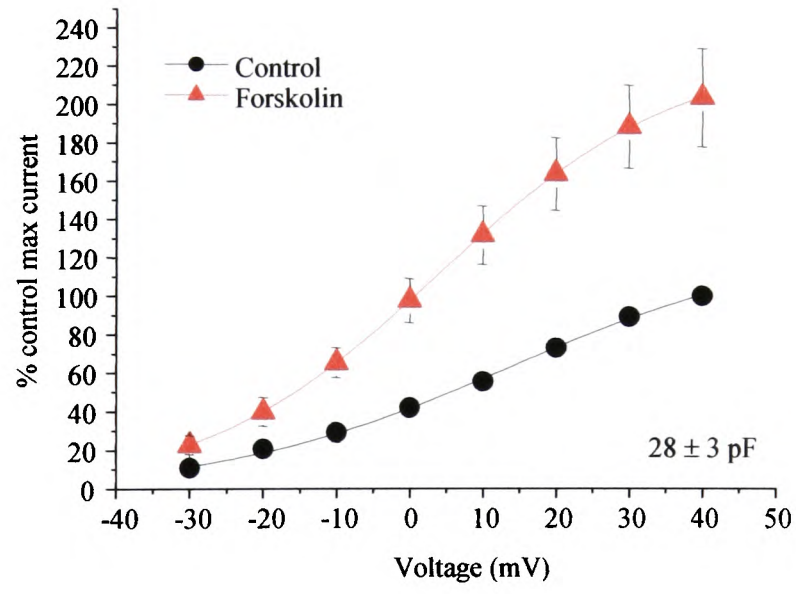

Figure 6.1 Page 262

The adenylate cyclase activator forskolin (10 μM) increased the amplitude of $I_{K(}$(a, 300 ms at 40 mV) over most of the range of both depolarisation duration (b) and voltage (c). I_K activated with both brief (>10 ms) and long depolarisation were increased in the presence of forskolin (n=6, $P<0.05$) and I_K amplitude activated with a 700 ms depolarisation was approximately doubled (b). A similar augmentation of I_K was found at most voltages, (n=6, $P<0.05$), and in addition the $V_{1/2}$ was shifted from 14 ± 5 to 4 ± 7 mV (n=6, $P<0.05$), without altering activation slope.

a,

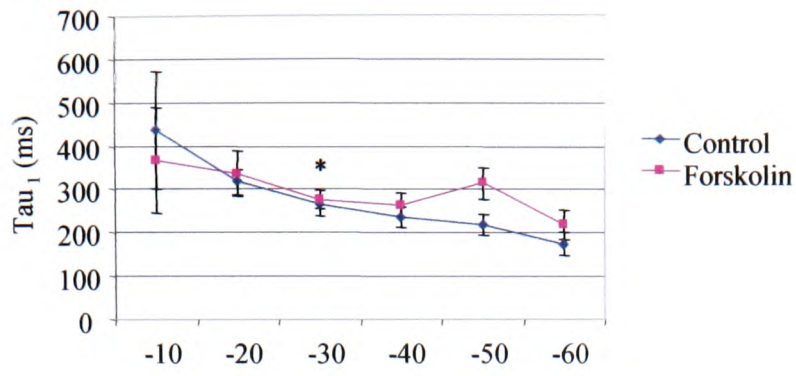

b,

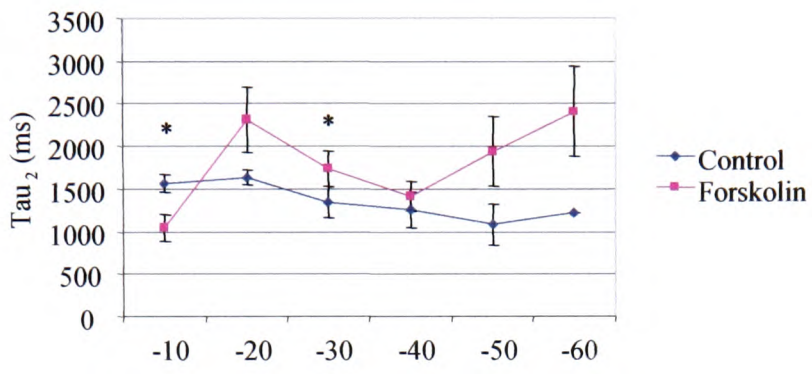

c,

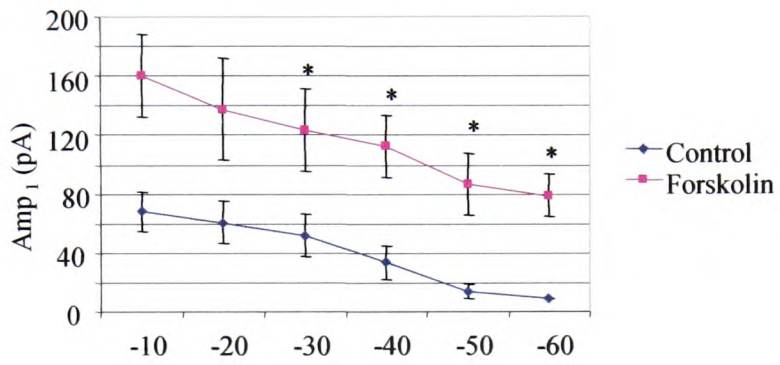

d,

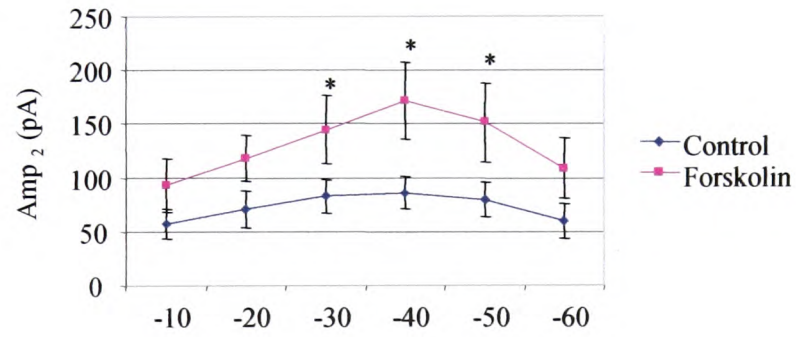

28 ± 3 pF

Figure 6.2 Page 263

The effect of forskolin (10 μM) upon Tau_1 and Tau_2 of I_K decay (a and b respectively), at various voltages and the effect upon the associated Amp_1 and Amp_2 (c and d). Forskolin did not obviously alter the rate of decay of the tail current (n=6), although there maybe a slight prolongation of the time-constants at some voltages (a and b). Forskolin tended to increase both Amp_1 and Amp_2 , being a significant effect in 7 (*) of 12 ($P<0.05$, n=6).

a,

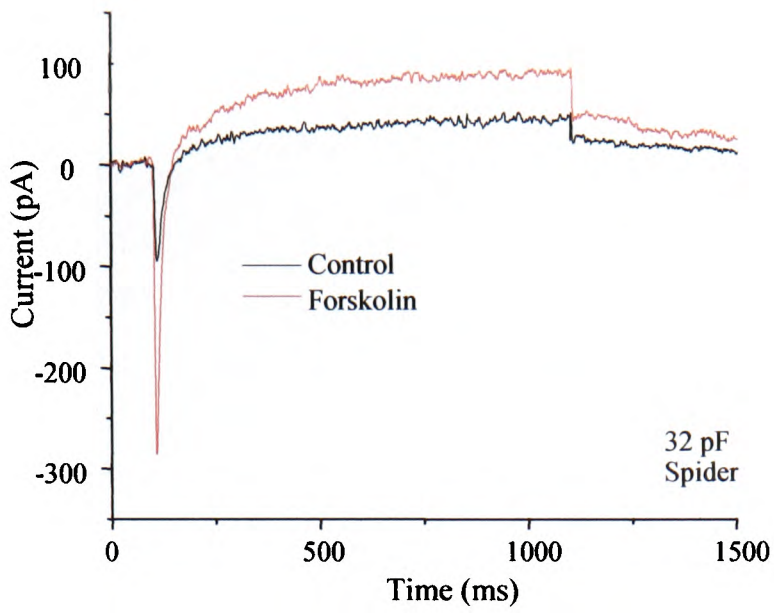

b,

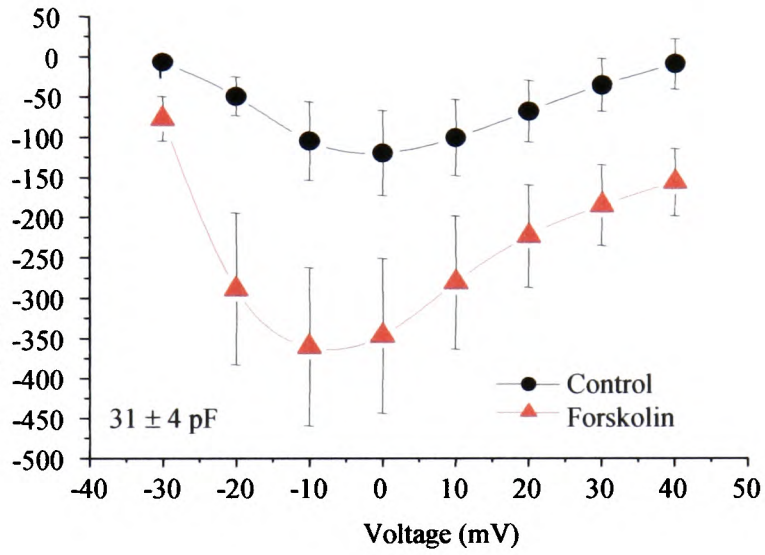

Figure 6.3 Page 264

Upon depolarisation to 0 mV (a), the instantaneous inward I_{CaL} is increased by 10 μM forskolin, as is the outward current during the rest of the depolarisation and the tail current. I_{CaL} was increased upon depolarisation between -20 and +30 mV (n=5, $P<0.05$) and shifted the maximal current activated from 0 to -10 mV.

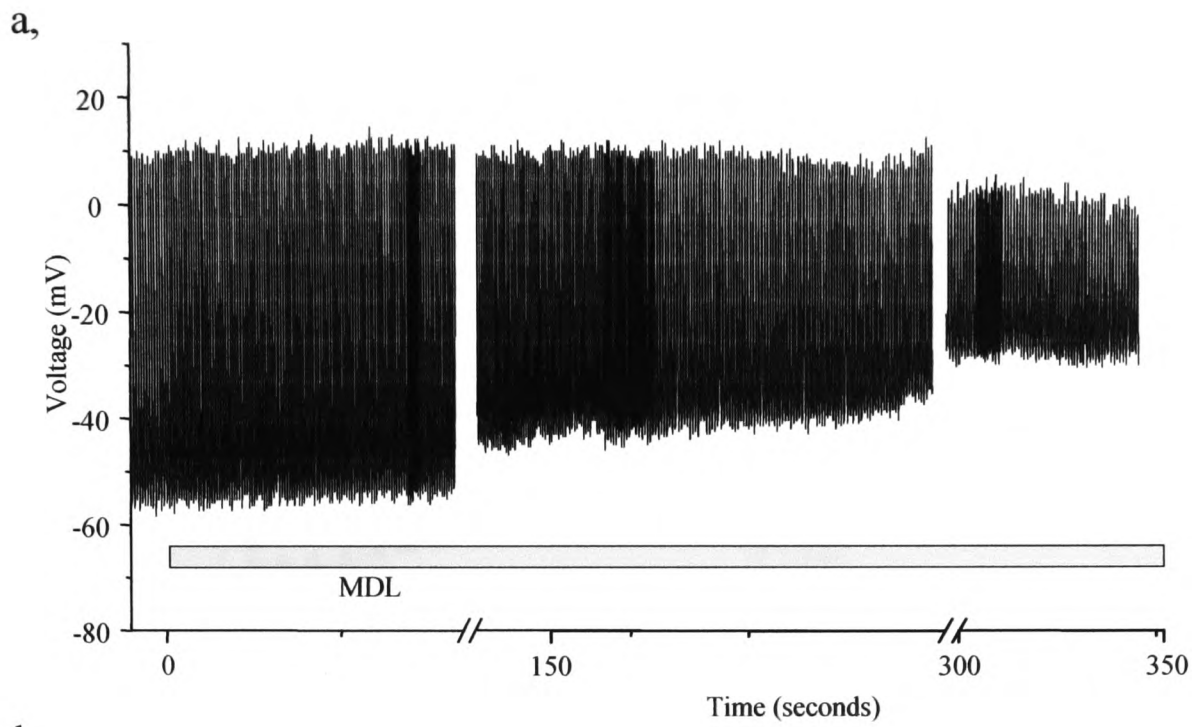

Figure 6.4 Page 265

Effect of AC inhibition upon spontaneous action potentials. MDL (10 μM) caused a gradual reduction of action potential amplitude (a), in this case over a period of 350 seconds, resulting in low voltage oscillations (b) and quiescence. A similar effect was found in 4 sino-atrial node cells, becoming quiescent in the presence of MDL, over a period of between 2 and 6 minutes. SQ 22536 (250 μM) caused a gradual reduction in the action potential amplitude of isolated sino-atrial node cells (c), and significantly reduced beating rate after 1 minute ($n=2$, $P<0.05$).

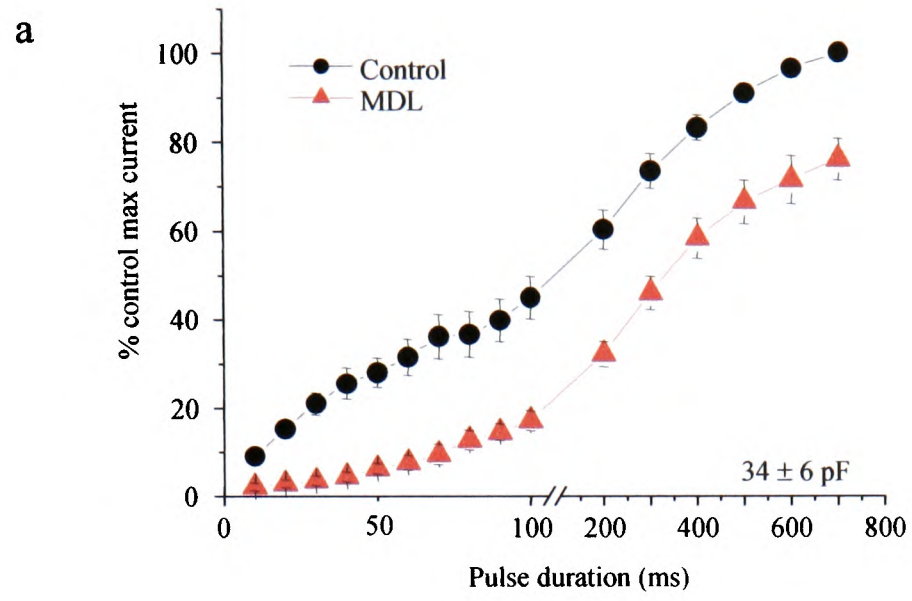

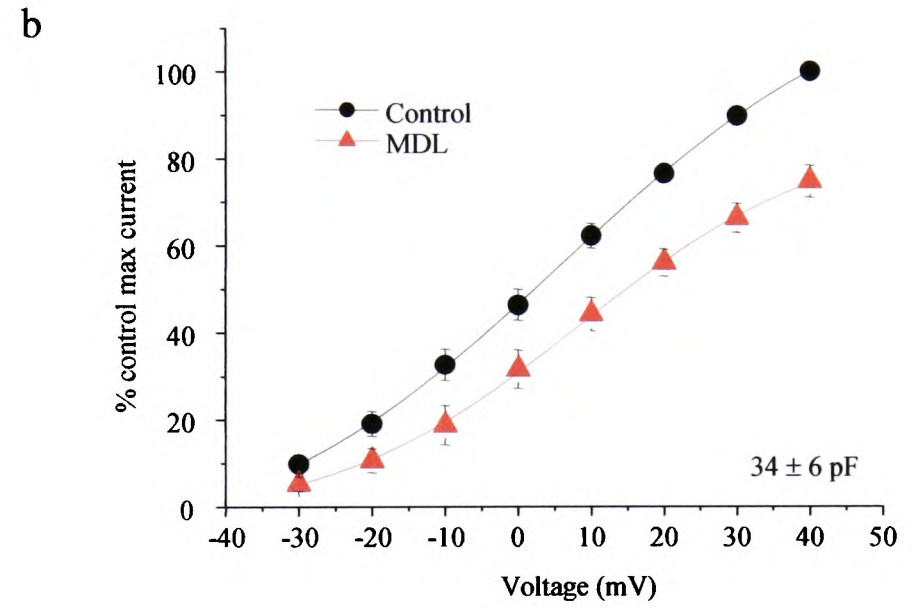

Figure 6.5 Page 266

10 μM MDL reduced the amplitude of both the time-dependent (a) and the voltage-dependent (b) activation of I_K. Both I_K activated with brief (as short of 10 ms) and prolonged depolarisation were reduced in the presence of MDL (n=7, $P<0.05$). Note the almost complete inhibition of I_K activation with depolarisations briefer than 70 ms. MDL also reduced I_K activated at voltages between -30 and +40 mV, without causing a significant alteration in either $V_{1/2}$ or activation slope (n=7).

a,

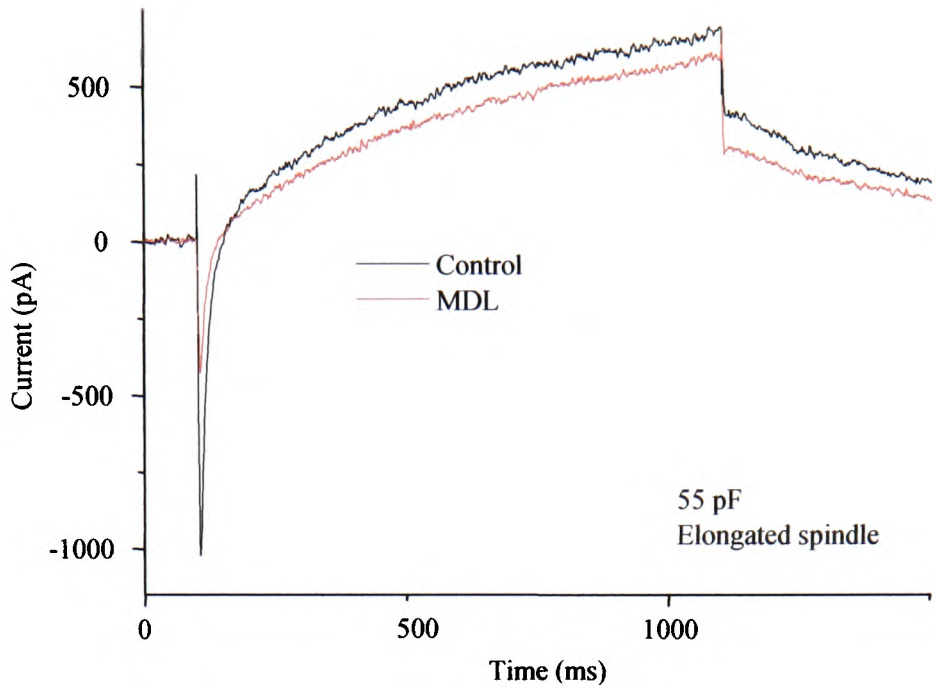

b,

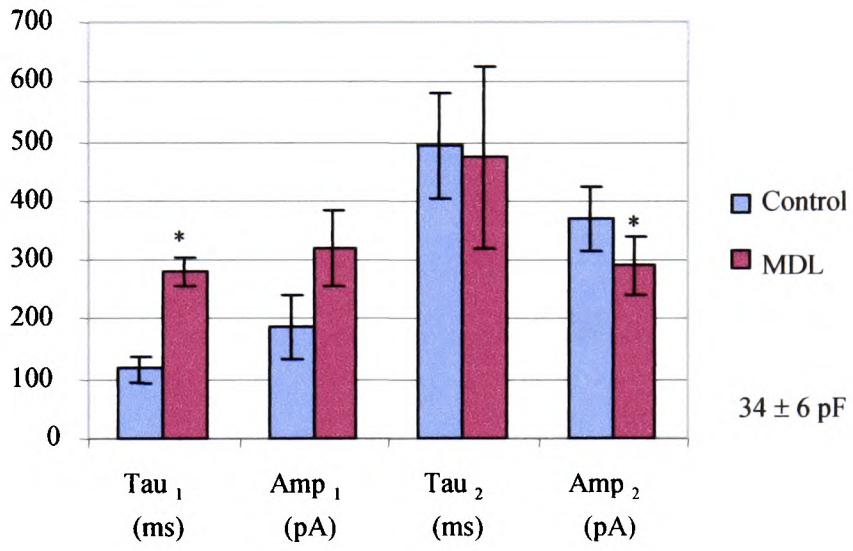

Figure 6.6 Page 267

The AC inhibitor MDL (10 μM) reduced the instantaneous inward current, outward current during the depolarisation and the tail current amplitude (a). MDL also altered the decay of the I_K tail current (b), by prolonging Tau_1 and reducing Amp_2 (n=7, P<0.05).

a,

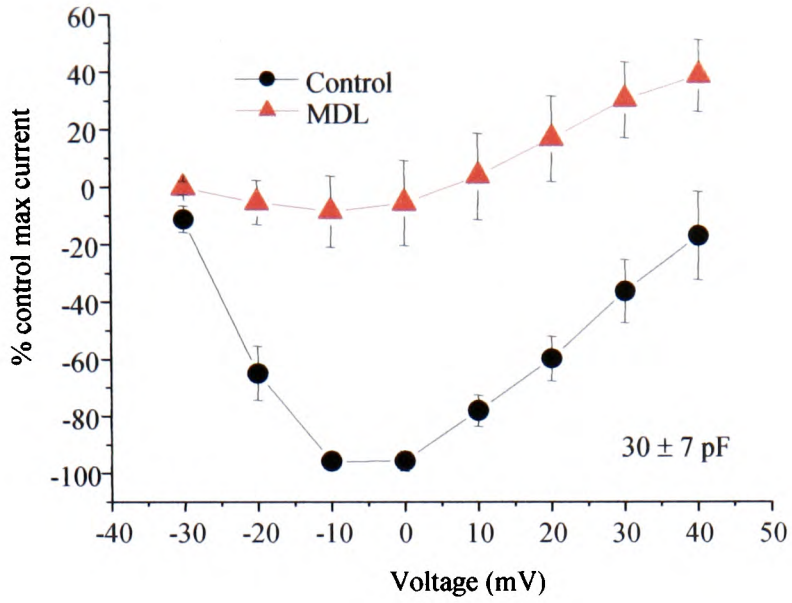

b,

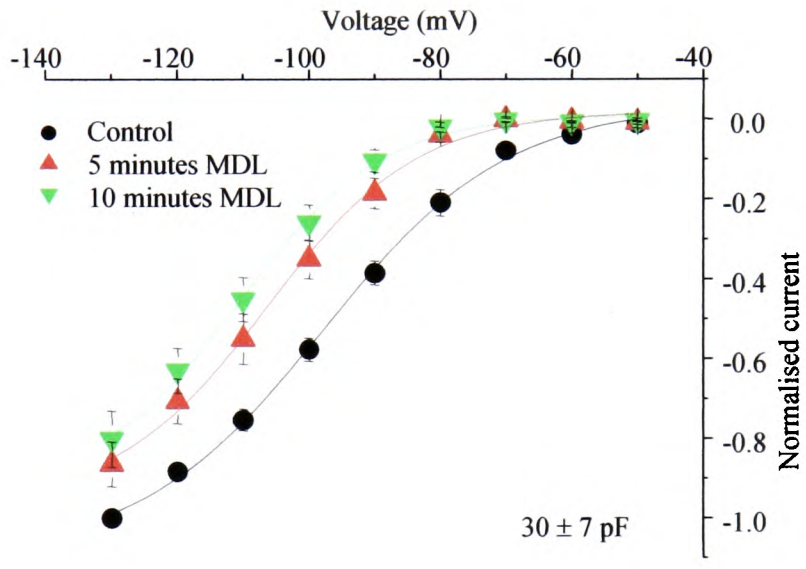

c,

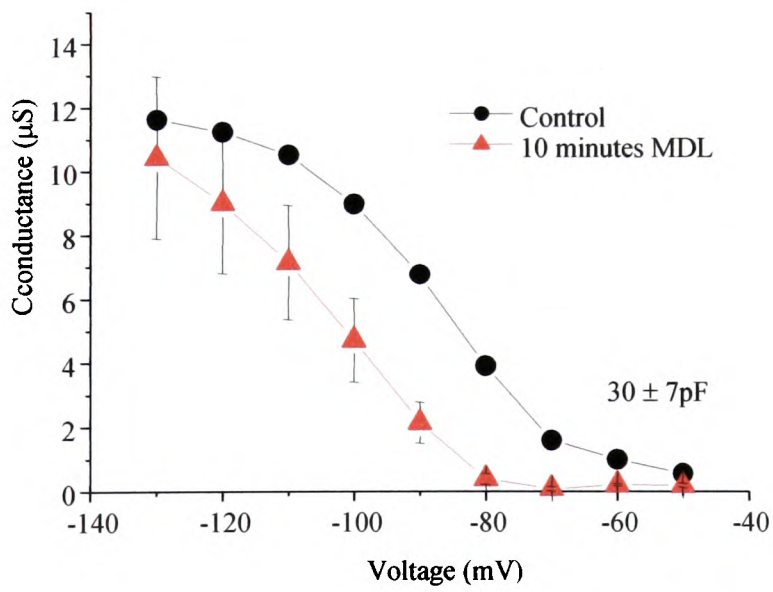

Figure 6.7 Page 268

MDL reduced I_{CaL} (a) and shifted the activation of I_f to more hyperpolarised potentials. MDL 10 µM reduced I_{CaL} activated with depolarisation ranging between -30 and +40 mV (n=5, P<0.05), without altering the voltage which activates maximal I_{CaL} (-10 mV). MDL almost totally abolished I_{CaL}, as very little inward current remains. MDL shifted the $V_{1/2}$ of I_f to more hyperpolarised potentials (n=5, P<0.05) by approximately 10 mV (b), this was found to be a time-dependent effect of MDL upon I_f (c). Activation slope was not altered.

a,

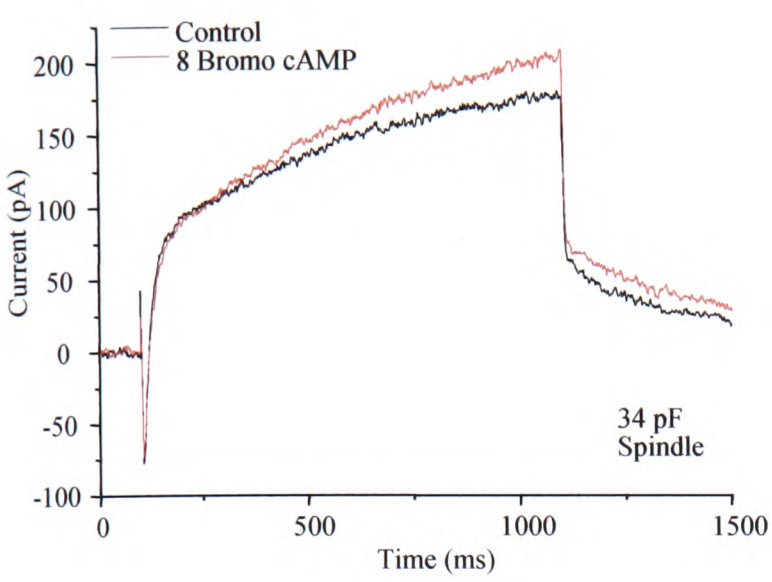

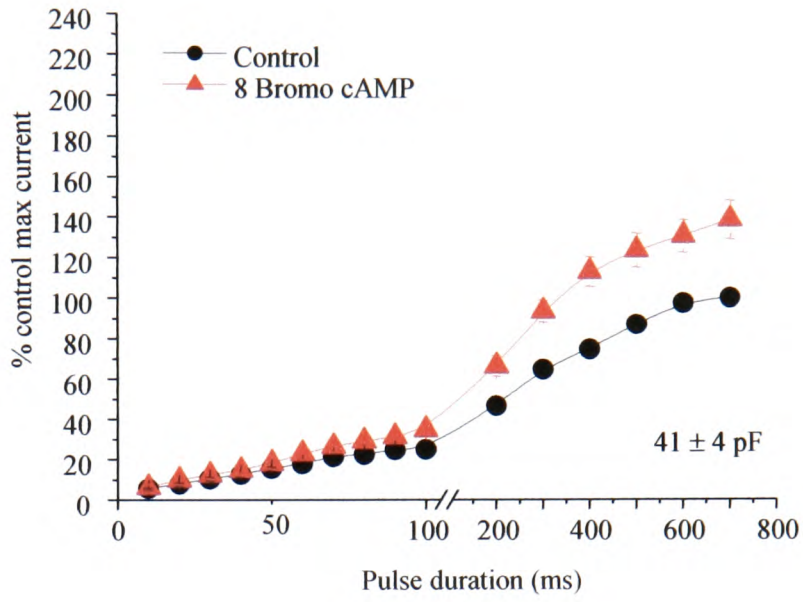

b,

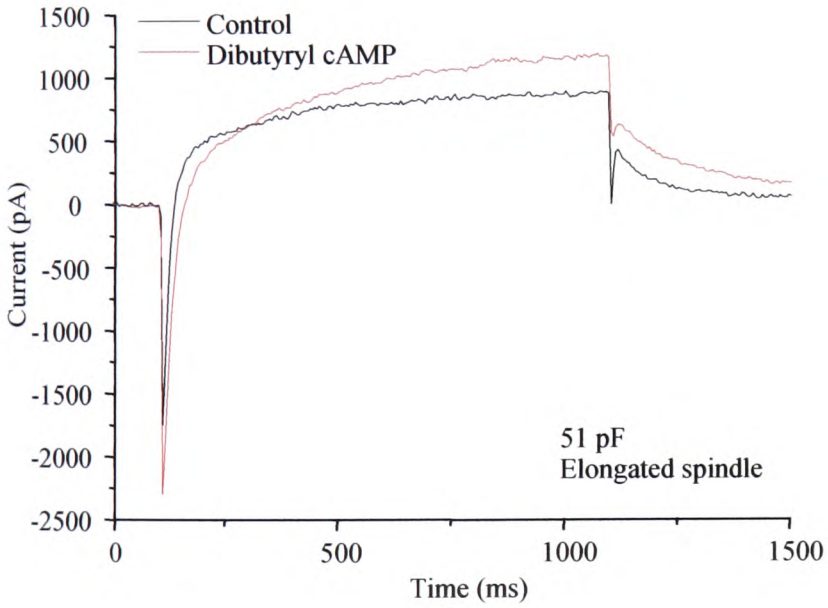

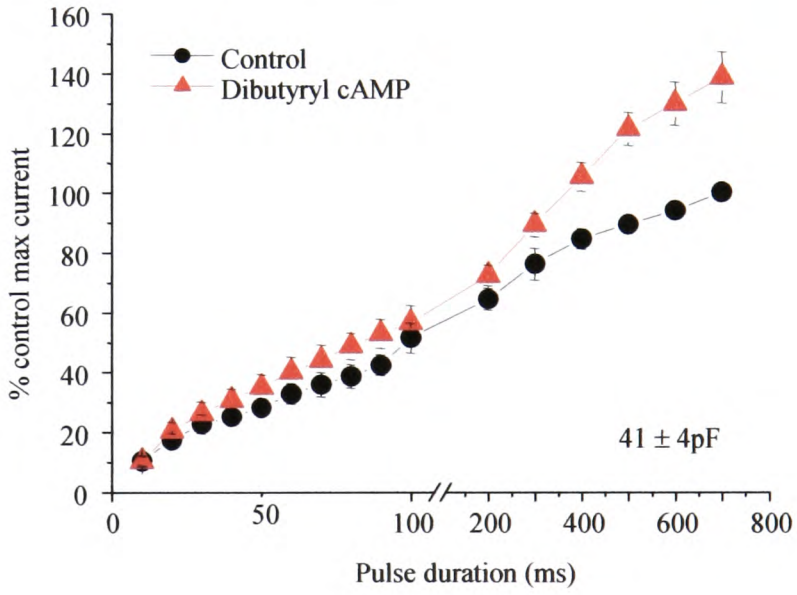

Figure 6.8 Page 269

The cell permeant cAMP analogues 8 bromo cAMP (a) and dibutyryl cAMP (b) increased the amplitude of the outward current activated upon depolarisation and the tail current amplitude (left panel). 8 bromo cAMP and dibutyryl cAMP were used at 500 μM and 1 mM. 8 bromo cAMP was found to increase the I_K amplitude (n=6, $P<0.05$) activated by depolarisations of 40 ms and longer (excluding 50 ms). Dibutyryl cAMP was similarly found to increase I_K activated with depolarisations greater than 20 ms (n=4, $P<0.05$)

a,

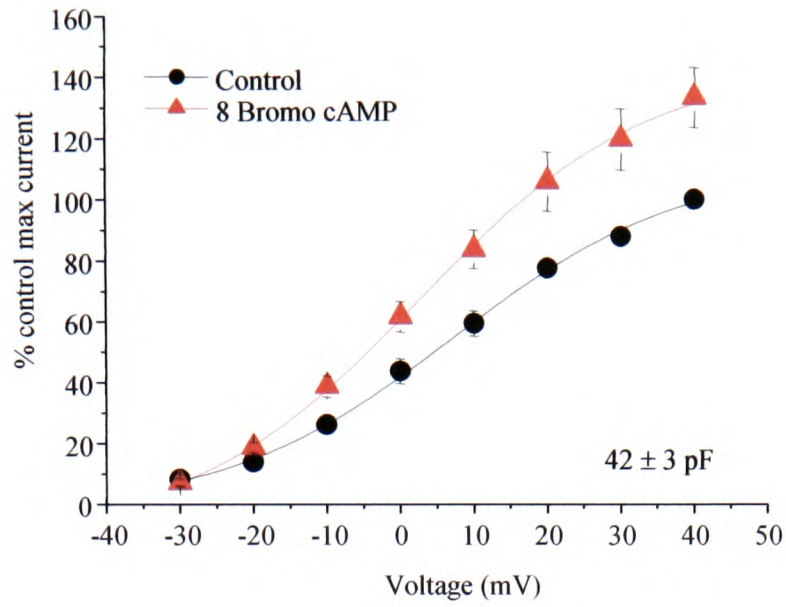

b,

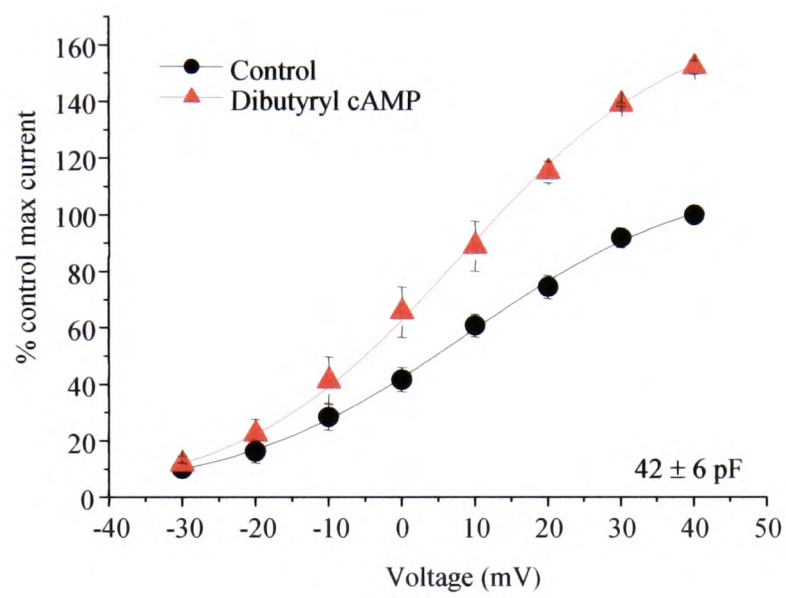

c,

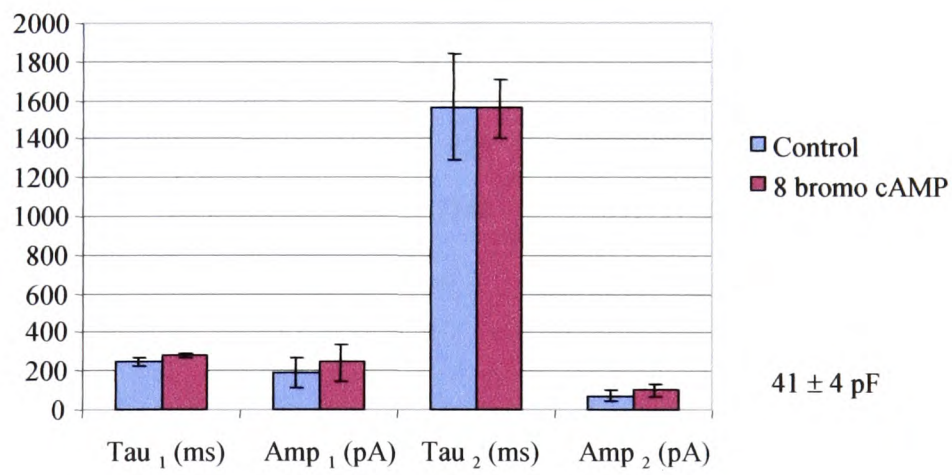

Figure 6.9 Page 270

Dibutyryl cAMP (500 μM) and 8 bromo cAMP (1 mM) increased I_K activated with depolarisation greater than –20 and +10 mV respectively (n=5 and 3, $P<0.05$). Dibutyryl cAMP caused a 5 mV shift in the $V_{1/2}$ ($P<0.05$), but the was no effect of 8 bromo cAMP upon $V_{1/2}$ and neither affect slope of activation. The I_K tail current deactivation kinetics at –40 mV are also shown (c), however 8 bromo cAMP appears to have no effect upon the time-constants or the amplitudes of decay (n=4).

a,

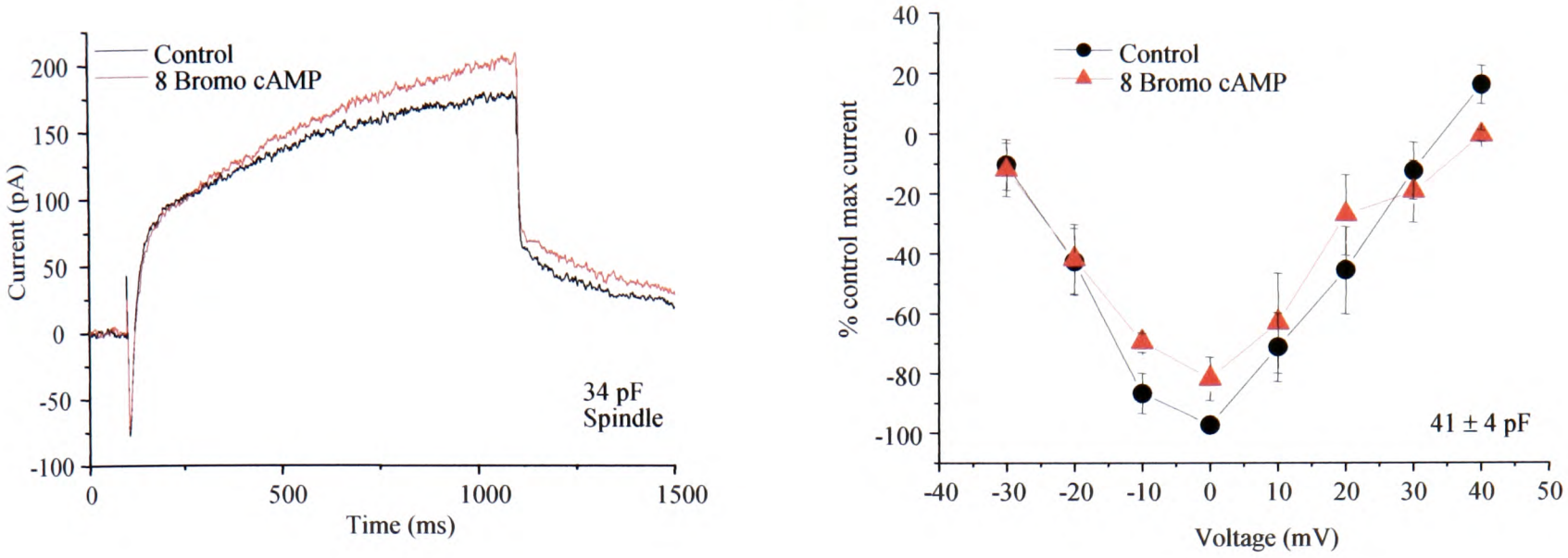

b,

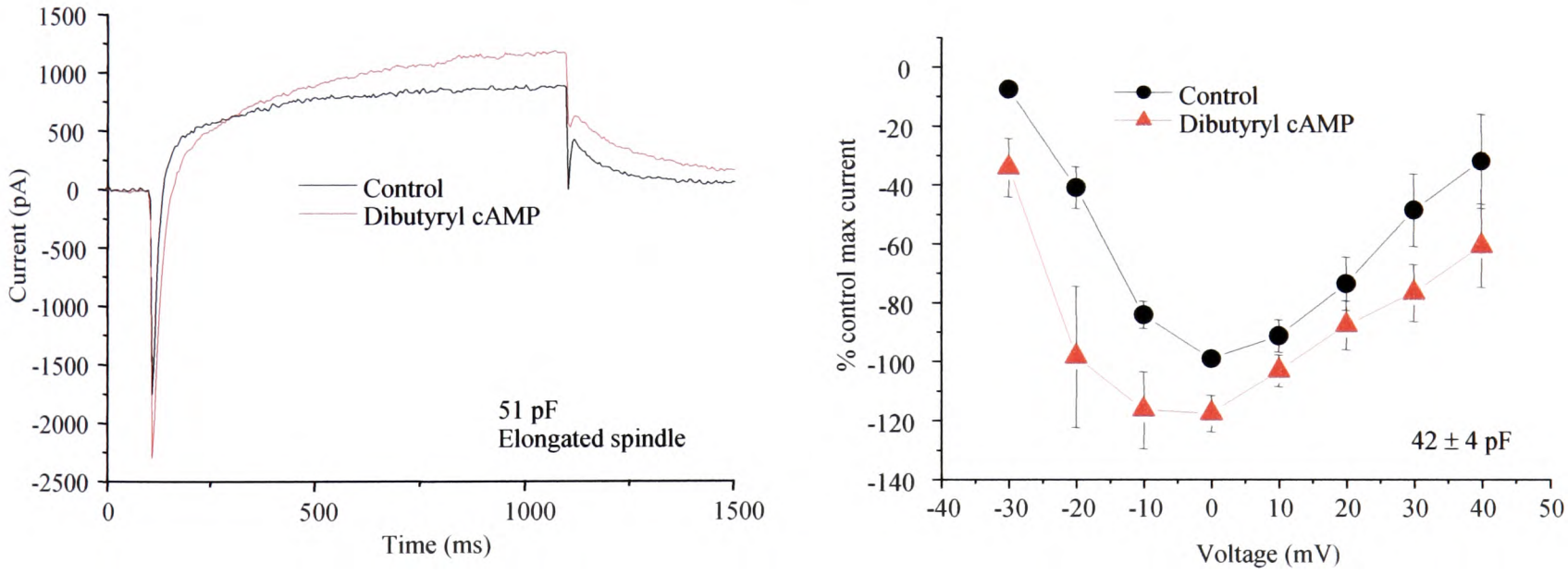

Figure 6.10 Page 271

The cell permeant cAMP analogues 500 μM 8 bromo cAMP (a) and 1 mM dibutyryl cAMP (b) tended to increase the amplitude of the inward I_{CaL} activated immediately upon depolarisation (left panel). 8 bromo cAMP however was not found to increase I_{CaL} amplitude (n=3), but the dibutyryl cAMP analogue increased I_{CaL} between –20 and +10 mV (n=4, $P<0.05$), without changing the voltage which maximally activated I_{CaL} (0 mV).

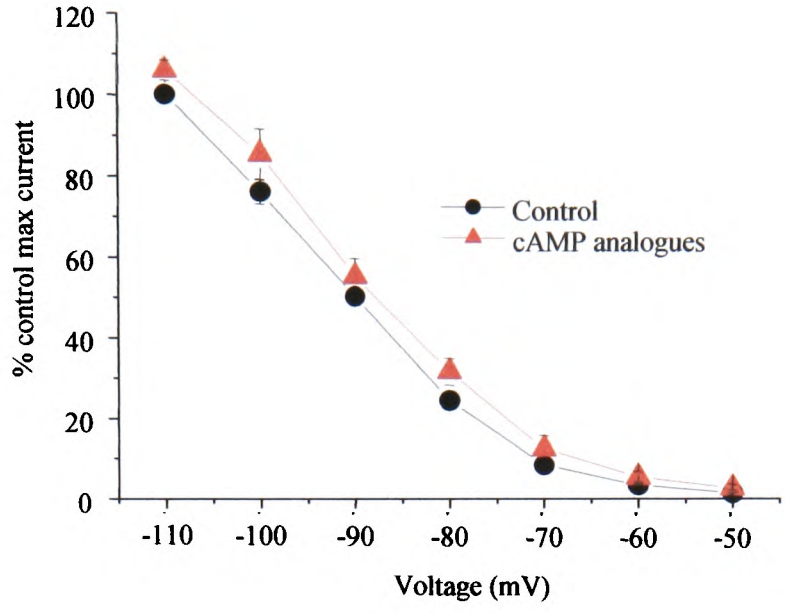

Figure 6.11

Grouped data found cAMP analogues, 500 μM 8 bromo cAMP (n=3) and 100 μM SP-cAMP (n=2), to have shifted the voltage dependent activation of I_f to slightly more depolarised potentials. This effect was quantified and the $V_{1/2}$ was found to be shifted from –97 ± 2 to –92 ± 1 mV (n=5, $P<0.05$), without altering the activation slope of I_f.

Agent	Target	Current	Affect
Forskolin	AC	Various	AC activation increased I_{Ks}, I_{Kr}
MDL	AC	Various	AC inhibition reduced beating rate, I_K, I_{CaL} and shifted I_f
cAMP analogues	cAMP sensitive pathways	Various	Slight increase in I_{Ks} and shift of I_f

Figure 6.12 Page 273
Summary table of findings in this chapter. Forskolin was used at 1 μM, MDL at 10 μM, whilst the cAMP analogues (dibutyryl, 8 bromo and SP) were used at 500 μM, 1 mM and 100 μM.

CHAPTER 7: Kinase regulation of I_K

Protein kinase activity modulates many intracellular components and this includes ion channels, which in the sino-atrial node define spontaneous action potential generation. Phosphorylation of ion channels tends to increase the amplitude of current and therefore protein kinase inhibitors generally reduce current. Sarcolemmal ion channels are regulated by protein phosphorylation; the net phosphorylation state is a balance between kinase (phosphorylation) and phosphatase (dephosphorylation) activity (Accili, Redaelli et al. 1997; Lemaire, Piot et al. 1998; Matsubayashi, Matsuura et al. 1999). Inhibition of dephosphorylation by phosphatase antagonism has been found to stimulate kinase activity upon various currents of the sino-atrial node (Accili, Redaelli et al. 1997; Lemaire, Piot et al. 1998; Matsubayashi, Matsuura et al. 1999).

PKA regulation of ionic currents of the sino-atrial node

There is evidence for a basal AC turnover, from acetylcholine I_{CaL} inhibition of non-stimulated sino-atrial node cells (Petit-Jacques, Bois et al. 1993; Habuchi, Yamamoto et al. 1996; Zaza, Robinson et al. 1996) and so PKA maybe consistently active. PKA regulation may have a comparatively large role in the sino-atrial node, as there appears to be a basal AC turnover and hence PKA regulation of pacemaking currents, as parasympathetic agonists only have activity upon I_{CaL} after sympathetic preconditioning in ventricular myocytes (Freeman and Kass 1993). Phosphorylation of ion channels and phospholamban (a SR calcium pump inhibitor element) by PKA, alters respectively the ionic and calcium handling characteristics of the sino-atrial node and consequently modify pacemaking rate.

Sympathetic tone initiates the cytosolic release of G_s, causing AC activation, cAMP production and hence PKA activation. I_{CaL} is also predominantly regulated by this cAMP dependent protein kinase (Reuter and Wollert 1967; Trautwein and Kameyama 1986; DiFrancesco and Tortora 1991; Tanaka, Clark et al. 1996; Bois, Renaudon et al. 1997).

Both components of the delayed rectifier potassium current are regulated by PKA activity, which can be initiated by β-adrenoceptor stimulation, direct AC activation, cAMP addition or introduction of the catalytic subunit of PKA (Giles, Nakajima et al. 1989; Lei and Brown 1996). The enhancement of the slow component I_{Ks} shows strong temperature dependency, unlike I_{CaL} measured from the same ventricular cell, and this may indicate slightly different PKA mediated augmentation mechanisms (Walsh and Kass 1988; Walsh, Begenisich et al. 1989). However regulation of sino-atrial node I_K appear to be temperature independent (Freeman and Kass 1993), and so similar PKA modulation pathways of I_K and I_{CaL} seem possible. Anchoring proteins are thought to be involved in the differentiation PKA modulation of I_K and I_{CaL}, possibly by localising the catalytic PKA subunit to the vicinity of I_{CaL} but not I_K (Kamp and Hell 2000). ERG regulation by PKA has been reported to be variable (Kiehn, Karle et al. 1998; Spector, Curran et al. 1996), with some studies describing a reduction in current upon PKA activity. But the native current I_{Kr} is predominately up-regulated by PKA, via a cAMP pathway (Kiehn, Karle et al. 1998) and direct evidence with radioactive phosphate has identified PKA mediated phosphorylation to enhance I_{Kr} (Cui, Kagan et al 2001). I_{Kr} augmentation upon β-adrenoceptor stimulation of PKA activity has recently been described to be

partially mediated through a reduction of voltage dependent I_{Kr} rectification (Brown and Difrancesco 1980; Heath and Terrar 2000).

Other currents involved in pacemaking are altered by PKA, such as I_{st} and I_{NCX} (Guo 1997), two inward currents that contribute to diastolic depolarisation. Both these currents are enlarged by PKA phosphorylation, via a cAMP dependent pathway and would therefore increase the rate of diastolic depolarisation and spontaneous action potential generation (Brown and Difrancesco 1980; Nicoll, Longoni et al. 1990; Heath and Terrar 2000; Mitsuiye, Shinagawa et al. 2000; Perchenet, Hinde et al. 2000). I_f is modulated by AC activation, but this is independent of PKA, as cAMP analogues that actually inhibit PKA activity, still cause a positive shift in the $V_{1/2}$ of I_f (DiFrancesco and Tortora 1991; Bois, Renaudon et al. 1997).

The role of PKC

There are some studies that claim exclusive modulation of I_{CaL} by PKA (Tanaka, Clark et al. 1996), but others disagree and have described complex PKC regulation of I_{CaL} which demonstrates cross-talk with the PKA pathway (Kamp and Hell 2000). PKC and PKA may exhibit cross-talk in phosphorylative regulation of ion channels. The PKA mediated augmentation of I_{Kr}, may be dependent upon calcium and PKC activity (Heath and Terrar 2000), possibly by PKA phosphorylation of calcium handling elements, resulting in increased calcium and hence PKC activation.

There is additional evidence for PKC linking ionic and calcium mechanisms involved in the pacemaking of the heart, as PKC appears to elevate cellular calcium levels (Satoh 1994; Satoh 1995) after being activated by adrenergic agonists.

Calcium activates PKC, and the high calcium level in the sino-atrial node (Calcium and the SR, page 209; (Tohse, Kameyama et al. 1987; Way, Chou et al. 2000; Rigg, Mattick et al. 2003) caused elevated PKC activity. PKC activity and calcium appear to be closely related in the sino-atrial node, being a point of cross-talk between the calcium/contraction and the kinase phosphorylation pathways.

I_{Ks} is regulated by PKC activation, with the phosphorylation site being located at the N102 amino-acid in $KCNQ_1$ (Varnum, Busch et al. 1993). In parallel with whole I_K, the effects upon I_{Ks} are calcium dependent (Walsh, Arena et al. 1991; Walsh and Kass 1991), and increase the open probability of these channels (Tohse, Kameyama et al. 1990). I_{Kr} also has some degree of PKC regulation, as co-expression of human ERG with α-adrenoceptors that activate the PKC cascade (Tohse, Kameyama et al. 1987; Walsh and Kass 1988), caused $V_{1/2}$ of I_{Kr} to be modified upon adrenoceptor stimulation (Jiang, Dun et al. 1999).

PKC has been found to regulate I_{CaL} by various groups (Hartzell, Hirayama et al. 1995), including (Guo, Giles et al. 2000) who found sino-atrial node spontaneous activity to be accelerated by H_2O_2 via a PKC dependent pathway.

Calmodulin and calmodulin kinase regulation of sino-atrial node ionic currents

High calcium concentrations in the sino-atrial node can directly regulate some ion channels, I_{CaL} is inactivated by calcium for example, but calcium also activates ubiquitous cellular regulatory elements such as calmodulin (CaM). Vieth, Nho et al (1993) found calcium binding to CaM to cause translocation to cellular membranes (SR and sarcolemmal) where the CaM alters the function of various channels:

including I_{CaL} (Wu, Dzhura et al. 2001), I_f (Liu and Huizinga 1994; Rigg, Mattick et al. 2003), I_K (Nitta, Furukawa et al. 1994) and the SR calcium pump SERCA (Narayanan and Xu 1997). Calcium activated CaM is not an enzyme, but an ubiquitous molecule for which numerous proteins have binding sites for. Binding of CaM to cellular proteins alters the function of the proteins, by causing conformational changes, hence CaM acts as a regulator. The formation of a calcium-CaM complex (and possibly CaMK) appears to regulate AC (Piascik, Babich et al. 1983; Piascik, Babich et al. 1986; Narayanan and Xu 1997). Calcium sensitive PKC can also regulate AC (see review by (Defer, Best-Belpomme et al. 2000). The cross-talk of CaM, PKA (via AC regulation) and calcium adds another level of complexity to regulation of ionic currents.

The situation is further complicated by the actions of a calmodulin kinase (CaMK) that is activated by the binding of the calcium-CaM complex. CaMK in the heart is generally of the second sub-type discovered ($CaMK_{II}$) and has been found to be vital to pacemaking and to regulate I_{CaL} (Vinogradova, Zhou et al. 2000), I_{Na} (Deschenes, Neyroud et al. 2002) and I_{NCX} (Isosaki, Minami et al. 1994). CaMK has been found to regulate phospholamban, and therefore SERCA, and ryanodine receptors (Wagner, Namiki et al. 1999) that mediate the uptake and release of calcium from the SR; CaMK therefore has important role in the modulation of calcium homeostasis (Calcium and the SR, page 209). The role of CaM and CaMK should definitely be considered when examining regulation of ionic currents involved in pacemaking.

Aims of chapter

The ionic currents of the sino-atrial node, and calcium handling mechanisms, appear to be under extensive kinase regulation. The basal turnover of AC and the relatively high cellular calcium levels of the sino-atrial node result in high PKA, PKC, CaM and CaMK activity before any autonomic control is considered. Phosphorylation of key cellular sites (I_{CaL}, PLB and I_K) will result in substantially different pacemaker characteristics and this chapter investigates various kinase pathways.

Results

Protein kinase inhibition with staurosporine.

Non-specific protein kinase inhibition with staurosporine reduced I_K components and I_{CaL}, indicating that phosphorylation associated with protein kinase activity augmented these currents (figure 7.1a). I_K showed time-dependent activation, with a component of activation between 0-80 ms (20 ± 5 % of control max current) and a subsequent phase activated with depolarisations greater than 70 ms (Description of I_K and other ionic currents, page 122). 300 nM staurosporine was initially added to the superfusing solutions and I_K activated with prolonged depolarisations was reduced from 178 ± 38 to 119 ± 28 pA (n=5, $P<0.05$), a reduction of 33 ± 6 % (figure 7.1b), while there was little or no change of I_K activated with brief depolarisations. The reduction of I_K by staurosporine (300 nM) was statistically significant with depolarisation of 70 ms and longer (n=5). In accordance with literature in the area (Heath and Terrar 2000), non-specific inhibition of protein kinase was also attempted

with 3 μM staurosporine (figure 7.2a). The findings from these experiments upon I_K were broadly similar to those with 300 nM, but paradoxically the higher concentration (x 10) of staurosporine appeared to inhibit I_K less (figure 7.1a and 8.2a). I_K activated with depolarisations greater than 200 ms was reduced by this concentration of staurosporine ($n=6$, $P<0.05$) and the maximal current (figure 7.1c) being reduced by 19 ± 4 % (196 ± 43 to 159 ± 38 pA). I_K activated with brief depolarisations (40 ms) was not significantly reduced; 28 ± 3 in control and 23 ± 6 pA in the presence of 3 μM staurosporine ($n=6$, $P>0.05$).

The voltage dependent activation of I_K was also studied and fitted with a sigmoid curve (figure 7.2b), having a $V_{1/2}$ of 7 ± 2 mV in control; this relationship was shifted to 13 ± 6 mV upon application of 300 nM staurosporine and maximal I_K was reduced from 205 ± 36 to 149 ± 32 pA ($n=5$, $P<0.05$) at +40 mV. Indeed I_K activated with depolarisation to –10 mV (from –40 mV) and greater were found to be significantly reduced ($n=5$). In the presence of 3 μM staurosporine the voltage dependent activation of I_K was altered (figure 7.2c), as the $V_{1/2}$ was shifted by 3 mV and the maximally activated current was reduced from 183 ± 43 to 160 ± 41 pA ($n=6$, $P<0.05$). Staurosporine reduced I_K activated with depolarisation greater than +10 mV, and –30 mV ($n=6$, $P<0.05$). In summary, staurosporine reduced I_K activated with extended depolarisations only. Staurosporine (300 nM) did not alter either of the I_K tail current decay time-constants (figure 7.3a), or associated amplitudes ($n=5$, $P>0.05$).

When considering I_{CaL} staurosporine (300 nM) was found to reduce the amplitude of this inward current (figure 7.3b) activated throughout the voltage range

–30 to +40 mV (n=6, P<0.05). There was no shift of the voltage that activated maximal I_{CaL} (0 mV) upon staurosporine inhibition (39 ± 12 %). Inhibition of I_{CaL} with 3 μM was not studied.

In an additional 4 cells, I_{Kr} was blocked with E4031 (5 μM) before the addition of 300 nM staurosporine. This investigation found the E4031 resistant current to be depressed by staurosporine, to 84 ± 5 % (n=4, P<0.05) of the max E4031 resistant current (figure 7.4a). A similar reduction of maximal activated I_K in the presence of E4031 was identified when voltage dependent activation was considered (77 ± 9 %); E4031 resistant I_K activated by depolarisation to –10 mV and greater was reduced by staurosporine (n=4, P<0.05). There was no significant alteration in either the $V_{1/2}$ or the slope of activation of the E4031 resistant current, upon protein kinase inhibition with staurosporine (figure 7.4b).

K252a inhibition of protein kinases in the sino-atrial node.

An additional non-specific protein kinase inhibitor (250 nM K252a) was used to evaluate I_K and I_{CaL} regulation by phosphorylation in the sino-atrial node. However 250 nM K252a was actually found to increase the amplitude of I_K (figure 7.5a); possibly indicating phosphorylation causing an inhibitory effect upon I_K, which was removed upon inhibition by K252a or non-specific activity. I_K was activated with both time and voltage dependent activation protocols, with the usual characteristics (Description of I_K and other ionic currents, page 122). However, upon addition of K252a I_K activated with depolarisations longer than 200 ms (figure 7.5b) and greater than 0 mV (figure 7.5c) were amplified; 130 ± 6 % after a 700 ms depolarisation and 131 ± 9 % at +40 mV (n=5, P<0.05). There were no alterations to the time-constant

or amplitude of I_K decay upon exposure to K252a (figure 7.6a, n=5, P>0.05). This observation, with a change in the opposite direction with that of staurosporine, could indicate a complex kinase regulation of I_K, including phosphorylation induced reduction.

Interestingly, I_{CaL} was found to be reduced by 250 nM K252a (figure 7.6b), possibly indicating slightly different kinase regulations of I_K and I_{CaL}. I_{CaL} was reduced at all potentials, with no alterations in the voltage that activates maximal I_{CaL}, but a 74 ± 12 % reduction of maximal control I_{CaL} (n=6, P<0.05).

The non-specific inhibitor K252a has different protein kinase selectivity than staurosporine (Way, Chou et al. 2000). The lesser degree of inhibition of I_K with the higher concentration staurosporine might in some way agree with this theory, as low concentrations could inhibit an up-regulatory kinase, whereas high concentrations could additionally inhibit a down-regulatory kinase (Mamas and Terrar, unpublished data).

Protein kinase A inhibition with KT-5720.

The subtype of kinase that regulates I_K and I_{CaL} in the sino-atrial node was investigated, initially using the specific protein kinase A (cAMP sensitive) inhibitor KT-5720 (1 μM). The time-dependent activation of I_K was identified as described above, with a rapid and delayed phase of activation. When the sino-atrial node cells were treated with KT-5720 (1 μM) the phase of I_K activated with brief depolarisation was almost abolished, from 19 ± 3 to 5 ± 3 % of control max current (figure 7.7b, n=5, P<0.05). There may have been some additional partial inhibition of I_K activated

with more prolonged depolarisations; maximal current was activated with a 700 ms depolarisation and was reduced to 68 ± 6 % (n=5, P<0.05). This indicates that I_K activated with brief depolarisation is already augmented by PKA phosphorylation, whereas there is only a slight degree of enlargement of I_K activated with more prolonged depolarisation; this finding correlates with basal AC turnover (Adenylate cyclase, page 240) augmenting I_{Kr}.

There was a corresponding reduction of I_K activated with various voltage depolarisations (figure 7.8a). 1 μM KT-5720 was found to reduce maximally activated I_K (at +40 mV) to 74 ± 3 % (n=5, P<0.05) and in addition lowered I_K activated at most voltages (-20 to +40 mV). There was no alteration in either the $V_{1/2}$ or the slope of I_K activation upon KT-5720 treatment.

I_{CaL} was reduced by 1 μM KT-5720 (figure 7.8b), I_{CaL} was reduced at all potentials, with no alterations in the voltage that activates maximal I_{CaL} (0 mV), but was reduced to 43 ± 8 % of maximal control I_{CaL} (n=6, P<0.05).

The effects of the PKC inhibitor Ro-31-8220.

The role of the subtype of protein kinase were also investigated, as some subtypes are activated by intracellular calcium and could therefore provide an important link between sino-atrial node calcium handling and phosphorylation state of ion channels.

The effects PKC inhibitors were studied, in this case Ro-31-8220 (50 nM) was utilised as it has high selectivity for PKC (Way, Chou et al. 2000). Ro-31-8220 (50 nM) was found to reduce the amplitude of I_K activated with depolarisation of 60 ms

and longer (figure 7.9b, n=5, P<0.05); no reduction was found at 40 ms, but maximum control current was reduced to 77 ± 9 % (n=5, P<0.05). This indicates I_K activated with prolonged depolarisations are reduced by PKC inhibition. This implies that PKC augments I_{Ks} (figure 7.10a), with the $V_{1/2}$ defined as –10 ± 3 mV and the slope of activation was 31 ± 6 mV; this voltage dependency indicated that I_K was activating at quite negative potentials and progressively enlarging throughout the voltage range. Ro-31-8220 (50 nM) reduced maximal I_K to 73 ± 7 % (n=5, P<0.05), shifted $V_{1/2}$ to –4 ± 13 mV (n=5, P>0.05) and altered the slope factor to 26 ± 9 mV (n=5, P>0.05). I_{CaL} was reduced in the presence of PKC inhibition by 50 nM Ro-31-8220, but maximal inhibition at 0 mV to 85 ± 2 % (n=5, P<0.05) of control. PKC inhibition reduced I_{CaL} at voltages between –30 and 0 mV (figure 7.10b), considerably less I_{CaL} reduction than that mediated by PKA inhibition.

Bisindolymaleimide I inhibition of PKC and the effects upon I_K components and I_{CaL}.

The protein kinase inhibitor bisindolymaleimide I (200 nM) was utilised, having been described as PKC selective (Way, Chou et al. 2000). I_K was time-dependently activated, with a 40 ms depolarisation activating 44 ± 5 pA (24 ± 4 % of control max) and 700 ms depolarisation producing an I_K tail current of 187 ± 29 pA (figure 7.11b, n=8). In the presence of bisindolymaleimide I both I_K activated with short and prolonged depolarisation was inhibited, reducing the 40 and 700 ms currents to 28 ± 4 and 152 ± 24 pA (n=8, P<0.05). I_K activated with any depolarisation duration (10 to 700 ms) was reduced with bisindolymaleimide I (figure 7.11b). Maximally activated current (700 ms) was reduced to 81 ± 9 %, whereas the maximal voltage dependently activated current (at + 40 mV) was only 81 ± 11 % of control (n=8, P<0.05). The voltage dependent activation of I_K was reduced at all

potentials greater than –20 mV in the presence of 200 nM bisindolymaleimide I (n=8, P<0.05), without shifting the $V_{1/2}$ or slope of activation (figure 7.11c). Bisindolymaleimide I correspondingly reduced the amplitude of the time-constants of I_K decay; but only Amp_2 was significantly reduced (n=6, P<0.05), whilst the time-constants themselves were not altered (figure 7.12a).

I_{CaL} was also found to be marginally inhibited by bisindolymaleimide I, although it has been reported to demonstrate some specificity to PKC (figure 7.11a). I_{CaL} was activated over the voltage range –30 to +40 mV and was found to be biggest at 0 mV, exhibiting rough bell-shaped voltage dependency around this point (figure 7.12b). The form of the voltage dependent activation of I_{CaL} was not altered by bisindolymaleimide I (max at 0 mV and a bell-shaped relationship), but the magnitude of the current was slightly diminished at voltages between –10 and +10 mV (including max I_{CaL}), being 62 ± 18 % of control (n=6, P<0.05). This indicates a degree of PKC regulation of I_{CaL}, possibly mediating PKA regulation as described by Heath an Terrar (2000) for I_{Kr} or a non-selective action of bisindolymaleimide I.

CaMK inhibition in the sino-atrial node.

The calcium sensitive protein kinase inhibitor calmodulin kinase (CaMK) was also investigated. KN-93 is an effective inhibitor of calmodulin kinase (Hagiwara and Irisawa 1989; Rigg, Mattick et al. 2003) and the structurally similar compound KN-92 was used, as this has a lower potency upon CaMK, using the same mechanism of inhibition. The effect (if any) of KN-92 should therefore be a fraction of the KN-93 effect upon I_K (figure 7.13). I_K activated with brief depolarisation (40 ms) was reduced to 37 ± 5 % (n=5, P<0.05) of control by 1 μM KN-93 (figure 7.14a), but KN-

92 (1 μM) did not diminish the corresponding current (figure 7.14b, n=3). KN-92 did reduce I_K activated with depolarisation of 50 and 60 ms (n=3, P<0.05) and there was a reduction trend at all durations. KN-93 reduced I_K activated with any duration depolarisation and maximally activated I_K (700 ms depolarisation) was reduced to 46 ± 7 % (n=5, P<0.05). Evidence for the reduction of the non- I_{Kr} component of I_K by CaMK inhibition has been gained by using E4031 (5 μM) to eliminate I_{Kr} (figure 7.16b). The E4031 resistant current was reduced at all depolarisation durations greater than 80 ms (n=3, P<0.05), with maximal E4031 resistant I_K (measured with a 700 ms depolarisation) being reduced to 51 ± 5 % of control (n=3, P<0.05).

The voltage dependent activation of I_K was similarly affected by KN-93 and KN-92 (both at 1 μM), causing reductions in I_K activated with depolarisation to +40 mV of 51 ± 11 % (n=5, P<0.05) and 84 ± 6 % (n=3, P<0.05) of respective controls (figure 7.15). I_K was reduced at all potentials by KN-93, but only at potentials greater than –10 mV with KN-92 (n=5 and 3, P<0.05). Both the KN-93 and KN-92 shift tended towards the I_K $V_{1/2}$ to more positive potentials, causing shifts of 10 ± 2 (P<0.05) and 4 ± 2 mV (P>0.05) respectively. The decay of I_K was investigated in the presence of KN-93 (figure 7.16a) and although the Tau's were not altered (119 and 521 ms), the amplitude of Tau_2 was reduced to 53 ± 12 % of control (n=6, P<0.05). The E4031 (5 μM) resistant current was also subjected to voltage-dependent investigation and KN-93 was found to reduce the current to 61 ± 7 % of control (n=3, P<0.05), and was reduced by KN-93 at all voltages greater than –20 mV (figure 7.16c). This was associated with a 4 mV shift in the $V_{1/2}$ from 16 to 20 mV (n=3, P<0.05), which even in control is a relatively positive value but this is probably due to I_{Kr} inhibition. The regulation of I_{CaL} by CaMK was also investigated. In some ways

regulation of a calcium channel by a calcium sensitive kinase seems likely, although calcium induced augmentation of calcium current would result in a positive feedback cycle. KN-93 (used at a concentration of 1 μM) was found to reduce I_{CaL} at potentials between –20 and 0 mV (figure 7.17a), including maximal voltages of maximal I_{CaL} activation, with the reduction at 0 mV being of 54 ± 17 % (n=5, $P<0.05$). The less potent but structurally similar compound KN-92 did not reduce I_{CaL} at any voltage (n=3, figure 7.17b).

Modulation of I_f by CaM.

Calmodulin (CaM), which activates CaMK, has been found to be a regulator or various ion channels (such as I_f) and other intracellular proteins (Rigg, Mattick et al. 2003). CaM is activated by calcium. CaM does not phosphorylate proteins, but rather interacts directly with them at specific binding domains, such as in the I_{Na} (Deschenes, Neyroud et al. 2002), I_{NCX} (Isosaki, Minami et al. 1994), I_{CaL} (Wu, Dzhura et al. 2001) and I_f (Rigg, Mattick et al. 2003). The association of CaM with channel proteins alters channel function. Calmidazolium (25 μM) and W7 (10 μM) are both effective CaM antagonists that have been used to describe the role of CaM in the regulation of I_f (Hagiwara and Irisawa 1989; Rigg, Mattick et al. 2003). Figure 7.18a shows that CaM inhibition with calmidazolium (25 μM) shifted the $V_{1/2}$ of I_f from –99 ± 3 to –104 ± 3 mV (n=6, $P<0.05$), without altering the slope of activation from 11 ± 2 mV (n=5). W7 is structurally different to calmidazolium but causes a similar negative shift in the voltage dependent activation of I_f. Upon exposure of W7 treated sino-atrial node cells with forskolin (10 μM), the negative shift in the voltage dependent activation of I_f was partially reversed (figure 7.18b), by shifting the $V_{1/2}$ by 7 mV (n=6, $P<0.05$).

Discussion

Sino-atrial node function has primarily been investigated in isolated cells, which are not autonomically regulated. Therefore kinase activity instigated by both sympathetic and parasympathetic nervous systems maybe absent. Isolated sino-atrial node cells are thought to have comparatively high calcium levels (Calcium and the SR, page 209; Verheijck 2000) and a basal AC turnover, which elevates intracellular cAMP (Adenylate cyclase, page 240). These two intracellular components are known to activate kinases, calcium stimulates PKC and CaMK (as well as CaM), whilst cAMP stimulates PKA activity. There are other kinases present, such as mitogen activated protein kinase etc, but have not been studied. Kinase activity in isolated sino-atrial node cells was investigated, using various inhibitors (non-selective and selective) to attempt to define the role kinase subtypes in the regulation of some of the ionic currents involved in the spontaneous development of action potentials.

Regulation of I_K by kinase activity in the sino-atrial node

Both I_{Kr} and I_{Ks} are regulated by protein phosphorylation, but this study found broad protein kinase inhibition to reduce only I_{Ks}. The literature indicates a basal enlargement of both I_{Kr} and I_{Ks}, but there is controversy regarding the type of kinase regulation of these components and kinase sub-type specific inhibition of the components of I_K probably underlies this unexpected result. I_{Kr} was found by Heath and Terrar (1996) to be PKA regulated, although this process was calcium dependent (see below). Others have directly described PKA regulation of I_{Kr} and the molecular correspondent ERG (Kiehn, Karle et al. 1998; Cui, Kagan et al. 2001); some have assigned exclusive regulation of I_{Kr} by PKA. There are some reports however that find I_{Kr} to additionally be regulated by PKC (Jiang, Dun et al. 1999), possibly being

related to PKC being closely related to cellular calcium (Satoh 1994) which has wide ranging intracellular activities (Calcium and the SR, page 209) including regulation of AC (Luthi, Bal et al. 1998). Basal AC turnover has been implicated in the sino-atrial node, hence elevating cAMP and therefore PKA activity at rest. I_{Kr} was found to be sensitive to AC inhibition and was postulated to be due to basal PKA augmentation of I_{Kr}. This is in agreement with the finding of this chapter that specific PKA inhibition reduced I_{Kr}. Heath and Terrar (2000) proposed that the PKA augmentation of I_{Kr} was mediated by phosphorylation of calcium handling apparatus, which resulted in elevated calcium and PKC activation; PKC was hypothesised to be an intermediate in the PKA augmentation of I_{Kr}. This study found I_{Kr} to be sensitive to both PKA and PKC inhibition, but primarily PKA, therefore possibly indicating a different mechanism of regulation. ERG has multiple phosphorylation sites (Bian, Cui et al. 2001; Cui, Kagan et al. 2001), and high PKA activity in the sino-atrial node (due to elevated AC turnover), may result in an additional site to be.

The slowly activating component of I_K, I_{Ks} has been found to be enlarged by both PKA and PKC mediated phosphorylation in this study, but the PKA inhibitor mediated reduction of I_{Ks} was of smaller magnitude. Sino-atrial node I_{Ks} enhancement maybe via a similar pathway to I_{CaL}, unlike I_{Ks} in ventricular myocytes (Freeman and Kass 1993) and a recent study by Marx, Kurokawa wt al (2002) found $KCNQ_1$ (the molecular correlate of I_{Ks}) regulation by PKA to mediate cardiac action potential abbreviation. I_{Ks} modulation by PKC is calcium dependent (Tohse, Kameyama et al. 1990), increases the probability of channel opening upon stimulation. PKC regulation of I_{Ks} is generally thought to predominant over other kinase activity, however this study has found CaMK to have a large regulatory role in the sino-atrial node. This is in agreement with Vinogradova, Zhou et al (2000), which

found CaMK activity to be vital to spontaneous action potential generation, although this was interpreted to be the result of enhancement of I_{CaL}. I_K has been previously described to be CaMK regulated (Nitta, Furukawa et al. 1994). In this study I_{Kr} was separated and was found to be reduced by over 75 % by CaMK inhibition and I_K activated with prolonged depolarisations (primarily I_{Ks}) was approximately halved; both I_{Kr} and I_{Ks} appear to be regulated by multiple kinases. The classic definition was that PKA primarily modulated I_{Kr} and PKC for I_{Ks} (Tohse, Kameyama et al. 1987; Kiehn, Karle et al. 1998), but this appears to be too simple a dogma for the kinase regulation of I_K in the sino-atrial node. However, both delayed rectifier currents were reduced to a greater degree by CaMK inhibition; this calcium-CaM sensitive kinase may therefore play a large role in the regulation of sino-atrial node I_K that has not been fully realised previously. There is possible cross-talk between calcium sensitive and other kinase pathways, creating a complex integrated I_K regulatory system.

Unpublished data from this laboratory has found I_K to be augmented in guinea-pig ventricular myocytes, by protein kinase inhibitors such as chlerythrin (Mamas and Terrar, unpublished data). This maybe similar to the observed effect of K252a, possibly indicating a protein kinase (specific sub-type) mediated reduction in I_K. This hypothesis requires further investigation.

Kinase regulation of I_{CaL} in the sino-atrial node

The L-type calcium current was one of the first ionic currents to be found to be modulated by protein kinase activity (Reuter and Wollert 1967) and the cAMP/PKA modulation of I_{CaL} in this study was again demonstrated in sino-atrial node cells (as well as Petit-Jacques, Bois et al. 1993). The magnitude of I_{CaL} was suppressed upon PKA inhibition. However, the voltage dependent activation remained indicating basal PKA phosphorylation of ion channel, which amplified

conductance, rather than kinase activity which altered activation or inactivation gates. The resting AC turnover, cAMP production and PKA activity is likely to be important in sino-atrial node (Petit-Jacques, Bois et al. 1993; Guo, Ono et al. 1995).

This study also identified a possible PKC augmentation of I_{CaL}, as both PKC inhibitors caused a slight reduction of the amplitude of I_{CaL} at voltages near maximal activation. There is previous evidence that suggests PKC I_{CaL} regulation (Hartzell, Hirayama et al. 1995), such as Guo, Giles et al (2000) finding that I_{CaL} augmentation via a PKC pathway accelerated of spontaneous activity of rabbit sino-atrial. Dual regulation of I_{CaL} by PKA and PKC has been identified in this study and others (Kurokawa, Murray et al. 2002). There have been various reports that the PKA and PKC kinase pathways interact with each other at some point (Kamp and Hell 2000), possibly via calcium regulation of AC (Luthi 1999), and PKC regulation may occur in isolated sino-atrial node cells indirectly through PKA modulation.

An intermediate degree of I_{CaL} inhibition (between PKA and PKC) was brought about by CaMK inhibition and it is likely that the activity of this kinase is closely linked to that of PKC, as they both share calcium sensitivity. However CaM, which activates CaMK, has an inhibitory effect upon AC (Piascik, Babich et al. 1983; Piascik, Babich et al. 1986) opposed to the calcium activation of AC (see review by Defer, Best-Belpomme et al 2000). Wu, MacMillan et al (1999) and Wu, Dzhura et al (2001) described a CaMK dependent enlargement of I_{CaL}, which was similar to this study and appeared to be dependent upon SR function, indicating SR calcium release activated CaMK and subsequent regulatory pathways. In addition, Xiao, Cheng et al (1994) described the voltage and calcium dependent modification of I_{CaL} characteristics to be abolished when CaMK was inhibited; co-localisation of CaMK and I_{CaL} were also observed. CaMK activity has been found to be essential for sino-

atrial node function (Vinogradova, Zhou et al. 2000) and inhibition of I_{CaL} upon CaMK blockade would certainly compromise action potential generation.

Kinase regulation of I_f in the sino-atrial node

The work upon I_f presented here, is sequential to the study by Rigg, Mattick et al (2003), in which I_f was found to be regulated by calcium and CaM (independent of CaMK), mediating fine tuning of I_f and its role in the sino-atrial node. CaM inhibition was found to negatively shift the voltage-dependent activation of I_f (Hagiwara and Irisawa 1989; Rigg, Mattick et al. 2003). Forskolin has been previously been found to shift the $V_{1/2}$ of I_f by various amounts (DiFrancesco and Tortora 1991; Rigg, Heath et al. 2000). The inhibition of I_f function by CaM inhibition was partially reversed by addition of forskolin which would increase cellular cAMP, which binds directly to the HCN channel and modifies voltage-dependent activation (DiFrancesco 1999).

The phosphorylative regulation of sino-atrial node ionic currents is complex and integrated. PKA, PKC and CaMK appear to modulate various ionic currents, including I_{Kr} and I_{Ks}, as well as I_{CaL}. Phosphorylation tends to increase current magnitude of these currents, without alteration of voltage dependency. The classical interpretation of I_{Kr} and I_{CaL} being regulated by PKA and I_{Ks} by PKC, has some creditability, but these kinase pathways appear to interact possibly at the level of cellular calcium and/or regulation of AC. The role of CaMK appears to be large in the sino-atrial node, as inhibition considerably reduced both I_K components and I_{CaL}; the role of CaMK in the sino-atrial node needs to be further investigated. Kinase modulation of ionic currents in the sino-atrial node alters current magnitude and therefore contribution to spontaneous action potential generation; regulation was investigated in the absence of autonomic stimulation, which increases kinase activity.

a,

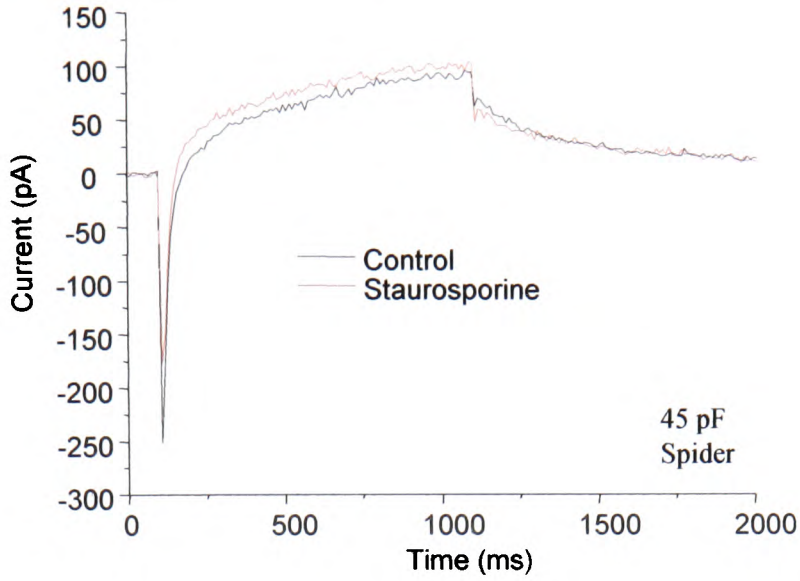

b,

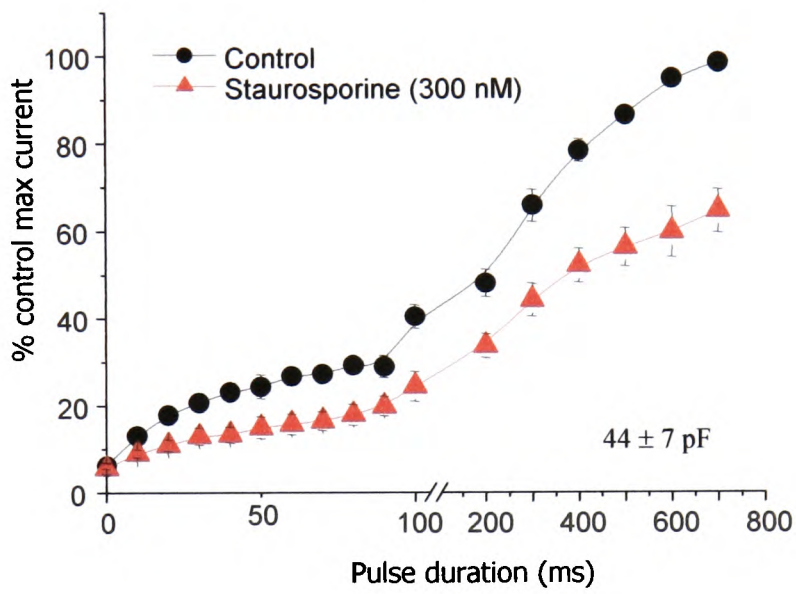

c,

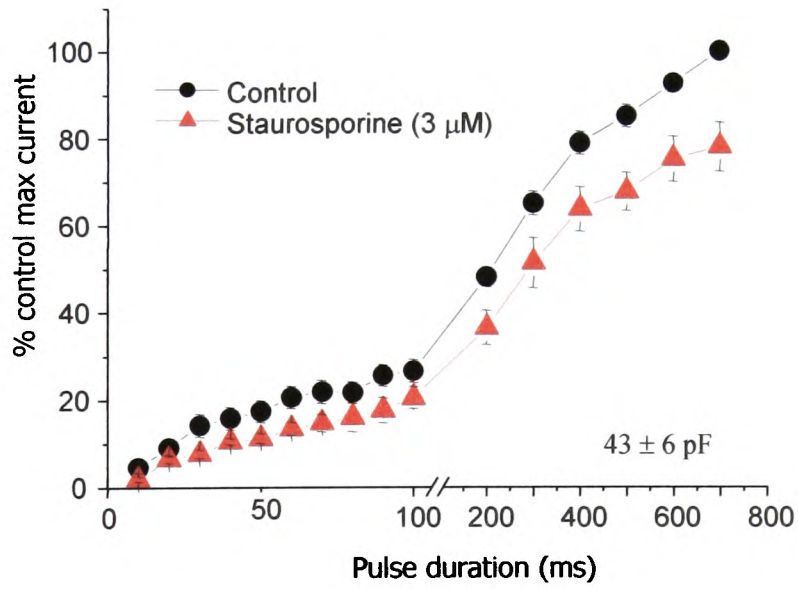

Figure 7.1 Page 293

Staurosporine reduced the amplitude of outward I_K tail current (a). The effect of staurosporine upon I_K was investigated at two concentrations; 300 nM (b) and 3 μM (c). 300 nM staurosporine was found to reduce I_K activated with depolarisation longer than 50 ms ($n=5$, $P<0.05$), excluding 60 ms, whereas 3 μM staurosporine reduced I_K activated with depolarisation of 200 ms and longer ($n=5$, $P<0.05$).

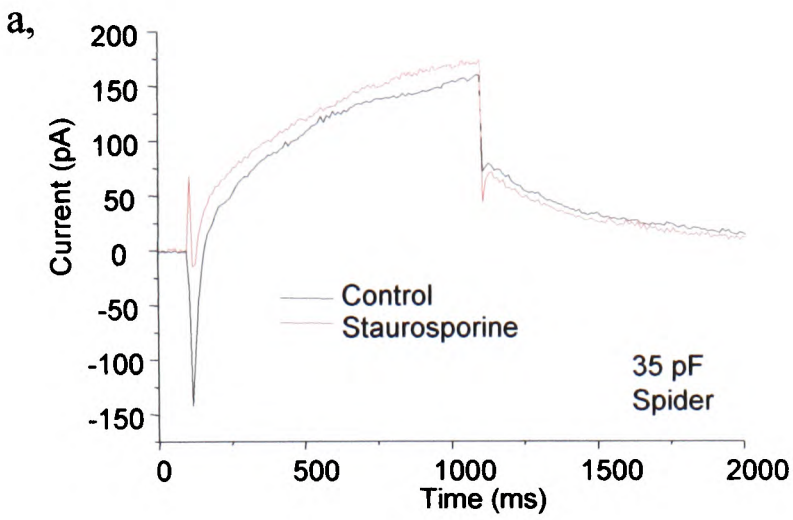

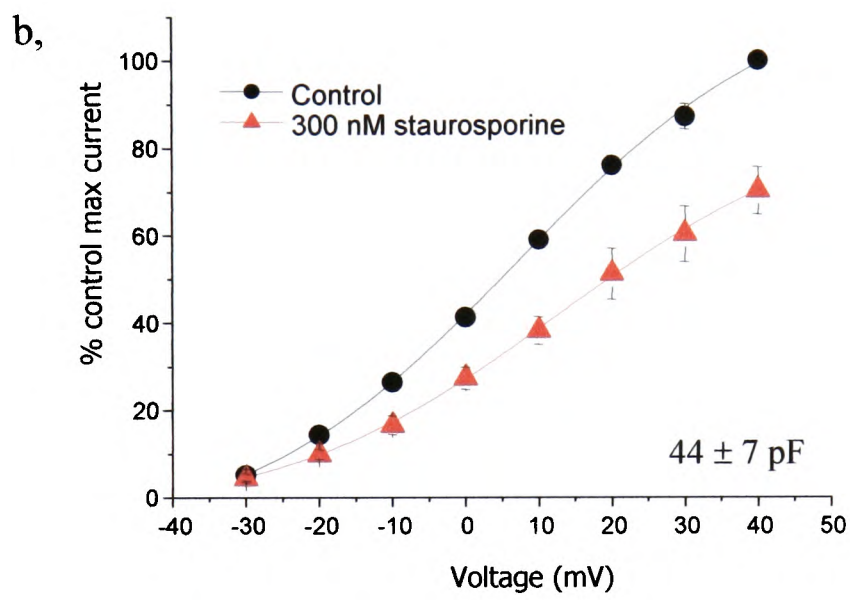

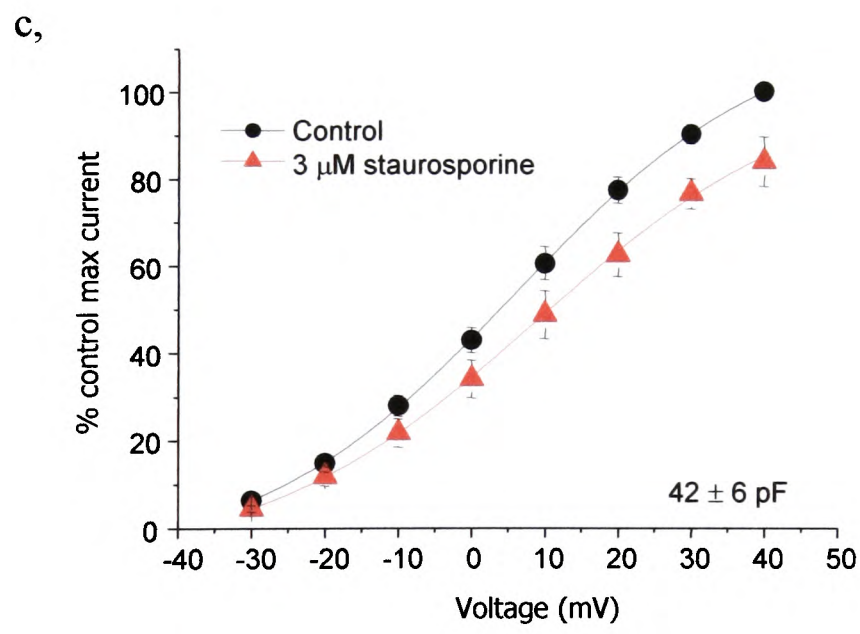

Figure 7.2 Page 294

Staurosporine reduced the amplitude of the outward I_K tail current (a). The effect of staurosporine upon I_K was investigated at two concentrations; 300 nM (b) and 3 μM (c). 300 nM staurosporine (b) was found to reduce I_K activated with depolarisation to -10 mV and greater ($n=5$, $P<0.05$) and shifted the $V_{1/2}$ from 7 ± 3 to 13 ± 3 mV ($P<0.05$), without changing the activation slope. Whereas 3 μM staurosporine (c) reduce I_K activated with depolarisation to -30, 10 mV and greater ($n=6$, $P<0.05$); however there was no change of $V_{1/2}$ or activation slope with 3 μM staurosporine.

a,

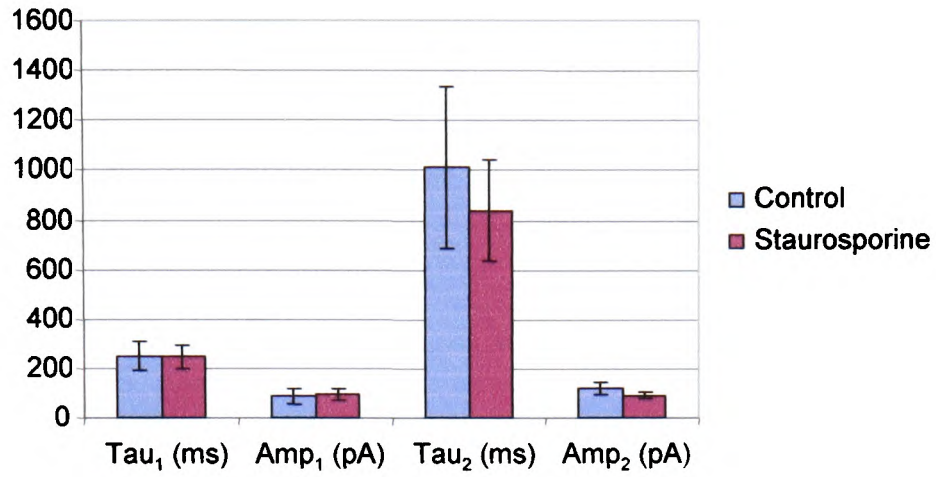

b,

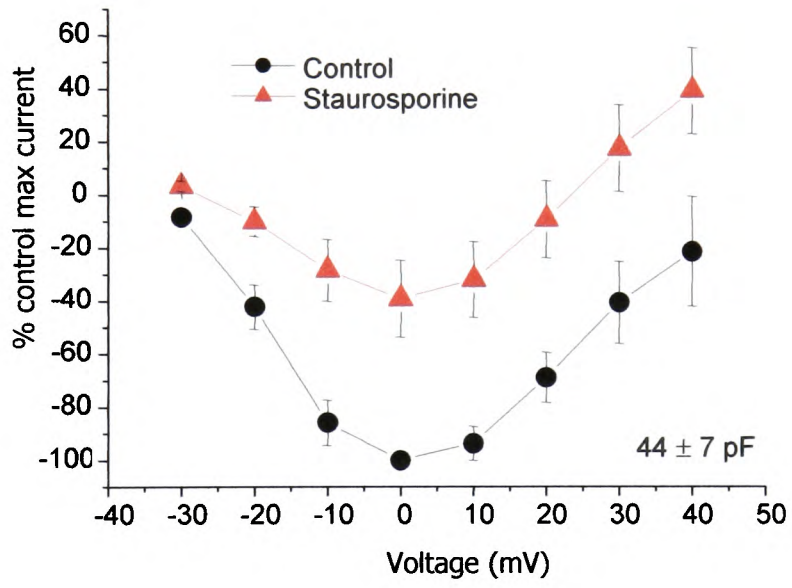

Figure 7.3 Page 295

Staurosporine (300 nM) did not alter the I_K tail current decay (a) but substantially reduced I_{CaL} (b). Neither time-constant or associated amplitudes of I_K decay was altered in the presence of staurosporine (n=6). I_{CaL} was reduced by staurosporine at voltages ranging between -30 and +40 mV (n=6, $P<0.05$). Staurosporine did not alter the voltage at which the maximal I_{CaL} was activated (0 mV).

a,

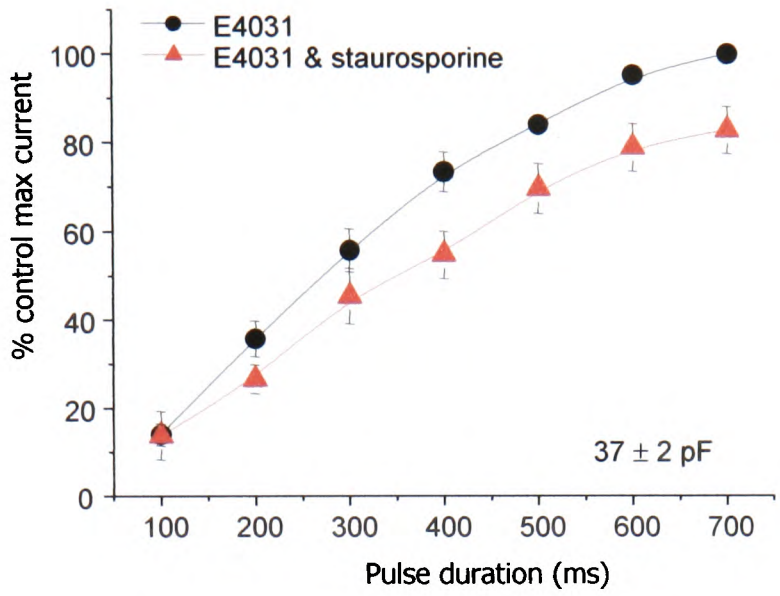

b,

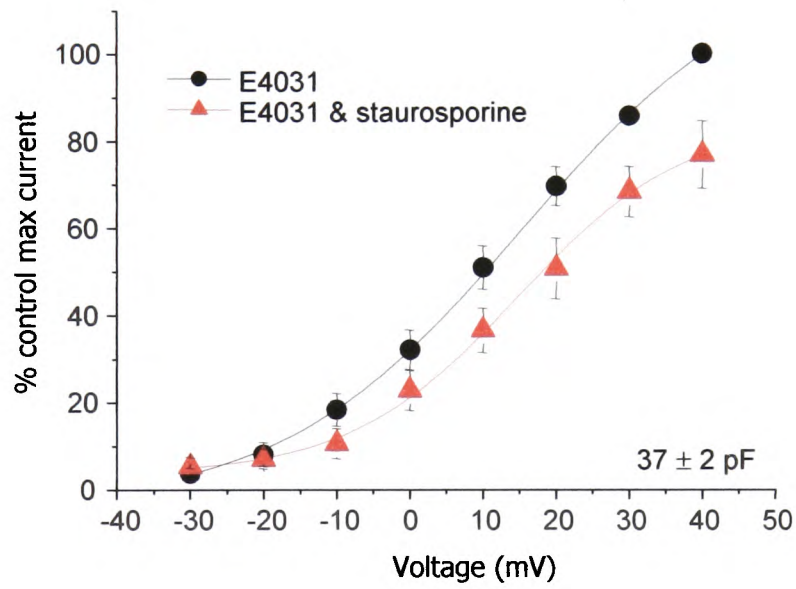

Figure 7.4 Page 296

Staurosporine (300 nM) reduced the amplitude of the current resistant to E4031 (5 μM). In the presence of E4031, staurosporine reduced I_K activated with depolarisation of 200 ms and longer (a), reducing maximal I_K to approximately 80 % of control (n=4, $P<0.05$). The E4031 resistant current was activated in a voltage dependent manner (b) and staurosporine reduced the I_K amplitude at voltages greater than -10 mV(n=5, $P<0.05$), without changing $V_{1/2}$ or activation slope.

a,

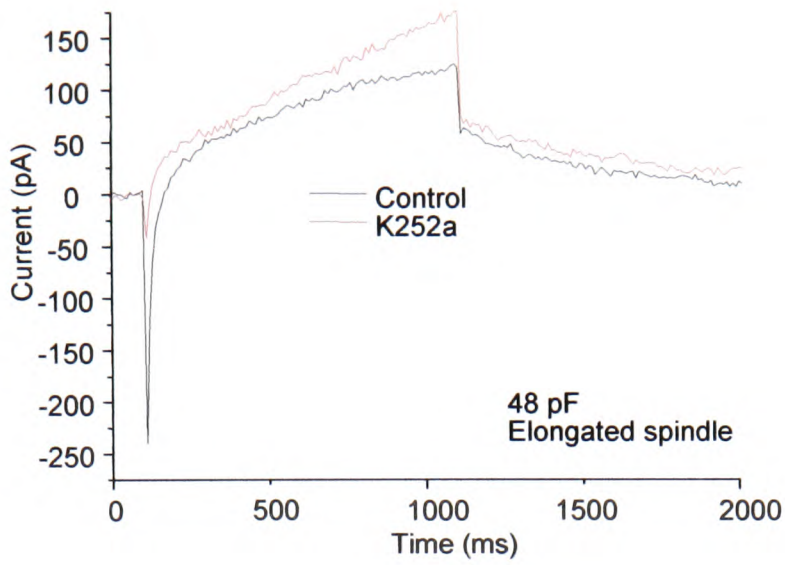

b,

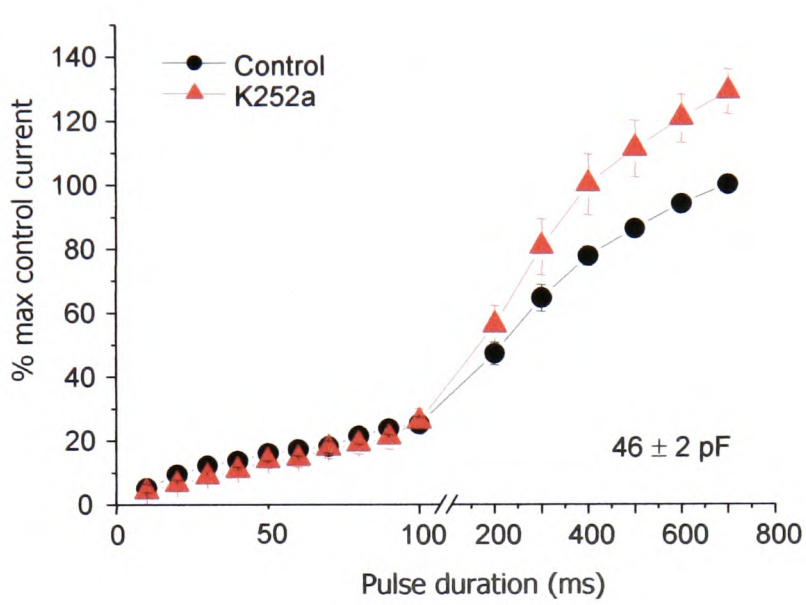

c,

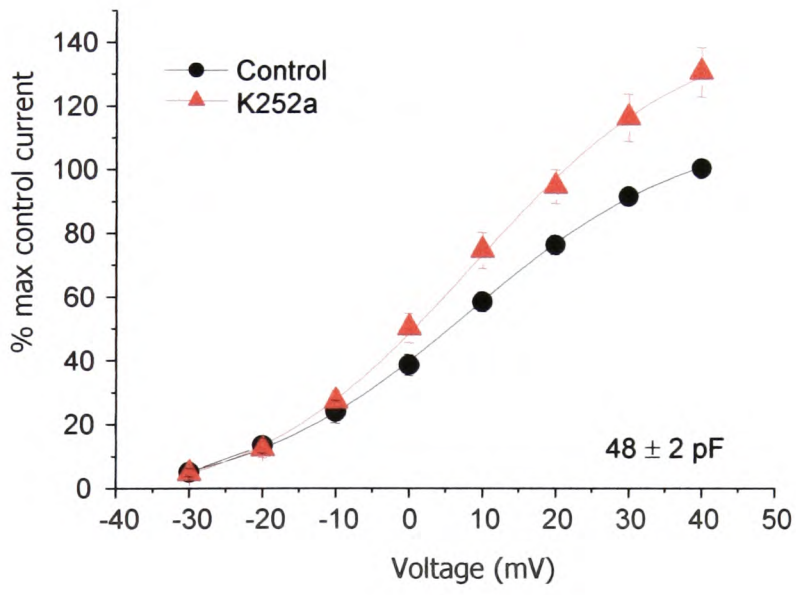

Figure 7.5 Page 297

K252a (250 nM) reduced I_{CaL} activated upon depolarisation, but increased the amplitude of I_K (a). K252a was found to increase the amplitude of I_K activated with depolarisations of 200 ms and longer (n=5, $P<0.05$), but had no effect upon I_K activated with brief depolarisation (b). K252a also increased I_K activated with depolarisation to 0 mV and greater (n=6, $P<0.05$), without altering the $V_{1/2}$ or activation slope of I_K (c).

a,

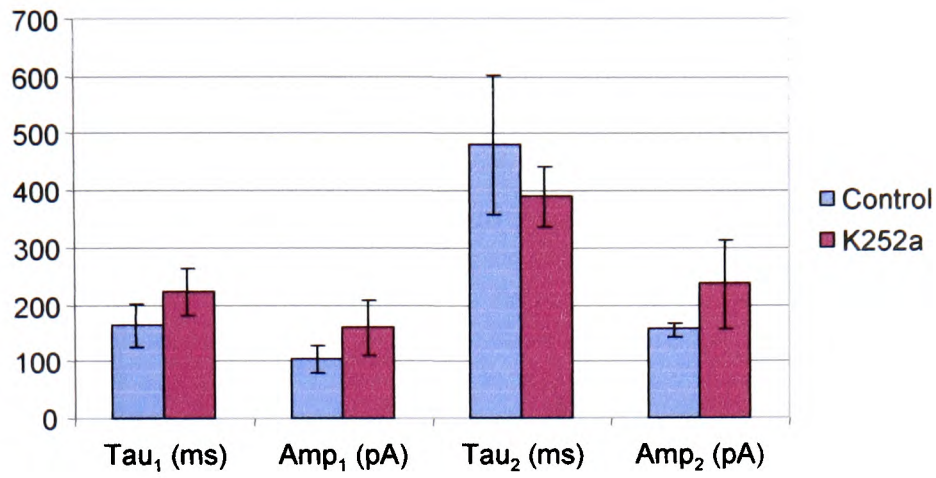

b,

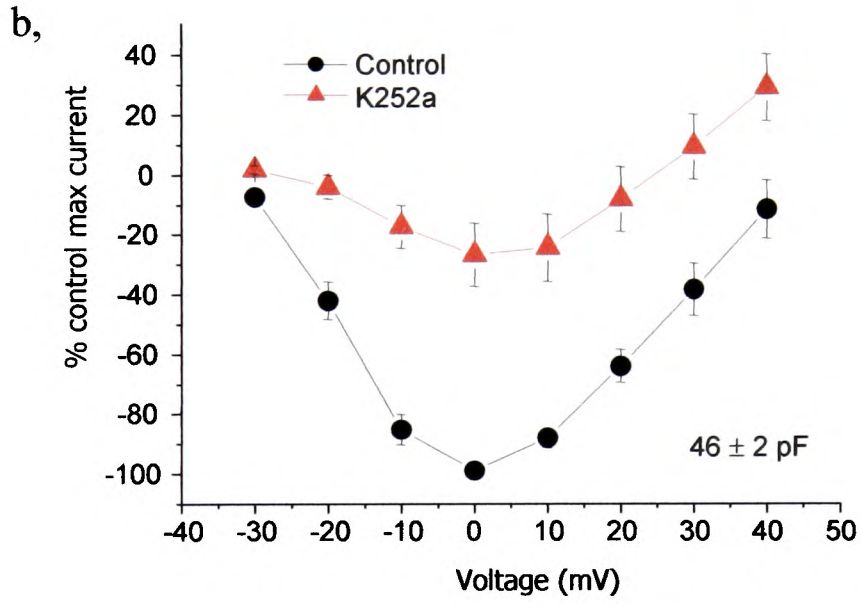

Figure 7.6 Page 298

K252a (250 nM) was found to not effect the kinetics of I_K tail current decay (a, n=6), but a large reduction of I_{CaL} was observed at all voltages tested (n=6, $P<0.05$). K252a did not alter the voltage at which I_{CaL} was maximal (0 mV).

a,

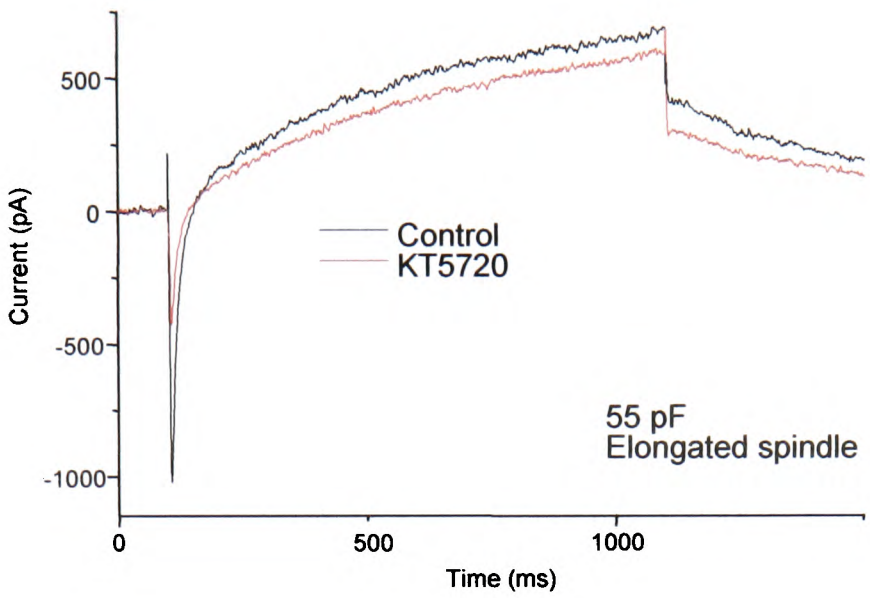

b,

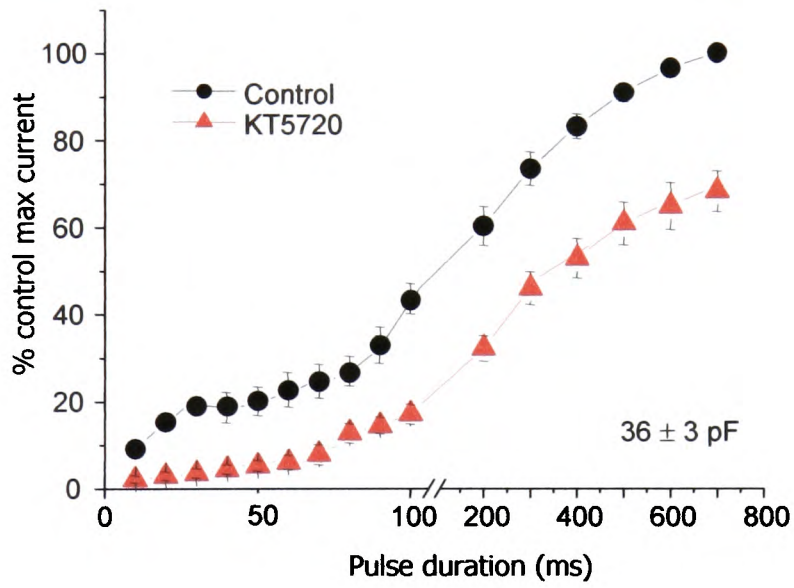

Figure 7.7 Page 299

KT5720 (1 μM) reduced the amplitude of the outward current activated upon depolarisation and the I_K tail current (a). Further investigation identified KT5720 to reduce I_K activated with depolarisation of 10 ms and longer (n=5, $P<0.05$).

a,

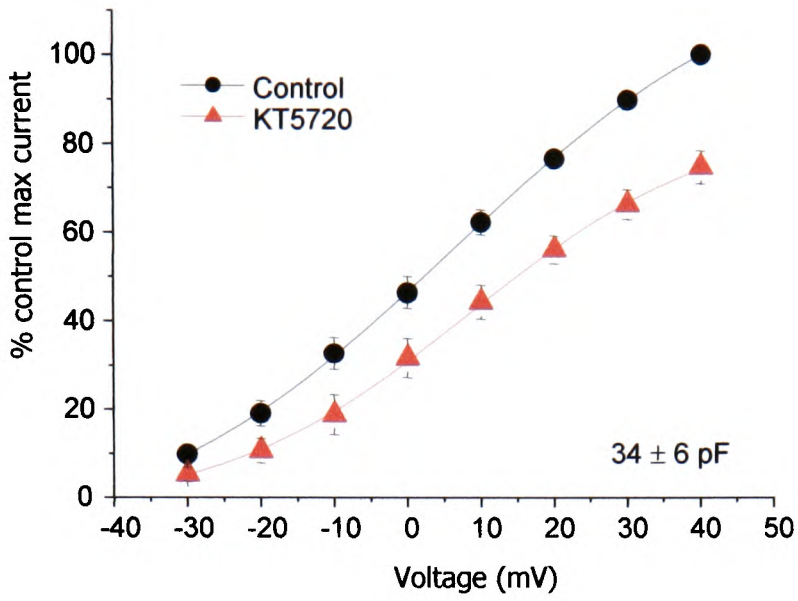

b,

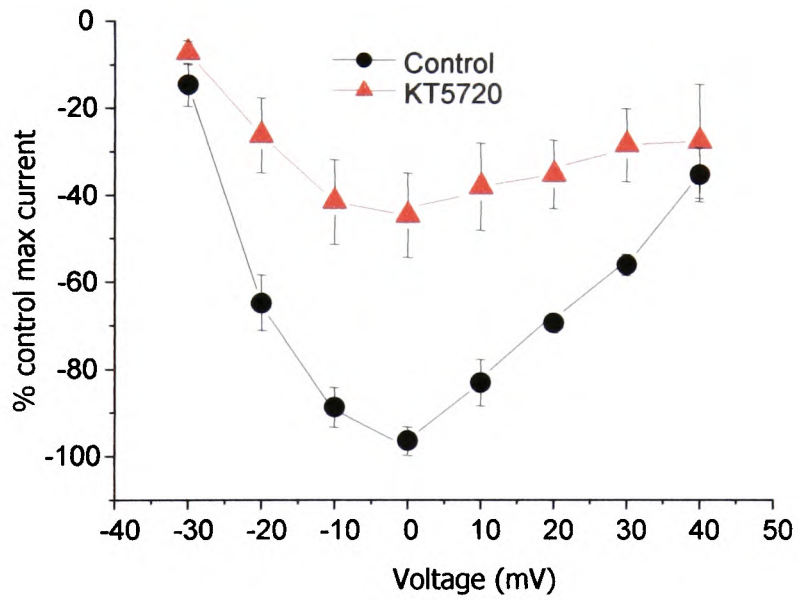

Figure 7.8 Page 300

I_K was voltage-dependently activated over the range -30 to +40 mV and KT5720 (1 μM) was found to reduce the amplitude all voltages (n=5, $P<0.05$), without altering either $V_{1/2}$ of activation slope (a); control 6 ± 3 and 22 ± 6 mV. KT5720 was also found to reduce I_{CaL} amplitude, activated upon depolarisation in the voltage range -20 to +30 mV (n=5, $P<0.05$), without shifting the voltage which activated maximal I_{CaL} from 0 mV (b).

a,

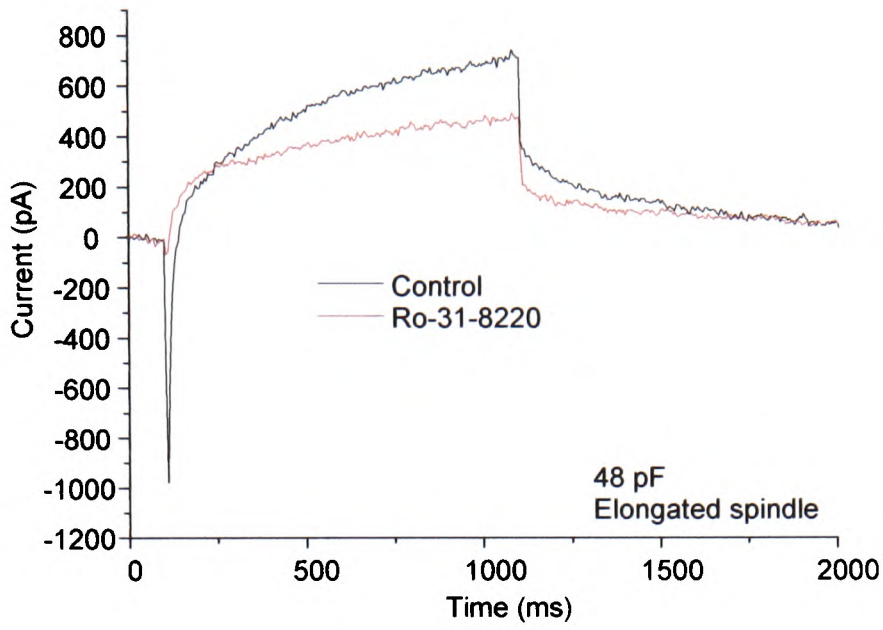

b,

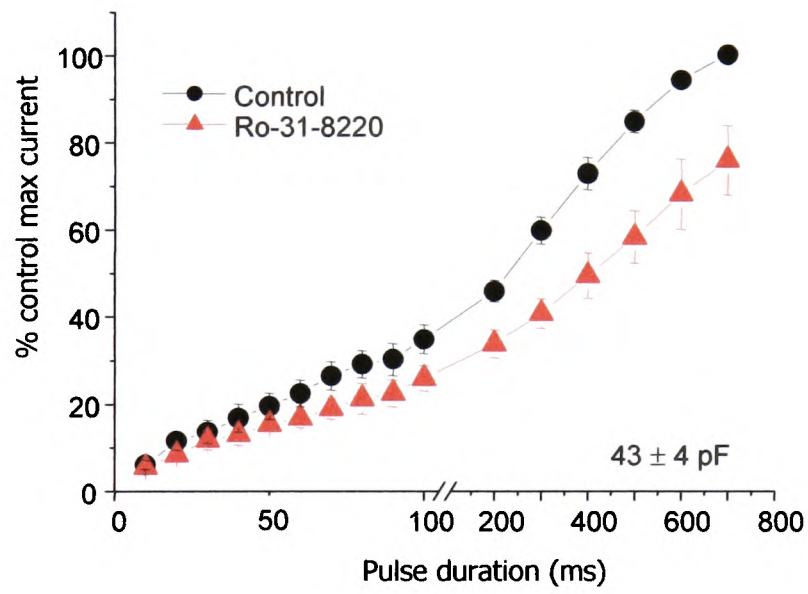

Figure 7.9 Page 301

Ro-31-8220 (50 nM) can be seen to reduce both the initial inward current and the subsequent outward current activated upon depolarisation (a, 1000 ms step to 0 mV). Further study (b) found Ro-31-8220 to reduce I_K activated with depolarisation longer than 40 ms (n=5, $P<0.05$).

a,

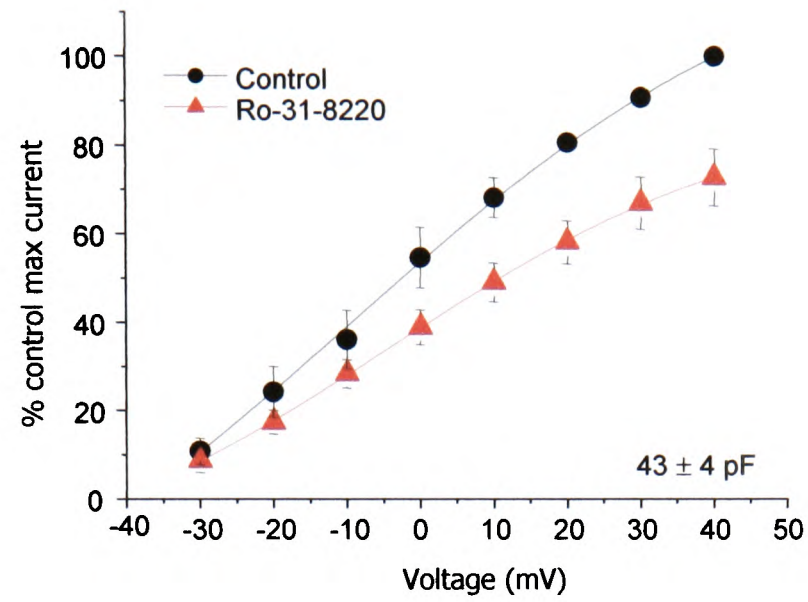

b,

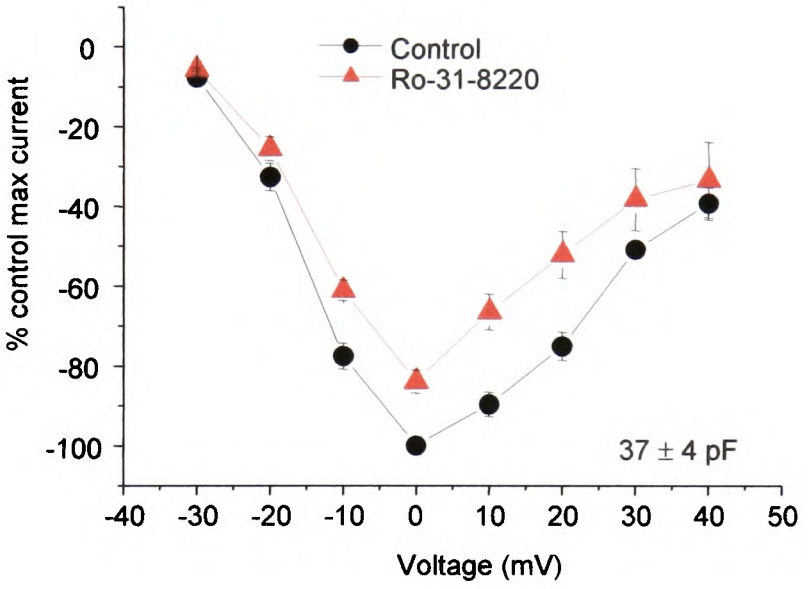

Figure 7.10 Page 302

Ro-31-8220 (50 nM) reduced I_K (a) and I_{CaL} (b), both of which are activated upon depolarisation. I_K activated with depolarisation between 0 and +40 mV was reduced by Ro-31-8220 (n=5, $P<0.05$), without altering the control values of $V_{1/2}$ or activation slope of I_K (a). I_{CaL} amplitude was reduced between -30 and 0 mV by Ro-31-8220 (n=4, $P<0.05$), without altering the voltage which activated maximal I_{CaL} (0 mV).

a,

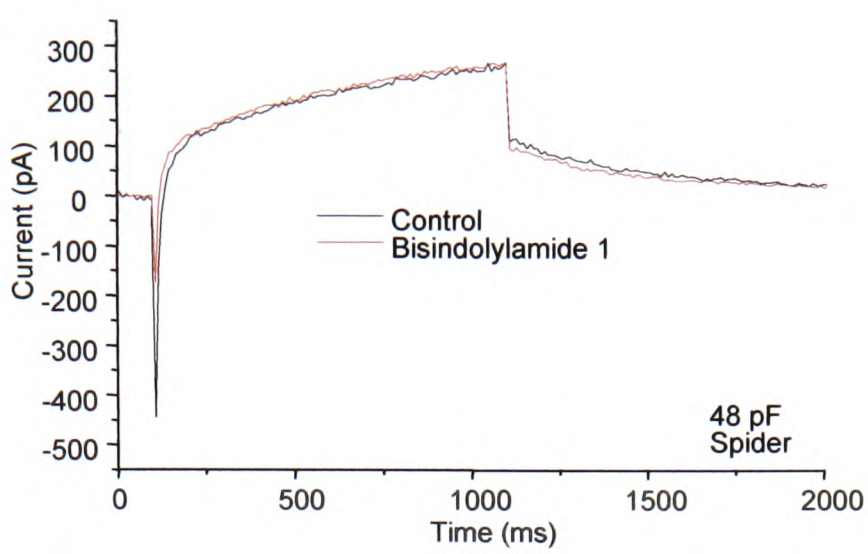

b,

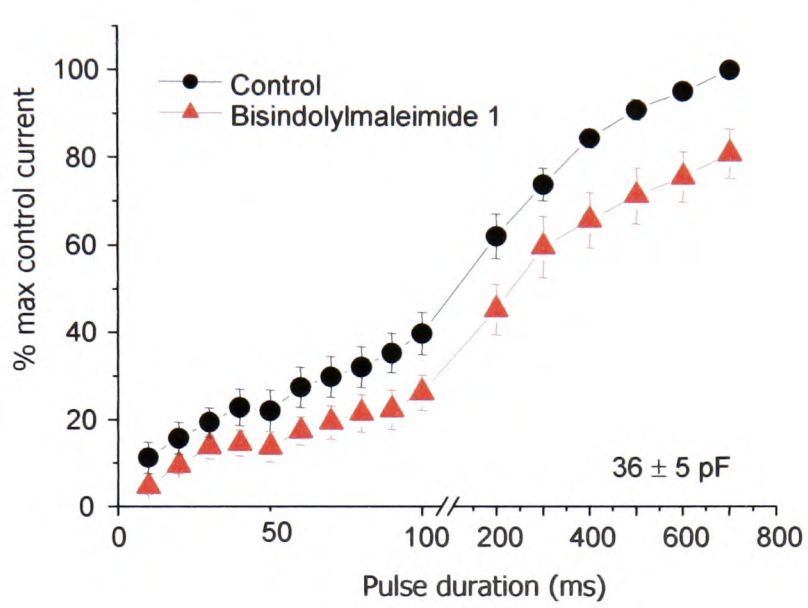

c,

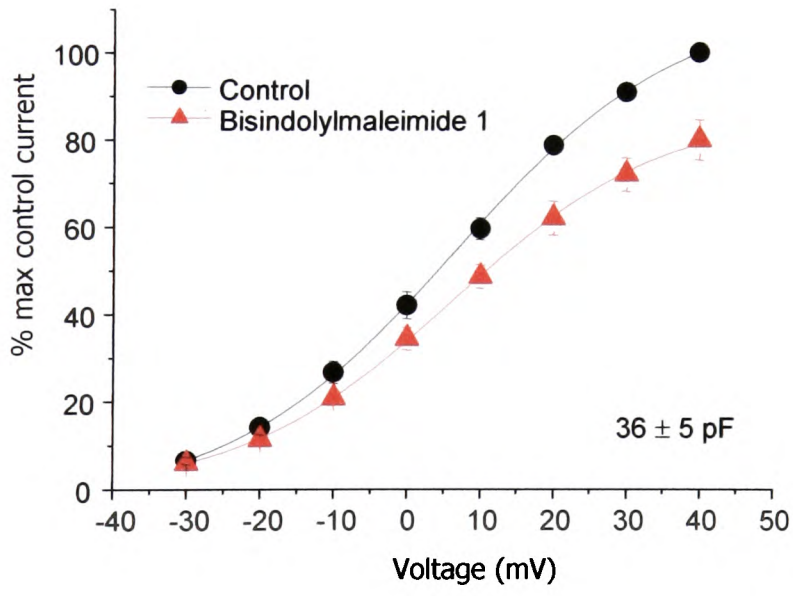

Figure 7.11 Page 303

Bisindolylmaleimide 1 (200 nM) was found to reduce the I_K tail current activated upon depolarisation (a). When bisindolylmaleimide 1 was found to reduce I_K at all duration of depolarisation (b) between 10 and 700 ms (n=8, $P<0.05$). Similarly bisindolylmaleimide 1 reduced I_K activated with depolarisation of -20 mV and greater (n=8, $P<0.05$), without effecting $V_{1/2}$ and activation slope (c).

a,

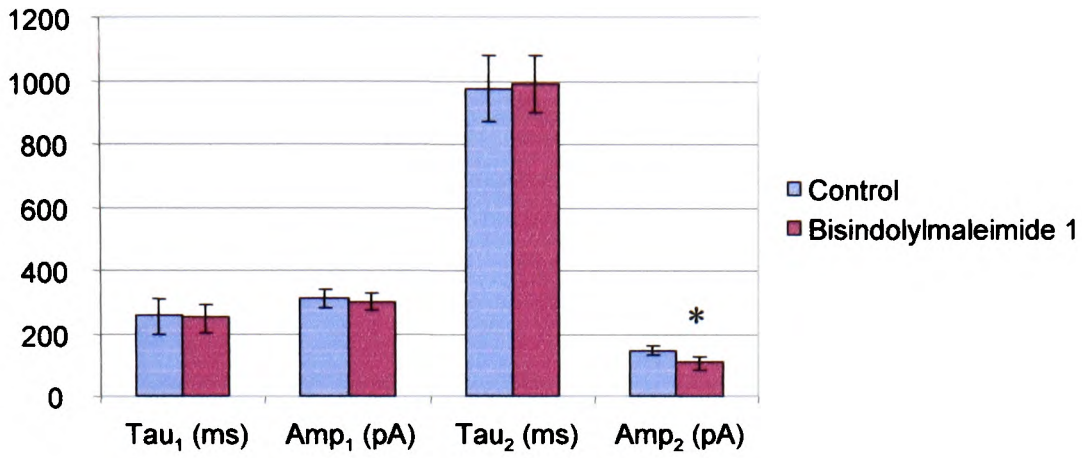

b,

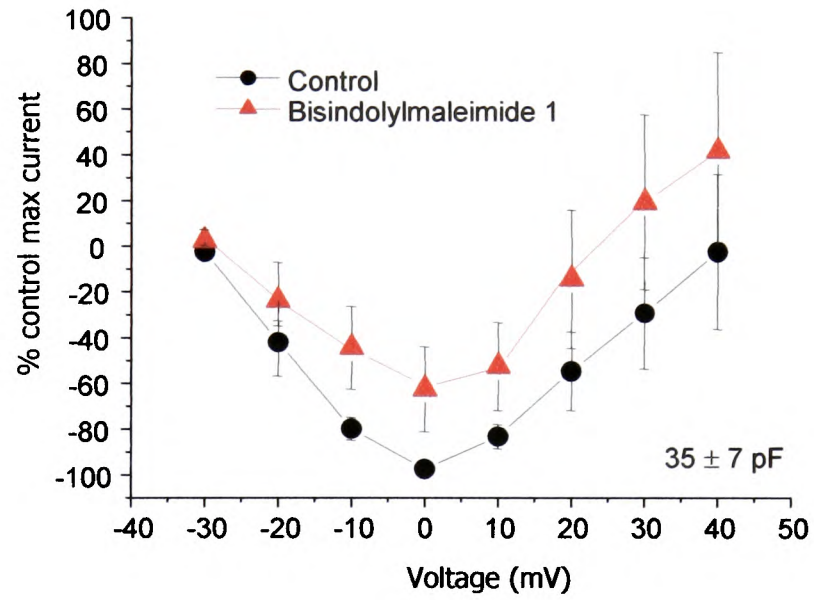

Figure 7.12 Page 304

Bisindolylmaleimide 1 (200 nM) was found to not effect the rate of I_K tail current decay (a), but Amp_2 was reduced (n=6, $P<0.05$). At some voltages (between -10 to 10 mV) bisindolylmaleimide 1 cause a reduction in the amplitude of I_{CaL} (n=6, $P<0.05$), without shifting the voltage which maximally activated I_{CaL} (b).

a,

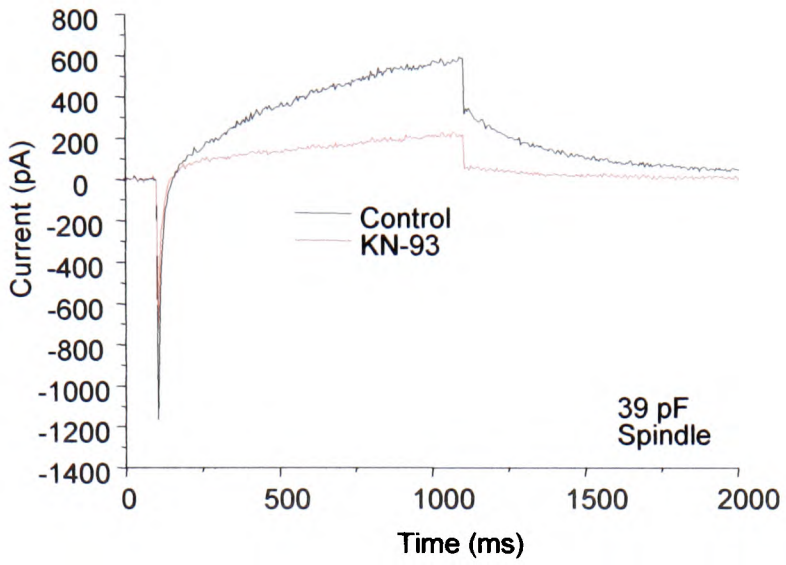

b,

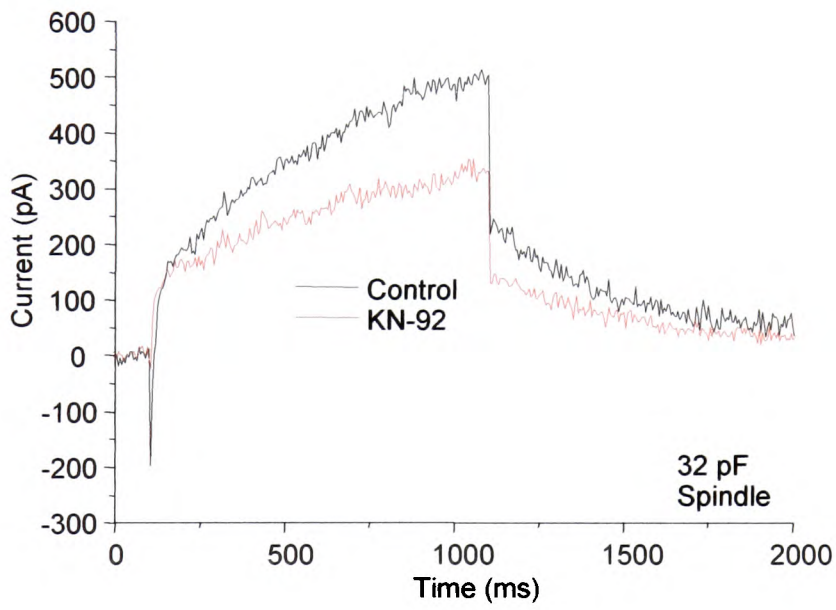

Figure 7.13 Page 305

Both the calmodulin kinase inhibitor KN-93 (a) and a closely related compound KN-92 (b) reduced the amplitude of the outward current (including tail current) activated upon depolarisation. Both KN-93 and KN-92 were used at 1 μM.

a,

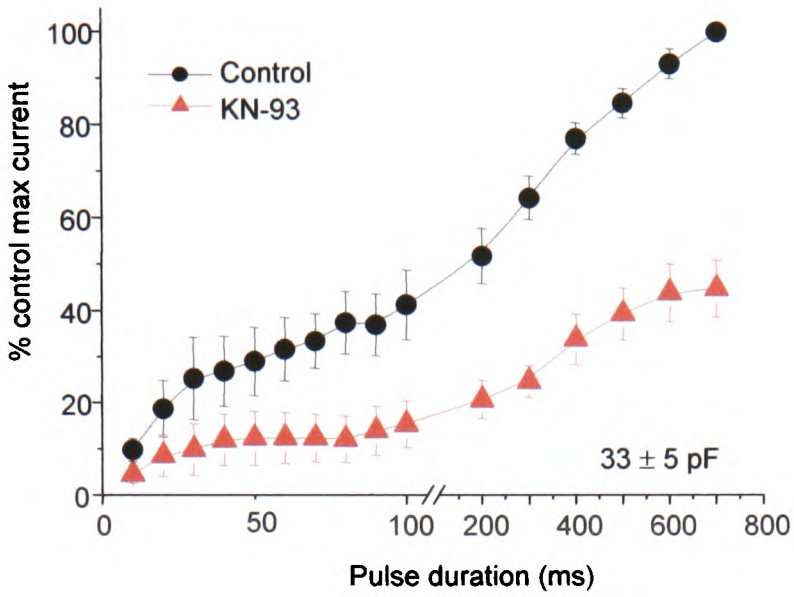

b,

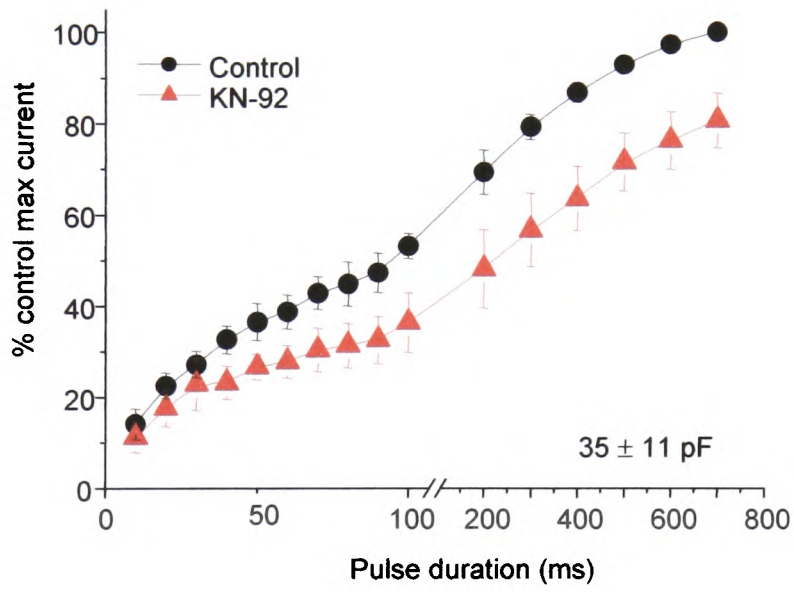

Figure 7.14 Page 306

Both KN-93 (a) and KN-92 (b) tended to reduce the amplitude of I_K activated with any duration depolarisation. Both KN-93 and KN-92 were used at 1 μM. I_K activated with any duration depolarisation was reduced by KN-93 ($n=5$, $P<0.05$), only I_K activated with depolarisation of 50 and 60 ms were reduced by KN-92 ($n=3$, $P<0.05$). Note the large degree of I_K inhibition by KN-93, reducing maximal I_K activated to approximately 50 % (a).

a,

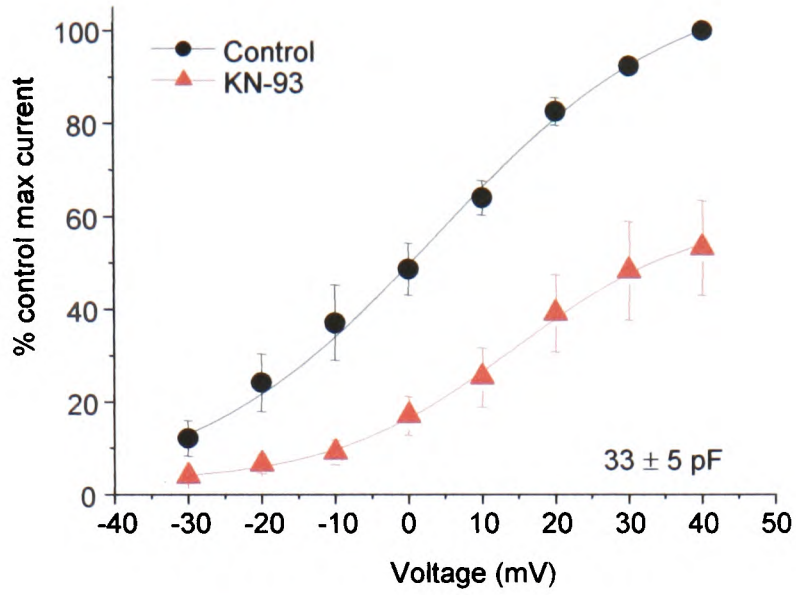

b,

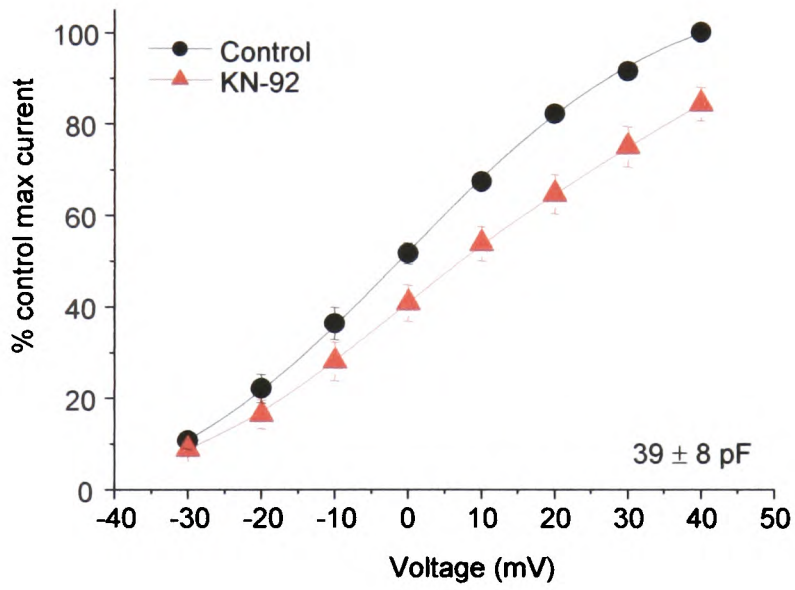

Figure 7.15 Page 307

Both KN-93 (a) and KN-92 (b) reduced the amplitude of I_K activated at various voltages. Both KN-93 and KN-92 were used at 1 μM. KN-93 reduced the amplitude of I_K activated with any voltage depolarisation (n=5, $P<0.05$), and shifted the $V_{1/2}$ from 4 ± 4 to 13 ± 5 mV ($P<0.05$), without changing the activation slope (a). Note the large degree of I_K inhibition by KN-93, reducing maximal I_K activated to approximately 50 % (a). KN-92 reduced I_K activated with depolarisation to -10 mV and greater (n=3, $P<0.05$), without altering $V_{1/2}$ or activation slope (b).

a,

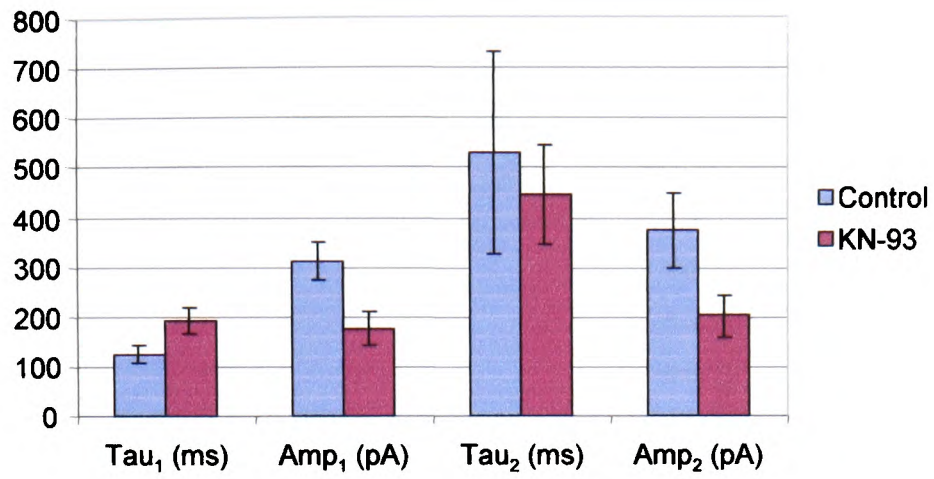

b,

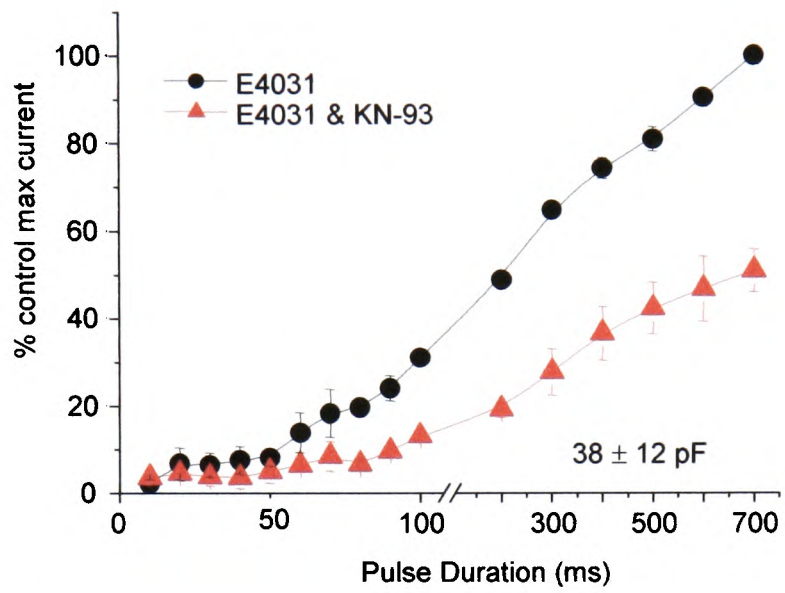

c,

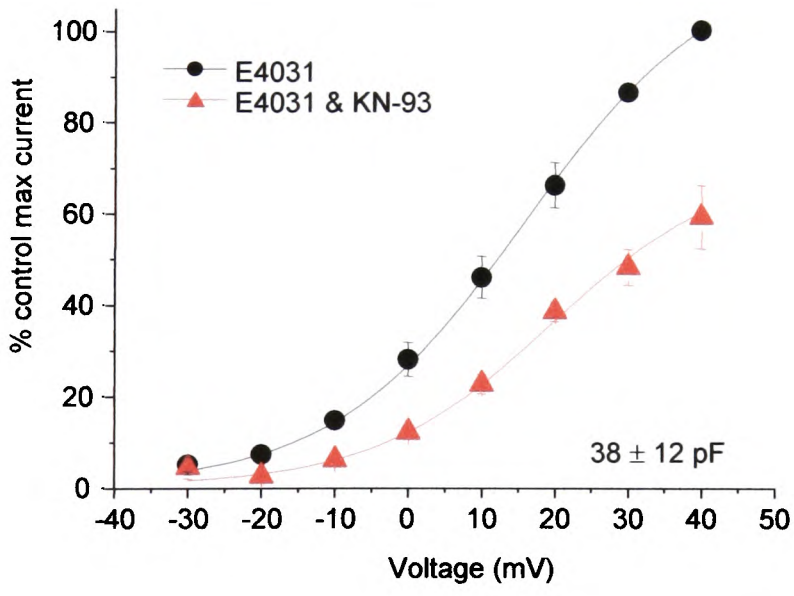

Figure 7.16 Page 308

KN-93 (1 μM) did not alter the time-constants of I_K tail current decay (a), but Amp_2 was reduced (n=6, P<0.05). In the presence of 5 μM E4031, KN-93 reduced I_K activated with depolarisation of 80 ms and greater (n=3, P<0.05), causing a large reduction in I_K similar to that in the absence of E4031 (b). After E4031 exposure, KN-93 reduced the amplitude of I_K activated with depolarisations greater than -20 mV (n=3, P<0.05), without altering the $V_{1/2}$ or activation slope (c).

a,

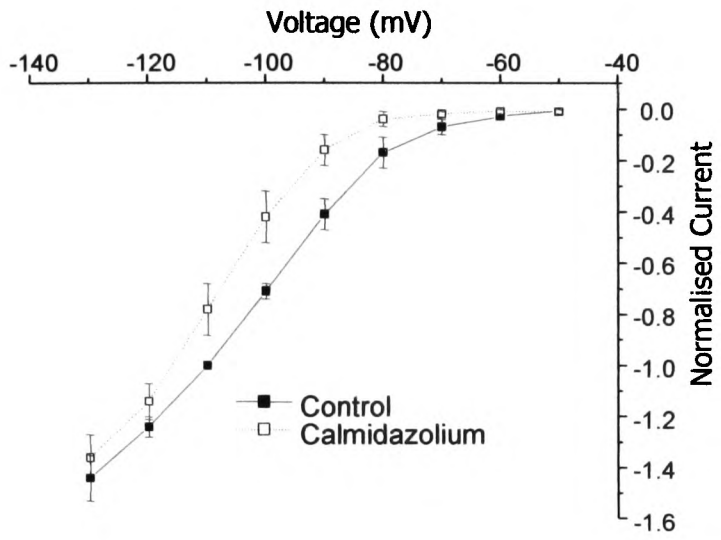

b,

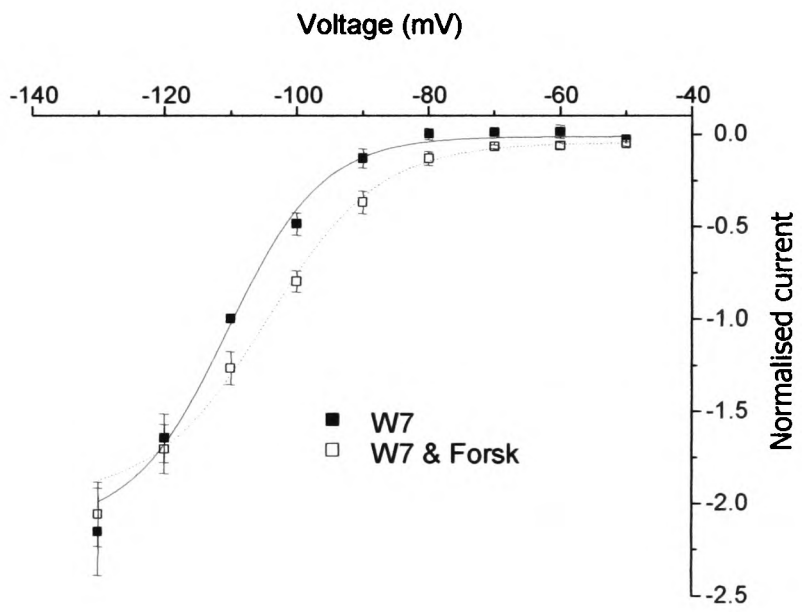

Figure 7.18 Page 310

The calmodulin antagonist calmidazolium (25 μM) shifted the $V_{1/2}$ of I_f from -99 ± 3 to -104 ± 3 mV (n=6, P<0.05), without changing the activation slope of I_f (a). The effect of another calmodulin antagonist W7 (10 μM) causing a negative shift of I_f activation, was partially negated upon addition of 1 μM forskolin (b), which shifted the $V_{1/2}$ by 7 mV to more depolarised voltage (n=6, P<0.05)

Agent	Target	Current	Affect
Staurosporine	Protein kinase	Various	Kinase inhibition reduced I_{Ks} and I_{CaL}
K252a	Protein kinase	Various	Kinase inhibition increased I_{Ks}, but reduced I_{CaL}
KT5720	PKA	Various	PKA inhibition reduced I_K
Ro-31-8220	PKA	Various	PKA inhibition reduced I_K
Bisindolyl-maleimide 1	PKC	Various	PKC inhibition reduced I_K
KN-93	$CaMK_{II}$	Various	$CaMK_{II}$ inhibition cause a large reduction of I_{Kr} and I_{Ks}
Calmidazolium /W7 then Forskolin	CaM	I_f	CaM inhibition shifted I_f $V_{1/2}$ to a more negative voltage, forskolin partially reversed this shift.

Figure 7.19 Page 311

Summary table of findings in this chapter. Stauroporine was used at 300 nM and 3 μM, K252a at 250 nM, KT5720 at 1 μM, Ro-31-8220 at 50 nM, Bisindolylmaleimide 1 at 200 nM, both KN-93 and KN-92 at 1 μM, calmidazolium at 25 μM, W7 at 10 μM and forskolin at 1 μM.

CHAPTER 8: β-adrenergic stimulation

The heart rate is well controlled by the autonomic nervous system (Irisawa, Brown et al. 1993); the parasympathetic prevailing tone slows spontaneous action potential generation, whilst sympathetic stimulation (and circulating hormones such as adrenaline) increase heart rate. The parasympathetic nervous tone is primarily transduced via sarcolemmal muscarinic receptors, whereas sympathetic stimuli employ adrenoceptors.

Stimulation of the adrenergic pathway causes positive inotrophy and chronotrophy; large increases in contraction and rates of beating. Other studies and findings presented previously indicate basal AC turnover in the sino-atrial node (Arch and Newsholme 1976; Defer, Best-Belpomme et al. 2000). This activity would simulate a slight β-adrenergic tone, primarily augmenting the inward currents as mentioned previously in the absence of autonomic stimuli. β-adrenergic agonists modify various ionic channels involved in pacemaking (including increasing I_{CaL}), SR calcium load, but decrease the myofibril calcium sensitivity. These major effects are mediated through the β_1-adrenoceptors, but other subtypes may have some physiological role (Bramich, Edwards et al. 1990; Choate, Edwards et al. 1993). β-adrenergic agonists activate cAMP production (Calaghan, White et al. 1998; Wang and Dhalla 2000) with consequent activation of PKA and phosphorylation of key protein targets (Bers 1993): 1) sarcolemmal ion channels 2) phospholamban 3) troponin. Alterations in the relative contribution of ionic currents during diastolic depolarisation and the action potential modify pacemaking rate. In addition, alterations of other key proteins change the manner in which calcium is handled and the resultant increase in cellular calcium more than compensates for reduced myofibril calcium sensitivity. The adenylate cyclase chapter (page 240) found I_{Kr}, I_{Ks},

I_f and presumably I_{NCX} to be calcium sensitive (Hagiwara and Irisawa 1989; Satoh 1994; Heath and Terrar 2000; Verkerk, Wilders et al. 2002) and identified cAMP modulation of I_{Kr}, I_{Ks}, I_f and I_{CaL} (Emerick and Agnew 1989; Perez-Reyes, Yuan et al. 1994; Xiong, Sperelakis et al. 1994; Cui, Kagan et al. 2001). To effect an increase in beating rate the inward currents (I_f, I_{NCX} and I_{CaL} etc) must be increased relatively more than the repolarising currents (I_{Kr} and I_{Ks}). It is not clear whether the β-agonists induced increase in beating rate is primarily due to increased cellular calcium, or the cAMP/PKA phosphorylation of ionic channels (such as I_{CaL}). The SR has been identified by a number of studies to facilitate the β-adrenoceptor agonist increase in beating rate (Hata, Noda et al. 1996; Rigg and Terrar 1996; Ju and Allen 1999), finding that SR calcium content defined beating rate. The alternate α-adrenergic pathway works via a parallel intracellular pathway and should be briefly mentioned, as α_1-receptors are at a similar density to β_1-adrenoceptors (Benfey 1990; Tohse, Nakaya et al. 1992; Takei, Ikegaki et al. 1999). Calcium is again central and α-adrenergic stimulation increases calcium sensitivity via a pathway involving the conversion of PIP_3 to IP_3 and DAG; IP_3 itself initiates calcium release from stores (Schmitz, Eschenhagen et al. 1991). Autonomic regulation of sino-atrial node cells maybe mediated by a AC/cAMP/PKA pathway resulting in ion channel phosphorylation, or via a more indirect manner utilising SR calcium release, which has not bee fully categorised, but would probably involve the activation of calcium sensitive protein kinases.

GTP-binding proteins were found to have roles in the cellular pathways passing autonomic signals, as both β-adrenergic and muscarinic agonists (isoprenaline and acetylcholine in these experiments) bind to their respective receptors and transmit

most of their cellular message by the release of GTP-binding protein sub-units. There are various GTP-binding protein subunits, but two subunits have opposing effects upon AC after autonomic stimuli activate; isoprenaline activates AC (via G_s), whilst acetylcholine has the opposing effect upon AC, via the inhibitory subunit (G_i). Acetylcholine can also bind directly to I_{KAch} channels, evoking a hyperpolarizing current (Boyett, Kodama et al. 1995; Renaudon, Bois et al. 1997), but both G_s and G_i have more rapid direct effects independent of AC (Yatani, Codina et al. 1987; Yatani, Codina et al. 1987).

Upon β-adrenergic stimulation heart rate is increased and this must by definition be associated with an increased rate of diastolic depolarisation, and therefore a greater amplification of inward ionic currents compared to any augmentation of outward currents. In regard to the inward depolarising currents, isoprenaline has been found to augment the contribution to diastolic depolarisation of I_f (DiFrancesco and Tromba 1987; Renaudon, Bois et al. 1997), I_{CaL} (Kamp and Hell 2000; Mangoni, Couette et al. 2003), I_{St} (Mitsuiye, Shinagawa et al. 2000), I_{NCX} (Perchenet, Hinde et al. 2000) and I_{bNa} (Noble, Denyer et al. 1992). There is at least one inward current which is thought to be unaffected by isoprenaline, as most (but not all) studies have found I_{CaT} to be unaffected by β-adrenoceptor agonists (Tytgat, Nilius et al. 1988). Isoprenaline can augment the role of inward currents during diastolic depolarisation by two major mechanisms; the direct amplification of inward currents, and/or the shifting of voltage dependency to one at which there is more current flowing during the sino-atrial node action potential. I_f and I_{CaL} probably adopt both mechanisms, as I_f activation is shifted to more depolarised potentials, in some cases max amplitude has been found to be increased; the deactivation of I_{CaL} is

shifted, so that the window current is greater, which partially causes the increased I_{CaL} amplitude (Zaza, Robinson et al. 1996). The outward currents affected by isoprenaline are primarily I_{Kr} and I_{Ks}, as the delayed rectifier current is the major repolarising current. I_{Kr} has been described to be augmented in few studies (Kiehn, Karle et al. 1998; Heath and Terrar 2000) and none in the sino-atrial node, however the studies that found I_{Kr} enhancement adopted elegant methods to minimise intracellular dialysis. (Heath and Terrar 2000) found I_{Kr} to be augmented in ventricular myocytes, partially by a reduction in voltage dependent rectification. There is an increase in I_{Ks} amplitude in the presence of isoprenaline, whether this is an effect of the shift in voltage dependency, an increase in the single channel current or an increase in the number of functional channels has not been identified. The relative contribution of I_{Kr} and I_{Ks} to repolarisation has been found to be altered in the presence of β-adrenergic stimulation (Sanguinetti and Jurkiewicz 1991; Sanguinetti, Jurkiewicz et al. 1991). The role of I_{Kr} diminished, indicating a relatively larger increase in the slow component of the delayed rectifier potassium current; this however may be a facet of (Sanguinetti and Jurkiewicz 1991) using conventional patch techniques, therefore not observing I_{Kr} enhancement by isoprenaline. In summary, β-adrenergic stimulation has a net effect of increasing the relative contribution of the depolarising currents, hence increasing the rate of spontaneous action potential generation.

Aims of this chapter

The role of the second messengers cAMP and calcium, which are present at high levels in the guinea-pig sino-atrial node, in the β-adrenergic enhancement will be investigated.

Results

The sympathomimetic agent isoprenaline was used to evaluate the effect of β-adrenergic stimulation upon beating rate of an isolated atrial preparation (including the sino-atrial node). After atrial preparations had developed a stable beating rate (187 ± 2 bpm, n=3), the concentration of isoprenaline ranging from 1 nM to 100 nM was gradually increased in the organ bath. The beating rate of these preparations increased almost immediately (figure 8.1a) and continued to rise in subsequent minutes. The rate of the isoprenaline-stimulated preparation was related to concentration (figure 8.1b); IC_{50} 2 ± 1 nM. The effect upon rate of beating was near maximal with isoprenaline additions of 50 nM and greater; 100 nM isoprenaline caused a 168 ± 6 % of control (n=3, $P<0.05$) increase in beating rate, over 10 minutes to have risen from 188 ± 6 to 315 ± 5 bpm (n=3).

In a similar set of experiments atrial preparations were initially treated with nickel (50 μM), which selectively blocks I_{CaT} and then exposed to the same range of isoprenaline concentrations (1 to 100 nM). 50 μM nickel tended to reduce the beating rate of the atrial preparations (~15 %) of the 2 preparations tested (figure 8.1c). Subsequent exposure to increasing concentrations of isoprenaline caused a concentration dependent increase in beating rate from 148 ± 6 to 264 ± 18 bpm with 100 nM isoprenaline (n=2, $P<0.05$). Note that the maximal 100 nM induced beating rate in the presence of nickel, is not as fast as in the absence of nickel.

The effects of the β-adrenergic agonist isoprenaline upon spontaneous activity of isolated sino-atrial node cells were studied. Sino-atrial node action potentials were recorded from spontaneous cells using the current clamp configuration of the patch amplifier. Isoprenaline has been found to increase the action potential amplitude, repolarisation and beating rate of the sino-atrial node cells (figure 8.2a); overshoot 27 ± 3 mV, most diastolic potential -65 ± 7 mV, action potential amplitude 92 ± 10 mV, beating rate 233 ± 13 bpm, APD_{50} 36 ± 5 ms and APD_{90} 59 ± 8 ms ($P<0.05$, n=3) in the presence of isoprenaline. It should be noted that such stimulation can introduce alternans (see oscillation of the most negative potential in figure 8.2a), a syndrome which is associated with variable SR calcium release and hence variations in action potential amplitude (reviewed by (Blatter, Kockskamper et al. 2003).

In addition to the measurement of these action potential parameters, the 1st derivative of action potential voltage was calculated. The 1st derivative measured the change in voltage against the change in time (dV/dT) and returns a value that describes the rate of voltage change; depolarisation gives a positive term, whilst repolarisation returns a negative value and magnitude describes rate of change in V/s. During control recordings the 1st derivative of voltage varied between –1 and around 5, with a brief peak at 4.3 V/s associated with the fastest period of the action potential upstroke, followed by a slowly developing (-1.1 V/s) trough during repolarisation (figure 8.2b). This trough became deeper as repolarisation progressed, as there was an initial small plateau-like period in this action potential and reduced as the most negative potential was approached. After the most negative potential diastolic depolarisation was attained, a very slow depolarisation, which gives a very slight positive 1st derivative term (~ 0.5 V/s). Isoprenaline (100 nM) accelerates pacemaking and alters various action potential parameters (see above and figure

8.2b). Isoprenaline (100 nM) therefore altered the 1st derivative; the time between each action potential is reduced in isoprenaline, however the general form of events is similar; rapid peak, followed by a progressive trough and then a period of slight positive values. The major difference between control and isoprenaline treated values of 1st derivative are the magnitudes (figure 8.2b). The peak associated with the action potential upstroke returned a much larger dV/dT value, being approximately 12 V/s, which is 227 ± 24 % of control (n=3, P<0.05). This peak appears to be slightly quicker than in control. Repolarisation again appears to be biphasic, with an initial repolarisation of –0.5 to -1 V/s and a ensuing repolarisation phase of –2 to –2.5 V/s; which is 172 ± 16 % of control (n=3, P<0.05). After peak repolarisation, dV/dT falls rapidly to values slightly positive to 0 and diastolic depolarisation maybe seen to occur at a slightly faster rate than in control. The dV/dT depolarisation peak, repolarisation trough and period of gradual depolarisation can all be seen to be abbreviated; this facilitates the isoprenaline-induced increase in sino-atrial node beating rate. The major isoprenaline induced changes in action potentials morphology are summarised in figure 8.2c.

Isolated sino-atrial node cells were voltage clamped and subjected to depolarisation of a range of durations (10-700 ms). The I_K tail current was measured upon repolarisation and two-phases of time-dependent activation were identified; these correspond closely to I_{Kr} and I_{Ks} (Description of I_K and other ionic currents, page 122). A 40 ms depolarisation activated 29 ± 13 pA, whilst a 700 ms depolarisation activated 206 ± 41 pA (n=8) and was defined as the maximal control current. Upon exposure of these sino-atrial node cells to 100 nM isoprenaline, the amplitude of the I_K tail currents was increased (figure 8.3a). The I_K augmentation by

isoprenaline occurred at all duration of depolarisation; 78 ± 13 pA (n=8, P<0.05) and 399 ± 52 pA (n=8, P<0.05) at 40 ms and 700ms respectively. Isoprenaline (100 nM) caused a 194 ± 25 % increase in the maximal control current (n=8, P<0.05). These data indicate that I_{Kr} is increased and imply that I_{Ks} is enlarged by isoprenaline.

These cells were also subjected to depolarisation to various voltages, -30 to +40 mV and the amount of I_K activated was evaluated according to the tail current amplitude upon repolarisation. I_K was voltage dependently activated, having a $V_{1/2}$ of 9 ± 2 mV and a activation slope of 19 ± 7 mV (n=12), being activated more rapidly between –10 and +20 mV, than the extremes of the voltage range, hence was sigmoidal in form. When isoprenaline (100 nM) was included in the superfusing solution, I_K was increased (figure 8.4a), with both the outward current activated during the depolarisation and the tail current upon repolarisation, being substantially increased. I_K was evaluated to be increased by 100 nM isoprenaline at every voltage depolarisation; isoprenaline increased I_K by 203 ± 35 % (n=12, P<0.05), from 283 ± 43 to 571 ± 78 pA at +40 mV (n=12, P<0.05). Isoprenaline shifted the $V_{1/2}$ of I_K voltage dependent activation towards 0 mV (2 ± 1 mV; n=12, P<0.05) without changing the slope of activation (17 ± 3 mV; n=12, P>0.05). I_K appear to progressively activate as the depolarisation was extended in the presence of isoprenaline.

It is apparent from figure 8.3a that there is greater outward current during the depolarisation after the treatment of sino-atrial node cells with isoprenaline. This outward current activates more rapidly in the presence of isoprenaline; this has been quantified over the voltage range –30 to +40 mV using single exponential curve

fitting (Methods, page 60; figure 8.4b). The time-constant of activation were quicken in the presence of isoprenaline when I_K was activated with depolarisation positive to 0 mV; at +40 mV the value was 312 ± 14 ms in control and 244 ± 21 ms in the presence of isoprenaline (n=9, P<0.05). In addition, the amplitude associated with these time-constant was found to be increased by isoprenaline over the same voltage range (figure 8.4c, n=9, P<0.05). The magnitude of increase is similar to that of I_K measured by the tail current amplitude; tail current amplitude was increased by 194 ± 25/203 ± 35 %, whilst activation constant amplitude was 181 ± 20 % of control at +40 mV. Unlike the time-constants of activation, those of I_K tail current deactivation were not altered in the presence of isoprenaline (figure 8.6); 176 ± 24, 811 ± 149 ms in control and 183 ± 25, 851 ± 150 ms in the presence of isoprenaline (figure 8.6, n=12, P>0.05). The time-constants were measured over the voltage range –60 to -10 mV and no alteration was found at any potential (n=12, P>0.05). Similarly to activation, the amplitude associated with these time-constants were augmented by isoprenaline (figure 8.6); Amp_1 from 228 ± 48 to 413 ± 81 pA and Amp_2 from 143 ± 34 to 315 ± 69 pA (n=12, P<0.05). Amp_2 was increased at voltages –60 to -10 mV, whereas Amp_2 were only increased in the voltage range –30 to –40 mV.

An envelope of tails test was used to describe the contribution of I_{Kr} and I_{Ks} in the presence of isoprenaline. This describes the tail current amplitude as a ratio against the outward current activated during the depolarisation, and is plotted with respect to the duration of depolarisation. The ratio was found to be relatively large (>1) after brief depolarisations and gradually become smaller as the depolarisation was prolonged. Isoprenaline treated I_K was found to be similar, overlaying in many points, the control envelop of tails test (figure 8.7, n=10, 6). This indicates that there

are multiple components contributing to I_K in the presence of isoprenaline and that the relative contribution is similar to I_K in the absence of stimulation.

The deactivation of I_K was modelled, as previously described (Description of I_K and other ionic currents, page 122), using the deactivation time-constants describing I_K deactivation upon repolarisation to –60 mV in the presence of isoprenaline. I_K does not decay fully before the activation of the subsequent action potential and an amount of residual decaying I_K tail current will remain and over a period of a few action potentials I_K will accumulate until the system becomes stable. A fast beating rate is simulated in this model, but a beating rate of over 300 bpm was described in isolated atrial preparations treated with 100 nM isoprenaline, so this model is physiologically relevant. The deactivation time-constants of I_K have been found to be 209 ± 18 and 2952 ± 31 ms upon repolarisation to –60 mV in the presence of isoprenaline, having amplitudes of 203 ± 10 and 60 ± 8 pA (n=6). These parameters are used to describe the decay of I_K and 10 action potentials were modelled (figure 8.7). The I_K activated by the simulated action potential did not fully decay before the subsequent I_K activation, and subsequent action potentials contributed more decaying I_K to the outward current; therefore a residual outward I_K developed over the first 10 action potentials was 515 pA (and was in fact still growing). It should be noted that this model is unlikely to be quantitatively accurate, but it does indicate the likelihood of residual I_K contributing to subsequent action potential repolarisation. This residual I_K will influence pacemaking in the presence of isoprenaline.

The I_{Kr} specific inhibitor E4031 (5 μM) was used to eliminate I_{Kr} from the I_K tail current, isolating an E4031 resistant current (almost analogous to I_{Ks}). This E4031 resistant current was measured with a range of depolarisation durations (100-700 ms), with the I_K tail current being quantified upon repolarisation. The E4031 resistant current was found to rapidly increase in amplitude activate with depolarisation briefer than 500 ms, and continue to activate as the depolarisation was extended to the longest duration (figure 8.8a); maximal E4031 resistant current was not activated. Depolarisation of 700 ms activated a 223 ± 18 pA tail current, whereas in the presence of 100 nM isoprenaline the maximal E4031 resistant current was 397 ± 32 pA (n=6, $P<0.05$). The maximal E4031 resistant I_K was increased by 178 ± 13 % and a similar augmentation occurred at all duration depolarisation (n=6, $P<0.05$). The E4031 resistant I_K continued to rapidly activated with depolarisations of 500 ms and longer.

Sino-atrial node cells treated with 5 μM E4031 were subjected to depolarisation to variable voltages (-30 to +40 mV) and E4031 resistant current was measured. The E4031 resistant I_K was voltage dependently activated, having a $V_{1/2}$ of 11 ± 4 mV and a activation slope of 21 ± 8 mV (n=7), being activated most rapidly at voltages above 0 mV. When isoprenaline (100 nM) was introduced, the E4031 resistant current was increased (figure 8.8b); isoprenaline increased E4031 resistant I_K by 149 ± 12 % (n=7, $P<0.05$), from 247 ± 36 to 368 ± 51 pA at +40 mV (n=7, $P<0.05$). Isoprenaline also shifted the $V_{1/2}$ of E4031 resistant I_K voltage dependent activation 9 mV more negative than in control (isoprenaline 2 ± 8 mV; n=7, $P<0.05$), without changing the slope of activation (21 ± 14 mV; n=7, $P>0.05$).

The effects of isoprenaline (100 nM) upon the voltage dependent activation of I_{CaL} were also investigated. In control conditions the inward I_{CaL} was voltage dependently activated, around 0 mV where I_{CaL} was maximal (342 ± 76 pA, n=10). In the presence of isoprenaline however, maximal I_{CaL} was activated at –10 mV (figure 8.9) and was at least double the amplitude at all voltages measured (n=10, $P<0.05$); I_{CaL} was 817 ± 122 pA at –10 mV in the presence of isoprenaline. In addition to an isoprenaline induced increase in amplitude, there was also a quickening of I_{CaL} activation (figure 8.10a). The time taken for the maximal inward I_{CaL} to develop after the depolarisation was recorded in the absence and presence of isoprenaline. The time taken to attain maximal I_{CaL} was recorded and was voltage dependent; at negative voltages the time was relatively long (14 ± 2 ms at –30 mV), but as the depolarisation became stronger, the duration to maximal I_{CaL} became briefer (5 ± 2 ms at +40 mV). A similar relationship was described in when these cells were treated with isoprenaline (100 nM), however the time-taken to attain maximal I_{CaL} was more brief with voltages between –20 and +20 mV (figure 8.10b, n=5, $P<0.05$); for example control duration at 0 mV was 8 ± 1 and in the presence of isoprenaline this value was reduced to 5 ± 0 ms (n=5, $P<0.05$).

I_f was activated by hyperpolarisations to between –50 and –110 mV from a holding potential of –40 mV. I_f was measured as the time-dependently activating inward current (Description of I_K and other ionic currents, page 122). I_f was voltage dependently activated, with activation happening most rapidly between –70 and –110 mV and less extensive at the extremes of the voltage range. The reversal potential of I_f has been previously described in guinea pig sino-atrial node cells (chapter 3.1) and conductance has been used to describe I_f (figure 8.11). The control guinea pig sino-

atrial node I_f $V_{1/2}$ was -97 ± 2 mV and had a slope activation factor of 10 ± 2 mV. Figure 8.11 shows that conductance was enlarged with 100 nM isoprenaline (120 ± 2 % at –110 mV, n=6, P<0.05), voltage dependent activation of I_f is shifted by 9 mV to more depolarised potentials (-88 ± 2 mV; n=6, P<0.01), and extended the slope of activation (13 ± 2 mV; n=6, P<0.05).

The effects of the I_{Kr} specific inhibitor E4031 upon the beating rate of sino-atrial node cells previously exposed to 100 nM isoprenaline were investigated. Action potential amplitude (73 ± 7 to 92 ± 7 mV) and beating rate were increased from 140 ± 8 to 252 ± 3 bpm upon exposure of the sino-atrial node cell to isoprenaline (figure 8.12a) and this became stable after 5 minutes. The inclusion of 5 μM E4031 into the superfusing solution did not appear to alter the beating rate of the isoprenaline treated sino-atrial node cells; 252 ± 3 in isoprenaline and 251 ± 8 bpm in isoprenaline and E4031 (n=3, P>0.05). There also was no alteration in the action potential amplitude (89 ± 2) within 5 minutes or any other parameters; overshoot 27 ± 0 mV, most diastolic potential -61 ± 2 mV, APD_{50} 53 ± 9 ms and APD_{90} 82 ± 10 ms (n=3)

E4031 was used to describe I_{Kr} (the sensitive current) and give a good approximation of I_{Ks} as the resistant current (Description of I_K and other ionic currents, page 122). 6 sino-atrial node cells were exposed to 100 nM isoprenaline before I_{Kr} and I_{Ks} were described in this manner. When pre-treated with isoprenaline the E4301 sensitive current displayed similar time-dependent activation as in control (figure 8.13a); being maximally activated by brief depolarisations (40 ms), and only slightly reduced during depolarisations of 700 ms. The maximal E4031 sensitive

current occurs over a range of duration depolarisation and the currents are expressed as a % maximal current, however the greatest value that E4031 sensitive current attain are approximately 75 %. The isoprenaline treated E4031 sensitive current is actually bigger at the very brief 10 ms depolarisation (n=15, 7; unpaired t-test, $P<0.05$), but at all other duration depolarisation there is no difference in the time-dependent activation. Although the time-dependent activation of I_K was similar, the amplitude of the E4031 sensitive current was larger in the presence of isoprenaline with all duration depolarisations; at 40 and 700 ms E4031 sensitive current was found to be 72 ± 11 and 65 ± 19 pA (n=15), but with isoprenaline treatment these values were 101 ± 17 and 119 ± 34 pA (n=7, $P<0.05$). These data indicate that the amplitude, but not the time-dependent activation of the E4031 sensitive current was modified by isoprenaline.

Isoprenaline did however modify the voltage-dependent activation of the E4031 sensitive current. The E4031 sensitive current has been described in Description of I_K and other ionic currents (page 122) to be rapidly activated by relatively negative depolarisations (-30 to –10 mV) and to display rectification upon depolarisation greater than +20 mV. Upon addition of isoprenaline the voltage-dependent activation of the E4031 sensitive current was found to be very similar to control with depolarisation between –30 and 0 mV, however at more depolarised potentials the current-voltage relationship diverged (figure 8.13b). At these more depolarised voltages the isoprenaline treated E4031 sensitive current continued to activate, although at a much-reduced rate, whereas the control E4031 sensitive current diminished; significantly different at voltages above +30 mV (n=18, 6; unpaired t-test, $P<0.05$). The voltage dependency of the control was described by the $V_{1/2}$,

which was –23 ± 11 mV, with an activation slope of 8 ± 6 mV (assessed between –30 and +20 mV to exclude rectification), however such evaluation of isoprenaline treated E4031 sensitive current fails due to the non-sigmoidal current-voltage relationship. This current is activated strongly at the most negative potentials and voltage dependent activation gradually declines; this is not a sigmoidal relationship. The voltage dependency can be compared to I_K and the E4031 resistant current; I_K $V_{1/2}$ 5 ± 1 and slope 16 ± 1 mV (n=14), E4031 resistant $V_{1/2}$ 15 ± 2 and slope 13 ± 1 mV (figure 8.14, n=10). The E4031 sensitive current activated in the presence of isoprenaline was considerably larger than that of control data at all potentials (n=18, 6; unpaired t-test, $P<0.05$); at +20 mV control E4031 sensitive current was 181 ± 16 pA, whereas this value was 62 ± 15 pA in the presence of isoprenaline (n=18, 6; unpaired t-test, $P<0.05$). Isoprenaline increased the amplitude and reduced the voltage dependent rectification of the E4031 sensitive current.

The time-dependent rectification of the E4031 sensitive current (I_{Kr}) also appeared to be altered in the presence of isoprenaline. E4031 sensitive current recorded during a depolarisation may progressively shrink during the period of depolarisation, this is known as time-dependent rectification (Description of I_K and other ionic current, page 122; figure 8.15a). Tail current amplitude is not normally greater than pulse current. However in the presence of isoprenaline, there were no appearances of time-dependent rectification of the E4031 sensitive current (figure 8.15b) and the tail current often appeared to be of greater amplitude than the pulse current.

Treatment with BAPTA-AM substantially reduced I_K to approximately halve the amplitude of control I_K activated with both brief and prolonged depolarisations (Calcium and the SR, page 209). Buffering of intracellular calcium therefore inhibits I_{Kr} and I_{Ks} (Tohse, Kameyama et al. 1987; Heath and Terrar 2000). In the continued presence of BAPTA-AM (10 μM) sino-atrial node cells were exposed to 100 nM isoprenaline. This caused the amplitude of I_K activated with each duration depolarisation to be augmented (figure 8.16a, n=6, $P<0.05$); BAPTA-AM treated 40 and 700 ms depolarisation induced I_K was 117 ± 12 and 260 ± 34 pA, but upon additional exposure to isoprenaline these values were increased to 145 ± 17 and 507 ± 63 pA (n=6, $P<0.05$). The maximal current activated in the presence of BAPTA-AM was increased by isoprenaline to 195 ± 9 % of control (n=6, $P<0.05$). I_K activated with brief depolarisation was increased in the presence of isoprenaline (in addition to BAPTA-AM), indicating an I_{Kr} amplification, however an additional phase of I_K augmented occurred with more prolonged depolarisations, implying an effect upon I_{Ks}.

BAPTA-AM treated I_K was also investigated in regard to its voltage-dependent activation and the $V_{1/2}$ was found to be +5 ± 2 mV, with a +21 ± 4 mV slope of activation (n=6). The maximal current activated was 312 ± 41 pA (n=6) recorded at +40 mV. Isoprenaline was subsequently included in superfusing solutions and the effect upon I_K recorded (figure 8.16b). Isoprenaline increased the I_K tail current activated with a +40 mV depolarisation to 518 ± 59 pA, 166 ± 6 % of control (n=6, $P<0.05$) and this amplification was apparent at each voltage (figure 8.16b, n=6, $P<0.05$). In addition the voltage dependent activation of I_K was altered, in the

presence of BAPTA-AM the $V_{1/2}$ was +5 ± 2 mV, but after the addition of isoprenaline this had been shifted 11 mV to -6 ± 5 mV (n=6, P<0.05).

The I_{CaL} was also measured in the presence of BAPTA-AM and BAPTA-AM/isoprenaline. The voltage-dependent activation of I_{CaL} was maximal around 0 mV (576 ± 86 pA) and displayed a rough bell-shaped activation curve (figure 8.17b). Upon additional introduction of isoprenaline, I_{CaL} was increased at all voltages and had a maximal effect of increasing I_{CaL} at 0 mV to 258 ± 33 % of control amplitude, measuring 1486 ± 222 pA (n=4, P<0.05). This indicates that the isoprenaline augmentation of I_{CaL} is not calcium dependent.

I_K was measured in isolated sino-atrial node cells were recorded (figure 8.18a), before they were exposed initially to nifedipine, then in the presence of nifedipine and then a nifedipine/isoprenaline concoction. The addition of nifedipine reduced the amplitude of I_K measured all duration depolarisation greater than 10 ms (n=11, P<0.05) as described in Description of I_K and other ionic currents (page 122). Upon additional introduction of 100 nM isoprenaline I_K was augmented, but only when the duration of depolarisation activating I_K was 100 ms or longer (figure 8.18b). 40 and 700 ms depolarisations in the presence of nifedipine activated I_K of 23 ± 4 pA and 180 ± 33 pA, but upon isoprenaline inclusion these magnitudes were 30 ± 5 pA (n=5, P>0.05) and 322 ± 58 (n=5, P<0.05). The maximally activated nifedipine current (700 ms) was increased to 179 ± 22 % (n=5, P<0.05) by isoprenaline. This indicates that I_{Ks}, but probably not I_{Kr}, was increased by isoprenaline in the presence of nifedipine.

The voltage dependent activation of I_K was also studied in the absence of any drugs, with nifedipine and a nifedipine/isoprenaline mixture (figure 8.18c). Nifedipine caused a slight but significant reduction to I_K at all potentials (n=12, $P<0.05$), however isoprenaline subsequent greatly increased I_K. In the presence of nifedipine the $V_{1/2}$ and activation slope were 10 ± 3 and 16 ± 2 mV (10 ± 3 and 14 ± 2 mV in control), and 9 ± 6 and 14 ± 3 mV in the presence of the nifedipine/isoprenaline mixture (n=5, $P>0.05$). In summary, nifedipine did not block the isoprenaline stimulated voltage dependent activation of I_K, although I_K amplitude was diminshed.

I_K is reduced when the SR calcium released is inhibited using 2 μM ryanodine. The role of the SR in the isoprenaline-mediated augmentation of I_K was investigated, by administering ryanodine and then a ryanodine/isoprenaline mixture (figure 8.19a). The currents are normalised to maximal current in the presence of ryanodine, which was 231 ± 43 pA activated with a 700 ms depolarisation (n=5). In the presence of ryanodine, isoprenaline (100 nM) increased the amplitude of I_K activated with depolarisation of 100 ms and longer (figure 8.19b, n=5, $P<0.05$); the 700 ms depolarisation activated isoprenaline treated I_K (in the continued presence of ryanodine), which was 134 ± 6 %, which was equivalent to 310 ± 46 pA. These data indicate that isoprenaline, in the presence of ryanodine, was able to moderately increase I_{Ks}.

Isoprenaline similarly increased the amplitude of I_K in the presence of ryanodine activated at various voltages (-30 to +40 mV), increasing the maximal current recorded at +40 mV from 263 ± 50 to 347 ± 58 pA (n=5, $P<0.05$), an increase

of 132 ± 7 % (figure 8.20a). There was no alteration of $V_{1/2}$ or slope of activation from control values of 5 ± 4 and 23 ± 8 mV (n=5).

The effect of isoprenaline upon I_{CaL} was also investigated in the presence of ryanodine (figure 8.20b). Ryanodine did not alter the voltage dependent activation of I_{CaL}, the maximal current was still activated at 0 mV (181 ± 16 pA). The addition of isoprenaline increased the amplitude of I_{CaL}; maximal I_{CaL} was activated at –10 mV and was increased by 372 ± 79 % to 673 ± 65 pA (n=5, $P<0.05$). I_{CaL} was increased by isoprenaline (in the presence of ryanodine) between –30 and +10 mV (n=5, $P<0.05$). This indicates that isoprenaline does not mediate augmentation of I_{CaL} via SR calcium release.

The AC inhibitor MDL reduced I_{Kr}, with possible additional effects upon I_{Ks} (Adenylate cyclase, page 240). When MDL (10 μM) treated sino-atrial node cells were subsequently exposed to isoprenaline, there was a slight increase in I_K activated with both brief and prolonged depolarisations (figure 8.21a), which at 700 ms was of 132 ± 5 % (n=5, $P<0.05$). The augmentation maybe primarily of I_{Kr}, reversing the MDL mediated reduction. An increase in voltage dependent activation of I_K was also observed when sino-atrial node cells continuously superfused with MDL, where exposed to isoprenaline (figure 8.22). The effect of isoprenaline upon the maximal amplitude was not particularly large at +40 mV, 212 ± 34 to 259 ± 43 pA (figure 8.22b, n=4, $P<0.05$). However the $V_{1/2}$ was shifted in the presence of isoprenaline (in addition to MDL) from 4 ± 1 to -7 ± 8 mV (n=4, $P<0.05$) and the activation slope altered from 15 ± 1 to 21 ± 12 mV (n=4, $P>0.05$). Note that the activation of I_K at –

30 and –20 mV was surprising large in the presence of MDL and isoprenaline, compared to MDL treated I_K activated at these voltages.

MDL almost abolished I_{CaL} (Adenylate cyclase, page 240), however isoprenaline was able to relieved the MDL-inhibition of I_{CaL} voltage dependent activation; I_{CaL} was enlarged by isoprenaline from 83 ± 18 to 346 ± 86 pA (417 ± 131 %) at –10 mV by isoprenaline in the presence of MDL (n=4, $P<0.05$). I_{CaL} has normally been maximally activated at 0 mV, but maximal I_{CaL} was activated in both situations by depolarisations to –10 mV (figure 8.22b).

Discussion

Autonomic regulation of heart rate is fundamental to effective circulation. Parasympathetic tone dominates the innervation of the sino-atrial node, lowering the heart rate by low concentration release of acetylcholine. Such acetylcholine concentrations inhibit AC (via muscarinic receptors), reducing cellular cAMP; causing a negative shift of I_f and reducing PKA mediated phosphorylation of I_K (Tohse, Kameyama et al. 1987; Heath and Terrar 2000), I_{CaL} (Perez-Reyes, Yuan et al. 1994; Hartzell, Hirayama et al. 1995). Parasympathetic stimuli alter the contribution of ionic currents to pacemaking, to favour the outward repolarising currents and hence delay spontaneous action potential generation. Higher concentrations of acetylcholine can directly open I_{KAch}, which act as flood gates to the potassium concentration gradient, resulting in rapid membrane hyperpolarisation to the reversal potential of potassium (Description of I_K and other ionic currents, page 122) and hence quiescence (figure 8.23).

The alternate arm of the autonomic nervous system mediates the fight or flight response, by the activation of β-adrenoceptor by noradrenalin or circulating hormones. Isoprenaline mimics these actions by activating cardiac β-adrenoceptors and the down-stream intracellular cascades. As many groups before, isoprenaline was found to concentration-dependently increase beating rate of sino-atrial node cells (Giles, Nakajima et al. 1989; Lei, Brown et al. 2000), in this case to approximately 175 % of control rates in both atrial preparations (315 bpm) and isolated sino-atrial node cells (252 bpm). The rate of diastolic depolarisation was not measured in this study, but the trend of the 1st derivative of voltage to be slightly more steep in that phase can be observed (figure 8.2b). (Rigg and Terrar 1996) found this to be significant, as isoprenaline increased the rate of diastolic depolarisation was increased by isoprenaline (100 nM) from 2 ± 0 (this value was approximately 2 ± 1 in this study) to 4 ± 1 V/s.

Isoprenaline was found to increase the most diastolic potential and the overshoot of the sino-atrial node action potential, as previously described by Brown and Difrancesco (1980), Lei, Brown et al (2000). This results in an amplification of action potential amplitude. It should be considered that the more negative voltages in the presence of isoprenaline may increase the number of I_{Na} channels (if present) which are recovering from voltage dependent inactivation each diastolic period. This could result in the more rapid upstroke of the action potential in the presence of isoprenaline being a result of the increased recruitment of I_{Na}. There is however no evidence for the presence of I_{Na} in the guinea-pig sino-atrial node cells, unlike those from other species (Mangoni, Couette et al. 2003). The rapid polarisation of the membrane is brought about by activation of inward I_{CaL} (for depolarisation) and outward I_K (for repolarisation); extensive isoprenaline augmentation of these currents

could underlie the more positive overshoot and more negative most diastolic potential. The rate of polarisation is certainly increased, which would fit with I_{CaL} and I_K augmentation, as the 1st derivative of voltage indicates increase polarisation rates approximately 225 and 175 %. Sympathetic stimulation reduces action potential duration, to facilitate a higher beating rate, as the relative duration of action potential to the end of diastole remains stable.

During sympathetic stimulation sino-atrial node cells (and all cardiac cell types) can experience a situation called alternans; this presents itself as variability in action potential amplitude, as can be seen in figure 8.2a. This observation is due to variable SR calcium release (Blatter, Kockskamper et al. 2003), causing rapid alterations of the ionic currents involved in defining action potential amplitude. This state is not pathophysiological, but may be associated with SR calcium overload and therefore can deteriorate *in vivo* into development of after-depolarisations. Alternans also indicates that rapid variations in SR calcium release have large effects upon sino-atrial node action potential, indicating calcium sensitive regulation of ion channels.

Some groups have found the isoprenaline augmentation of beating rate to be dependent upon aspects related to the calcium handling. Vinogradova, Bogdanov et al (2002) found local SR calcium release events (sparks) to be increased by isoprenaline, when these sparks where inhibited by ryanodine, isoprenaline did not increase beating rate (even in the presence of I_{CaL} enlargement). I_{CaT} maybe involved in this process as I_{CaT} activated during diastolic depolarisation causes a local increase of calcium near the SR that may cause calcium sparks, activate I_{NCX} and promote depolarisation (Huser, Blatter et al. 2000). When I_{CaT} was blocked with low concentration of nickel, beating rate was reduced (Description of I_K and other ionic currents, page 122), but upon subsequent isoprenaline addition, beating rate was

similarly increased. I_{CaT} has therefore been found to have a role in pacemaking (Huser, Blatter et al. 2000), however this can be surpassed by β-adrenoceptor activation, which appears to not alter I_{CaT} in pacemaking (Tytgat, Nilius et al. 1988).

The relative contribution of the components of the delayed rectifier potassium current have been investigated in the presence of isoprenaline, as previous literature indicates that I_{Ks} may have a greater role during β-adrenoceptor activation (Sanguinetti and Jurkiewicz 1991; Lei, Cooper et al. 2002). The beating rates of isoprenaline pre-treated sino-atrial node cells were found to not be effected by the blockade of I_{Kr}, presumably indicating only a minor (if any) role for I_{Kr} in pacemaking during β-adrenoceptor stimulation (Sanguinetti and Jurkiewicz 1991). It should be considered that the I_{Kr} specific blocker E4031 has been reported to be less effective in the presence of isoprenaline (Heath and Terrar 1996); still the role of I_{Kr} must be substantially less in the presence of isoprenaline.

As previous studies described (Giles, Nakajima et al. 1989; Sanguinetti and Jurkiewicz 1991; Heath and Terrar 1996) and the action potential data indicated, I_K was enhanced by isoprenaline. Augmentation of this outward current could of facilitated the increased rate of sino-atrial node action potential repolarisation and subsequent enhanced negativity of the most diastolic potential. The rate of I_K activation was accelerated (at least the depolarisation activated outward current) at positive potentials, which would abbreviate the isoprenaline-treated action potential. Therefore both amplitude and rate of I_K activation are altered by isoprenaline to maximise outward current. Lei and Brown (1996) identified a 10 mV negative shift in the voltage-dependent activation of I_K in rabbit sino-atrial node cells (without alteration of slope), which closely parallels the 8 mV shift finding by this study in guinea-pig sino-atrial node cells. Unlike the study by Lei, Brown et al (2000), no

quickening of I_K deactivation was observed upon treatment with isoprenaline (Heath and Terrar 1996). All studies identified an isoprenaline-induced increase in I_K amplitude. If I_K deactivation quickened, the inward currents would become more dominant earlier in diastolic depolarisation and thus increase the rate of spontaneous action potential generation; absence of this observation brings this hypothesis into question and suggests a relative augmentation of inward currents. An additional consideration is that Lei et al used 20 nM isoprenaline, whereas (Heath and Terrar 1996) and this study used 100 nM; a difference in isoprenaline sensitivity of I_K components, which define the decay constants, maybe an alternative explanation.

In the working model of I_K decay (Description of I_K and other ionic currents, page 122), the residual I_K during a train of action potentials is predicted; lingering I_K develops due to incomplete decay of I_K from the preceding action potential. In this model the heart rate is simulated to be 300 bpm, which is within the range described upon β-adrenoceptor agonism, and the deactivation of I_K was that recorded upon repolarisation of I_K to –60 mV in the presence of isoprenaline; Tau_1 1209 ms and Tau_2 2952 ms. When these parameters were factored into the model, the residual I_K (the minimum I_K flowing after 10 action potentials) was found to be > 0.5 nA. This is a very large current, as currents as small as 3 pA are thought to have a role in pacemaking when not stimulated (DiFrancesco 1991). This could easily be an underestimation of residual I_K, as the model system does not appear to be at equilibrium after 10 action potentials; the basal I_K is still rapidly increasing. The limitations of this model should be recognised, as it is developed from very basic parameters, however a large residual I_K component may well play a part in isoprenaline stimulated pacemaking.

Using the perforated patch configuration of patch clamp, both I_{Kr} and I_{Ks} have been found to be augmented by isoprenaline (figure 8.3) This is a similar finding to that of forskolin activation of AC, causing I_{Kr} enhancement (Heath and Terrar 2000) Description of I_K and other ionic currents, page 122). Few groups have identified the enhancement of the rapid component of I_K, as previous less elegant techniques disturb the cytosolic composition to a greater degree (Sanguinetti and Jurkiewicz 1991; Heath and Terrar 1994; Lei and Brown 1996). I_{Ks} appears to be more ruggedly modulated by isoprenaline and all previous studies have therefore identified enlargement (Sanguinetti and Jurkiewicz 1991; Lei and Brown 1996). The relative contribution of I_K components in the absence of stimulation has identified a dual role in sino-atrial node (Anumonwo, Freeman et al. 1992), whereas in rabbit I_K is predominately I_{Kr} (Lei and Brown 1996). Upon adrenergic stimulation the relative contribution of I_{Kr} and I_{Ks} alters, favouring the more slowly activating component (Sanguinetti and Jurkiewicz 1991; Lei, Cooper et al. 2002) and therefore increasing the role of I_{Ks} in the action potential repolarisation (see above). However previous studies may have confused this situation by using techniques that would not have registered the isoprenaline enhancement of I_{Kr}. The envelope of tails test indicated that there were still two (or more) I_K components in the presence of isoprenaline, and that the relative contribution of these components (to time-dependent activation of I_K) appeared similar to that recorded in control conditions. This is an indication of similar enhancement of I_{Kr} and I_{Ks} by isoprenaline.

More direct evidence of I_{Ks} enlargement by isoprenaline was acquired in the presence of I_{Kr} inhibition. The delayed rectifier potassium current resistant to E4031, effectively I_{Ks} was found to activate at positive voltages and only with prolonged depolarisations; similar to the voltage and dependent activation of I_{Ks} described

previously (Sanguinetti and Jurkiewicz 1991; Lei, Cooper et al. 2002). The E4031 resistant delayed rectifier current was increased by isoprenaline, causing a 9 mV negative shift in the voltage dependent activation and 80 % increase of this current activated with prolonged depolarisation. The shift in the voltage dependent activation of I_{Ks} transforms this component to one that would be activated more effectively in a sino-atrial node action potential. I_{Ks} is larger than I_{Kr} in guinea pig sino-atrial node (Anumonwo, Freeman et al. 1992; Lei, Cooper et al. 2002) and is activated in a similar voltage range in the presence when stimulated by isoprenaline, and so the large I_{Ks} could swamp the relatively small I_{Kr} component.

The E4031 sensitive current (I_{Kr}) is rapidly activated (as measured by the tail current) and then the amplitude becomes relatively stable as depolarisation is prolonged. This relationship is not altered in the presence of isoprenaline, however the E4031 sensitive current is substantially larger. The increase in amplitude by isoprenaline maybe partly due to the reduction in the voltage and time-dependent rectification (figure 8.13b, 9.15; (Heath and Terrar 1996)); I_{Kr} would be increased at depolarised voltages and prevent dwindling during the action potential. The removal of the negative current-voltage relationship of I_{Kr} at positive potentials (voltage dependent rectification) by isoprenaline, has found to be mediated by the calcium dependent inhibition of C-terminal rectification of the ERG protein (Heath and Terrar 1996). Calcium is vital for I_{Kr} enhancement by isoprenaline, probably indicating a calcium dependent kinase activity being involved in the removal of I_{Kr} voltage dependent rectification. Removal of rectification may augment I_{Kr}, however the current was enlarged at all voltages and so channel phosphorylation induced amplification was also involved (Brum, Flockerzi et al. 1983; Heath and Terrar 1996).

β-adrenergic agonist have for a long time been known to increase the amplitude of I_{CaL} in various cardiac myocytes (Reuter and Wollert 1967; Brum, Flockerzi et al. 1983; Trautwein and Kameyama 1986; Tanaka, Clark et al. 1996) and this study finds this to be the case in sino-atrial node cells. Peak I_{CaL} was more than doubled by isoprenaline. The voltage of maximum I_{CaL} activation was shifted to a slightly more negative potential by isoprenaline (figure 8.9), as has been previously described (Brum, Flockerzi et al. 1983; Brum, Osterrieder et al. 1984; Trautwein and Kameyama 1986). I_{CaL} enhancement has previously been found to be determined by a shift in voltage dependent deactivation, increasing the window current (Brum, Osterrieder et al. 1984), where calcium passes through I_{CaL} between activation and deactivation. The time-course of I_{CaL} activation was also accelerated by isoprenaline (Brum, Osterrieder et al. 1984), quicken the time to reach max I_{CaL} after depolarisation is initiated. All the above effects of isoprenaline tend to enhance the amplitude of I_{CaL}. In the presence of isoprenaline PKA would be activated, with subsequent phosphorylation of phopsholamban and I_{CaL} (Osterrieder, Brum et al. 1982); the calcium handling of the sino-atrial node would therefore be altered. Calcium handling (especially SR calcium release) appear to have an important role in sino-atrial node pacemaking (Rigg, Heath et al. 2000). The positive chronotrophic effect of isoprenaline (and other β-adrenoceptor agonists) was originally postulated by (Brown and Difrancesco 1980) to be caused by calcium current amplification, in association with a shift in I_f voltage-dependency. It appears that I_{CaL} although vital in all action potentials, does not define the rate of beating; however the role of I_f is still contentious. Isoprenaline (and forskolin) have been found to shift the voltage-dependent activation of I_f to more physiological voltages (this study; (DiFrancesco and Tromba 1987; Renaudon, Bois et al. 1997), via stimulation of cAMP production,

which directly interacts with the HCN channel. There is also probably an AC tone in sino-atrial node cells (Adenylate cyclase, page 240) which would physiologically increase the importance of I_f during normal pacemaking, by shifting the $V_{1/2}$ to more depolarised voltages. Specific inhibition of I_f reduced beating rate of isolated cells by ~15 % (Description of I_K and other ionic currents, page 122), this indicates a role (but not a large one) in normal pacemaking. Upon adrenergic activation I_f would be enhanced by the increased cellular cAMP, and the enhanced most negative potential (see above) would activate additional I_f, therefore increasing the relative contribution of inward I_f to pacemaking (DiFrancesco 1987; DiFrancesco 1991).

The buffering of cytosolic calcium has been found to severely reduce the amplitude of both I_{Kr} and I_{Ks} (chapter 4;(Tohse, Kameyama et al. 1987; Walsh, Arena et al. 1991). This study used the AM ester of BAPTA to load the sino-atrial node cell with calcium buffer and identified I_K inhibition in excess of 50 % (Calcium and the SR, page 209). The speed and effectiveness of BAPTA to reduce calcium in the sub-sarcolemmal domain, where the calcium sensitive ionic channels will be regulated should be questioned, as local concentrations around cytosolic release sites (both on the sarcolemma and the SR) will be very high (Verheijck 2000). BAPTA did however significantly reduce the amplitude of both I_K components, and upon subsequent exposure to isoprenaline definitely increased I_{Ks} and probably I_{Kr} (figure 8.16). Isoprenaline treatment was associated with a 9 mV shift in the voltage dependent activation of I_K and a significant amplification. These data imply both components of I_K to be sensitive to cytosolic calcium concentration, with isoprenaline augmentation to be slightly reduced compared to control, hence implying an isoprenaline augmentation partially dependent upon calcium. Calcium buffering did not reduce I_{CaL} amplitude, indicating cytosolic calcium concentration to not effect

I_{CaL}. I_{CaL} exhibits calcium dependent inactivation, however the very high local concentration around the channels upon activation, may not be effectively buffered by BAPTA. Upon exposure to isoprenaline of BAPTA pre-treated sino-atrial node cells, I_{CaL} was increased to a similar degree as in the absence of cytosolic calcium buffering. There was however no alteration in the voltage that activated maximum isoprenaline enhanced I_{CaL} in the presence of BAPTA. This indicates that I_{CaL} is insensitive to cytosolic calcium and is augmented by isoprenaline in a calcium independent manner; this correlates with the many reports of PKA phosphorylation of I_{CaL} (Osterrieder, Brum et al. 1982; Perez-Reyes, Yuan et al. 1994; Kamp and Hell 2000).

An alternative mechanism to reduce cellular calcium is to eliminate sarcolemmal calcium entry pathways, such as the L-type calcium channel. I_{CaL} is associated with a brief inward current upon depolarisation and can fully blocked by nifedipine. The addition of nifedipine reduced I_K, however this is thought to be due to a reduction in cellular calcium (as I_K is calcium sensitive), rather than a direct inhibition. An additional consideration is that I_{CaL} is thought to act a trigger for the release of SR calcium (Bers 1993), so when the I_{CaL} trigger is blocked, SR calcium release maybe inhibited/abolished. In the continued presence of nifedipine block of I_{CaL} (and hence depressed SR calcium release), isoprenaline was found to only effect I_{Ks}. There was an absence of isoprenaline amplification of I_{Kr}, and the effect upon I_{Ks} (in the presence of nifedipine) was of reduced amplitude compared to control. This indicated that I_{Kr} is augmented by a nifedipine sensitive mechanism, but it is at this point unknown whether this is directly related to I_{CaL} or via SR calcium release. I_{Ks} amplification by isoprenaline also appears to be primarily mediated by a calcium dependent mechanism.

Further investigation of the I_K effects of isoprenaline when trigger calcium (I_{CaL}) is not blocked, but the SR calcium release is inhibited with ryanodine. When SR calcium release is inhibited, only the slow component of I_K is reduced (Rigg and Terrar 1996), with no effect upon I_{Kr} or I_{CaL} being observed. Isoprenaline increased the ryanodine pre-treated I_{CaL}, similarly to previous exposure to nifedipine, shifting the voltage of maximal activation to a slightly more negative potential and causing enlargement greater than 100 % (Vinogradova, Bogdanov et al. 2002). The effects of isoprenaline upon I_K were severely reduced in the presence of ryanodine, as isoprenaline also caused only a slight increase of I_{Ks} (130 %) and had no effect upon I_{Kr} (figure 8.19). The large majority of I_K augmentation by isoprenaline can therefore be attributed to a SR dependent pathway. Calcium has been identified to modulate I_K (Calcium and the SR, page 209; (Tohse, Kameyama et al. 1987; Tohse, Kameyama et al. 1990), with most of the studies indicating the involvement of a calcium sensitive kinase, such as PKC or calmodulin kinase (Walsh and Kass 1988; Tohse, Kameyama et al. 1990; Nitta, Furukawa et al. 1994). The amplitude of I_K maybe closely related to the beating rate of the sino-atrial node, as isoprenaline augmentation of rate has also been found to be a SR dependent process (Hancox and Levi 1994; Rigg and Terrar 1996; Huser, Blatter et al. 2000; Lipsius, Huser et al. 2001).

Sino-atrial node cells are thought to have an intrinsic turnover of AC, and hence cAMP production, in the absence of any stimulation (Adenylate cyclase, page 240). When the AC inhibitor MDL is used to reduce cAMP production, I_{CaL}, I_f, I_{Kr} but not I_{Ks} were reduced in amplitude (Adenylate cyclase, page 240). In these investigation MDL was present at all times (so AC was inhibited), but then isoprenaline was introduced into the system; this caused an increase in all the currents (I_f was not measured) that MDL previously reduced (not I_{Ks}). I_{CaL} has been found to

be regulated by PKA and so I_{CaL} enhancement upon the reversal of the MDL inhibition of AC by isoprenaline, replenishing cellular cAMP levels, should be expected. A similar argument for I_{Kr} enhancement can be applied, indicating that in the absence of stimulation the inherent cAMP production enlarges I_{Kr}. There maybe some I_{Ks} enhancement by isoprenaline in the presence of MDL, however there is little confidence from these findings; this however in some ways makes some sense. MDL did not reduce the amplitude of I_{Ks}, although the effects upon I_{Kr}, I_f and I_{CaL} indicate that cAMP concentration was reduced; this implies I_{Ks} is not regulated by these low concentrations of cAMP (and presumably PKA). MDL reduces AC turnover, however isoprenaline would have to compete to increase cAMP production, possibly resulting in a cAMP level not dissimilar to control. This could explain the effect upon I_{Kr}, but not I_{Ks}, with isoprenaline in the presence of MDL.

There are a number of studies which have found I_{Ks} to be regulated by the calcium sensitive PKC (Walsh and Kass 1988; Tohse, Kameyama et al. 1990), however SR calcium dependent modulation of I_{Kr} has also been identified in this study. The calcium released from the SR may however take part in other intracellular pathways, other than PKC activation such as CaM and CaMK activation, which appear to have large roles in ion channel regulation. AC has been found to be calcium regulated (Luthi and McCormick 1999; Rigg, Mattick et al. 2003) and so inhibition of SR calcium release could reduce I_{Kr}, via a reduction in cAMP production and therefore PKA activation. I_{Ks} does not appear to be regulated by the low concentrations of cAMP, but is augmented by isoprenaline in a SR dependent manner, which maybe related to the SR calcium activation of PKC and CaM (Walsh and Kass 1988; Vinogradova, Zhou et al. 2000; Mamas and Terrar 2001).

a,

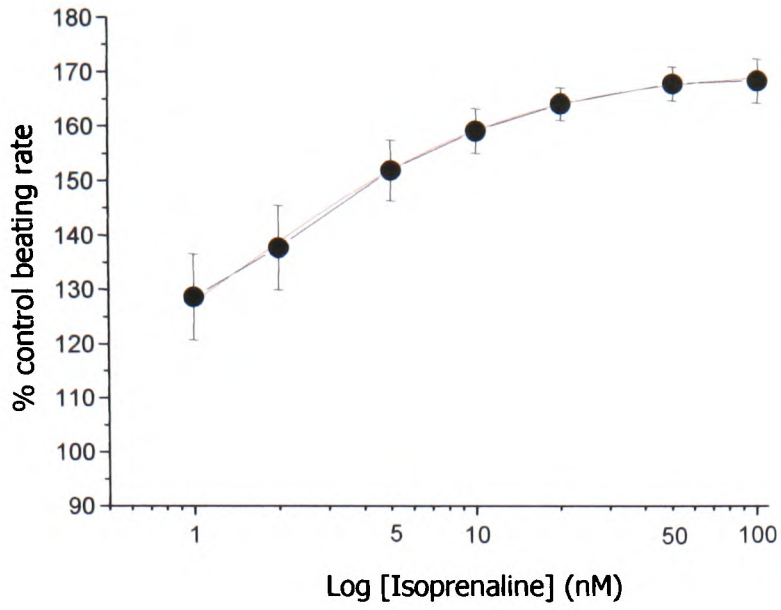

b,

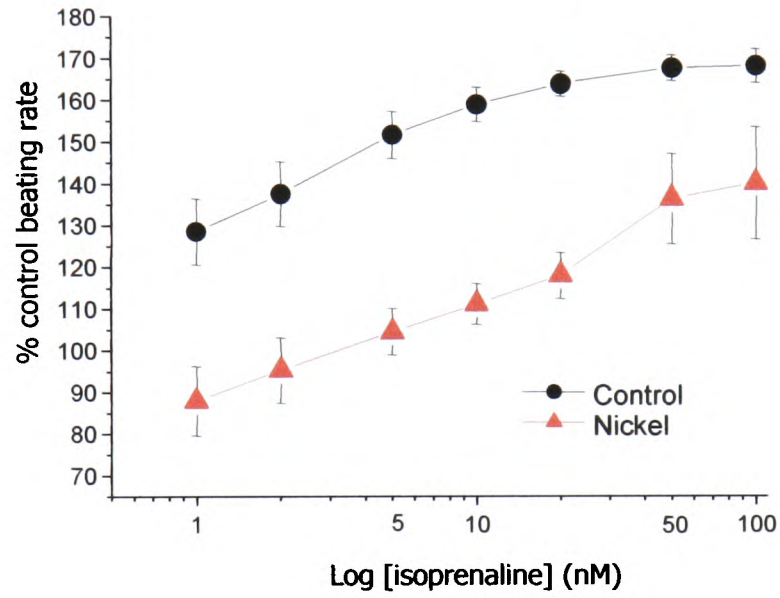

Figure 8.1 Page 343

Isoprenaline (1-100 nM) increased the beating rate of isolated atrial preparations (a), with an IC_{50} of 2 ± 1 nM (n=3). Although 50 μM nickel reduced the beating rate of atrial preparations, it did not prohibit the isoprenaline mediated increase in beating rate (b); 100 nM isoprenline increased beating rate from 187 ± 2 to 315 ± 5 bpm (n=3, $P<0.05$), whereas the same isoprenaline concentration increased nickel pre-treated atrial preparations from 148 ± 6 to 264 ± 18 bpm (n=2, $P<0.05$).

a,

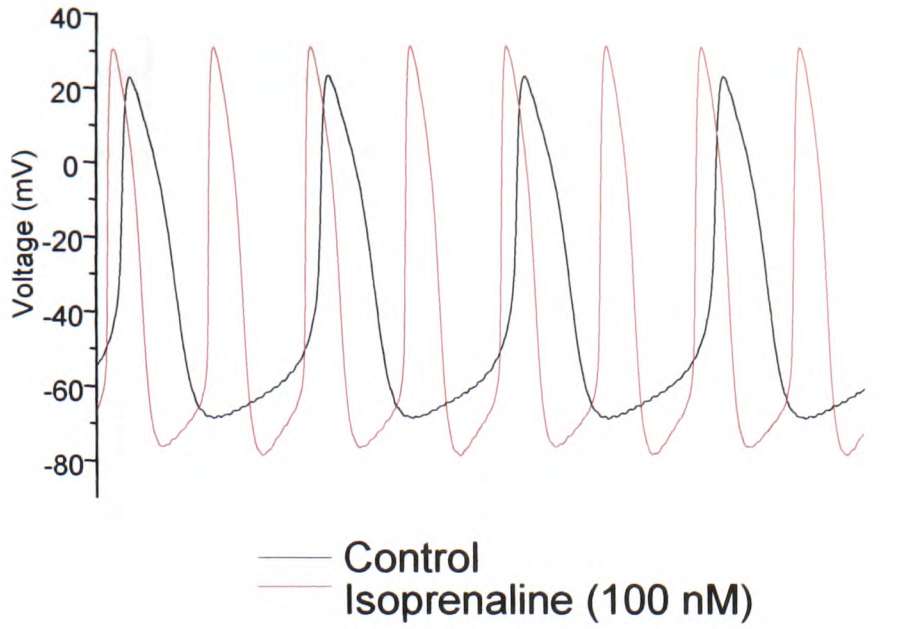

b,

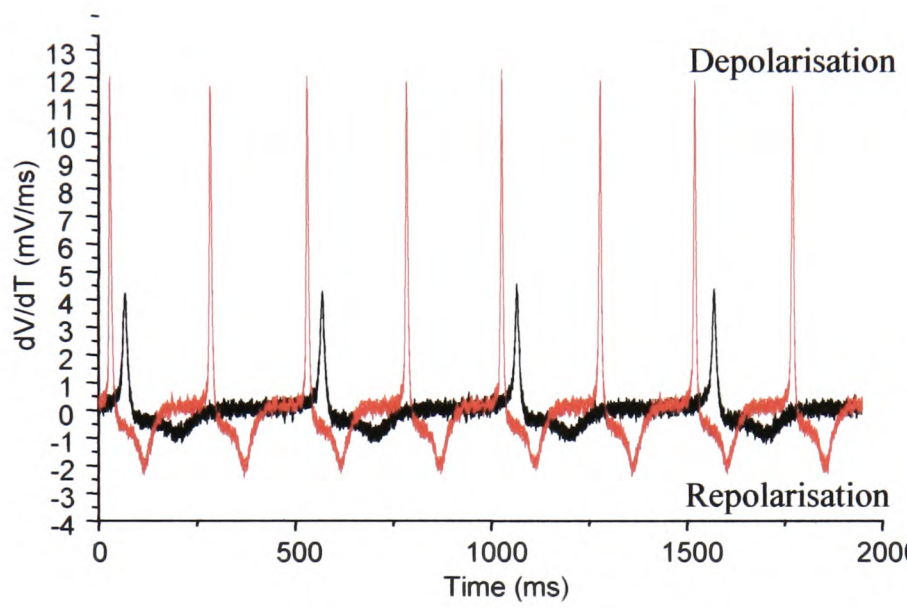

c,

	Rate (bpm)	MDP (mV)	% dV/dT max	OS (mV)	% dV/dT min
Control	144 ± 13	-55 ± 7	100 ± 0	18 ± 3	100 ± 0
Isoprenaline	233 ± 13	-65 ± 7	227 ± 24	27 ± 3	172 ± 16

Figure 8.2 Page 344

Isoprenaline (100 nM) increased the rate of spontaneous action potential generation of isolated sino-atrial node cells (a) and increased various action potential parameters (b and c). The 1st derivitive of voltage was mathematically calculated in the absence and presence of isoprenaline. Various action potential parameters were measured (c) and were found to all be different after the addition of isoprenaline (n=3, $P<0.05$); MDP most diastolic potential, dV/dT 1st derivitive of voltage, OS overshoot.

a,

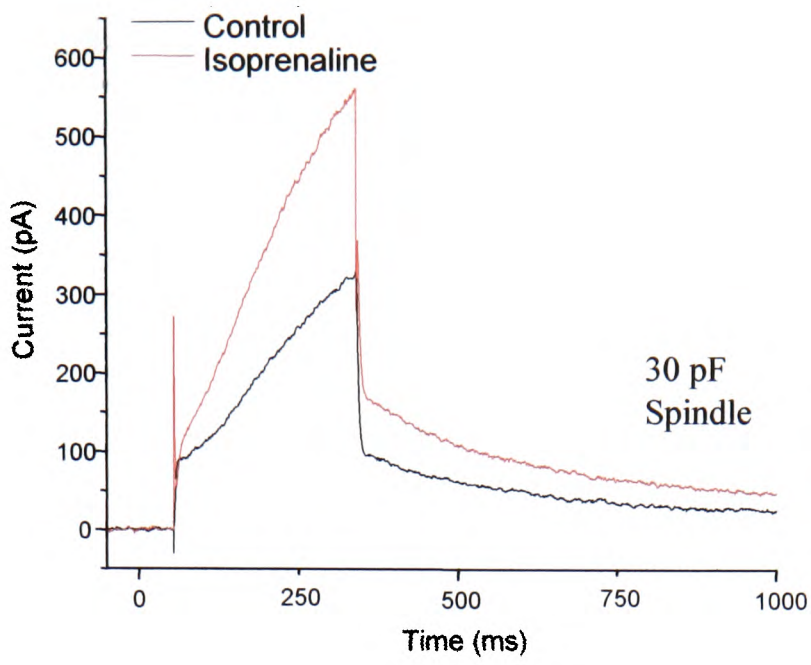

b,

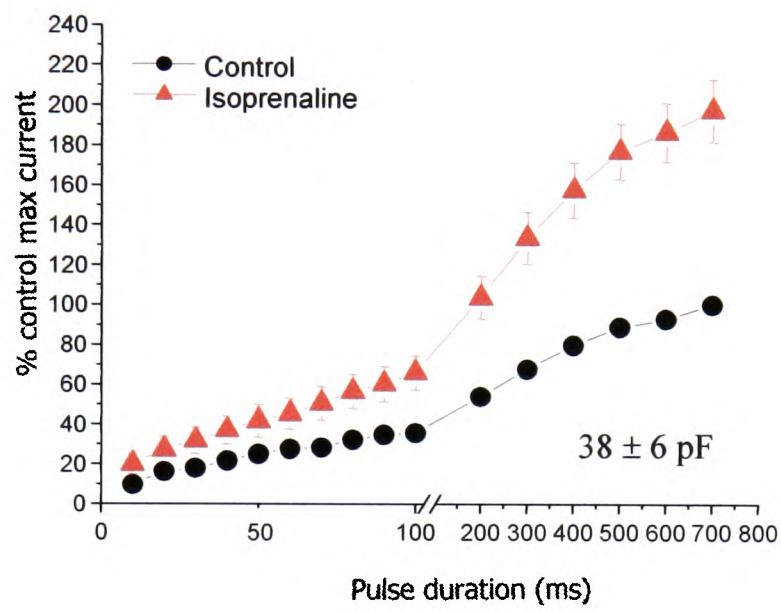

Figure 8.3 Page 345

Isoprenaline (100 nM) increased the amplitude of the pulse (300 ms) and the tail current (a), to an approximately comparable degree. Currents activated with depolarisation from 10 to 700 ms (b) were all increased upon exposure to 100 nM isoprenaline (n=8, $P<0.05$). Note the expanded time-scale between 0-100 ms.

a,

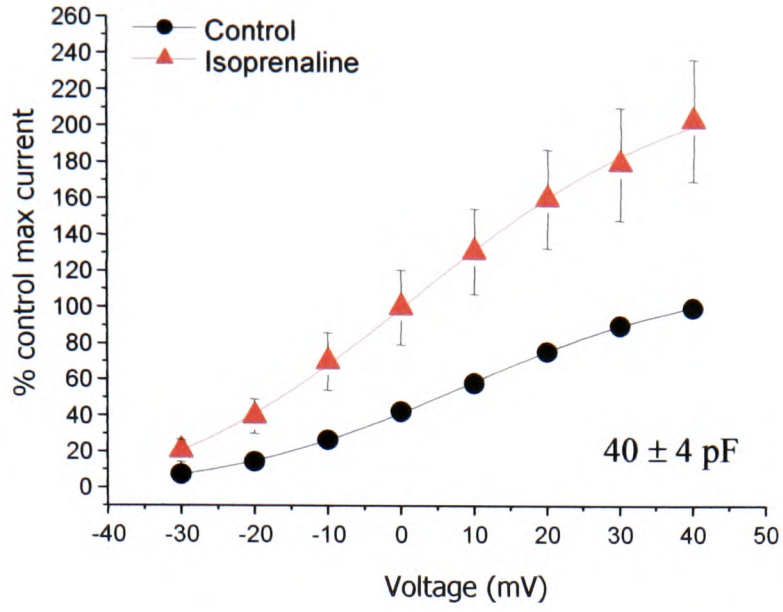

b,

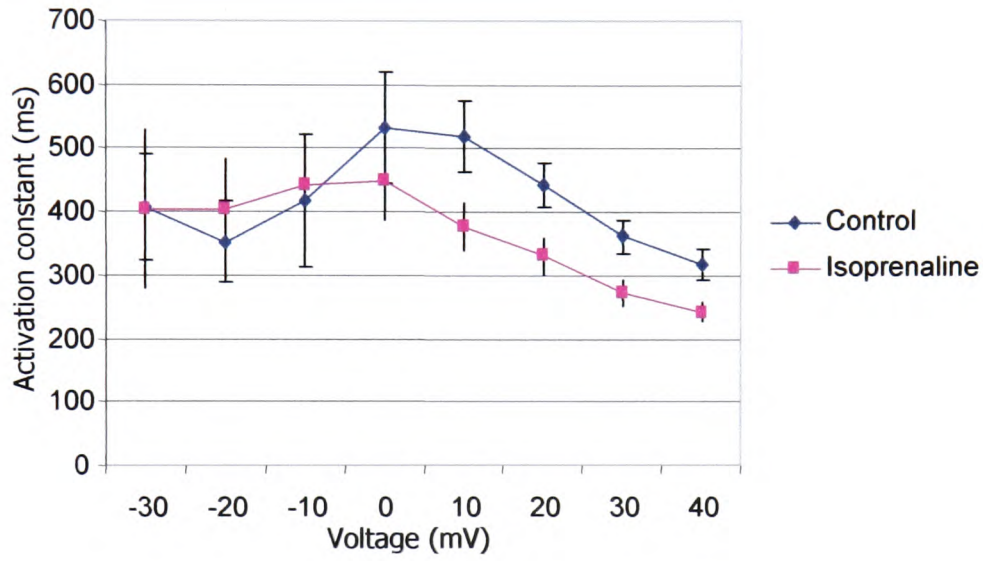

c,

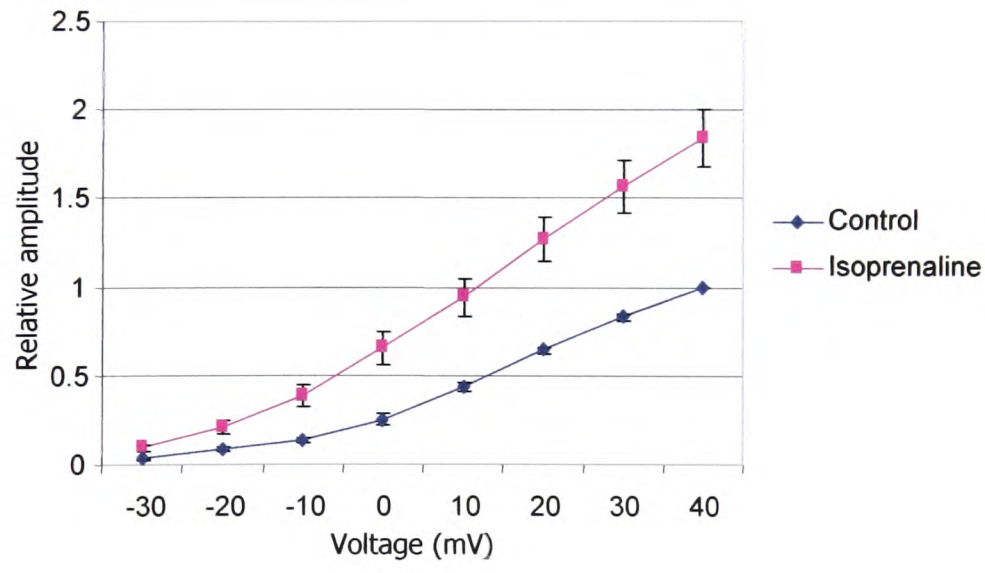

Figure 8.4 Page 346

Isoprenaline (100 nM) increased the voltage dependent activation of I_K tail current (a), in the voltage range –30 to +40 mV (n=12, P<0.05). Isoprenaline also shifted the $V_{1/2}$ from 9 ± 2 to 2 ± 1 mV, without altering the slope of activation (n=12, P<0.05). Depolarisation activated outward current was fitted with a single exponential from 100 ms after voltage step (avoiding transient inward current). The activation constant of outward pulse current was quickened in the presence of isoprenaline (b), in the voltage range 0-40 mV (n=8, P<0.05). Amplitudes of the exponential components fitted to activation were increased by isoprenaline (c), similarly to tail currents (a), being approximately doubled (n=9, P<0.05).

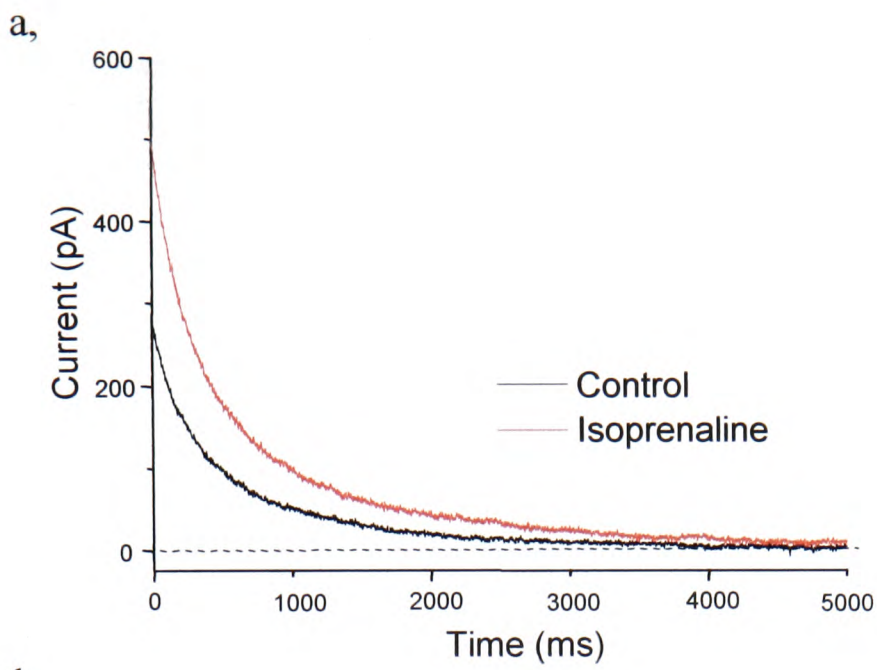

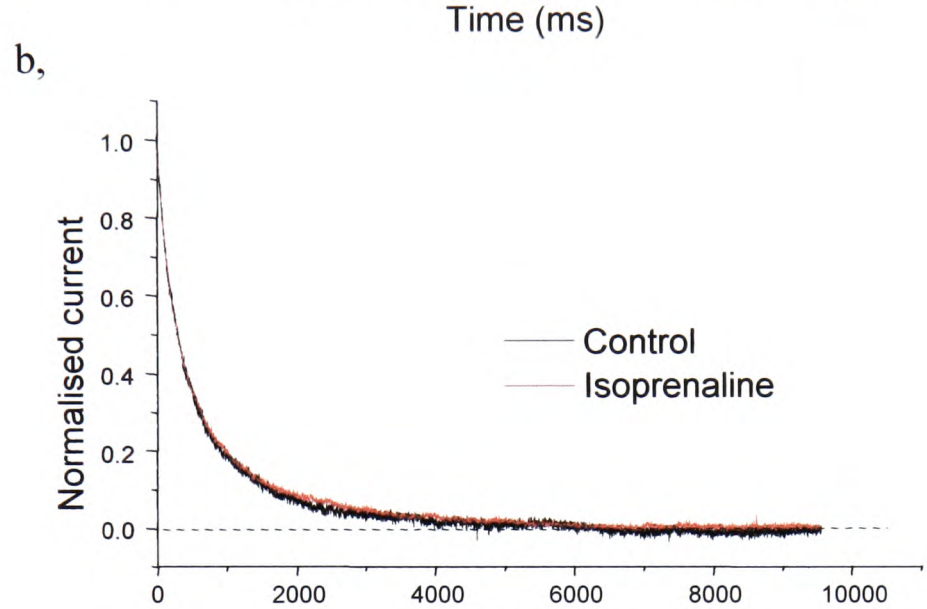

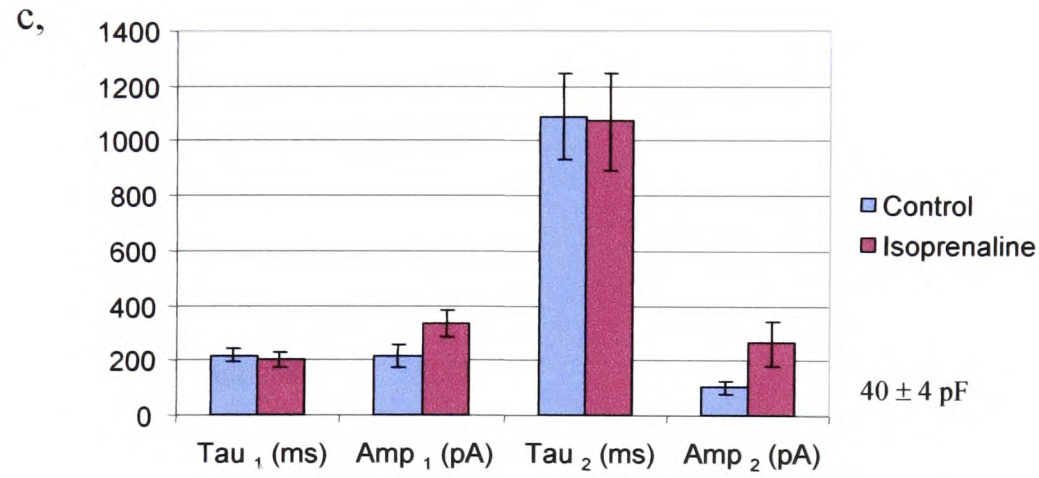

Figure 8.5 Page 347

I_K tail current decay in the presence of isoprenaline (100 nM). Tail current amplitude is greater in the presence of isoprenaline (a), but when control and isoprenaline treated tail currents are normalised, decay overlaps fully (b). Decay was quantified using a bi-exponential curve (n=12); the 2 decay time-constants, Tau_1 (176 ± 24 ms) and Tau_2 (811 ± 149 ms) were not altered by isoprenaline (c), however Amp_1 and Amp_2 were increased (n=12, $P<0.05$).

a,

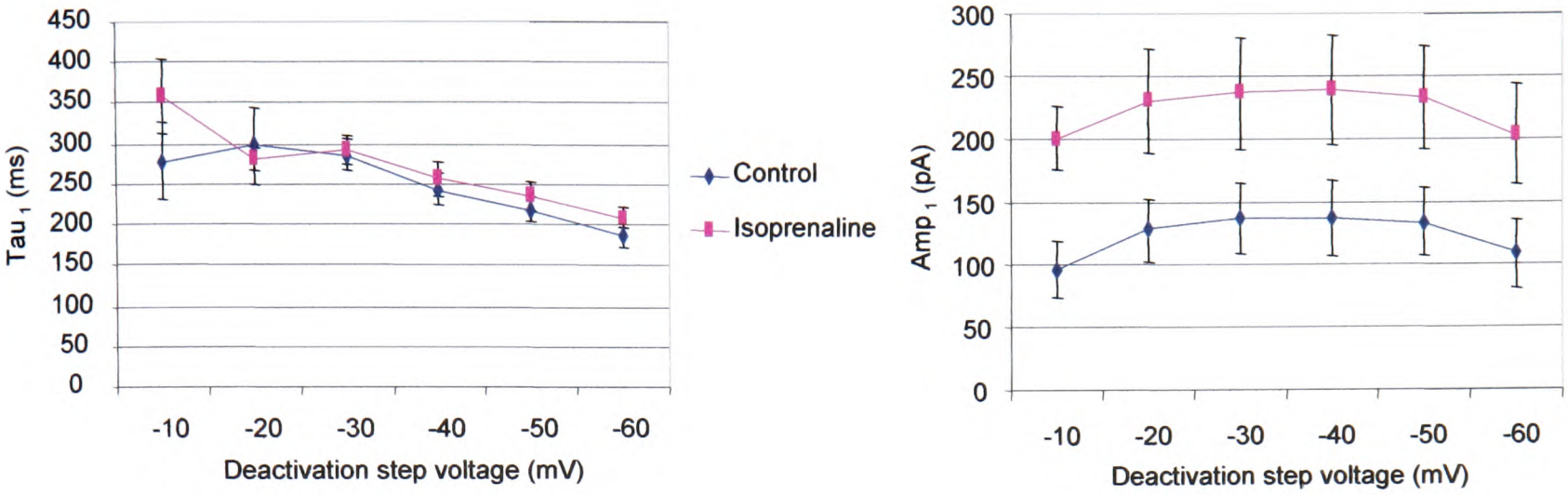

b,

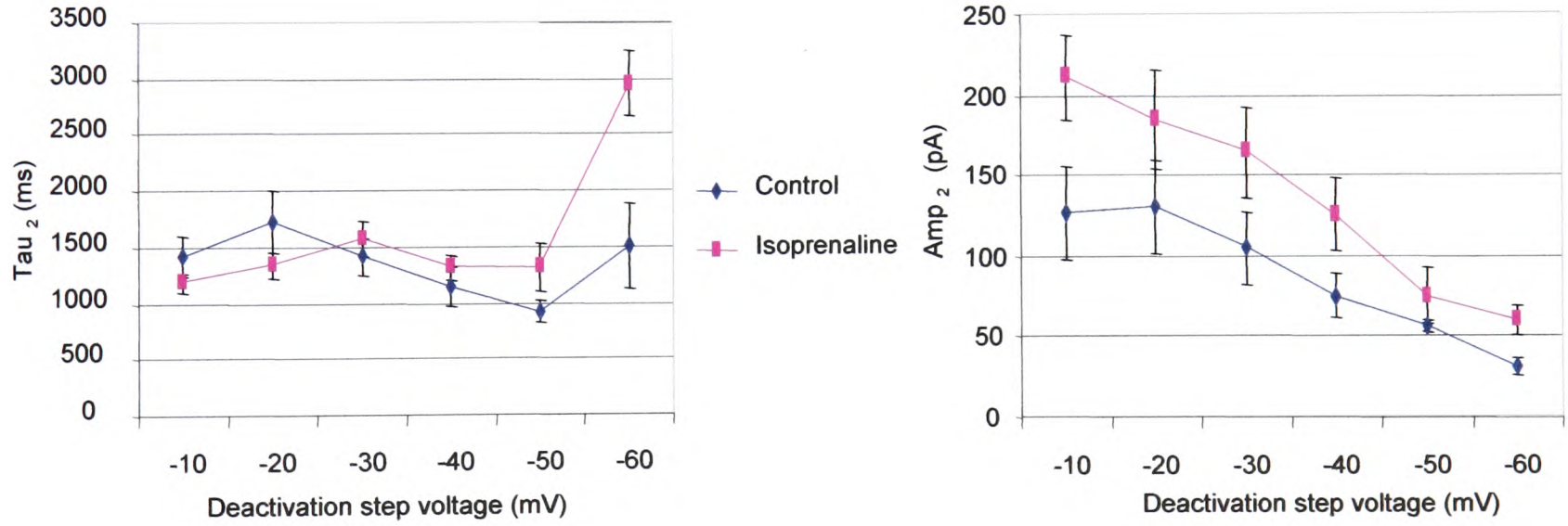

Figure 8.6

100 nM isoprenaline altered the amplitudes (right panel) but not the time-constant (left panel) of the fast (a) and the slow (b) phases of tail current deactivation (n=6, $P<0.05$). Amp_1 was increased at -30 and -40 mV ($P<0.05$, n=6).

a,

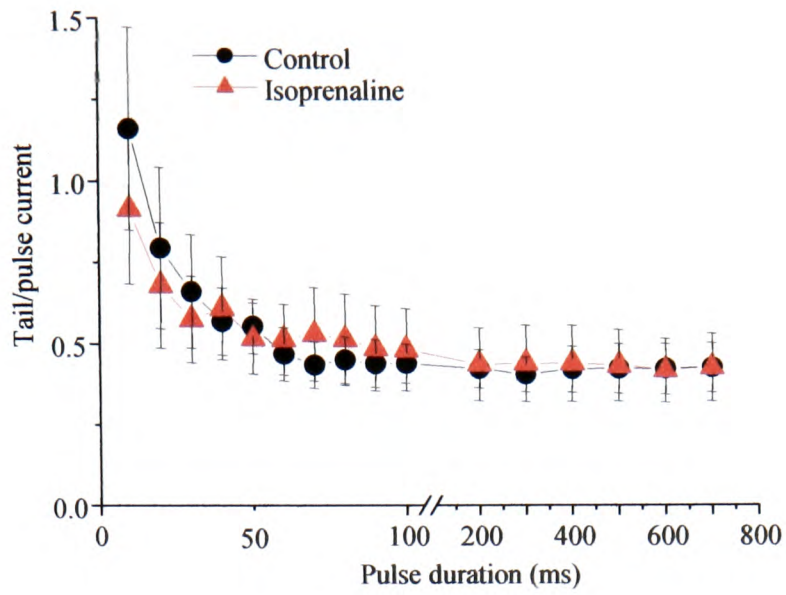

b,

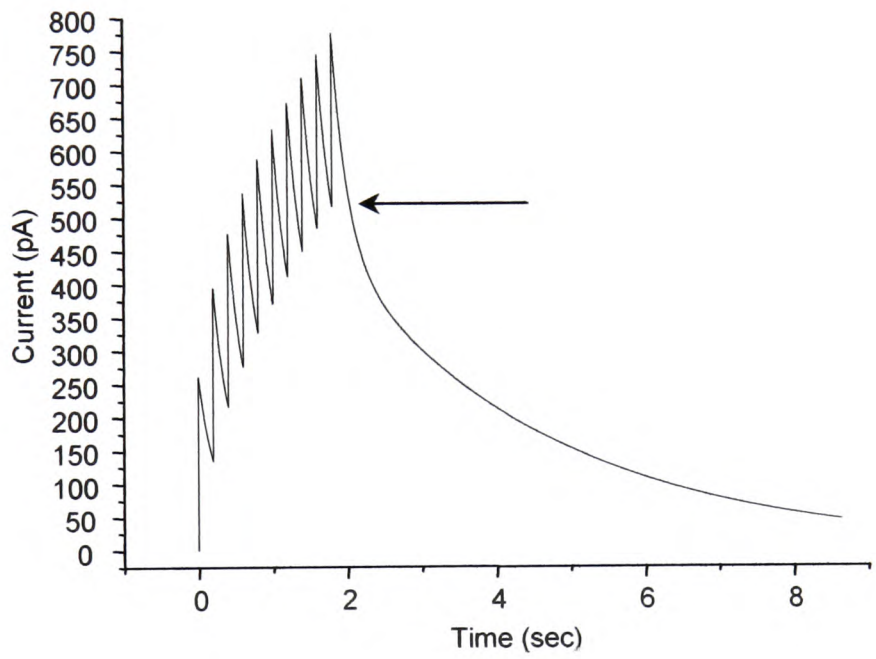

Figure 8.7 Page 349

There was no difference between the envelop of tails test in the absence and presence of 100 nM isoprenaline (n=10 and 6), as the relationships almost overlap throughout the range of depolarisation durations (a). Simulation of I_K tail current decay during a period of 10 action potentials. I_K tail current deactivation to –60 mV time-constants of 209 and 2952 ms, amplitudes of 203 and 60 pA (n=6). These were incorporated into a simulation of I_K decay (b), in which the virtual sino-atrial node cell was stimulated with isoprenaline beating at 300 bpm, basal I_K after 10 action potentials was 515 pA (arrow) and was still developing.

a,

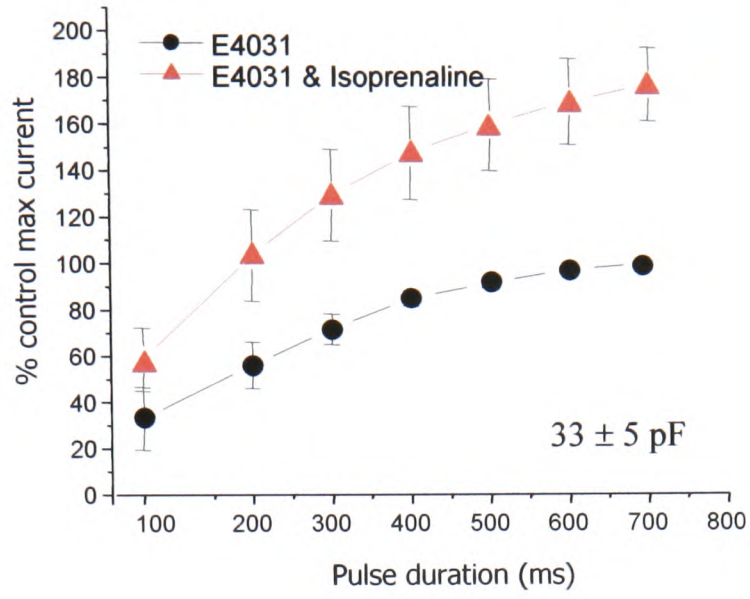

b,

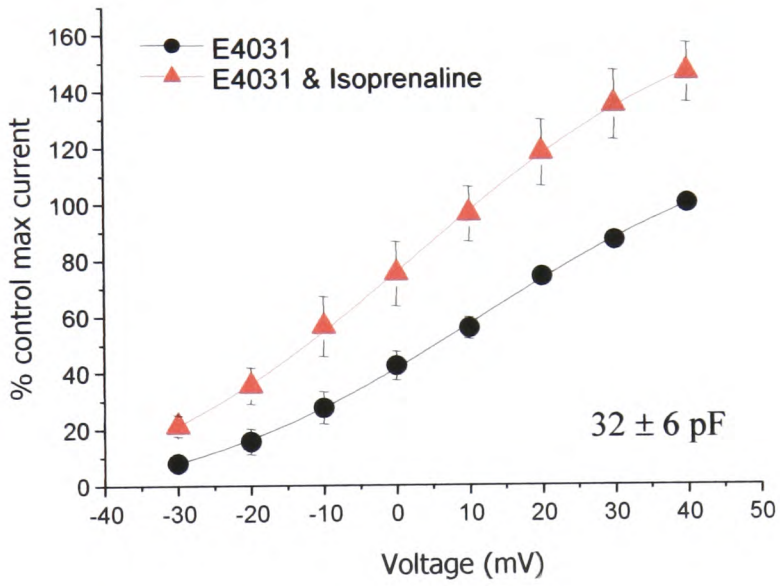

Figure 8.8

E4031 (5 μM) pre-treated sino-atrial node cells were exposed to 100 nM isoprenaline and the effects upon the time (a) and voltage-dependent (b) activation of I_K were investigated. Isoprenaline increased the amplitude of E4031 exposed I_K tail current, activated with depolarisation of between 100 and 700 ms ($n=6$, $P<0.05$). I_K activated in the presence of E4031 was increased at all voltages (-30 to +40 mV) after the 100 nM isoprenaline ($n=7$, $P<0.05$); $V_{1/2}$ was also shifted from 11 ± 4 to 2 ± 8 mV ($n=7$, $P<0.05$), without altering the slope of activation.

a,

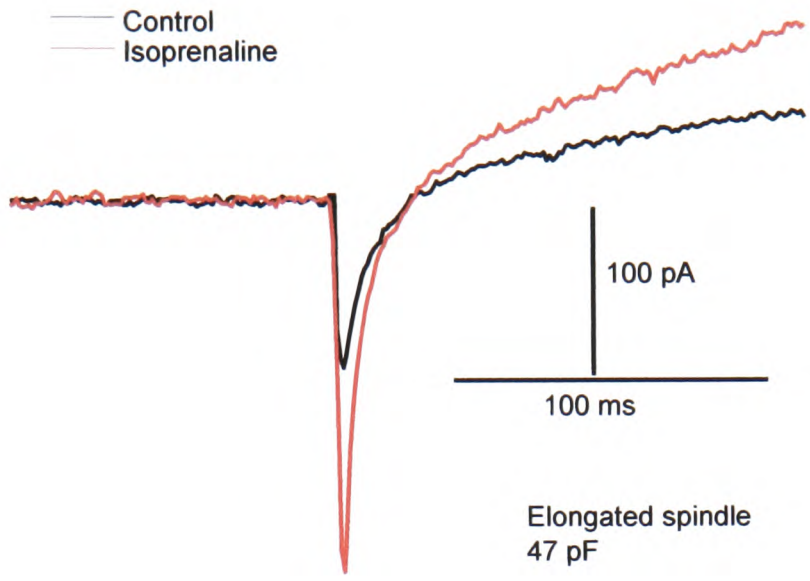

b,

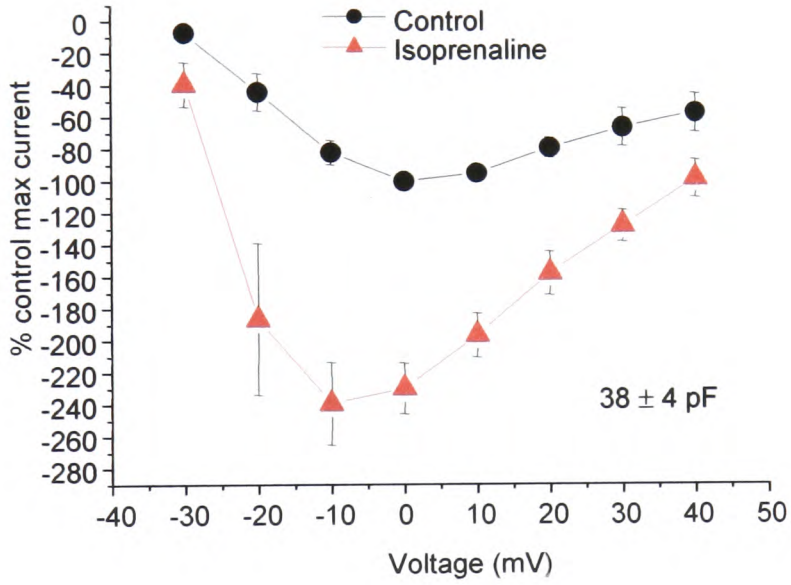

Figure 8.9 Page 351

The amplitude of the transient inward current activated upon depolarisation (0 mV), which is composed mostly of I_{CaL}, is augmented by exposure of 100 nM isoprenaline (a). I_{CaL} activated by depolarisation to any voltage (-30 to +40 mV) was increased in the presence of isoprenaline (n=10, $P<0.05$), with maximum I_{CaL} (at 0 mV) being increase by 250 % (b).

a,

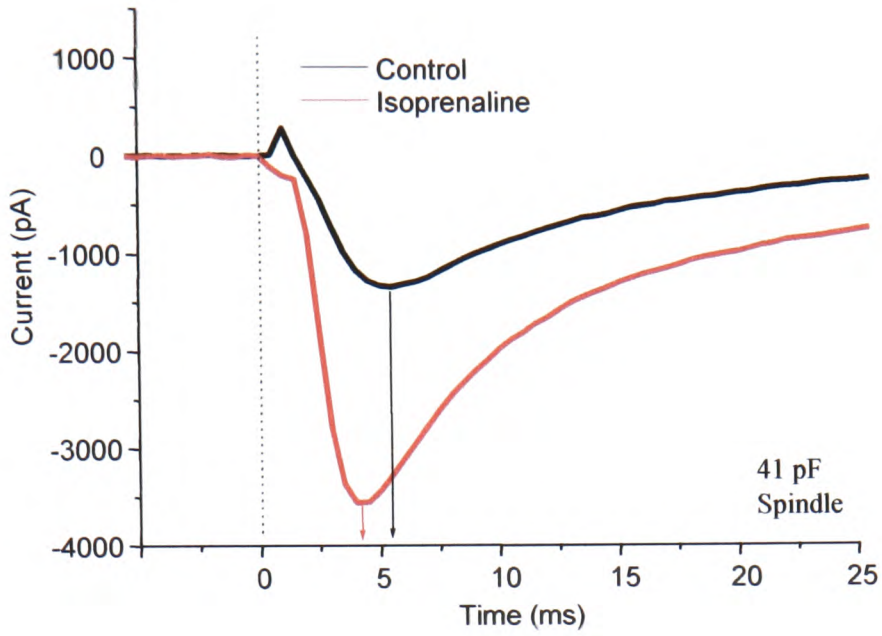

b,

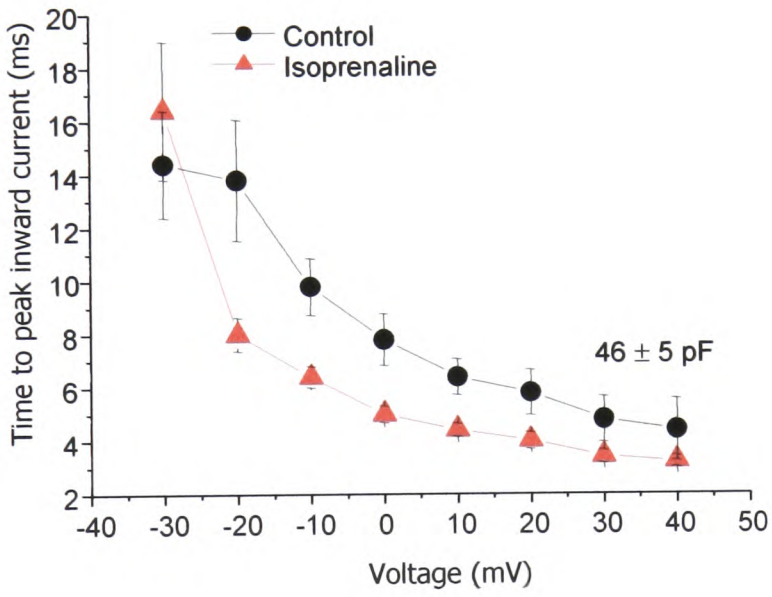

Figure 8.10 Page 352

I_{CaL} activation is accelerated in the presence of 100 nM isoprenaline, as the time to peak inward I_{CaL} becomes quicker (a). Depolarisation is initiated at the dotted line, this example was during a depolarisation to 0 mV. The time to peak inward current was found to be shorter at potentials between –20 to +20 mV (n=5, $P<0.05$), generally becoming more rapid as depolarisation was extended (b).

a,

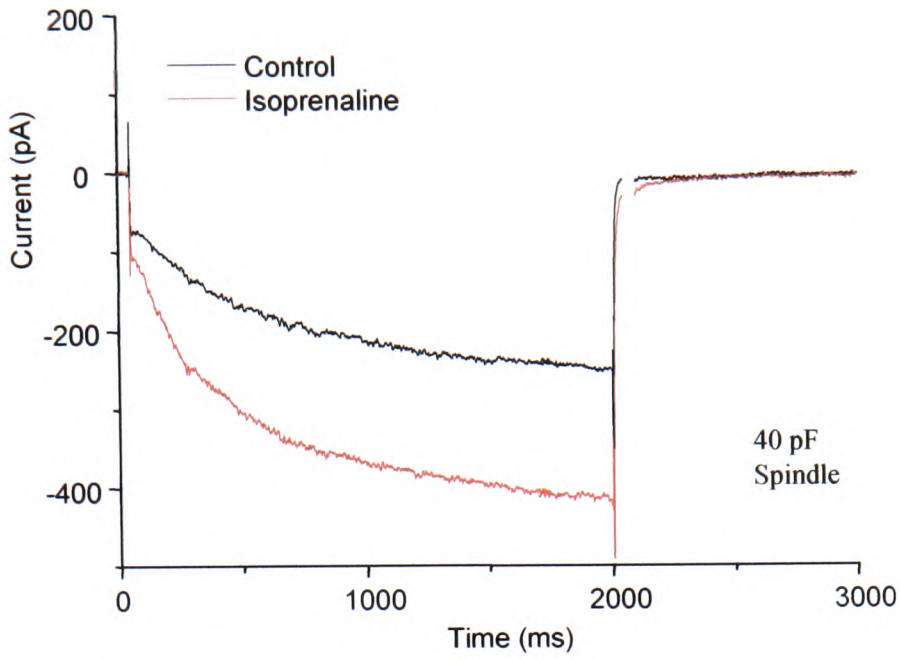

b,

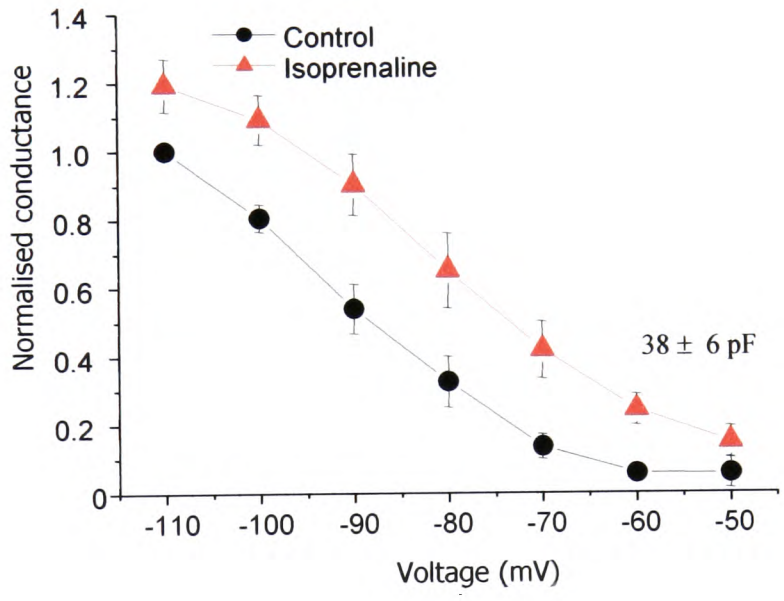

Figure 8.11 Page 353

I_f amplitude was increased by 100 nM isoprenaline (a) and voltage dependent activation of conductance was shifted to more positive voltages (b). I_f activated upon hyperpolarisation to –80 mV was measured as the time-dependently activating inward current. The $V_{1/2}$ of the conductance-voltage relationship was shifted from -97 ± 2 to -88 ± 2 mV (n=6, $P<0.01$) by isoprenaline, but decreased the activation slope from 10 ± 2 to 13 ± 2 mV (n=6, $P<0.05$).

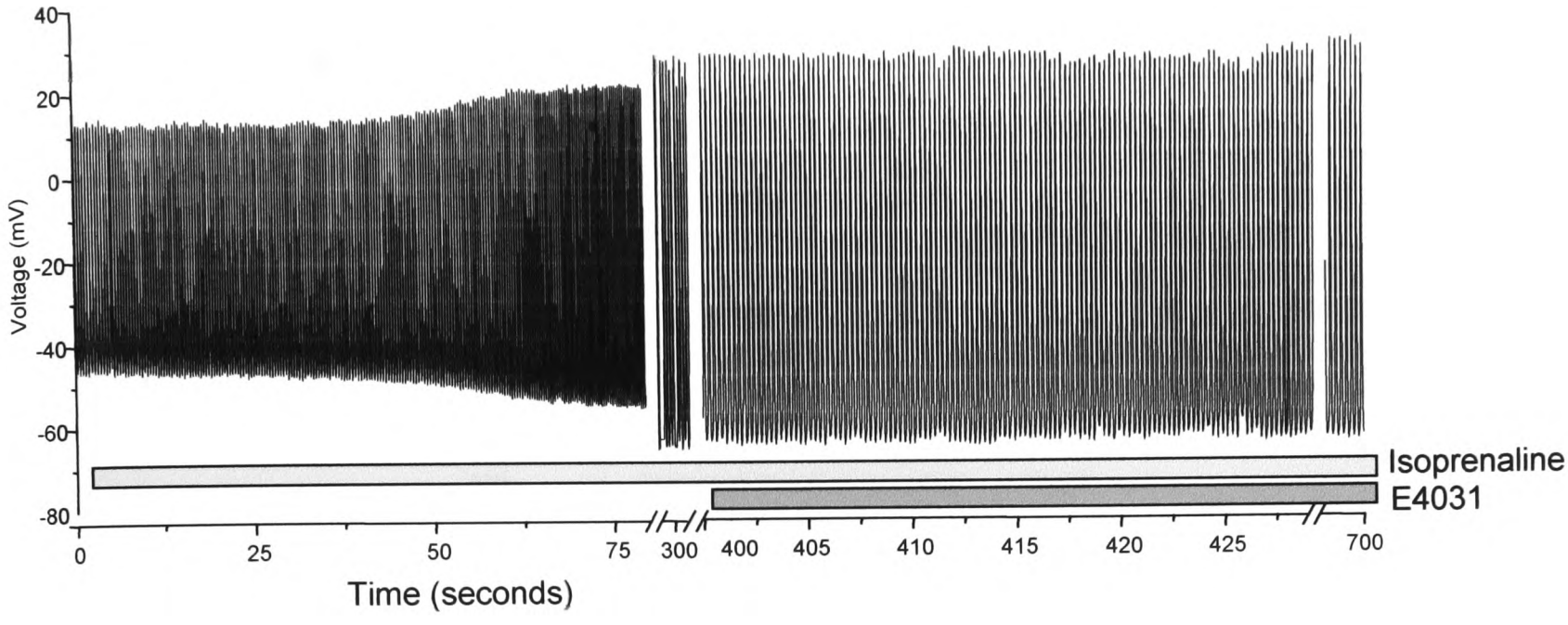

Figure 8.12 Page 354

Isoprenaline (100 nM) increased the action potential amplitude and rate of spontaneous beating of isolated sino-atrial node cells (a, left) and this was not altered with subsequent exposure of these cells to 5 μM E4031 (a, right). Note the 4 regions in this figure have different time-scales.

a,

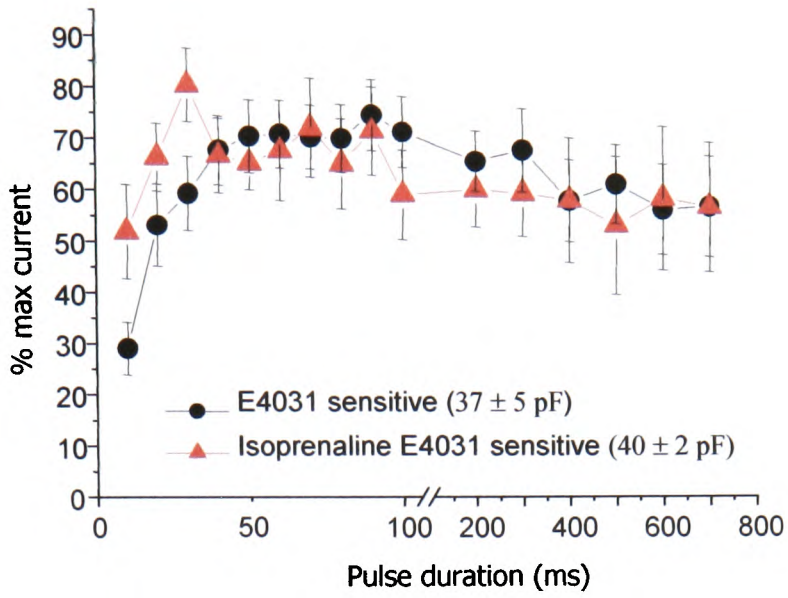

b,

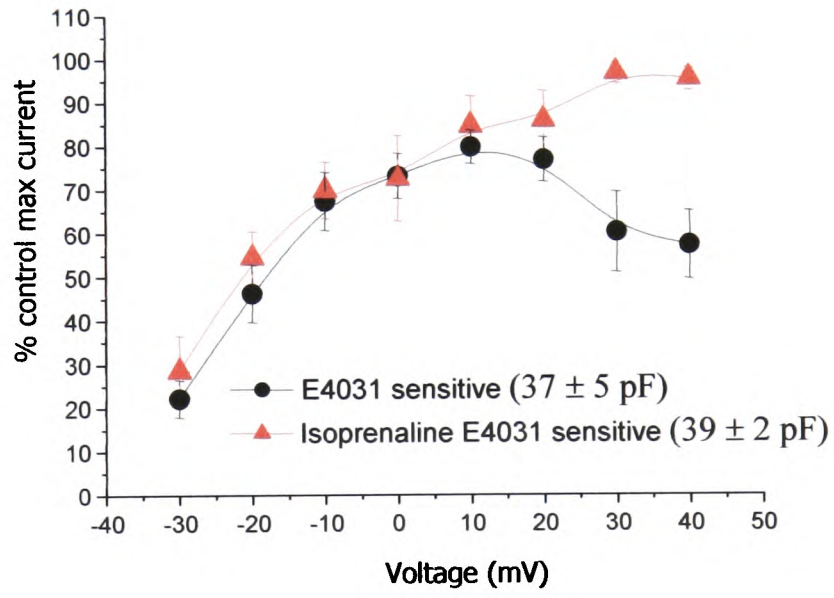

Figure 8.13

Time and voltage dependent activation of the E4031 (5 μM) sensitive current in the absence and presence of 100 nM isoprenaline. Time-dependent activation is similar in the presence of isoprenaline (a), except it is increased upon 10 ms depolarisation (n=15 and 7, $P<0.05$ unpaired t-test). Voltage dependent activation of the E4031 sensitive current is similar between –30 and +20 mV, where upon isoprenaline treated current continued to increase, whereas control diminished with further depolarisation (n=18 and 6, $P<0.05$ unpaired t-test).

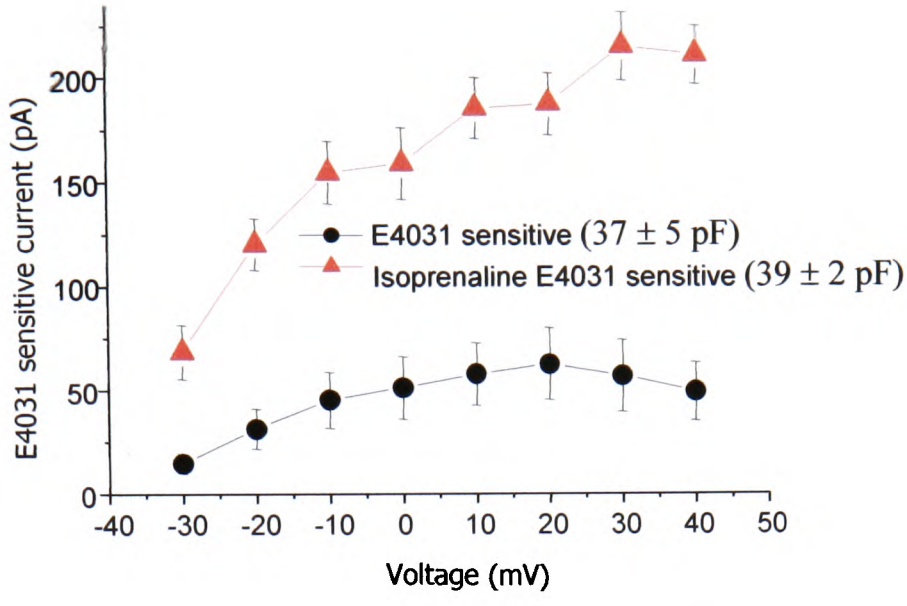

Figure 8.14 Page 356

Isoprenaline (100 nM) increased the absolute current amplitude of the E4031 sensitive current at all voltages tested (n=18 and 6, P<0.05 unpaired T-test).

a,

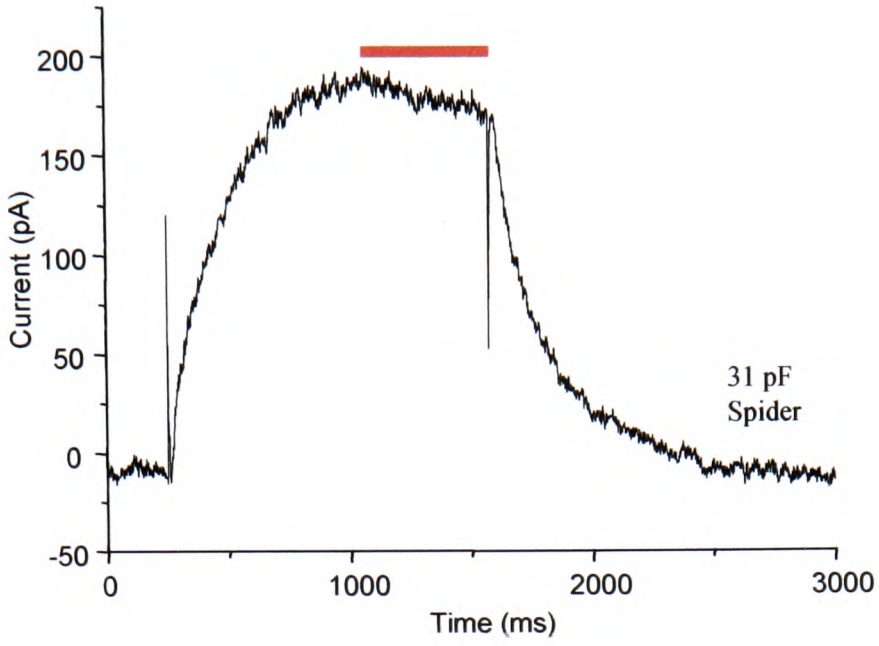

b,

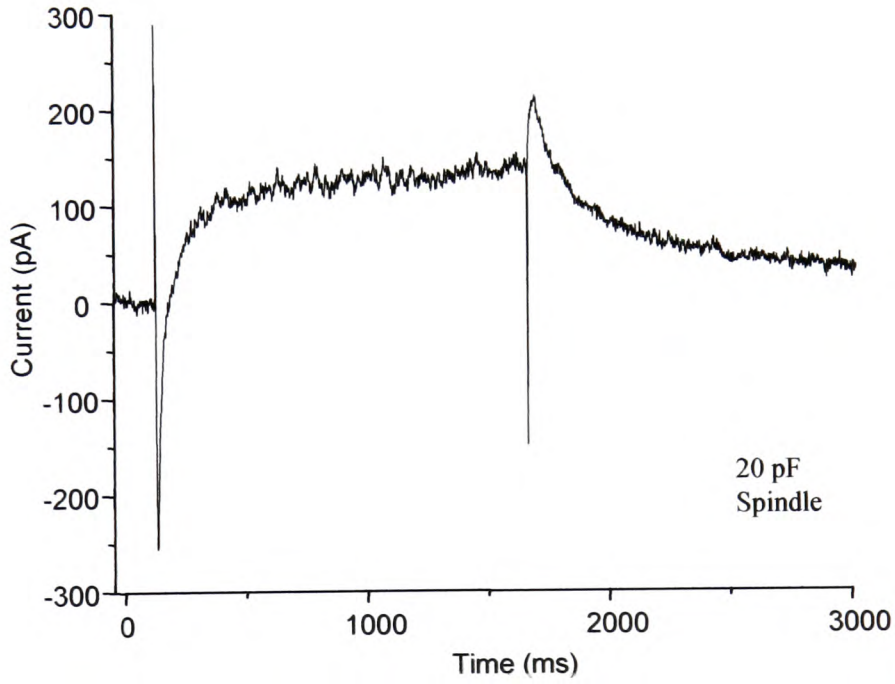

Figure 8.15 Page 357

Reduction in the outward current during depolarisation (+10 mV, a, below red bar), was eliminated in the presence of 100 nM isoprenaline (b). The outward currents of some of the sino-atrial node cells population demonstrate a reduction in current during prolonged depolarisations, but none of the isoprenaline treated currents displayed this characteristic. Note in isoprenaline the rapid activation of the E4031 sensitive current and the tail current exceeds the pulse current (b).

a,

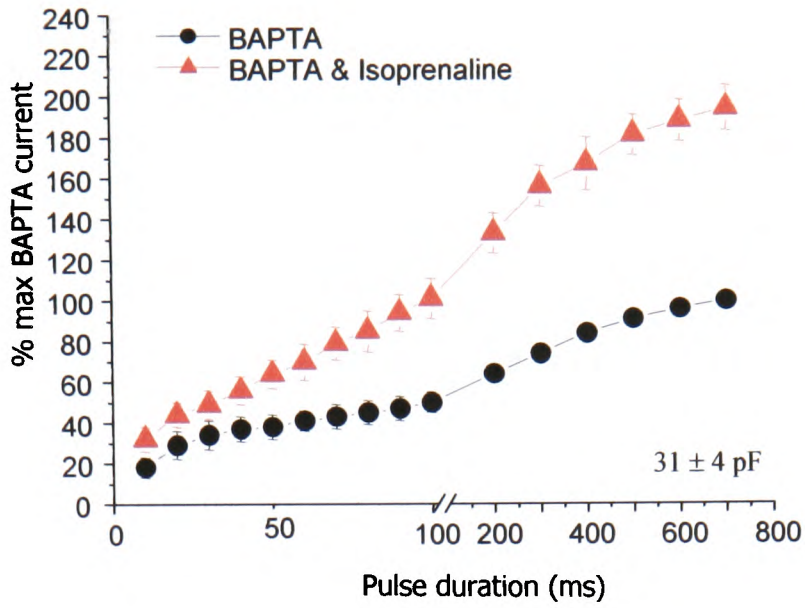

b,

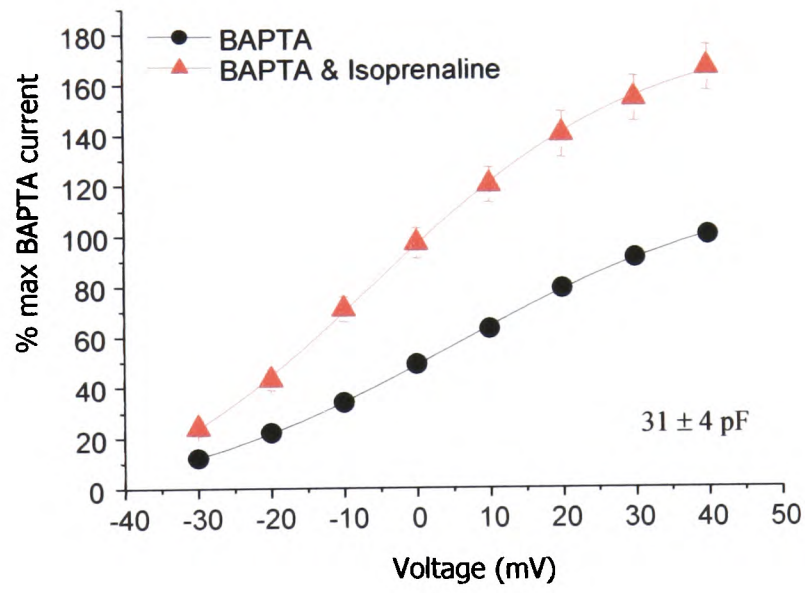

Figure 8.16 Page 358

Isoprenaline (100 nM) increased the time (a) and voltage (b) dependent activation of I_K in the presence of BAPTA-AM (10 μM). Tail current amplitudes associated with depolarisation ranging in duration from 10 to 700 ms (a), in the presence of BAPTA, were found to be increased by isoprenaline (n=6, $P<0.05$). Isoprenaline increased I_K at all voltages (b, n=6, $P<0.05$). Isoprenaline exposure shifted the $V_{1/2}$ of I_K activation in the presence of BAPTA by 11 mV from 5 ± 3 to –6 ± 5 mV (n=6, $P<0.05$), without altering the slope of activation.

a,

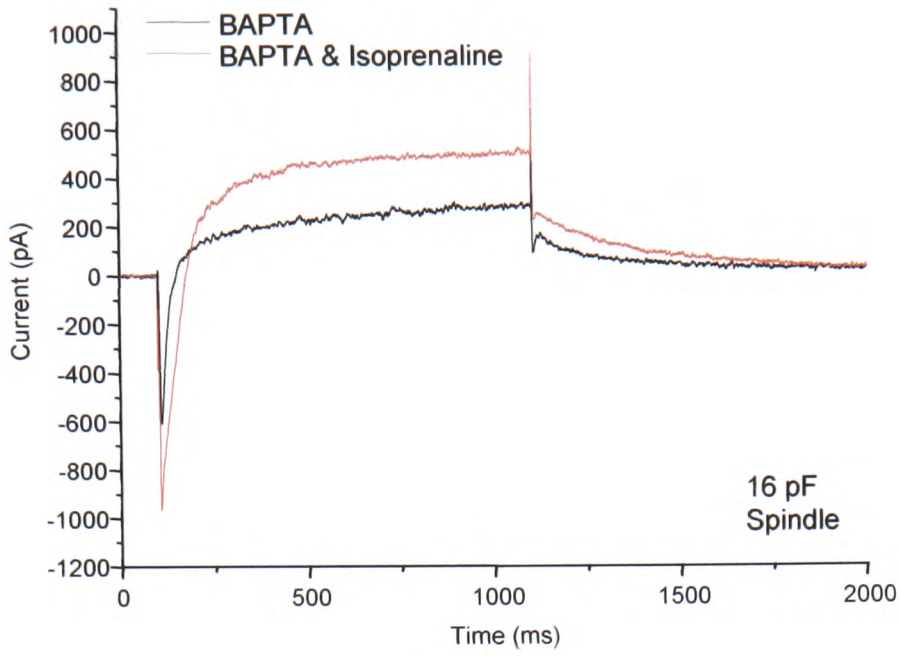

b,

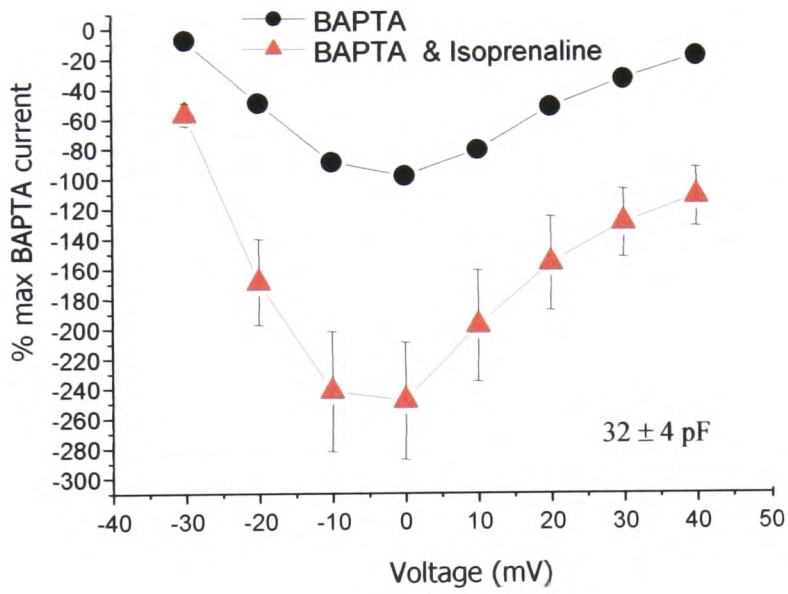

Figure 8.17 Page 359

Isoprenaline (100 nM) increased the BAPTA-AM (10 μM) treated I_{CaL} amplitude (a), and subsequent I_K (depolarisation to 0 mV). Isoprenaline was found to increase I_{CaL} at all voltages (-30 to +40 mV) in the presence of BAPTA (n=4, $P<0.05$), without changing the voltage which activated maximal I_{CaL} (0 mV).

a,

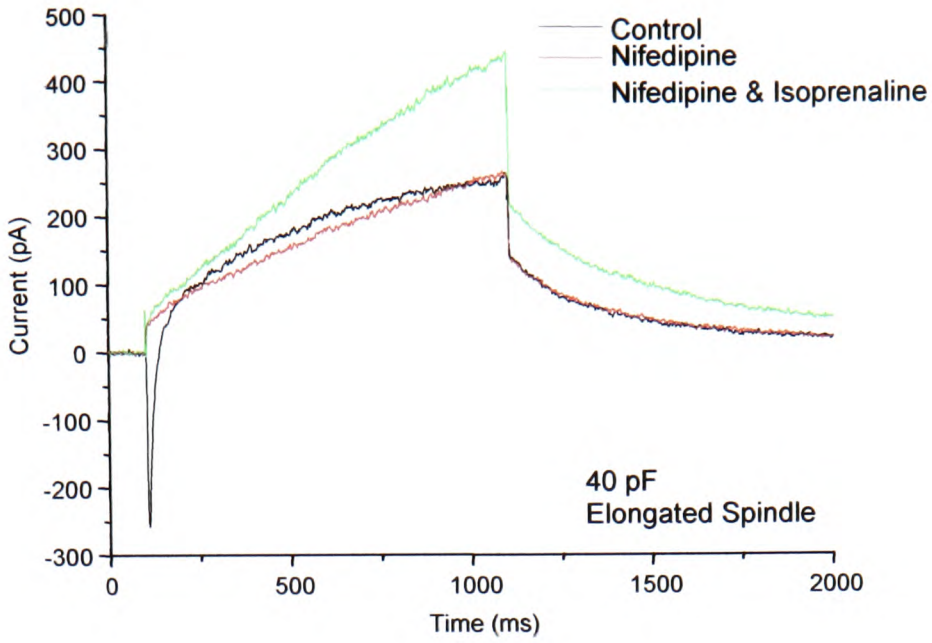

b,

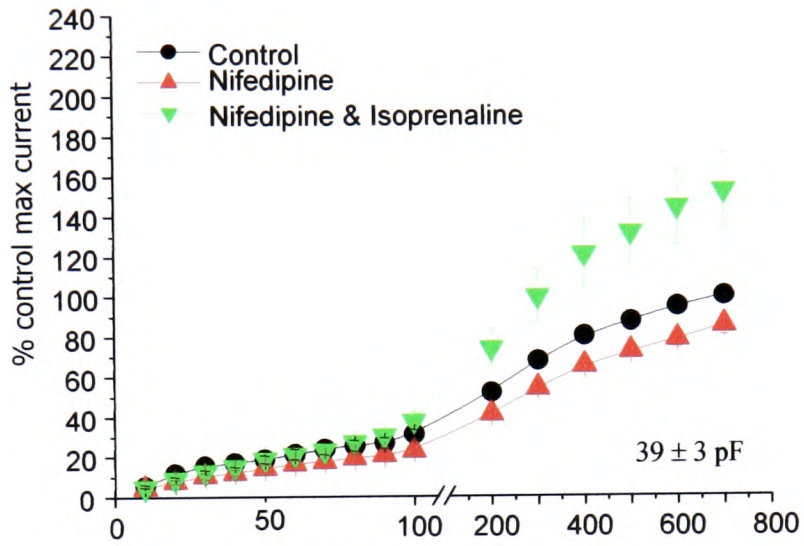

c,

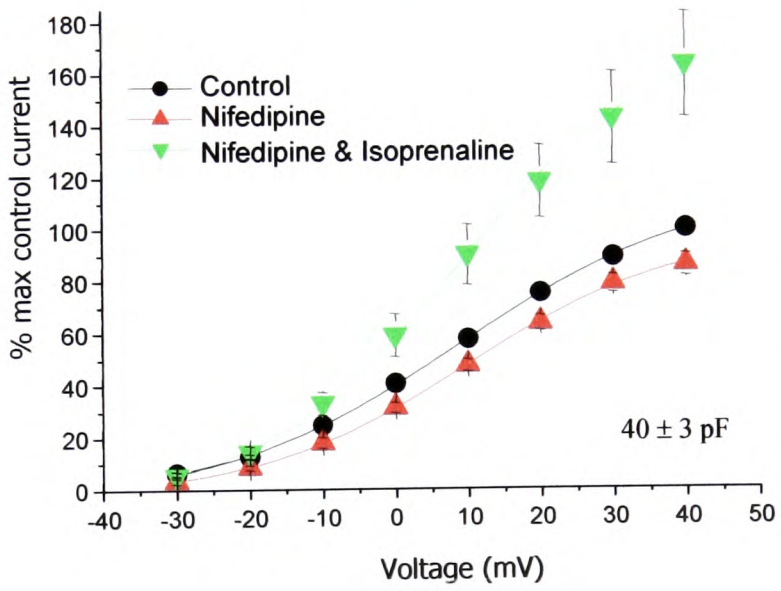

Figure 8.18 Page 360

Isoprenaline (100 nM) increased I_K in the presence of nifedipine (5 μM). Upon depolarisations to 0 mV (a) nifedipine blocks I_{CaL}, having little effect upon I_K, but isoprenaline subsequently increased I_K. Nifedipine caused a slight reduction in the amplitude of I_K activated with various depolarisation durations, greater than 10 ms (b, n=11, $P<0.05$). Isoprenaline subsequently increased I_K activated with depolarisations of 100 ms and longer (n=11 and 5, $P<0.05$). Nifedipine caused a similar slight reduction in the voltage dependent activation of I_K (c), which was overcome by isoprenaline and exceeded control. There was no alteration of either the $V_{1/2}$ or the activation slope; control 9 ± 6 and 14 ± 4 mV (n=12).

a,

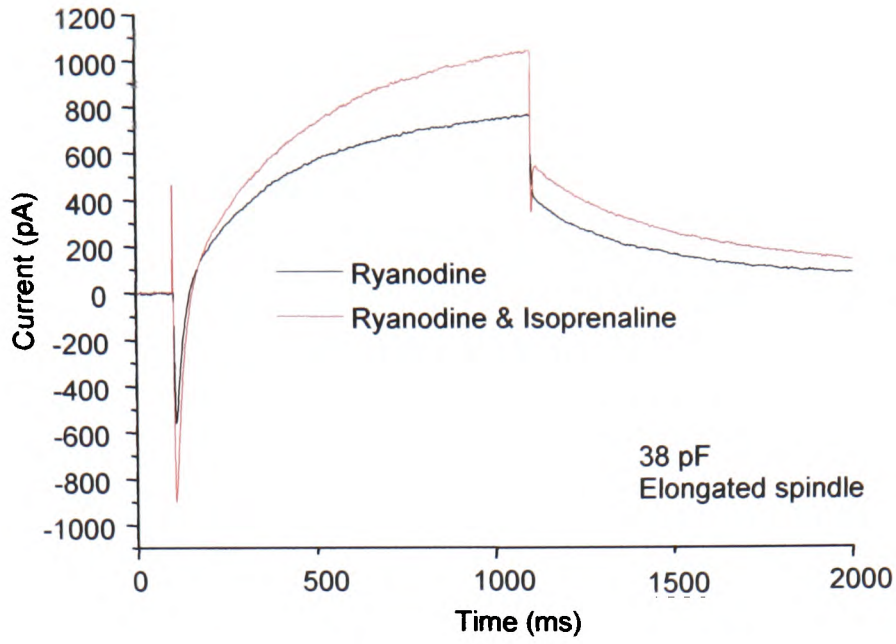

b,

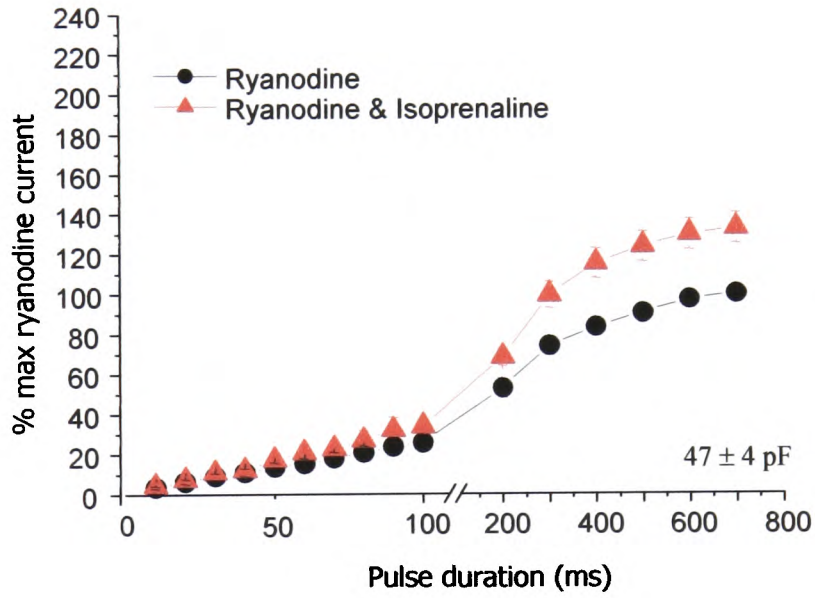

Figure 8.19 Page 361

100 nM isoprenaline increased I_K in the presence of ryanodine (2 μM). The outward current activated upon depolarisations to 0 mV in the presence of ryanodine (a), was increased in the presence of additional isoprenaline. When sino-atrial node cells were treated with ryanodine (b), only the current activated by depolarisations (to +40 mV) of greater than 90 ms duration were increased by isoprenaline (n=5, $P<0.05$).

a,

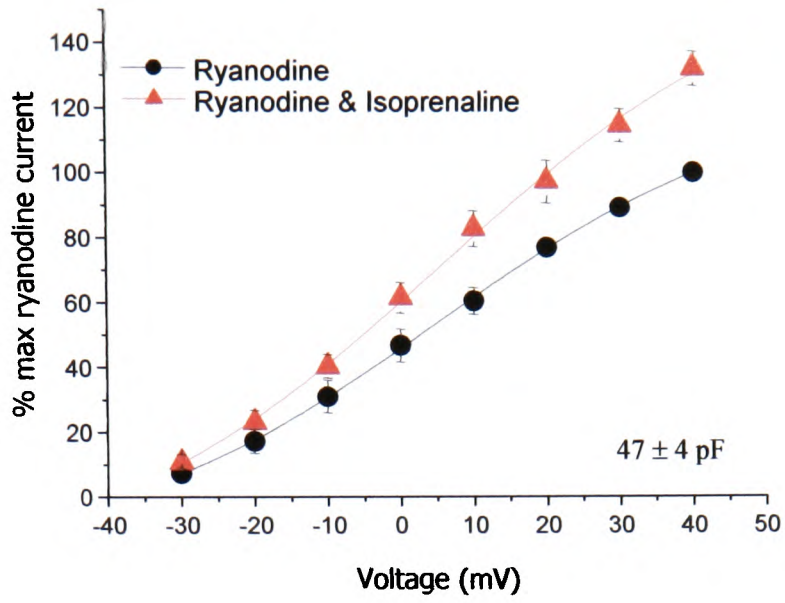

b,

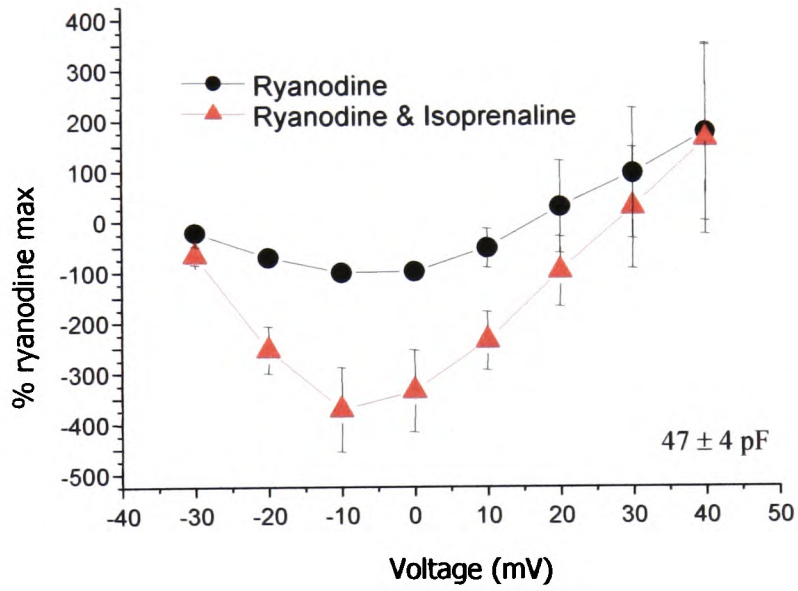

Figure 8.20 Page 362

Isoprenaline increased the voltage dependent activation of I_K (a) and I_{CaL} (b) previously treated with ryanodine (2 μM). Isoprenaline (100 nM) caused a slight increase in the amplitude of I_K (pretreated with ryanodine) at all voltages (n=5, $P<0.05$), without altering the $V_{1/2}$ or activation slope; control 5 ± 4 and 22 ± 10 mV (n=5). Isoprenaline was found to increase I_{CaL} between -30 to +10 mV in the presence of ryanodine (n=5, $P<0.05$), without changing the voltage which activated maximal I_{CaL} (-10 mV).

a,

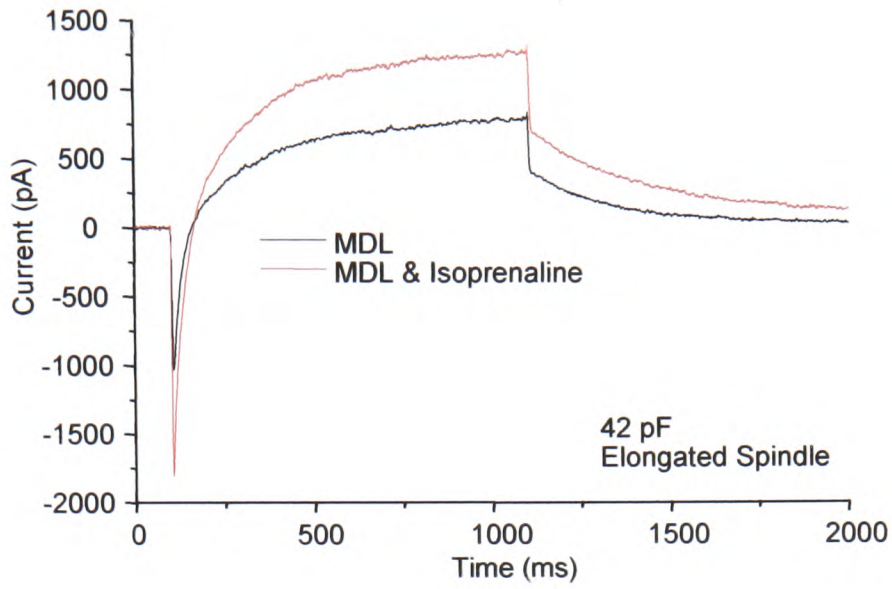

b,

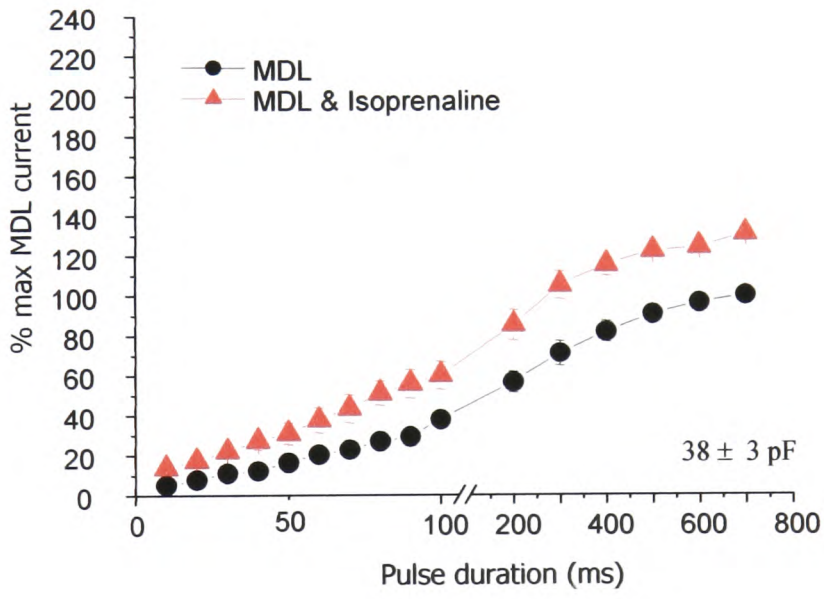

Figure 8.21

100 nM isoprenaline increased I_K in the presence of MDL (10 μM). The outward current activated upon depolarisations to 0 mV in the presence of MDL (a), was increased in the additional presence of isoprenaline. When sino-atrial node cells were treated with MDL, isoprenaline was able to increase I_K activated with depolarisation of any duration (b, n=5, $P<0.05$), however the isoprenaline augmentation is relatively meagre.

a,

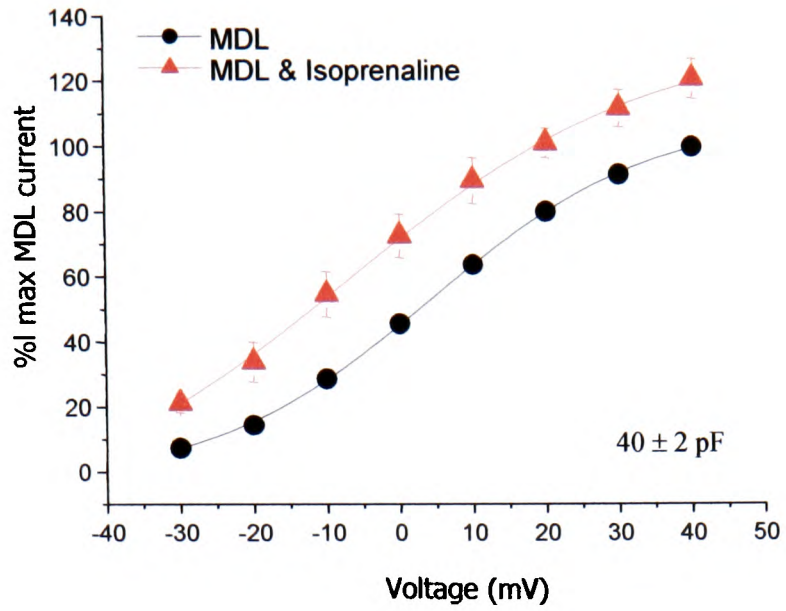

b,

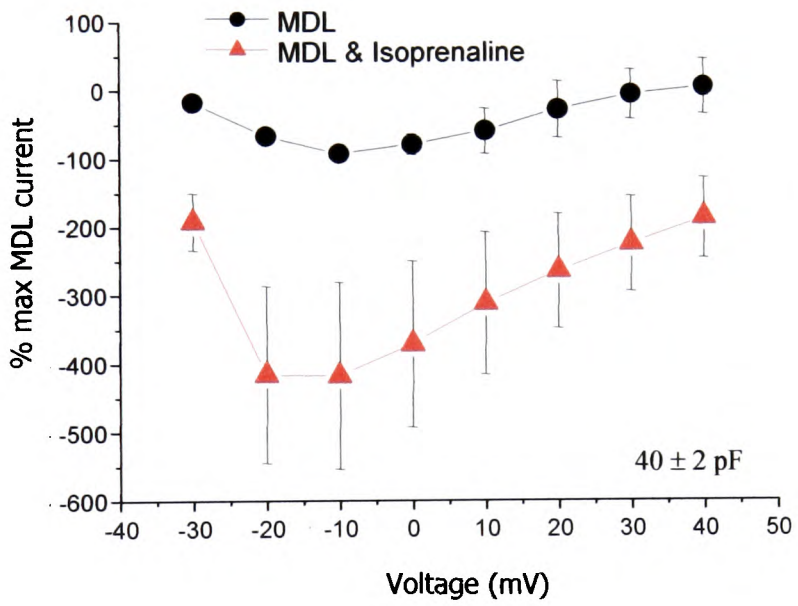

Figure 8.22 Page 364

In the presence of MDL (10 μM), isoprenaline (100 nM) increased both I_K (a) and I_{CaL} (b). Isoprenaline also shifted the $V_{1/2}$ of the MDL treated I_K activation from 4 ± 1 to –8 ± 10 mV ($P<0.05$, n=4), without altering the activation slope. Isoprenaline was found to increase I_{CaL} at voltages (-30 to +40 mV) in the presence of MDL (n=4, $P<0.05$), without changing the voltage which activated maximal I_{CaL} (-10 mV).

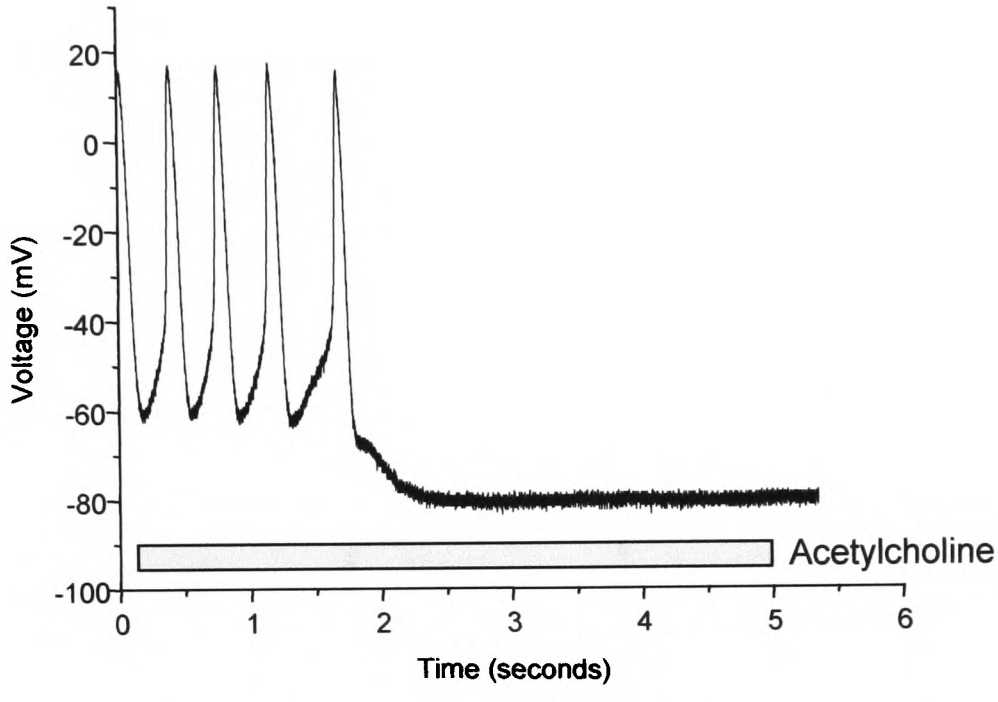

Figure 8.23 Page 365

Upon rapid switch exposure of an isolated sino-atrial node cell to acetylcholine (5 μM), the generation of spontaneous activity failed and the cell became quiescent (b).

Agent	Target	Current	Affect
Isoprenaline	β-adrenoceptors	Various	Accelerate pacemaking
Isoprenaline	β-adrenoceptors	I_{Kr} and I_{Ks}	Similarly increased in amplitude
Isoprenaline	β-adrenoceptors	I_{CaL}	Increased amplitude, activated quicker and max current at -10 mV
Isoprenaline	β-adrenoceptors	I_f	Increased amplitude and 9 mV depolarised shift in $V_{1/2}$
E4031 with isoprenaline	E4031 sensitive	I_{Kr}	Increased E4031 sensitive current amplitude, reduction in rectification
BAPTA then isoprenaline	Cytosolic calcium	Various	Isoprenaline I_K augmentation similar amplitude to control
Nifedipine then isoprenaline	I_{CaL} calcium	Various	Isoprenaline I_K augmentation slightly reduced compared with control
Ryanodine then isoprenaline	SR calcium	Various	Comparatively small increase in I_K
MDL then isoprenaline	AC	Various	Comparatively small increase in I_K

Figure 8.24 Page 366
Summary table of findings in this chapter. Isoprenaline was used at 100 nM, E4031 at 5 μM, BAPTA-AM at 10 μM, nifedipine at 5 μM, ryanodine at 2 μM and MDL at 10 μM.

CHAPTER 9: General discussion

The investigations presented in this thesis describe some of the characteristics of the two components of the delayed rectifier potassium current, I_{Kr} and I_{Ks}, in guinea-pig sino-atrial node cells, and allow evaluation of their relative contribution to pacemaking. In addition the possible regulation of these currents by calcium, both by trans-sarcolemmal and that released from the SR, have been investigated. The role of AC activity and cAMP has also been studied. Finally, the mechanism of β-adrenergic enhancement of I_{Kr} and I_{Ks} has been studied.

Most of the initial investigation into the sino-atrial node was undertaken upon rabbit sino-atrial node cells. There are currently a number of different species in which the sino-atrial node is studied, including the guinea-pig (as in this study), but most studies still use rabbit sino-atrial node cells. There are some differences in the ion channel density between species, with the most important being the greater amount of I_{Ks} compared to I_{Kr} in guinea-pig (versus the rabbit) sino-atrial node cells (Anumonwo, Freeman et al 1992). There are other differences, such as the absence of I_{TO} in guinea-pig cells compared to the presence in rabbit (Boyett, Honjo et al 1998), but the general sequence of ion channel activation is very similar. This is one of the few large studies of ion currents involved in the guinea-pig sino-atrial node.

The second messenger pathways involving calcium and cAMP appear to be delicately balanced in sino-atrial node cells and leaching of patch pipette contents in and/or cellular components out, disrupts these regulation systems. Throughout this study the use of perforated patch recordings from sino-atrial node cells has allowed investigation without the disruption of intracellular regulation pathways, hence

avoiding run-down that plagues whole-cell recordings. This study therefore more faithfully describes the intrinsic regulation of ionic currents in the sino-atrial node.

Although activation of I_{Kr} and I_{Ks} occurs over approximately similar voltage ranges and depolarisation durations, I_{Kr} is activated by smaller voltages (Anumonwo, Freeman et al. 1992) and by shorter depolarisations. In this study the slightly different activation characteristics and the use of E4031, a selective inhibitor of I_{Kr}, have been use to separate the two components (I_{Kr} and I_{Ks}) of the delayed rectifier potassium current. Neither E4031 nor thiopentone (a relatively selective inhibitor of I_{Ks}) caused quiescence of atrial preparations, although 8 of 9 isolated sino-atrial node cells ceased in the presence of I_{Kr} inhibition, but partial I_{Ks} inhibition only reduce the beating rate.

Immunohistochemical investigation found both of the channels that underlie I_{Kr} (ERG) and I_{Ks} ($KvLQT_1$ synonymous with $KCNQ_1$), to be localised primarily to the sarcolemmal membrane in sino-atrial node cells (and other cardiac myocytes). This implies these channel proteins are localised to the outer cell membrane and could form functional channels perhaps in association with the appropriate accessory sub-units; $miRP_1$ and minK respectively (Curran, Splawski et al. 1995; Barhanin, Lesage et al. 1996).

I_{Kr} and I_{Ks} were electrophysiologically defined in this study according to their voltage dependent activation over the range –30 to +40 mV. In the absence of any inhibitors, a sigmoidal voltage dependent activation was described, having a $V_{1/2}$ of 6 mV. The E4031 sensitive current (I_{Kr}) was found to have a $V_{1/2}$ of –23 mV, whilst the

E4031 resistant current (I_{Ks}) had a $V_{1/2}$ of 20 mV. This indicates that the $V_{1/2}$ of the delayed rectifier potassium current (6 mV) reflects a combination of the $V_{1/2}$'s of I_{Kr} and I_{Ks}, in which I_{Ks} has slightly larger weighting. The duration of the depolarisation that activates these currents was also investigated (10 to 700 ms) and by using E4031, I_{Kr} was found to activated by brief depolarisations (maximal after 60 ms depolarisation), whereas I_{Ks} was progressively activated with depolarisation of 70-80 ms and longer. In the absence of inhibitors, two phases of delayed rectifier potassium current activation can be identified as the depolarisation duration is extended, the 1st rapidly activating (activation rate constant of 8 ms) and a 2nd phase progressively activating after depolarisation greater than 70-80 ms. The bi-phasic activation has been described previously (Anumonwo, Freeman et al. 1992; Lei, Brown et al. 2000). In sino-atrial node cells from the guinea-pig, maximally activated I_{Kr} was only 35 % of the amplitude of I_{Ks} non-maximally activated with a 700 ms depolarisation.

Buffering of cytosolic calcium with BAPTA was found to reduce the amplitude of the both components of the delayed rectifier potassium current. These data indicate that calcium is involved in the regulation pathway of both I_{Kr} and I_{Ks}, but do not provide information concerning the source of the regulating calcium. Inhibition of calcium release from the SR with ryanodine caused a reduction in the amplitude of I_{Ks}, whilst inhibition of trans-sarcolemmal flux through I_{CaL} (nifedipine) reduced both components. It therefore appears that both calcium entering the sino-atrial node cell and that released from the SR regulate the delayed rectifier potassium current, although the system appears complex and mechanisms of regulation may vary with different components. Procedures that increase calcium, increase atrial preparation beating rate, whilst inhibition of SR function and I_{CaT} in isolated sino-

atrial node cells lowers the rate of action potential generation (Huser, Blatter et al. 2000), but does not stop spontaneous activity. Isolated sino-atrial node cells rapidly cease to beat in the presence of the fast calcium chelator BAPTA. These data imply that the level of cytosolic calcium is directly related to automaticity of the sino-atrial node cell; actions to increase cellular calcium increase rate and reducing calcium slows (or stops) spontaneous activity. There is a parallel between the calcium regulation of I_K and calcium dependent effect upon beating rate; it is possible that I_K regulation alters beating rate via a calcium dependent mechanism, although the involvement of additional calcium-dependent pathways can not be excluded. This effect maybe mediated by calcium sensitive adenylate cyclase, altering cellular cAMP levels and subsequently protein kinase regulation of I_K, although other mechanisms such as calmodulin-dependent protein kinase may also be involved.

To test the possibility that adenylate cyclase activity modulates I_K, probably via a protein kinase regulation cascade, this enzyme was specifically activated using forskolin. Using the perforated patch clamp technique, both I_{Kr} and I_{Ks} were found to be augmented by forskolin. A +6 mV shift in the $V_{1/2}$ for I_f, gave evidence for increased cellular concentrations of cAMP. The regulation of I_{Kr} appears to be very sensitive to the presence of intracellular components, which are lost with conventional ruptured patch clamp techniques. This study is one of the few that has identified forskolin augmentation of the I_{Kr} (Heath and Terrar 2000); the studies that have observed an increase in I_{Kr}, all utilise techniques that minimise cytosolic dialysis. I_{Kr} was increased by 140 %, whereas delayed rectifier potassium current activated with a 700 ms depolarisation was increased by 190 % in the presence of forskolin. Inhibition of adenylate cyclase by MDL caused a -14 mV shift in the $V_{1/2}$ of I_f and

therefore indicated a substantial reduction in cAMP levels. In the presence of MDL I_{Kr} was reduced, but there appeared to be little (if any) depression of I_{Ks}. The adenylate cyclase activation and inhibition data taken together could imply that there is a basal turnover of this enzyme, producing a higher non-stimulated level of cAMP than expected. Basal cAMP could be near maximally enhancing I_{Kr}, but not having much effect upon I_{Ks}. These assumptions fit with I_{Ks} being primarily enhanced by activation and only I_{Kr} being reduced by inhibition of adenylate cyclase.

If the assumption of basal adenylate cyclase is valid, this would constitutively activate cAMP sensitive protein kinase PKA. Numerous studies of I_f by DiFrancesco's group point towards a high resting level of cAMP, as they find a relatively positive $V_{1/2}$ and have identified acetylcholine (which inhibits adenylate cyclase via G_i) to cause a negative shift in $V_{1/2}$ in the absence of pre-stimulation (DiFrancesco and Tromba 1987). Adenylate cyclase turnover is also suggested by I_{CaL} being reduced by acetylcholine in sino-atrial node, but not in the ventricle (Petit-Jacques, Bois et al. 1993; Habuchi, Nishio et al. 1996; Zaza, Robinson et al. 1996). The other major cellular 2nd messenger calcium is also thought to be at high concentration in the sino-atrial node (Verheijck 2000) and therefore processes regulated by this ubiquitous intermediate will also be intrinsically activated. Various protein kinases are sensitive to calcium and cAMP (classically PKC and PKA respectively). In the sino-atrial node a large degree of basal protein target phosphorylation should be expected, for example, of ion channels. In this study non-specific protein kinase inhibition was generally found to reduce both I_{Kr} and I_{Ks}, indicating the hypothesised basal kinase activity. PKA specific inhibition using KT-5720 was found to severely inhibit I_{Kr}, with a comparatively slight reduction of I_{Ks},

whereas PKC inhibition using 2 separate drugs was found to reduce both I_{Kr} and I_{Ks}. This is consistent with the suggestion that there is a large amount of basal PKA mediated I_{Kr} enhancement, which agrees with the adenylate cyclase data, but little PKA regulation of I_{Ks}. Both I_{Kr} and I_{Ks} are regulated by the calcium sensitive PKC, in the absence of stimulation, indicating similar basal PKC phosphorylation of the ERG and $KvLQT_1$ channels. In addition to PKA and PKC, CaMK was investigated and it turned out that inhibition caused a severe inhibition of both I_{Kr} and I_{Ks}, indicating an additional calcium sensitive phosphorylative regulation. The I_K regulation investigated in this thesis, has all been in some way dependent upon cellular calcium; PKC and CaM are directly activated by calcium, whereas PKA (via calcium regulation of AC) and CaMK (via CaM) are indirectly regulated by calcium. There appear to be multiple calcium and cAMP sensitive kinase regulations of both components of the delayed rectifier potassium current, but PKA and CaMK appear to have greater roles under these conditions.

The β-adrenoceptor agonist isoprenaline (100 nM) was found not only to increase the rate of spontaneous action potential generation by 62 %, but also the amplitude of the sino-atrial node action potentials (by 19 mV). This presumably is a result of isoprenaline mediated-augmentation of the ionic currents which underlie the depolarisation and repolarisation phases of the sino-atrial node action potential, which are I_{CaL} and the delayed rectifier potassium current respectively. Voltage clamp experiments confirmed that both of these current were enlarged by isoprenaline. When the components of the delayed rectifier potassium current were separated, I_{Ks} was enlarged by isoprenaline to a greater extent than I_{Kr}. A significant isoprenaline augmentation of I_{Kr} was found (Brown, Kimura et al. 1984; Heath and Terrar 2000),

which many previous studies have missed (Sanguinetti and Jurkiewicz 1991; Sanguinetti, Jurkiewicz et al. 1991). This finding was probably due to the perforated patch clamp technique which was used in this study (see above). In isoprenaline treated sino-atrial node cells, the beating rate was accelerated, however I_{Kr} specific inhibition did not actually reduce the rate, implying I_{Kr} had a smaller role in isoprenaline treated cells compared to control conditions. However, using the envelope of tails test, there appeared to be little difference in the tail current to step current ratio (at any duration) in the absence and the presence of isoprenaline, indicating a similar relative contribution of I_{Kr} and I_{Ks}. Although these results seem confusing, the altered action potential amplitude (I_{CaL} augmentation caused a greater overshoot) may cause a preferential activation of I_{Ks}; I_{Kr} displays marked rectification at positive voltages, whereas I_{Ks} continues to voltage dependently activate. Isoprenaline treatment has been found to reduce I_{Kr} voltage-dependent rectification at positive potentials and increase the amplitude of I_{Kr} (Heath and Terrar 2000).

To investigate the mechanism of isoprenaline mediated augmentation of I_{Kr} and I_{Ks}, various agents were used to compromise specific cellular mechanisms before exposure of these cells to isoprenaline. The % increase in these currents was compared to control results. Isoprenaline increased both components of the delayed rectifier potassium current in the presence of BAPTA. This may be a SR mediated effect, but I_{CaL} was greatly increased and so sub-sarcolemmal calcium concentrations would be elevated and it is possible that buffering of subsarcolemmal calcium by BAPTA may not be quick enough. In the presence of calcium release and entry inhibitors, only I_{Ks} was augmented by isoprenaline. This indicates that I_{Kr} regulation is precisely dependent on intracellular components (as described previously) and that

calcium regulation (possibly via calmodulin kinase) mediates at least part of the isoprenaline enlargement of I_{Kr}. The regulation of I_{Kr} appears very fragile, with actions that disturb various cellular functions abolishing the isoprenaline augmentation. I_{Ks} regulation, and hence augmentation by isoprenaline, appears to be a more robust mechanism. The amplitude of the I_{Ks} augmentation was diminished in the presence of calcium entry inhibitors, and to a lesser extent, release inhibitors. Calcium entry inhibition would in part also compromise SR calcium release, as the trigger for release would be absent. The effect of SR inhibition limiting the action of isoprenaline upon I_{Ks}, implies a substantial role for the SR in this process. Finally adenylate cyclase activity was inhibited and when these sino-atrial node cells were treated with isoprenaline both I_{Kr} and I_{Ks} were still enlarged, but to approximately a third of the control augmentation. It therefore appears that adenylate cyclase activity is important in the amplification of the delayed rectifier potassium current, but inhibition can be partially overcome with isoprenaline.

Future Work

As extensive as this study was, there remain areas in which further investigation should be directed. The main focus of future work should be to define the AC subtype that is present in the guinea-pig sino-atrial node, there is evidence for calcium up-regulated AC sub-types in other tissue (Luthi and McCormick 1999). Investigation of the whole heart did not identify this sub-type as the most prevalent, however differential AC subtype in the sino-atrial node appears probable. If a calcium up-regulated AC subtype were identified, then a link between intracellular pathways that involve the second messengers calcium and cAMP would be established. Both calcium and cAMP are thought to be at a high concentration in the

sino-atrial node and the interplay between regulation pathways which involve these two second messengers is likely to be fundamental in understanding the function of the sino-atrial node.

REFERENCES

Accili, E. A. and D. DiFrancesco (1996). "Inhibition of the hyperpolarization-activated current (if) of rabbit SA node myocytes by niflumic acid." Pflugers Arch **431**(5): 757-62.

Accili, E. A., G. Redaelli, et al. (1997). "Differential control of the hyperpolarization-activated current (i(f)) by cAMP gating and phosphatase inhibition in rabbit sino-atrial node myocytes." J Physiol **500 (Pt 3)**: 643-51.

Ahlijanian, M. K., R. E. Westenbroek, et al. (1990). "Subunit structure and localization of dihydropyridine-sensitive calcium channels in mammalian brain, spinal cord, and retina." Neuron **4**(6): 819-32.

Ahn, H. S., D. Eardley, et al. (1986). "Effects of several newer cardiotonic drugs on cardiac cyclic AMP metabolism." Biochem Pharmacol **35**(7): 1113-21.

Altomare, C., B. Terragni, et al. (2003). "Heteromeric HCN1-HCN4 channels: a comparison with native pacemaker channels from the rabbit sinoatrial node." J Physiol **549**(Pt 2): 347-59.

Anumonwo, J. M., M. Delmar, et al. (1994). "Is the "funny" current funnier than we thought?" J Cardiovasc Electrophysiol **5**(4): 394-6.

Anumonwo, J. M., L. C. Freeman, et al. (1992). "Delayed rectification in single cells isolated from guinea pig sinoatrial node." Am J Physiol **262**(3 Pt 2): H921-5.

Anumonwo, J. M., Y. N. Tallini, et al. (2001). "Action potential characteristics and arrhythmogenic properties of the cardiac conduction system of the murine heart." Circ Res **89**(4): 329-35.

Arch, J. R. and E. A. Newsholme (1976). "Activities and some properties of adenylate cyclase and phosphodiesterase in muscle, liver and nervous tissues from vertebrates and invertebrates in relation to the control of the concentration of adenosine 3':5'-cyclic monophosphate." Biochem J **158**(3): 603-22.

Arena, J. P., K. B. Walsh, et al. (1990). "Measurement, block, and modulation of potassium channel currents in the heart." Prog Clin Biol Res **334**: 43-63.

Babenko, A. and G. Vassort (1997). "Enhancement of the ATP-sensitive K+ current by extracellular ATP in rat ventricular myocytes. Involvement of adenylyl cyclase-induced subsarcolemmal ATP depletion." Circ Res **80**(4): 589-600.

Barbuti, A., M. Baruscotti, et al. (1999). "Action of internal pronase on the f-channel kinetics in the rabbit SA node." J Physiol **520 Pt 3**: 737-44.

Barhanin, J., F. Lesage, et al. (1996). "K(V)LQT1 and lsK (minK) proteins associate to form the I(Ks) cardiac potassium current." Nature **384**(6604): 78-80.

Benfey, B. G. (1990). "Function of myocardial alpha-adrenoceptors." Life Sci **46**(11): 743-57.

Benson, D. W., D. W. Wang, et al. (2003). "Congenital sick sinus syndrome caused by recessive mutations in the cardiac sodium channel gene (SCN5A)." J Clin Invest **112**(7): 1019-28.

Bers, D. M. (1993). Excitation-contraction coupling and cardiac contratile force, Kluwer Acedemic Publishers.

Bers, D. M. and E. Perez-Reyes (1999). "Ca channels in cardiac myocytes: structure and function in Ca influx and intracellular Ca release." Cardiovasc Res **42**(2): 339-60.

Bers, D. M., K. D. Philipson, et al. (1980). "Sodium-calcium exchange and sidedness of isolated cardiac sarcolemmal vesicles." Biochim Biophys Acta **601**(2): 358-71.

Bian, J., J. Cui, et al. (2001). "HERG K(+) channel activity is regulated by changes in phosphatidyl inositol 4,5-bisphosphate." Circ Res **89**(12): 1168-76.

Blatter, L. A., J. Kockskamper, et al. (2003). "Local calcium gradients during excitation-contraction coupling and alternans in atrial myocytes." J Physiol **546**(Pt 1): 19-31.

Bois, P., B. Renaudon, et al. (1997). "Activation of f-channels by cAMP analogues in macropatches from rabbit sino-atrial node myocytes." J Physiol **501 (Pt 3)**: 565-71.

Bosch, R. F., R. Gaspo, et al. (1998). "Effects of the chromanol 293B, a selective blocker of the slow, component of the delayed rectifier K+ current, on repolarization in human and guinea pig ventricular myocytes." Cardiovasc Res **38**(2): 441-50.

BoSmith, R. E., I. Briggs, et al. (1993). "Inhibitory actions of ZENECA ZD7288 on whole-cell hyperpolarization activated inward current (If) in guinea-pig dissociated sinoatrial node cells." Br J Pharmacol **110**(1): 343-9.

Bouman, L. N. and H. J. Jongsma (1986). "Structure and function of the sino-atrial node: a review." Eur Heart J 7(2): 94-104.

Boyett, M. R. (1986). "Current concepts on the electrophysiology of the myocardium." J Perinat Med **14**(6): 349-54.

Boyett, M. R., H. Honjo, et al. (2000). "The sinoatrial node, a heterogeneous pacemaker structure." Cardiovasc Res **47**(4): 658-87.

Boyett, M. R., H. Honjo, et al. (1998). "Regional differences in effects of 4-aminopyridine within the sinoatrial node." Am J Physiol **275**(4 Pt 2): H1158-68.

Boyett, M. R., I. Kodama, et al. (1995). "Ionic basis of the chronotropic effect of acetylcholine on the rabbit sinoatrial node." Cardiovascular Research **29**(6): 867-78.

Boyett, M. R., H. Honjo, et al. (1998). "Regional differences in effects of 4-aminopyridine within the sinoatrial node." Am J Physiol **275**(4 Pt 2): H1158-68.

Brahmajothi, M. V., M. J. Morales, et al. (1997). "Heterogeneity in K+ channel transcript expression detected in isolated ferret cardiac myocytes." Pacing Clin Electrophysiol **20**(2 Pt 2): 388-96.

Brahmajothi, M. V., M. J. Morales, et al. (1997). "Regional localization of ERG, the channel protein responsible for the rapid component of the delayed rectifier, K+ current in the ferret heart." Circ Res **81**(1): 128-35.

Bramich, N. J., F. R. Edwards, et al. (1990). "Sympathetic nerve stimulation and applied transmitters on the sinus venosus of the toad." J Physiol **429**: 349-75.

Brown, H. and D. Difrancesco (1980). "Voltage-clamp investigations of membrane currents underlying pace-maker activity in rabbit sino-atrial node." J Physiol **308**: 331-51.

Brown, H. F., D. DiFrancesco, et al. (1979). "How does adrenaline accelerate the heart?" Nature **280**(5719): 235-6.

Brown, H. F., J. Kimura, et al. (1984). "The ionic currents underlying pacemaker activity in rabbit sino-atrial node: experimental results and computer simulations." Proc R Soc Lond B Biol Sci **222**(1228): 329-47.

Brown, H. F., D. Noble, et al. (1986). "Relationship between the transient inward current and slow inward currents in the sino-atrial node of the rabbit." J Physiol **370**: 299-315.

Brum, G., V. Flockerzi, et al. (1983). "Injection of catalytic subunit of cAMP-dependent protein kinase into isolated cardiac myocytes." Pflugers Arch **398**(2): 147-54.

Brum, G., W. Osterrieder, et al. (1984). "Beta-adrenergic increase in the calcium conductance of cardiac myocytes studied with the patch clamp." Pflugers Arch **401**(2): 111-8.

Budd, S. L. and D. G. Nicholls (1996). "Mitochondria, calcium regulation, and acute glutamate excitotoxicity in cultured cerebellar granule cells." J Neurochem **67**(6): 2282-91.

Calaghan, S., E. White, et al. (1998). "Preservation of the in vivo phosphorylation status of phospholamban in the heart: evidence for a site-specific difference in the dephosphorylation of phospholamban." Biochem Biophys Res Commun **248**(3): 701-5.

Calaghan, S. C., E. White, et al. (1998). "Co-ordinated changes in cAMP, phosphorylated phospholamban, Ca2+ and contraction following beta-adrenergic stimulation of rat heart." Pflugers Arch **436**(6): 948-56.

Campbell, D. L., R. L. Rasmusson, et al. (1993). "The calcium-independent transient outward potassium current in isolated ferret right ventricular myocytes. I. Basic characterization and kinetic analysis." J Gen Physiol **101**(4): 571-601.

Carmeliet, E. (1993). "K+ channels and control of ventricular repolarization in the heart." Fundam Clin Pharmacol **7**(1): 19-28.

Carmeliet, E. (1993). "Use-dependent block of the delayed K+ current in rabbit ventricular myocytes." Cardiovasc Drugs Ther **7 Suppl 3**: 599-604.

Catterall, W. A. (1988). "Molecular properties of voltage-sensitive sodium and calcium channels." Braz J Med Biol Res **21**(6): 1129-44.

Chapman, R. A. and J. Tunstall (1980). "The interaction of sodium and calcium ions at the cell membrane and the control of contractile strength in frog atrial muscle." J Physiol **305**: 109-23.

Cheng, J., K. Kamiya, et al. (1999). "Heterogeneous distribution of the two components of delayed rectifier K+ current: a potential mechanism of the

proarrhythmic effects of methanesulfonanilideclass III agents." Cardiovasc Res **43**(1): 135-47.

Chinn, K. (1993). "Two delayed rectifiers in guinea pig ventricular myocytes distinguished by tail current kinetics." J Pharmacol Exp Ther **264**(2): 553-60.

Choate, J. K., F. R. Edwards, et al. (1993). "Effects of sympathetic nerve stimulation on the sino-atrial node of the guinea-pig." J Physiol **471**: 707-27.

Choate, J. K., M. Klemm, et al. (1993). "Sympathetic and parasympathetic neuromuscular junctions in the guinea-pig sino-atrial node." J Auton Nerv Syst **44**(1): 1-15.

Clark, R. B., R. A. Bouchard, et al. (1996). "Action potential duration modulates calcium influx, Na(+)-Ca2+ exchange, and intracellular calcium release in rat ventricular myocytes." Ann N Y Acad Sci **779**: 417-29.

Clay, J. R., A. Ogbaghebriel, et al. (1995). "A quantitative description of the E-4031-sensitive repolarization current in rabbit ventricular myocytes." Biophys J **69**(5): 1830-7.

Cooper, D. M., N. Mons, et al. (1995). "Adenylyl cyclases and the interaction between calcium and cAMP signalling." Nature **374**(6521): 421-4.

Coronado, R., J. Morrissette, et al. (1994). "Structure and function of ryanodine receptors." Am J Physiol **266**(6 Pt 1): C1485-504.

Cui, J., A. Kagan, et al. (2001). "Analysis of the cyclic nucleotide binding domain of the HERG potassium channel and interactions with KCNE2." J Biol Chem **276**(20): 17244-51.

Cui, Y. and D. H. Zhao (1995). "Effects of isoprenaline on delayed rectifier potassium current in isolated guinea pig ventricular myocytes." Zhongguo Yao Li Xue Bao **16**(6): 502-4.

Curran, M. E., I. Splawski, et al. (1995). "A molecular basis for cardiac arrhythmia: HERG mutations cause long QT syndrome." Cell **80**(5): 795-803.

Davis, L. M., H. L. Kanter, et al. (1994). "Distinct gap junction protein phenotypes in cardiac tissues with disparate conduction properties." J Am Coll Cardiol **24**(4): 1124-32.

Davis, L. M., M. E. Rodefeld, et al. (1995). "Gap junction protein phenotypes of the human heart and conduction system." J Cardiovasc Electrophysiol **6**(10 Pt 1): 813-22.

Defer, N., M. Best-Belpomme, et al. (2000). "Tissue specificity and physiological relevance of various isoforms of adenylyl cyclase." Am J Physiol Renal Physiol **279**(3): F400-16.

Denyer, J. C. and H. F. Brown (1990). "Rabbit sino-atrial node cells: isolation and electrophysiological properties." J Physiol **428**: 405-24.

Deschenes, I., N. Neyroud, et al. (2002). "Isoform-specific modulation of voltage-gated Na(+) channels by calmodulin." Circ Res **90**(4): E49-57.

Dhein, S., C. J. van Koppen, et al. (2001). "Muscarinic receptors in the mammalian heart." Pharmacol Res **44**(3): 161-82.

DiFrancesco, D. (1987). "The pacemaker current in the sinus node." Eur Heart J **8 Suppl L**: 19-23.

DiFrancesco, D. (1991). "The contribution of the 'pacemaker' current (if) to generation of spontaneous activity in rabbit sino-atrial node myocytes." J Physiol **434**: 23-40.

DiFrancesco, D. (1999). "Dual allosteric modulation of pacemaker (f) channels by cAMP and voltage in rabbit SA node." J Physiol **515 (Pt 2)**: 367-76.

DiFrancesco, D. and M. Mangoni (1994). "Modulation of single hyperpolarization-activated channels (i(f)) by cAMP in the rabbit sino-atrial node." J Physiol **474**(3): 473-82.

DiFrancesco, D. and C. Ojeda (1980). "Properties of the current if in the sino-atrial node of the rabbit compared with those of the current iK, in Purkinje fibres." J Physiol **308**: 353-67.

DiFrancesco, D. and P. Tortora (1991). "Direct activation of cardiac pacemaker channels by intracellular cyclic AMP." Nature **351**(6322): 145-7.

DiFrancesco, D. and C. Tromba (1987). "Acetylcholine inhibits activation of the cardiac hyperpolarizing-activated current, if." Pflugers Arch **410**(1-2): 139-42.

Ding, W. G., F. Toyoda, et al. (2002). "Blocking action of chromanol 293B on the slow component of delayed rectifier K(+) current in guinea-pig sino-atrial node cells." Br J Pharmacol **137**(2): 253-62.

Doerr, T., R. Denger, et al. (1989). "Calcium currents in single SA nodal cells of the rabbit heart studied with action potential clamp." Pflugers Arch **413**(6): 599-603.

Dokos, S., B. G. Celler, et al. (1993). "Modification of DiFrancesco-Noble equations to simulate the effects of vagal stimulation on in vivo mammalian sinoatrial node electrical activity." Ann Biomed Eng **21**(4): 321-35.

Emerick, M. C. and W. S. Agnew (1989). "Identification of phosphorylation sites for adenosine 3',5'-cyclic phosphate dependent protein kinase on the voltage-sensitive sodium channel from Electrophorus electricus." Biochemistry **28**(21): 8367-80.

England, S. K., V. N. Uebele, et al. (1995). "Characterization of a voltage-gated K+ channel beta subunit expressed in human heart." Proc Natl Acad Sci U S A **92**(14): 6309-13.

Fedida, D., F. S. Chen, et al. (1998). "The 1997 Stevenson Award Lecture. Cardiac K+ channel gating: cloned delayed rectifier mechanisms and drug modulation." Can J Physiol Pharmacol **76**(2): 77-89.

Ferrario, M., M. Sanguinetti, et al. (1991). "[Use of surgical staplers in surgery of the colon: personal experience]." G Chir **12**(3): 187-8.

Ferretti, M. E., D. Sonetti, et al. (1996). "MDL 12330A inhibits the non-neuronal adenylyl cyclase from the freshwater snail Planorbarius corneus, but the neuronal enzyme is activated by this compound." Neurosci Lett **207**(3): 191-4.

Findlay, I. (1994). "The ATP sensitive potassium channel of cardiac muscle and action potential shortening during metabolic stress." Cardiovasc Res **28**(6): 760-1.

Fischmeister, R., M. Brocas-Randolph, et al. (1986). "A dual effect of cardiac glycosides on Ca current in single cells of frog heart." Pflugers Arch **406**(3): 340-2.

Fischmeister, R. and H. C. Hartzell (1986). "Mechanism of action of acetylcholine on calcium current in single cells from frog ventricle." J Physiol **376**: 183-202.

Fischmeister, R. and H. C. Hartzell (1990). "Regulation of calcium current by low-Km cyclic AMP phosphodiesterases in cardiac cells." Mol Pharmacol **38**(3): 426-33.

Frank, J. S., G. Mottino, et al. (1992). "Distribution of the Na(+)-Ca2+ exchange protein in mammalian cardiac myocytes: an immunofluorescence and immunocolloidal gold-labeling study." J Cell Biol **117**(2): 337-45.

Freeman, L. C. and R. S. Kass (1993). "Delayed rectifier potassium channels in ventricle and sinoatrial node of the guinea pig: molecular and regulatory properties." Cardiovasc Drugs Ther **7 Suppl 3**: 627-35.

Freeman, L. C., W. M. Kwok, et al. (1992). "Phosphorylation-independent regulation of cardiac IK by guanine nucleotides and isoproterenol." Am J Physiol **262**(4 Pt 2): H1298-302.

Gao, J., R. T. Mathias, et al. (1992). "Isoprenaline, Ca2+ and the Na(+)-K+ pump in guinea-pig ventricular myocytes." J Physiol **449**: 689-704.

Gathercole, D. V., D. J. Colling, et al. (2000). "Immunogold-labeled L-type calcium channels are clustered in the surface plasma membrane overlying junctional

sarcoplasmic reticulum in guinea-pig myocytes-implications for excitation-contraction coupling in cardiac muscle." J Mol Cell Cardiol **32**(11): 1981-94.

Giles, W., T. Nakajima, et al. (1989). "Modulation of the delayed rectifier K+ current by isoprenaline in bull-frog atrial myocytes." J Physiol **415**: 233-49.

Giles, W. and Y. Shimoni (1989). "Comparison of sodium-calcium exchanger and transient inward currents in single cells from rabbit ventricle." J Physiol **417**: 465-81.

Gintant, G. A. (1995). "Regional differences in IK density in canine left ventricle: role of IK,s in electrical heterogeneity." Am J Physiol **268**(2 Pt 2): H604-13.

Gintant, G. A., N. B. Datyner, et al. (1985). "Gating of delayed rectification in acutely isolated canine cardiac Purkinje myocytes. Evidence for a single voltage-gated conductance." Biophys J **48**(6): 1059-64.

Golard, A. and S. A. Siegelbaum (1993). "Kinetic basis for the voltage-dependent inhibition of N-type calcium current by somatostatin and norepinephrine in chick sympathetic neurons." J Neurosci **13**(9): 3884-94.

Gould, R. P. and T. Powell (1972). "Intact isolated muscle cells from the adult rat heart." J Physiol **225**(2): 16P-19P.

Granzier, H. and S. Labeit (2002). "Cardiac titin: an adjustable multi-functional spring." J Physiol **541**(Pt 2): 335-42.

Guo, J., W. R. Giles, et al. (2000). "Effect of hydrogen peroxide on the membrane currents of sinoatrial node cells from rabbit heart." Am J Physiol Heart Circ Physiol **279**(3): H992-9.

Guo, J., T. Mitsuiye, et al. (1997). "The sustained inward current in sino-atrial node cells of guinea-pig heart." Pflugers Arch **433**(4): 390-6.

Guo, J. and A. Noma (1997). "Existence of a low-threshold and sustained inward current in rabbit atrio-ventricular node cells." Jpn J Physiol **47**(4): 355-9.

Guo, J., K. Ono, et al. (1995). "A sustained inward current activated at the diastolic potential range in rabbit sino-atrial node cells." J Physiol **483 (Pt 1)**: 1-13.

Habuchi, Y., M. Nishio, et al. (1996). "Regulation by acetylcholine of Ca2+ current in rabbit atrioventricular node cells." Am J Physiol **271**(6 Pt 2): H2274-82.

Habuchi, Y., T. Yamamoto, et al. (1996). "Modulation of L-type Ca current by denopamine, a nonparenteral partial beta 1 stimulant, in rabbit ventricular cells." Naunyn Schmiedebergs Arch Pharmacol **354**(4): 437-43.

Hagiwara, N. and H. Irisawa (1989). "Modulation by intracellular Ca2+ of the hyperpolarization-activated inward current in rabbit single sino-atrial node cells." J Physiol **409**: 121-41.

Hagiwara, N., H. Irisawa, et al. (1988). "Contribution of two types of calcium currents to the pacemaker potentials of rabbit sino-atrial node cells." J Physiol **395**: 233-53.

Hagiwara, N., H. Irisawa, et al. (1992). "Background current in sino-atrial node cells of the rabbit heart." J Physiol **448**: 53-72.

Hancox, J. C. and C. Howarth (1995). "The actions of nickel on membrane currents activated by hyperpolarisation in single cells from the rabbit atrioventricular node." Gen Pharmacol **26**(8): 1727-34.

Hancox, J. C. and A. J. Levi (1994). "L-type calcium current in rod- and spindle-shaped myocytes isolated from rabbit atrioventricular node." Am J Physiol **267**(5 Pt 2): H1670-80.

Hartzell, H. C., Y. Hirayama, et al. (1995). "Effects of protein phosphatase and kinase inhibitors on the cardiac L-type Ca current suggest two sites are phosphorylated by protein kinase A and another protein kinase." J Gen Physiol **106**(3): 393-414.

Hata, T., T. Noda, et al. (1996). "The role of Ca2+ release from sarcoplasmic reticulum in the regulation of sinoatrial node automaticity." Heart Vessels **11**(5): 234-41.

Hata, Y., T. Sakamoto, et al. (1998). "Effects of thapsigargin and KCl on the O2 use of the excised blood-perfused rat heart." J Mol Cell Cardiol **30**(10): 2137-43.

Hauswirth, O., R. E. McAllister, et al. (1969). "Reconstruction of the actions of adrenaline and calcium on cardiac pacemaker potentials." J Physiol **204**(2): 126P+.

Heath, B. M. and D. A. Terrar (1994). "Effect of glibenclamide, forskolin, and isoprenaline on the parallel activation of KATP and reduction of IK by cromakalim in cardiac myocytes." Cardiovasc Res **28**(6): 818-22.

Heath, B. M. and D. A. Terrar (1996). "The deactivation kinetics of the delayed rectifier components IKr and IKs in guinea-pig isolated ventricular myocytes." Exp Physiol **81**(4): 605-21.

Heath, B. M. and D. A. Terrar (1996). "Separation of the components of the delayed rectifier potassium current using selective blockers of IKr and IKs in guinea-pig isolated ventricular myocytes." Exp Physiol **81**(4): 587-603.

Heath, B. M. and D. A. Terrar (2000). "Protein kinase C enhances the rapidly activating delayed rectifier potassium current, IKr, through a reduction in C-type inactivation in guinea-pig ventricular myocytes." J Physiol **522 Pt 3**: 391-402.

Herring, N., L. Rigg, et al. (2001). "NO-cGMP pathway increases the hyperpolarisation-activated current, I(f), and heart rate during adrenergic stimulation." Cardiovasc Res **52**(3): 446-53.

Hirano, Y., H. A. Fozzard, et al. (1989). "Characteristics of L- and T-type Ca2+ currents in canine cardiac Purkinje cells." Am J Physiol **256**(5 Pt 2): H1478-92.

Hirano, Y., H. A. Fozzard, et al. (1989). "Inactivation properties of T-type calcium current in canine cardiac Purkinje cells." Biophys J **56**(5): 1007-16.

Honjo, H., M. R. Boyett, et al. (1996). "Correlation between electrical activity and the size of rabbit sino-atrial node cells." J Physiol **496 (Pt 3)**: 795-808.

Honjo, H., M. Lei, et al. (1999). "Heterogeneity of 4-aminopyridine-sensitive current in rabbit sinoatrial node cells." Am J Physiol **276**(4 Pt 2): H1295-304.

Hori, Y., T. Takamoto, et al. (1989). "Monoclonal antibody to phospholamban isolated from bovine cardiac muscle." J Clin Lab Immunol **30**(4): 163-8.

Hove-Madsen, L., P. F. Mery, et al. (1996). "Regulation of myocardial calcium channels by cyclic AMP metabolism." Basic Res Cardiol **91 Suppl 2**: 1-8.

Howarth, F. C., A. J. Levi, et al. (1996). "Characteristics of the delayed rectifier K current compared in myocytes isolated from the atrioventricular node and ventricle of the rabbit heart." Pflugers Arch **431**(5): 713-22.

Huser, J., L. A. Blatter, et al. (2000). "Intracellular Ca2+ release contributes to automaticity in cat atrial pacemaker cells." J Physiol **524 Pt 2**: 415-22.

Iijima, T. and N. Taira (1989). "Mechanisms of beta-adrenoceptor mediated increase in delayed rectifier potassium current." Tohoku J Exp Med **159**(4): 277-81.

Irisawa, H. (1987). "Membrane currents in cardiac pacemaker tissue." Experientia **43**(11-12): 1131-5.

Irisawa, H., H. F. Brown, et al. (1993). "Cardiac pacemaking in the sinoatrial node." Physiol Rev **73**(1): 197-227.

Isacoff, E., D. Papazian, et al. (1990). "Molecular studies of voltage-gated potassium channels." Cold Spring Harb Symp Quant Biol **55**: 9-17.

Isacoff, E. Y., Y. N. Jan, et al. (1990). "Evidence for the formation of heteromultimeric potassium channels in Xenopus oocytes." Nature **345**(6275): 530-4.

Ishii, K., T. Yamagishi, et al. (1994). "Cloning and functional expression of a cardiac inward rectifier K+ channel." FEBS Lett **338**(1): 107-11.

Isosaki, M., N. Minami, et al. (1994). "Pharmacological evidence for regulation of Na(+)-Ca++ exchange by Ca++/calmodulin-dependent protein kinase in

isolated bovine adrenal medullary cells." J Pharmacol Exp Ther **270**(1): 104-10.

Ito, H. and K. Ono (1995). "A rapidly activating delayed rectifier K+ channel in rabbit sinoatrial node cells." Am J Physiol **269**(2 Pt 2): H443-52.

Janiak, R. and B. Lewartowski (1996). "Early after-depolarisations induced by noradrenaline may be initiated by calcium released from sarcoplasmic reticulum." Mol Cell Biochem **163-164**: 125-30.

Jewett, P. H., S. D. Leonard, et al. (1973). "Chicken cardiac muscle: its elusive extended junctional sarcoplasmic reticulum and sarcoplasmic reticulum fenestrations." J Cell Biol **56**(2): 595-600.

Jiang, M., W. Dun, et al. (1999). "Use-dependent 'agonist' effect of azimilide on the HERG channel." J Pharmacol Exp Ther **291**(3): 1324-36.

Jorgensen, A. O. and L. R. Jones (1987). "Immunoelectron microscopical localization of phospholamban in adult canine ventricular muscle." J Cell Biol **104**(5): 1343-52.

Josephson, I. R., A. Guia, et al. (2002). "Modulation of the conductance of unitary cardiac L-type Ca(2+) channels by conditioning voltage and divalent ions." Biophys J **83**(5): 2587-94.

Ju, Y. K. and D. G. Allen (1998). "Intracellular calcium and Na+-Ca2+ exchange current in isolated toad pacemaker cells." J Physiol **508 (Pt 1)**: 153-66.

Ju, Y. K. and D. G. Allen (1999). "How does beta-adrenergic stimulation increase the heart rate? The role of intracellular Ca2+ release in amphibian pacemaker cells." J Physiol **516 (Pt 3)**: 793-804.

Ju, Y. K. and D. G. Allen (2000). "The distribution of calcium in toad cardiac pacemaker cells during spontaneous firing." Pflugers Arch **441**(2-3): 219-27.

Kamp, T. J. and J. W. Hell (2000). "Regulation of cardiac L-type calcium channels by protein kinase A and protein kinase C." Circ Res **87**(12): 1095-102.

Kiehn, J., C. Karle, et al. (1998). "HERG potassium channel activation is shifted by phorbol esters via protein kinase A-dependent pathways." J Biol Chem **273**(39): 25285-91.

Kiehn, J., B. Wible, et al. (1995). "Cloned human inward rectifier K+ channel as a target for class III methanesulfonanilides." Circ Res **77**(6): 1151-5.

Kodama, I., M. R. Nikmaram, et al. (1997). "Regional differences in the role of the Ca2+ and Na+ currents in pacemaker activity in the sinoatrial node." Am J Physiol **272**(6 Pt 2): H2793-806.

Komas, N., A. Le Bec, et al. (1991). "Cardiac cGMP-stimulated cyclic nucleotide phosphodiesterases: effects of cGMP analogues and drugs." Eur J Pharmacol **206**(1): 5-13.

Kurachi, Y., Y. Asano, et al. (1989). "Cardiac Ca current does not run down and is very sensitive to isoprenaline in the nystatin-method of whole cell recording." Naunyn Schmiedebergs Arch Pharmacol **340**(2): 219-22.

Kurokawa, H., P. A. Murray, et al. (2002). "Propofol attenuates beta-adrenoreceptor-mediated signal transduction via a protein kinase C-dependent pathway in cardiomyocytes." Anesthesiology **96**(3): 688-98.

Kyrozis, A. and D. B. Reichling (1995). "Perforated-patch recording with gramicidin avoids artifactual changes in intracellular chloride concentration." J Neurosci Methods **57**(1): 27-35.

Lei, M. and H. F. Brown (1996). "Two components of the delayed rectifier potassium current, IK, in rabbit sino-atrial node cells." Exp Physiol **81**(5): 725-41.

Lei, M., H. F. Brown, et al. (2000). "Modulation of delayed rectifier potassium current, iK, by isoprenaline in rabbit isolated pacemaker cells." Exp Physiol **85**(1): 27-35.

Lei, M., P. J. Cooper, et al. (2002). "Role of the 293b-sensitive, slowly activating delayed rectifier potassium current, i(Ks), in pacemaker activity of rabbit isolated sino-atrial node cells." Cardiovasc Res **53**(1): 68-79.

Lemaire, S., C. Piot, et al. (1998). "Heart rate as a determinant of L-type Ca2+ channel activity: mechanisms and implication in force-frequency relation." Basic Res Cardiol **93 Suppl 1**: 51-9.

Leuranguer, V., A. Monteil, et al. (2000). "T-type calcium currents in rat cardiomyocytes during postnatal development: contribution to hormone secretion." Am J Physiol Heart Circ Physiol **279**(5): H2540-8.

Li, J., J. Qu, et al. (1997). "Ionic basis of ryanodine's negative chronotropic effect on pacemaker cells isolated from the sinoatrial node." Am J Physiol **273**(5 Pt 2): H2481-9.

Lindner, M., T. Bohle, et al. (2002). "Ca2+-handling in heart failure--a review focusing on Ca2+ sparks." Basic Res Cardiol **97 Suppl 1**: I79-82.

Lipp, P. and E. Niggli (1994). "Modulation of Ca2+ release in cultured neonatal rat cardiac myocytes. Insight from subcellular release patterns revealed by confocal microscopy." Circ Res **74**(5): 979-90.

Lipsius, S. L., J. Huser, et al. (2001). "Intracellular Ca2+ release sparks atrial pacemaker activity." News Physiol Sci **16**: 101-6.

Liu, L. W. and J. D. Huizinga (1994). "Canine colonic circular muscle generates action potentials without the pacemaker component." Can J Physiol Pharmacol **72**(1): 70-81.

Lo, C. F. and R. Numann (1998). "Independent and exclusive modulation of cardiac delayed rectifying K+ current by protein kinase C and protein kinase A." Circ Res **83**(10): 995-1002.

Luthi, A., T. Bal, et al. (1998). "Periodicity of thalamic spindle waves is abolished by ZD7288,a blocker of Ih." J Neurophysiol **79**(6): 3284-9.

Luthi, A. and D. A. McCormick (1998). "Periodicity of thalamic synchronized oscillations: the role of Ca2+-mediated upregulation of Ih." Neuron **20**(3): 553-63.

Luthi, A. and D. A. McCormick (1999). "Ca(2+)-mediated up-regulation of Ih in the thalamus. How cell-intrinsic ionic currents may shape network activity." Ann N Y Acad Sci **868**: 765-9.

Luthi, A. and D. A. McCormick (1999). "Modulation of a pacemaker current through Ca(2+)-induced stimulation of cAMP production." Nat Neurosci **2**(7): 634-41.

Mamas, M. A. and D. A. Terrar (2001). "Inotropic actions of protein kinase C activation by phorbol dibutyrate in guinea-pig isolated ventricular myocytes." Exp Physiol **86**(5): 561-70.

Mangoni, M. E., B. Couette, et al. (2003). "Functional role of L-type Cav1.3 Ca2+ channels in cardiac pacemaker activity." Proc Natl Acad Sci U S A **100**(9): 5543-8.

Mangoni, M. E. and J. Nargeot (2001). "Properties of the hyperpolarization-activated current (I(f)) in isolated mouse sino-atrial cells." Cardiovasc Res **52**(1): 51-64.

Marcus, D. C., H. Sunose, et al. (1997). "P2U purinergic receptor inhibits apical IsK/KvLQT1 channel via protein kinase C in vestibular dark cells." Am J Physiol **273**(6 Pt 1): C2022-9.

Martinez, M. L., M. P. Heredia, et al. (1999). "Expression of T-type Ca(2+) channels in ventricular cells from hypertrophied rat hearts." J Mol Cell Cardiol **31**(9): 1617-25.

Marx, S. O., J. Kurokawa, et al. (2002). "Requirement of a macromolecular signaling complex for beta adrenergic receptor modulation of the KCNQ1-KCNE1 potassium channel." Science **295**(5554): 496-9.

Matsubayashi, T., H. Matsuura, et al. (1999). "On the mechanism of the enhancement of delayed rectifier K+ current by extracellular ATP in guinea-pig ventricular myocytes." Pflugers Arch **437**(5): 635-42.

Matsuura, H. and T. Ehara (1997). "Selective enhancement of the slow component of delayed rectifier K+ current in guinea-pig atrial cells by external ATP." J Physiol **503 (Pt 1)**: 45-54.

Matsuura, H., T. Ehara, et al. (2002). "Rapidly and slowly activating components of delayed rectifier K(+) current in guinea-pig sino-atrial node pacemaker cells." J Physiol **540**(Pt 3): 815-30.

Matsuura, H., T. Ehara, et al. (1987). "An analysis of the delayed outward current in single ventricular cells of the guinea-pig." Pflugers Arch **410**(6): 596-603.

Matsuura, H., Y. Tsuruhara, et al. (1996). "Enhancement of delayed rectifier K+ current by P2-purinoceptor stimulation in guinea-pig atrial cells." J Physiol **490 (Pt 3)**: 647-58.

McDonald, T. V., Z. Yu, et al. (1997). "A minK-HERG complex regulates the cardiac potassium current I(Kr)." Nature **388**(6639): 289-92.

Misquitta, C. M., D. P. Mack, et al. (1999). "Sarco/endoplasmic reticulum Ca2+ (SERCA)-pumps: link to heart beats and calcium waves." Cell Calcium **25**(4): 277-90.

Misquitta, C. M., A. Sing, et al. (1999). "Control of sarcoplasmic/endoplasmic-reticulum Ca2+ pump expression in cardiac and smooth muscle." Biochem J **338 (Pt 1)**: 167-73.

Mitsuiye, T., J. Guo, et al. (1999). "Nicardipine-sensitive Na+-mediated single channel currents in guinea-pig sinoatrial node pacemaker cells." J Physiol **521 Pt 1**: 69-79.

Mitsuiye, T., Y. Shinagawa, et al. (2000). "Sustained inward current during pacemaker depolarization in mammalian sinoatrial node cells." Circ Res **87**(2): 88-91.

Morace, G., M. Sanguinetti, et al. (1995). "In vitro susceptibility of Candida species isolated from patients with haematological malignancies." Mycoses **38**(1-2): 59-67.

Narayanan, N. and A. Xu (1997). "Phosphorylation and regulation of the Ca(2+)-pumping ATPase in cardiac sarcoplasmic reticulum by calcium/calmodulin-dependent protein kinase." Basic Res Cardiol **92 Suppl 1**: 25-35.

Nerbonne, J. M. (2000). "Molecular basis of functional voltage-gated K+ channel diversity in the mammalian myocardium." J Physiol **525 Pt 2**: 285-98.

Nicoll, D. A., S. Longoni, et al. (1990). "Molecular cloning and functional expression of the cardiac sarcolemmal Na(+)-Ca2+ exchanger." Science **250**(4980): 562-5.

Nitta, J., T. Furukawa, et al. (1994). "Subcellular mechanism for Ca(2+)-dependent enhancement of delayed rectifier K+ current in isolated membrane patches of guinea pig ventricular myocytes." Circ Res **74**(1): 96-104.

Okada, T. (1976). "Effect of verapamil on electrical activities of SA node, ventricular muscle and Purkinje fibers in isolated rabbit hearts." Jpn Circ J **40**(4): 329-41.

Ono, K. and H. Ito (1995). "Role of rapidly activating delayed rectifier K+ current in sinoatrial node pacemaker activity." Am J Physiol **269**(2 Pt 2): H453-62

Ono, K., S. Shibata, et al. (2000). "Properties of the delayed rectifier potassium current in porcine sino-atrial node cells." J Physiol (Lond) **524**(Pt 1): 51-62.

Opie, L. H., C. Muller, et al. (1980). "Evidence for role of cyclic AMP as second messenger of arrhythmogenic effects of beta-stimulation." Adv Cyclic Nucleotide Res **12**: 63-9.

Osterrieder, W., G. Brum, et al. (1982). "Injection of subunits of cyclic AMP-dependent protein kinase into cardiac myocytes modulates Ca2+ current." Nature **298**(5874): 576-8.

Pan, B. S., J. D. Hannon, et al. (1999). "Effects of isoproterenol on twitch contraction of wild type and phospholamban-deficient murine ventricular myocardium." J Mol Cell Cardiol **31**(1): 159-66.

Parratt, J. R. and K. A. Kane (1994). "KATP channels in ischaemic preconditioning." Cardiovasc Res **28**(6): 783-7.

Perchenet, L., A. K. Hinde, et al. (2000). "Stimulation of Na/Ca exchange by the beta-adrenergic/protein kinase A pathway in guinea-pig ventricular myocytes at 37 degrees C." Pflugers Arch **439**(6): 822-8.

Perez-Reyes, E., W. Yuan, et al. (1994). "Regulation of the cloned L-type cardiac calcium channel by cyclic-AMP-dependent protein kinase." FEBS Lett **342**(2): 119-23.

Petit-Jacques, J., P. Bois, et al. (1993). "Mechanism of muscarinic control of the high-threshold calcium current in rabbit sino-atrial node myocytes." Pflugers Arch **423**(1-2): 21-7.

Philipson, K. D., D. M. Bers, et al. (1980). "Binding of Ca2+ and Na+ to sarcolemmal membranes: relation to control of myocardial contractility." Am J Physiol **238**(3): H373-8.

Piascik, M. T., M. Babich, et al. (1986). "Calmodulin activation and calcium regulation of parotid gland adenylate cyclase." Am J Physiol **250**(4 Pt 1): C642-5.

Piascik, M. T., M. Babich, et al. (1983). "Calmodulin stimulation and calcium regulation of smooth muscle adenylate cyclase activity." J Biol Chem **258**(18): 10913-8.

Pitts, B. J. (1979). "Stoichiometry of sodium-calcium exchange in cardiac sarcolemmal vesicles. Coupling to the sodium pump." J Biol Chem **254**(14): 6232-5.

Po, S., S. Roberds, et al. (1993). "Heteromultimeric assembly of human potassium channels. Molecular basis of a transient outward current?" Circ Res **72**(6): 1326-36.

Powell, T., M. F. Sturridge, et al. (1981). "Intact individual heart cells isolated from human ventricular tissue." Br Med J (Clin Res Ed) **283**(6298): 1013-5.

Powell, T., D. A. Terrar, et al. (1980). "Electrical properties of individual cells isolated from adult rat ventricular myocardium." J Physiol **302**: 131-53.

Protas, L. and R. B. Robinson (2000). "Mibefradil, an I(Ca,T) blocker, effectively blocks I(Ca,L) in rabbit sinus node cells." Eur J Pharmacol **401**(1): 27-30.

Pusch, M., R. Magrassi, et al. (1998). "Activation and inactivation of homomeric KvLQT1 potassium channels." Biophys J **75**(2): 785-92.

Qu, Y. and D. L. Campbell (1998). "Modulation of L-type calcium current kinetics by sarcoplasmic reticulum calcium release in ferret isolated right ventricular myocytes." Can J Cardiol **14**(2): 263-72.

Rakovic, T. (2000). Biophysics, Boston, USA.

Rasmusson, R. L., M. J. Morales, et al. (1998). "Inactivation of voltage-gated cardiac K+ channels." Circ Res **82**(7): 739-50.

Renaudon, B., J. Bescond, et al. (1998). "Nucleotide modulation of f-channel activity in rabbit sino-atrial node myocytes." Receptors Channels **5**(5): 315-22.

Renaudon, B., P. Bois, et al. (1997). "Acetylcholine modulates I(f) and IK(ACh) via different pathways in rabbit sino-atrial node cells." J Mol Cell Cardiol **29**(3): 969-75.

Reuter, H. and U. Wollert (1967). "[On the effect of various sympathomimetic amines on contractility and Ca-45-uptake of isolated guinea pig auricles]." Naunyn Schmiedebergs Arch Exp Pathol Pharmakol **258**(3): 288-96.

Rigg, L., B. M. Heath, et al. (2000). "Localisation and functional significance of ryanodine receptors during beta-adrenoceptor stimulation in the guinea-pig sino-atrial node." Cardiovasc Res **48**(2): 254-64.

Rigg, L., P. A. Mattick, et al. (2003). "Modulation of the hyperpolarization-activated current (I(f)) by calcium and calmodulin in the guinea-pig sino-atrial node." Cardiovasc Res **57**(2): 497-504.

Rigg, L. and D. A. Terrar (1996). "Possible role of calcium release from the sarcoplasmic reticulum in pacemaking in guinea-pig sino-atrial node." Exp Physiol **81**(5): 877-80.

Robinson, R. B. and S. A. Siegelbaum (2003). "HYPERPOLARIZATION-ACTIVATED CATION CURRENTS: From Molecules to Physiological Function." Annu Rev Physiol **65**: 453-80.

Roche, J. P., R. Westenbroek, et al. (2002). "Antibodies and a cysteine-modifying reagent show correspondence of M current in neurons to KCNQ2 and KCNQ3 K+ channels." Br J Pharmacol **137**(8): 1173-86.

Rubenstein, D. S., J. P. Zbilut, et al. (1993). "Phase-dependent properties of the cardiac sarcoplasmic reticulum oscillator in cat right atrium: a mechanism contributing to dysrhythmias induced by Ca2+ overload." Exp Physiol **78**(1): 79-93.

Salata, J. J., N. K. Jurkiewicz, et al. (1996). "IK of rabbit ventricle is composed of two currents: evidence for IKs." Am J Physiol **271**(6 Pt 2): H2477-89.

Sanguinetti, M. C., M. E. Curran, et al. (1996). "Coassembly of K(V)LQT1 and minK (IsK) proteins to form cardiac I(Ks) potassium channel." Nature **384**(6604): 80-3.

Sanguinetti, M. C., C. Jiang, et al. (1995). "A mechanistic link between an inherited and an acquired cardiac arrhythmia: HERG encodes the IKr potassium channel." Cell **81**(2): 299-307.

Sanguinetti, M. C. and N. K. Jurkiewicz (1990). "Two components of cardiac delayed rectifier K+ current. Differential sensitivity to block by class III antiarrhythmic agents." J Gen Physiol **96**(1): 195-215.

Sanguinetti, M. C. and N. K. Jurkiewicz (1991). "Delayed rectifier outward K+ current is composed of two currents in guinea pig atrial cells." Am J Physiol **260**(2 Pt 2): H393-9.

Sanguinetti, M. C., N. K. Jurkiewicz, et al. (1991). "Isoproterenol antagonizes prolongation of refractory period by the class III antiarrhythmic agent E-4031 in guinea pig myocytes. Mechanism of action." Circ Res **68**(1): 77-84.

Sato, Y., D. G. Ferguson, et al. (1998). "Cardiac-specific overexpression of mouse cardiac calsequestrin is associated with depressed cardiovascular function and hypertrophy in transgenic mice." J Biol Chem **273**(43): 28470-7.

Satoh, H. (1994). "Elevation of intracellular Ca2+ concentration by protein kinase C stimulation in isolated single rabbit sino-atrial node cells." Gen Pharmacol **25**(2): 325-32.

Satoh, H. (1995). "Role of T-type Ca2+ channel inhibitors in the pacemaker depolarization in rabbit sino-atrial nodal cells." Gen Pharmacol **26**(3): 581-7.

Schmalhofer, W. A., J. Bao, et al. (2002). "Identification of a new class of inhibitors of the voltage-gated potassium channel, Kv1.3, with immunosuppressant properties." Biochemistry **41**(24): 7781-94.

Schmitz, W., T. Eschenhagen, et al. (1991). "The role of alpha 1-adrenergic and muscarinic receptors in cardiac function." Eur Heart J **12 Suppl F**: 83-7.

Schnee, M. E. and B. S. Brown (1998). "Selectivity of linopirdine (DuP 996), a neurotransmitter release enhancer, in blocking voltage-dependent and calcium-activated potassium currents in hippocampal neurons." J Pharmacol Exp Ther **286**(2): 709-17.

Seamon, K. B. and J. W. Daly (1981). "Forskolin: a unique diterpene activator of cyclic AMP-generating systems." J Cyclic Nucleotide Res **7**(4): 201-24.

Seamon, K. B., W. Padgett, et al. (1981). "Forskolin: unique diterpene activator of adenylate cyclase in membranes and in intact cells." Proc Natl Acad Sci U S A **78**(6): 3363-7.

Seebohm, G., C. Lerche, et al. (2001). "Dependence of I(Ks) biophysical properties on the expression system." Pflugers Arch **442**(6): 891-5.

Shah, N., N. Than, et al. (1994). "The role of the sarcoplasmic reticulum in the response of isolated ferret cardiac muscle to beta-adrenergic stimulation." Exp Physiol **79**(6): 929-41.

Sharma, O. P., J. A. Flores, et al. (1994). "Cellular basis for follicle-stimulating hormone-stimulated calcium signaling in single rat Sertoli cells: possible dissociation from effects of adenosine 3',5'-monophosphate." Endocrinology **134**(4): 1915-23.

Shi, W., R. Wymore, et al. (1999). "Distribution and prevalence of hyperpolarization-activated cation channel (HCN) mRNA expression in cardiac tissues." Circ Res **85**(1): e1-6.

Shibasaki, T. (1987). "Conductance and kinetics of delayed rectifier potassium channels in nodal cells of the rabbit heart." J Physiol **387**: 227-50.

Shinagawa, Y., H. Satoh, et al. (2000). "The sustained inward current and inward rectifier K+ current in pacemaker cells dissociated from rat sinoatrial node." J Physiol **523 Pt 3**: 593-605.

Sipido, K. R., M. Maes, et al. (1997). "Low efficiency of Ca2+ entry through the Na(+)-Ca2+ exchanger as trigger for Ca2+ release from the sarcoplasmic reticulum. A comparison between L-type Ca2+ current and reverse-mode Na(+)-Ca2+ exchange." Circ Res **81**(6): 1034-44.

Smith, G. D., J. E. Keizer, et al. (1998). "A simple numerical model of calcium spark formation and detection in cardiac myocytes." Biophys J **75**(1): 15-32.

Snyders, D. J., M. M. Tamkun, et al. (1993). "A rapidly activating and slowly inactivating potassium channel cloned from human heart. Functional analysis after stable mammalian cell culture expression." J Gen Physiol **101**(4): 513-43.

Sommer, J. R. and E. A. Johnson (1968). "Cardiac muscle. A comparative study of Purkinje fibers and ventricular fibers." J Cell Biol **36**(3): 497-526.

Song, L. S., A. Guia, et al. (2002). "Ca(2+) signaling in cardiac myocytes overexpressing the alpha(1) subunit of L-type Ca(2+) channel." Circ Res **90**(2): 174-81.

Song, L. S., M. D. Stern, et al. (1997). "Partial depletion of sarcoplasmic reticulum calcium does not prevent calcium sparks in rat ventricular myocytes." J Physiol **505 (Pt 3)**: 665-75.

Spector, P. S., M. E. Curran, et al. (1996). "Fast inactivation causes rectification of the IKr channel." J Gen Physiol **107**(5): 611-9.

Stern, M. D., G. Pizarro, et al. (1997). "Local control model of excitation-contraction coupling in skeletal muscle." J Gen Physiol **110**(4): 415-40.

Suessbrich, H. and A. E. Busch (1999). "The IKs channel: coassembly of IsK (minK) and KvLQT1 proteins." Rev Physiol Biochem Pharmacol **137**: 191-226.

Swan, H., M. Viitasalo, et al. (1999). "Sinus node function and ventricular repolarization during exercise stress test in long QT syndrome patients with KvLQT1 and HERG potassium channel defects." J Am Coll Cardiol **34**(3): 823-9.

Takagishi, Y., K. Yasui, et al. (2000). "Species-specific difference in distribution of voltage-gated L-type Ca(2+) channels of cardiac myocytes." Am J Physiol Cell Physiol **279**(6): C1963-9.

Takei, R., I. Ikegaki, et al. (1999). "Naftopidil, a novel alpha1-adrenoceptor antagonist, displays selective inhibition of canine prostatic pressure and high affinity binding to cloned human alpha1-adrenoceptors." Jpn J Pharmacol **79**(4): 447-54.

Tanaka, H., R. B. Clark, et al. (1996). "Positive chronotropic responses of rabbit sino-atrial node cells to flash photolysis of caged isoproterenol and cyclic AMP." Proc R Soc Lond B Biol Sci **263**(1368): 241-8.

Terrar, D. and L. Rigg (2000). "What determines the initiation of the heartbeat?" J Physiol **524 Pt 2**: 316.

Tesmer, J. J. and S. R. Sprang (1998). "The structure, catalytic mechanism and regulation of adenylyl cyclase." Curr Opin Struct Biol **8**(6): 713-9.

Tohse, N., M. Kameyama, et al. (1987). "Intracellular Ca2+ and protein kinase C modulate K+ current in guinea pig heart cells." Am J Physiol **253**(5 Pt 2): H1321-4.

Tohse, N., M. Kameyama, et al. (1990). "Protein kinase C activation enhances the delayed rectifier potassium current in guinea-pig heart cells." J Mol Cell Cardiol **22**(6): 725-34.

Tohse, N., H. Nakaya, et al. (1992). "Alpha 1-adrenoceptor stimulation enhances the delayed rectifier K+ current of guinea pig ventricular cells through the activation of protein kinase C." Circ Res **71**(6): 1441-6.

Trautwein, W. and M. Kameyama (1986). "Intracellular control of calcium and potassium currents in cardiac cells." Jpn Heart J **27 Suppl 1**: 31-50.

Tsien, R. W. (1983). "Calcium channels in excitable cell membranes." Annu Rev Physiol **45**: 341-58.

Tsien, R. W., B. P. Bean, et al. (1983). "Calcium channels: mechanisms of beta-adrenergic modulation and ion permeation." Cold Spring Harb Symp Quant Biol **48 Pt 1**: 201-12.

Tsien, R. W., P. Hess, et al. (1987). "Calcium channels: mechanisms of selectivity, permeation, and block." Annu Rev Biophys Biophys Chem **16**: 265-90.

Tytgat, J., B. Nilius, et al. (1988). "The T-type Ca channel in guinea-pig ventricular myocytes is insensitive to isoproterenol." Pflugers Arch **411**(6): 704-6.

Tytgat, J., J. Vereecke, et al. (1990). "A combined study of sodium current and T-type calcium current in isolated cardiac cells." Pflugers Arch **417**(2): 142-8.

Tytgat, J., J. Vereecke, et al. (1990). "Mechanism of cardiac T-type Ca channel blockade by amiloride." J Pharmacol Exp Ther **254**(2): 546-51.

Vaccari, T., A. Moroni, et al. (1999). "The human gene coding for HCN2, a pacemaker channel of the heart." Biochim Biophys Acta **1446**(3): 419-25.

Varnum, M. D., A. E. Busch, et al. (1993). "The min K channel underlies the cardiac potassium current IKs and mediates species-specific responses to protein kinase C." Proc Natl Acad Sci U S A **90**(24): 11528-32.

Vassalle, M. (1987). "Contribution of the Na+/K+-pump to the membrane potential." Experientia **43**(11-12): 1135-40.

Vassalle, M. (1995). "The pacemaker current (I(f)) does not play an important role in regulating SA node pacemaker activity." Cardiovasc Res **30**(2): 309-10.

Verheijck, E. E. (2000). EWGCCE, Bern, Switzerland.

Verheijck, E. E., A. C. van Ginneken, et al. (1995). "Effects of delayed rectifier current blockade by E-4031 on impulse generation in single sinoatrial nodal myocytes of the rabbit." Circ Res **76**(4): 607-15.

Verkerk, A. O., R. Wilders, et al. (2002). "Ca(2+)-activated Cl(-) current in rabbit sinoatrial node cells." J Physiol **540**(Pt 1): 105-17.

Vieth, W. R., K. Nho, et al. (1993). "Dual role of calmodulin in excitable cells." Ann Biomed Eng **21**(6): 669-77.

Vinogradova, T. M., K. Y. Bogdanov, et al. (2002). "beta-Adrenergic stimulation modulates ryanodine receptor Ca(2+) release during diastolic depolarization to accelerate pacemaker activity in rabbit sinoatrial nodal cells." Circ Res **90**(1): 73-9.

Vinogradova, T. M., K. Y. Bogdanov, et al. (2002). "Novel perspectives on the beating rate of the heart." Circ Res **91**(4): e3.

Vinogradova, T. M., Y. Y. Zhou, et al. (2000). "Sinoatrial node pacemaker activity requires Ca(2+)/calmodulin-dependent protein kinase II activation." Circ Res **87**(9): 760-7.

Wagner, M. B., T. Namiki, et al. (1999). "Electrical interactions among real cardiac cells and cell models in a linear strand." Am J Physiol **276**(2 Pt 2): H391-400.

Walsh, K. B., J. P. Arena, et al. (1991). "Delayed-rectifier potassium channel activity in isolated membrane patches of guinea pig ventricular myocytes." Am J Physiol **260**(4 Pt 2): H1390-3.

Walsh, K. B., T. B. Begenisich, et al. (1989). "Beta-adrenergic modulation of cardiac ion channels. Differential temperature sensitivity of potassium and calcium currents." J Gen Physiol **93**(5): 841-54.

Walsh, K. B. and R. S. Kass (1988). "Regulation of a heart potassium channel by protein kinase A and C." Science **242**(4875): 67-9.

Walsh, K. B. and R. S. Kass (1991). "Distinct voltage-dependent regulation of a heart-delayed IK by protein kinases A and C." Am J Physiol **261**(6 Pt 1): C1081-90.

Wang, Q., M. E. Curran, et al. (1996). "Positional cloning of a novel potassium channel gene: KVLQT1 mutations cause cardiac arrhythmias." Nat Genet **12**(1): 17-23.

Wang, X. and N. S. Dhalla (2000). "Modification of beta-adrenoceptor signal transduction pathway by genetic manipulation and heart failure." Mol Cell Biochem **214**(1-2): 131-55.

Watanabe, E. I., H. Honjo, et al. (1995). "Modulation of pacemaker activity of sinoatrial node cells by electrical load imposed by an atrial cell model." American Journal of Physiology **269**(5 Pt 2): H1735-42.

Way, K. J., E. Chou, et al. (2000). "Identification of PKC-isoform-specific biological actions using pharmacological approaches." Trends Pharmacol Sci **21**(5): 181-7.

Wickenden, A. (2002). "K(+) channels as therapeutic drug targets." Pharmacol Ther **94**(1-2): 157-82.

Wieland (1986). Phalloidotoxins. New York, Springer-Verlag.

Wier, W. G. (1990). "Cytoplasmic [Ca2+] in mammalian ventricle: dynamic control by cellular processes." Annu Rev Physiol **52**: 467-85.

Wu, J., R. B. Schuessler, et al. (2001). "Morphological and membrane characteristics of spider and spindle cells isolated from rabbit sinus node." Am J Physiol Heart Circ Physiol **280**(3): H1232-40.

Wu, Y., I. Dzhura, et al. (2001). "Calmodulin kinase and a calmodulin-binding 'IQ' domain facilitate L-type Ca2+ current in rabbit ventricular myocytes by a common mechanism." J Physiol **535**(Pt 3): 679-87.

Wu, Y., L. B. MacMillan, et al. (1999). "CaM kinase augments cardiac L-type Ca2+ current: a cellular mechanism for long Q-T arrhythmias." Am J Physiol **276**(6 Pt 2): H2168-78.

Wymore, R. S., G. A. Gintant, et al. (1997). "Tissue and species distribution of mRNA for the IKr-like K+ channel, erg." Circ Res **80**(2): 261-8.

Xiao, R. P., H. Cheng, et al. (1994). "Dual regulation of Ca2+/calmodulin-dependent kinase II activity by membrane voltage and by calcium influx." Proc Natl Acad Sci U S A **91**(20): 9659-63.

Xiong, Z., N. Sperelakis, et al. (1994). "Isoproterenol modulates the calcium channels through two different mechanisms in smooth-muscle cells from rabbit portal vein." Pflugers Arch **428**(2): 105-13.

Xiong, Z., N. Sperelakis, et al. (1994). "Regulation of L-type calcium channels by cyclic nucleotides and phosphorylation in smooth muscle cells from rabbit portal vein." J Vasc Res **31**(5): 271-9.

Yanagihara, K. and H. Irisawa (1980). "Inward current activated during hyperpolarization in the rabbit sinoatrial node cell." Pflugers Arch **385**(1): 11-9.

Yang, H. T., D. Tweedie, et al. (2002). "The ryanodine receptor modulates the spontaneous beating rate of cardiomyocytes during development." Proc Natl Acad Sci U S A **99**(14): 9225-30.

Yasui, K., W. Liu, et al. (2001). "I(f) current and spontaneous activity in mouse embryonic ventricular myocytes." Circ Res **88**(5): 536-42.

Yatani, A., J. Codina, et al. (1987). "Direct activation of mammalian atrial muscarinic potassium channels by GTP regulatory protein Gk." Science **235**(4785): 207-11.

Yatani, A., J. Codina, et al. (1987). "A G protein directly regulates mammalian cardiac calcium channels." Science **238**(4831): 1288-92.

Yatani, A., C. L. Seidel, et al. (1987). "Whole-cell and single-channel calcium currents of isolated smooth muscle cells from saphenous vein." Circ Res **60**(4): 523-33.

Yatani, A., D. L. Wilson, et al. (1983). "Recovery of Ca currents from inactivation: the roles of Ca influx, membrane potential, and cellular metabolism." Cell Mol Neurobiol **3**(4): 381-95.

Zaritsky, J. J., J. B. Redell, et al. (2001). "The consequences of disrupting cardiac inwardly rectifying K(+) current (I(K1)) as revealed by the targeted deletion of the murine Kir2.1 and Kir2.2 genes." J Physiol **533**(Pt 3): 697-710.

Zaza, A., G. Maccaferri, et al. (1991). "Intracellular calcium does not directly modulate cardiac pacemaker (if) channels." Pflugers Arch **419**(6): 662-4.

Zaza, A., R. B. Robinson, et al. (1996). "Basal responses of the L-type Ca2+ and hyperpolarization-activated currents to autonomic agonists in the rabbit sino-atrial node." J Physiol **491 (Pt 2)**: 347-55.

Zaza, A., M. Micheletti, et al. (1997). "Ionic currents during sustained pacemaker activity in rabbit sino-atrial myocytes." J Physiol **505 (Pt 3)**: 677-88.

Zhang, H. and M. Vassalle (2001). "Role of I(K) and I(f) in the pacemaker mechanisms of sino-atrial node myocytes." Can J Physiol Pharmacol **79**(12): 963-76.

Zhang, H., A. V. Holden, et al. (2000). "Mathematical models of action potentials in the periphery and center of the rabbit sinoatrial node." Am J Physiol Heart Circ Physiol **279**(1): H397-421.

Zhou, Z. and S. L. Lipsius (1994). "T-type calcium current in latent pacemaker cells isolated from cat right atrium." J Mol Cell Cardiol **26**(9): 1211-9.